

# **Identification and Characterisation of Cell Division Proteins in *Staphylococcus aureus***

By

Azhar F. Kabli MSc  
(University of Sheffield)

A thesis submitted for the degree of Doctor of Philosophy

December 2013

Department of Molecular Biology and Biotechnology,  
University of Sheffield, Firth Court, Western Bank, Sheffield, S10 2TN

## Summary

Cell division is a vital process that is required for bacterial proliferation and is thus an important target for the development of new antimicrobial agents. Bacterial cell division has mainly been studied in rod-shaped microorganisms, where a complex macromolecular machine, termed the divisome, mediates the division process. Cell division requires the coordination of components from the cytoplasm, through the membrane, to the cell wall where synthesis of new peptidoglycan takes place. *Escherichia coli* and *Bacillus subtilis* divisomes involve multiple essential components, mostly of unknown function. *Staphylococcus aureus* is a coccus that divides by binary fission in three orthogonal planes. The cell division machinery of *S. aureus* has been initially mapped as it is a clinically significant pathogen that poses a serious threat to public health due to resistance to current antibiotics. Indeed, the search for new drug targets against *S. aureus* is crucial.

In this study, *S. aureus* cell division components DivIC and FtsL were identified as members of a novel class of cell wall-binding proteins, and their affinity for the cell wall was shown to be enhanced by the presence of wall teichoic acids. A GFP fusion analysis and immunolocalisation experiments demonstrated that DivIC and FtsL may transiently localise to the division site and their localisation patterns suggest that they may identify previous or potential planes of division by recognising specific forms of peptidoglycan architecture. Attempts to determine the roles of *divIC* and *ftsL* in *S. aureus* using in-frame deletions and conditional lethal mutants of these genes were unsuccessful. Identifying the roles of DivIC and FtsL in *S. aureus* will enhance the utility of these proteins as putative antimicrobial targets.

## **Acknowledgements**

I would like to thank Prof. Simon Foster for giving me the opportunity to be part of his research group and for all his guidance and support throughout my project. I would like to thank Dr. Sveta Sedelnikova for help with protein crystallisation. I would like to acknowledge several people who aided me in this project; in particular, I thank Dr. Amy Bottomley and Dr. Gareth McVicker for technical assistance, Dr. Robert Turner for helping with peptidoglycan purification, Dr. Stéphane Mesnage for helping me with gel filtration and Western blotting and Dr. Victoria Kent, Dr. Richard Wheeler and Victoria Lund for assisting me with microscopy. I would like to thank all the past and present members of the Foster laboratory who have made working in this lab so enjoyable, especially Ashley Davies, Calum Chisnell, Alex Williams, Tomasz Prajsnar, Emma Johnson, Felix Weihs and Caroline Busch.

I extend special thanks and gratitude to my amazing husband, Esam, without whom completing my PhD would have been much more difficult. I would also like to express particular gratitude to my parents for their constant support, help, love, encouragement and motivation, and for being there no matter what. Special appreciation goes to my brother, Ahmad, and to my sisters, Amani and Abrar, for their love and support, as well as their understanding when I did not call them regularly. A special dedication goes to the joy of my life, my daughter Tala, for her patience with me being away and busy all the time.

I am also incredibly grateful to all my fantastic friends for keeping me smiling, especially Heba, Laila, Lulwa and Lina.

This work was funded by the Ministry of Higher Education of Saudi Arabia.

## Abbreviations

3D	three dimensional
°C	Degrees Celsius
μF	Microfarad
μg	Microgram
μl	Microlitres
μm	Micromolar
A	Absorbance
a.a	Amino acids
ADA	3-amino-D-ala
AFM	Atomic force microscopy
Ala	Alanine
Amp	Ampicillin
AP	Alkaline phosphatase
APS	Ammonium persulphate
Asp	Aspartic acid
attB	<u>A</u> ttachment site in the <u>b</u> acterial genome
ATc	Anhydrotetracycline
ATP	Adenosine triphosphate
ATPase	Adenosine triphosphate hydrolase
attP	<u>A</u> ttachment site in the <u>p</u> hage genome
BHI	Brain heart infusion
bp	Base pair
BPr	Baird-Parker medium
BSA	Bovine serum albumin
Cat	Chloramphenicol
CBD	Cell wall-binding domain
CFP	Cyan fluorescent protein
CHAP	<u>C</u> ysteine, <u>h</u> istidine-dependent <u>a</u> midohydrolase/ <u>p</u> eptidase
CIP	Calf intestinal alkaline phosphatase
d	Days

dH <sub>2</sub> O	Deionised water
DMSO	Dimethyl sulphoxide
DNA	Dexoyribonuclic acid
DNase	Deoxyribonuclease
dNTP	Dexoyribonucleoside-5'-triphosphate
dsDNA	Double stranded dexoyribonuclic acid
ECL	Enhanced chemiluminescent
EDTA	Ethylenediaminetetraacetic acid
Ery	Erythromycin
FITC	Fluorescein isothiocyanate
FPLC	Fast-performance liquid chromatography
FRAP	Fluorescence recovery after photobleaching
FRET	Förster resonance energy transfer
Fts	Filamentous temperature sensitive
g	Grams
GDP	Guanosine diphosphate
GFP	Green fluorescent protein
GlcNAc	N-acetylglucosamine
Glu	Glutamic acid
GTE	Glucose-Tris-EDTA
GTP	Guanosine triphosphate
GTPase	Guanosine triphosphate hydrolase
GW	Glycine-tryptophan
h	Hours
HADA	7-hydroxycoumarin 3-carboxylic acid (HCC-OH) attached to ADA
His	Histidine
HMW	High molecular weight
IgG	Immunoglobulin G
<i>int</i>	Integrase gene
IPTG	Isopropyl beta-D-1-thiogalactopyranoside
Kan	Kanamycin

K <sub>av</sub>	Partition coefficient
Kb	Kilobase pairs
K <sub>d</sub>	Dissociation constant
kDa	Kilodaltons
kV	Kilovolts
l	Litre
LB	Luria-Bertani medium
Lin	Lincomycin
LMP	Low melting point
LMW	Low molecular weight
LTA	Lipoteichoic acid
M	Molar
mA	Milliamps
max	Maximum
MCS	Multiple cloning site
mg	Milligrams
min	Minutes
ml	Millilitres
mM	Millimolar
mol	Moles
MDRSA	Multi-drug-resistant <i>S. aureus</i>
MRSA	Methicillin-resistant <i>S. aureus</i>
MurNAc	N-acetylmuramic acid
MW	Molecular weight
NA	Nutrient agar
NB	Nutrient broth
NBT	Nitroblue tetrazolium
NCBI	National Centre for Biotechnology Information
Neo	Neomycin
ng	Nanograms
nm	Nanometres

NMR	Nuclear magnetic resonance
Noc	Nucleoid occlusion factor
OD <sub>600</sub>	Optical density at 600 nm
PAGE	Polyacrylamide gel electrophoresis
PBP	Penicillin-binding protein
PBS	Phosphate buffered saline
PCR	Polymerase chain reaction
Pfu	Plaque forming units
PG	Peptidoglycan
pI	Isoelectric point
P <sub>pcn</sub>	Penicillinase promoter
P <sub>Spac</sub>	Spac promoter
P <sub>xyl</sub>	Xylose-inducible promoter
pmol	Picomoles
PVDF	Polyvinylidene difluoride
RBB	Remazol brilliant blue
RBS	ribosome binding site
RNA	Ribonucleic acid
RNase	Ribonucleic acid hydrolase
rpm	Revolutions per minute
RT	Room temperature
s	Seconds
SCO	Single crossover
sdH <sub>2</sub> O	Sterilised deionised water
SDM	Site-directed mutagenesis
SDS	Sodium dodecyl sulphate
SEC	Size exclusion chromatography
SEDS	Separation, elongation, division and sporulation family
Spec	Spectinomycin
SPOR	Sporulation-related repeat
SPR	Surface Plasmon resonance

TAE	Tris-acetate EDTA
Taq	Thermostable DNA polymerase derived from <i>Thermus aquaticus</i>
TBS	Tris buffered saline
TBSI	Tris buffered saline containing a protease inhibitor cocktail
TBST	Tris buffered saline tween
TEM	Transmission electron microscopy
TEMED	N,N,N',N'-tetramethyl-ethylenediamine
Tet	Tetracycline
TMDH	Transposon-mediated differential Hybridisation
Tris	Tris (hydroxymethyl) aminomethane
tRNA	Transfer RNA
Ts	Temperature sensitive
TSA	Tryptone soya agar
TSB	Tryptone soya broth
TSST1	Toxic shock syndrome toxin 1
U	Enzyme unit
UK	United Kingdom
US	United States
UV	Ultraviolet
V	Volts
v/v	Volume for volume
VISA	Vancomycin-insensitive <i>S. aureus</i>
VRE	Vancomycin-resistant <i>Enterococcus</i>
VRSA	Vancomycin-resistant <i>S. aureus</i>
w/v	Weight for volume
WTA	Wall teichoic acid
X-Gal	5'-bromo-4-chloro-3-indolyl-beta-D-galactopyranoside
xg	times gravity
Φ	Phage
Ω	Ohms



## Table of Contents

	Page number
Title page	i
Summary	ii
Acknowledgments	iii
Abbreviations	iv
Table of contents	ix
List of figures	xv
List of tables	xviii
<b>Chapter 1 Introduction</b>	<b>1-56</b>
1.1. Cell division	1
1.2. The importance of bacterial cell division	3
1.3. Temporal control of bacterial cell division	3
1.4. Cylindrical elongation in rod-shaped bacteria	4
1.5. The cell division machinery	8
1.5.1. The Z-ring	8
1.5.2. Selection of the division sites	13
1.5.2.1. The Min system	13
1.5.2.2. Nucleoid occlusion	16
1.5.3. Proteins that interact with FtsZ	17
1.5.3.1. FtsA	17
1.5.3.2. ZipA	20
1.5.3.3. ZapA	21
1.5.3.4. EzrA	22
1.5.3.5. SepF	23
1.5.3.6. Recently identified FtsZ-interacting proteins: ZipN, ZapB and ZapC	23
1.5.4. Late cell division proteins	25
1.5.4.1. FtsW	25
1.5.4.2. Penicillin binding proteins (PBPs)	26
1.5.4.3. FtsK	28
1.5.4.4. FtsL	29
1.5.4.5. FtsB/DivIC	31
1.5.4.6. FtsQ/DivIB	33
1.5.4.7. FtsN	34
1.5.4.8. FtsEX	36
1.5.4.9. GpsB (YpsB)	37
1.6. The separation of daughter cells	38
1.7. The late cell division proteins assembly pathway	40
1.8. Importance of cell division in drug development	40

1.9. Cell division in cocci	43
1.9.1. <i>S. aureus</i> as a cell division model	46
1.10. Staphylococcal species	48
1.11. <i>S. aureus</i>	50
1.11.1. <i>S. aureus</i> infection	50
1.11.2. Virulence factors	51
1.11.3. Antibiotic resistance	52
1.12. Study aims	56

## **Chapter 2 Materials and Methods** **57-107**

2.1. Media	57
2.1.1 Baird-Parker (BPr)	57
2.1.2 Brain Heart Infusion (BHI)	57
2.1.3 Luria-Bertani (LB)	57
2.1.4 LK	57
2.1.5 Nutrient agar (NA)	57
2.1.6 Nutrient broth (NB)	58
2.1.7 Tryptic soya broth (TSB)	58
2.1.8 Tryptic soya agar (TSA)	58
2.2. Antibiotics	58
2.3. Bacterial strains and plasmids	59
2.3.1 <i>S. aureus</i> strains	59
2.3.2 <i>E. coli</i> strains	60
2.3.3 <i>B. subtilis</i> strains	60
2.3.4 Plasmids	61
2.4. Buffers and stock solutions	63
2.4.1 Phage buffer	63
2.4.2 Phosphate buffered saline (PBS)	63
2.4.3 TAE (50x)	63
2.4.4 Tris buffered saline (TBS)	64
2.4.5 QIAGEN buffers	64
2.4.5.1 QIAGEN Buffer P1	64
2.4.5.2 QIAGEN Buffer P2	64
2.4.5.3 QIAGEN Buffer P3	64
2.4.5.4 QIAGEN Buffer EB	64
2.4.5.5 QIAGEN Buffer N3, QG, PB and PE	64
2.4.6 HiTrap purification buffers	65
2.4.6.1 0.1 M Sodium PO <sub>4</sub> Buffer	65
2.4.6.2 START buffer	65
2.4.6.3 Elution buffer	65
2.4.7 SDS-PAGE solutions	65
2.4.7.1 SDS-PAGE reservoir buffer (10x)	65
2.4.7.2 SDS-PAGE loading buffer (2x)	66
2.4.7.3 Coomassie Blue stain	66
2.4.7.4 Coomassie destain	66
2.4.7.5 Renaturing gel solution	66

2.4.7.6 Renaturing gel stain (10x)	67
2.4.8 Western blotting buffer	67
2.4.8.1 Blotting buffer	67
2.4.8.2 TBST (20x)	67
2.4.8.3 Blocking buffer	67
2.4.8.4 Alkaline Phosphatase buffer	68
2.4.8.5 GTE	68
2.4.8.6 TBSI	68
2.5. Enzymes and chemicals	68
2.6. Centrifugation	69
2.7. Determining bacterial cell density	69
2.7.1 Spectrophotometric measurement (OD <sub>600</sub> )	69
2.8. DNA purification technique	70
2.8.1 Genomic DNA extraction	70
2.8.2 Small scale plasmid purification	70
2.8.3 Large scale plasmid purification	71
2.8.4 Gel extraction of DNA	71
2.8.5 PCR purification	72
2.8.6 Ethanol precipitation of DNA	72
2.9. <i>In vitro</i> DNA manipulation techniques	73
2.9.1 Polymerase chain reaction (PCR) techniques	73
2.9.1.1 Primer design	73
2.9.1.2 PCR amplification	80
2.9.1.3 Colony PCR screening of <i>E. coli</i>	81
2.9.1.4 Colony PCR screening of <i>S. aureus</i>	81
2.9.2 TOPO TA cloning	81
2.9.3 QuickChange site-directed mutagenesis	82
2.9.3.1 Mutant strand synthesis reaction	82
2.9.3.2 Amplification products digestion	83
2.9.4 Restriction endonuclease digestion	83
2.9.5 Phosphate treatment of vector DNA	83
2.9.6 Ligation of DNA	83
2.9.7 Agarose gel electrophoresis	84
2.9.8 DNA sequencing	85
2.10. Transformation techniques	85
2.10.1 Transformation of <i>E. coli</i>	85
2.10.1.1 Preparation of electrocompetent <i>E. coli</i> cells	85
2.10.1.2 Electroporation of DNA into <i>E. coli</i> competent cells	86
2.10.2 Transformation of <i>S. aureus</i>	86
2.10.2.1 Preparation of electrocompetent <i>S. aureus</i> RN4220 cells	86
2.10.2.2 Electroporation of DNA into <i>S. aureus</i> RN4220 competent cells	87
2.10.3 Phage techniques	87
2.10.3.1 Bacteriophage	87
2.10.3.2 Preparation of phage lysate	87
2.10.3.3 Determination of phage titre	88
2.10.3.4 Phage transduction	88
2.11. Protein analysis	88
2.11.1 SDS-PAGE	88

2.11.2	Coomassie staining	91
2.11.3	Gel drying	91
2.11.4	Western blot	91
2.11.5	Bradford estimation of protein concentration	92
2.11.6	Mini-scale protein extraction of <i>S. aureus</i>	93
2.11.7	Preparation of bacterial whole cell lysate	94
2.12.	Production of recombinant proteins	94
2.12.1	Expression in <i>E.coli</i> BL21 (DE3)	94
2.12.2	Analysis of recombinant induction and solubility	95
2.12.3	Separation of the soluble and insoluble material	95
2.12.4	HiTrap™column for protein purification	96
2.12.5	Protein dialysis	96
2.12.5.1	Preparation of the dialysis membrane	96
2.12.5.2	Dialysis of the recombinant protein	97
2.13.	Generation of antibodies	97
2.13.1	Production of antibodies	97
2.13.2	Removal of cross-reactive antibodies	97
2.13.2.1	<i>E.coli</i> lysate treatment	97
2.14.	Peptidoglycan hydrolase assays	98
2.14.1	Peptidoglycan preparation	98
2.14.1.1	Peptidoglycan preparation from Gram-positive bacteria	98
2.14.1.2	Peptidoglycan preparation from <i>E.coli</i>	99
2.14.2	Staining of purified peptidoglycan	100
2.14.2.1	Staining with Procion Red	100
2.14.2.2	Staining with Remazol Brilliant Blue	100
2.14.3	Renaturing gel analysis	101
2.14.3.1	Renaturing SDS-PAGE	101
2.14.3.2	Analysis of peptidoglycan hydrolase by renaturing SDS-PAGE	101
2.14.4	Native zymogram assay	101
2.14.5	RBB release assay	102
2.15.	Size exclusion chromatography by FPLC	102
2.16.	Cell fractionation	105
2.17.	Preparation of sample for light microscopy	105
2.17.1	Fluorescence microscopy	106
2.17.2	Fluorescent labeling of nascent cell wall synthesis	106
2.17.3	Immunofluorescence	107
<b>Chapter 3 Analysis of DivIC and FtsL function</b>		<b>108-156</b>
3.1	Introduction	108
3.1.1	Aim of this chapter	110
3.2	Results	110
3.2.1	Bioinformatic analysis of cell division proteins	110
3.2.1.1	Bioinformatic analysis of DivIC	111
3.2.1.2	Bioinformatic analysis of FtsL	113
3.2.2	Expression of the soluble domains of DivIC and FtsL	113
3.2.2.1	pET overexpression system	118
3.2.2.2	Construction of the DivIC and FtsL expression plasmids	118

3.2.2.3 Overexpression of the recombinant proteins in <i>E. coli</i>	119
3.2.2.4 Purification of recombinant proteins by HiTrap™ column	121
3.2.3 Oligomerisation state of <i>S. aureus</i> recombinant proteins	123
3.2.4 Biochemical activity of recombinant proteins	126
3.2.4.1 Analysis of the peptidoglycan hydrolase activity of <i>S. aureus</i> recombinant proteins	126
3.2.4.2 Mapping the potential active site of <i>S. aureus</i> DivIC	130
3.2.4.2.1 Production of the recombinant <i>S. aureus</i> DivIC fragment	130
3.2.4.2.2 Site-directed mutagenesis of <i>S. aureus</i> DivIC	132
3.2.4.2.3 Analysis of the peptidoglycan hydrolase activity of SDMs	137
3.2.4.3 Analysis of peptidoglycan hydrolysis using other techniques	139
3.2.4.3.1 Native zymogram analysis	139
3.2.4.3.2 RBB release assay	141
3.2.4.4 Peptidoglycan binding analysis	141
3.2.4.4.1 Affinity binding assay	141
3.2.5 Structural analysis	146
3.3 Discussion	150
3.3.1 Oligomeric states of DivIC and FtsL	150
3.3.2 DivIC and FtsL peptidoglycan hydrolase activity	151
3.3.3 DivIC and FtsL peptidoglycan binding activity	153
3.4 Future work	156

## **Chapter 4 Localisation of *S. aureus* DivIC and FtsL** **157-199**

4.1 Introduction	157
4.1.1 Aims of this chapter	160
4.2 Results	160
4.2.1 Generation of anti-DivIC and anti-FtsL antibodies	160
4.2.2 Subcellular localisation of DivIC and FtsL	166
4.2.2.1 Western blot analysis of subcellular fractions	166
4.2.2.2 Localisation of <i>S. aureus</i> GFP-tagged proteins	169
4.2.2.2.1 Localisation of <i>S. aureus</i> DivIC-GFP+	169
4.2.2.2.2 Localisation of <i>S. aureus</i> FtsL-GFP+	183
4.2.3 DivIC and FtsL overexpression in <i>S. aureus</i>	184
4.2.3.1 pLOW system	184
4.2.3.2 Construction of overexpression plasmid	186
4.2.3.3 Induction of protein expression	189
4.2.3.4 Phenotypic effect of DivIC and FtsL overexpression in <i>S. aureus</i>	191
4.2.4 Immunolocalisation of <i>S. aureus</i> DivIC and FtsL	193
4.2.4.1 Immunolocalisation of <i>S. aureus</i> DivIC	193
4.2.4.2 Immunolocalisation of <i>S. aureus</i> FtsL	193
4.3 Discussion	197
4.3.1 Localisation of DivIC in <i>S. aureus</i>	197
4.3.2 Localisation of FtsL in <i>S. aureus</i>	199
4.4 Future work	199

## **Chapter 5 Analysis of the roles of DivIC and FtsL** **201-247**

5.1	Introduction	201
5.1.1	Aims of this chapter	202
5.2	Results	203
5.2.1	Construction of <i>S. aureus divIC</i> and <i>ftsL</i> conditional lethal mutants	203
5.2.1.1	Construction of an integration plasmid containing P <sub>spac</sub>	203
5.2.1.2	Construction of regulatable copies of <i>divIC</i> and <i>ftsL</i>	204
5.2.2	Construction of <i>S. aureus divIC</i> and <i>ftsL</i> deletion mutants	217
5.2.3	Complementation of the <i>S. aureus divIC</i> and <i>ftsL</i> in-frame deletion mutants	242
5.3	Discussion	245
5.3.1	The essentiality of <i>divIC</i> and <i>ftsL</i> in <i>S. aureus</i>	245
5.4	Future work	247
<b>Chapter 6 General discussion</b>		<b>248-260</b>
6.1	Conservation of the bacterial divisome	248
6.2	<i>S. aureus</i> , a model of cell division	251
6.3	Cell wall-binding proteins	254
6.4	Cell division as an antibacterial target	257
6.5	Future work	259
<b>References</b>		<b>261-284</b>

Enclosed CD-ROM contains an electronic copy of this thesis and movies showing Z-stack images. Images may be better seen electronically.

## List of Figures

<b>Figure 1.1</b> Cell wall assembly in rod- and coccus-shaped gram-positive bacteria	2
<b>Figure 1.2</b> Elongation machinery of <i>B. subtilis</i> and <i>E. coli</i>	7
<b>Figure 1.3</b> Cell division machinery of <i>B. subtilis</i> and <i>E. coli</i>	9
<b>Figure 1.4</b> Interaction maps of cell division complex	10
<b>Figure 1.5</b> The Min system in <i>E. coli</i> and <i>B. subtilis</i>	14
<b>Figure 1.6</b> The nucleoid occlusion system in rod-shaped bacteria	18
<b>Figure 1.7</b> Timeline of introduction and subsequent development of resistance by <i>S. aureus</i> to commonly used antibiotics	53
<b>Figure 2.1</b> Calibration curve for Bradford assay	93
<b>Figure 2.2</b> Calibration curves of gel filtration standards	104
<b>Figure 3.1</b> Bioinformatic analysis of <i>S. aureus</i> and <i>B. subtilis</i> DivIC	114
<b>Figure 3.2</b> Bioinformatic analysis of <i>S. aureus</i> and <i>B. subtilis</i> FtsL	116
<b>Figure 3.3</b> Construction of <i>S. aureus</i> and <i>B. subtilis</i> protein overexpression plasmids	120
<b>Figure 3.4</b> Production and purification of recombinant proteins	122
<b>Figure 3.5</b> <i>S. aureus</i> DivIC oligomerisation	124
<b>Figure 3.6</b> <i>S. aureus</i> FtsL oligomerisation	125
<b>Figure 3.7</b> Zymogram analysis of <i>S. aureus</i> DivIC and FtsL	127
<b>Figure 3.8</b> <i>divIC</i> mutant overexpression plasmids	131
<b>Figure 3.9</b> Production and purification of truncated DivIC <sub>Sa</sub> fragment and site-directed mutant proteins	133
<b>Figure 3.10</b> DivIC orthologs	135
<b>Figure 3.11</b> Zymogram analyses of <i>S. aureus</i> DivIC site-directed mutants	138
<b>Figure 3.12</b> Native zymogram analysis	140
<b>Figure 3.13</b> RBB release assay	142
<b>Figure 3.14</b> Cell wall affinity binding assay of DivIC <sub>Sa</sub> , FtsL <sub>Sa</sub> and FtsL <sub>Ba</sub>	144
<b>Figure 3.15</b> Cell wall affinity binding assays of <i>S. aureus</i> DivIC mutants	145
<b>Figure 3.16</b> Initial crystallization condition screening results for recombinant <i>S. aureus</i> DivIC	149

<b>Figure 4.1</b> Reactivity of polyclonal $\alpha$ -DivIC antibodies	161
<b>Figure 4.2</b> Reactivity of polyclonal $\alpha$ -FtsL antibodies	163
<b>Figure 4.3</b> Subcellular localisation of DivIC and FtsL in <i>S. aureus</i>	167
<b>Figure 4.4</b> Construction of a <i>S. aureus divIC-gfp+</i> strain	170
<b>Figure 4.5</b> Map of pGL485, the <i>lacI</i> expression plasmid	172
<b>Figure 4.6</b> Functionality of the DivIC-GFP+ fusion in <i>S. aureus</i>	174
<b>Figure 4.7</b> Localisation of DivIC-GFP+ fusion in <i>S. aureus</i>	175
<b>Figure 4.8</b> Localisation of DivIC-GFP+ fusion in <i>S. aureus</i>	178
<b>Figure 4.9</b> Localisation patterns of DivIC-GFP+ fusion in <i>S. aureus</i>	180
<b>Figure 4.10</b> Western blot analysis of a DivIC-GFP+ fusion in <i>S. aureus</i>	182
<b>Figure 4.11</b> Construction of a <i>S. aureus ftsL-gfp+</i> strain	185
<b>Figure 4.12</b> Construction of pAFK4 (pLOW- <i>S. aureus divIC</i> ) plasmid	187
<b>Figure 4.13</b> Construction of pAFK5 (pLOW- <i>S. aureus ftsL</i> ) plasmid	188
<b>Figure 4.14</b> Western blot analysis of AFK4 (SH1000 <i>spa::kan</i> pAFK4) and AFK12 (SH1000 <i>spa::kan</i> pAFK5)	190
<b>Figure 4.15</b> Phenotypic effect of DivIC and FtsL overexpression in <i>S. aureus</i>	192
<b>Figure 4.16</b> Immunolocalisation of DivIC in <i>S. aureus</i>	194
<b>Figure 4.17</b> Immunolocalisation of DivIC in <i>S. aureus</i>	196
<b>Figure 5.1</b> Construction of the P <sub>Spac</sub> -pCL84 plasmid (pAFK7)	205
<b>Figure 5.2</b> Construction of pAFK10 (P <sub>Spac</sub> - <i>divIC</i> -pCL84)	207
<b>Figure 5.3</b> Construction of pAFK11 (P <sub>Spac</sub> - <i>ftsL</i> -pCL84)	208
<b>Figure 5.4</b> Construction of the P <sub>Spac</sub> - <i>divIC</i> plasmid pAFK12	210
<b>Figure 5.5</b> Construction of the P <sub>Spac</sub> - <i>ftsL</i> plasmid pAFK13	211
<b>Figure 5.6</b> Map of the integrative plasmid, pKASBAR	213
<b>Figure 5.7</b> Construction of the integration plasmids pGM073 and pAFK22	214
<b>Figure 5.8</b> Construction of the pAFK16 (P <sub>Spac</sub> - <i>divIC</i> -pAFK22) plasmid	215
<b>Figure 5.9</b> Construction of the pAFK17 (P <sub>Spac</sub> - <i>ftsL</i> -pAFK22) plasmid	216
<b>Figure 5.10</b> Integration of pAFK16 into the <i>S. aureus</i> chromosome	218
<b>Figure 5.11</b> Integration of pAFK17 into the <i>S. aureus</i> chromosome	220



<b>Figure 5.12</b> Construction of the <i>S. aureus divIC</i> in-frame deletion plasmid, pAFK8	222
<b>Figure 5.13</b> Construction of the <i>S. aureus divIC</i> in-frame deletion plasmid, pAFK9	224
<b>Figure 5.14</b> Construction of the <i>S. aureus divIC</i> in-frame deletion plasmid, pAFK14	229
<b>Figure 5.15</b> Construction of the <i>S. aureus divIC</i> in-frame deletion plasmid, pAFK15	231
<b>Figure 5.16</b> Construction of the pAFK14 and pAFK15 plasmids in <i>S. aureus</i>	234
<b>Figure 5.17</b> Homologous recombination of pAFK14 into the <i>S. aureus</i> SH1000 chromosome	235
<b>Figure 5.18</b> Homologous recombination of pAFK15 into the <i>S. aureus</i> SH1000 chromosome	237
<b>Figure 5.19</b> Creation of the <i>divIC</i> deletion in <i>S. aureus</i> SH1000	240
<b>Figure 5.20</b> Creation of the <i>ftsL</i> deletion in <i>S. aureus</i> SH1000	241
<b>Figure 5.21</b> Creation of the conditional <i>S. aureus divIC</i> lethal mutant	243
<b>Figure 5.22</b> Creation of the conditional <i>S. aureus ftsL</i> lethal mutant	244
<b>Figure 6.1</b> Cell division machinery of <i>S. aureus</i>	250
<b>Figure 6.2</b> <i>S. aureus</i> cell wall architecture and maturation	252

## List of Tables

<b>Table 1.1</b> Conservation of cell division genes between <i>S. aureus</i> and <i>B. subtilis</i>	49
<b>Table 2.1</b> Antibiotic stock solutions and concentrations	58
<b>Table 2.2</b> <i>S. aureus</i> strains used in this study	59
<b>Table 2.3</b> <i>E. coli</i> strains used in this study	60
<b>Table 2.4</b> <i>B. subtilis</i> strain used in this study	60
<b>Table 2.5</b> Plasmids used in this study	61
<b>Table 2.6</b> Stock solutions and concentrations	68
<b>Table 2.7</b> Primers used in this study for DNA amplification by PCR	74
<b>Table 2.8</b> DNA fragments used as size markers for agarose gel electrophoresis	84
<b>Table 2.9</b> Protein size standards used in this study	90
<b>Table 2.10</b> Gel filtration size standards	103
<b>Table 2.11</b> Fluorescence filter sets used	106
<b>Table 3.1</b> Bioinformatic analysis summary	112
<b>Table 6.1</b> Conservation of divisome components across species	249

# Chapter 1

## Introduction

### 1.1. Cell division

Cell division is a vital process for maintaining the growth and proliferation of organisms. The time between each cell division is referred to as a cell cycle. During this period, the cell duplicates its constituents and distributes them between two cells to ensure that genetic information is passed from parent to daughter. Most prokaryotic cells undergo a cell division process known as binary fission, which permits the cell to split in the middle, resulting in two equal daughter cells (Madigan and Martinko, 2006; Sievers and Errington, 2000a; Errington *et al.*, 2003). In general, the prokaryotic cell begins the division process by duplicating its DNA, and chromosome segregation along with cell elongation (to two times its size) follows. A septum is then formed in the middle of the cell, the cell splits into two daughter cells, and the process is repeated over and over again (Figure 1.1) (Madigan and Martinko, 2006; Sievers and Errington, 2000a; Errington *et al.*, 2003). Eukaryotes and prokaryotes share some common features of cell division, such as DNA replication and chromosome segregation; however, the mechanisms used to accomplish these processes vary between the two types of organisms (Fletcher *et al.*, 2007). In eukaryotic cells, the microtubule-organising centres mediate chromosome separation and organisation (Goshima and Kimura, 2010). In contrast, DNA replication and chromosome separation occur simultaneously during prokaryotic cell division (Toro and Shapiro, 2010). Cytokinesis and full cell separation in both eukaryotes and prokaryotes occurs through the formation of a contractile ring-like structure. In eukaryotes, this structure consists of 1,000-2,000 actin filaments (Kamasaki *et al.*, 2007; van den Ent *et al.*, 2001), whereas in prokaryotes, the tubulin-like ring structure is smaller (Erickson, 1997; Raychaudhuri, 1999; Lan *et al.*, 2009). Thus, the cell division process between eukaryotes and prokaryotes has some differences and similarities; this chapter will focus on prokaryotic cell division.

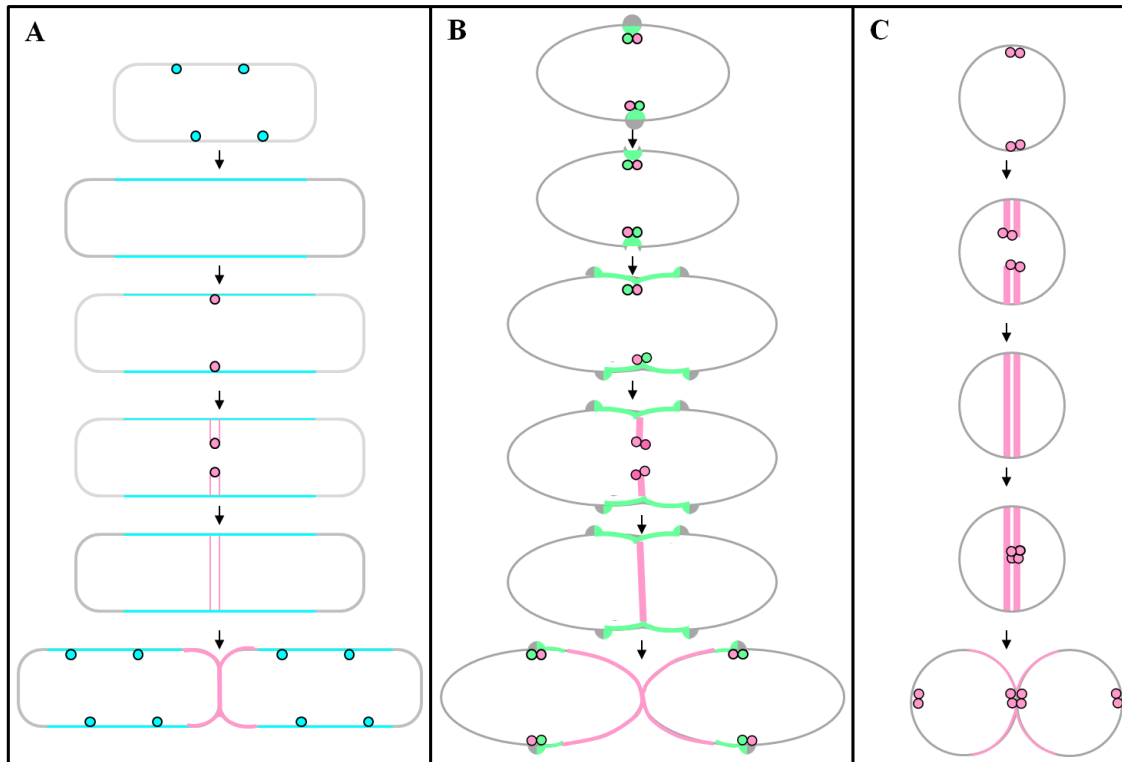


**Figure 1.1 Cell wall assembly in rod- and coccus-shaped gram-positive bacteria**

Schematic representations of cell wall assembly in gram-positive rods (e.g., *B. subtilis*, A), ovococci (e.g., *Streptococcus pneumoniae*, B) and true cocci (e.g., *S. aureus*, C). The parental cell wall is represented in grey; the nascent lateral cell wall is represented in cyan. The new peripheral cell wall and the new septal cell wall are represented in green and pink, respectively. The elongation machinery is shown in cyan with a black outline; the peripheral synthesis machinery is shown in green with black outlines. The septal synthesis machinery is represented in pink with a black outline. Adapted from (Zapun *et al.*, 2008; Pinho *et al.*, 2013).

## 1.2. The importance of bacterial cell division

Bacterial cell division has primarily been studied in model rod-shaped microorganisms, including Gram-positive bacilli, such as *B. subtilis*, and Gram-negative bacilli, such as *E. coli*. A complex macromolecular machine, called the divisome, mediates the cell division process. Many of the divisome components are essential for bacterial cell viability. Ten cell division genes have been found to be essential in *E. coli* (Buddelmeijer and Beckwith, 2002), *B. subtilis* (Kobayashi *et al.*, 2003) and *Caulobacter crescentus* (Goley *et al.*, 2011). Six cell division genes have been identified to be essential genes in *S. pneumoniae* (Song *et al.*, 2005).

Cell division is conserved between prokaryotes; however, the mechanisms differ. The differences are likely due to the shape and envelope structure of the bacterial cells. The key components of the cell division machinery, such as the FtsZ protein, are highly conserved among bacterial species whereas others vary significantly (Angert, 2005). Some bacterial species do not divide by binary fission, and in others, alternative mechanisms of division may be used only under certain conditions, such as stress (Angert, 2005). These alternative mechanisms include budding, as observed in proteobacteria, such as *Ancalomicrobium*, *Hyphomonas* and *Pedomicrobium* (Angert, 2005), and multiple offspring formation, as seen in *Metabacterium polyspora*, in which multiple endospores are formed by asymmetric division (Angert and Losick, 1998). *Streptomyces* produces branched filaments through hyphal growth, and these filaments contain multiple nuclei that will occasionally septate (Chater, 1993). In cell wall-deficient, L-form *B. subtilis*, propagation occurs without the cell division machinery and instead proceeds through an extrusion-resolution mechanism (Leaver *et al.*, 2009).

## 1.3. Temporal control of bacterial cell division

Cell division in bacteria must be coordinated to guarantee that cells are partitioned equally to realise their developmental fate (Lutkenhaus and Addinall, 1997). The division of *Enterococcus hirae* is initiated independently of chromosome replication and growth rate but occurs at a consistent cell volume (Gibson *et al.*, 1983). In addition, *B. subtilis* and *E. coli* reach a certain cell length before the chromosome begins to dissociate, a process that is a prerequisite for the formation of the septum

(Donachie and Begg, 1989; Sharpe *et al.*, 1998). To ensure that cells are coordinating their size with their growth rate, a mechanism must exist to detect nutrient availability so that it may be communicated to the divisome, allowing appropriate timing of septum formation initiation (Wang and Levin, 2009). The growth rate appears to affect the assembly of FtsZ proteins and the period between formation of the ring and cytokinesis, indicating that cell size is regulated by growth rate through the polymerisation of FtsZ (Den Blaauwen *et al.*, 1999; Weart and Levin, 2003). The glucolipid biosynthesis pathway has been described in *B. subtilis* and works as a metabolic sensor to coordinate the size of the cell with its growth rate (Weart *et al.*, 2007). An important component of this pathway is the effector protein, UgtP, a glucosyltransferase that has been shown to inhibit the assembly of FtsZ *in vitro* and regulate the formation of the Z-ring *in vivo*.

UgtP ensures that the cell reaches a certain mass, the “critical mass”, before cytokinesis is initiated (Weart *et al.*, 2007). Two enzymes, PgcA and GtaB, provide nutritional information directly to the divisome, suspending division until cells reach the critical mass (Weart *et al.*, 2007). The expression and midcell localisation of UgtP is altered by the availability of nutrients, thereby guaranteeing that inhibition of division is coupled to growth rate (Weart *et al.*, 2007). *B. subtilis* cells deficient in *ugtP* generate small daughter cells with disruptions in FtsZ assembly; thus, cell division and chromosome segregation are perturbed (Weart *et al.*, 2007). *E. coli* cells lacking the *pgcA* homologue, *pgm*, show a similar phenotype (Lu and Kleckner, 1994). Recently an UgtP homologue, OpgH has been described in *E. coli*, which acts as a nutrient-dependant regulator of the cell size. It localises at the division site in high nutrient media and disrupts FtsZ assembly, thus halting cell division and increasing the size of the cell (Hill *et al.*, 2013).

#### **1.4. Cylindrical elongation in rod-shaped bacteria**

Rod-shaped bacteria, such as *B. subtilis* and *E. coli*, increase in cell size by increasing in cell length before division (Grover *et al.*, 1977). The mode of peptidoglycan synthesis changes from an elongating status, sustaining a constant cell diameter, to a reduction in the diameter of the cell at a specific location, resulting in septum formation and cell constriction (Grover *et al.*, 1977). Cell

constriction and elongation depends on the local activity of a protein complex that incorporates peptidoglycan precursors using the old cell wall as a template (den Blaauwen *et al.*, 2008). Early studies on bacterial shape presumed that shape was defined by the cell wall, which functions as an exoskeleton (Holtje, 1998; Nanninga, 1998). However, recent studies have shown that many proteins are involved in controlling cell morphology (den Blaauwen *et al.*, 2008). Mutations in the *mreB*, *mreC*, *mreD*, *rodA*, *pbp-2a* or *pbp-H* genes in *B. subtilis* (Levin *et al.*, 1992; Henriques *et al.*, 1998; Wei *et al.*, 2003; Leaver and Errington, 2005), *mreB*, *mreC*, *mreD* or *rodA* genes in *E. coli* (Matsuzawa *et al.*, 1973; Wachi *et al.*, 1987; Wachi *et al.*, 1989) and *mreB*, *mreC*, *mreD* or *rodA* genes in *Salmonella typhimurium* (Costa and Anton, 1999; Normark, 1969) result in spherical cells. Furthermore, mutation of the RodA homologue in the ovococcus, *Streptococcus thermophilus*, leads to spherical growth (Thibessard *et al.*, 2002). MreB and its *B. subtilis* paralogues MreBH and Mbl have been identified as actin homologues that form dynamic bundle filaments (Dempwolff *et al.*, 2011), indicating a role of the MreB family as cytoskeletal components that organise lateral peptidoglycan synthesis (Figge *et al.*, 2004; Defeu Soufo and Graumann, 2004; Daniel and Errington, 2003; Shih *et al.*, 2003; van den Ent *et al.*, 2001; Jones *et al.*, 2001). The integral proteins MreC and MreD are believed to stabilise the MreB cytoskeleton by linking the cytosolic MreB filaments to the extracellular peptidoglycan synthesis machinery (Leaver and Errington, 2005; Divakaruni *et al.*, 2005; Kruse *et al.*, 2005). The elongation machinery is believed to involve penicillin-binding proteins (PBPs), which are associated with cell wall synthesis and the SEDS (shape, elongation, division and sporulation) protein RodA (Ishino *et al.*, 1986; Henriques *et al.*, 1998; Real *et al.*, 2008). SEDS proteins are usually present in the same operon as the class B PBPs, and their function is to translocate the peptidoglycan precursors from the cytoplasm to the extracellular site of synthesis (Ehlert and Holtje, 1996). A fluorescent derivative of vancomycin that stains nascent peptidoglycan synthesis (Pinho and Errington, 2003) has demonstrated a cylindrical incorporation pattern of labelling in *B. subtilis* (Daniel and Errington, 2003; Tiyanont *et al.*, 2006), *E. coli* (Varma *et al.*, 2007) and *C. crescentus* (Divakaruni *et al.*, 2007). However, current data suggest no overall pattern of synthesis but a discontinuous and patchy incorporation in *E. coli* and *C. crescentus* (Turner *et al.*, 2013). Recent studies using total internal reflection fluorescence

microscopy have shown that MreB does not form a helical cytoskeletal structure but forms distinct foci, moving perpendicular and bidirectionally along the cell axis of *B. subtilis* (Dominguez-Escobar *et al.*, 2011; Garner *et al.*, 2011). The peptidoglycan precursors have been shown to localise in an identical arrangement to MreB (Dominguez-Escobar *et al.*, 2011). The inhibition of cell wall synthesis hinders the motility of MreB (Garner *et al.*, 2011), indicating that cell wall synthesis drives MreB dynamics. The localisation of MreB is dependent upon RodA, MreC and MreD, and the association of the MreBCD complex is essential for lateral bacterial growth (Kruse *et al.*, 2005). MreC has been shown to localise in a manner similar to MreB in both *B. subtilis* and *C. crescentus* (Leaver and Errington, 2005; Divakaruni *et al.*, 2005; Dye *et al.*, 2005). Direct interactions between MreC, MreD, MreB, RodA and PBPs have been demonstrated by bacterial two-hybrid and pull-down assays (Kruse *et al.*, 2005; Leaver and Errington, 2005; van den Ent *et al.*, 2006; Kawai *et al.*, 2009; White *et al.*, 2010). Additionally, proteins that are involved in the synthesis of wall teichoic acid (WTA) interact with MreB, MreC and MreD (Mohammadi *et al.*, 2007; Formstone *et al.*, 2008; White *et al.*, 2010).

Lateral cell wall synthesis is conducted by a complex of proteins (Figure 1.2), including cytoskeletal components (MreB, MreC and MreD), to ensure insertion of new peptidoglycan material into the existing cell wall. Proteins such as PBPs and RodA also participate in the synthesis of the cell wall and insertion of new peptidoglycan material into the old lateral cell wall. Recent studies have shown that RodZ localises in a pattern similar to MreB in *E. coli*, *B. subtilis* and *C. crescentus* (Shiomi *et al.*, 2008; Alyahya *et al.*, 2009), and the absence of RodZ results in spherical cells and the misassembly of MreB (Shiomi *et al.*, 2008; Bendezu *et al.*, 2009). RodZ interacts with RodA, MreB and MreD, indicating its involvement in the elongation machinery (van den Ent *et al.*, 2010; White *et al.*, 2010). In *E. coli*, pseudorevertants of  $\Delta rodZ$  mutants acquired a near-wild-type rod-shaped phenotype, suggesting that RodZ is not the only protein required for cell wall elongation (Niba *et al.*, 2010).



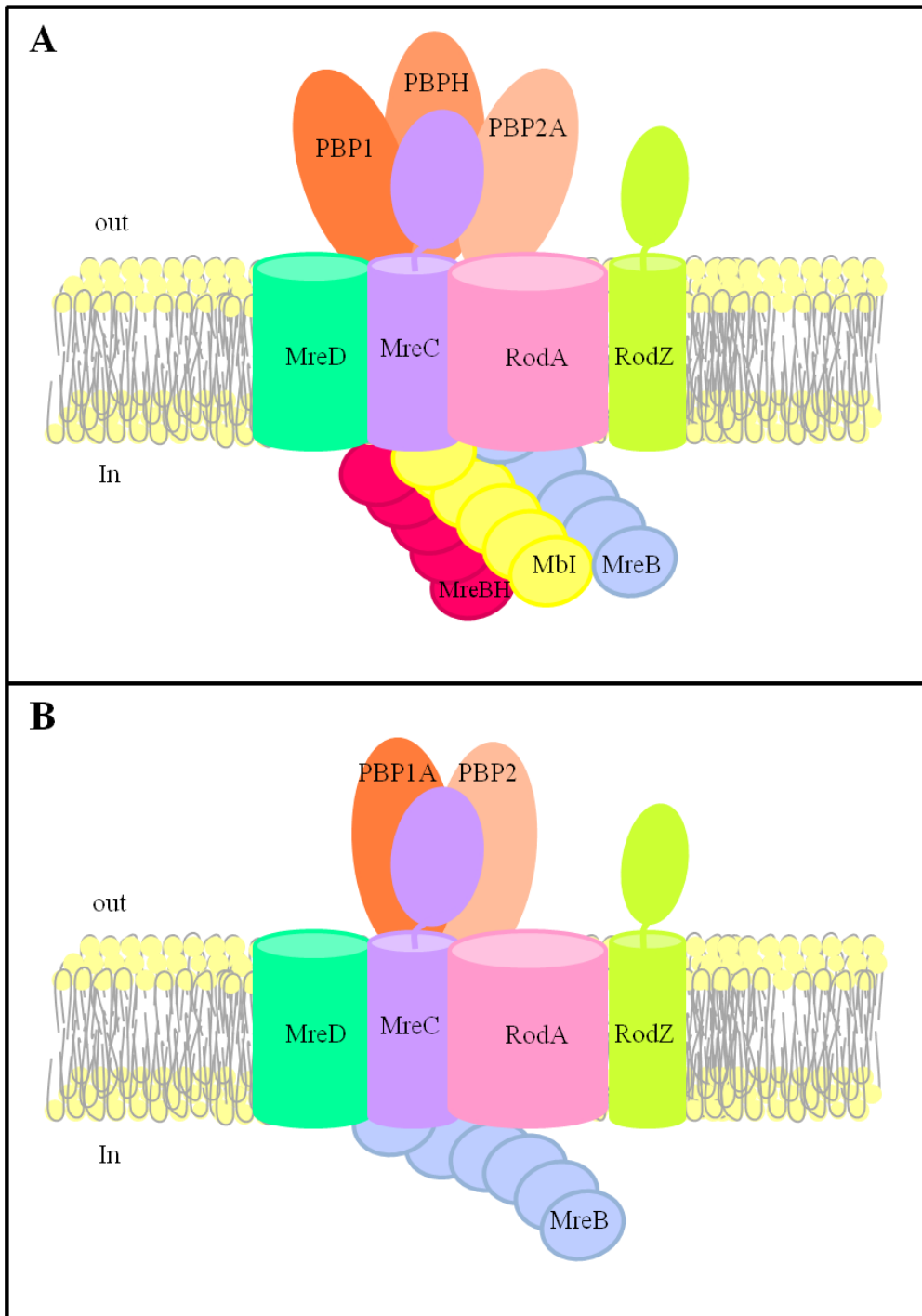


**Figure 1.2 Elongation machineries of *B. subtilis* and *E. coli***

Schematic representations of the elongation machineries in *B. subtilis* (A) and *E. coli* (B). The components were determined based on protein-protein interactions and localisation at the midcell. Not all known interactions between the elongation components are shown here. Adapted from (Chastanet and Carballido-Lopez, 2012; Carballido-Lopez and Formstone, 2007; Typas *et al.*, 2011).

## 1.5. The cell division machinery

As mentioned above, the cell division machinery has been mainly studied in rod-shaped bacteria. Many of the divisome components have been identified, but their precise molecular functions remain poorly understood (Gueiros-Filho and Losick, 2002; Daniel *et al.*, 1998). The study of these components is complicated due to the complexity of the cell division process and the lethality of gene mutations. Biochemical assays, *in vivo* imaging, structural determination, mutation, conditional mutation and two-hybrid analysis have been very useful in identifying novel cell division components and elucidating their function. Some differences in divisome composition have been found between *E. coli* and *B. subtilis* (Figure 1.3), and some of the components are conserved between the two species.

The cell division apparatus (the divisome) is composed of many proteins, several of which are Fts (filamentous temperature sensitive) that are found in the septal site (Bramhill, 1997; Weiss, 2004). In the absence of one of these essential Fts proteins, the bacterial cells cannot proliferate, leading to elongated filamentous cells and death (van den Ent and Lowe, 2000; Hale and de Boer, 1997).

The divisome proteins can be categorised into two groups based on their localisation and timing of participation in division; the FtsZ interacting proteins, such as FtsA, ZipA (in *E. coli*), ZapA (in *B. subtilis* and *E. coli*) and EzrA (in Gram-positive bacteria), interact directly, whereas the late division proteins depend on the FtsZ interacting proteins for localisation to the division site (Daniel *et al.*, 2006). The interactions between cell division apparatus proteins have been demonstrated by the bacterial/yeast two-hybrid system in *S. aureus* (Figure 1.4A) (Steele *et al.*, 2011), *S. pneumoniae* (Figure 1.4B) (Maggi *et al.* 2008), *B. subtilis* (Figure 1.4C) (Daniel *et al.*, 2006), and *E. coli* (Figure 1.4D) (Di Lallo *et al.*, 2003).

### 1.5.1. The Z-ring

The FtsZ protein is a GTPase, and monomers of the protein assemble and polymerise into a Z-ring structure at the potential site of cytokinesis (Di Lallo *et al.*, 2003; Gueiros and Losick, 2002).

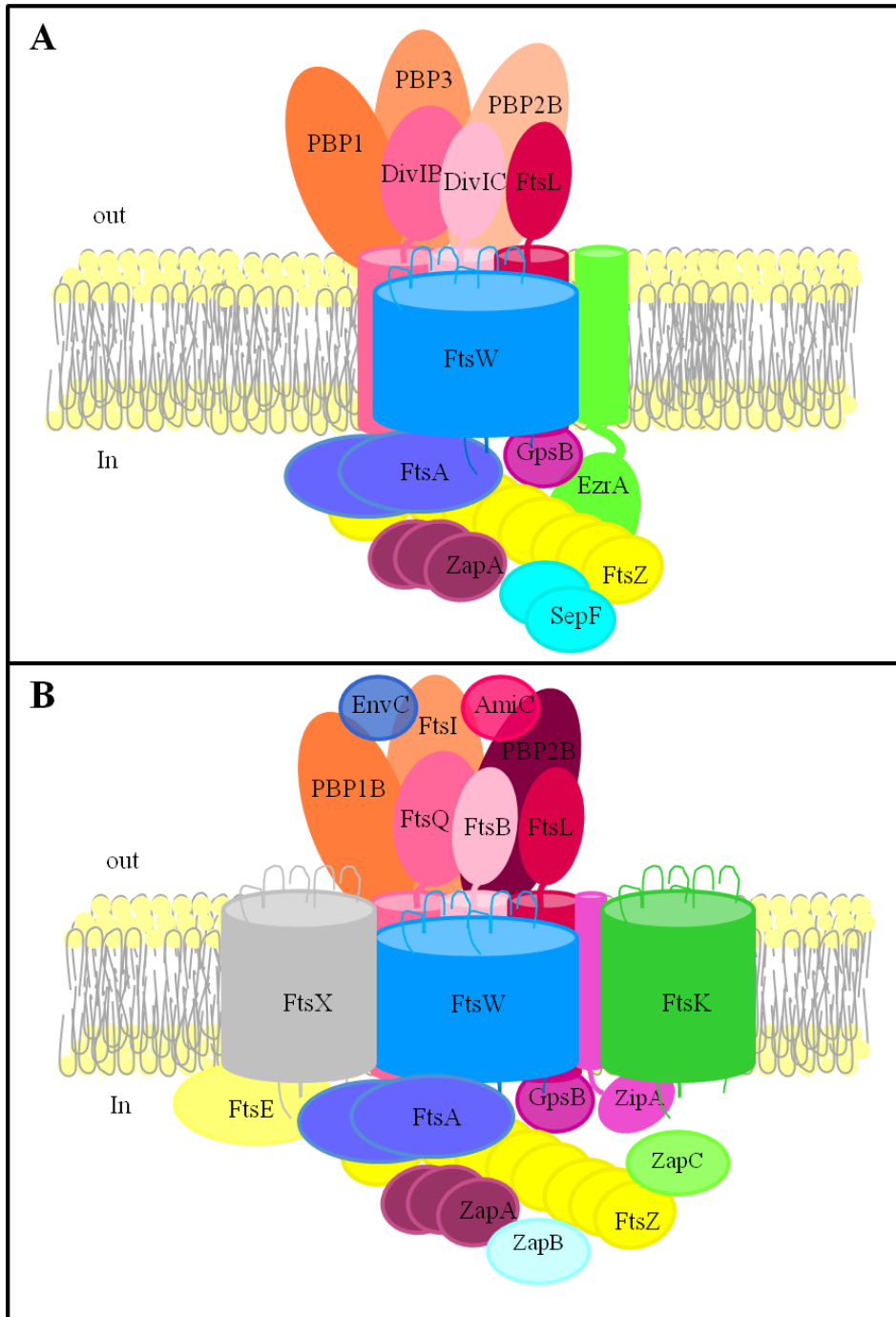


**Figure 1.3 Cell division machineries of *B. subtilis* and *E. coli***

Schematic representations of the cell division machineries in *B. subtilis* (A) and *E. coli* (B). The components were determined based on protein-protein interactions and localisation at the midcell using fluorescent protein fusions or immunolocalisation. Not all known interactions between the division components are shown here. Analogues are shown in the same colours. Adapted from (Carballido-Lopez and Formstone, 2007; Gamba *et al.*, 2009; Adams and Errington, 2009; Errington *et al.*, 2003; de Blaauwen *et al.*, 2008).

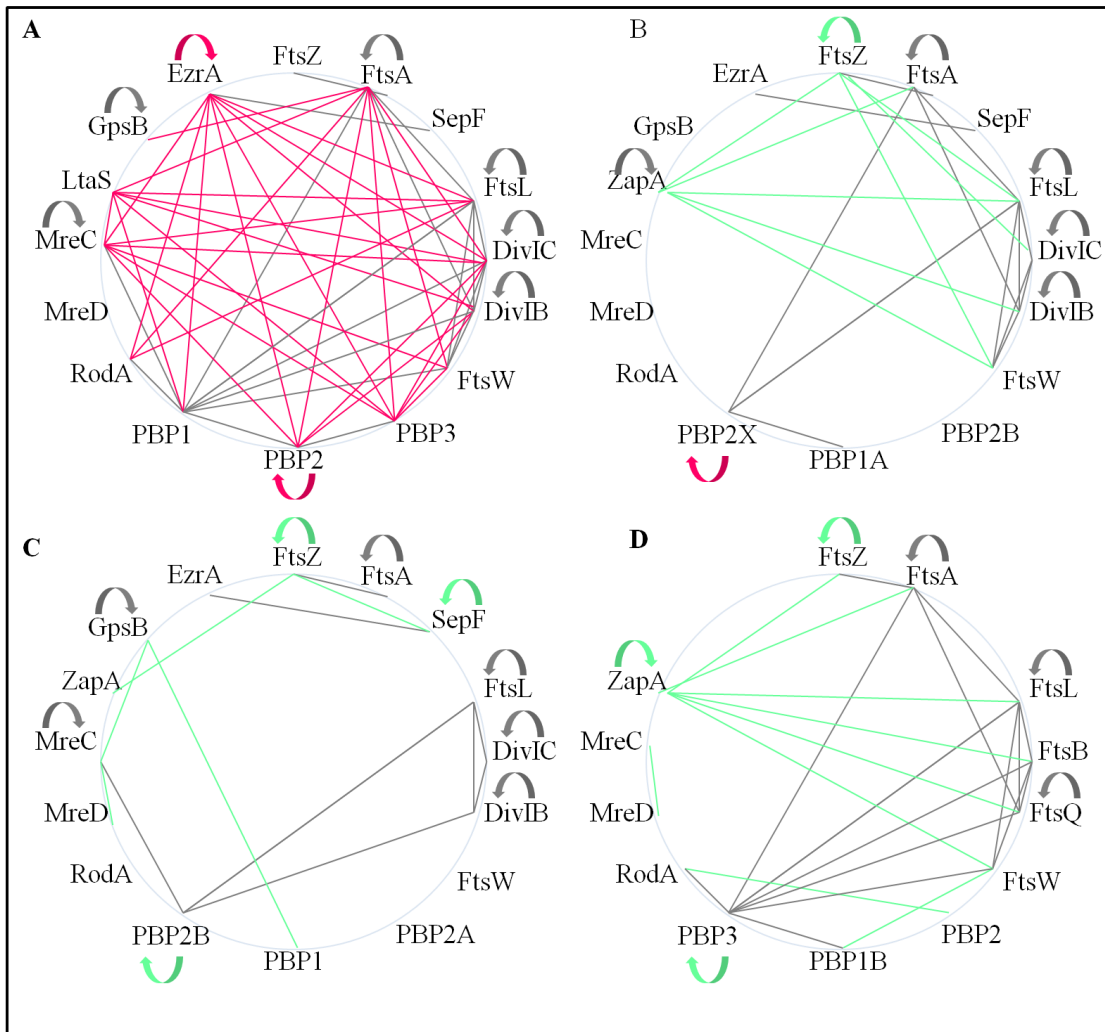


**Figure 1.4 Interaction maps of cell division components**

- A. The interaction map between cell division components in *S. aureus* was determined using the bacterial-two hybrid system
- B. Interaction map between cell division components in *S. pneumoniae* was determined using the bacterial/yeast-two hybrid system.
- C. Interaction map between cell division components in *B. subtilis* was determined using the bacterial/yeast-two hybrid system.
- D. Interaction map between cell division components in *E. coli* was determined using the bacterial/yeast-two hybrid system.

Curved arrows signify self-interactions. Interactions that are observed in other species are signified by grey lines, and interactions that are novel in *S. aureus* are indicated by pink lines. Interactions that are observed in other species but not in *S. aureus* are signified by green lines. An absence of lines between proteins in other species does not indicate negative results, as not all proteins have been studied to determine their interactions.

(Steele *et al.*, 2011; Maggi *et al.*, 2008; Daniel *et al.*, 2006; Karimova *et al.*, 2005).

GTP hydrolysis (Scheffers *et al.*, 2002) is initiated through the binding of the FtsZ amino-terminal to GTP (Singh *et al.*, 2007). This process is highly conserved among many organisms, such as archaea and bacteria, with the exception of Chlamydiae, *Ureaplasma urealyticum* and *Aeropyrum pernix* (Beech *et al.* 2000; Margolin, 2000). FtsZ has also been found in higher plants and plays an important role in chloroplast division (Osteryoung *et al.*, 1998). FtsZ is potentially one of the most important proteins in the divisome (Vaughan *et al.*, 2004; Sievers and Errington, 2000b; Singh *et al.*, 2007) and is the only cell division protein that is conserved in microorganisms that lack a cell wall, e.g., *Mycoplasma* (Wang and Lutkenhaus, 1996).

FtsZ is a homologue of the mammalian protein tubulin (Scheffers *et al.*, 2002). It is a soluble cytoplasmic protein (Hale and de Boer, 1997) that is associated with the early stage of bacterial cell division (Errington *et al.*, 2003). FtsZ serves as a scaffold (Levin and Losick, 1994) and directs cell division components to the division site using the energy release associated with its function in GTP hydrolysis (Daniel and Errington, 2000; Lucet *et al.*, 2000; Gueiros-Filho and Losick, 2002). Binding of the FtsZ protein to GTP induces polymerisation of the protein that then activates GTP hydrolysis (Ruiz-Avila *et al.*, 2013).

FtsZ was first identified as an essential protein in *E. coli* when temperature-sensitive (Ts) mutant filament cells failed to form complete septa and did not divide properly (Lutkenhaus *et al.*, 1980; Dai and Lutkenhaus, 1991). Conditional mutation of FtsZ in *B. subtilis* also resulted in the failure to divide and form a complete septum, indicating the importance of this protein in *B. subtilis* division (Beall and Lutkenhaus, 1991). In both organisms, the filament cells demonstrated normal cell elongation, DNA replication and chromosome separation; however, they failed to form complete septa, leading to cell lysis (Lutkenhaus *et al.*, 1980, Dai and Lutkenhaus, 1991, Beall and Lutkenhaus, 1991). In *ftsZ*<sup>-</sup> *B. subtilis* cells, no division was observed, and the bilateral peptidoglycans were synthesised continuously, resulting in long filamentous cells (Pinho and Errington, 2003).

A recent study using photoactivated localisation microscopy has shown that the Z-ring in *E. coli* is a compressed helical structure composed of loose, overlapping bundles of protofilaments (Fu *et al.*, 2010). In *B. subtilis* cells that overproduce FtsZ or in misshapen vegetative and vegetative growing cells, FtsZ has a helical-like polymer (Thanedar and Margolin, 2004, Sun and Margolin, 1998, Ma *et al.*, 1996, Jones *et al.*, 2001).

Using cryoelectron microscopy in *C. crescentus*, the FtsZ-ring was found to consist of short, independent protofilaments (~100 nm) located next to the division site in an irregular pattern (Li *et al.*, 2007). Approximately 30 % of FtsZ in *B. subtilis* and *E. coli* was found as a ring structure, and the rest of the protein was diffused in the cytoplasm (Anderson *et al.*, 2004). Fluorescence recovery after photobleaching (FRAP) analysis using a FtsZ-green fluorescence protein (GFP) fusion has revealed that the Z-rings in *E. coli* and *B. subtilis* are very dynamic; the fluorescence recovery of *B. subtilis* and *E. coli* was 8 s and 9 s, respectively (Anderson *et al.*, 2004; Stricker *et al.*, 2002b). Atomic force microscopy (AFM) of the FtsZ-ring in the presence of GTP has shown the importance of GTP in regulating the exchange rate of the FtsZ monomer. The rate of exchange is slower in the presence of GDP, aluminium fluoride and non-hydrolysable nucleotide analogues (Mingorance *et al.*, 2005). The organisation of FtsZ into a helical structure has been demonstrated by time-lapse microscopy in *E. coli* and *B. subtilis* (Thanedar and Margolin, 2004; Peters *et al.*, 2007). Photoactivation single molecule tracking in *E. coli* has shown that the FtsZ molecules move in a helical motion outside the Z-ring structure, whereas in the Z-ring, the molecules are motionless (Niu and Yu, 2008). Recently, the architecture of the Z-ring in *B. subtilis* and *S. aureus* has been visualised using three-dimensional (3D)-structured illumination microscopy. The Z-ring in these two organisms consisted of a heterogeneous distribution of FtsZ proteins, and the distribution was subjected to changes prior to and during the formation of the FtsZ-ring (Strauss *et al.*, 2012).

Resolution of the FtsZ crystal structure from *Methanococcus jannaschii* confirmed that the protein was a structural homologue of tubulin and suggested a cytoskeletal function for FtsZ (Lowe and Amos, 1998). In the presence of GTP *in vitro*, FtsZ assembled into filaments in a manner similar to assembly at the N-terminal GTP-

binding site of tubulin; however, the C-terminal domain of FtsZ does not share sequence similarity with tubulin ((Mukherjee and Lutkenhaus, 1998). Unlike tubulin protofilaments, FtsZ protofilaments do not assemble into microtubules because the loops on the surface of the FtsZ protein do not make lateral contacts between the protofilaments (Erickson *et al.*, 1996).

FtsZ was the first cell division protein found to be localised at the midpoint of the cell. Using immunogold electron microscopy, a ring-like structure was observed in *E. coli* (Bi and Lutkenhaus, 1991). Immunofluorescence and GFP fusion analysis have shown that the FtsZ-ring is located at the site of division in many bacterial species (Levin and Losick, 1996; Addinall *et al.*, 1997; Wang and Lutkenhaus, 1996; Ma *et al.*, 1996). Cells lacking *ftsZ* are unable to induce the localisation of the rest of the division apparatus to the mid-point of the cell (Di Lallo *et al.*, 2003).

### **1.5.2. Selection of division sites**

The correct selection of the division site and the formation of the FtsZ-ring are regulated by the Min system and nucleoid occlusion, both of which prevent Z-ring assembly at the cell poles. These mechanisms allow division to occur at the midcell as the default site (Weiss, 2004). The precise timing of Z-ring formation and placement of the septum at the midcell is crucial for ensuring that each daughter cell inherits one copy of the genome. The FtsZ-ring formation at the midcell occurs with high fidelity, as the standard deviation for the middle position in *E. coli* is 2.6 % and in *B. subtilis* is 2.2 % (Migocki *et al.*, 2002; Yu and Margolin, 1999).

#### **1.5.2.1. The Min system**

The Min system is so named because of a mutation in the *E. coli minCDE* operon that resulted in minicells lacking a nucleoid, which was due to Z-ring formation at the cell poles (de Boer *et al.*, 1989). The overexpression of MinCD blocks division, and filament cells with no septa form (de Boer *et al.*, 1992b). The Min system in *E. coli* (Figure 1.5A) consists of three proteins, MinC, MinD and MinE, that hinder septation at the cell poles (Hu *et al.*, 1999).

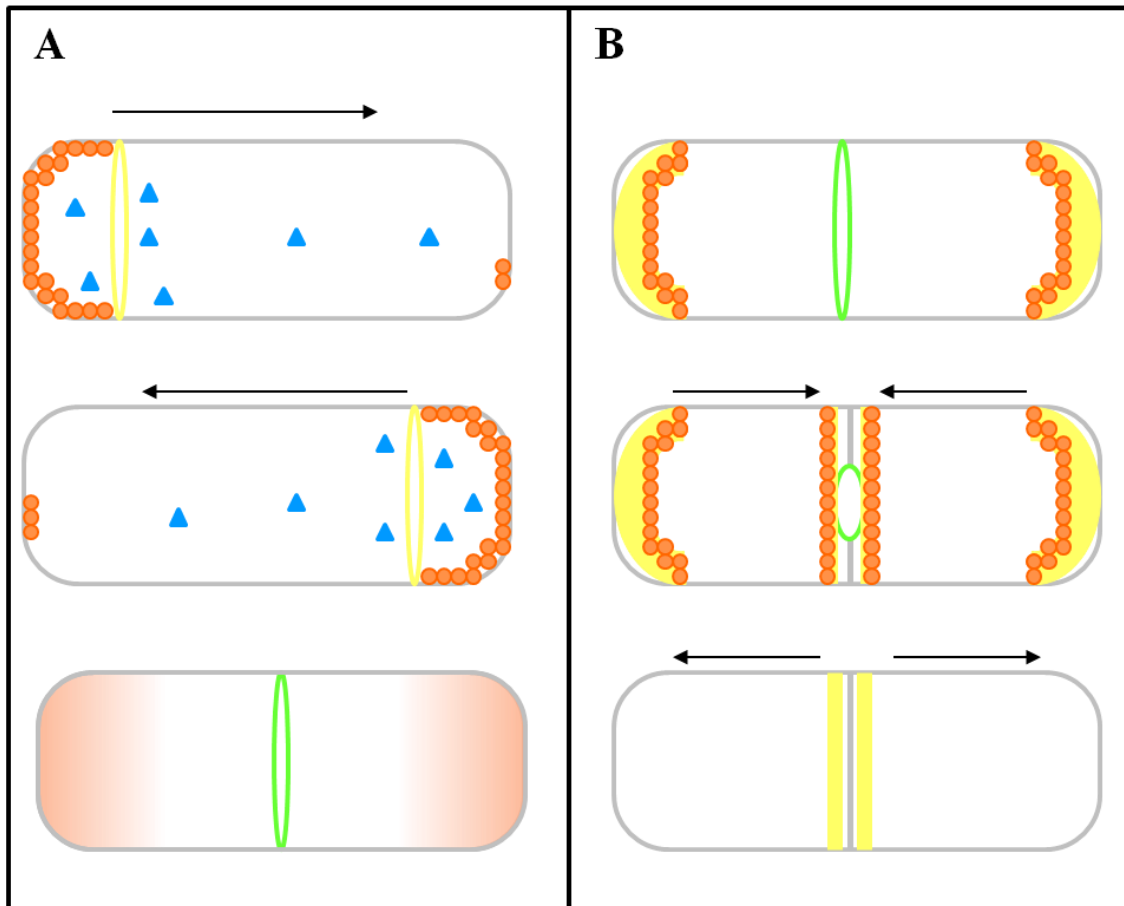


**Figure 1.5 The Min systems in *E. coli* and *B. subtilis***

Schematic representations of the Min system in *E. coli* (A) and *B. subtilis* (B). The Min system hinders division at the cell poles.

A. In *E. coli*, MinCD (orange) oscillates between cell poles to prevent divisome assembly away from the midcell. MinCD is released from the membrane by MinE (yellow), which is triggered by ATP (blue) hydrolysis. Once the nucleotide is exchanged in the cytosol, MinCD assembles at the opposite pole. The concentration of MinCD is highest at the cell poles, where it builds division restriction zones.

B. In *B. subtilis*, the MinCD complex (orange) is recruited to the poles and to the midcell by the DivIVA/MinJ complex (yellow). DivIVA is stable at the midcell while the septum constricts.

Adapted from (Lutkenhaus, 2012; Rothfield *et al.*, 2005).



The amino terminal domain of MinC interacts with FtsZ to inhibit its polymerisation, and the carboxy terminal domain of MinC mediates interaction and dimerisation with itself (Hu and Lutkenhaus, 2000). The overexpression of MinC prevents cell division (de Boer *et al.*, 1992b); however, the GTPase is not hindered, indicating that MinC only inhibits the association of the protofilaments into bundles and not their assembly (Erickson *et al.*, 2010).

MinD is a monomeric peripheral membrane protein that binds and hydrolyses ATP (de Boer *et al.*, 1991). MinD also associates with MinC at the membrane and triggers MinC to inactivate division at the cell poles (de Boer *et al.*, 1991). MinE is a topological specificity factor that gives MinC its site specificity and thus inhibits division at the midcell (de Boer *et al.*, 1991; de Boer *et al.*, 1992b). The MinE N-terminus interacts electrostatically with the cell membrane, and this interaction is stabilised by the C-terminal region of the protein. The MinE-membrane interaction also gives the protein its topological specificity and is crucial for the dynamic functioning of the Min system, as verified by mutational studies with the MinE protein (Hsieh *et al.*, 2010). MinCD serves as a negative regulator of the formation of the Z-ring, which is spatially coordinated by the MinE protein (Erickson *et al.*, 2010).

Fluorescence imaging using GFP fusions has provided insight into MinCDE mechanisms of action. MinD movement from pole to pole is dependent upon MinE, with a periodicity of roughly 20 s (Hu and Lutkenhaus, 1999; Raskin and de Boer, 1999a). MinD has been shown to move in a helical track as a protein filament *in vivo* and *in vitro* when ATP is present. It binds to phospholipid vesicles, suggesting that polymerisation of the protein into helical filaments reflects the dynamic action of MinD (Hu *et al.*, 2002; Shih *et al.*, 2003; Suefuji *et al.*, 2002). MinC also moves from one pole to another; however, the interaction of MinC with MinD makes this a passive movement and prevents FtsZ from assembling at the midcell (Hu and Lutkenhaus, 1999; Raskin and de Boer, 1999b). MinE demonstrates a ring-like structure near the midcell, but it does not remain there; it moves from one cell pole to another (Fu *et al.*, 2001). In addition, MinE stimulates the movement of MinCD between the cell poles and stimulates

the ATPase activity of MinD, releasing the MinC from the membrane (Fu *et al.*, 2001; Hale *et al.*, 2001; Suefuji *et al.*, 2002; Lackner *et al.*, 2003). MinC and MinE compete for the MinD binding site, and binding of one of the proteins prevents the other from binding, and it disassociates from the complex (Ma *et al.*, 2004). MinE prevents MinCD from localising at the division site, and MinD assembles at one cell pole and then reassembles at the opposite cell pole on the membrane. Consequently, the MinE concentration at the cell poles is low, and when the concentration is low at the midcell and high at the cell poles, pole-specific FtsZ depolymerisation is initiated (Meinhardt & de Boer, 2001).

A homologue of the MinCD system was found in *B. subtilis* (Figure 1.5B), and this homologue prevented polar division, although a MinE homologue was not present (Varley and Stewart, 1992). Movement of the MinD protein between the poles in *B. subtilis* was not observed, indicating that the mechanism of Z-ring formation is different from that of *E. coli* (Marston *et al.*, 1998). DivIVA is the topological specificity factor in *B. subtilis*, and this protein has a similar role to MinE (Edwards and Errington, 1997; Cha and Stewart, 1997). DivIVA is recruited to the site of division at a later stage of septum formation, and the protein remains at the newly formed cell poles (Edwards and Errington, 1997). In *B. subtilis*, MinCD is recruited to the cell poles by DivIVA through a new component of the selection system, MinJ, and the MinCD complex remains at the poles to stop future division at these sites (Bramkamp *et al.*, 2008). DivIVA binds to phospholipids similar to the *E. coli* MinE, and the N-terminal domain of the protein binds to the cell membrane. In mutants with an abnormal cell shape, DivIVA assembled near the most curved part of the cell membrane (Lenarcic *et al.*, 2009). Certain *Clostridia* have DivIVA and MinE proteins, but the mechanisms of selection of these proteins are not clear (Errington *et al.*, 2003). Other bacterial species, such as Gram-positive cocci, do not have a Min system (Margolin, 2001).

#### **1.5.2.2. Nucleoid occlusion**

The nucleoid occlusion model was proposed as a mechanism for the spatial control of bacterial cell division. Studies have found that division is inhibited at locations where nucleoids are present, and these structures disrupt DNA segregation or

replication (Mulder and Woldringh, 1989; Woldringh *et al.*, 1990). In a rod-shaped bacterial cell that has undergone cell division, DNA replication and segregation, three sites are vacant of Z-ring formation, and DNA is absent: the two cell poles and the midcell (Figure 1.6A) (Errington *et al.*, 2003). Because division at the cell poles is inhibited by the Min system, the only site for Z-ring formation is the midcell. Thus, nucleoid occlusion could provide the spatial and temporal regulation of cell division because the midcell is free from DNA and only created after proper DNA segregation of the newly replicated nucleoids has occurred (Errington *et al.*, 2003) (Figure 1.6B).

Certain effectors of nucleoid occlusion have been determined in *B. subtilis* and *E. coli* (Bernhardt & de Boer, 2005; Wu & Errington, 2004). In *B. subtilis*, the nucleoid occlusion factor (Noc) is a non-specific DNA-binding protein that colocalises with the nucleoid and prevents the assembly of the cell division machinery, thereby preventing division in the region that is occupied by the nucleoid (Wu and Errington, 2004). A recent study in *B. subtilis* has shown that Noc recognises a consensus Noc-binding DNA sequence that is present in 70 distinct regions of the chromosome (Wu *et al.*, 2009). The *E. coli* protein SlmA has been shown to be an inhibitor of division associated with the nucleoid. This function of SlmA was found via screening for lethal mutations in combination with an impaired Min system. SlmA binds DNA similar to Noc and also colocalises with the cell nucleoid (Bernhardt and de Boer, 2005). Although Noc and SlmA are considered functional analogues, they do not share sequence homology, and they belong to different DNA-binding protein families (Wu and Errington, 2011). The resolution of the crystal structure of SlmA has assisted in the recognition of the DNA-binding site and the molecular mechanism of *E. coli* nucleoid occlusion via the assembly of the FtsZ polymer (Cho *et al.*, 2011; Tonthat *et al.*, 2011; Cho and Bernhardt, 2013).

### **1.5.3. Proteins that interact with FtsZ**

#### **1.5.3.1. FtsA**

FtsA is considered the second-most conserved cell division protein (Rothfield *et al.*, 1999); however, it is not found in mycoplasma, cyanobacteria or mycobacteria (Margolin, 2000).

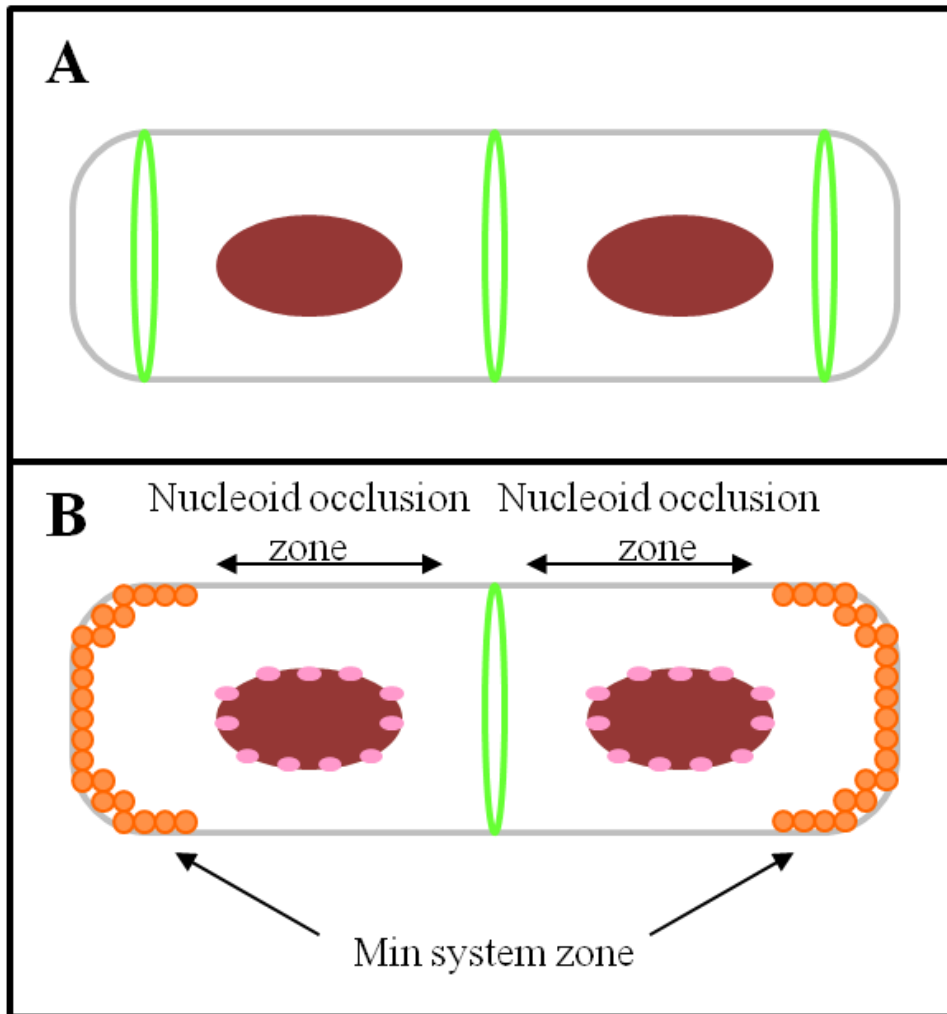


**Figure 1.6 The nucleoid occlusion system in rod-shaped bacteria**

Schematic representations of the nucleoid occlusion system.

A. Once the bacterial cell undergoes cell division, DNA replication and segregation, there are three sites that remain vacant for Z-ring formation (green) and at which DNA is absent: the cell poles and the midcell.

B. Negative regulation of Z-ring formation occurs to prevent the polymerisation of FtsZ in the wrong areas. The Min system (orange) prevents division at the poles, while nucleoid occlusion proteins (pink) prevent Z-ring formation over the separated nucleoids.

Adapted from (Rothfield *et al.*, 2005; Errington *et al.*, 2003).

FtsA is a positive regulator of FtsZ and one of the earliest proteins recruited to the division site (Singh *et al.*, 2007; Haeusser *et al.*, 2004). The *ftsA* gene is commonly found upstream of *ftsZ*. In many bacteria, *ftsA* is surrounded by cell wall biosynthesis and cell division genes, indicating that *ftsA* encodes a protein that may interact with FtsZ directly (Dai and Lutkenhaus, 1992). Although the function of FtsA has not yet been defined, it is believed that FtsA interacts with FtsZ directly. The protein was first detected using the yeast two-hybrid system (Wang *et al.*, 1997). FtsA was shown to interact with the highly conserved FtsZ carboxy-terminal region (Din *et al.*, 1998), and many FtsA-conserved residues are required for this interaction (Pichoff and Lutkenhaus, 2007). Consequently, the localisation of FtsA-GFP to the division site is dependent upon the interaction with FtsZ (Feucht *et al.*, 2001; Ma *et al.*, 1996; Addinall and Lutkenhaus, 1996). The interaction of FtsA with FtsZ is critical for the recruitment of the division apparatus to the division site to facilitate septum formation (van den Ent and Lowe, 2000), as the inactivation of FtsA prevented the recruitment of these proteins to the division site. Thus, division protein localisation is dependent on FtsA (Errington *et al.*, 2003), suggesting a role for FtsA in the early stage of cell division. *ftsA* has been found to be an essential gene in *E. coli* and other bacteria, such as *S. pneumoniae* and *B. subtilis*; however, in *B. subtilis*, although the deletion of this gene leads to severe defects in cell division, slow growth is possible (Margolin 2000; Beall and Lutkenhaus, 1992).

An examination of the FtsA primary sequence suggests that FtsA belongs to the actin/Hsp70/sugar kinase ATPase superfamily (Bork *et al.*, 1992). The *Thermotoga maritima* FtsA crystal structure is similar to the actin family of proteins, which have ATPase activity (Hale and de Boer, 1997; van den Ent and Lowe, 2000). FtsA is a peripheral membrane protein containing a C-terminal amphipathic helix that is conserved in many bacteria and targets the protein to the membrane (Pichoff and Lutkenhaus, 2005). All organisms using FtsZ-ring formation need the ring to be anchored to the membrane, and FtsA and other proteins are anticipated to tether FtsZ to the membrane. However, the exact mode of action is unknown (Pichoff and Lutkenhaus, 2005). FtsA was found to interact with a number of cell division proteins (Maggi *et al.*, 2008; Karimova *et al.*, 2005; Di Lallo *et al.*, 2003), and it

was proposed that FtsA uses the energy released from ATP hydrolysis to drive the process of cell constriction (Errington *et al.*, 2003). *In vitro*, the *B. subtilis* FtsA forms a dimer, binds to ATP and hydrolyses the molecule (Feucht *et al.*, 2001). In *S. pneumoniae*, the recombinant FtsA polymerises in a nucleotide-dependent manner, generating long helices that are assembled by a pair of filaments (Lara *et al.*, 2005). In the cytoplasm of *E. coli*, FtsA is phosphorylated and binds to ATP, whereas the membrane-bound FtsA is not phosphorylated and cannot bind to ATP (Sanchez *et al.*, 1994). Moreover, mutations in the *E. coli* FtsA protein have suggested that neither ATP binding nor phosphorylation are important for FtsA, but these processes may play a regulatory role in the FtsA action on septation (Sanchez *et al.*, 1994). The cellular ratio of FtsA to FtsZ appears to be important for proper division to occur (Dai and Lutkenhaus 1992). The cellular ratio of FtsA: FtsZ is 1:5 in *B. subtilis* (Feucht *et al.*, 2001), 1:1.5 in *S. pneumoniae* (Lara *et al.*, 2005) and 1:100 in *E. coli* (Dai and Lutkenhaus, 1991).

### **1.5.3.2. ZipA**

ZipA was first described in *E. coli* as an integral inner membrane protein, as determined using an affinity-blotting assay (Hale and de Boer, 1997). Although ZipA is essential in *E. coli*, it is poorly conserved in other bacteria (Hale and de Boer, 1997). ZipA is absent in *B. subtilis* (Gueiros-Filho and Losick, 2002), and a homologue in *Haemophilus influenzae* has been identified (Raychaudhuri, 1999). ZipA has an N-terminal domain that anchors the protein to the inner cell membrane and a large C-terminal domain that is located in the cytoplasm (Hale and de Boer, 1999). The resolution of the C-terminal structure of the *E. coli* ZipA protein demonstrated a hydrophobic cavity that was shown to be important in ZipA binding to the extreme C-terminus of FtsZ *in vivo* and *in vitro* (Mosyak *et al.*, 2000, Moy *et al.*, 2000).

Immunolocalisation studies have revealed the presence of ZipA at the early stage of the cell division process in an FtsZ-dependent but FtsA-independent manner, indicating that ZipA is important in the recruitment of other cell division

components to the septal site (Hale and de Boer, 1997; Hale and de Boer 1999; Hale and de Boer, 2002). The FtsZ-ring is constructed in the presence of ZipA or FtsA but not in the absence of these proteins. This finding suggests a functional redundancy, as FtsA or ZipA can tether FtsZ to the membrane. However, both proteins are required for the recruitment of other cell division components (Pichoff & Lutkenhaus, 2002). ZipA was essential for stabilising FtsZ polymers and enhancing FtsZ bundles (RayChaudhuri 1999), suggesting the involvement of this protein in promoting the FtsZ-ring assembly and/or maintaining the stability of the ring. FRAP has revealed that the ZipA protein is highly dynamic with rapid and regular exchanges between the membrane and FtsZ-ring (Stricker et al., 2002).

#### **1.5.3.3. ZapA**

The ZapA protein was identified in *B. subtilis* as a factor that promotes the formation of the FtsZ-ring through its ability to repress the inhibition of cell division caused by MinD overproduction (Gueiros-Filho and Losick, 2002). ZapA is a cytoplasmic protein that is localised at the division site in both *B. subtilis* and *E. coli* and is involved in the formation of the FtsZ-ring (Gueiros-Filho and Losick, 2002). ZapA is highly conserved and has orthologues in various bacteria, including *P. aeruginosa* (Gueiros-Filho and Losick, 2002, Small *et al.*, 2007). The localisation of *B. subtilis* ZapA is FtsZ-dependent (Gueiros-Filho and Losick, 2002). Although this protein is not essential, its absence causes severe blockage in division when its absence is combined with the absence of the EzrA or DivIVA protein (Gueiros-Filho and Losick, 2002). ZapA interacts directly *in vitro* with FtsZ, suppressing its GTPase activity and sustaining the polymerisation of FtsZ to stabilise the Z-ring and induce the bundling of FtsZ polymers (Hale and de Boer, 1997; Hale and de Boer, 2002; Gueiros-Filho and Losick, 2002, Small *et al.*, 2007). ZapA was able to compensate for the inhibitory action of MinC on FtsZ polymerisation *in vitro* (Scheffers, 2008). The resolution of the ZapA crystal structure from *P. aeruginosa* has shown that the protein forms homodimers and tetramers via the C-terminal coiled coil regions (Low *et al.*, 2004). Biochemical, cytological and biophysical analyses have shown that ZapA may play a role in early Z-ring assembly or in the late stage of cell separation (Gueiros-Filho and Losick,

2002) because ZapA was shown to cross-link the FtsZ polymers in addition to bundling and stabilising the Z-ring (Monahan *et al.*, 2009; Dajkovic *et al.*, 2010).

#### 1.5.3.4. EzrA

The EzrA protein was first identified in *B. subtilis* when nonsense mutations in the *ezrA* gene were shown to rescue the viability of the Ts *ftsZ* mutants at non-permissive temperatures (Levin *et al.*, 1999). EzrA is a transmembrane protein that is conserved among the low GC Gram positive bacteria (Haeusser *et al.*, 2004; Singh *et al.*, 2007; Levin *et al.*, 1999). The *ezrA* gene is not essential in *B. subtilis*, but the *ezrA* mutation was lethal in the absence of some cell division genes, including *zapA*, *sepF*, *noc* and *gpsB* (Gueiros-Filho & Losick, 2002; Wu & Errington, 2004; Hamoen *et al.*, 2006; Claessen *et al.*, 2008), indicating that the *B. subtilis* EzrA protein is required for efficient cell division. In *ezrA*<sup>-</sup> *B. subtilis* cells, division was interrupted, causing an increase in cell size, and filaments with no septa were observed (Levin *et al.*, 1999; Chung *et al.*, 2004; Claessen *et al.*, 2008). A recent study showed that EzrA is essential for *S. aureus* cell growth (Steele *et al.*, 2011). Although the function of EzrA is not well understood, it is presumed to be a negative regulator of FtsZ-ring formation (Levin *et al.*, 1999). In *ezrA* null mutants, the *B. subtilis* cells contained multiple medial and polar FtsZ-rings and had reduced concentrations of FtsZ that prevented Z-ring formation (Levin *et al.*, 1999). EzrA has been shown to interact with the conserved C-terminal domain of FtsZ, and the polymerisation of FtsZ is disrupted by EzrA bundling of the protofilaments (Levin *et al.*, 1999; Haeusser *et al.*, 2004; Chung *et al.*, 2007; Singh *et al.*, 2007), even with only a two-fold higher expression of *ezrA*. However, EzrA cannot disrupt the previously formed ring at the division site (Haeusser *et al.*, 2004). EzrA localises to the division site in a FtsZ-dependent manner in *B. subtilis* (Levin *et al.*, 1999). Recently, *S. aureus* EzrA-GFP and EzrA-mCherry analysis showed that EzrA colocalised with FtsZ at the midcell (Steele *et al.*, 2011; Jorge *et al.*, 2011). Seven conserved amino acid residues have been identified in *B. subtilis* EzrA, and these are essential for proper localisation at the midcell (Haeusser *et al.*, 2007). Mutations in these residues affect the localisation of EzrA but not the ability of the protein to halt FtsZ assembly at the poles (Haeusser *et al.*, 2007). The absence of *S. aureus* EzrA results in a blockade in peptidoglycan synthesis, and thus, the cell division



machinery is delocalised (Steele *et al.*, 2011; Jorge *et al.*, 2011). These data indicate that EzrA may have a positive role in *S. aureus* cell division. In addition, EzrA was suggested to have a role in *B. subtilis* cell elongation, as *ezrA*<sup>-</sup> *B. subtilis* cells have a reduced cell diameter (Claessen *et al.*, 2008). Homo-polymerisation of EzrA has been suggested to occur in *B. subtilis* (Haeusser *et al.*, 2004) and *S. aureus* (Steele *et al.*, 2011).

#### **1.5.3.5. SepF**

Two independent studies have identified SepF as a cell division protein in *B. subtilis* (Hamoen *et al.*, 2006; Ishikawa *et al.*, 2006). SepF is a well-conserved protein in Gram-positive bacteria (Adams and Errington, 2009). Although it is not essential in *B. subtilis*, it is required for cell division in the absence of EzrA (Hamoen *et al.*, 2006) or FtsA (Ishikawa *et al.*, 2006). Deletion of *B. subtilis* SepF affects the maturation of the septum, resulting in an aberrant septum (Hamoen *et al.*, 2006). In contrast, deletion of *S. pneumoniae* SepF affects cell morphology, resulting in the occurrence of minicells, cells with multiple septa and elongated cells (Fadda *et al.*, 2003). The overproduction of SepF in *B. subtilis* was able to compensate for the absence of FtsA, implying redundant roles (Ishikawa *et al.*, 2006). Yeast two-hybrid assays and affinity chromatography have shown a direct interaction between SepF and FtsZ (Ishikawa *et al.*, 2006; Hamoen *et al.*, 2006). Further investigation of the interactions between FtsZ and SepF showed that the interaction was mediated by the C-terminal tail of FtsZ (Singh *et al.*, 2008). SepF localisation to the division site is dependent on FtsZ, but it is not a late acting division protein (Hamoen *et al.*, 2006; Ishikawa *et al.*, 2006). SepF induces FtsZ polymerisation, bundling of the protofilament and suppression of FtsZ GTPase activity (Singh *et al.*, 2008). A recent study has found that the protein forms a large ring-like structure (50 nm in diameter). The SepF rings cause the FtsZ protofilaments to bundle into long tubular structures, suggesting a role of SepF in the arrangement of FtsZ filaments (Gundogdu *et al.*, 2011).

#### **1.5.3.6. Recently identified FtsZ-interacting proteins: ZipN, ZapB and ZapC**

The *zipN* gene was identified in *Synechococcus* as an important cell division protein, and it is also present in cyanobacteria and plant chloroplasts (Koksharova

and Wolk, 2002). This gene is essential for the viability of *Synechococcus* (Mazouni *et al.*, 2004). The ZipN protein has an N-terminal DnaJ domain that is responsible for interacting with the Z-ring and localisation of the protein to the septum (Mazouni *et al.*, 2004). ZipN was shown to interact with several cell division proteins, such as SepF, FtsZ, FtsQ and FtsI, as well as with itself, indicating that the protein may function similarly to FtsA in cell division, as no FtsA homologue has been identified in cyanobacteria or chloroplasts (Marbouty *et al.*, 2009).

The *zapB* gene was first identified in *E. coli*, and its product was considered to participate in cell division (Ebersbach *et al.*, 2008). The deletion of this gene resulted in filamentous *E. coli* cells and impaired division, confirming its role in cell division (Ebersbach *et al.*, 2008). ZapB was shown to interact with itself, FtsZ and ZapA via the ZipB N-terminal domain and to be recruited to the division site through interaction with ZapA (Ebersbach *et al.*, 2008; Galli and Gerdes, 2010; Galli and Gerdes, 2012). Consequently, the localisation of ZapB to the midcell is dependent upon ZapA and FtsZ but independent of ZipA, FtsA and FtsI (Ebersbach *et al.*, 2008; Galli and Gerdes, 2010). The overproduction of ZapA delocalises ZapB and impairs the FtsZ helical-structure (Galli and Gerdes, 2011). In *in vitro* and *in vivo* analysis, ZapB strongly interacted with ZapA, resulting in reduced interaction between ZapA and FtsZ, suggesting that ZapA favours ZapA-ZapB complexes rather than ZapA-FtsZ complexes (Galli and Gerdes, 2012). High-resolution 3D reconstruction microscopy has shown that the ZapB ring contracts slightly before the Z-ring (Galli and Gerdes, 2010). Homologues of ZapB are found in  $\gamma$ -proteobacteria and contain coiled-coil domains that polymerise into large filaments (Ebersbach *et al.*, 2008).

Recent studies by two independent groups have identified a cell division protein, ZapC, in *E. coli* by cytological and genetic screening (Hale *et al.*, 2011; Durand-Heredia *et al.*, 2011). Localisation of ZapC to the septum is FtsZ-dependent and is not dependent on the other FtsZ-interacting proteins, FtsA, ZipA or ZipB (Durand-Heredia *et al.*, 2011; Hale *et al.*, 2011). Moreover, the localisation of ZapA, ZapB and FtsZ are not affected by ZapC deletion, suggesting that ZapC is not required

for ZapA and ZapB recruitment to the division site (Galli and Gerdes, 2012). The overproduction of ZapC negatively impacts cell division, resulting in impaired FtsZ assembly and atypical ring formation, such as spirals, spots or rod-like structures (Durand-Heredia *et al.*, 2011; Hale *et al.*, 2011). These studies suggest a role for ZapC in FtsZ-ring regulation. ZapC acts as a positive regulator in addition to ZapA in the assembly of the FtsZ protein (Galli and Gerdes, 2012) and has been shown to interact with FtsZ *in vivo* (Hale *et al.*, 2011; Durand-Heredia *et al.*, 2011). ZapC induces FtsZ protofilament bundling (Durand-Heredia *et al.*, 2011; Hale *et al.*, 2011) and suppresses the GTPase activity of FtsZ (Hale *et al.*, 2011), thereby improving the stability of the Z-ring. The absence of ZapC affects *E. coli* cell morphology, as the cells are elongated to some extent (Galli and Gerdes, 2012; Hale *et al.*, 2011).

#### **1.5.4. Late cell division proteins**

Almost all of the remaining cell division components that are recruited to the midcell after the Z-ring has been formed contain at least one transmembrane domain. Cytokinesis in bacteria necessitates the synthesis, remodelling and degradation of bacterial peptidoglycans to facilitate septum formation and splitting of daughter cells. Nearly all of the late cell division proteins are involved in these functions.

##### **1.5.4.1. FtsW**

FtsW is a cell division protein that is part of the SEDS family of proteins (Gerard *et al.*, 2002; Real *et al.*, 2008). These proteins are connected to the membrane via 10 transmembrane spans (Ikeda *et al.*, 1989; Gerard *et al.*, 2002; Lara and Ayala, 2002). The genes encoding the SEDS proteins are usually related to genes encoding class B PBPs; in *E. coli*, FtsW is located in the same operon as FtsI and RodA, and another SEDS protein is located in an operon with PBP2 (Tamaki *et al.*, 1980; Ishino *et al.*, 1989; Boyle *et al.*, 1997). Mutations in SEDS proteins and class B PBPs have a similar phenotype, implying a functional relationship (Margolin, 2000; Errington *et al.*, 2003). Indeed, an investigation of sequenced bacterial genomes revealed a perfect presence-absence correlation between FtsI (PBP3) and FtsW, indicating that these proteins are closely linked (Henriques *et al.*, 1998). In *E. coli*

cells, *ftsW* mutants demonstrate the importance of this protein in both the early and late stages of cell division (Khattar *et al.*, 1997). *In vitro* and *in vivo* studies, including co-immunoprecipitation assays, Förster resonance energy transfer (FRET) analyses, peptide-based assays and bacterial-two hybrid systems (Fraipont *et al.*, 2011; Datta *et al.*, 2006; Karimova *et al.*, 2005; Di Lallo *et al.*, 2003), have shown a direct interaction between PBP3 and FtsW. In *E. coli*, a monofunctional glycosyltransferase, MgtA, which is engaged in glycan strand elongation, has been shown to interact with FtsI and FtsW (Derouaux *et al.*, 2008). FtsW is essential for FtsI recruitment to the septum in *E. coli* and *Mycobacterium tuberculosis* (Mercer and Weiss, 2002; Datta *et al.*, 2006). SEDS proteins have been proposed to act as flippases, which function in the translocation of lipid II-linked peptidoglycan precursors from the cytoplasm to the external peptidoglycan-synthesising complex (Holtje, 1998). The *E. coli* MurJ (MviN) protein, which is not a member of the SEDS family, is a peptidoglycan lipid II flippase (Ruiz, 2008; Inoue *et al.*, 2008). These studies suggest that FtsW may have another role in cell division. A recent study in *E. coli* showed that the transportation of lipid II requires FtsW (Mohammadi *et al.*, 2011). Moreover, purified FtsW induces the translocation of lipid II in biogenic membranes, indicating that FtsW may be a division-specific lipid II transporter (Mohammadi *et al.*, 2011).

#### **1.5.4.2. Penicillin binding proteins (PBPs)**

Cell division requires PBPs to synthesise the septum, which will form the new daughter cell poles. Several bacteria contain multiple PBPs, and they have some functional redundancies. *E. coli* has 12 PBPs, *B. subtilis* has 16 PBPs, and cocci have from 4 to 7 PBPs (Wei *et al.*, 2003; Pinho and Errington, 2005; Zapun *et al.*, 2008). High molecular weight (HMW) PBPs are grouped into class A PBPs, including PBP1a and PBP1b, and class B PBPs, including PBP2 and PBP3 (FtsI) (Palomeque-Messia *et al.*, 1991; Goffin and Ghuysen, 1998). Class A PBPs are considered bifunctional proteins, as their N-terminal domain has glycosyl transferase activity, and their C-terminal domain show transpeptidase activity. This bifunctional action allows the enzymes to participate in the formation of cross-links within peptidoglycans (transpeptidation) and the elongation of glycan strands

(transglycosylation) (Goffin and Ghuysen, 1998; Daniel *et al.*, 2006; Wei *et al.*, 2003; Scheffers and Errington, 2004). However, class B PBPs are much smaller and only act as transpeptidases (Goffin and Ghuysen, 1998). Low molecular weight (LMW) PBPs possess D, D-carboxypeptidase activity and have a role in regulating glycan strand cross-links (Goffin and Ghuysen, 1998; McPherson *et al.*, 2001).

The HMW class B PBPs are essential for *E. coli* cell division and play specific roles in peptidoglycan synthesis (Spratt, 1975). Mutation of FtsI (PBP3) leads to the formation of long filaments, as cell elongation is continuous without cell division (Spratt, 1977). PBP2 mutation leads to the formation of round cells, as cylinder peptidoglycan synthesis is lost (Spratt, 1975). A functional homologue has been identified in *B. subtilis* based on sequence homology and the conservation of the gene position (Yanouri *et al.*, 1993). Cell division in *B. subtilis* cells that are depleted of PBP2B is blocked (Daniel *et al.*, 2000). Immunolocalisation studies have shown that FtsI and PBP2B are localised at the division septa during division (Weiss *et al.*, 1997; Weiss *et al.*, 1999; Daniel *et al.*, 2000). The elucidation of the PBP2x crystal structure has revealed the expected fold for a transpeptidase (Pares *et al.*, 1996), and immunolocalisation studies have shown that PBP2x localises in the middle of *S. pneumoniae* cells (Zapun *et al.*, 2008).

*E. coli* FtsI is a penicillin binding protein (588 amino acids) consisting of a large C-terminal domain and a short N-terminal membrane anchor (Weiss *et al.*, 1999). The N-terminal membrane anchor is necessary for FtsI localisation at the division site and cell division (Weiss *et al.*, 1999). Site-directed mutagenesis in the non-penicillin-binding domain results in FtsI destabilisation and loss of function, but the exact function of this domain is largely unknown (Goffin *et al.*, 1996). This finding suggests that the non-penicillin-binding domain is involved in the correct folding of the catalytic domain (Marrec-Fairley *et al.*, 2000). The transpeptidase domain of *C. crescentus* PBP3 is needed for proper localisation of the protein to the division site (Costa *et al.*, 2008). Treatment with  $\beta$ -lactam antibiotics prevents FtsI (in *E. coli*) and PBP2B (in *B. subtilis*) from associating with the septum (Wang *et al.*, 1998; Daniel and Errington, 2000; Claessen *et al.*, 2008). In *E. coli*, FtsZ and FtsA are responsible for FtsI localisation at the midcell, and localisation of PBP2 to the S.

*aureus* midcell is dependent upon FtsZ (Pinho and Errington, 2005). Numerous interactions have been identified between FtsI (and PBP2B) and other cell division components (Daniel *et al.*, 2006; Di Lallo *et al.*, 2003; Karimova *et al.*, 2005). In *B. subtilis*, PBP2B depletion results in reduced levels of FtsL and DivIC (Daniel *et al.*, 2006).

In *E. coli*, class A HMW PBPs are involved in septal and lateral synthesis of peptidoglycans (Goffin and Ghuysen, 1998; Wei *et al.*, 2003; Scheffers and Errington, 2004; Daniel *et al.*, 2006). Nevertheless, class A PBP1 shuttles between the lateral cell wall and the division septum throughout cell growth, indicating an important role of PBP1 in cell division (Claessen *et al.*, 2008). Mutation of *B. subtilis* PBP1 leads to filamentous growth due to impairment in the formation of the septum and a subsequent block in cell division (Pedersen *et al.*, 1999). PBP1 localisation at the division site depends on different cell division proteins, such as PBP2, FtsZ, DivIB, DivIC and FtsL and is involved in the formation of asymmetric septa (Scheffers and Errington, 2004).

#### **1.5.4.3. FtsK**

FtsK is a highly conserved cell division protein in eubacteria and has homologues in archaea (Bigot *et al.*, 2007). The protein is important in DNA segregation (Grenga *et al.*, 2008). The C-terminal domain of FtsK is located in the cytoplasm and is separated from the N-terminal domain by a linker that has variable length and sequence (Errington *et al.*, 2003; Grenga *et al.*, 2008). The N-terminal domain targets the protein to the division site, is involved in the interaction with other divisome components, such as FtsL and FtsQ and is essential for *E. coli* but not *B. subtilis* division (Draper *et al.*, 1998; Yu *et al.*, 1998). The N-terminal domain is poorly conserved at the sequence level, and the lack of conservation could elucidate the differences observed in the FtsK N-terminal domain between bacterial species (Bigot *et al.*, 2007). The C-terminal domain of FtsK is important in cell division, particularly in chromosome segregation, and allows the translocation of DNA in an ATP-dependent manner (Yu *et al.*, 1998; Aussel *et al.*, 2002). These studies suggest that FtsK is involved in transporting DNA to the closing septum (Saleh *et al.*, 1996;

Aussel *et al.*, 2002; Pease *et al.*, 2005). Furthermore, the C-terminal region of FtsK has been shown to be involved in promoting the resolution of chromosome dimers (Aussel *et al.*, 2002; Bigot *et al.*, 2004). The localisation of FtsK at the midcell is necessary for the recruitment of other cell division proteins to the division site (Grenga *et al.*, 2008).

#### 1.5.4.4. FtsL

Two independent groups have identified a poorly conserved gene, *ftsL*, in *E. coli* (Ueki *et al.*, 1992; Guzman *et al.*, 1992). The gene encodes a small transmembrane protein that contains a coiled-coil motif in its C-terminal domain, suggesting a function in protein-protein interactions (Guzman *et al.*, 1992). There is only slight similarity in the FtsL sequence between *E. coli* and *B. subtilis*; however, these sequences are considered homologues based on several factors, including their predicted transmembrane topology, depletion phenotype, gene size and location of genes that are immediately upstream of *pbpB* (Daniel *et al.*, 1996; Daniel *et al.*, 1998). No homologue of *ftsL* has been found in bacteria lacking cell walls (Margolin, 2000). This finding suggests that the protein might be involved in cell wall synthesis and/or remodelling. FtsL is essential for cell division in *E. coli* and *B. subtilis*, as depletion of the protein leads to filamentous growth and eventually cell death (Guzman *et al.*, 1992; Daniel *et al.*, 1998). Studies suggest that FtsL is also likely to be essential in *S. pneumoniae* (Le Gouellec *et al.*, 2008).

FtsL consists of a short N-terminal tail, a transmembrane segment and a relatively large extracellular domain (Guzman *et al.*, 1992; Daniel *et al.*, 1998). Heterologous domain swapping has revealed that the transmembrane and N-terminal domains are required for the function and localisation of FtsL in *E. coli* (Guzman *et al.*, 1997; Ghigo and Beckwith, 2000). Mutagenesis of *ftsL* in *B. subtilis* has shown that few, if any, of the FtsL residues are critical for its function, implying a structural role rather than a catalytic role in cell division (Sievers and Errington, 2000a). Protein-protein interaction studies have shown that FtsL interacts with several cell division proteins (Sievers and Errington, 2000a; Sievers and Errington, 2000b; Di Lallo *et al.*, 2003; Karimova *et al.*, 2005; Daniel *et al.*, 2006; Maggi *et al.*, 2008). FtsL, FtsB

and FtsQ form a complex in *E. coli* independently of their localisation at the division site (Buddelmeijer & Beckwith, 2004), and this trimeric complex is conserved in all bacterial species in which cell division protein interactions have been investigated (Buddelmeijer and Beckwith, 2004; Noirclerc-Savoie *et al.*, 2005; Daniel *et al.*, 2006; D'Ulisse *et al.*, 2007), suggesting a functional importance. *In vitro*, the trimeric FtsL, DivIC and DivIB complex was reconstituted in *S. pneumoniae* (Noirclerc-Savoie *et al.*, 2005), and bacterial two-hybrid assays revealed that FtsL interacted directly with DivIC and DivIB (Karimova *et al.*, 2005; Daniel *et al.*, 2006). Furthermore, FtsL has been shown to interact with itself and form a dimer (Ghigo & Beckwith, 2000; Karimova *et al.*, 2005; Daniel *et al.*, 2006). The interactions between FtsL, DivIC and DivIB promote their stabilisation and recruitment to the division site. FtsL levels are reduced in *B. subtilis* cells in the absence of DivIB at elevated temperatures, and the overexpression of *ftsL* rescues the temperature sensitivity phenotype of *divIB* mutants in *B. subtilis* and *S. pneumoniae* at non-permissive conditions (Daniel & Errington, 2000; Le Gouellec *et al.*, 2008). These data suggest the involvement of DivIB in stabilising FtsL. The overproduction of FtsL also rescues the delayed Z-ring constriction observed in *ezrA*-depleted *B. subtilis* cells, indicating a synergistic role of FtsL and EzrA in regulating Z-ring formation (Kawai and Ogasawara, 2006). The assembly of DivIC, DivIB and PBP2B at the division site in *B. subtilis* is hindered by the depletion of FtsL (Daniel *et al.*, 1998; Daniel & Errington, 2000). Similar patterns of localisation dependency have been observed in these proteins in *E. coli* (Ghigo *et al.*, 1999; Buddelmeijer *et al.*, 2002).

FtsL is an intrinsically unstable protein (Robson *et al.*, 2002; Daniel & Errington, 2000). In *B. subtilis*, FtsL is unstable at high temperatures in Ts and null *divIB* mutants, suggesting that DivIB may protect FtsL from degradation at high temperatures (Daniel and Errington, 2000). The N-terminal cytoplasmic domain of FtsL in *B. subtilis* has been found to serve as a signal for protein degradation that is to some extent mediated by RasP (YluC), a membrane metalloprotease (Bramkamp *et al.*, 2006; Bramkamp *et al.*, 2008). However, FtsL cleavage by RasP is stabilised by DivIC (Wadenpohl and Bramkamp, 2010). *rasP* mutant cells are shorter due to early initiation of cell division, indicating that FtsL is normally rate limiting for *B. subtilis* division (Bramkamp *et al.*, 2006; Bramkamp *et al.*, 2008). The transcription



of *ftsL* is regulated by DnaA, a DNA replication initiation protein, which interrupts cell division when DNA replication is perturbed (Goranov *et al.*, 2005). At the early stage of the division process, the FtsL protein can actually assemble at the division site to form a ring that remains until the late division stages (Sievers and Errington, 2000b). FtsL levels in the *E. coli* cell are affected by the depletion of *ftsB* (Gonzalez and Beckwith, 2009).

#### 1.5.4.5. FtsB/DivIC

The *divIC* gene was first described in *B. subtilis* (Levin and Losick, 1994). This gene encodes an FtsL-like protein that is essential for division at various temperatures, just as the N-terminal and transmembrane domains are necessary for DivIC to function at high temperatures (Levin and Losick, 1994; Katis and Wake, 1999; Sievers and Errington, 2000a). DivIC is intrinsically unstable, similar to FtsL (Robson *et al.*, 2002). Interaction studies have shown a direct interaction between DivIC and FtsL through their C-terminal domains, which contain a leucine zipper-like motif (Guzman *et al.*, 1992; Sievers and Errington, 2000a; Daniel *et al.*, 2006; Wadenpohl and Bramkamp, 2010); however, biochemical data have also shown that they do not interact (Robson *et al.*, 2002). *B. subtilis* DivIC localises at the division site and requires FtsL for proper septal localisation (Katis *et al.*, 1997; Daniel *et al.*, 1998), and depletion of FtsL results in reduced levels of DivIC in the cell, suggesting that the stability of DivIC is dependent upon its interaction with FtsL (Daniel *et al.*, 1998). No significant reduction in *B. subtilis* DivIC was observed in the absence of both DivIB and FtsL, but in the absence of FtsL and presence of DivIB, DivIC was reduced, indicating that DivIB might act as a negative regulator of DivIC (Daniel *et al.*, 2006).

FtsB was first identified in *E. coli* and *Vibrio cholerae* based on a search of *ftsL*-like genes. This protein is weakly homologous to the *Bacillus halodurans divIC* gene (Buddelmeijer *et al.*, 2002; Errington *et al.*, 2003). FtsB is an essential cell division protein in both *E. coli* and *V. cholerae*, and septal localisation is co-dependent on FtsL (Buddelmeijer and Beckwith, 2002). FtsB is a small transmembrane protein with a predicted topology similar to FtsL and DivIC, e.g., containing a leucine zipper-like domain in the extracellular C-terminal region (Katis

*et al.*, 1997; Buddelmeijer and Beckwith, 2004; Gonzalez and Beckwith, 2009; Robichon *et al.*, 2011). The C-terminus of FtsB in *E. coli* is important for the interaction with FtsQ, whereas the N-terminus is essential for the interaction with FtsL and the stability of the FtsQ/FtsL/FtsB trimeric complex (Gonzalez and Beckwith, 2009). Immunoprecipitation studies have shown that FtsL and FtsB/DivIC can form a complex without the presence of FtsQ/DivIB (Noirclerc-Savoie *et al.*, 2005; Gonzalez and Beckwith, 2009). The leucine zipper-like motif in both proteins is required for proper interactions between the proteins (Robichon *et al.*, 2011). However, truncated FtsB missing almost half of its leucine zipper-like motif is still able to bind to FtsL (Gonzalez and Beckwith, 2009). This dimeric complex of FtsL/FtsB is required for the recruitment of FtsI and FtsW to the division site (Gonzalez and Beckwith, 2009). Depletion of FtsB causes the degradation of FtsL (Buddelmeijer *et al.* 2002; Gonzalez and Beckwith 2009), and conversely, depletion of FtsL in *E. coli* results in degradation of the C-terminus of FtsB (Gonzalez and Beckwith, 2009). This finding indicates that both FtsB and FtsL are dependent upon each other for stability and likely, their localisation. DivIC also stabilises FtsL against RasP cleavage, and this regulated degradation is believed to participate in cell division control (Bramkamp *et al.*, 2006; Wadenpohl and Bramkamp, 2010; Robichon *et al.*, 2011). Furthermore, FtsB stability is also dependent upon FtsQ in *E. coli* (Gonzalez & Beckwith, 2009). The  $\beta$ -domain of *S. pneumoniae* DivIB interacts with the C-terminal region of the dimeric FtsB/FtsL complex (Masson *et al.*, 2009).

In *B. subtilis* and *S. pneumoniae* cells, DivIC is abundant (Noirclerc-Savoie *et al.*, 2005; Katis and Wake, 1999; Katis *et al.*, 1997). The presence of DivIC at the midcell was demonstrated in *S. pneumoniae* and *B. subtilis* using immunolocalisation studies, which revealed the early localisation of DivIC, even before the septum had formed and before other late division proteins were recruited (Noirclerc-Savoie *et al.*, 2005; Katis *et al.*, 1997). In contrast, FtsB in *E. coli* does not localise at the division site until it is recruited by FtsQ (Daniel *et al.*, 1998). Recently, a model of the FtsB/FtsL/FtsQ interaction has been proposed, suggesting that the proteins exist as either a trimeric or hexameric complex, with the latter more applicable than the trimeric complex (Villanelo *et al.*, 2011); however, this hypothesis requires further investigation. The interaction between FtsQ/DivIB and

the dimeric complex FtsB/DivC-FtsL is believed to be important to stabilise the complex (Masson *et al.*, 2009), and these proteins together act as a scaffold for other cell division proteins.

#### 1.5.4.6. FtsQ/DivIB

*ftsQ* is located upstream of *ftsA* and *ftsZ* in many bacteria, but there is little conservation of the sequence (Harry and Wake, 1989; Beall, and Lutkenhaus, 1989). *E. coli* FtsQ has been found to be essential in cell division, and the overproduction of this protein results in filamentation (Carson *et al.*, 1991). DivIB is suggested to be a homologue of FtsQ in *B. subtilis* based on gene size similarities, membrane topology and chromosomal location (Harry *et al.*, 1994). *B. subtilis* DivIB is only essential for growth at higher temperatures, but it is necessary for proper sporulation at all temperatures (Beall and Lutkenhaus, 1989; Harry *et al.*, 1993). In *S. pneumoniae*, DivIB is dispensable for growth in rich media, but *divIB* mutants have altered cell morphology such that long chains of cells form and do not grow in nutrient-limited media (Le Gouellec *et al.*, 2008).

*ftsQ/divIB* is often located in an operon of genes that is involved in the synthesis of peptidoglycan precursors (Zapun *et al.*, 2008), and no homologues of FtsQ/DivIB are found in bacteria lacking cell walls (Margolin, 2000). Furthermore, FtsQ shares a weak sequence similarity with MplI, a peptidoglycan-recycling factor (Mengin-Lecreulx *et al.*, 1996). In *S. pneumoniae*,  $\Delta divIB$  mutants are sensitive to  $\beta$ -lactam inhibitors, which target cell wall synthesis (Le Gouellec *et al.*, 2008). *divIB* null mutants in *B. subtilis* produce atypical thick septa at the cell poles during sporulation; such septa are similar to those produced in mutants with a defect in the production of sporulation-specific septal peptidoglycan hydrolases (Thompson *et al.*, 2006). These data suggest that the protein might be involved in cell wall synthesis and/or remodelling. L-form *E. coli* can grow and divide normally, even with a defective FtsQ protein, indicating that FtsQ is not required for division in bacteria lacking cell walls (Siddiqui *et al.*, 2006).

DivIB/FtsQ is a transmembrane protein that is composed of a short cytoplasmic N-

terminal tail, a hydrophobic membrane-spanning domain and a long extracellular C-terminus (Carson *et al.*, 1991; Buddelmeijer *et al.*, 1998; Katis and Wake 1999; Chen *et al.*, 2002). The replacement of the extracellular domain of FtsQ/DivIB has demonstrated the importance of this domain for the function of the protein in both *E. coli* and *B. subtilis* (Buddelmeijer *et al.*, 1998; Katis and Wake, 1999; Chen *et al.*, 2002). Furthermore, the transmembrane segment is required for the septal localisation of FtsQ/DivIB in *E. coli* and *B. subtilis* but is not required for viability (Scheffers *et al.*, 2007; Wadsworth *et al.*, 2008). The interaction of FtsQ with several cell division proteins occurs through the cytoplasmic tail, extracellular domain and/or transmembrane segment (Karimova *et al.*, 2005; D'Ulisse *et al.*, 2007; van den Ent *et al.*, 2008).

DivIB is present in *B. subtilis* cells at a high abundance (5,000 molecules per cell) (Rowland *et al.*, 1997), whereas in *E. coli*, FtsQ is present at 25-50 molecules per cell (Carson *et al.*, 1991). These data suggest that DivIB is involved in cell wall synthesis, and the number of molecules in Gram-positive bacteria reflect the requirement of a thicker cell wall (Katis & Wake, 1999). In *S. pneumoniae*, there are approximately 200 DivIB molecules per cell (Noirclerc-Savoie *et al.*, 2005). Interaction studies have shown that FtsQ is an integral part of the division apparatus. Two-hybrid and co-immunoprecipitation studies have shown that *E. coli* FtsQ interacts directly with several cell division components, including FtsA, FtsK, FtsX, FtsL, FtsB, FtsW, FtsN and FtsI (D'Ulisse *et al.*, 2007; Karimova *et al.*, 2005; Buddelmeijer & Beckwith, 2004; Di Lallo *et al.*, 2003). Mutagenesis analyses and resolution of the periplasmic domain of FtsQ from *Yersinia enterocolitica* and *E. coli* have shown two distinct domains within this region; one is required for the interaction of FtsQ with proteins that are recruited by FtsQ to the septum, and the other is required for the interaction of FtsQ with proteins that are involved in localising FtsQ to the septum (van den Ent *et al.*, 2008).

#### **1.5.4.7. FtsN**

FtsN has been identified in *E. coli* as an essential cell division protein, as gene depletion leads to filamentous growth (Dai *et al.*, 1993). Overexpression of the protein compensates for Ts *ftsA* and *ftsK* mutants and partially compensates for Ts

*ftsQ* and *ftsI* mutants (Dai *et al.*, 1993; Goehring *et al.*, 2007). Nevertheless, in the absence of FtsN, suppressor mutants of FtsA are viable (Bernard *et al.*, 2007). The transmembrane segment and N-terminal cytoplasmic domain are necessary for the suppression of FtsA, FtsK, FtsI and FtsQ mutations (Goehring *et al.*, 2007). FtsN is poorly conserved and found among *Haemophilus* species and enteric bacteria (Errington *et al.*, 2003). However, FtsN has recently been found in proteobacteria, with some sequence differences (Moll and Thanbichler, 2009). The protein consists of a large periplasmic C-terminal domain, a transmembrane domain and a short cytoplasmic N-terminal domain (Dai *et al.*, 1996). The C-terminal periplasmic domain is required for FtsN binding to peptidoglycans (Ursinus *et al.*, 2004; Muller *et al.*, 2007) and its localisation to the septum (Dai *et al.*, 1996) and is dependent upon FtsI, FtsZ, FtsA, FtsQ and FtsK (Addinall *et al.*, 1997; Ursinus *et al.*, 2004). The C-terminal domain of FtsN encodes a sporulation-related repeat (SPOR) domain that mediates localisation to the division site, and the domain localisation is dependent upon the amidases that are associated with cell division (Arends *et al.*, 2010; Moll and Thanbichler, 2009; Gerding *et al.*, 2009). However, the FtsN C-terminal domain is not essential for cell division (Ursinus *et al.*, 2004).

Bacterial two-hybrid assays have shown multiple interactions of FtsN with other cell division proteins, including FtsL, FtsI, FtsW, FtsQ and FtsA (Di Lallo *et al.*, 2003; Karimova *et al.*, 2005). The recruitment of FtsQ, FtsL, FtsI and FtsA to the divisome is independent of FtsN, indicating that FtsN is the last essential component of the division apparatus to be recruited to the septum (Chen & Beckwith, 2001; Goehring *et al.*, 2007). Thus, FtsN may be involved in stabilising the divisome along with FtsK (Goehring *et al.*, 2007). In addition, FtsN has been shown to interact with PBP1A and PBP1B through its N-terminal domain (Muller *et al.*, 2007), as well as with MtgA, a lytic transglycosylase (Derouaux *et al.*, 2008). These interactions stimulate the transglycosylase and transpeptidase activities of the PBP1B protein, suggesting the involvement of FtsN in peptidoglycan turnover (Muller *et al.*, 2007).

#### 1.5.4.8. FtsEX

The highly conserved FtsEX complex is predicted to be an ABC transporter (de Leeuw *et al.*, 1999; Schmidt *et al.*, 2004). The genes are arranged in one operon along with *ftsY*, the product of which regulates the release of signal recognition particles from the cytoplasmic membrane (de Leeuw *et al.*, 1999). *ftsX* encodes for an integral membrane protein, whereas *ftsE* encodes a cytoplasmic ATPase that is associated with FtsX (de Leeuw *et al.*, 1999). In *M. tuberculosis*, FtsE has been shown to bind to ATP, verifying that the protein functions as a nucleotide-binding protein (Mir *et al.*, 2006). *E. coli* FtsE/X localises to the division septum, and the localisation of FtsX is dependent upon FtsZ, FtsA and ZipA but not FtsI, FtsL or FtsQ (Schmidt *et al.*, 2004). Defects in *E. coli* cell division in the absence of *ftsEX* are salt-dependent (Schmidt *et al.*, 2004). In conditions lacking salt, cell division is hindered, and the downstream genes of FtsEX (FtsI, FtsN, FtsQ and FtsK) do not localise to the division site. However, the localisation of the upstream genes, FtsA and ZipA, are not affected (Schmidt *et al.*, 2004). The *E. coli* FtsEX protein is osmoremedial in addition to being salt remedial (Reddy, 2007). This finding suggests that FtsEX is directly associated with the stability of the divisome at a relatively early stage of the division process and specifically in low-salt and low-osmolarity conditions (Schmidt *et al.*, 2004; Reddy, 2007). The division defect can be restored in *E. coli* *ftsEX*-null mutants by overexpressing FtsZ, FtsA and FtsQ together or by overexpressing FtsN alone (Reddy, 2007). FtsX can localise to the division site in the absence of FtsE, indicating that FtsX targets FtsEX to the division site (Arends *et al.*, 2009). Bacterial two-hybrid analyses have shown that FtsX interacts with FtsQ and FtsA (Karimova *et al.*, 2005), and co-immunoprecipitation analyses have shown that FtsE interacts with FtsZ (Corbin *et al.*, 2007). The Z-ring is poorly formed in FtsE mutants with lesions in the ATPase domain; however, the assembly of the divisome is not affected in these mutants (Arends *et al.*, 2009). These data imply that FtsEX utilises ATP to support the formation of the Z-ring (Arends *et al.*, 2009). Mutants of either FtsE and/or FtsX in *Flavobacterium johnsoniae*, *Aeromonas hydrophila* and *Neisseria gonorrhoeae* have also revealed defects in division, arguing that FtsEX function in division is conserved in these organisms (Ramirez-Arcos *et al.*, 2001; Merino *et al.*, 2001; Kempf and McBride 2000; Bernatchez *et al.*, 2000). Depletion of FtsEX in *B. subtilis* cells does not

affect division, but entry into sporulation was delayed, and an aberrant symmetric septum was formed (Garti-Levi *et al.*, 2008).

A recent study suggested that the FtsEX complex is involved in the coordination of peptidoglycan remodelling, as these proteins regulate the hydrolysis of the cell wall at the division site (Yang *et al.*, 2011). FtsX and FtsE are essential proteins in *S. pneumoniae*, and depletion of either gene leads to defects in *S. pneumoniae* division; the cells become spherical in shape, and atypical placement of the division septa occurs (Sham *et al.*, 2011; Sham *et al.*, 2013). The large periplasmic loop of *S. pneumoniae* FtsX interacts with the coiled-coil domain of PcsB and is believed to act as an amidase or endopeptidase (Ng *et al.*, 2004; Sham *et al.*, 2013). Furthermore, the periplasmic loop of *E. coli* FtsX interacts directly with EnvC, a peptidoglycan hydrolase, and this interaction is responsible for the recruitment of EnvC to the division site (Yang *et al.*, 2011). *ftsEX* mutants with a defect in the ATPase domain are able to recruit EnvC to the septum, but the cells cannot separate, suggesting that the activation of amidase through EnvC is affected by the conformational changes of the FtsEX complex (Yang *et al.*, 2011).

#### **1.5.4.9. GpsB (YpsB)**

*gpsB* was first identified in *B. subtilis* as a paralogue of *divIVA*, with homologues present in many Gram-positive bacteria as a result of a gene duplication event (Tavares *et al.*, 2008). The N-terminal regions of DivIVA and GpsB share high sequence similarity, and both contain central coiled-coil domains. However, the coiled-coil and C-terminal domains have low sequence similarity (Tavares *et al.*, 2008; Claessen *et al.*, 2008). Furthermore, GpsB proteins are distinguished from DivIVA by exhibiting a highly conserved and shorter-length C-terminus (Tavares *et al.*, 2008). Subcellular localisation studies have shown that GpsB is associated with membrane and cytoplasmic fractions, and fluorescence microscopy has shown the localisation of the protein at the division site (Tavares *et al.*, 2008). The recruitment of GpsB to the division site is dependent upon FtsZ, FtsA, PBP2B and DivIC, and the N-terminus of the protein is likely responsible for its localisation (Tavares *et al.*, 2008). GpsB and PBP1 alternate between both the lateral and division sites during the cell cycle, suggesting that GpsB and EzrA coordinate cell elongation and

division in *B. subtilis* (Claessen *et al.*, 2008). GpsB is not essential for the formation of the septum and is not retained at the newly formed cell poles (Tavares *et al.*, 2008). However, deletion of both *gpsB* and *ezrA* leads to severe defects in both lateral and septal synthesis of peptidoglycans as a result of perturbed localisation of PBP1 (Claessen *et al.*, 2008).

An analysis of the sequenced genome revealed that *ponA*, which encodes PBP1, is usually closely located to the *gpsB* gene on the chromosome of many bacteria (Tavares *et al.* 2008). In many bacteria that lack the *gpsB* gene (mostly enterobacteria), PBP1 orthologues contain the highly conserved residues of the N-terminal domain of GpsB and DivIVA, suggesting an association between the two proteins (Tavares *et al.* 2008). Indeed, a direct interaction between GpsB and PBP1 has been shown using bacterial two-hybrid analysis, and interactions between GpsB and EzrA and MreC have also been demonstrated (Claessen *et al.* 2008).

### **1.6. The separation of daughter cells**

The separation of daughter cells is dependent upon cell wall hydrolases (e.g., autolysins), which cleave the peptidoglycan layer that connects the two daughter cells. The specific mechanisms of the regulation of cell separation are not well known; however, in many bacteria, there is a link between the failure of cell partition and the lack of autolysins (Yamada *et al.*, 1996). The process is relatively complicated because the constriction mechanism varies between Gram-negative and Gram-positive bacteria, and the constriction of the outer membrane, cell wall and cell membrane are coordinately organised. In Gram-negative bacteria (e.g., *E. coli*), cell division occurs by a gradual constriction of the cylindrical part of the cell wall (Errington *et al.*, 2003; Uehara and Bernhardt, 2011). In Gram-positive bacteria (e.g., *B. subtilis*), the new cross-wall forms from the cylindrical cell wall, and cell separation occurs after completion of septation (Foster and Popham, 2001; Errington *et al.*, 2003). Nevertheless, numerous factors have been found to participate in the separation of daughter cells in Gram-negative and Gram-positive bacteria.

Several enzymes have been observed to participate in *E. coli* cell separation, and the most important are the LytC-type periplasmic peptidoglycan amidases



AmiA/B/C (Peters *et al.*, 2011; Uehara and Bernhardt, 2011; Yang *et al.*, 2012). AmiC localises to the midcell through its N-terminal binding to FtsN (Bernhardt and de Boer, 2003) and cleaves the septal peptidoglycans, inducing cell separation (Heidrich *et al.*, 2001). Furthermore, the LytM factors EnvC and NlpD are associated with cell division in *E. coli* (Uehara and Bernhardt, 2011). A previous study suggested that EnvC is involved in daughter cell separation as a zinc metalloprotease (Bernhardt and de Boer, 2004). However, recent studies have shown that both EnvC and NlpD localise to the septum (Uehara *et al.*, 2009) and activate amidases (Uehara *et al.*, 2010; Yang *et al.*, 2012). The activation of AmiA and AmiB by EnvC and AmiC by NlpD has been observed by *in vitro* cell wall cleavage assays (Uehara *et al.*, 2010). When septal peptidoglycan synthesis was blocked in *E. coli*, amidases were not able to localise to the division ring, yet NlpD and EnvC were shown to localise (Peters *et al.*, 2011). Consequently, the spatial and temporal regulation of cell separation occurs by coupling the activation of peptidoglycan hydrolase activity with the assembly of the division apparatus.

Recent studies have characterised the *C. crescentus* DipM protein (Goley *et al.*, 2010; Poggio *et al.*, 2010; Moll *et al.*, 2010). The C-terminus of DipM contains LytM endopeptidase domains, and the hydrolysis of peptidoglycans has been illustrated in gel-based assays (Moll *et al.*, 2010). DipM localises at the division site once division is initiated, and this localisation is dependent upon FtsZ (Goley *et al.*, 2010; Poggio *et al.*, 2010; Moll *et al.*, 2010) and FtsN (Moll *et al.*, 2010). Furthermore, two-hybrid and co-immunoprecipitation assays have shown a direct interaction between DipM and FtsN, indicating the involvement of DipM in cell division (Moll *et al.*, 2010). Inactivation of the *dipM* gene causes major defects in outer membrane invagination and delays cytoplasmic constriction and daughter cell separation (Moll *et al.*, 2010). Depletion of *dipM* causes morphological abnormalities, including thickening of the septal peptidoglycans and blebbing of the outer membrane at the division sites. These observations suggest a role of DipM in envelope invagination during cell division via septal peptidoglycan hydrolysis (Goley *et al.*, 2010).

Many autolysins have been proposed to have a role in the separation of daughter cells; however, a direct interaction between autolysins and divisome components

has not been illustrated. In *B. subtilis*, LytF, LytE and CwlS were shown to localise at the cell separation sites and poles during the late stage of cell growth (Fukushima *et al.*, 2006). In *Mycobacterium smegmatis*, RipA-depleted cells demonstrated branching and chaining of cells, indicating a failure in the separation of the cells (Hett *et al.* 2008). RipA is an endopeptidase that localises to the septum (Hett *et al.*, 2007). In addition, the *S. aureus* autolysin Atl localises as a ring-like structure at the presumptive site of cell separation (Yamada *et al.*, 1996). Cse of *S. thermophilus* localises to the mature septa, and its absence results in the formation of long chains of cells (Layec *et al.*, 2009). The above findings suggest the possibility of direct interactions between autolysins and the components of the divisome, but this assumption requires further investigation.

### **1.7. The late cell division protein assembly pathway**

The study of the assembly pathway of the late cell division proteins has identified notable differences between *B. subtilis* and *E. coli*. Recruitment of late cell division proteins occurs in a linear hierarchy: FtsE/X-FtsK-FtsQ-FtsB/FtsL-FtsW-FtsI-FtsN, in which the recruitment of FtsE/FtsX and FtsB/FtsL is co-dependent (Buddelmeijer and Beckwith, 2002; Errington *et al.*, 2003; Goehring and Beckwith, 2005). Nevertheless, lack of this linear recruitment of *E. coli* division proteins is possible (Vicente and Rico, 2006). Premature targeting approaches have demonstrated that assembly of most of the late division proteins can occur independently of their upstream proteins, indicating that the linear assembly model is imprecise (Goehring *et al.*, 2006). The linear model in *E. coli* is not conserved in *B. subtilis* or *S. pneumoniae* (Errington *et al.*, 2003; Morlot *et al.*, 2004). In *B. subtilis*, the recruitment of late division proteins appears to be interdependent. Mutation or depletion of one of the proteins leads to blockade of protein assembly at the division site, reflecting their dependency but not temporal order of assembly (Errington *et al.*, 2003).

### **1.8. Importance of cell division in drug development**

Treatment of bacterial diseases is becoming problematic due to the emergence of antibiotic resistance by pathogenic bacteria, such as *S. aureus*, *Enterococcus*

*faecalis* and *S. pneumoniae* (McDevitt *et al.*, 2002). Most of the essential divisome components are conserved and present in a wide range of bacterial species. Thus, the cell division apparatus may be an interesting target for the development of new therapeutic agents (McDevitt *et al.*, 2002). Numerous compounds have been shown to inhibit cell division, and they are under investigation as potential antimicrobial agents (McDevitt *et al.*, 2002; Beuria *et al.*, 2009; Schaffner-Barbero *et al.*, 2011).  $\beta$ -lactam antibiotics are the most widely utilised antibiotics due to several factors, including low cost, high effectiveness and minimal side effects (Wilke *et al.*, 2005). The effect of penicillin on many bacteria is effective even at low concentrations. Penicillin promotes cell filamentation, suggesting that it induces a block in cell division (Gardner, 1940; Fisher, 1946).  $\beta$ -lactams are functional analogues of D-alanyl-D-alanine, as they block the active site of PBPs by irreversible acylation of serine, preventing the final transpeptidation of nascent peptidoglycans and interfering with cell wall synthesis (Blumberg and Strominger, 1974). This process results in the accumulation of peptidoglycan precursors that activate autolysins and hydrolyse the old peptidoglycans in the absence of nascent peptidoglycan synthesis, leading to cell lysis (Kitano and Tomasz, 1979). Furazlocillin is a  $\beta$ -lactam antibiotic that targets FtsI (PBP3) (Gootz *et al.*, 1979) and inhibits the formation of the septum by blocking peptidoglycan synthesis (Schmidt *et al.*, 1981; Olijhoek *et al.*, 1982). The  $\beta$ -lactam cephalexin induces cells to undergo rapid lysis at the division sites (Chung *et al.*, 2009; Chung *et al.*, 2011). The assembly of the divisome must be complete for the cell to lyse, including the recruitment of FtsN by FtsI, and FtsN then recruits autolysins to separate the daughter cells (Chung *et al.*, 2009). The rapid lysis caused by cephalexin is due to FtsI blockade that does not disrupt divisome component recruitment and consequent autolysin activation (Chung *et al.*, 2009). Mutations in FtsI make many bacteria resistant to  $\beta$ -lactams and have only slight effects on bacterial survival (Hedge and Spratt, 1985; Nagai *et al.*, 2002; Kishii *et al.*, 2010).

An equally important PBP drug target is FtsZ due to its importance in recruiting all other divisome components to the midcell. Viriditoxin, a natural compound that is isolated from *Aspergillus viridinutans*, was identified by fluorescence-based assays as an FtsZ inhibitor (Wang *et al.*, 2003; Park *et al.*, 2011). Viriditoxin blocks the polymerisation of FtsZ and its GTPase activity and has been shown to hinder cell

division in Gram-positive pathogens, such as methicillin-resistant *S. aureus* (MRSA) and vancomycin-resistant *Enterococci* (VRE) without disturbing the viability of eukaryotic HeLa cells (Wang *et al.*, 2003; Park *et al.*, 2011). A similar inhibitory effect on FtsZ and subsequent growth cessation in clinically relevant pathogens has been described for food products, such as cinnamaldehyde (Domadia *et al.*, 2007) and curcumin (Rai *et al.*, 2008), and for the natural compounds from *Chrysosphaeum taylori* (Plaza *et al.*, 2010). The C-terminal tail of FtsZ is involved in interactions with many divisome components; however, cinnamaldehyde was found to also bind to the C-terminal tail, inhibiting the binding site and preventing the recruitment of the division proteins (Domadia *et al.*, 2007). Sanguinarine is an antimicrobial from *Sanguinaria canadensis* that binds to FtsZ to perturb Z-ring formation in Gram-positive and Gram-negative bacteria (Beuria *et al.*, 2005).

Several FtsZ inhibitors have been shown to destabilise FtsZ protofilaments and suppress FtsZ GTPase activity, causing a reduction in the formation of the FtsZ-ring and filamentation in a wide range of bacteria, including pathogenic species (Ito *et al.*, 2006; Jaiswal *et al.*, 2007; Shimotohno *et al.*, 2010; Hemaiswarya *et al.*, 2011). A high-throughput protein-based screening analysis has identified Zantrins, a group of compounds that have GTPase inhibitory effects (Margalit *et al.*, 2004). Some of these compounds inhibit the polymerisation of FtsZ, and others stabilise the protofilaments and inhibit their depolymerisation (Margalit *et al.*, 2004). An *in vitro* study has identified several compounds that affect FtsZ assembly, including OTBA(3-{5-[4-oxo-2-thioxo-3-(3-trifluoromethyl-phenyl)-thiazolidin-5-ylidenemethyl]-furan-2-yl}-benzoic acid), which induces the assembly of FtsZ (Beuria *et al.*, 2009).

PC190723, a small synthetic antibacterial, has also been found to alter the dynamics of FtsZ assembly in *B. subtilis*, MRSA and multi-drug-resistant *S. aureus* (MDRSA). PC190723 induced the assembly of FtsZ polymers into coiled protofilaments, bundles, ribbons and toroids (Ohashi *et al.*, 1999; Haydon *et al.*, 2008; Andreu *et al.*, 2010; Adams *et al.*, 2011). PC190723 has been shown to suppress the GTPase activity of FtsZ and demonstrates selective *in vivo* bactericidal activity, as it protected mice infected with a fatal dose of *S. aureus* (Haydon *et al.*, 2008). GTP analogues can prevent the polymerisation of FtsZ with

minimal effect on host cell tubulin assembly (Lappchen *et al.*, 2005). Antisense oligodeoxynucleotides repress the expression of *ftsZ* and thus affect cell viability (Tan *et al.*, 2004).

Studies have investigated inhibitors of FtsZ protein-protein interactions by screening a library of approximately 250,000 compounds and have identified several small molecules that bind to ZipA and prevent its binding to FtsZ, resulting in inhibition of cell division (Sutherland *et al.*, 2003; Jennings *et al.*, 2004a; Jennings *et al.*, 2004b). Screening of a phage display library using *P. aeruginosa* FtsA has led to the identification of two consensus peptide sequences that block the ATPase activity of FtsA. This information could be useful for targeting other cell division components and for developing new inhibitors against other proteins (Paradis-Bleau *et al.*, 2005).

### **1.9. Cell division in cocci**

The cell division process has mostly been investigated in rod-shaped microorganisms, particularly *E. coli* and *B. subtilis*. Although the cell division process among prokaryotes is likely conserved, much information can be obtained from comparative studies of morphologically diverse bacteria (Zapun *et al.*, 2008). Coccus-shaped bacteria lack cylindrical elongation, making them a simple model for studying cell division (Zapun *et al.*, 2008). Cell wall synthesis in rod-shaped bacteria occurs in two stages: first, elongation of the cell and doubling of the cell size, which is mediated by MreB, and second, division after septum formation at the midcell region, which is mediated by FtsZ (Carballido-Lopez and Formstone, 2007) (Figure 1.1A). MreB assembles to form dynamic bundle filaments at the cell periphery and has been proposed to act as a scaffold for the elongation machinery components, such as MreC and MreD (Jones *et al.*, 2001; Defeu-Soufo and Graumann, 2004; Carballido-Lopez and Formstone, 2007; Dempwolff *et al.*, 2011). A comprehensive examination of sequenced bacterial genomes has identified a link between absence of *mreB* and a non-rod-like shape; however, chlamydia and some cyanobacteria do not adhere to this association, as both are subjected to morphological changes that are mediated by MreB (Daniel and Errington, 2003). These observations suggest a molecular basis for the absence of cylindrical cell wall

synthesis in coccus-shaped organisms (Daniel and Errington, 2003). Cell wall synthesis in cocci is dependent upon FtsZ, which thus determines morphology and accounts for the synthesis of each daughter cell (Zapun *et al.*, 2008). There is relevance in investigating division in cocci because many species are common human pathogens, including *S. aureus*, *N. gonorrhoeae*, *Neisseria meningitidis* and *S. pneumoniae*, and understanding their division will help identify novel antimicrobial targets.

There are two classes of cocci, true cocci, such as *staphylococci*, *Neisseria* or *micrococci*, which are truly round and oval cocci (ovococci), such as *lactococci*, *enterococci* or *streptococci*, which are elongated ellipsoids. Both cocci types have different mechanisms of cell wall synthesis during their life cycle (Zapun *et al.*, 2008). Annular outgrowth of peptidoglycans surrounds the middle of the ovococcus cell and is known as the equatorial ring (Higgins and Shockman, 1970; Tomasz *et al.*, 1964). During cell division in ovococci, a small ingrowth below the equatorial ring occurs before the initiation of septum formation. The equatorial ring splits in two and the two rings separate as new peripheral cell wall forms. The small annular ingrowth remains equidistant from the separating equatorial rings and then begins to grow centripetally to form the septum. Once the septum is completely formed, the cells split to form two new daughter cells. The peripheral synthesis of the cell wall before the formation of the septum suggests that the ovococcus has two sites of peptidoglycan synthesis during division (Figure 1.1B) (Higgins and Shockman, 1970). Further experiments have supported this assumption. Ts mutants grown at restrictive temperatures and cells treated with division-inhibiting concentrations of antibiotics form long filaments, suggesting longitudinal growth in the absence of septation (Lleo *et al.*, 1990; Gibson *et al.*, 1983; Higgins *et al.*, 1974). When cell division is blocked in truly round cocci, filamentation of the cells is not observed because true coccus cells are only subjected to one mode of cell wall synthesis (Figure 1.1C) (Pinho and Errington, 2003; Lleo *et al.*, 1990; Gibson *et al.*, 1983; Higgins *et al.*, 1974).

The selection of the division site in true cocci is complicated in comparison with rod-shaped bacteria and elongated cocci, as midcell division occurs in one parallel plane to produce single chains of cells (Zapun *et al.*, 2008). In contrast, true cocci have the capability to divide in an infinite number of theoretical planes with a maximum diameter within the cell (Zapun *et al.*, 2008). However, coccus division in more than one plane is not common and can occur in two perpendicular planes to form tetrads or flat sheets of cells, as seen in *Neisseria*, *Micrococcus*, *Pediococcus* or *Lampropedia* (Zapun *et al.*, 2008). Division in three orthogonal planes can also occur to produce cuboidal packs of eight cells, as seen in *Staphylococci* or *Sarcina*. However, the latter produce regular packs of cells, whereas *Staphylococci* proceed through incomplete cell division that causes the appearance of cell clusters (Begg and Donachie, 1998; Giesbrecht *et al.*, 1998; Murray *et al.*, 1983; Tzagoloff and Novick, 1977). The recognition of previous and potential division planes by cocci is still not well understood. Recently, epigenetic information in *S. aureus* has been suggested to be contained within its cell wall. The large bands of equatorial peptidoglycans and less distinct orthogonal bands that are observed in *S. aureus* peptidoglycans act as physical indicators of sequential orthogonal division planes (Turner *et al.*, 2010). *S. aureus* cells lacking Noc form multiple Z-rings that are not placed in orthogonal planes, indicating that the nucleoid occlusion is involved in choosing the plane of the next septum (Veiga *et al.*, 2011).

Fluorescent vancomycin staining of *S. aureus* has confirmed the previous suggestion that peptidoglycan synthesis occurs exclusively at the division site (Pinho and Errington, 2003). In the absence of FtsZ, peptidoglycans are delocalised over the entire *S. aureus* cell surface, most likely caused by the delocalisation of divisome components (Pinho and Errington, 2003). In *S. pneumoniae*, the localisation of peptidoglycan synthesis using fluorescent vancomycin labelling verified that peptidoglycan synthesis also occurred at the midcell (Ng *et al.*, 2004; Daniel and Errington, 2003). Despite these data, because ovoids have two types of division-specific mechanisms of peptidoglycan synthesis, the proteins that are involved in the synthesis of peptidoglycans, such as PBPs, can be organised into two separate systems (Zapun *et al.*, 2008). The two peptidoglycan synthesis systems in *S. pneumoniae* were initially assumed to localise in different places

throughout the cell cycle (Morlot *et al.*, 2003), but immunofluorescence microscopy has shown that all *S. pneumoniae* PBPs are localised in the middle of the cell during the cell cycle. This finding suggests a common localisation of the two distinct systems (Zapun *et al.*, 2008).

*S. aureus* has four PBPs, and three of them were shown to localise to the middle of the cell (Pinho and Errington, 2005; Pereira *et al.*, 2007b; Atilano *et al.*, 2010). Non-essential HMW class B PBP3 localisation in *S. aureus* has not yet been demonstrated, but PBP3 is unlikely to localise somewhere other than the midcell (Zapun *et al.*, 2008). The localisation of PBPs from other true cocci has not yet been determined; however, *N. gonorrhoeae* and *N. meningitidis* have only four defined PBPs, suggesting one mode of peptidoglycan synthesis (Stefanova *et al.*, 2004; Barbour, 1981; Nolan and Hildebrandt, 1979). Accordingly, cell division in true cocci may be a simple system because it lacks the cylindrical elongation process and thus, the presence of one of the division-specific peptidoglycan synthesis systems. This model can therefore help in classifying novel drugs targeting molecules essential for bacterial division and growth in clinically relevant organisms.

### **1.9.1. *S. aureus* as a cell division model**

Because *S. aureus* is a major human pathogen and causes a serious threat to public health due to high incidences of resistance to current antibiotics, developing new antibiotics is necessary. Most of the existing antibiotics and inhibitors are directed at DNA, protein synthesis and cell wall components (Wang *et al.*, 2003). Discovery of essential genes is crucial for the development of novel antimicrobials, thus making cell division an attractive model of study, as it is an essential process in all bacteria. The simple cycle and morphology of *S. aureus* cells make *S. aureus* an appropriate model for studying the process of cell division. *S. aureus* is closely related to the model organism *B. subtilis*, and thus, it is presumed that the two organisms have conserved cell division mechanisms (Steele *et al.*, 2011). Both organisms vary in their cell shape, and *S. aureus* is a simpler organism, as mentioned above. *S. aureus* as true cocci is not subjected to a different mode of cell division than rod-shaped



organisms (Zapun *et al.*, 2008). The synthesis of peptidoglycans between division cycles in rods is specific to the lateral cell wall and leads to elongation (Carballido-Lopez and Formstone, 2007). Once the cell has doubled in length, which is followed by the segregation of the chromosome, cell wall synthesis occurs at the midcell, causing formation of the septum and resulting in division (Adams and Errington, 2009). Mutation of genes involved in cell elongation (e.g., *mreB*, *mreC*, *mreD*, *pbp-2a*, *pbp-H* or *rodA*) results in the formation of spherical cells (Levin *et al.*, 1992; Henriques *et al.*, 1998; Wei *et al.*, 2003; Leaver & Errington, 2005). Sphere-shaped *S. aureus* cells do not undergo the elongation phase of growth, as they lack the MreB homologue and only synthesise peptidoglycan at the septum (Pinho & Errington, 2003; Zapun *et al.*, 2008). Although *S. aureus* has homologues of *mreC*, *mreD* and *rodA*, the genes are not essential, as they are in *B. subtilis* (Zapun *et al.*, 2008). In *B. subtilis*, these genes have been proposed to play a role in the cell division process (Henriques *et al.*, 1998; Lee and Stewart, 2003; Formstone and Errington, 2005).

*S. aureus* does not sporulate as does *B. subtilis*, which changes from vegetative growth, in which septation is dependent on FtsZ at the midcell, to sporulation, which causes polar septation during starvation (Carballido-Lopez and Formstone, 2007). The Z-ring constructs near the cell pole during sporulation form asymmetric septum (Ben-Yehuda and Losick, 2002). Asymmetric division then occurs, producing a mother cell and small forespores that mature into metabolically inactive spores and are able to survive in extreme conditions (Frandsen *et al.*, 1999). The division machinery that is associated with asymmetric division is similar to the machinery utilised in vegetative septation. Several other sporulation-specific proteins are also involved in asymmetric septum formation, such as SpoIIA, SpoIIE and SpoIIG (Feucht *et al.*, 1996; Piggot and Hilbert, 2004). Therefore, studying the role of the division proteins in *B. subtilis* is complicated because *B. subtilis* has a sporulation mechanism.

As mentioned previously (Section 1.9), *S. aureus* as a true coccus has a single mechanism of cell wall synthesis and division and therefore has less functional redundancy between the proteins associated with cell division and peptidoglycan synthesis than *B. subtilis*. This fact makes the study of the role of these proteins in cell division less complicated. A comparison of the cell division genes between *B.*

*subtilis* and *S. aureus* has shown that most of the division components are well conserved (Table 1.1) (Chaudhuri *et al.*, 2009). Homologues of all the essential genes used in cell division in *B. subtilis* are putatively essential for *S. aureus* growth; however, some of the non-essential genes are not conserved. Furthermore, homologues of some non-essential genes of *B. subtilis*, such as *gpsB* and *sepF*, have been found to be potentially essential in *S. aureus*, suggesting reduced redundancy (Chaudhuri *et al.*, 2009). A recent study showed that the homologue of the non-essential *ezrA* gene in *B. subtilis* is essential for the growth and division of *S. aureus* (Steele *et al.*, 2011). *S. aureus* has fewer genes encoding PBPs than *B. subtilis* and could indicate a single mode of peptidoglycan synthesis in *S. aureus* (Zapun *et al.*, 2008). The multiple PBPs in *B. subtilis* have definite roles in elongation, spore formation and septum formation (Claessen *et al.*, 2008), indicating dual roles of PBPs in *B. subtilis* and possibly rods in general. The Min system is not present in many Gram-positive cocci (Margolin 2001). Although the *minC* and *minD* genes are essential in *B. subtilis* and absent in *S. aureus*, a homologue of these genes, *divIVA*, is present in *S. aureus* but is not essential for *S. aureus* viability, chromosome segregation or morphology (Pinho and Errington 2004). The absence of the Min system in *S. aureus* reflects the absence of DNA at the cell poles, which prevents division in spherical bacteria. In *B. subtilis*, *noc* and *minD* double-mutants affect cell survival (Wu & Errington, 2004). Recent work has shown that Noc is not essential for growth in *S. aureus* but is required for inhibiting Z-ring formation over nucleoids, hence preventing nucleoid bisection by the septa (Veiga *et al.* 2011).

### **1.1. Staphylococcal species**

Staphylococci are gram-positive, spherical bacteria that have a diameter of approximately 0.5-1.5  $\mu\text{m}$  (Harris *et al.*, 2002; Hennekinne *et al.*, 2012). These bacteria are immobile, facultative, non-spore forming anaerobes and some strains are resistant to disinfectants and heat (Hennekinne *et al.*, 2012). The cells divide in three perpendicular planes (Tzagoloff and Novick, 1977), forming clusters (from which their nomenclature is derived).

	<i>B. subtilis</i> gene	Essentiality in <i>B. subtilis</i>	<i>S. aureus</i> homologue (NCTC 8325)	Identity/similarity of the gene product	Essentiality in <i>S. aureus</i>
Chromosome segregation	<i>parE</i>	Essential (Huang <i>et al.</i> , 1998)	SAOUHSC_01351	71/85	Essential (Chaudhuri <i>et al.</i> , 2009)
	<i>parC</i>	Essential (Huang <i>et al.</i> , 1998)	SAOUHSC_01352	59/76	Essential (Chaudhuri <i>et al.</i> , 2009)
Septa placement	<i>divIVA</i>	Essential (Cha and Stewart, 1997)	<i>divIVA</i>	41/72	Not essential (Pinho and Errington, 2004)
	<i>noc</i>	Not essential (Wu and Errington, 2004)	SAOUHSC_03049	48/65	Not essential (Veiga <i>et al.</i> , 2011)
Z-ring formation	<i>ftsZ</i>	Essential (Beall and Lutkenhaus, 1991)	<i>ftsZ</i>	63/76	Essential (Pinho & Errington, 2003)
	<i>ftsA</i>	Essential* (Beall and Lutkenhaus, 1992)	<i>ftsA</i>	32/55	Essential (Ko, 2006; Chaudhuri <i>et al.</i> , 2009)
	<i>ezrA</i>	Not essential (Levin <i>et al.</i> , 1999)	SAOUHSC_01827	22/55	Essential (Steele <i>et al.</i> , 2011)
	<i>zapA</i>	Not essential (Gueiros-Filho & Losick, 2002)	SAOUHSC_01096	49/68	Not essential (Chaudhuri <i>et al.</i> , 2009)
	<i>sepF</i>	Essential <sup>‡</sup> (Hamoen <i>et al.</i> , 2006)	SAOUHSC_01154	70/86	Essential (Chaudhuri <i>et al.</i> , 2009)
Late division proteins	<i>ftsL</i>	Essential (Daniel <i>et al.</i> , 1998)	SAOUHSC_01144	23/42	Essential (Chaudhuri <i>et al.</i> , 2009)
	<i>divIC</i>	Essential (Levin & Losick, 1994)	SAOUHSC_00482	23/41	Essential (Chaudhuri <i>et al.</i> , 2009)
	<i>divIB</i>	Essential <sup>§</sup> (Beall and Lutkenhaus, 1989)	SAOUHSC_01148	28/52	Essential (Chaudhuri <i>et al.</i> , 2009)
	<i>ftsW</i>	Essential (Kobayashi <i>et al.</i> , 2003)	SAOUHSC_01063	28/45	Essential (Chaudhuri <i>et al.</i> , 2009)
	<i>gpsB</i>	Not essential (Claessen <i>et al.</i> , 2008)	SAOUHSC_01462	63/81	Essential (Chaudhuri <i>et al.</i> , 2009)
PBPS (peptidoglycan biosynthesis)	<i>ponA</i>	Essential <sup>‡</sup> (Murray <i>et al.</i> , 1998)	<i>pbpB</i>	37/56	Essential (Pinho <i>et al.</i> , 2001)
	<i>pbpB</i>	Essential (Daniel <i>et al.</i> , 1996)	<i>pbpA</i>	40/60	Essential (Chaudhuri <i>et al.</i> , 2009)
	<i>pbpA</i>	Not essential (Murray <i>et al.</i> , 1997)	<i>pbpC</i>	44/63	Not essential (Pinho <i>et al.</i> , 2000)
Teichoic acid biosynthesis	<i>ltaS</i>	Not essential (Kobayashi <i>et al.</i> , 2003)	<i>ltaS</i>	57/73	Essential (Grundling and Schneewind, 2007b)
	<i>tagG</i>	Essential (Lazarevic and Karamata, 1995)	<i>tagG</i> ( <i>tarG</i> )	37/60	Essential (Swoboda <i>et al.</i> , 2009; Chaudhuri <i>et al.</i> , 2009)
Elongation	<i>rodA</i>	Essential (Henriques <i>et al.</i> , 1998)	SAOUHSC_02319	31/51	Not essential (Chaudhuri <i>et al.</i> , 2009)
	<i>mreD</i>	Essential (Leaver and Errington, 2005)	SAOUHSC_01758	29/54	Not essential (Chaudhuri <i>et al.</i> , 2009)
	<i>mreC</i>	Essential (Leaver and Errington, 2005)	SAOUHSC_01759	36/58	Not essential (Chaudhuri <i>et al.</i> , 2009)
Lipid membrane biosynthesis	<i>plsY</i>	Essential (Hunt <i>et al.</i> , 2006)	SAOUHSC_01350	46/66	Essential (Chaudhuri <i>et al.</i> , 2009)

**Table 1.1 Conservation of cell division genes between *S. aureus* and *B. subtilis***

\* *B. subtilis* *ftsA* (Beall & Lutkenhaus, 1992) and *sepF* (Hamoen *et al.*, 2006) mutants were viable; however, they show severe defects in cell division, cell morphology and growth. Thus, the genes are classified as essential.

§ *B. subtilis* *divIB* is only essential at elevated temperatures.

‡ The *ponA* gene in *B. subtilis* is only essential for cell growth and sporulation in divalent cation-deficient media (Murray *et al.*, 1998).

In 1880, Sir Alexander Ogston, a Scottish surgeon, identified this genus and named it *Staphylococcus* from the Greek words *staphylo*, meaning “bunch of grapes”, and *kokkos*, meaning “grain” (Archer, 1998). These bacteria can be distinguished from *micrococcus*, which produces acid aerobically, by the oxidation-fermentation test. They can grow in media that contains 7.5% NaCl, making high-salt media the media of choice for *Staphylococcus* (Madigan & Martinko, 2006; Harris *et al.*, 2002). Furthermore, one of the features that distinguish this genus from other gram-positive cocci is the catalase test, which is positive in the presence of staphylococci and negative in the presence of streptococci (Madigan & Martinko, 2006).

The *Staphylococcus* genus comprises approximately 40 species, most of which are harmless and reside on human mucous membranes and skin (DeLeo *et al.*, 2009). However, five species in this genus are considered as potential pathogens: *S. aureus*, *Staphylococcus saprophyticus*, *Staphylococcus epidermidis*, *Staphylococcus hominis* and *Staphylococcus haemolyticus* (Hennekinne *et al.*, 2012).

## **1.2. *S. aureus***

*S. aureus* is a species of the genus *Staphylococcus*, family Staphylococcaceae, order Bacillales, class Cocci, phylum Firmicutes, kingdom Bacteria and domain Bacteria (Ludwig, 2009). *S. aureus* has a circular chromosome of approximately 2.8 Mbp (Lowy, 1998; Harris *et al.*, 2002). Its colonies are distinct from those of other staphylococcal species, as they contain a golden yellow pigment. Moreover, *S. aureus* can be distinguished from other staphylococcal species by the DNase and coagulase tests (Madigan and Martinko, 2006; Lowy, 1998).

### **1.2.1. *S. aureus* infections**

*S. aureus* is considered to be an opportunistic pathogen, and over the past 30 years, hospital-acquired and community-associated *S. aureus* infections have increased dramatically (Hennekinne *et al.*, 2012). This bacterium is usually found as normal flora on the skin or in the upper respiratory tract, although it mostly colonises the mucous membranes of the nasal cavity (Archer, 1998; Hennekinne *et al.*, 2012). The risk of infection is raised in intravenous drug users and those undergoing

surgery, as well as in immunocompromised and diabetic patients (Madigan and Martinko, 2006; Archer, 1998; Howell and Phillips, 2007; Hennekinne *et al.*, 2012). *S. aureus* is responsible for a wide range of infections and diseases, such as mild skin infections (e.g., folliculitis, impetigo and cellulitis), invasive diseases (e.g., osteomyelitis, wound infections and metastatic complications) and toxin-mediated diseases (e.g., toxic shock syndrome, food poisoning and scalded skin syndrome), where colonisation precedes the infections (Archer, 1998; Lowy, 1998; von Kockritz-Blickwede *et al.*, 2008; Hennekinne *et al.*, 2012). In some animals (e.g., cows, goats and sheep), *S. aureus* causes mastitis, which is economically important (Le Marechal *et al.*, 2011). Approximately 30% of the healthy population carry *S. aureus*, which can asymptotically colonise the skin of human hosts (Peacock *et al.*, 2001; Hennekinne *et al.*, 2012). However, a break or puncture of the skin allows the bacteria to enter the soft tissue or the bloodstream and cause infections (Lowy, 1998).

### **1.2.2. Virulence factors**

The wide range of diseases caused by *S. aureus* are the result of a multitude of virulence factors expressed by the bacteria. Many surface proteins bind to host extracellular matrix molecules (Harris *et al.*, 2002; Lowy, 1998; Foster and Hook, 1998), allowing colonisation in the anterior nares (Garcia-Lara *et al.*, 2005). Indeed, colonisation of the pathogen in the anterior nares could be due to adhesins or the indirect help of teichoic acid (Garcia-Lara *et al.*, 2005). Surface proteins also act as immune evasion molecules. Protein A, which acts as an adhesion, binds to the Fc part of antibodies, preventing recognition by the host immune system (Uhlen *et al.*, 1984; Harris *et al.*, 2002). *S. aureus* can also produce several toxins including cytotoxins, leukotoxins and haemolysins that lyse cells and provoke proinflammatory responses. For example, exotoxins A and B are involved in scalded skin syndrome, and toxic shock syndrome toxin 1 (TSST1) is involved in toxic shock syndrome (Lowy, 1998; Harris *et al.*, 2002; Foster, 2005). Other virulence factors that are released by *S. aureus* are extracellular enzymes such as proteases, coagulase and lipases, which are thought to be involved in spreading the infection and damaging the host tissue (Foster, 2005).

### 1.2.3. Antibiotic resistance

Preceding the introduction of antibiotics, the mortality rate of infections caused by *S. aureus* was approximately 80% (Skinner, 1941), this rate declined to approximately 25% in 1944 (Jevons *et al.*, 1963), after the introduction of penicillin treatment (Dancer, 2008). However, a significant problem related to *S. aureus*, apart from it causing life-threatening diseases, is its resistance to different antibiotics (Figure 1.7) (Garcia-Lara *et al.*, 2005). This resistance has become a worldwide health issue that has jeopardised communities, increasing the high rate of *S. aureus* infection mortality to  $\sim > 30\%$  (Dancer, 2008). Penicillin-resistant *S. aureus* is the result of the inactivation of penicillin by  $\beta$ -lactamase, which hydrolyses the  $\beta$ -lactam ring. This was first identified in 1941, soon after the introduction of penicillin and by 1948, approximately 50% of isolates were resistant (Barber and Rozwadowska-Dowzenko, 1948; Lowy, 1998; Witte *et al.*, 2008). Approximately 5% of *S. aureus* isolates now show sensitivity to penicillin (Lowy, 1998). In the 1950s, *S. aureus* was found to also become resistant to many of the most commonly used antibiotics such as streptomycin, erythromycin, chloramphenicol and tetracycline (Lacey; 1975; Witte *et al.*, 2008). In order to combat the problem of penicillin resistance,  $\beta$ -lactamase-resistant semisynthetic penicillins, such as methicillin, cloxacillin and oxacillin, were developed (Rice, 2006). However, *S. aureus* became resistant to methicillin in 1961 in the United Kingdom (U.K.) and in 1969 in the United States (U.S.) (Jevons, 1961; Rice, 2006; McLean and Ness, 2008).

Methicillin resistance occurs via the acquisition of the *mecA* gene encoding PBP2a (Matsukawa, 2001; Fuda *et al.*, 2004; Dancer, 2008). The *S. aureus* PBPs are inactivated by  $\beta$ -lactam antibiotics and hence inhibiting peptidoglycan biosynthesis. However, PBP2a is capable of replacing the function of the four essential PBPs in the presence of  $\beta$ -lactam antibiotics, as the active site of PBP2a is modified and has low affinity to  $\beta$ -lactams (Lim and Strynadka, 2002; Meroueh *et al.*, 2003; Fuda *et al.*, 2004). MRSA has spread to over 70% in hospitals in the U.S. and Europe (Rice, 2006), causing a major threat to public health and making the development of an effective antimicrobial drug that can combat MRSA crucial (Fuda *et al.*, 2004).

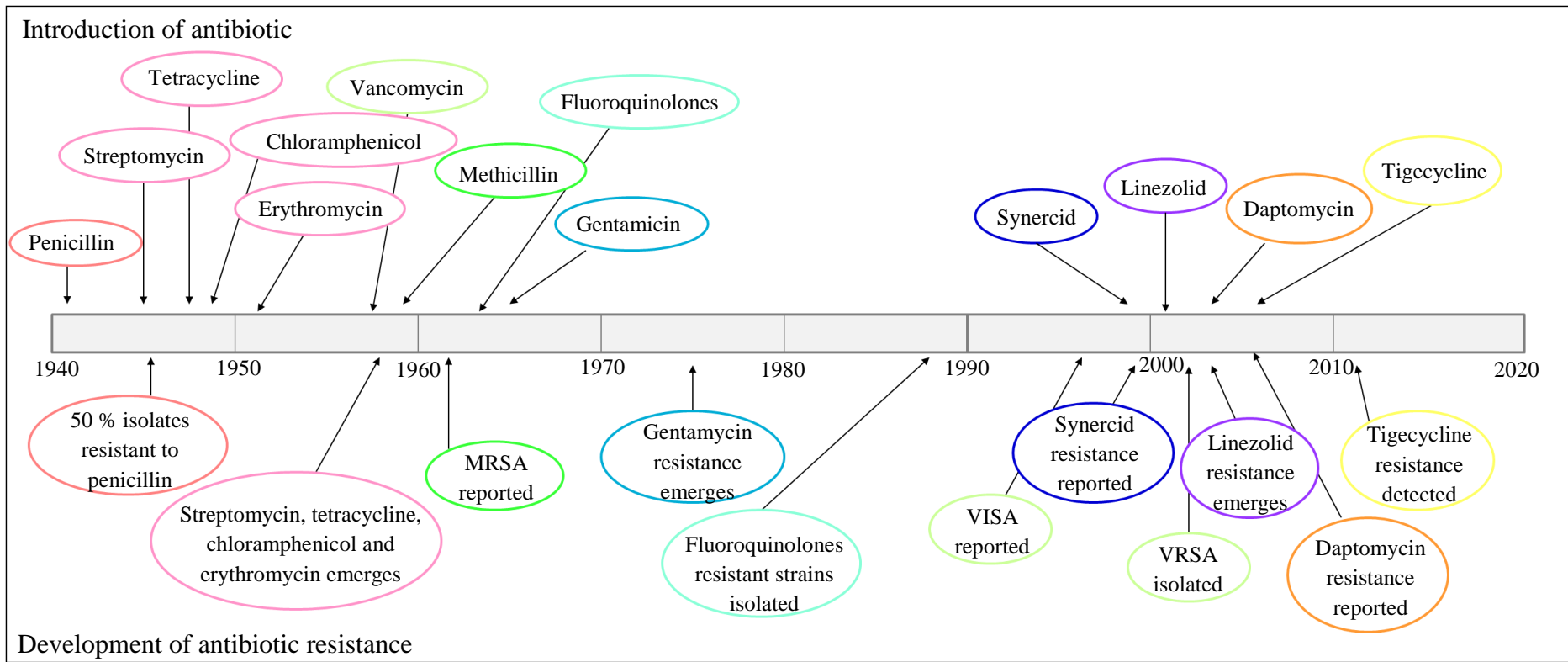


**Figure 1.7** Timeline of introduction and subsequent development of resistance by *S. aureus* to commonly used antibiotics

In 1964, gentamicin was introduced to treat MRSA cases in the U.K.; however, in the mid-1970s, resistance of *S. aureus* to gentamicin and related antibiotics, such as kanamycin and tobramycin, had been found in clinical isolates from Europe, the U.S. and Australia (Dowding, 1977; Naidoo and Noble, 1978; Storrs *et al.*, 1988; Wright *et al.*, 1998). The resistance to gentamicin is due to a bifunctional enzyme, gentamicin phosphotransferase/aminoglycoside 6'-N- acetyltransferase, which modifies the antibiotic, preventing binding to the 30S ribosomal target in the strain (Dowding, 1977; Rouch *et al.*, 1987).

Fluoroquinolone antibiotics such as ofloxacin, norfloxacin and ciprofloxacin were originally introduced in the late 1980s to treat infections caused by Gram-negative bacteria; however, the efficacy of the drug was poor, and hence, the activity against Gram-positive pathogens was poor as well (Entenza *et al.*, 1999; Khaliq and Zhanel, 2003). A new generation of fluoroquinolones, such as clinafloxacin, pefloxacin and sparfloxacin, was subsequently introduced to treat infections caused by Gram-positive pathogens (Entenza *et al.*, 1999; Khaliq and Zhanel, 2003). However, *S. aureus* and MRSA have easily developed resistance against fluoroquinolones (Greenberg *et al.*, 1987; Scaefler, 1989; Munoz-Bellido *et al.*, 1999) via mutation in DNA gyrase and overexpression of NorA, a multidrug efflux protein (Ng *et al.*, 1994; Ferrero *et al.*, 1995; Kaatz and Seo, 1997; Jacoby; 2005; Charbonneau *et al.*, 2006).

The glycopeptide vancomycin was first introduced in 1958 to treat drug-resistant pathogens (Cafferkey *et al.*, 1982). Vancomycin has a high affinity for the D-Ala-D-Ala terminus of the peptidoglycan precursor, blocking integration into peptidoglycan (Courvalin, 2006). VRE were first isolated as clinical strains in Europe in 1988 (Leclercq *et al.*, 1988; Uttley *et al.*, 1988). The resistance is due to the presence of the *vanA* operon that encodes the VanH dehydrogenase and VanA ligase, which are responsible for the synthesis of D-Ala-D-Lac that replaces D-Ala-D-Ala (Bugg *et al.*, 1991; Courvalin, 2006). Vancomycin-insensitive *S. aureus* (VISA) was found first in Japan in 1996 (Hiramatsu *et al.*, 1997; Smith *et al.*, 1999) and in 1999 in the U.S. (Rotun *et al.*, 1999; Hageman *et al.*, 2001). VISA is due to an alteration in the synthesis of peptidoglycan, which results in



thickening of the cell wall. The alteration in the cell wall sequesters vancomycin due to the production of nascent peptidoglycan and thus reduces the diffusion of vancomycin across the cell wall (Cui *et al.*, 2000; Cui *et al.*, 2006; Pereira *et al.*, 2007a). In 2002, vancomycin-resistant *S. aureus* (VRSA) were first isolated in the U.S. (Sievert *et al.*, 2008; Cui *et al.*, 2006). The full resistance to vancomycin was caused by the transfer of *vanA* from a co-existing VRE (Weigel *et al.*, 2003; Cui *et al.*, 2006). The incidence of VRSA is quite rare; however, the incidence of VRSA-MRSA combination strains is predicted to increase, posing a major threat to public health. Furthermore, VRSA is also resistant to other antibiotics, such as rifampin (Weigel *et al.*, 2003), causing a critical situation in the control of *S. aureus* infection and making the search for new antimicrobial agents imperative.

Few effective antibiotics (e.g. synergid, linezolid, daptomycin and tigecycline) have been introduced to treat both MRSA and VRSA. Synergid is a combination of two streptogramins (quinupristin and dalfopristin), which bind to the 50S ribosomal subunit and hence inhibit protein synthesis (Drew *et al.*, 2000). Resistance to synergid in clinical isolates from France and Spain has been reported (Werner *et al.*, 2001), due to a mutation in the L22 ribosomal protein (Malbruny *et al.*, 2002). Linezolid-resistant *S. aureus* strains were isolated in 2001, which was the same year that linezolid was introduced. The resistance is caused by a mutation in the 23S ribosomal target (Tsiodras *et al.*, 2001). Daptomycin is a cyclic lipopeptide that depolarises the cell membrane (Tally *et al.*, 1999; Silverman *et al.*, 2003). The drug was introduced in 2003 to treat *S. aureus* infection; however, in 2005, clinical isolates were found to be resistant to daptomycin (Mangili *et al.*, 2005; Hayden *et al.*, 2005). Resistance is caused by perturbation of the bacterial cell wall and cell membrane, reducing the surface binding of the drug and making the strain resistant to the depolymerisation effect of daptomycin (Bayer *et al.*, 2013). Tigecycline is a novel glycylicycline class of antimicrobial agents that is structurally similar to tetracycline but not affected by the tetracycline resistance mechanisms of ribosomal protection and efflux pump (Petersen *et al.*, 1999; Pankey, 2005; Verkade *et al.*, 2010). After the introduction of tigecycline in 2006, surveillance of reported resistance suggested that resistance to this antibiotic had not occurred in clinical isolates as of 2008 (Rodloff *et al.*, 2008). However, cases

of tigecycline-resistant *S. aureus* have been reported recently in the U.K. (Hope *et al.*, 2010, Kreis *et al.*, 2013).

### **1.3. Study aims**

Although the mechanism of cell division is conserved between organisms, cell division in *S. aureus* is still not well understood. This project aimed to identify the role of some *S. aureus* cell division proteins, particularly the bitopic proteins, in division. Specifically, DivIC and FtsL in *S. aureus* were chosen for examination. Experiments were performed using different molecular and biochemical assays to study biochemical function and localisation in the cell. The interaction between these proteins and the bacterial cell wall was also investigated and emphasised the importance of these proteins in the cell division process.

## Materials and methods

### 2.1. Media

Media were prepared using deionised water (dH<sub>2</sub>O) and sterilised by autoclaving for 20 min at 121°C and 15 pounds per square inch.

#### 2.1.1 Baird-Parker (BPr)

Baird-Parker Agar Base (Oxoid) 63 g l<sup>-1</sup>

Egg Yolk Emulsion (VWR) 50 ml l<sup>-1</sup>

(Egg Yolk Emulsion was added after cooling the agar to 50°C).

#### 2.1.2 Brain Heart Infusion (BHI)

BHI (Oxoid) 37 g l<sup>-1</sup>

1.5 % (w/v) Oxoid agar No. 1 was added to make BHI agar.

#### 2.1.3 Luria-Bertani (LB)

Tryptone (Oxoid) 10 g l<sup>-1</sup>

Yeast extracts (Oxoid) 5 g l<sup>-1</sup>

NaCl 10 g l<sup>-1</sup>

1.5 % (w/v) Oxoid agar No. 1 was added to make LB agar.

#### 2.1.4 LK

Tryptone (Oxoid) 10 g l<sup>-1</sup>

Yeast extracts (Oxoid) 5 g l<sup>-1</sup>

KCl 7 g l<sup>-1</sup>

1 % (w/v) Oxoid agar No. 1 was added to make LK bottom agar.

0.7 % (w/v) Oxoid agar No. 1 was added to make LK top agar.

#### 2.1.5 Nutrient agar (NA)

Nutrient agar (Oxoid) 28 g l<sup>-1</sup>

### 2.1.6 Nutrient broth (NB)

Nutrient broth (Oxoid) 13 g l<sup>-1</sup>

### 2.1.7 Tryptic soya broth (TSB)

Tryptic soya broth (Oxoid) 30 g l<sup>-1</sup>

### 2.1.8 Tryptic soya agar (TSA)

Tryptic soya agar 30 g l<sup>-1</sup>

## 2.2 Antibiotics

The antibiotics (Table 2.1) used in this study were prepared from stock solutions, which were filter-sterilised (0.2 µm pore size) and stored at -20°C. The antibiotic stock solution was added just before use to the liquid media, whilst in agar plates, the media were first cooled to below 50°C and then the antibiotic solutions were added.

Antibiotics	Dissolved in	Stock concentration (mg ml <sup>-1</sup> )	<i>S. aureus</i> working concentration (µg ml <sup>-1</sup> )	<i>E. coli</i> working concentration (µg ml <sup>-1</sup> )
Ampicillin (Amp)	H <sub>2</sub> O	100	-	100
Anhydrotetracycline (ATc)	100 % (v/v) ethanol	150	1	-
Chloramphenicol (Cat)	100 % (v/v) ethanol	30	30 or 10	15
Erythromycin (Ery)	100 % (v/v) ethanol	5	5	-
Kanamycin (Kan)	H <sub>2</sub> O	50	50	-
Lincomycin (Lin)	50 % (v/v) ethanol	25	25	-
Neomycin (Neo)	H <sub>2</sub> O	50	50	-
Spectinomycin (Spec)	H <sub>2</sub> O	100	-	100
Tetracycline (Tet)	100 % (v/v) ethanol	5	5	-

**Table 2.1 Antibiotic stock solutions and concentrations**

## 2.3 Bacterial strains and plasmids

### 2.3.1 *S. aureus* strains

The bacteria used in this study were obtained from glycerol stocks and were grown on agar plates. The *S. aureus* strains used in this study (Table 2.2) were grown on BHI or TSA plates (Sigma) from  $-80^{\circ}\text{C}$  Microbank (Pro-lab Diagnostics) stocks. The plates contained antibiotics to maintain resistance markers. For short-term storage, the plates were kept at  $4^{\circ}\text{C}$ . A single colony was stored in Microbank beads at  $-80^{\circ}\text{C}$  for long-term storage.

For bacterial growth in liquid media, the strains were grown aerobically at  $37^{\circ}\text{C}$ . In addition, strains containing temperature-sensitive plasmids were grown at  $25-30^{\circ}\text{C}$ . A single colony was used to inoculate 5 ml of media in a sterile 25 ml universal tube. The culture was grown overnight at  $37^{\circ}\text{C}$  on a rotary shaker at 250 rpm. This culture was then used to inoculate fresh media in a sterile conical flask to an  $\text{OD}_{600}$  of 0.05. The strains were then grown to exponential phase at  $37^{\circ}\text{C}$  on a rotary shaker at 250 rpm.

Strain	Relevant genotype/Markers	Source
RN4220	Restriction deficient transformation recipient	Kreiswirth <i>et al.</i> , 1983
SH1000	Functional <i>rsbU</i> <sup>+</sup> derivative of 8325-4	Horsburgh <i>et al.</i> , 2002
CYL316	RN4220/pYL112Δ19, a plasmid carrying the L45a integrase gene, Cat <sup>R</sup>	Lee <i>et al.</i> , 1991
SJF2978	SH1000 <i>spa::kan</i> , Kan <sup>R</sup>	A gift from G. Buist
SJF3830	Newman <i>spa</i> <sup>-</sup> <i>sbi</i> <sup>-</sup> , Kan <sup>R</sup> , Ery <sup>R</sup>	Lab stock
SJF3189	SH1000 pGL485, Cat <sup>R</sup>	X. Ma, unpublished
AFK1	SH1000 <i>divIC-GFP</i> , Ery <sup>R</sup>	This study
AFK2	SH1000 <i>spa::kan divIC-GFP</i> , Ery <sup>R</sup> , Kan <sup>R</sup>	This study
AFK3	SH1000 pAFK4, Ery <sup>R</sup>	This study
AFK4	SH1000 <i>spa::kan</i> pAFK4, Ery <sup>R</sup> , Kan <sup>R</sup>	This study
AFK5	SH1000 <i>divIC-GFP</i> pGL485, Ery <sup>R</sup> , Cat <sup>R</sup>	This study
AFK6	SH1000 <i>spa::kan divIC-GFP</i> pGL485, Ery <sup>R</sup> , Kan <sup>R</sup> , Cat <sup>R</sup>	This study
AFK7	SH1000 pAFK14 <i>geh::Pspac-divIC</i> , Cat <sup>R</sup> , Tet <sup>R</sup>	This study
AFK8	SH1000 pAFK15 <i>geh::Pspac-ftsL</i> , Cat <sup>R</sup> , Tet <sup>R</sup>	This study
AFK9	RN4220 pAFK4, Ery <sup>R</sup>	This study
AFK10	RN4220 pAFK5, Ery <sup>R</sup>	This study
AFK11	SH1000 pAFK5, Ery <sup>R</sup>	This study
AFK12	SH1000 <i>spa::kan</i> pAFK5, Ery <sup>R</sup> , Kan <sup>R</sup>	This study
AFK13	RN4220 pAFK14, Cat <sup>R</sup>	This study
AFK14	RN4220 pAFK15, Cat <sup>R</sup>	This study
AFK15	SH1000 pAFK14, Cat <sup>R</sup>	This study
AFK16	SH1000 pAFK15, Cat <sup>R</sup>	This study

AFK17	RN4220 pCL112Δ19 <i>geh::pAFK16</i> , Tet <sup>R</sup>	This study
AFK18	RN4220 pCL112Δ19 <i>geh::pAFK17</i> , Tet <sup>R</sup>	This study
AFK19	SH1000 <i>geh::pAFK16</i> , Tet <sup>R</sup>	This study
AFK20	SH1000 <i>geh::pAFK17</i> , Tet <sup>R</sup>	This study
AFK21	SH1000 pAFK14 SCO, Cat <sup>R</sup>	This study
AFK22	SH1000 pAFK15 SCO, Cat <sup>R</sup>	This study

**Table 2.2 *S. aureus* strains used in this study**

Cat<sup>R</sup>, chloramphenicol resistant; Ery<sup>R</sup>, erythromycin resistant; Kan<sup>R</sup>, kanamycin resistant; Tet<sup>R</sup>, tetracycline resistant, SCO, single crossover.

### 2.3.2 *E. coli* strains

The *E. coli* strains used in this study (Table 2.3) were grown aerobically at 37°C. Standard growth and storage conditions were the same as for *S. aureus* strains (Section 2.3.1) except that LB agar or broth was used as the growth media.

Strain	Relevant genotype/Markers	Source
TOP10	F- <i>mcr</i> Δ ( <i>mrr-hsdRMS-mcrBC</i> ) ϕ 80 <i>lacZ</i> Δ <i>M15</i> Δ <i>lacX74</i> <i>recA1</i> <i>deo</i> <i>araD139</i> Δ( <i>ara-leu</i> ) 7697 <i>galK</i> <i>rpsL</i> (Str <sup>R</sup> ) <i>endA1</i> <i>nupG</i>	Invitrogen
BL21 (DE3)	F <sup>-</sup> <i>ompT</i> <i>hsdS<sub>B</sub></i> ( <i>r<sub>B</sub><sup>-</sup></i> <i>m<sub>B</sub><sup>-</sup></i> ) <i>gal</i> <i>dcm</i> <i>lacY1</i> (DE3)	Novagen

**Table 2.3 *E. coli* strains used in this study**

### 2.3.3 *B. subtilis* strains

The *B. subtilis* strain used in this study (Table 2.4) was grown at 37°C. Standard growth and storage conditions were the same as for *S. aureus* strains (Section 2.3.1) except that NB agar or broth was used as the growth media.

Strain	Relevant genotype/Markers	Source
168 HR	<i>trpC2</i>	Kindly provided by H. Rogers

**Table 2.4 *B. subtilis* strain used in this study**

### 2.3.4 Plasmids:

The plasmids used in this study are listed in Table 2.5. All plasmid DNA was purified using QIAGEN kits as described in the manufacturer's instructions (Section 2.8.2 and Section 2.8.3) and was stored in dH<sub>2</sub>O or elution buffer at -20°C.

Plasmid	Relevant genotype/Markers	Source
pET-21d	His <sub>6</sub> -tag overexpression vector; Amp <sup>R</sup>	Novagen
pMUTIN-GFP+	Insertion vector carrying Spac promoter and <i>GFP+</i> gene; Amp <sup>R</sup> ( <i>E. coli</i> ), Ery <sup>R</sup> ( <i>S. aureus</i> )	Kaltwasser <i>et al.</i> , 2002
pGL485	Cat <sup>R</sup> derivative of <i>E. coli-S. aureus</i> shuttle vector pMJ8426, containing <i>E. coli lacI</i> gene under the control of a constitutive promoter; Spec <sup>R</sup> ( <i>E. coli</i> ), Cat <sup>R</sup> ( <i>S. aureus</i> )	J. Garcia-Lara, unpublished
pLOW	<i>E. coli-S. aureus</i> shuttle vector carrying the Spac promoter. Low copy number plasmid; Amp <sup>R</sup> ( <i>E. coli</i> ), Ery <sup>R</sup> ( <i>S. aureus</i> )	Liew <i>et al.</i> , 2010
pCR <sup>TM</sup> 2.1-TOPO <sup>®</sup>	Linear vector for TA cloning, covalently bound to topoisomerase I; Amp <sup>R</sup> , Kan <sup>R</sup>	Invitrogen
pMAD	Low copy number shuttle vector containing temperature-sensitive replication origin in <i>S. aureus</i> and <i>bgaB</i> gene constitutively expressing thermostable β-galactosidase; Ery <sup>R</sup> ( <i>S. aureus</i> ), Amp <sup>R</sup> ( <i>E. coli</i> )	Arnaud <i>et al.</i> , 2004
pIMAY	Shuttle vector with a temperature-sensitive origin of replication in <i>S. aureus</i> and carrying an inducible <i>secY</i> antisense RNA; Cat <sup>R</sup>	Monk <i>et al.</i> , 2012
pCL84	Vector for integration into <i>S. aureus</i> lipase gene ( <i>geh</i> ), <i>attP</i> ; Tet <sup>R</sup> ( <i>S. aureus</i> ), Spec <sup>R</sup> ( <i>E. coli</i> )	Lee <i>et al.</i> , 1991
pAISH1	Tet <sup>R</sup> derivative of pMUTIN4; Tet <sup>R</sup> ( <i>S. aureus</i> ), Amp <sup>R</sup> ( <i>E. coli</i> )	Aish, 2003
pKASBAR	Hybrid vector of pCL84 and pUC18 for integration into <i>S. aureus</i> lipase gene ( <i>geh</i> ), <i>attP</i> ; Tet <sup>R</sup> ( <i>S. aureus</i> ), Spec <sup>R</sup> ( <i>E. coli</i> )	K. Wacnik and B. Salamaga, unpublished
pGM073	pKASBAR derivative with improved MCS containing <i>ezrA-psmOrange</i> ; <i>attP</i> , Tet <sup>R</sup> ( <i>S. aureus</i> ), Amp <sup>R</sup> ( <i>E. coli</i> )	G. McVicker, unpublished
pGL617	pMUTIN-GFP+ containing <i>S. aureus divIC</i> ; Ery <sup>R</sup> ( <i>S. aureus</i> ), Amp <sup>R</sup> ( <i>E. coli</i> )	J. Garcia-Lara, unpublished
pGL618	pMUTIN-GFP+ containing <i>S. aureus ftsL</i> ; Ery <sup>R</sup> ( <i>S. aureus</i> ), Amp <sup>R</sup> ( <i>E. coli</i> )	J. Garcia-Lara, unpublished
pALB26	pET-21d containing a 251 bp fragment of <i>S. aureus divIC</i> corresponding to nucleotides 143-393; Amp <sup>R</sup>	Kabli, 2009
pAFK18	pET-21d containing a 251 bp fragment of <i>S. aureus divIC</i> corresponding to nucleotides 143-393; with a point mutation in nucleotides 300 (C to G) and 301 (G to C); Amp <sup>R</sup>	This study
pAFK19	pET-21d containing a 251 bp fragment of <i>S. aureus divIC</i> corresponding to nucleotides 143-393; with a point mutation in nucleotide 273 (G to A); Amp <sup>R</sup>	This study
pAFK20	pET-21d containing a 251 bp fragment of <i>S. aureus divIC</i> corresponding to nucleotides 143-393; with a point mutation in nucleotides 310 (T to G) and 311(A to C); Amp <sup>R</sup>	This study
pALB27	pET-21d containing a 230 bp fragment of <i>S. aureus ftsL</i> corresponding to nucleotides 173-402; Amp <sup>R</sup>	Kabli, 2009

pAFK1	pET-21d containing a 224 bp fragment of <i>B. subtilis divIC</i> corresponding to nucleotides 152-375; Amp <sup>R</sup>	This study
pAFK2	pET-21d containing a 210 bp fragment of <i>B. subtilis ftsL</i> corresponding to nucleotides 142-351; Amp <sup>R</sup>	This study
pAFK3	pET-21d containing a 212 bp fragment of <i>S. aureus divIC</i> corresponding to nucleotides 143-354; Amp <sup>R</sup>	This study
pAFK4	pLOW carrying a 420 bp fragment containing RBS and coding region of <i>S. aureus divIC</i> ; Amp <sup>R</sup>	This study
pAFK5	pLOW carrying a 430 bp fragment containing RBS and coding region of <i>S. aureus ftsL</i> ; Amp <sup>R</sup>	This study
pAFK7	pCL84 carrying the Spac promoter; Tet <sup>R</sup> ( <i>S. aureus</i> ), Spec <sup>R</sup> ( <i>E. coli</i> )	This study
pAFK8	pMAD containing a 0.99 Kb fragment of <i>S. aureus divIC</i> upstream region fused in frame to 1 Kb fragment of <i>S. aureus divIC</i> downstream region; Amp <sup>R</sup> ( <i>E. coli</i> ), Ery <sup>R</sup> ( <i>S. aureus</i> )	This study
pAFK9	pMAD containing a 1 Kb fragment of <i>S. aureus ftsL</i> upstream region fused in frame to 1.1 Kb fragment of <i>S. aureus ftsL</i> downstream region; Amp <sup>R</sup> ( <i>E. coli</i> ), Ery <sup>R</sup> ( <i>S. aureus</i> )	This study
pAFK10	pAFK7 carrying a 408 bp fragment containing RBS and 5' region of <i>S. aureus divIC</i> ; Amp <sup>R</sup> ( <i>E. coli</i> ), Tet <sup>R</sup> ( <i>S. aureus</i> )	This study
pAFK11	pAFK7 carrying a 418 bp fragment containing RBS and 5' region of <i>S. aureus ftsL</i> ; Amp <sup>R</sup> ( <i>E. coli</i> ), Tet <sup>R</sup> ( <i>S. aureus</i> )	This study
pAFK12	pAISH1 carrying a 408 bp fragment containing RBS and 5' region of <i>S. aureus divIC</i> ; Amp <sup>R</sup> ( <i>E. coli</i> ), Tet <sup>R</sup> ( <i>S. aureus</i> )	This study
pAFK13	pAISH1 carrying a 418 bp fragment containing RBS and 5' region of <i>S. aureus ftsL</i> ; Amp <sup>R</sup> ( <i>E. coli</i> ), Tet <sup>R</sup> ( <i>S. aureus</i> )	This study
pAFK14	pIMAY containing a 0.99 Kb fragment of <i>S. aureus divIC</i> upstream region fused in frame to 1 Kb fragment of <i>S. aureus divIC</i> downstream region; Cat <sup>R</sup>	This study
pAFK15	pIMAY containing a 1 Kb fragment of <i>S. aureus ftsL</i> upstream region fused in frame to 1.1 Kb fragment of <i>S. aureus ftsL</i> downstream region; Cat <sup>R</sup>	This study
pAFK16	pAFK22 carrying Spac promoter and a 408 bp fragment containing RBS and 5' region of <i>S. aureus divIC</i> ; Amp <sup>R</sup> ( <i>E. coli</i> ), Tet <sup>R</sup> ( <i>S. aureus</i> )	This study
pAFK17	pAFK22 carrying Spac promoter and a 418 bp fragment containing RBS and 5' region of <i>S. aureus divIC</i> ; Amp <sup>R</sup> ( <i>E. coli</i> ), Tet <sup>R</sup> ( <i>S. aureus</i> )	This study
pAFK22	pGM073 derivative; attP, Tet <sup>R</sup> ( <i>S. aureus</i> ), Amp <sup>R</sup> ( <i>E. coli</i> )	This study

**Table 2.5 Plasmids used in this study**

Amp<sup>R</sup>, ampicillin; Cat<sup>R</sup>, chloramphenicol resistant; Ery<sup>R</sup>, erythromycin resistant; Kan<sup>R</sup>, kanamycin resistant; Spec<sup>R</sup>, spectinomycin resistant; Tet<sup>R</sup>, tetracycline resistant. The nucleotide numbers correspond to *S. aureus* strain NCTC 8325-4 and *B. subtilis* strain 168.



## 2.4 Buffers and stock solutions

All buffers and solutions were prepared using dH<sub>2</sub>O, sterilised if required and stored at room temperature or at 4°C. Unless otherwise mentioned, all the methods in this Chapter can be found in Sambrook and Russell (2001).

### 2.4.1 Phage buffer

MgSO <sub>4</sub>	1 mM
CaCl <sub>2</sub>	4 mM
Tris-HCl pH 7.8	50 mM
NaCl	0.6 % (w/v)
Gelatin	0.1 % (w/v)

### 2.4.2 Phosphate buffered saline (PBS)

NaCl	8 g l <sup>-1</sup>
Na <sub>2</sub> HPO <sub>4</sub>	1.4 g l <sup>-1</sup>
KCl	0.2 g l <sup>-1</sup>
KH <sub>2</sub> PO <sub>4</sub>	0.2 g l <sup>-1</sup>

The pH was adjusted to 7.4 using NaOH.

### 2.4.3 TAE (50x)

Trisma base	242 g l <sup>-1</sup>
Glacial acetic acid	0.57 % (v/v)
Na <sub>2</sub> EDTA pH 8.0	0.05 M

The buffer was diluted to 1:50 with dH<sub>2</sub>O before use.

#### **2.4.4 Tris buffered saline (TBS)**

Tris-HCL pH7.5	50 mM
NaCl	100 mM

#### **2.4.5 QIAGEN buffers**

##### **2.4.5.1 QIAGEN Buffer P1**

Tris-HCl pH 8	50 mM
EDTA	10 mM
RNase A	100 $\mu\text{g ml}^{-1}$

##### **2.4.5.2 QIAGEN Buffer P2**

NaOH	200 mM
SDS	1 % (w/v)

##### **2.4.5.3 QIAGEN Buffer P3**

Potassium acetate pH 5.5	3.0 M
--------------------------	-------

##### **2.4.5.4 QIAGEN Buffer EB**

Tris-HCl pH 8.5	10 mM
-----------------	-------

##### **2.4.5.5 QIAGEN Buffer N3, QG,PB and PE**

Supplied in the QIAquick kit; details not provided.

## 2.4.6 HiTrap purification buffers

### 2.4.6.1 0.1M Sodium PO<sub>4</sub> Buffer

1M Na <sub>2</sub> HPO <sub>4</sub>	31.6 ml
1M NaH <sub>2</sub> PO <sub>4</sub>	68.4 ml
dH <sub>2</sub> O	900 ml

The pH of the buffer was adjusted to 7.2, and the buffer was autoclaved at 121°C for 20 min at 15 pounds per square inch.

### 2.4.6.2 START buffer

NaPO <sub>4</sub>	0.1 M
NaCl	0.5 M
sdH <sub>2</sub> O	up to 1L
(+/-) Urea	8 M

### 2.4.6.3 Elution buffer

START buffer containing:

Imidazole	0.5 M
(+/-) Urea	8 M

## 2.4.7 SDS-PAGE solutions

### 2.4.7.1 SDS-PAGE reservoir buffer (10x)

Glycine	144 g l <sup>-1</sup>
Tris base	30.3 g l <sup>-1</sup>
SDS	10 g l <sup>-1</sup>

The buffer was diluted to 1:10 with dH<sub>2</sub>O before use.

#### **2.4.7.2 SDS-PAGE loading buffer (2x)**

Tris-HCl pH 6.8	0.62 M
SDS	10 % (w/v)
Glycerol	20 % (v/v)
Bromophenol blue	0.1 % (w/v)

Fresh 10 % (v/v) β-mercaptoethanol was added to the buffer just before use.

#### **2.4.7.3 Coomassie Blue stain**

Coomassie blue	0.1 % (w/v)
Methanol	5 % (v/v)
Glacial acetic acid	10 % (v/v)

#### **2.4.7.4 Coomassie destain**

Methanol	5 % (v/v)
Glacial acetic acid	10 % (v/v)

#### **2.4.7.5 Renaturing gel solution**

Triton X-100	0.1 % (v/v)
MgCl <sub>2</sub>	10 mM
Tris-HCl (pH 7.5) / Sodium citrate (pH 5)	25 mM

To bring the solution to the desired volume, dH<sub>2</sub>O was used.

#### **2.4.7.6 Renaturing gel stain (10x)**

Methylene Blue	4 g
2 M (+/-) KOH	3.58 ml
dH <sub>2</sub> O	up to 400 ml

The buffer was diluted to 1:50 with dH<sub>2</sub>O before use.

#### **2.4.8 Western blotting buffers**

##### **2.4.8.1 Blotting buffer**

Trisma base	2.4 g l <sup>-1</sup>
Glycine	11.26 g l <sup>-1</sup>
Methanol	20 % (v/v)

The buffer was chilled to 4°C before use.

##### **2.4.8.2 TBST (20x)**

Trisma base	48.4 g l <sup>-1</sup>
NaCl	20 g l <sup>-1</sup>
Tween-20	2 % (v/v)

The pH was adjusted to 7.6 and the buffer was diluted 1:20 with dH<sub>2</sub>O before use.

##### **2.4.8.3 Blocking buffer**

Dried skimmed milk powder (Oxoid)	5 % (w/v)
-----------------------------------	-----------

Dissolved in 1xTBST

#### 2.4.8.4 Alkaline Phosphatase buffer

Tris-HCl pH 9.5	0.1 M
NaCl	5.8 g l <sup>-1</sup>
MgCl <sub>2</sub> .6H <sub>2</sub> O	10.2 g l <sup>-1</sup>

#### 2.4.9 GTE

Glucose	50 mM
EDTA	10 mM
Tris-HCl pH7.5	20 mM

#### 2.4.10 TBSI

Tris-HCl pH7.5	50 mM
NaCl	0.1 M
Protease inhibitor cocktail (Roche)	1 tablet

### 2.5 Enzymes and chemicals

All the enzymes and chemical used in this study were of analytical grade and purchased from Thermo-Fisher Scientific, Roche or Sigma unless otherwise stated. All restriction enzymes, T4 ligase, DNase, dNTPs and appropriate buffers for DNA manipulation were purchased from New England Biolabs, Promega, Fermentas, Roche or Thermo-Fisher Scientific. Storage conditions and concentrations of stock solutions are listed in Table 2.6

Stock solution	Storage	Concentration	Dissolved in
Lysostaphin	-20°C	5 mg ml <sup>-1</sup>	20mM sodium acetate
Lysozyme	-20°C	10 mg ml <sup>-1</sup>	dH <sub>2</sub> O

Mutanolysin	-20°C	0.5 mg ml <sup>-1</sup>	dH <sub>2</sub> O
Isopropyl β-D-1-thiogalactopyranoside (IPTG)	-20°C	1 M	dH <sub>2</sub> O
5-bromo-4-chloro-3-indolyl-β-D-galactopyranoside (X-Gal)	-20°C, wrapped in foil	40 mg ml <sup>-1</sup>	DMSO
α-Chymotrypsin	-20°C	100 μg ml <sup>-1</sup>	50 mM Sodium phosphate
Formaldehyde	4°C, short term	16 % (w/v)	PBS at 60°C
Glutaraldehyde	-20°C	25 % (w/v)	dH <sub>2</sub> O

**Table 2.6 Stock solutions and concentrations**

## 2.6 Centrifugation

The following centrifuges were used for harvesting cells or precipitated material.

- i. Eppendorf microfuge 5415D; max volume of 2 ml, max speed of 13,200 rpm (10,000 x g).
  - ii. Sigma centrifuge 4K15C; max volume of 50 ml, max speed of 5,100 rpm (5525 x g).
  - iii. Jouan centrifuge JAC50.10; max volume of 50 ml, max speed of 13,000 rpm (10,000 x g).
  - iv. Avanti™ J25I (Beckman); max volumes and speeds depend on the rotor.
    - JA-20; max volume of 50 ml, max speed of 20,000 rpm (48,384 x g).
    - JA-10.5; max volume of 500 ml, max speed of 10,000 rpm (18,480 x g).
  - v. Beckman Ultracentrifuge Optima LE-80k; maximum volumes and speeds depend on the rotor.
    - 70.1Ti: max volume of 12 ml, max speed of 70,000 rpm (450,000 x g).
- Centrifugation was carried out at room temperature unless otherwise noted.

## 2.7 Determining bacterial cell density

### 2.7.1 Spectrophotometric measurement (OD<sub>600</sub>)

To quantify bacterial yield, spectrophotometric measurements at 600 nm (OD<sub>600</sub>) were carried out using either a Jenway 6100 spectrophotometer or a Biochrom WPA Biowave

DNA spectrophotometer. Culture samples were diluted 1:10 in sterile culture medium when necessary.

## **2.8 DNA purification techniques**

### **2.8.1 Genomic DNA extraction**

*S. aureus* and *B. subtilis* DNA was purified using a DNeasy blood and tissue kit (QIAGEN). First, 1 ml was taken from a 5 ml overnight culture and centrifuged for 10 min at 14,000 rpm. The pellet was washed with 1 ml sdH<sub>2</sub>O and re-centrifuged. The cell pellet was re-suspended in 180 µl sdH<sub>2</sub>O. Then, 10 µg of lysostaphin was added to *S. aureus* cells and 20 µg of lysozyme was added to *B. subtilis* cells and the samples were incubated at 37°C for 1 h. The protocol described in the manual was then followed, and the sample was stored at -20°C.

### **2.8.2 Small scale plasmid purification**

Small-scale plasmid purification from *E. coli* or *S. aureus* was accomplished using the QIAGEN QIAprep<sup>TM</sup> Spin column kit. Cells from a 5 ml overnight culture of *E. coli* or *S. aureus* were centrifuged at 4°C and 5,100 rpm for 10 min and the pellet was re-suspended in 250 µl of buffer P1 containing RNase A (100 µg ml<sup>-1</sup>). For *S. aureus* plasmid isolation, 5 µl of 5 mg ml<sup>-1</sup> lysostaphin was added and the sample was incubated for 30 min to 1 h at 37°C on a rotary shaker. Then, 250 µl of buffer P2 was added to lyse the cells and the sample was mixed by inverting the tube 4-6 times. Cell lysis was stopped by adding 350 µl of neutralising buffer N3 and the tube was immediately mixed as before. The mixture was then centrifuged at RT at 13,000 rpm for 10 min to remove cell debris. The supernatant was transferred to a QIAprep spin column and centrifuged for 1 min at RT at 13,000 rpm, and the flow-through was discarded. Then, 500 µl of buffer PB was added to wash the column and re-centrifuged. The flow-through was discarded; 750 µl of buffer PE was added, and the column was re-centrifuged. The flow-through was discarded, and the column was centrifuged for an additional 1 min to remove residual buffer. The column was then placed into a clean microcentrifuge tube. Then, 50 µl of buffer EB was added to the column centre to elute the DNA and the column was incubated for 1 min. The sample was then centrifuged as before and then stored at -20°C.



### 2.8.3 Large scale plasmid purification

Large-scale plasmid purification from *E. coli* or *S. aureus* was accomplished using the QIAGEN QIAprep™ Midiprep kit. Cells from a 100 ml overnight culture of *E. coli* or *S. aureus* were harvested by centrifugation at 4°C at 5,100 rpm for 10 min. The pellet was re-suspended in 25 ml PBS and centrifuged as before. The pellet was re-suspended in 4 ml of buffer P1 with RNase A (100µg ml<sup>-1</sup>), and the sample was vortexed. For *S. aureus* plasmid isolation, 15 µl of 5 mg ml<sup>-1</sup> lysostaphin was added and the sample was incubated for 30 min to 1 h at 37°C on a rotary shaker. Then, 4 ml of buffer P2 was added to lyse the cells and the sample was mixed gently by inverting the tube 4-6 times. Cell lysis was stopped by adding 4 ml of chilled buffer P3, and the tube was immediately mixed as before. The sample was incubated on ice for 15 min. Cell debris was then removed by centrifugation at 4°C at 9,500 rpm for 30 min. The supernatant was transferred into a pre-equilibrated QIAGEN tip 100 with 4 ml QBT buffer. The QIAGEN tip was washed twice with 10 ml QC buffer, and the DNA was eluted with 5 ml QF buffer. Then, 3.5 ml isopropanol was added to precipitate the plasmid DNA and the sample was mixed and centrifuged immediately at 4°C at 9,500 rpm for 30 min. The supernatant was cautiously discarded, and the DNA pellet was washed with 5 ml 70 % (v/v) ethanol and re-centrifuged. The supernatant was cautiously discarded, and the plasmid DNA pellet was air dried, dissolved in 200 µl sterile dH<sub>2</sub>O and stored at -20°C.

### 2.8.4 Gel extraction of DNA

DNA was separated using a 1% (w/v) TAE agarose gel, which was then stained with ethidium bromide and the DNA was visualised by a UV transilluminator. The DNA fragment of interest was excised from the agarose gel using a clean and sharp scalpel blade. The DNA was then isolated using the QIAquick gel extraction kit (QIAGEN). The gel slice was placed in a universal tube and weighed, and 3 volumes of Buffer QG were added to 1 volume of the gel. The mixture was incubated at 50°C until the gel was completely dissolved. Then, 1 gel volume of isopropanol was added to the sample to enhance the purification of small DNA molecules. The mixture was then transferred to a QIAquick spin column to bind the DNA and was centrifuged at 13,000 rpm for 1 min. The flow-through was discarded, and 500 µl of Buffer QG was added and centrifuged at 13,000 rpm for 1 min to remove any remaining agarose. Next, 750 µl of

Buffer PE was added to the QIAquick column and the column was centrifuged at 13,000 rpm for 1 min. The flow-through was discarded, and the column was centrifuged for an additional 1 min to eliminate any residual ethanol. The QIAquick spin column was transferred to a microcentrifuge tube and the DNA was eluted by adding 50 µl of Buffer EB by centrifugation at 13,000 rpm for 1 min. To verify the presence of the desired DNA in the flow-through, 2-5 µl was separated on a 1 % (w/v) agarose gel and viewed under UV transillumination. The sample was then stored at  $-20^{\circ}\text{C}$ .

### **2.8.5 PCR purification**

A QIAquick PCR purification kit (QIAGEN) was used to purify the DNA fragment from the PCR and enzymatic reactions. First, 5 volumes of buffer PB were added to 1 volume of the PCR sample. The sample mixture was placed into a QIAquick spin column and centrifuged at 13,000 rpm for 1 min, and the flow-through was discarded. The sample was washed with 750 µl of buffer PE, re-centrifuged and transferred to a microcentrifuge tube. Then, 50 µl of buffer EB was added to the column to elute the DNA by centrifugation. Finally, 2-5 µl of the DNA sample was separated on a 1 % (w/v) agarose gel, viewed by UV transillumination and stored at  $-20^{\circ}\text{C}$ .

### **2.8.6 Ethanol precipitation of DNA**

To improve the efficacy of transformation into *E. coli* after DNA ligation, 0.1 volume of 3 M sodium acetate, pH 5.2, and 2.5 volumes of 100 % (v/v) ethanol were added to the DNA mixture and transferred to an eppendorf tube. Next, 0.05 volumes of glycogen (Roche,  $20\text{ mg ml}^{-1}$ ) was added to aid in visualising the DNA pellet. The sample mixture was incubated overnight at  $-20^{\circ}\text{C}$ . The precipitated DNA sample was recovered by centrifugation at 13,000 rpm at  $4^{\circ}\text{C}$  for 20 min. The pellet was washed with 70 % (v/v) ethanol twice by centrifugation as described above. The supernatant was discarded, and the pellet was air dried for 5 min next to a flame. The pellet was then re-suspended in the desired volume of  $\text{sdH}_2\text{O}$ .

## **2.9 *In vitro* DNA manipulation techniques**

### **2.9.1 Polymerase chain reaction (PCR) techniques**

#### **2.9.1.1 Primer design**

The primers used in this study (Table 2.7) for PCR amplification were designed as short oligonucleotides (20-40 nucleotides) that were built according to the DNA sequences of *S. aureus* 8325-4 or *B. subtilis* 168. Convenient restriction enzyme sites were included when necessary at the 5' ends of the primers to allow for cloning. When needed, 6 bases (T or A) were added to permit efficient digestion by the restriction enzymes at these sites. NetPrimer software ([www.premierbiosoft.com/netprimer](http://www.premierbiosoft.com/netprimer)) was used to design the primers. The software predicts the annealing temperature and potential dimerisation and cross-dimerisation sites. Mutagenic oligonucleotide primers (~55 nucleotides long) containing the required mutation were designed using the QuikChange® Primer Design Program ([www.stratagene.com/sdmdesigner/default.aspx](http://www.stratagene.com/sdmdesigner/default.aspx)). The primers were manufactured by Eurofins MWG operon (<http://www.eurofinsdna.com>) and stored at -20°C in sdH<sub>2</sub>O as 100 µM stock solutions or as 10 µM working solutions.

Primer	Sequence (5'-3')	Application	Source
ALB19	ATAAT <u>ACCATGGCT</u> AAAATGGATGCGTATGATCG	Amplification of the extracellular domain of <i>S. aureus ftsL</i> . Forward primer	Kabli, 2009
ALB20	ATAATA <u>CTCGAGAT</u> TTTTTGGCTTCGCCATTACT	Amplification of the extracellular domain of <i>S. aureus ftsL</i> . Reverse primer	Kabli, 2009
ALB21	ATAAT <u>ACCATGGCT</u> AAACATCGCAATGATATTGAT	Amplification of the extracellular domain of <i>S. aureus divIC</i> . Forward primer	Kabli, 2009
ALB22	ATAAT <u>TCTCGAGT</u> TTTTTTCGAAGATTTGAGCT	Amplification of the extracellular domain of <i>S. aureus divIC</i> . Reverse primer	Kabli, 2009
ALB23	TGTGAGCGGATAACAATCCCC	Sequencing of inserts in pET21-d. Forward primer	Bottomley, 2011
ALB24	TTCCTTTCGGGCTTTGTTAGCAG	Sequencing of inserts in pET21-d. Reverse primer	Bottomley, 2011
AK1	ATAAT <u>ACCATGGCT</u> TACATCTTCCCTTAGTGCAAAA	Amplification of the extracellular domain of <i>B. subtilis divIC</i> . Forward primer	This study
AK2	ATAATA <u>CTCGAGCT</u> TGCTCTTCTTCTCCACAT	Amplification of the extracellular domain of <i>B. subtilis divIC</i> . Reverse primer	This study
AK3	ATAAT <u>ACCATGGCT</u> TATGCGGCATATCAAACC	Amplification of extracellular domain of <i>B. subtilis ftsL</i> . Forward primer	This study
AK4	ATAAT <u>TACTCGAGT</u> TCCTGTATGTTTTTCACTTTTT	Amplification of extracellular domain of <i>B. subtilis ftsL</i> .	This study

		Reverse primer	
AK5	ATAAT <u>ACCATGGCT</u> AAACATCGCAATGATATTGAT	Amplification of extracellular domain of <i>S. aureus divIC</i> <sup>Δ118-30</sup> . Forward primer	This study
AK6	ATAATA <u>CTCGAGTGGCAACCT</u> AAAAATCACTT	Amplification of extracellular domain of <i>S. aureus divIC</i> <sup>Δ118-30</sup> . Reverse primer	This study
AK7	GAAGAAATTGCGTTAAAAGAAAAGTTGAATAATCTGAATAAC AAAGATTACATTGAAAAA	Mutagenic sense primer to create <i>S. aureus divIC</i> <sup>D92N</sup> , forward primer	This study
AK8	TTTTTCAATGTAATCTTTGTTATTCAGATTATTCAACTTTTCTTT AACGCAATTTCTTC	Mutagenic antisense primer to create <i>S. aureus divIC</i> <sup>D92N</sup> , Reverse primer	This study
AK9	CATTGAAAAAATTGCGCGTGATGATGCTTACTTAAGCAACAAA GGTGAAGTG	Mutagenic sense primer to create <i>S. aureus divIC</i> <sup>Y104A</sup> , forward primer	This study
AK10	CACTTCACCTTTGTTGCTTAAGTAAGCATCATCACGCGCAATTT TTCAATG	Mutagenic antisense primer to create <i>S. aureus divIC</i> <sup>Y104A</sup> . Reverse primer	This study
ALB43	GACAAAGATTACATTGAAAAAATTGCGGCTGATGATTACTT AAGCAACAAAGG	Mutagenic sense primer to create <i>S. aureus divIC</i> <sup>R101A</sup> Forward primer	Bottomley, unpublished
ALB44	CCTTTGTTGCTTAAGTAATAATCATCAGCCGCAATTTTTTCAATC TAATCTTTGTC	Mutagenic antisense primer to create <i>S. aureus divIC</i> <sup>R101A</sup> , Reverse primer	Bottomley, unpublished
AK11	ATAATAGGATCCAGGAGGTGACAAGCAAGCAATGAAAAAT	Amplification of <i>S. aureus</i> 5' <i>divIC</i> and RBS. Forward primer	This study

AK12	ATAATAG <u>AATCCT</u> TATTTTTTCGAAGATTTTGAGCTAGACG	Amplification of <i>S. aureus</i> 5' <i>divIC</i> and RBS. Reverse primer	This study
AK13	ATAATAG <u>GATCC</u> AGGAGGCAATTTATATGGCTGTAG	Amplification of <i>S. aureus</i> 5' <i>ftsL</i> and RBS. Forward primer	This study
AK14	ATAATAG <u>GATTCT</u> TAAATTTTTTGCTTCGCCATTACTACGCACT ACC	Amplification of <i>S. aureus</i> 5' <i>ftsL</i> and RBS. Reverse primer	This study
AK15	ATAATAG <u>GATCC</u> CTACATCTTCCCTTAGTGC	Amplification of extracellular domain of <i>B. subtilis divIC</i> . Forward primer	This study
AK16	ATAATAG <u>TCGAC</u> CTTGCTCTTCTTCTCCACATTG	Amplification of extracellular domain of <i>B. subtilis divIC</i> . Reverse primer	This study
AK17	GACCTGCAGGCATGCCTG	Sequencing of inserts in pLOW. Forward primer	This study
AK18	GTTTTCCAGTCACGACGTTG	Sequencing of inserts in pLOW. Reverse primer	This study
AK19	CCTCTGCTAAAATTCCTG	Sequencing of inserts in pMUTIN+GFP. Forward primer	This study
AK20	ACGGGAAAAGCATTGAACAC	Sequencing of inserts in pMUTIN+GFP. Reverse primer	This study
AK21	ATAATAG <u>GATCC</u> CTTTGATTACGCAAGTT	Amplification of region upstream of <i>S. aureus divIC</i> . Forward primer	This study
AK22	ATAATAG <u>CGGCC</u> CGCCTCCAATTTACGCTT	Amplification of region upstream of <i>S. aureus divIC</i> . Reverse primer	This study
AK23	ATAATAG <u>CGGCC</u> CGCAGGATTTATTTAACATAGTCAA	Amplification of region downstream of <i>S. aureus divIC</i> . Forward primer	This study

AK24	ATAATAG <u>AATTC</u> AATACGATACATAAATAGTT	Amplification of region downstream of <i>S. aureus divIC</i> . Forward primer	This study
AK25	ATAATAGGATCCCTTTTCGAAGATATTGCTG	Amplification of region upstream of <i>S. aureus ftsL</i> . Forward primer	This study
AK26	ATAATAGCGGCCGCATTGCTCCTATT	Amplification of region upstream of <i>S. aureus ftsL</i> . Reverse primer	This study
AK27	ATAATAGCGGCCGCAAGGTAGTGCCTAGTAATGGCGAAG	Amplification of region downstream of <i>S. aureus ftsL</i> . Forward primer	This study
AK28	ATAATAG <u>AATTC</u> CCATAATATCTCTATGTCCAG	Amplification of region downstream of <i>S. aureus ftsL</i> . Reverse primer	This study
AK29	ATAATAC <u>CCGGG</u> TGGAGGTGACAAGCAATGAAAAAT	Amplification of <i>S. aureus 5' divIC</i> and RBS. Forward primer	This study
AK30	ATAATAC <u>CCGGG</u> TATTTTTTCGAAGATTTTGAGC	Amplification of <i>S. aureus 5' divIC</i> and RBS. Reverse primer	This study
AK31	ATAATAC <u>CCGGG</u> TAAGGAGCAATTTATAATGGCTG	Amplification of <i>S. aureus 5' ftsL</i> and RBS. Forward primer	This study
AK32	ATAATAC <u>CCGGG</u> TAAATTTTTTGCTTCGCC	Amplification of <i>S. aureus 5' ftsL</i> and RBS. Reverse primer	This study
AK33	GTCTCCGACCATCAGGCACC	Sequencing of inserts in pCL84 Forward primer	This study
AK34	CAAGTTAATCCCATCCTTCTATG	Sequencing of inserts in pCL84 Reverse primer	This study
AK35	ATAATAGGTAC <u>CC</u> TTTGATTACGCAAG	Amplification of region upstream of <i>S. aureus divIC</i> . Forward primer	This study

AK36	ATAATAGAGCTCAATACGATACATAATAG	Amplification of region downstream of <i>S. aureus divIC</i> . Reverse primer	This study
AK37	ATAATAGAATTCCTTTCGAAGATATTGC	Amplification of region upstream of <i>S. aureus ftsL</i> . Forward primer	This study
AK38	ATAATAGACGTCCATAATATCTCTA	Amplification of region downstream of <i>S. aureus ftsL</i> . Reverse primer	This study
AK39	TTTTTTGGGCCCATCGTTAAGGGATCAAC	Amplification of P <sub>Spac</sub> region and MCS fragment. Forward primer	This study
AK40	TTTTTTGCGATCGCCACAGTAGTTCATCACCA	Amplification of P <sub>Spac</sub> region and MCS fragment. Reverse primer	This study
AK41	TAAGTTGGGTAACGCCAGG	Sequencing of inserts in pGM073. Forward primer	This study
AK42	AGGGCAAACGCTTGTGG	Sequencing of inserts in pGM073. Forward primer	This study
AK43	GATGGCTTCACACTGTTAGATG	Amplification of region outside the upstream of <i>S. aureus divIC</i> . Forward primer	This study
AK44	AAATCCTAGTTTATTACGTGTTGA	Amplification of region outside the downstream of <i>S. aureus divIC</i> . Reverse primer	This study
AK45	GGGATAGAGAACTTGGGAATGAT	Amplification of region outside the upstream of <i>S. aureus ftsL</i> . Forward primer	This study



AK46	GATTCACCCCAACCGAC	Amplification of region outside the downstream of <i>S. aureus fisL</i> . Reverse primer	This study
MCSFWD	TACATGTCAAGAATAAACTGCCAAAGC	Sequencing of inserts in pIMAY. Forward primer	Monk <i>et al.</i> , 2012
MCSREV	AATACCTGTGACGGAAGATCACTTCG	Sequencing of inserts in pIMAY. Reverse primer	Monk <i>et al.</i> , 2012
ALB128	TTTTTT <u>AGATCT</u> ATCGTTAAGGGATCAACTTT	Amplification of P <sub>Spac</sub> region and MCS fragment. Forward primer	Bottomley, unpublished
ALB127	TTTTTT <u>GGATCCC</u> CACAGTAGTTCATCACCA	Amplification of P <sub>Spac</sub> region and MCS fragment. Reverse primer	Bottomley, unpublished

**Table 2.7 Primers used in this study for DNA amplification by PCR.** The restriction sites are underlined.

### 2.9.1.2 PCR amplification

PCR amplification reactions were carried out using high-fidelity Extensor PCR ReddyMix™ (Thermo Scientific). A final working reaction volume of 25 µl contained the following:

DNA polymerase	1.25 U
MgCl <sub>2</sub>	2.25 mM
dNTPs	0.5 mM (each)
Precipitant and red dye for electrophoresis	

The following components were mixed together on ice in sterilised 0.2 ml thin-walled PCR tubes:

High-fidelity Extensor Master Mix (Thermo Scientific)	12.5µl
Forward primer	200 nM
Reverse primer	200 nM
Template DNA	100 ng

An appropriate volume of sdH<sub>2</sub>O was added to give a 1x concentration of PCR ReddyMix.

The amplification was achieved by using a TC-3000 (Techne) PCR machine. The lid was preheated to 105°C for 4 min, and the thermal cycling programme was as follows:

1 cycle	Initial denaturation	95°C	5 min
30 cycles	Denaturation	95°C	30 s
	Annealing	49-55°C	30 s – 1 min
	Extension	72°C	1 min per Kb (1 min minimum)
1 cycle	Final extension	72°C	5 min

The reaction products were stored at -20°C.

### **2.9.1.3 Colony PCR screening of *E. coli***

Primers and  $\text{sdH}_2\text{O}$  were added to PCR ReddyMix in 0.2 ml thin-walled PCR tubes as described in section 2.9.1.2 without the addition of template DNA. Using a sterile pipette tip, a single colony was patched onto an agar plate with or without antibiotics and then introduced into a PCR reaction tube. The PCR reaction was performed as described above.

### **2.9.1.4 Colony PCR screening of *S. aureus***

Primers and  $\text{sdH}_2\text{O}$  were added to PCR ReddyMix in 0.2 ml thin-walled PCR tubes as described in section 2.8.1.2 without the addition of template DNA. Using a sterile pipette tip, a single colony was streaked onto an agar plate with or without antibiotics and then introduced into a PCR reaction tube. An additional step was added to lyse the cells as follows:

37°C	15 min
99°C	20 min
4°C	1 min
99°C	2 min
4°C	1 min

The PCR reaction was performed as described above.

### **2.9.2 TOPO TA cloning**

According to the manufacturer's instructions, purified PCR products were cloned directly into pCR2.1-TOPO (Invitrogen). First, 0.5-4  $\mu\text{l}$  of fresh PCR product was added to 1  $\mu\text{l}$  of the dilute salt solution (supplied in the kit), and DNase free water was added to a final volume of 5  $\mu\text{l}$ . Then, 1  $\mu\text{l}$  of pCR2.1-TOPO vector was added to the mixture and the reaction was incubated at room temperature for 10 min. The reaction mixture was then used directly to transform electrocompetent *E. coli* cells.

## 2.9.3 QuickChange site-directed mutagenesis

### 2.9.3.1 Mutant strand synthesis reaction

The QuickChange II Site-Directed Mutagenesis kit (Stratagene) was used to create a site-specific mutation in a specific gene, using mutagenic primers containing the desired mutation (Section 2.9.1.1; Table 2.7). Purified plasmid containing the desired insert was used as template DNA. The following components were added, on ice, to a 0.2 ml thin-walled PCR tube:

10x reaction buffer	5 $\mu$ l
DNA	5-50 ng
Mutagenic forward primer	125 ng
Mutagenic reverse primer	125 ng
dNTP mix	1 $\mu$ l
sdH <sub>2</sub> O	up to 50 $\mu$ l
<i>PfuUltra</i> HF DNA polymerase (2.5U/ $\mu$ l)	1 $\mu$ l

The amplification was carried out using a TC-3000 (Techne) PCR machine. The lid was preheated to 95°C and the thermal cycling programme was as follows:

1 cycle	Initial denaturation	95°C	30 s
30 cycle	Denaturation	95°C	30 s
	Annealing	T <sub>m</sub> -5 °C	1 min
	Extension	68 °C	1 min/plasmid length (Kb)
1 cycle	Final extension	68 °C	5 min

Following amplification, the reactions were placed on ice for 2 min to cool the reactions down to  $\leq 37^\circ\text{C}$ . The amplification products were examined on a 1 % (w/v) agarose gel and stored at  $-20^\circ\text{C}$ .

### **2.9.3.2 Amplification products digestion**

To digest the parental dsDNA (non-mutated), 1  $\mu\text{l}$  of *Dpn* I restriction enzyme ( $10 \text{ U } \mu\text{l}^{-1}$ ) was added to the amplification reaction and mixed by pipetting up and down. The mixture was centrifuged for 1 min at room temperature at 13,000 rpm, and the reactions were incubated for 1 h at  $37^\circ\text{C}$ . Then, 1  $\mu\text{l}$  of the *Dpn* I digested sample was added to 50  $\mu\text{l}$  of electrocompetent cells, and the procedures described in Section 2.10.1.2 were followed.

### **2.9.4 Restriction endonuclease digestion**

Restriction enzymes were purchased from New England Biolabs or Promega. DNA digestion was carried out according to the manufacturer's instructions using the buffers supplied by the manufacturer. The reaction mixture was incubated at the appropriate temperature and time according to the enzyme used. If the digested products were to be used in a subsequent cloning reaction, then the restriction enzymes were inactivated at  $65^\circ\text{C}$  for 15 min and removed by using the QIAquick PCR purification kit (Section 2.8.5).

### **2.9.5 Phosphatase treatment of vector DNA**

Digested vector DNA was treated with calf intestinal alkaline phosphatase (CIP) to reduce self-ligation by removing the 5'  $\text{PO}_4$  from the DNA. According to the manufacturer's instructions, phosphatase and the provided buffer was directly added to the restriction endonuclease digestion of the vector. The reaction mixture was then incubated at  $37^\circ\text{C}$  for 1 h. Another 1  $\mu\text{l}$  phosphatase was added and the reaction mixture was incubated for an additional 30 min. The CIP phosphatase was removed by using the QIAquick PCR purification kit (Section 2.8.5), and the purified dephosphorylated vector was stored at  $-20^\circ\text{C}$ .

### **2.9.6 Ligation of DNA**

Insert and vector DNA were restriction digested by endonucleases. When required, 5' phosphate groups were removed from plasmid DNA by phosphatase treatment. Vector DNA and insert were ligated at different ratios and the ligations were performed in a 10  $\mu\text{l}$  volume with 1  $\mu\text{l}$  of 10x T4 DNA ligase buffer and 1  $\mu\text{l}$  of  $3 \text{ U } \mu\text{l}^{-1}$  T4 DNA ligase

(Promega). The reactions were incubated at room temperature for approximately 2 h or 16°C overnight. The ligation mixtures were purified by ethanol precipitation (Section 2.8.6) and were then used to transform electrocompetent cells. As a negative control, a ligation reaction mixture was prepared as described above, but without insert DNA.

### 2.9.7 Agarose gel electrophoresis

DNA samples were usually separated in 1% (w/v) agarose gels in 1x TAE buffer. To get a sharper resolution of smaller DNA fragments (<230bp), samples were separated in 1.5% (w/v) agarose gels in 1x TAE buffer. Horizontally submerged agarose gels were poured and run using various size horizontal electrophoresis tanks (Life Technologies, Scie-Plas). 5-15µl of ethidium bromide (10mg ml<sup>-1</sup>; BioRad or Sigma), dependent on the gel size was added to the molten gel to allow the DNA visualization.

DNA samples were mixed with one fifth their volume of 6 × DNA loading buffer (ThermoScientific) and then loaded into the wells of the agarose gel. Gels were run for 45 min to 2 h at 100 V at room temperature, DNA was viewed using an UV transilluminator at 260 nm and photographed using the UVi Tec Digital camera and UVi Doc Gel documentation system. The concentration and size of the DNA fragments were estimated by co-electrophoresing 5 µl of DNA ladder (ThermoScientific; Table 2.8).

Marker	DNA fragment size (bp)
1 Kb DNA ladder (ThermoScientific)	10,000
	8,000
	6,000
	5,000
	4,000
	3,000
	2,500
	2,000
	1,500
	1,000
	750
	500

	250
2-log DNA ladder (New England Biolabs)	10,000
	8,000
	6,000
	5,000
	4,000
	3,000
	2,000
	1,500
	1,200
	1,000
	900
	800
	700
	600
	500
	400
	300
200	
100	

**Table 2.8 DNA fragments used as size markers for agarose gel electrophoresis**

### **2.9.8 DNA sequencing**

Plasmids and PCR products used in this study were sequenced by the Core Genetics Service, University of Sheffield, using the primers listed in Table 2.7. Sequencing traces were analysed using Finch TV software (Geospiza).

## **2.10 Transformation techniques**

### **2.10.1 Transformation of *E. coli***

#### **2.10.1.1 Preparation of electrocompetent *E. coli* cells**

*E. coli* TOP10 or BL21 (DE3) was streaked for single colonies on LB agar plates and grown overnight at 37°C. A single colony was inoculated into 5 ml LB and incubated overnight at 37°C at 250 rpm. The overnight culture was used to inoculate 400 ml LB to

an OD<sub>600</sub> of 0.05 and was incubated at 37°C and 250 rpm until the OD<sub>600</sub> was between 0.5-0.7. The culture was immediately cooled on an ice-slurry for 15-20 min. The cells were harvested by centrifugation in 4x100 ml aliquots at 5,100 rpm, 4°C, for 10 min. The pellets were washed three times with 25 ml of ice-cold sterile dH<sub>2</sub>O and vortexed at the initial step only to re-suspend the pellets; they were then centrifuged at 5,100 rpm, 4°C, for 10 min. The supernatant was discarded, the 4 samples were mixed together into one tube, and 50% (v/v) ice-cold glycerol was added to the sample with a final concentration of 10% (v/v). The cells were divided into 50 µl aliquots, snap-frozen in liquid nitrogen and stored at – 80°C.

### **2.10.1.2 Electroporation of DNA into *E. coli* competent cells**

First, 50 µl aliquots of *E. coli* electrocompetent cells were thawed on ice and 5 to 10 µl (~1 ng) of plasmid DNA was added. The mixture was then transferred into a 1 mm pre-chilled (Bio-Rad) electroporation cuvette. Electroporation was performed using a Gene Pulser system set at 200 Ω, 1.75 kV and 25 µF. The cells were recovered immediately by the addition of 400 µl of ice-cold LB followed by growth for 60 min at 37°C and 250 rpm. Finally, 100 µl aliquots of the cells were spread on LB selective plates and incubated at 37°C overnight.

## **2.10.2 Transformation of *S. aureus***

### **2.10.2.1 Preparation of electrocompetent *S. aureus* RN4220 cells**

*S. aureus* RN4220 was streaked for single colonies on BHI agar plates and grown overnight at 37°C. A single colony was inoculated into 400 ml BHI and incubated for 10-12 h at 37°C, 250 rpm. This culture was used to inoculate 400 ml of pre-warmed, fresh BHI to an OD<sub>600</sub> of 0.1. The samples were incubated at 37°C, 250 rpm, for 60-90 min, until the OD<sub>600</sub> was between 0.4-0.6. The cells were harvested by centrifugation in 4x 100 ml aliquots at 5,100 rpm at room temperature for 10 min. The pellets were washed 3 times with 25 ml of ice-cold sdH<sub>2</sub>O by centrifugation at 5,100 rpm, 4°C, for 10 min. The supernatant was discarded, the 4 samples were mixed together into one tube, and 20 ml of 10% (v/v) glycerol was added to the sample. The samples were centrifuged at 5,100 rpm



at room temperature for 10 min. The cell pellets were then re-suspended in 10 ml of 10 % (v/v) glycerol, incubated for 30 min at room temperature and recovered by centrifugation at 5100 rpm at room temperature for 10 min. The pellets were re-suspended in 400 µl 10% (v/v) glycerol and then divided into 50 µl aliquots and used immediately for transformation.

### **2.10.2.2 Electroporation of DNA into *S. aureus* RN4220 competent cells**

Approximately 1 µg plasmid DNA was added to a 50 µl aliquot of *S. aureus* electrocompetent cells. The mixture was then transferred into 1 mm electroporation cuvettes (Bio-Rad). Electroporation was performed using a Gene Pulser system set at 100 Ω, 2.3 kV and 25 µF. The cells were recovered immediately by the addition of 1 ml of pre-warmed BHI followed by growth for 3 h at 37°C (unless otherwise stated) and 250 rpm. Finally, 150 - 200 µl aliquots of the cells were spread onto BHI selective plates and incubated at 37°C (unless otherwise stated) for 48 h.

### **2.10.3 Phage techniques**

#### **2.10.3.1 Bacteriophage**

The bacteriophage Φ11 (Mani *et al.*, 1993) was used for phage transduction of *S. aureus*. This phage is specific for *S. aureus*. It is a temperate-transducing phage of serological group B that requires Ca<sup>2+</sup> ions for infection maintenance and has an approximate genome size of 45 Kb (Novick, 1991).

#### **2.10.3.2 Preparation of phage lysate**

The donor *S. aureus* strain was grown at 37°C overnight in 5 ml BHI containing appropriate antibiotics. Using this overnight culture, cells were inoculated to an OD<sub>600</sub> of 0.2 in 5 ml BHI in a 50 ml conical flask. Then, 5 ml of phage buffer and 100 µl of stock phage lysate (Φ11) were added and the sample mixture was incubated at 30°C for 4-6 h on a rotary shaker at 30 rpm. Once cleared, the lysate was filter sterilised (0.2 µm pore size) and then stored at 4°C.

### **2.10.3.3 Determination of phage titre**

*S. aureus* SH1000 strain was grown in 5 ml BHI to an OD<sub>600</sub> of ~0.5 at 37°C, 250 rpm. The phage lysate was serially diluted in phage buffer, and 100 µl of diluted phage was then mixed with a 400 µl culture and 50 µl of 1 M CaCl<sub>2</sub>. The phage mixture was incubated at room temperature for 10 min without rotation, and then 5 ml of phage top agar was added to the mixture, overlaying a phage bottom agar plate. The plates were incubated 48 h at 37°C, and the number of plaques were counted. A successful lysate was in the range of 10<sup>-7</sup> – 10<sup>-10</sup> plaque forming units (pfu) per ml.

### **2.10.3.4 Phage transduction**

The recipient *S. aureus* strain was grown overnight in 50 ml LK and harvested by centrifugation at 5,100 rpm at room temperature for 10 min. The pellet was re-suspended in 1 ml LK. Then, 500 µl of recipient cells were mixed with 500 µl of phage lysate and 1 ml of LK containing 10 mM CaCl<sub>2</sub>. A control mixture that did not contain phage lysate was also prepared. The mixture was incubated at 37°C for 25 min without rotation followed by incubation for 15 min at 37°C, 250 rpm. Then, 1 ml of ice-cold 0.02 M sodium citrate was added to the mixture and placed on ice for 5 min before harvesting the cells at 5100 rpm for 10 min at room temperature. The pellet was re-suspended in 1 ml of 0.02 M sodium citrate and incubated on ice for 45 min to 1 h. Next, 150 µl and 100 µl aliquots were spread onto LK agar plates containing 0.05% (w/v) sodium citrate and incubated at 37°C for 2 h. The plates were overlaid with 5 ml of LK top agar containing a 6x normal concentration of selective antibiotic and incubated at 37°C for 24-72 h. To ensure that they possessed the correct resistance profile, colonies were picked and streaked onto BHI agar plates with appropriate antibiotics.

## **2.11 Protein analysis**

### **2.11.1 SDS-PAGE**

Resolving gels were prepared using the following components. Note that Ammonium persulphate (APS) and N,N,N',N'-tetramethyl-ethylenediamine (TEMED) were added

immediately before pouring the gel:

**15 % (w/v) resolving gel**

dH <sub>2</sub> O	2.4 ml
1.5 M Tris-HCl (pH8.8)	2.5 ml
10 % (w/v) SDS	100 µl
30 % (w/v) Acrylamide/Bis (37.5:1,BioRad)	5 ml
10 % (w/v) APS	100 µl
TEMED	20 µl

**11 % (w/v) resolving gel**

dH <sub>2</sub> O	3.5 ml
1.5 M Tris-HCl (pH8.8)	2.5 ml
10 % (w/v) SDS	100 µl
30 % (w/v) Acrylamide/Bis (37.5:1,BioRad)	4 ml
10 % (w/v) APS	100 µl
TEMED	20 µl

The components were placed in a 20 ml sterile universal tube, mixed gently to avoid air bubbles, and then loaded into the gel casting apparatus (Bio-Rad Mini-Protean II gel slabs). A layer of isopropanol was added on the top of the gel to isolate the gel from the air. Once the gel formed, the isopropanol was drained onto a tissue paper and the gel was washed with dH<sub>2</sub>O. A stacking gel was then made and applied on top as follows:

dH <sub>2</sub> O	2.5 ml
0.5 M Tris-HCl (pH 6.8)	0.62 ml
10 % (w/v) SDS	50 µl
30 % (w/v) Acrylamide/Bis (37.5:1BioRad)	0.83 µl
10 % (w/v) APS	50 µl
TEMED	5 µl

A Bio-Rad plastic comb was placed immediately into the gel to construct the wells and also to isolate the gel from the air. Once the gel solidified, it was transferred to a Protean II (BioRad) protein gel-running tank and submerged in 1x SDS-PAGE

reservoir buffer. The comb was removed, and 5-20  $\mu$ l samples were loaded onto the wells. In addition, 10  $\mu$ l of Dalton Mark VII- L (Sigma), Ultra-Low range (Sigma), Prestained ColorBurst™ (Sigma) or Color Marker Ultra-Low Range (Sigma) protein size markers (Table 2.9) were loaded. The proteins were then separated by electrophoresis at 150 V until the blue dye front of the sample buffer was at the base of the gel plate.

Marker	Protein or Band colour	Molecular Mass (kDa)
Dalton Mark VII-L (Sigma)	Bovine serum albumin	66.0
	Ovalbumin	45.0
	Glyceraldehyde-3-phosphate dehydrogenase	36.0
	Carbonic anhydrase	29.0
	Trypsinogen	24.0
	Soybean trypsin inhibitor	20.1
	$\alpha$ -Lactalbumin	14.5
Ultra-Low Range (Sigma)	Triose phosphate isomerase	26.6
	Myoglobin	17.0
	$\alpha$ -Lactalbumin	14.5
	Aprotinin	6.5
	Insulin chain B	3.496
	Bradykinin	1.06
Prestained ColorBurst™ (Sigma)	Violet	210.0
	Pink	90.0
	Blue	65.0
	Pink	40
	Orange	30
	Blue	20
	Pink	13
	Blue	8
Color Marker Ultra-Low Range (Sigma)	Triose phosphate isomerase	26.6
	Myoglobin	17.0
	$\alpha$ -Lactalbumin	14.5
	Aprotinin	6.5
	Insulin chain B	3.496
	Bradykinin	1.06

**Table 2.9 Protein size standards used in this study**

### **2.11.2 Coomassie staining**

When the electrophoresis was complete, the gel was placed in Coomassie Blue stain for approximately 30 min to visualise the proteins. The gel was de-stained in two volumes of Coomassie destain solution overnight or until the background was clear and then placed in water before being dried (Section 2.11.3). The molecular masses of the proteins were estimated by comparison to protein standards of known mass.

### **2.11.3 Gel drying**

The SDS gels were dried between two sheets of DryEase mini Cellophane (Invitrogen), which had been pre-soaked in Gel-Dry<sup>TM</sup> Drying solution (Invitrogen). A mini-gel drying frame and base (Novex) was used to hold the gel plus the drying sheets and were left at room temperature until completely dry. The renaturing gels were dried between two sheets of DryEase mini Cellophane (Invitrogen), which had been pre-soaked in 10% (v/v) glycerol using the same gel drying apparatus as above. The gels were photographed when they were dry.

### **2.11.4 Western blot**

Protein samples were separated by SDS-PAGE as previously described (Section 2.11.1). Immunoblot polyvinylidene difluoride (PVDF) membrane (BioRad) or Amersham<sup>TM</sup>Hybond<sup>TM</sup>-ECL membrane (GE Healthcare) was cut to the same size as the SDS-PAGE gel. The PVDF membrane was submerged briefly in 100% (v/v) methanol, rinsed in sdH<sub>2</sub>O and then equilibrated in blotting buffer for 10 min before use. The nitrocellulose membrane was wetted briefly in dH<sub>2</sub>O and then equilibrated in blotting buffer for 10 min before use. Proteins were transferred from the gel to the membrane by electroblotting in cold blotting buffer using a Mini Trans-Blot apparatus (BioRad) at 60 V for 60 min. The membrane was dried on blotting paper for 5 min and then blocked in blocking buffer for 1 h at room temperature or overnight at 4°C with gentle shaking. The blot was briefly rinsed twice with TBST and then washed with TBST for 15 min. The washing step was repeated twice at 5 min intervals. The membrane was then incubated in

blocking buffer containing the primary antibody at an appropriate dilution for 2 h at room temperature or overnight at 4°C with gentle shaking. The primary antibody solution was washed with TBST three times as described previously. If PVDF was used, then the blot was incubated in blocking buffer containing 1:10,000 alkaline phosphatase conjugated goat  $\alpha$ -rabbit secondary antibody (Sigma). If the membrane was nitrocellulose, the blot was incubated in blocking solution containing 1:20,000 horseradish peroxidase conjugated goat anti-rabbit secondary antibody (Sigma) for 1 h at room temperature or overnight at 4°C with gentle shaking. The unbound secondary antibody solution was removed by washing the blot with TBST three times as described previously. The PVDF membrane was equilibrated in alkaline phosphatase buffer (Section 2.4.8.4) for 5 min. The blot was developed by submerging it in alkaline phosphatase buffer containing BCIP/NBT (Roche) and incubated in the dark without shaking until the required degree of stained bands was observed. The reaction was stopped by the addition of equal volumes of 1 M Tris-HCl, pH 7.5, and 0.5 M EDTA, dried on blotting paper and scanned using an EPSON Perfection 3170 scanner. However, when a nitrocellulose membrane was used, the excess blotting buffer was drained from the membrane. Equal volumes of enhanced chemiluminescent (ECL) substrate reagent 1 and ECL substrate reagent 2 were mixed in the dark room, poured on top of the entire surface of the membrane and incubated at room temperature for 5 min. Excess reagent was drained and the blot was wrapped in clingfilm while ensuring that no air bubbles were trapped between the blot and the clingfilm. The wrapped blot was placed in a film cassette, Amersham Hyperfilm™ ECL (GE Healthcare) was placed on top of the wrapped blot, and the film was exposed for 30 s. The film was then immediately developed by submerging it in developer until the bands appeared; then film was rinsed in dH<sub>2</sub>O, submerged in fixer and rinsed in dH<sub>2</sub>O again. The exposure of the film was repeated, varying the exposure time as needed for optimal detection of proteins. The developed films were air-dried.

### **2.11.5 Bradford estimation of protein concentration**

Bovine serum albumin (BSA) was used to prepare a protein standard curve (Figure 2.1). To prepare the standards, 0, 2, 5, 10 and 20  $\mu$ g of BSA (1.45 mg ml<sup>-1</sup>; BIO-RAD) were added to dH<sub>2</sub>O to a final volume of 800  $\mu$ l. Then, 200  $\mu$ l of Bio-Rad Protein assay dye was added, mixed by inversion and incubated at room temperature

for 5 min. The samples were then transferred into spectrophotometer cuvettes, and  $A_{595}$  was measured using a Jenway 6100 spectrophotometer. To calibrate the spectrophotometer to zero, a 0  $\mu\text{g}$  BSA sample was used. The samples were diluted into  $\text{dH}_2\text{O}$  to a final volume of 800  $\mu\text{l}$  in a spectrophotometer cuvettes and 200  $\mu\text{l}$  of Bio-Rad Protean assay dye was added; the samples were mixed as before and incubated at room temperature for 5 min.  $A_{595}$  was measured and protein concentrations were determined from the standard curve.

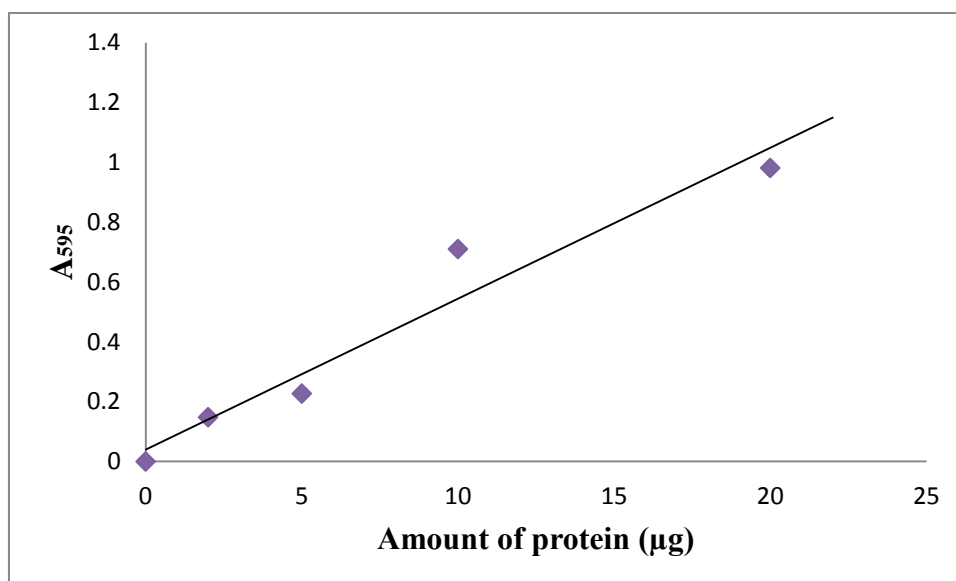


**Figure 2.1 Calibration curve for Bradford assay**

Absorbance of 1 ml standard protein solutions of BSA at 595 nm. The linear regression line was used for estimation of the protein concentration of the samples (shown in black).

#### **2.11.6 Mini-scale protein extraction of *S. aureus***

A single colony of a freshly streaked plate was used to inoculate 5 ml of BHI containing appropriate antibiotics and incubated overnight at  $37^\circ\text{C}$ , 250 rpm. The overnight culture was used to re-inoculate a desired volume of BHI containing appropriate antibiotics in the presence or absence of inducer (IPTG) to an  $\text{OD}_{600}$  of 0.05. The culture was incubated at  $37^\circ\text{C}$ , 250 rpm, to an  $\text{OD}_{600}$  of 0.5. The cells were harvested by centrifugation for 10 min at  $4^\circ\text{C}$ , 5,100 rpm, and the resulting pellet was re-suspended in an appropriate volume of PBS. The sample was then transferred into FastPrep tubes (MP Biomedicals), and the cells were broken using a FastPrep

instrument (MP Biomedicals) set at speed 6 for 40 s, 10 runs, with cooling for 5 min on ice between runs. The FastPrep beads were allowed to settle, and the samples were recovered from tubes and transferred into fresh microcentrifuge tubes. The sample was then centrifuged for 5 min at 13,000 rpm, 4°C. The supernatant was transferred again to a fresh microcentrifuge tube and kept as the soluble fraction while the pellet was re-suspended in an appropriate volume of PBS and kept as the insoluble fraction. Finally, 10 µl of the sample was analysed by SDS-PAGE (Section 2.11.1).

### **2.11.7 Preparation of bacterial whole cell lysate**

A single colony from a freshly streaked plate was used to inoculate 5 ml of BHI containing appropriate antibiotics and incubated overnight at 37°C, 250 rpm. The overnight culture was used to re-inoculate a desired volume of BHI containing appropriate antibiotics in the presence or absence of an inducer (IPTG) to an OD<sub>600</sub> of 0.05. The culture was incubated at 37°C, 250 rpm, to an OD<sub>600</sub> of 0.5. The cells were harvested by centrifugation for 10 min at 4°C, 5,100 rpm, and the resulting pellet was re-suspended in an appropriate amount of sample loading buffer (Section 2.4.7.2), boiled for 10 min, centrifuged for 3 min at 13,000 rpm at room temperature, and then analysed by SDS-PAGE (Section 2.11.1).

## **2.12 Production of recombinant proteins**

### **2.12.1 Expression in *E. coli* BL21 (DE3)**

A single colony of *E. coli* BL21 containing the pET21-d overexpression plasmid with the desired insert was inoculated in 5 ml LB containing 5 µl of ampicillin (100 µg ml<sup>-1</sup>) and incubated overnight at 37°C, 250 rpm. The culture was used to inoculate 100 ml LB with 100 µg ml<sup>-1</sup> ampicillin if small-scale purification was required and 1 l LB with 100 µg ml<sup>-1</sup> ampicillin if large-scale purification was required. The cultures were grown to an OD<sub>600</sub> of 0.05 and then incubated at 37°C, 250 rpm, until an OD<sub>600</sub> of 0.4-0.6 was reached. Then, 1 mM IPTG was added to the culture to induce the expression of the protein, and the cells were incubated for 3 to 4 h. The cells were then harvested by centrifugation at



4°C, 5,100 rpm, for 10 min. The supernatant was discarded, and the pellet was stored at -20°C.

### **2.12.2 Analysis of recombinant protein induction and solubility**

During the preparation of the cells in section 2.12.1, 1 ml of culture was removed before the addition of 1 mM IPTG (uninduced sample), and then 2 samples of 1 ml were removed after the 3 h incubation with IPTG (induced sample). The cells were harvested by centrifugation at 13,000 rpm for 5 min at room temperature and the supernatant was discarded. The uninduced sample and one of the induced samples were re-suspended in SDS sample loading buffer, boiled for 10 min and centrifuged for 3 min at 13,000 rpm to pellet any insoluble material. Then, 15 µl of each sample was analysed by SDS-PAGE to confirm the overexpression of the recombinant protein. To determine the solubility of the recombinant protein, the second induced culture pellet was re-suspended in START buffer and 1 mg ml<sup>-1</sup> lysozyme was added. The sample was incubated at room temperature for 1 h and then sonicated (Sanyo soniprep 150) three times for 10 s. The sample was then centrifuged for 10 min at 13,000 rpm to separate the insoluble and the soluble material. The supernatant (soluble fraction) was transferred into a fresh microcentrifuge tube while the pellet (insoluble fraction) was re-suspended in START buffer containing 8 M urea. SDS loading buffer was added to both fractions, boiled for 10 min and centrifuged for 3 min at 13,000 rpm, room temperature. Finally, 15 µl of each fraction was separated by SDS-PAGE to verify which fraction contained the overexpressed protein.

### **2.12.3 Separation of the soluble and insoluble material**

Pellets from section 2.12.1 were thawed and re-suspended in 5 ml START buffer without urea. The suspension was freeze-thawed three times by placing the sample at -80°C for 10 min followed by thawing it completely on ice. The cells were broken by sonication, ten times for 10 s (Sanyo Soniprep 150), and then spun down at 10,000 rpm, 4°C, for 25 min. The supernatant (soluble fraction) was transferred into another tube through a 0.45 µm pore size sterilised filter and stored at 4°C. If the recombinant protein in section 2.11.2 was determined to be insoluble, then the pellet was re-suspended completely in 5 ml (for small-scale purification) or 30 ml (for large-scale purification) START buffer containing 8

M urea and then incubated at 4°C overnight. The sample was centrifuged at 10,000 rpm, 4°C, for 25 min to remove any unbroken cells. The resulting supernatant (solubilised proteins) was then filtered through a 0.45 µm pore size sterilised filter and stored at 4°C.

#### **2.12.4 HiTrap™ column for protein purification**

The Bio-Rad Econo Gradient system was used to purify the protein using a 5 ml HiTrap™ affinity column (GE Healthcare). The column was washed with 15 ml dH<sub>2</sub>O and charged with 20 ml 50 mM NiSO<sub>4</sub>, and then 15 ml of dH<sub>2</sub>O was flushed through the column to remove the excess unbound Ni<sup>2+</sup> ion. The system pumps and fraction collector tubing were flushed with START at a flow rate of 1.5 ml min<sup>-1</sup>. When the protein was insoluble (Section 2.12.2), 8 M urea was added to the START and elution buffers. The charged column was connected to the system (BioRad Econo Gradient pump) and was then equilibrated with 5 ml START buffer. The supernatant containing the His-tagged protein was applied to the column at a flow rate of 1 ml min<sup>-1</sup> and non-specifically bound proteins were removed by washing with 5 % (v/v) elution buffer until the absorbance returned to zero. The His-tagged protein was then eluted by increasing the gradient (5-100 % (v/v)) of the elution buffer containing 0.5 M imidazole at a flow rate of 1 ml min<sup>-1</sup>, with 1 ml fractions being collected. The eluted fractions were then analysed by SDS-PAGE. The HiTrap™ column was washed with 10 ml 50 mM EDTA to remove NiSO<sub>4</sub>. Then, 10 ml of dH<sub>2</sub>O was run through the column, and the column was then flushed with 10 ml of 20 % (v/v) ethanol and stored at 4°C.

#### **2.12.5 Protein dialysis**

#### **2.12.6 Preparation of the dialysis membrane**

For proteins with a molecular weight less than 12 kDa, benzoylated dialysis tubing (Sigma) with a cut-off of 2 kDa was used, whereas for proteins greater than 12 kDa, size 2 dialysis membrane tubing (Medicell International Ltd.) was used. Before use, the benzoylated dialysis tubing was incubated in 0.3 % (w/v) sodium sulphide at 70°C for 60 s and washed with sterile water pre-heated to 60°C for 2 min to remove the sulphur-containing compounds. To acidify the benzoylated tubing, the tubing was placed into a 0.2 % (v/v) sulphuric acid solution for 2 min followed by washing in hot water to

remove any residual acid. For long-term storage, the tubing was placed in sterile water containing 0.01 % (w/v) sodium azide at 4°C. The dialysis membrane tubing (Medicell International Ltd.) was boiled in 2 mM EDTA for 20 min and then washed in dH<sub>2</sub>O before use. For long-term storage, the EDTA-boiled dialysis tubing was placed in 50 % (v/v) ethanol and stored at 4°C.

### **2.12.7 Dialysis of the recombinant protein**

Fractions eluted in Section 2.12.4 containing the recombinant proteins were placed in dialysis tubing and dialysed in PBS buffer at 4°C for 12 h. The dialysis buffer was changed twice and dialysed for an additional 2 h each time. If the recombinant protein was insoluble, then 4 M urea was added to the dialysis buffer during the first dialysis. The buffer was then replaced by the fresh buffer containing 2 M urea, and dialysis was carried out for 12 h at 4°C. This step was repeated three times using fresh buffer each time; the buffers contained 1 M, 0.5 M and 0 M urea. After dialysis was complete, the recombinant protein fractions were removed from the tubing and 10 % (v/v) glycerol was added. Finally, 10 µl of the purified protein was analysed by SDS-PAGE, and the rest of the protein was separated into 200 µl aliquots and stored at -80°C.

## **2.13 Generation of antibodies**

### **2.13.1 Production of antibodies**

Polyclonal antibodies were raised in rabbits and affinity purified by BioServ (University of Sheffield).

### **2.13.2 Removal of cross-reactive antibodies**

#### **2.13.2.1 *E. coli* lysate treatment**

Cross-reactive antibodies were removed from the polyclonal antisera antibodies by incubating the antiserum with *E. coli* bacterial lysate. A single colony from a freshly streaked plate was used to inoculate 5 ml LB and incubated overnight at 37°C, 250 rpm. The overnight culture was used to inoculate 100 ml LB to an OD<sub>600</sub> of 0.05 and incubated at 37°C, 250 rpm, to saturation phase. The cells were harvested by centrifugation at 5,100

rpm, 4°C, for 10 min. The pellet was re-suspended in 3 ml re-suspension buffer (50 mM Tris-HCl pH 8, 10 mM EDTA pH 8) and stored at 4°C. The suspension was freeze-thawed several times by placing the sample at -80°C for 10 min followed by thawing it completely on ice. The cells were lysed by sonication, ten times for 20 s (Sanyo Soniprep 150) and then centrifuged at 5,100 rpm, 4°C, for 10 min. The supernatant was transferred into fresh tubes, and the lysates were stored at -20°C. Just before use, 0.5 ml of lysate was added to 1 ml of antibody preparation. The mixture was then incubated for 4 h at room temperature while rotating slowly. The treated antibody was then stored at -20°C.

## **2.14 Peptidoglycan hydrolase assay**

### **2.14.1 Peptidoglycan preparation**

#### **2.14.1.1 Peptidoglycan preparation from Gram-positive bacteria**

A single colony from a freshly streaked plate of either *S. aureus* SH1000 or *B. subtilis* HR was inoculated into 10 ml BHI or NB, respectively, and incubated overnight at 37°C, 250 rpm. The overnight culture was used to inoculate 2 l of either BHI or NB to an OD<sub>600</sub> of 0.05 and then incubated at 37°C, 250 rpm, until exponential phase (OD<sub>600</sub> 0.5-0.8). The cells were harvested by centrifugation for 10 min at 4°C, 8,000 rpm, and the pellet was re-suspended in 30 ml water. The cells were killed by boiling for 10 min. The cell preparations were then cooled, and peptidoglycan was purified from the lysed cells. For preparation of broken peptidoglycan sacculi from *S. aureus*, cells were boiled and then centrifuged for 10 min at 5,100 rpm, 4°C. The pellet was re-suspended in 10 ml dH<sub>2</sub>O and chilled on ice. Then, 1 ml of cell suspension was added to pre-chilled FastPrep tubes (MP Biomedicals) and the cells were lysed using a FastPrep instrument (MP Biomedicals) set at speed 6 for 40 s, 10 runs, with cooling on ice for 5 min between runs. The FastPrep beads were allowed to settle before the samples were recovered from the tubes and were then combined in a 50 ml Falcon tube. The beads were washed with dH<sub>2</sub>O vigorously 3 times. The beads were allowed to settle, and then the supernatant was recovered. Any remaining beads and unbroken cells were removed by centrifugation for 5 min at 2,000 rpm, 4°C. For the preparation of broken peptidoglycan sacculi from *B. subtilis*, the cells were disrupted by placing the cell suspension twice through a French pressure cell (Aminco, 180 MPa, 4°C). The protocol for purification of peptidoglycan from lysed cells from *S. aureus* or *B. subtilis* was

similar from this stage onwards. To harvest the cells, they were centrifuged for 10 min at room temperature, 14,000 rpm, and the pellet was re-suspended in 25 ml 5 % (w/v) SDS. The cells were boiled for 25 min, cooled, and then centrifuged for 15 min at room temperature, 10,000 rpm. The pellet was re-suspended in 4 % (w/v) SDS, boiled again for 15 min and centrifuged for 15 min at room temperature, 10,000 rpm. The pellet was washed several times until free of SDS by re-suspension in dH<sub>2</sub>O and centrifugation at 10,000 rpm for 15 min at room temperature. The pellet was re-suspended in 50 mM Tris-HCl (pH 7.5) containing 2 mg ml<sup>-1</sup> pronase, incubated for 90 min at 60°C and centrifuged for 15 min at room temperature at 10,000 rpm. The pellet was washed twice and then re-suspended in dH<sub>2</sub>O and stored at -20°C. To remove teichoic acids, the pellets were re-suspended in 250 µl hydrofluoric acid and incubated overnight at 4°C in microcentrifuge tubes. The samples were washed 6 times by re-suspension in dH<sub>2</sub>O and centrifugation at 14,000 rpm for 10 min at room temperature until the pH was greater than 4. The samples were re-suspended in dH<sub>2</sub>O and stored at -20°C.

#### **2.14.1.2 Peptidoglycan preparation from *E. coli***

A single colony from a freshly streaked plate of *E. coli* was inoculated into 10 ml LB and incubated overnight at 37°C while shaking at 250 rpm. The overnight culture was used to inoculate 2 l LB to an OD<sub>600</sub> of 0.05, and this culture was incubated at 37°C while shaking at 250 rpm until the exponential phase was reached (OD<sub>600</sub> 0.5-0.8). The cells were harvested by centrifugation for 10 min at 4°C at 8,000 rpm, and the pellet was re-suspended in 30 ml water. The cells were killed by boiling for 10 min and were then centrifuged for 10 min at 4°C at 8,000 rpm. The pellet was resuspended in 5 % (w/v) SDS and incubated at 55°C for 10 min. The cells were boiled for 30 min and harvested by ultracentrifugation at 62,000 rpm for 15 min at room temperature. The pellet was washed twice with 50 mM sodium phosphate buffer pH 7.3 followed by ultracentrifugation at 62,000 rpm for 15 min at room temperature. The cells were resuspended in sodium phosphate buffer containing 100 µg ml<sup>-1</sup> α-chymotrypsin and 0.05 % (w/v) sodium azide and were then incubated overnight at 37°C while shaking at 250 rpm. The cells were harvested by ultracentrifugation at 62,000 rpm for 15 min at room temperature. The pellet was resuspended in 5 % (w/v) SDS and incubated at 55°C for 10 min. The cells were boiled for 30 min and then harvested by ultracentrifugation for 15 min at room

temperature at 62,000 rpm. The pellet was washed three times with 50 mM sodium phosphate buffer pH 7.3 followed by ultracentrifugation at 62,000 rpm for 15 min at room temperature. The cells were resuspended in sdH<sub>2</sub>O containing 0.05 % (w/v) sodium azide and then stored at -20°C.

## **2.14.2 Staining of purified peptidoglycan**

### **2.14.2.1 Staining with Procion Red**

Purified peptidoglycan (10 mg ml<sup>-1</sup>) was re-suspended in 2 % (w/v) sodium chloride and incubated for 30 min at 60°C with constant shaking. Then, 0.1 M sodium hydroxide and 15 mg ml<sup>-1</sup> Procion Red MX5B (Sigma) were added, and the sample was incubated for 3 d at 60°C with constant shaking. Any unbound dye was then removed by washing repeatedly with sdH<sub>2</sub>O and centrifugation for 10 min at 14,000 rpm at room temperature. The sample was sonicated one time for one 10 s burst after each wash step to disrupt any insoluble dye particles that could have precipitated during the centrifugation step. Once the supernatant was clear, the Procion Red-labelled peptidoglycan was re-suspended in sdH<sub>2</sub>O and stored at -20°C.

### **2.14.2.2 Staining with Remazol Brilliant Blue**

Purified peptidoglycan (10 mg ml<sup>-1</sup>) was incubated with 20 mM Remazol Brilliant Blue R (RBB, Sigma) and 0.25 M sodium hydroxide overnight with gentle shaking at 37°C. Any unbound dye was then removed by washing several times with sdH<sub>2</sub>O and centrifugation for 10 min at 14,000 rpm at room temperature. The sample was sonicated one time for one 10 s burst after each washing step to disrupt any insoluble dye particles that could precipitate during the centrifugation step. Once the supernatant was clear and free of unbound dye, the RBB-labelled peptidoglycan was re-suspended in sdH<sub>2</sub>O and stored at -20°C.

### **2.14.3 Renaturing gel analysis**

#### **2.14.3.1 Renaturing SDS-PAGE**

Peptidoglycan hydrolase activity was detected by renaturing gel electrophoresis using purified *S. aureus* and *B. subtilis* cell walls (Section 2.14.1.1) as the substrates, which were incorporated into the resolving polyacrylamide gel (Section 2.11.1) to a final concentration of 0.1% (w/v). Electrophoresis was performed as described in Section 2.11.1. Samples were then run in duplicate lanes. When electrophoresis was complete, one lane was excised and stained with Coomassie Blue to visualise proteins (Section 2.11.2). The other lane was used to assay for peptidoglycan hydrolase activity (Section 2.14.3.2).

#### **2.14.3.2 Analysis of peptidoglycan hydrolases by renaturing SDS-PAGE**

The electrophoresed gels were rinsed in dH<sub>2</sub>O to remove the SDS and then incubated in renaturing solution (Section 2.4.7.5) for 30 min at room temperature with gentle shaking. The gels were then incubated in fresh renaturing solution overnight at 37°C with gentle shaking. Renatured gels were then rinsed in dH<sub>2</sub>O and stained in 1x renaturing stain (Section 2.4.7.6) for 3 h at room temperature, with gentle shaking. The gels were de-stained in dH<sub>2</sub>O until zones of clearing could be observed against a blue background, indicating peptidoglycan hydrolase activity.

#### **2.14.4 Native zymogram assay**

A 1% (w/v) low melting point (LMP) agarose gel (SIGMA) was melted in renaturing solution (pH 5) containing MgCl<sub>2</sub>. *S. aureus* cell walls pre-stained with Procion-Red MX5B (Section 2.14.2.1) or with RBB (Section 2.14.2.2) were added to the 1% (w/v) LMP agarose gel. The 1% (w/v) LMP agarose gel was poured onto the hydrophilic side of pre-warmed GelBond<sup>®</sup> film (Lonza) and allowed to set. After the thin solid layer of gel formed, 2 µl of a 1:2 serial dilution of protein was spotted on the gel and allowed to adsorb. The gel was then incubated in a humidifier overnight at 37°C. Zones of clearing within a dark background indicate peptidoglycan hydrolase activity. Unstained *S. aureus* cell walls were stained with renaturing stain for 3 h after the overnight incubation at 37°C.

The film was de-stained with dH<sub>2</sub>O until zones of clearing were observed and left to dry overnight at room temperature. The film was either scanned or photographed.

#### **2.14.5 RBB release assay**

First, 20 µl of RBB-labelled peptidoglycan (Section 2.14.2.2) and purified recombinant protein (0.1 mg ml<sup>-1</sup>) were incubated at 37°C for 60 min in 200 µl 20 mM sodium citrate (pH5) containing 1 mM MgCl<sub>2</sub>. The reaction was stopped by incubation at 95°C for 5 min. Then, soluble cleavage products were separated from the insoluble substrate by centrifugation for 20 min at 14,000 rpm at room temperature. The supernatant was collected, and the absorbance was measured at 595 nm using a Victor™ X3 multilabel reader.

#### **2.15 Size exclusion chromatography by FPLC**

The oligomerisation state of the purified recombinant proteins was determined by size exclusion chromatography (SEC) using an ÄKTA fast-performance liquid chromatography (FPLC) system (ÄKTA design, Amersham Bioscience). The mobile phases were 50 mM Sodium citrate containing 0.15 M NaCl or 50 mM Tris-HCl (pH 8) containing 0.15 M NaCl. This solution was prepared using MilliQ water and was degassed before use. Purified recombinant proteins were separated on Superdex™ 200 10/300 GL columns (Tricorn™ high performance columns) and eluted with 1.5 times the column volume of buffer at a flow rate of 0.5 ml min<sup>-1</sup>. Elutions of the purified recombinant proteins were detected by measuring the absorbance at 260 nm and 280 nm. Calibration curves were prepared by measuring the elution volumes of protein standards of known sizes (Gel Filtration Standards, GE Healthcare; Table 2.10) at pH 5 and pH 8. The partition coefficient ( $K_{av}$ ) was then calculated for the protein standards and plotted against the logarithm of their molecular weight (Figure 2.2). The molecular weight of recombinant protein samples was then estimated from the calibration curve after calculating its  $K_{av}$  from its elution volume using the following formula:

$$K_{av} = \frac{V_e - V_o}{V_t - V_o}$$



where:

$V_e$ : Elution volume of recombinant protein (ml).

$V_o$ : Void volume of the column (ml; 7 ml for Superdex 200™ 10/300 GL column).

$V_t$ : Total volume of the column (ml; 25 ml for Superdex™ 200 10/300 GL column).

Protein	Molecular Mass (kDa)
Aldolase	158.0
Ovalbumin	43.0
Ribonuclease A	13.7
Aprotinin	6.5

**Table 2.10 Gel filtration size standards**

P

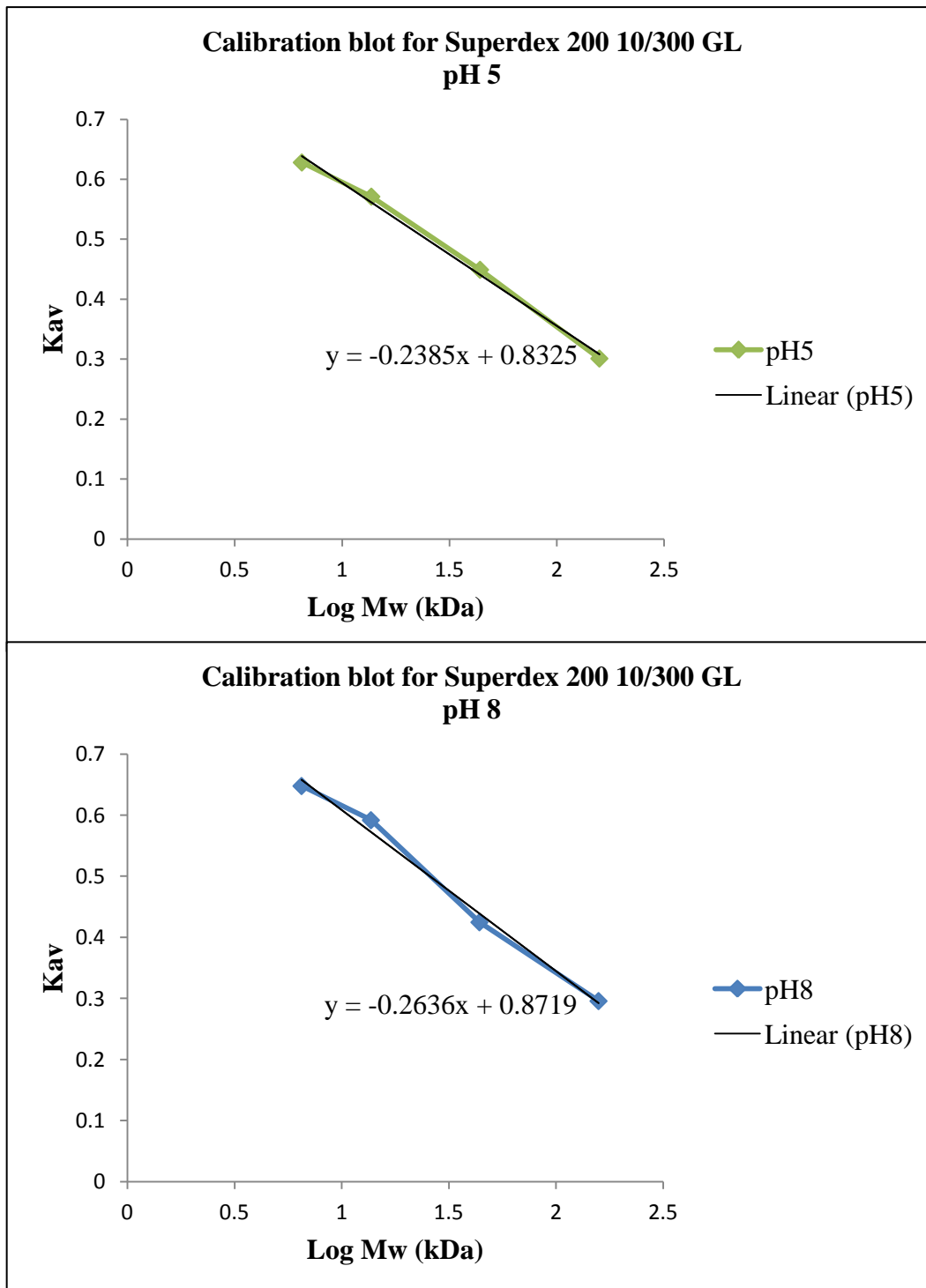


**Figure 2.2 Calibration curves of gel filtration standards**

The partition coefficient ( $K_{av}$ ) of the gel filtration standards was plotted against the log molecular weight (MW) at pH 5 (A) and pH 8 (B). A linear regression line (black) was used to calculate the log MW of the protein samples.

## 2.16 Cell fractionation

A single colony from a freshly streaked plate of *S. aureus* SH1000 *spa::kan* was used to inoculate 5 ml of BHI containing kanamycin (50 mg ml<sup>-1</sup>) and neomycin (50 mg ml<sup>-1</sup>). The overnight culture was used to inoculate 2 l of BHI to an OD<sub>600</sub> of 0.01 and was incubated at 37°C, 250 rpm, until cells reached the exponential phase (OD<sub>600</sub> 0.5). The cells were then harvested by centrifugation for 10 min at 8000 rpm, 4°C, and the pellet was washed three times by re-suspension in dH<sub>2</sub>O and centrifugation for 10 min at 8000 rpm, 4°C. The cells were then re-suspended in 5 ml TBSI (Section 2.4.10) and then transferred to pre-chilled FastPrep tubes (MP Biomedicals). The cells were lysed using the FastPrep instrument (MP Biomedicals) set at speed 6 for 40 s, 10 runs, with cooling for 5 min on ice between runs. The FastPrep beads were settled before samples were recovered from the tubes and were then combined in a 50 ml Falcon tube. The beads were washed 3 times with sdH<sub>2</sub>O by shaking vigorously. After the beads settled, the supernatant was recovered. Any remaining beads and un-lysed cells were removed by centrifugation at 2,000 rpm for 5 min, 4°C. The supernatant was then centrifuged twice for 10 min at 18,000 rpm, 4°C. The resulting pellets contain the cell wall fraction and any remaining un-lysed cells. The supernatant was transferred to ultracentrifuge tubes (Beckman), and cell membrane fractions were harvested by ultracentrifugation for 2 h at 50,000 rpm, 4°C. The remaining supernatant contained the cytoplasmic fraction. The membrane pellet was washed by re-suspension in TBSI followed by ultracentrifugation for 2 h at 50,000 rpm, 4°C. The fractions were re-suspended in TBSI and then stored at -20°C.

## 2.17 Preparation of samples for light microscopy

Samples of appropriate cultures, corresponding to an OD<sub>600</sub> of 0.5, were harvested by centrifugation for 3 min at 14,000 rpm, room temperature. The cells were washed in 1 ml dH<sub>2</sub>O and then harvested by centrifugation for 3 min at 14,000 rpm, room temperature. The cells were fixed by re-suspension in 500 µl PBS containing 2.7% (w/v) paraformaldehyde and 0.005% (v/v) glutaraldehyde, followed by incubation for 30 min at room temperature on a rotary shaker. The cells were washed 3 times by re-

suspension in 1 ml dH<sub>2</sub>O and centrifugation for 3 min at 14,000 rpm, room temperature. The cells were then re-suspended in an appropriate volume of GTE buffer (Section 2.4.9), and 5 µl was spotted onto poly-L-lysine glass slides (Sigma) and air-dried. Once dry, 10 µl of SlowFade® Gold antifade reagent (Invitrogen) was applied to the slide and a coverslip was placed on top, mounted and sealed with DPX mountant (BDH).

### 2.17.1 Fluorescence microscopy

Fluorescence images were acquired using an Olympus IX70 deconvolution microscope and SoftWoRx 3.5.0 software (Applied Precision). For the visualisation of each fluorophore, the appropriate filters were used (Table 2.11). The samples were prepared in the dark by wrapping the tubes in foil during fixation to prevent fluorophore bleaching and preparing the slide mounts using SlowFade® Gold antifade reagent (Invitrogen) to prolong the life of the fluorophore.

Filter	Excitation wavelength (nm)	Emission wavelength (nm)	Fluorophore used
DAPI	436/10	457/50	HADA
FITC-YFP	490/20	528/38	GFP
mRFP	580/20	630/60	AlexaFluor 594, Vancomycin

**Table 2.11 Fluorescence filter sets used**

### 2.17.2 Fluorescent labelling of nascent cell wall synthesis

Fluorescent vancomycin (Pinho and Errington 2003) or HADA (7-hydroxycoumarin 3-carboxylic acid (HCC-OH) attached to 3-amino-D-ala (ADA) (Kuru *et al.*, 2012) were used to label the nascent peptidoglycan. Vancomycin binds the terminal D-Ala D-Ala residues present on peptidoglycan pentapeptides not yet cross-linked. As the peptidoglycan moves away from the septum it becomes more processed and fewer D-ala D-Ala residues are available for binding. HADA is incorporated into peptidoglycan during its synthesis. When cells were labelled with vancomycin, they were transferred to a microfuge tube containing 10 µl of 100 µg ml<sup>-1</sup> 1:1 vancomycin: fluorescently

labelled vancomycin (at a final concentration of  $1 \mu\text{g ml}^{-1}$ ) and incubated while rotating for 5 min to 30 min at  $37^{\circ}\text{C}$ . When the cells were labelled with HADA,  $5 \mu\text{l}$  of  $100 \text{ mM}$  HADA was added to  $1 \text{ ml}$  of cells and incubated for 5 to 30 min while rotating at  $37^{\circ}\text{C}$ . The cells were then harvested by centrifugation at  $13,000 \text{ rpm}$  for 5 min at room temperature and washed 3 times in  $\text{sdH}_2\text{O}$ . The cells were then fixed (if required) as described in Section 2.17.

### **2.17.3 Immunofluorescence**

Cells were grown, harvested, and fixed as described in Section 2.17. The cells were then applied to poly-L-lysine slides (Sigma) and allowed to dry. Gentle lysis of cells was performed using lysostaphin at a range of concentrations from  $0 - 30 \text{ ng ml}^{-1}$  for 1 min. The cells were then washed 3 times in PBS as described in Section 2.16 and allowed to air dry. The cells were rehydrated with PBS and blocked with 2 % (w/v) BSA in PBS for 15 min and incubated overnight at  $4^{\circ}\text{C}$  with the primary antibody (rabbit anti-*S. aureus* DivIC or FtsL at 1:100 to 1:2000) in 2% (w/v) BSA in PBS. The primary antibody was not added to the control slides. The samples were washed 8 times with PBS, and then anti-rabbit IgG AlexaFluor 594 conjugate (Invitrogen) was added at 3:1000 in 2% (w/v) BSA in PBS. The slides were incubated in the dark for 2 h. The cells were then washed 8 times with PBS, and a coverslip was mounted in Slow Fade Gold and sealed with DPX (BDH).

## Chapter 3

### Analysis of DivIC and FtsL functions

#### 3.1. Introduction

Cell division is a vital process that is involved in the maintenance of bacterial growth and proliferation (Madigan and Martinko, 2006). Most prokaryotic cells are subject to a cell division mechanism that is known as binary fission. The cell starts the division process by duplicating its DNA, elongating to twice its size, forming a septum, and finally dividing (Figure 1.1) (Carballido-Lopez and Formstone, 2007). However, as a coccus, *S. aureus* does not follow exactly the same process, as it divides along three perpendicular planes, producing daughter cells that remain attached (Figure 1.1C) (Zapun et al., 2008, Tzagoloff and Novick, 1977, Pinho and Errington, 2003). Cell division comprises several essential components that are conserved across species (Weiss, 2004), and whose coordinated activity has been primarily studied in rod-shaped organisms (Sievers and Errington, 2000b; Weiss, 2004). Nonetheless, with the exception of penicillin-binding proteins (Sauvage *et al.*, 2008), the precise functions of most of these components are not well understood (Gueiros-Filho and Losick, 2002; Daniel *et al.*, 1998). The interaction between cell division components has been demonstrated using the bacterial/yeast two-hybrid system in *B. subtilis* (Daniel *et al.*, 2006) and in *E. coli* (Di Lallo *et al.*, 2003). In addition, studies in our laboratory using *S. aureus* have recently shown, by two-hybrid analysis that several homologues of cell division proteins from the rod-shaped organisms interact with each other (Figure 1.4A) (Steele *et al.*, 2011). Moreover, a number of these proteins are putatively essential for the viability of *S. aureus*, as shown by transposon-mediated differential hybridisation (TMDH) (Chaudhuri *et al.*, 2009). The homologous genes are essential and conserved across the species, suggesting the involvement of their protein products in the formation of the divisome complex.

The *divIC* gene is essential for *B. subtilis* survival as it is required for septum formation during sporulation and cell growth. A mutation in this gene causes defects in bacterial growth at all temperatures; the cells fail to separate and

eventually lyse (Levin and Losick, 1994; Robichon *et al.*, 2008). The *B. subtilis* DivIC is small bitopic protein that comprises 125 amino acids with hydrophobic amino acid residues that act as a membrane-spanning domain at the N-terminus and also leucine-zipper motif near the C-terminus (Levin and Losick, 1994). *E. coli* FtsB (DivIC) is a small bitopic protein of 103 amino acids with a cytoplasmic N-terminal domain of only 3 amino acid residues; this domain, along with the transmembrane fragment, is essential for interaction of the protein with FtsL. The periplasmic C-terminal domain, which contains a leucine zipper motif, is also required for protein-protein interactions, particularly the last 18 amino acid residues of this domain; the deletion of these residues decreases the binding affinity of FtsB to FtsQ (Buddelmeijer *et al.*, 2002; Gonzalez and Beckwith, 2009). The *E. coli* *ftsL* gene is located only fifteen base pairs upstream of the *ftsI* gene and is part of an operon. The *ftsL* gene was identified in *E. coli* and *B. subtilis* as essential as a null mutation in the gene inhibits cell division. The mutant cells fail to divide and continue to grow as long filaments. Before cell lysis, some cells appear as thick filaments with lumps, suggesting that this gene product is important for cell division and morphogenesis (Guzman *et al.*, 1992; Sievers and Errington, 2000a). *E. coli* and *B. subtilis* FtsL are small, bitopic membrane proteins (121 and 117 amino acids, respectively) comprising a single membrane-spanning domain, a short N-terminal cytoplasmic domain (34 amino acids) and a long C-terminal domain (Guzman *et al.*, 1992; Daniel *et al.*, 1998). A relatively low abundance of the FtsL protein, approximately 20-40 copies per cell, has been reported in *E. coli* (Guzman *et al.*, 1992). *B. subtilis* FtsL is predicted to contain a leucine zipper motif, which might be involved in the interaction with DivIC to form a heterodimeric complex (Daniel *et al.*, 1998). *E. coli* and *H. influenzae* FtsL also contain leucine zipper motifs in their respective C-terminal regions, and these motifs could be engaged in protein interactions to form homodimers or to form heterodimers with other cell division proteins (Ghigo and Beckwith, 2000). The DivIC and FtsL proteins recruit other cell division components to the site of division in *B. subtilis* (Daniel *et al.*, 2006) and *E. coli* (Gonzalez and Beckwith, 2009). The yeast two-hybrid system has demonstrated that full-length DivIC and FtsL interact with each other to form a dimeric complex (Sievers and Errington, 2000b, Daniel *et al.*, 2006), and this complex interacts with another cell division protein, DivIB, forming a trimeric complex (Daniel *et al.*, 2006, Noirclerc-Savoie *et al.*, 2005) that facilitates the

recruitment of other cell division proteins to the mid-cell (Daniel *et al.*, 2006, Gonzalez and Beckwith, 2009). The leucine zipper motifs of *S. pneumoniae* FtsL and DivIC are localised in their respective extracytoplasmic domains and are important for protein dimerisation (Noirclerc-Savoie *et al.*, 2005).

### 3.1.1. Aims of this chapter

- Overexpress and purify recombinant forms of the *S. aureus* and *B. subtilis* cell division proteins DivIC and FtsL;
- Investigate the biochemical activities of DivIC and FtsL;
- Map the potential DivIC active site

## 3.2. Results

### 3.2.1. Bioinformatic analysis of cell division proteins

Many cell division proteins are highly conserved between *B. subtilis* and *S. aureus*. A recent study revealed 351 essential genes in *S. aureus*, including putative cell division genes such as *divIC* and *ftsL*, that are homologues of essential genes in *B. subtilis* (Chaudhuri *et al.*, 2009). *S. aureus* DivIC and FtsL have direct homologues in *B. subtilis* (Levin and Losick, 1994; Sievers and Errington, 2000b) and structural homologues in *E. coli* (Gonzalez and Beckwith, 2009, Guzman *et al.*, 1992). The *S. aureus* genome sequences derived from *S. aureus* NCTC 8325 (NCBI database); the *divIC* and *ftsL* accession numbers are SAOUHSE\_00482 and SAOUHSE\_01144, respectively. The *B. subtilis* genomic sequences were obtained from the SubtiList World-Wide Web Server (<http://genolist.pasteur.fr/SubtiList/>). The *divIC* and *ftsL* accession numbers are BG10125 and BG10220, respectively. DivIC and FtsL are members of the DivIC superfamily of proteins, which are septum initiator proteins. DivIC and FtsL gene lengths and locations are listed in Table 3.1. An alignment of the *S. aureus* and *B. subtilis* DivIC protein sequences reveals that the proteins are 27% identical and 57% similar (Figure 3.1A), while alignment of the *S. aureus* and *B. subtilis* FtsL protein sequences revealed 27% identity and 49% similarity (Figure 3.2A). The DivIC and FtsL proteins from different bacterial species exhibit similar topologies, with a long extracellular C-terminal domain, a



membrane-spanning domain and a short N-terminal cytoplasmic domain (Katis *et al.*, 1997; Daniel *et al.*, 1998; Ghigo and Beckwith, 2000; Buddelmeijer *et al.*, 2002; Noirclerc-Savoie *et al.*, 2005).

### 3.2.1.1. Bioinformatic analysis of DivIC

In the *S. aureus* chromosome, *divIC* is located upstream of the S1 RNA binding domain protein and tRNA (Ile)-lysine synthase and downstream of an unknown protein and *yabN*, a tetrapyrrole methylase (Figure 3.1B). In *B. subtilis*, *divIC* is located downstream of *yabP* and *yapQ* (Figure 3.1B). These genes encode proteins of unknown function, but mutations in those genes resulted in a blockage of the final stage of the sporulation process (Fawcett *et al.*, 2000). *B. subtilis divIC* is located upstream of *yabR*, which encodes a protein of unknown function that is similar to polyribonucleotide nucleotidyltransferase and *trnSL-met1*, a tRNA gene (Figure 3.1B). *S. aureus* DivIC consists of 130 amino acids and has a molecular weight of 15.35 kDa and a predicted isoelectric point (pI) of 9.77 (Table 3.1). The *B. subtilis* DivIC protein is 125 amino acids in length, with a molecular weight of 14.58 kDa and a pI of 9.97 (Table 3.1). The SOSUI program can be used to predict a protein's secondary structure and distinguish between soluble and membrane proteins (Figure 3.1C/D). In addition, this program also predicts transmembrane helices (Hirokawa *et al.*, 1998). Bioinformatic analysis of *S. aureus* and *B. subtilis* DivIC using SOSUI revealed analogous transmembrane helices of 23 and 22 amino acids residues, respectively, between residues 34 and 56 in *S. aureus* and residues 38 and 59 in *B. subtilis* (Figure 3.1C). The coiled coil motif structure consists of 7 residues with a *a to g* periodicity, with a hydrophobic residue such as leucine at positions *a* and *d* and polar residues at the other positions (Tropsha *et al.*, 1991; Alber, 1992; Lupas, 1997; Vincent *et al.*, 2013). The leucine zipper motif facilitates protein-protein interactions, such as dimerisation via the hydrophobic surfaces of the coiled coil helices that is crucial for protein binding to DNA (Tropsha *et al.*, 1991; Alber, 1992; Lupas, 1997). *E. coli* FtsB contains a leucine zipper-like domain within its single coiled coil motif (Buddelmeijer *et al.*, 2002; Gonzalez and Beckwith, 2009) *B. subtilis* DivIC contains a leucine zipper motif near the C-terminus (Levin and Losick, 1994, Figure 3.1E). The *S. aureus* DivIC sequence was

Protein	Accession number	Genomic locus	Gene length (bp)	Protein length (a.a)	Molecular weight (kDa)	Predicted iso-electric point (pI)	C-terminal (Figure 3.1D and 3.2D) molecular weight (kDa)	C-terminal (Figure 3.1D and 3.2D) (pI)
<i>S. aureus</i> DivIC	SAOUHSC_00482	480218-480610	393	130	15.35	9.77	(57-130 a.a) 9.68	(57-130 a.a) 8.16
<i>B. subtilis</i> DivIC	BG10125	59.353-79.353	375	125	14.58	9.97	(60-125 a.a) 8.49	(60-125 a.a) 6.56
<i>S. aureus</i> FtsL	SAOUHSC_01144	1093492- 1093893	402	133	15.33	9.34	(67-133 a.a) 8.45	(67-133 a.a) 8.02
<i>B. subtilis</i> FtsL	BG10220	1571.076- 1591.076	351	117	12.93	10.08	(57-117 a.a) 7.80	(57-117 a.a) 8.22

**Table 3.1 Bioinformatic analysis summary**

previously analysed using the COILS server (Lupas, 1997), which detected two putative coiled-coil domains, one at the N-terminus and one at the C-terminus (Figure 3.1E).

### 3.2.1.2. Bioinformatic analysis of FtsL

In the *S. aureus* chromosome, *ftsL* is located upstream of *pbp1*, encoding penicillin-binding protein 1, and *mraY*, phospho-N-acetylmuramoyl-pentapeptide-transferase, both of which are involved in peptidoglycan biosynthesis, and downstream of *mraZ*, a putative cell division protein with unknown function, and *mraW*, an S-adenosyl-methyltransferase (Figure 3.2B). In *B. subtilis*, *ftsL* is situated downstream of *mraY* and *mraZ* and upstream of *pbpB*, penicillin-binding protein 2B, and *spoVD*, a penicillin-binding protein that regulates spore shape (Figure 3.2B). *S. aureus* FtsL is a protein of 133 amino acids with a molecular weight of 15.33 kDa and a pI of 9.34. *B. subtilis* FtsL consists of 117 amino acids and has a molecular weight of 12.93 kDa and a predicted pI of 10.08 (Table 3.1). Bioinformatic analysis of *S. aureus* and *B. subtilis* FtsL using SOSUI identified analogous transmembrane helices of 22 or 23 amino acid residues, respectively, situated between residues 45 to 66 of *S. aureus* FtsL and residues 34 and 56 of *B. subtilis* FtsL (Figure 3.2C/D). The COILS server was used to analyse the *S. aureus* and *B. subtilis* FtsL coiled-coil motifs (Lupas, 1997), and one putative coiled coil domain was identified (Figure 3.2E).

### 3.2.2. Expression of the soluble domains of DivIC and FtsL

The C-termini of DivIC and FtsL are important for the interactions of these proteins with themselves, each other and other cell division proteins. The C-terminus of *E. coli* FtsB (DivIC) is important for its interaction with FtsQ and contains a leucine zipper motif that is crucial for protein homo- or hetero-dimerisation (Gonzalez and Beckwith, 2009). The C-terminus of *E. coli* FtsL is required for the interaction of the FtsL/FtsB subcomplex with FtsQ and contains a coiled coil motif that is important for its interactions with FtsB and with itself (Ghigo and Beckwith, 2000; Gonzalez *et al.*, 2010).



- A. Alignment of the *S. aureus* and *B. subtilis* DivIC protein sequences using ClustalW with the BLOSUM62 scoring matrix. Asterisks indicate conserved residues, colons indicate conservative substitutions and full stops indicate semi-conservative substitutions. The C-terminal residues are shown in red. The transmembrane domains are indicated by green boxes. The predicted coiled coil domain is boxed, and the residue positions within the heptad repeat are labelled a to g.
- B. The chromosomal region of *divIC* in *S. aureus* and *B. subtilis*.
- C. Hydropathy plots of the *S. aureus* and *B. subtilis* DivIC protein generated by the SOSUI server. The transmembrane helices are indicated by green boxes
- D. A topological model of the *S. aureus* and *B. subtilis* DivIC protein generated by the SOSUI server. The C-terminal domains are indicated by red boxes.
- E. *S. aureus* and *B. subtilis* DivIC COILS results.

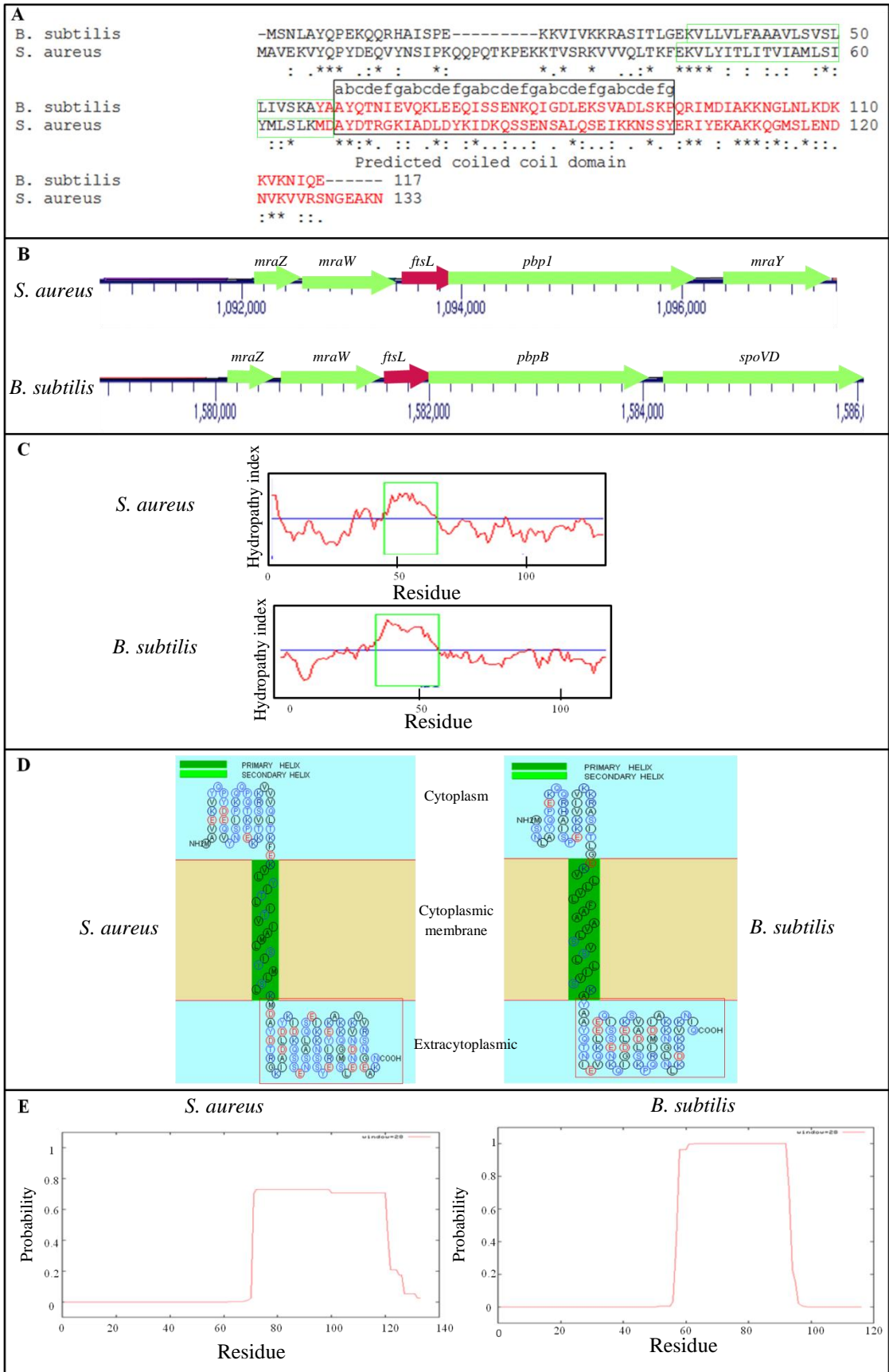


Figure 3.2 Bioinformatic analysis of *S. aureus* and *B. subtilis* FtsL

- A. Alignment of the *S. aureus* and *B. subtilis* FtsL protein sequences generated by ClustalW using the BLOSUM62 scoring matrix. Asterisks indicate conserved residues, colons indicate conservative substitutions and full stops indicate semi-conservative substitutions. The C-terminal residues are shown in red. The transmembrane domains are indicated by green boxes. The predicted coiled coil domain is boxed, and the residue positions within the heptad repeat are labelled a to g.
- B. The chromosomal region of *ftsL* in *S. aureus* and *B. subtilis*.
- C. Hydropathy plots of the *S. aureus* and *B. subtilis* FtsL proteins generated by the SOSUI server. The transmembrane helices are indicated by green boxes.
- D. A topological model of the *S. aureus* and *B. subtilis* FtsL protein generated by the SOSUI server. The C-terminal domains are indicated by red boxes.
- E. *S. aureus* and *B. subtilis* FtsL COILS results.

In *B. subtilis*, the external C-terminus of DivIC is important for its localisation at the division site and contains the leucine zipper motif that is required for its interaction with the leucine zipper motif of FtsL (Katis and Wake, 1999; Sievers and Errington, 2000a). The C-terminal domains of *B. subtilis* FtsL and DivIC form a heterodimer *in vitro* with a ratio of 1:1 (Sievers and Errington, 2000b; Masson *et al.*, 2009). In *S. pneumoniae*, the heterodimerisation of DivIC and FtsL could be forced by introducing an artificial coiled coil peptide into the extracellular domain (Noirclerc-Savoie *et al.*, 2005). These findings emphasise the functional importance of the C-terminal domains of DivIC and FtsL. The molecular weights and pI values of the C-terminal domains (Figure 3.1D and Figure 3.2D) are summarised in Table 3.1.

#### **3.2.2.1. pET overexpression system**

The pET overexpression system is an effective mechanism that relies on bacteriophage T7 RNA polymerase (Studier and Moffatt, 1986). The target gene is cloned under the control of the T7 promoter, which drives a high level of expression of the target protein in *E. coli*, such that the recombinant protein may comprise more than 50% of the total protein in the host cell within a few hours following induction. The desired gene is initially cloned in a host that does not express the T7 RNA polymerase. The construct is then transformed into an expression strain carrying the T7 RNA polymerase gene under the control of the *lacUV5* promoter. Gene expression can be induced by adding IPTG to the bacterial culture. pET-21d(+) is a translational fusion vector that contains a C-terminal 6×His tag, which facilitates the purification of the desired protein via nickel affinity chromatography. This vector contains a *lac* repressor to control the basal expression of the target gene. In addition, pET-21d(+) has a multiple cloning site and carries an ampicillin resistance gene to permit selection in the host strain (Novagen).

#### **3.2.2.2. Construction of the DivIC and FtsL expression plasmids**

To produce recombinant proteins, the desired genes from *B. subtilis* and *S. aureus* were cloned into the pET-21d(+) vector. The recombinant *S. aureus* *divIC* and *ftsL*



constructs were described previously (Kabli, 2009). The extracellular domains were identified based on topology predictions (Figure 3.1 and Figure 3.2), and primers were designed accordingly. The restriction enzymes *NcoI* and *XhoI* were chosen because they cut within the vector and not within the desired gene. As a result, *divIC* and *ftsL* were amplified from *S. aureus* SH1000 and *B. subtilis* 168 using primer pairs containing *NcoI* and *XhoI* restriction sites (Table 2.7). To ensure that the desired gene sequence was in frame, an additional C and T were appended to the *NcoI* restriction site. The extracellular domains of both *divIC* and *ftsL* were amplified, and the resulting PCR products were analysed by 1% (w/v) agarose electrophoresis (Section 2.8.7). The PCR fragments were excised from the gel, purified using a QIAquick Gel Extraction kit (Section 2.8.4) and digested with *NcoI* and *XhoI*. The plasmid was digested with the same enzymes, and the digested plasmid and PCR fragments were purified using a QIAquick PCR Purification kit (Section 2.8.5). The inserts were then ligated into the plasmid (Section 2.9.6), ethanol precipitated (Section 2.8.6) and transformed into electrocompetent *E. coli* TOP10 cells (Section 2.10.1, Figure 3.3A). The transformants were selected on LB agar containing 100 µg ml<sup>-1</sup> ampicillin. Positive clones were verified by colony PCR (data not shown) and by plasmid extraction using a QIAprep Spin Mini kit (Section 2.8.2) followed by digestion with *NcoI* and *XhoI*. The digested plasmids were separated by 1% agarose electrophoresis (Section 2.8.7), and the expected DNA band sizes corresponding to the inserts were observed (Figure 3.3B). Plasmids were also sequenced at the Core Genomic Facility, University of Sheffield, and the sequencing confirmed that no substitutions or frameshift mutations were introduced during PCR (data not shown).

### **3.2.2.3. Overexpression of recombinant proteins in *E. coli***

pALB26, pALB27, pAFK1 and pAFK2 were transformed into the expression strain, *E. coli* BL21 (DE3), by electroporation (Section 2.10.1). This strain carries the T7 RNA polymerase gene under the control of the *lacUV5* promoter, and T7 expression can be induced by the addition of IPTG. Furthermore, the absence of the *lon* protease and outer membrane proteases from this strain reduces the degradation of overexpressed proteins.

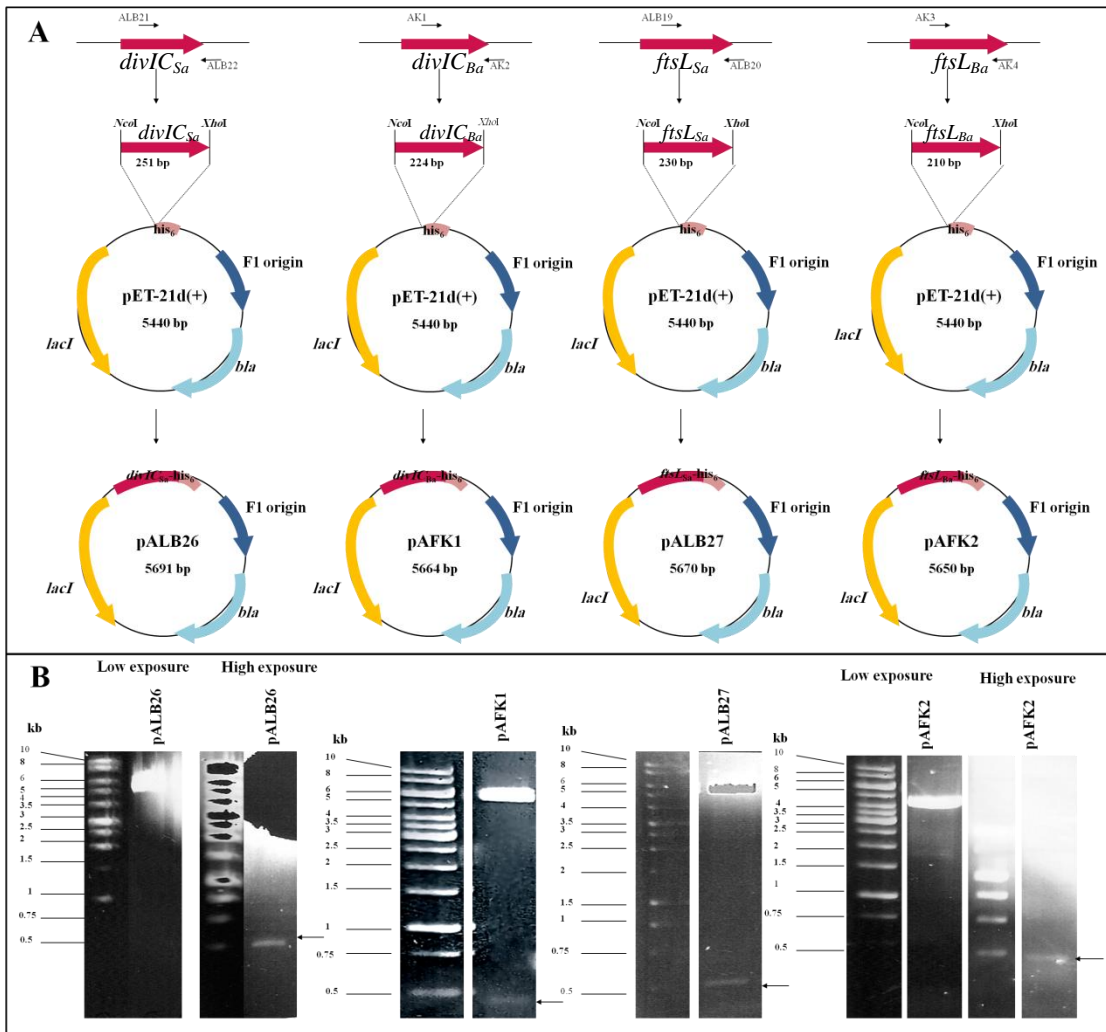


**Figure 3.3 Construction of *S. aureus* and *B. subtilis* protein overexpression plasmids**

A. Diagram illustrating the fusion of *S. aureus* and *B. subtilis* *divIC* and *ftsL* to 6×His in the pET21d vector.

B. pALB26, pAFK1, pALB27 and pAFK2 were digested with *Nco*I and *Xho*I and analysed by 1% (w/v) TAE agarose gel electrophoresis. The 5440 bp band corresponds to linearised pET21-d vector. Bands of 251 bp and 224 bp, corresponding to *S. aureus* and *B. subtilis* *divIC*, respectively, are marked by black arrows. Bands of 230 bp and 210 bp, corresponding to *S. aureus* and *B. subtilis* *ftsL*, respectively, are marked by black arrows.

Transformants were selected on LB agar containing 100  $\mu\text{g ml}^{-1}$  ampicillin, and positive clones were verified by PCR, digestion with *NcoI* and *XhoI* and DNA sequencing (data not shown). The recombinant proteins were overexpressed via the addition of 1 mM IPTG to the bacterial culture (Section 2.12.1). Samples were taken before and after the addition of 1 mM IPTG to evaluate the induction of the recombinant protein expression. The solubility of the recombinant proteins was assessed by lysing the induced cells as described in Section 2.12.2. The samples were analysed by electrophoresis on a 15% (w/v) SDS-PAGE gel (Section 2.11.1), followed by staining with Coomassie Blue (Section 2.11.2, Figure 3.4A). These analyses revealed bands of slightly less than 14 kDa for *S. aureus* DivIC (DivIC<sub>Sa</sub>) and FtsL (FtsL<sub>Sa</sub>) and *B. subtilis* FtsL (FtsL<sub>Bs</sub>) in the induced sample fraction, indicating successful overexpression. These bands correspond to masses that are slightly higher than expected. The presence of polar and charged amino acid residues in the C-termini of these recombinant proteins might affect their migration in SDS-PAGE. The induction and overexpression of *B. subtilis* DivIC (DivIC<sub>Bs</sub>) was unsuccessful; no band corresponding to the expected size was detected in induced culture (Figure 3.4A). The solubility analysis revealed that all of the recombinant proteins were present in the soluble fraction, and the solubility of the recombinant proteins was subsequently verified (data not shown).

#### **3.2.2.4. Purification of recombinant proteins using a HiTrap™ column**

As described in Section 2.12.4, the recombinant proteins were overexpressed by growing the cells until the exponential phase was reached, followed by induction with 1 mM IPTG for 3-6 h. The proteins were then purified by passage over a HiTrap™ affinity column (GE Healthcare). The column was pre-loaded with Ni Sepharose™ and charged with Ni<sup>2+</sup>, which facilitates the binding of the 6×His-tagged proteins. Unbound proteins were eluted with 5% (w/v) imidazole (Section 2.4.6.3). The recombinant proteins were eluted by increasing the imidazole concentration, collecting 1-ml fractions, and separating the proteins by 15% (w/v) SDS-PAGE. Fractions that contained bands of the expected sizes were collected, combined, dialysed in PBS (Section 2.12.5) and separated by 15% SDS-PAGE (Figure 3.4B).

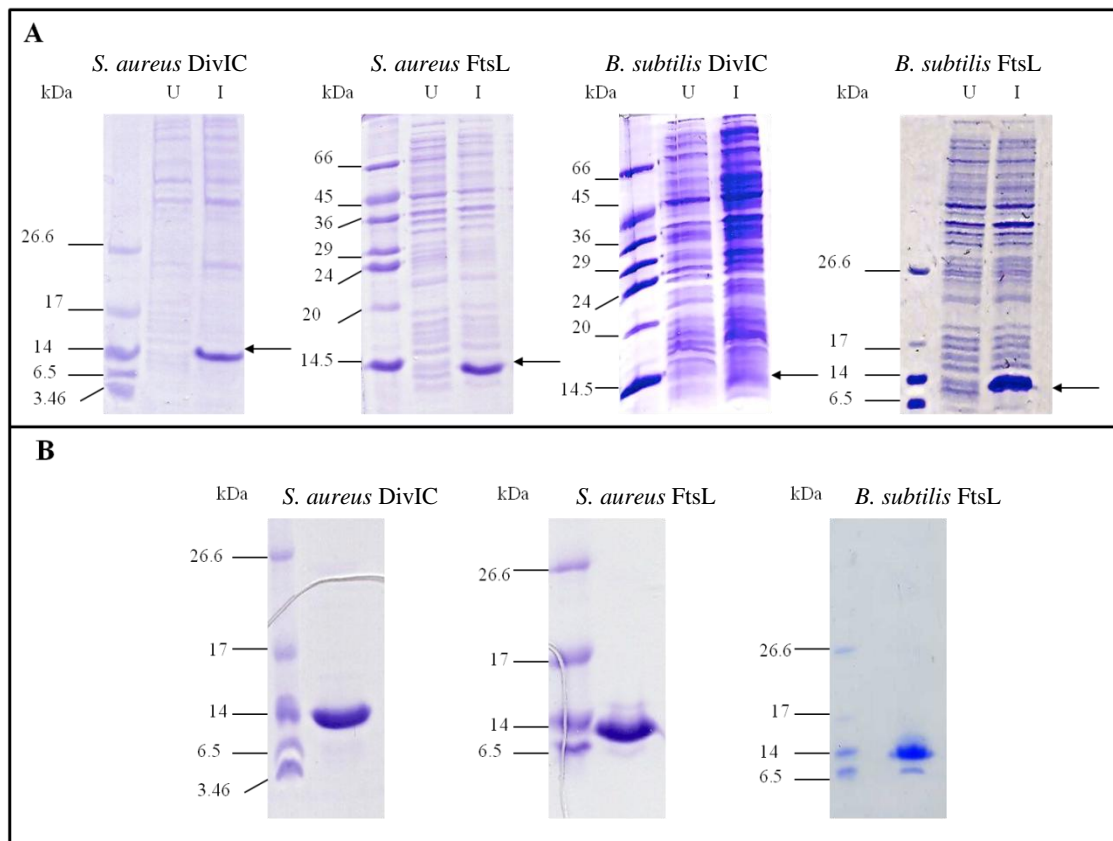


**Figure 3.4 Production and purification of recombinant proteins**

Recombinant proteins were overexpressed from pALB26, pALB27, pAFK1 and pAFK2 in BL21 (DE3) by induction with 1 mM IPTG.

A. Samples were taken before (Uninduced, U) and after (Induced, I) the addition of 1 mM IPTG. Whole cell lysates were analysed by 15% (w/v) SDS-PAGE. Black arrows indicate protein bands of the expected size. The solubility analysis revealed that all of the recombinant proteins were present in the soluble fraction, and the solubility of the recombinant proteins was subsequently verified (data not shown).  
 B. Purified recombinant proteins after nickel affinity chromatography and dialysis.

### 3.2.3. Oligomerisation state of *S. aureus* recombinant proteins

Size exclusion chromatography (SEC) was used to examine the oligomerisation state of recombinant DivIC<sub>Sa</sub> and FtsL<sub>Sa</sub>. A Superdex™ 200 10/300 GL column (Amersham Bioscience) was used to separate recombinant DivIC<sub>Sa</sub> and FtsL<sub>Sa</sub>. A total of 20 µg of the recombinant proteins was injected, and the absorbance was measured at 280 nm and 260 nm (Figure 3.5 I.A and II.A, Figure 3.6 I.A and II.A). Fractions corresponding to the major peaks were collected and analysed by 15% (w/v) SDS-PAGE to verify that a protein of the expected size was present (Figure 3.5 I.B and II.B and Figure 3.6 I.B and II.B). The molecular weights of the proteins in these fractions were determined by comparison with protein standards of known sizes (Gel Filtration Calibration Kit, GE Healthcare; Figure 2.2). Because the environmental pH can affect protein stability and dimerisation (Bose and Clark, 2005), the oligomerisation state of the recombinant proteins was assessed in both pH 5 and pH 8 buffers. DivIC<sub>Sa</sub> was eluted at 16.32 ml at pH 5 and DivIC<sub>Sa</sub> was eluted at 16.61 ml at pH 8. The predicted molecular weights of DivIC<sub>Sa</sub> in the pH 5 and pH 8 fractions were estimated to be ~ 20.89 and ~ 19.05 kDa, respectively, as described in Section 2.15. The predicted molecular weights of the proteins in these fractions were greater than that of the predicted DivIC<sub>Sa</sub> extracellular domain (9.68 kDa). This result suggests that recombinant DivIC<sub>Sa</sub> might exist as a dimer. The protein is predicted to contain two coiled-coil motifs (Figure 3.1E), which can mediate protein homodimerisation (Alber, 1992; Vincet *et al.*, 2013). FtsL<sub>Sa</sub> was eluted at 16.81 ml at pH 5 and 16.78 ml at pH 8. The estimated molecular weights of FtsL<sub>Sa</sub> in the pH 5 and pH 8 fractions were 16.03 and 17.66 kDa, respectively, larger than the predicted molecular weight of the FtsL<sub>Sa</sub> extracellular domain (8.45 kDa). This observation suggests that recombinant FtsL<sub>Sa</sub> might exist as a dimer. FtsL<sub>Sa</sub> is predicted to have a single coiled coil motif (Figure 3.2E).

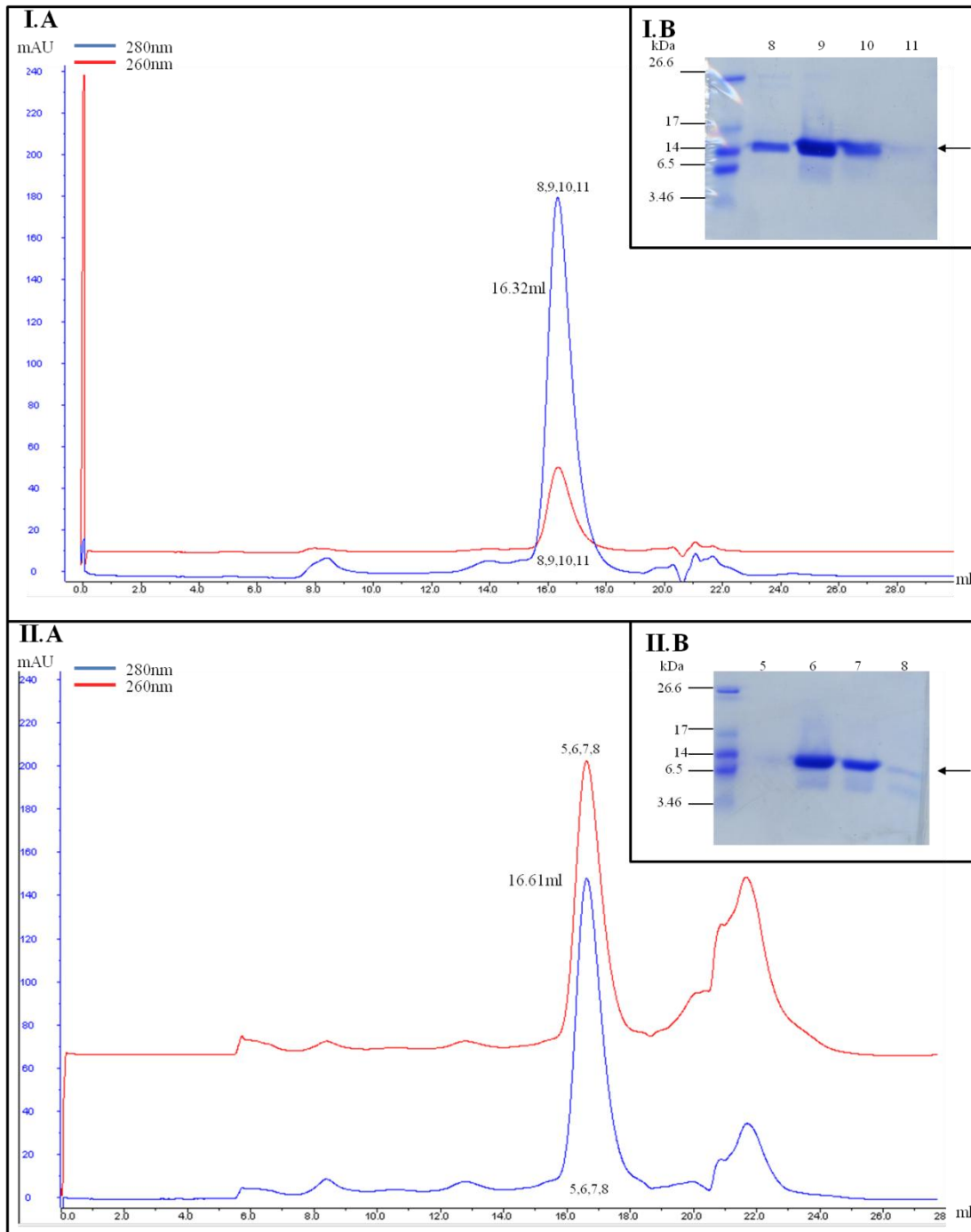


**Figure 3.5 *S. aureus* DivIC oligomerisation**

Recombinant protein was analysed by gel filtration on a Superdex™ 200 10/300 GL column (Amersham Biosciences). The absorbance was measured at 280 nm and 260 nm. The DivIC<sub>Sa</sub> chromatographic profiles at pH 5 (I.A) and pH 8 (II.A) are shown. Samples (10 µl) of the major peak fractions were analysed by 15% (w/v) SDS-PAGE (pH 5 (I.B) and pH 8 (II.B)). Black arrows indicate the DivIC<sub>Sa</sub> protein band.

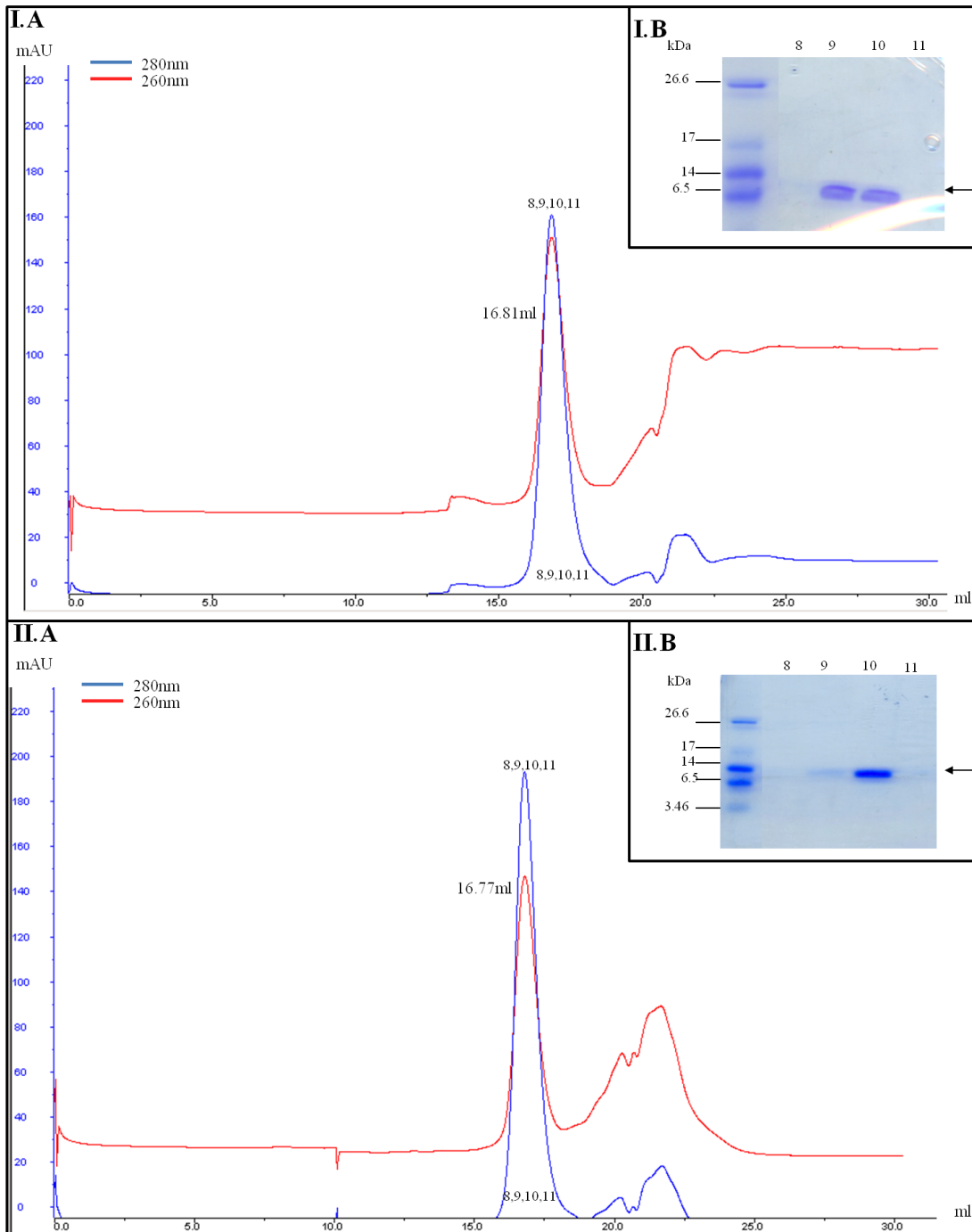


**Figure 3.6** *S. aureus* FtsL oligomerisation

Recombinant protein was analysed by gel filtration on a Superdex™ 200 10/300 GL column (Amersham Bioscience). Absorbance was measured at 280 nm and 260 nm. The FtsL<sub>Sa</sub> chromatographic profiles at pH 5 (I.A) and pH 8 (II.A) are shown. Samples (10 µl) of the major peak fractions were analysed by 15% (w/v) SDS-PAGE (pH 5 (I.B) and pH 8 (II.B)). Black arrows indicate the FtsL<sub>Sa</sub> protein band.

These findings suggest that the C-terminal domains of *S. aureus* DivIC and FtsL are important for the physiological functions of these proteins due to their roles in self-association and, potentially, interactions with other cell division proteins.

### **3.2.4. Biochemical activity of recombinant proteins**

#### **3.2.4.1. Analysis of the peptidoglycan hydrolase activity of *S. aureus* recombinant proteins**

Previous work in our lab on an *S. aureus* cell division protein, DivIB, revealed that the protein exhibited potential hydrolytic activity in a zymogram assay (Bottomley, 2011; Figure 3.7). Because DivIB, DivIC and FtsL are all bitopic membrane proteins with similar topologies (Carson *et al.*, 1991; Guzman *et al.*, 1997; Katis *et al.*, 1997; Daniel *et al.*, 1998; Chen *et al.*, 1999 Ghigo and Beckwith, 2000; Buddelmeijer *et al.*, 2002; Robson and King, 2006), we evaluated whether DivIC<sub>Sa</sub> and FtsL<sub>Sa</sub> were able to hydrolyse the cell wall. Zymogram analysis is the method of choice for examining the hydrolytic activity of recombinant proteins against purified bacterial cell walls. SDS-zymography is a qualitative technique that is used to determine the hydrolytic activity of enzymes in a renaturing SDS gel containing a substrate (Kleiner and Stetler-Stevenson 1994; Foster, 1992). The hydrolytic activity of DivIC<sub>Sa</sub> and FtsL<sub>Sa</sub> was analysed in a 15% (w/v) renaturing SDS gel containing purified bacterial cell walls as substrate (Section 2.14.3.2). The appearance of clear zones within the dark background indicated the hydrolytic activities of the enzymes. The molecular masses of the recombinant proteins were estimated in comparison to protein standards of known sizes that were separated by 15% (w/v) SDS-PAGE and stained with Coomassie Blue (Section 2.11.2).

The activities of DivIC<sub>Sa</sub> and FtsL<sub>Sa</sub> were assessed in pH 5 and pH 7.5 buffers as the environmental pH can affect enzymatic activity (Huard *et al.*, 2004). In addition, we investigated the influence of divalent cations on the activity of the proteins, as Mg<sup>2+</sup> has previously been reported to be crucial for hydrolase activity (Foster, 1992; Horsburgh *et al.*, 2003).



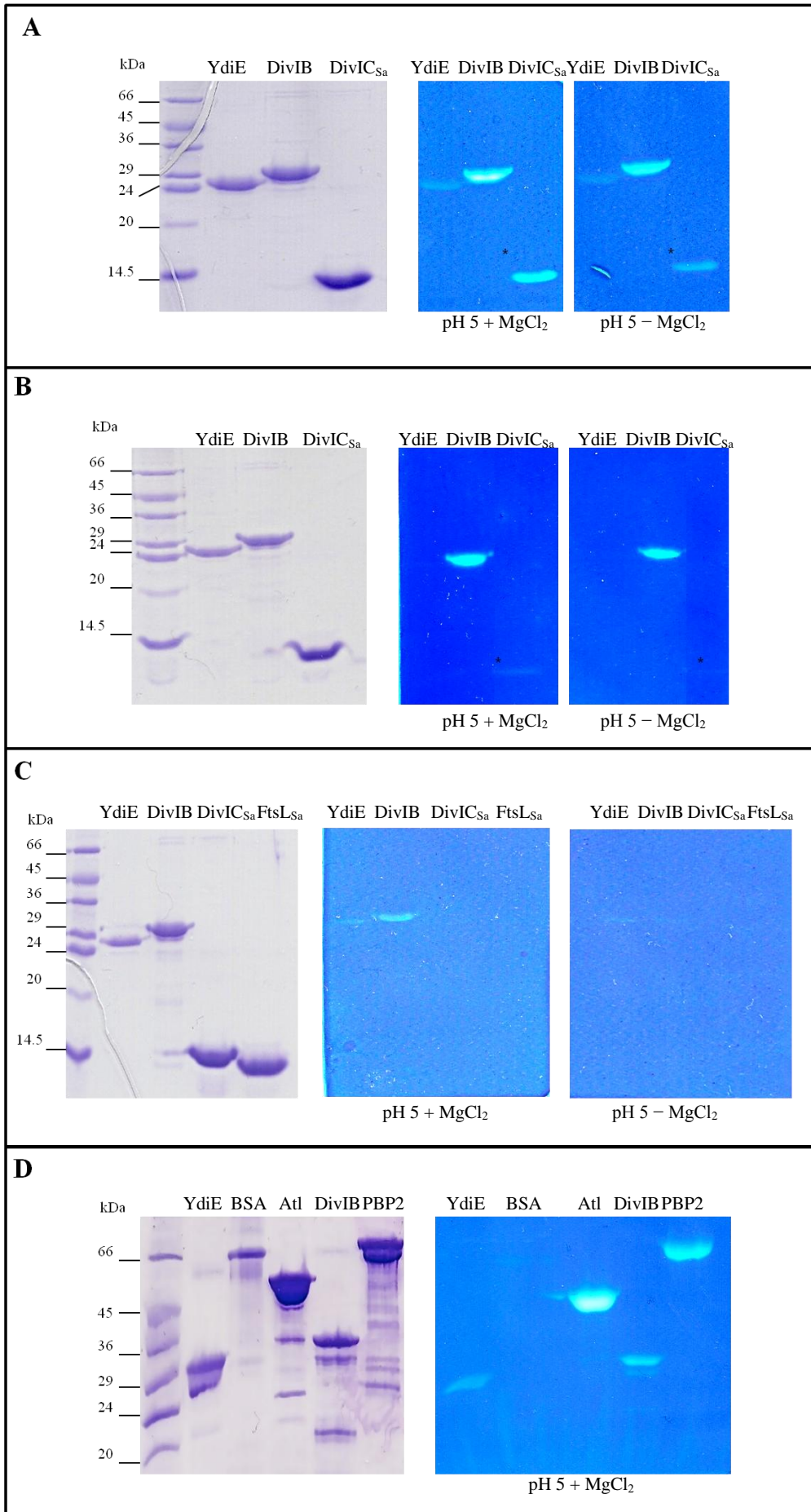


### **Figure 3.7 Zymogram analysis of *S. aureus* DivIC and FtsL**

A 15% (w/v) renaturing SDS gel containing 0.1% (w/v) purified *S. aureus* peptidoglycan as substrate. A total of 10 µg recombinant protein was used, and the gel was stained with Coomassie Blue (gels on the left) or renaturing stain (gels on the right). Protein renaturation was performed at pH 5 or pH 7.5 in the presence and absence of 10 mM MgCl<sub>2</sub>.

- A. SDS zymogram gel of DivIC<sub>Sa</sub> and controls at pH 5 with or without MgCl<sub>2</sub>.
- B. SDS zymogram gel of FtsL<sub>Sa</sub> and controls at pH 5 with or without MgCl<sub>2</sub>.
- C. SDS zymogram gel of DivIC<sub>Sa</sub> and FtsL<sub>Sa</sub> at pH 7.5 with or without MgCl<sub>2</sub>.
- D. SDS zymogram gel of controls at pH 5 with MgCl<sub>2</sub>.

DivIC<sub>Sa</sub> was observed to have hydrolytic activity in the presence of *S. aureus* peptidoglycan (PG) with wall teichoic acid (WTA) at pH 5 both with and without MgCl<sub>2</sub> (Figure 3.7A) but not at pH 7.5 with or without CaCl<sub>2</sub> (Figure 3.7C). The hydrolytic activity of DivIC<sub>Sa</sub> was enhanced by the presence of Mg<sup>2+</sup> in the incubation buffer. In contrast, FtsL<sub>Sa</sub> did not exhibit any hydrolytic activity in either pH buffer in the presence of *S. aureus* PG plus WTA (Figure 3.7B, Figure 3.7C). Thus, the production of a zone of clearing by DivIC<sub>Sa</sub> is likely specific because no activity was observed in the presence of FtsL<sub>Sa</sub> or other controls. Neither YdiE, a His-tagged *S. aureus* protein of unknown function, nor BSA produced a zone of clearing (Figure 3.7D). In contrast, DivIB, Atl (a His-tagged *S. aureus* autolysin) and PBP2 (a His-tagged cell division protein) produced obvious zones of clearing on a zymogram gel (Figure 3.7D). *B. subtilis* PG plus WTA was also used as substrate; however, neither DivIC<sub>Sa</sub> nor FtsL<sub>Sa</sub> produced any zone of clearing (data not shown). The peptidoglycan structures of *B. subtilis* and *S. aureus* differ in a number of ways, including in glycan chain length, stem peptide sequence and the composition of the cross-linkage between glycan strands. For instance, *S. aureus* peptidoglycan may end with reduced N-acetylmuramic acid (MurNAc) or N-acetylglucosamine (GlcNAc), while *B. subtilis* peptidoglycan may end with 1,6-anhydroMurNAc residues (Vollmer *et al.*, 2008). The amino acid at position three of the peptide stem may vary between species; in *B. subtilis*, amidated *meso*-A<sub>2</sub>pm is added to this position via the Mur ligases (Roten *et al.*, 1991; Atrih *et al.*, 1999). Moreover, the composition of the interpeptide bridge also varies between species; *S. aureus* has a pentaglycine bridge (Snowden and Perkins, 1991; Schneider *et al.*, 2004), whereas the cross-linkage between the stem peptides in *B. subtilis* comprises a peptide bridge between mesodiaminopimelic acid and D-alanine (Forrest *et al.*, 1991). The O-acetylation of the MurNAc residues of peptidoglycan in *S. aureus* is catalysed by the O-acetyltransferase OatA (Bera *et al.*, 2005). This modification can increase the resistance of *S. aureus* to lysozyme. Thus, certain hydrolases cannot hydrolyse *S. aureus* peptidoglycan (Bera *et al.*, 2005; Vollmer, 2008). *B. subtilis* peptidoglycan contains deacetylated glucosamine (GlcNdAc) and deacetylated muramic acid (MurNdAc) residues (Atrih *et al.*, 1999; Vollmer, 2008). These differences between *S. aureus* and *B. subtilis* peptidoglycan and the ability of DivIC<sub>Sa</sub> to hydrolyse the *S. aureus* cell wall but not the *B. subtilis* cell wall highlights the substrate specificity of these enzymes.

### 3.2.4.2. Mapping the potential active site of *S. aureus* DivIC

To identify the residues associated with DivIC<sub>Sa</sub> potential enzymatic activity, several forms of the extracytoplasmic domain, including a number of site-directed mutants and truncations, were produced (Figure 3.8A).

#### 3.2.4.2.1. Production of a recombinant *S. aureus* DivIC fragment

A truncated DivIC extracellular domain fragment (DivIC<sub>Sa</sub><sup>Δ118-130</sup>, Figure 3.8A) was produced using the pET system as described in Section 3.2.2.1. The last 13 amino acids at the C-terminus were deleted, as these polar and charged amino acid residues might affect the biochemical activity of the protein. AK5 and AK6 primers (Table 2.7) containing *Nco*I and *Xho*I sites, respectively, were used to amplify the truncated DivIC<sub>Sa</sub> extracellular domain from *S. aureus* SH1000 genomic DNA. The PCR product was excised from a 1.5% (w/v) agarose gel (Section 2.9.7), gel purified (Section 2.8.4) and digested with *Nco*I and *Xho*I. The plasmid was digested with the same enzymes, and the digested plasmid and PCR product were purified using a QIAquick PCR Purification kit (Section 2.8.5). The insert was then ligated into the plasmid (Section 2.9.6), the plasmid was ethanol precipitated (Section 2.8.6) and transformed into electrocompetent *E. coli* TOP10 cells (Section 2.10.1). Transformants were selected on LB agar containing 100 μg ml<sup>-1</sup> ampicillin, and positive clones were verified by colony PCR (data not shown). In addition, the plasmid was extracted using a QIAprep Spin Mini kit, followed by digestion with *Nco*I and *Xho*I. The digested plasmid was resolved by 1.5% (w/v) agarose gel electrophoresis and a DNA band corresponding to the expected size of the insert was observed (Figure 3.8B). The plasmid was also sequenced at the Core Genomic Facility, University of Sheffield to confirm that no substitutions or frameshift mutations were introduced during PCR (data not shown). pAFK3, which contains the *S. aureus* *divIC* truncated C-terminal domain (DivIC<sub>Sa</sub> Δ118-130), was transformed into the *E. coli* BL21 (DE3) expression strain by electroporation (Section 2.10.1). Transformants were selected on LB agar containing 100 μg ml<sup>-1</sup> ampicillin, and positive clones were verified by PCR, digestion with *Nco*I and *Xho*I and DNA sequencing (data not shown). The overexpression of the recombinant protein was induced by adding 1 mM IPTG to the bacterial culture (Section 2.12.1).

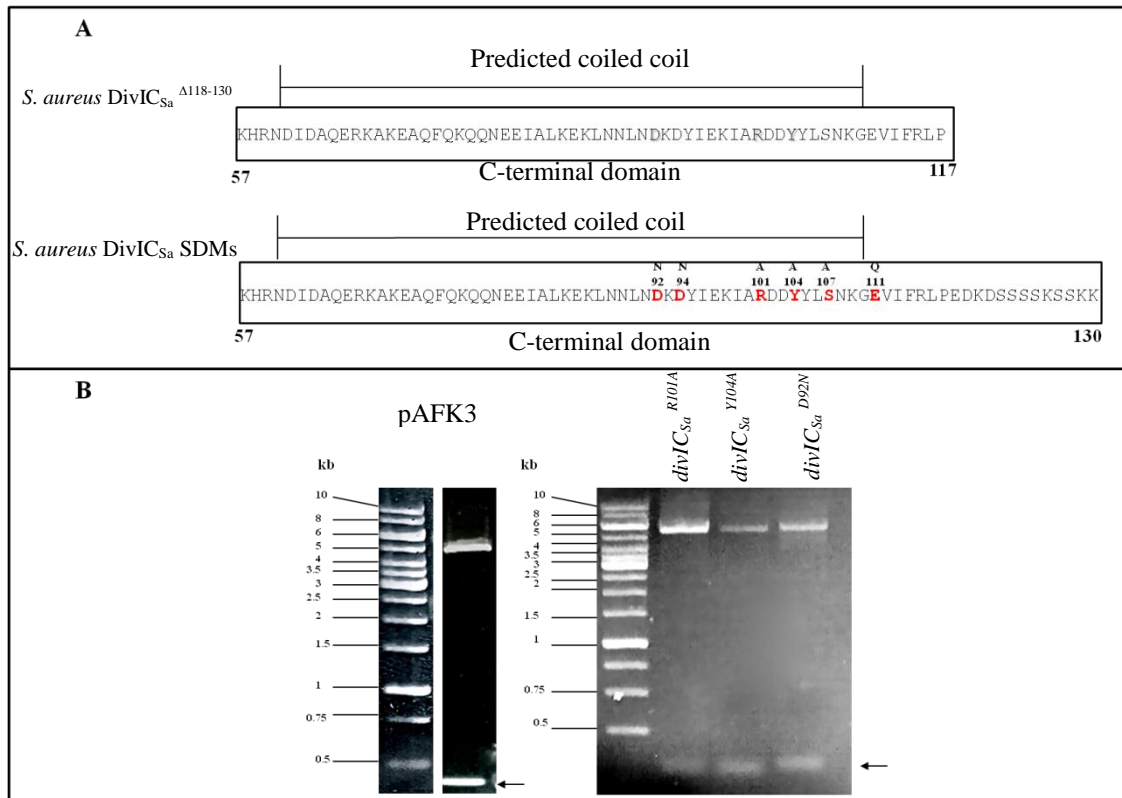


**Figure 3.8** *divIC* mutant overexpression plasmids

- A. Schematic diagram of the mutated forms of the *S. aureus* DivIC C-terminal domain fragment. Residues in red represent the point mutations.
- B. pAFK3 was restriction digested with *Nco*I and *Xho*I, and the DNA was separated by 1.5% (w/v) agarose gel electrophoresis. pAFK3 shows the linearised pET21-d vector at the expected size of 5540 bp and the *divIC*<sub>Sa</sub><sup>Δ118-130</sup> insert (indicated by a black arrow) at the expected size of 212 bp. The site-directed mutagenesis plasmids (*divIC*<sub>Sa</sub><sup>R101A</sup>, *divIC*<sub>Sa</sub><sup>Y104A</sup> and *divIC*<sub>Sa</sub><sup>D92N</sup>) were restriction digested with *Dpn*I, and the DNA was separated by 1% (w/v) agarose gel electrophoresis. The site-directed mutagenesis plasmids show the linearised pET21-d vector at the expected size of 5540 bp and the insert *divIC*<sub>Sa</sub><sup>R101A</sup>, *divIC*<sub>Sa</sub><sup>Y104A</sup> and *divIC*<sub>Sa</sub><sup>D92N</sup> (indicated by a black arrow) at the expected size of 251 bp.

Samples were taken before and after the addition of 1 mM IPTG, as described previously, to evaluate the expression of the recombinant protein. The solubility of the recombinant protein was determined by lysing the induced cells (Section 2.12.2). The samples were analysed by electrophoresis on a 15% (w/v) SDS-PAGE gel (Section 2.11.1), followed by staining with Coomassie Blue (Section 2.11.2, Figure 3.9A). The analysis revealed a band of ~10 kDa for the truncated DivIC<sub>Sa</sub> extracellular domain. This band was larger than the expected size (7.5 kDa) with the presence of polar and charged amino acid residues in the C-terminus of the recombinant protein potentially affecting migration in SDS-PAGE. A solubility analysis demonstrated that the recombinant protein was present in the soluble fraction, and the solubility of the recombinant protein was subsequently verified (data not shown). The His-tagged protein fragment was purified using a nickel affinity column, as described previously (Section 2.12.4). The column was washed with 5% (w/v) imidazole to elute unbound proteins, and the recombinant protein was eluted by increasing the imidazole concentration. Fractions (1 ml) were collected and analysed using 15% (w/v) SDS-PAGE. Fractions containing bands of the expected sizes were collected combined, dialysed in PBS (Section 2.12.5) and separated by 15% SDS-PAGE (Figure 3.9B).

#### **3.2.4.2.2. Site-directed mutagenesis of *S. aureus* DivIC**

The coordination and spatial organisation of essential residues in the active site is crucial for the catalytic activity of an enzyme (Wallace *et al.* 1996). Catalytic residues can vary among enzyme families, but these variations have distinct patterns. The pattern of catalytic residues consisting of an acid, base and nucleophile, is widely conserved and is known as the catalytic triad. The catalytic triad cleaves the ester or peptide bonds of a substrate by nucleophilic attack (Dodson and Wlodawer 1998). The best studied catalytic triad is the serine-histidine-aspartate triad present in lipases and serine proteases (Wallace *et al.* 1996). Each residue in the catalytic triad has a specific role in the catalytic process, and they are often distant from one another in the primary amino acid sequence of the enzyme.

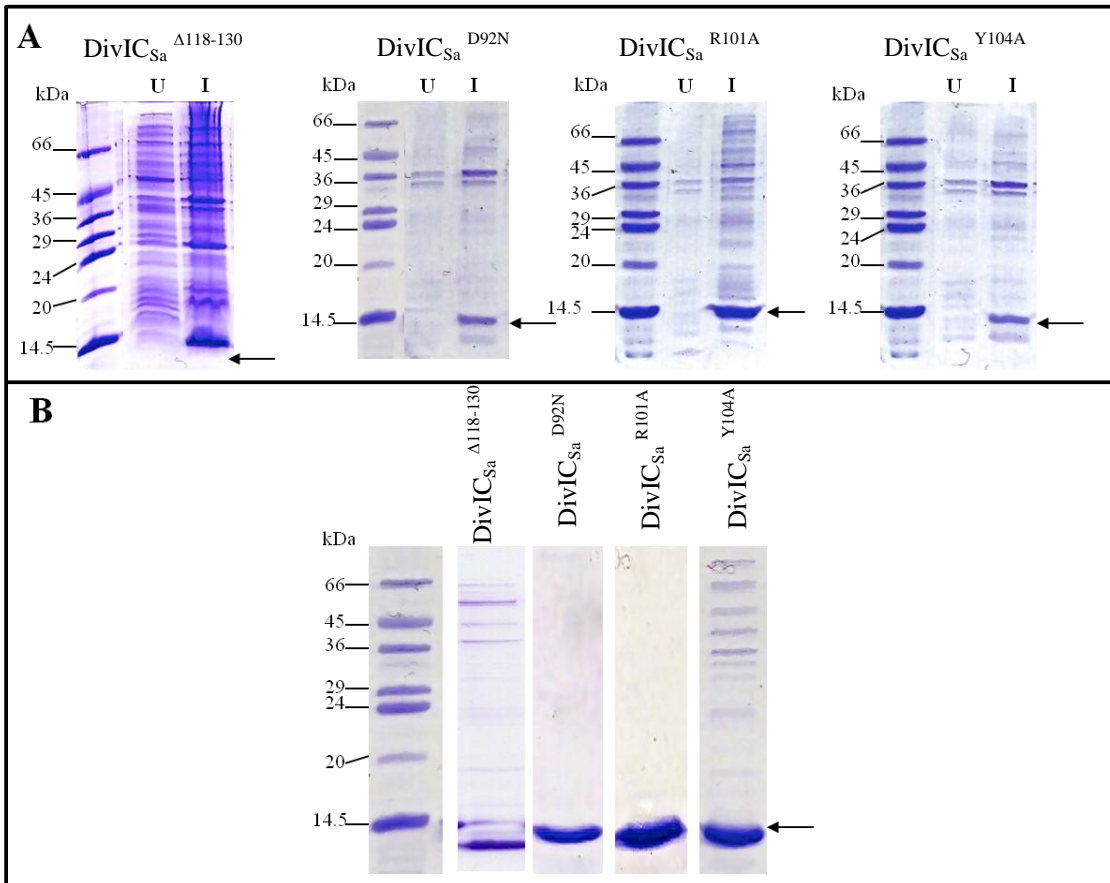


**Figure 3.9 Production and purification of truncated DivIC<sub>Sa</sub> fragment and site-directed mutant proteins**

The recombinant proteins were overexpressed from pAFK3, pALB26<sup>D92N</sup>, pALB26<sup>R101A</sup> and pALB26<sup>Y104A</sup> in BL21 (DE3) by induction with 1 mM IPTG.

A. Samples were taken before (Uninduced, U) and after (Induced, I) the addition of 1 mM IPTG. Whole-cell lysates were analysed by 15% (w/v) SDS-PAGE. Black arrows indicate protein bands of the expected size.

B. Purified recombinant proteins after nickel affinity chromatography and dialysis.

However, these residues can only cleave the relevant bond in the substrate if they are located in close spatial proximity as the result of a specific protein conformation (Dodson and Wlodawer 1998; Wallace *et al.* 1996). Catalytic triad variations include the substitution of the aspartate residue with glutamate in aspartyl dipeptidase (Ekici *et al.*, 2008) and the presence of a lysine residue instead of histidine in class A  $\beta$ -lactamases and PBPs (van der Linden *et al.*, 1994). Other enzymes achieve catalysis through a single active site residue, such as threonine or serine, as observed in the Ntn hydrolase superfamily (Ekici *et al.*, 2008). Amino acid sequence alignments (Bioinformatics analysis) of DivIC (Section 3.2.1) with its homologues in different bacterial species (Figure 3.10A) and different staphylococcal species (Figure 3.10B) revealed conserved residues. Conserved amino acid residues may be functionally relevant; e.g., they may be involved in the enzyme active site. Because DivIC is poorly conserved among bacterial species, both conserved and semi-conserved amino acids were targeted for site-directed mutagenesis. Aspartate (D) and glutamate (E) were mutated to asparagine (N) and glutamine (Q), respectively, because mutating acidic residues to neutral polar residues generally does not affect protein stability (Tokunaga *et al.*, 2008). All other selected conserved and semi-conserved residues were replaced by alanine (A).

Site-directed mutagenesis using the QuikChange II site-directed mutagenesis kit was used to introduce the site-specific mutations (Section 2.9.3). Mutagenic oligonucleotide primers containing the required mutations were designed (Table 2.7) using the QuikChange® Primer Design Program ([www.stratagene.com/sdmdesigner/default.aspx](http://www.stratagene.com/sdmdesigner/default.aspx)). The primers were extended via thermal cycling with *PfuUltra* high-fidelity DNA polymerase (Section 2.9.3.1), and a mutated plasmid with staggered nicks was produced. The mutated plasmid was treated with the endonuclease *DpnI* to digest the methylated parental DNA (Section 2.9.3.2; Figure 3.8B), followed by transformation into *E. coli* TOP10 electrocompetent cells for nick repair and selection on LB agar containing 100  $\mu\text{g ml}^{-1}$  ampicillin. To confirm the presence of the mutation, the plasmid was sequenced directly (Core Genomic Facility, University of Sheffield).



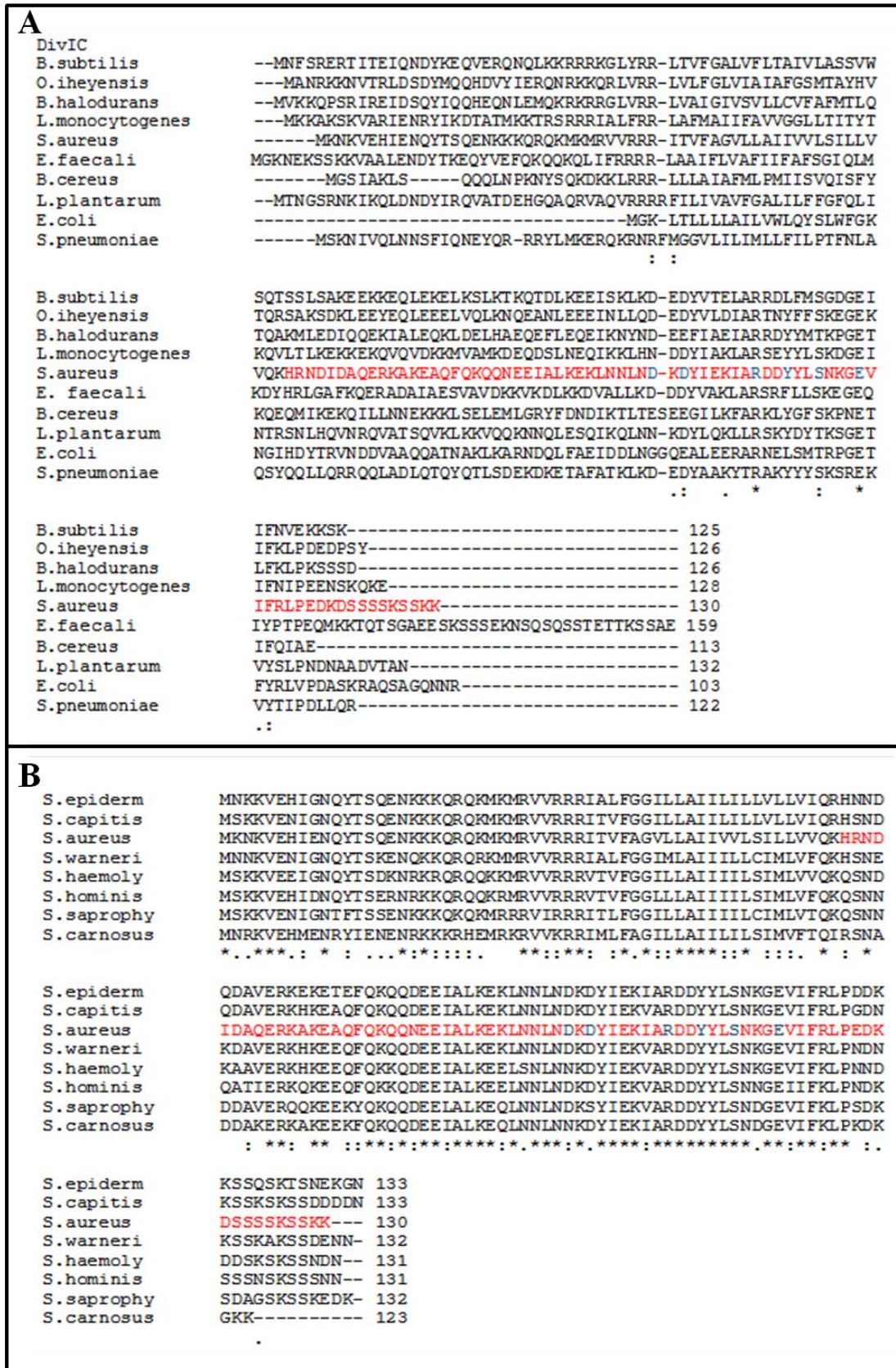


Figure 3.10 DivIC orthologs

**A.** A multiple sequence alignment (MSA) for DivIC proteins in different *species* was obtained using the ClustalW2 program. Organisms: *B. subtilis*, *Oceanobacillus iheyensis*, *B. halodurans*, *Listeria monocytogenes*, *S. aureus*, *E. faecalis*, *Bacillus cereus*, *Lactobacillus plantarum*, *E. coli*, and *S. pneumoniae*

**B.** A MSA for DivIC proteins in different species was obtained using the ClustalW2 program. Organisms: *S. epidermidis*, *Staphylococcus capitis*, *S. aureus*, *Staphylococcus warneri*, *S. haemolyticus*, *S. hominis*, *S. saprophyticus*, and *Staphylococcus carnosus*.

Asterisks indicate conserved residues, colons indicate conservative substitutions, and full stops indicate semi-conservative substitutions. The C-terminal residues are shown in red and the SDMs are shown in blue.

The plasmid construct was then transformed into *E. coli* BL21. Proteins were expressed by adding 1 mM IPTG to the culture. The induction of protein expression and solubility were tested as described previously (Section 2.12.2; Figure 3.9A), and the recombinant proteins were purified by nickel affinity chromatography (Section 2.12.4). The fractions were collected, pooled and dialysed against PBS (Section 2.12.5). The purity of the recombinant proteins was assessed by 15% (w/v) SDS-PAGE (Figure 3.9B).

### 3.2.4.2.3. Analysis of the peptidoglycan hydrolase activity of SDMs

Zymogram analysis (Section 2.14.3) was used to examine the potential peptidoglycan hydrolysis activity of the DivIC<sub>Sa</sub> mutants. Purified *S. aureus* cell wall was used as the substrate. The recombinant proteins were incubated in sodium citrate buffer at pH 5 in the presence and absence of MgCl<sub>2</sub>. In the presence of MgCl<sub>2</sub>, DivIC<sub>Sa</sub><sup>D92N</sup> produced a hydrolysis band, while DivIC<sub>Sa</sub><sup>R101A</sup> and DivIC<sub>Sa</sub><sup>Y104A</sup> produced weak hydrolysis bands (Figure 3.11A). In contrast, when MgCl<sub>2</sub> was absent from the renaturing solution, DivIC<sub>Sa</sub><sup>D92N</sup> produced weak zone of clearing, while DivIC<sub>Sa</sub><sup>R101A</sup> and DivIC<sub>Sa</sub><sup>Y104A</sup> had no detectable activities (Figure 3.11B). The activities of the recombinant proteins were clearly enhanced by the presence of Mg<sup>2+</sup> ions in the renaturing buffer. DivIC<sub>Sa</sub><sup>D92N</sup> exhibited wild-type activity, while DivIC<sub>Sa</sub><sup>R101A</sup> and DivIC<sub>Sa</sub><sup>Y104A</sup> displayed weaker hydrolytic activities. Replacing the conserved Arg<sup>101</sup> residue and the semi-conserved Tyr<sup>104</sup> residue with Ala inhibited the activity of the protein, suggesting that these residues are involved at the protein active site. A number of DivIC<sub>Sa</sub> SDMs (constructed by Amy Bottomley, University of Sheffield), including D94N, S107A and E111Q (Figure 3.8A), were also analysed by renaturation. None of these mutations impaired the enzymatic activity of the protein (data not shown). Thus, additional experiments were performed to map the protein active site and verify peptidoglycan hydrolase activity.

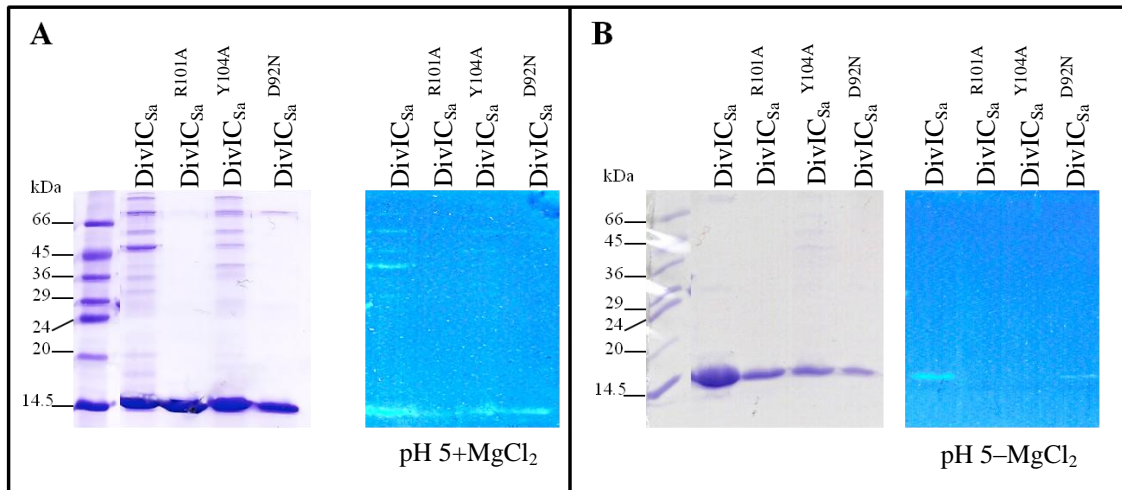


**Figure 3.11 Zymogram analyses of *S. aureus* DivIC site-directed mutants**

A 15% (w/v) renaturing SDS gel containing 0.1% (w/v) purified *S. aureus* peptidoglycan as a substrate is shown. A total of 10  $\mu$ g recombinant protein was used, and the gel was stained with Coomassie Blue (gels on the left) or renatured (gels on the right). Protein renaturation was performed at pH 5 in the presence and absence of 10 mM MgCl<sub>2</sub>.

A. SDS zymogram gel of DivIC<sub>Sa</sub> and its site-directed mutants at pH 5 with MgCl<sub>2</sub>.

B. SDS zymogram gel of DivIC<sub>Sa</sub> and its site-directed mutants at pH 5 without MgCl<sub>2</sub>.

### 3.2.4.3. Analysis of peptidoglycan hydrolysis using other techniques

#### 3.2.4.3.1. Native zymogram analysis

To verify the peptidoglycan hydrolase activity of DivIC and FtsL, we established a novel biochemical assay in which the proteins were not exposed to major physical or chemical changes, such as exposure to SDS, heat or 2-mercaptoethanol. The use of these factors could result in linearisation of the protein and the reduction of its disulphide bonds, consequently disrupting its enzymatic activity (Madigan and Martinko, 2006; Cadieux and Kadner, 1999). *S. aureus* cell walls that were unstained or prestained with Procion-Red MX-5B or RBB (Section 2.14.2) were used as substrates (Section 2.14.4) (Foster 1991, Zhou *et al.*, 1988). LMP agarose (0.1% (w/v), Sigma) was melted in renaturing solution (pH 5, with MgCl<sub>2</sub>) and cooled to 30°C; then, 1% (w/v) unstained or pre-stained *S. aureus* cell wall was added. The mixture was then poured onto the hydrophilic side of pre-warmed GelBond<sup>®</sup> film (Lonza) and allowed to set. Once a thin solid layer of gel had formed, 2 µl of 1:2 serial dilutions of protein were spotted on the gel and allowed to adsorb. The gel was then incubated in a humidifier overnight at 37°C. Zones of clearing within a dark background indicate peptidoglycan hydrolysis. Unstained *S. aureus* cell wall was stained with renaturing stain for 3 hr after incubation at 37°C, then destained with dH<sub>2</sub>O until zones of clearing were observed. YdiE was used as a negative control. Lysostaphin and mutanolysin were used as positive controls; both have strong hydrolase activity against the *S. aureus* cell wall (Kumar, 2008; Herbert *et al.*, 2007). Mutanolysin is preferred to lysostaphin as a positive control because the enzymatic activity of the latter decreases by 50% when MgCl<sub>2</sub> is added to the renaturing solution, whereas the enzymatic activity of mutanolysin increases in the presence of Mg<sup>2+</sup> ions (Zhou *et al.*, 1988; Yokogawa *et al.* 1974). A zone of clearing was readily apparent in the positive control compared to the recombinant proteins, which produced opaque spots (Figure 3.12A, Data not shown for prestained peptidoglycan with RBB). The opaque spots produced by the recombinant proteins appeared to be the result of precipitation rather than hydrolysis. As the activities of the recombinant proteins and the positive control were noticeably different, another gel was prepared in the same manner but was stained with crystal violet (Figure 3. 12B).

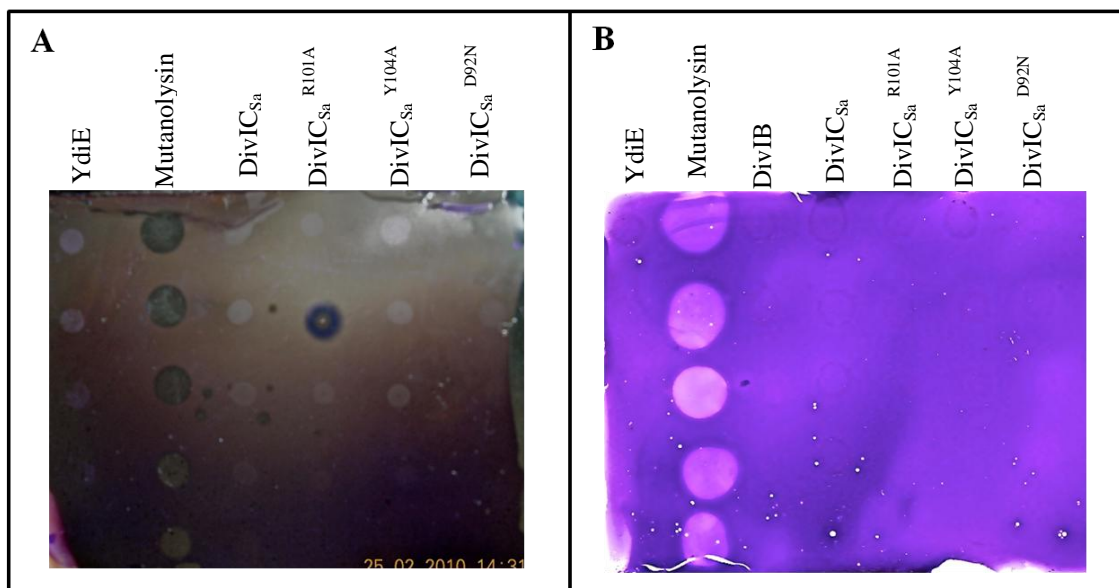


**Figure 3.12 Native zymogram analysis**

Native zymogram gels containing 1% (w/v) *S. aureus* cell wall, pre-stained with Procion-Red MX-5 (A) or pre-stained with Procion-Red MX-5B and then stained with crystal violet (B). A series of 1:2 dilutions of each protein (2  $\mu$ l) with an initial concentration of 1 mg ml<sup>-1</sup> were spotted on the native zymogram gel and then incubated for 3 h at 37°C. The gels were photographed or scanned immediately after incubation.

The positive control yielded clear zones, while YdiE, DivIC<sub>Sa</sub> and its mutants produced opaque zones on the gel. Because this experiment did not expose the protein to any denaturation factors that would disrupt its enzymatic activity, the lack of observed clearing suggests that DivIC<sub>Sa</sub> may not be a true peptidoglycan hydrolase.

#### **3.2.4.3.2. RBB release assay**

A semi-quantitative method, called a dye release assay (Zhou *et al.*, 1988; Morlot *et al.*, 2010; Uehara *et al.*, 2010), was used to verify the hydrolase activity of the recombinant protein. The peptidoglycan substrate was dyed with RBB, which binds to the glycan hydroxyl group to form a stable linkage (Zhou *et al.*, 1988). The release of soluble dyed products from the substrate through the hydrolytic activity of the enzyme was then measured (Morlot *et al.*, 2010; Uehara *et al.*, 2010). Several different substrates were tested, namely *S. aureus*, *B. subtilis* and *E. coli* peptidoglycans. A 20- $\mu$ l aliquot of 10 mg l<sup>-1</sup> RBB-stained substrate was incubated with 0.1 mg l<sup>-1</sup> recombinant protein for 30 min at 37°C in 200  $\mu$ l of 1 $\times$  PBS plus 20 mM MgCl<sub>2</sub>. The reactions were then stopped by incubation at 95°C for 5 min. Insoluble substrate was removed by centrifugation at 14,000 rpm at RT for 20 min. The absorbance of the free soluble dye-coupled materials in the supernatant was measured at 595 nm (Section 2.14.5) (Morlot *et al.*, 2010; Uehara *et al.*, 2010). Peptidoglycan only and proteins only were used as negative controls, while mutanolysin was used as positive control. Mutanolysin released the dye-coupled product in the supernatant, signifying peptidoglycan hydrolysis, whereas DivIC<sub>Sa</sub>, DivIC<sub>Sa</sub> SDMs, DivIC<sub>Sa</sub> <sup>$\Delta$ 118-130</sup> or FtsL (Figure 3.13) did not display hydrolase activities under any conditions, similar to the results of the negative controls.

#### **3.2.4.4. Peptidoglycan binding analysis**

##### **3.2.4.4.1. Affinity binding assay**

The capability of DivIC<sub>Sa</sub> to hydrolyse peptidoglycan was not clear. Both the recombinant protein and the mutant proteins produced unambiguous zones of clearing on zymogram gels, but no hydrolase activities were detected in a native zymogram assay or RBB release assay.

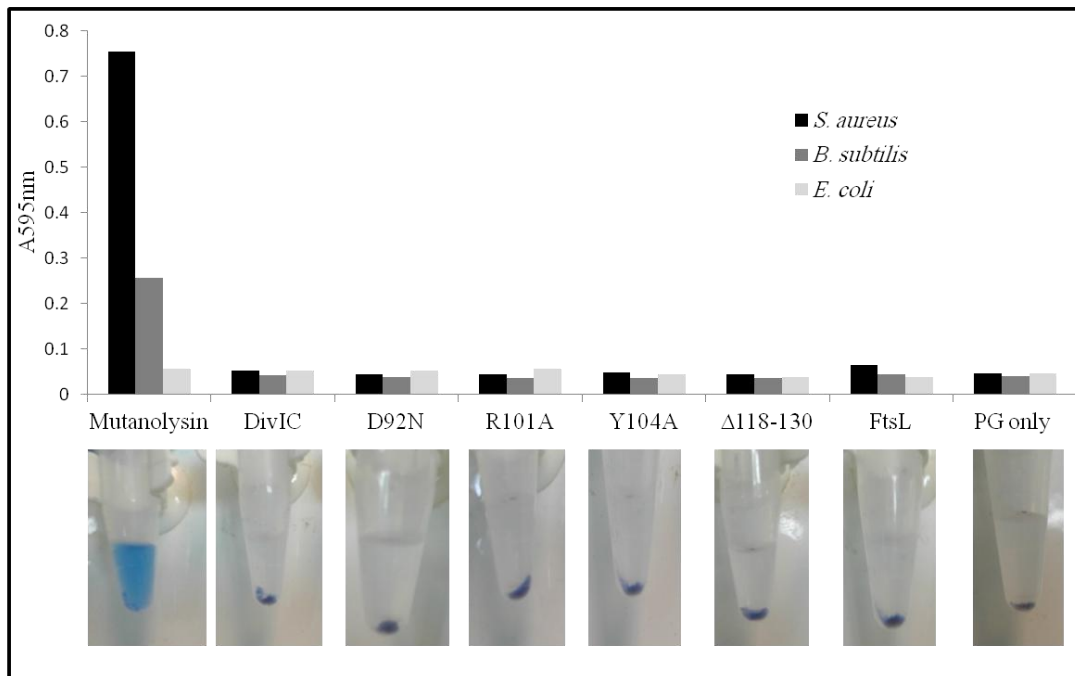


**Figure 3.13 RBB release assay**

A Semi-quantitative RBB release assay was performed to investigate peptidoglycan hydrolysis. RBB pre-stained PG (from *S. aureus*, *B. subtilis* or *E. coli*) was incubated with the designated proteins ( $0.1 \text{ mg ml}^{-1}$ ) for 30 min at  $37^\circ\text{C}$ . Undigested peptidoglycan was removed by centrifugation, and the absorbance of the free soluble dye-coupled materials in the supernatant was measured at 595nm. The images below the graph show the reaction tubes after the incubation and centrifugation steps.



The zones of clearing observed in the zymography assay seem likely to have been produced due to the strong binding of the proteins to peptidoglycan, which prevents the dye from accessing the substrate. A similar phenomenon was observed for proteins that bind to cell walls and enhance the hydrolytic activity of other hydrolases. These proteins produce a (false) positive zymogram signal but do not display detectable hydrolase activity in solution-based assays (Bernhardt and de Boer, 2004; Morlot *et al.*, 2010; Uehara *et al.*, 2010; Gutierrez *et al.*, 2010). Therefore, we investigated whether DivIC<sub>Sa</sub> could bind to peptidoglycan using a qualitative affinity binding analysis (Kern *et al.*, 2008). In brief, 0.1 mg ml<sup>-1</sup> of purified protein was mixed with different peptidoglycan concentrations in a 20 mM sodium citrate buffer, pH 5, containing 1 mM MgCl<sub>2</sub> and incubated for 2 h on a rotary shaker at 37°C. The mixture was then centrifuged for 10 min at 14,000 rpm. To remove non-specifically bound proteins from the peptidoglycan, the pellet was washed with 200 µl buffer and centrifuged again.

Both the supernatant (S) and pellet (P) fractions were boiled in SDS loading buffer and analysed by 15% (w/v) SDS-PAGE. If bound to peptidoglycan, the protein will appear in the pellet fraction rather than the supernatant; otherwise, the protein will remain in the supernatant fraction. The protein interactions with peptidoglycan (PG) in the presence and absence of WTA were examined. DivIC<sub>Sa</sub> binds to *S. aureus* PG in a concentration-dependent manner; as the PG concentration decreases, increasing amounts of DivIC<sub>Sa</sub> appear in the supernatant fraction (Figure 3.14A). In the presence of WTA, DivIC<sub>Sa</sub> was found in the pellet fraction when incubated with *S. aureus* (Figure 3.14A) and *B. subtilis* PG (Figure 3.14B), suggesting that the binding affinity of DivIC<sub>Sa</sub> for peptidoglycan is enhanced by binding to WTA and that this binding is not substrate-specific. The binding domain of DivIC was then mapped using the previously constructed mutants (Section 3.2.4.2.1 and Section 3.2.4.2.2). The binding affinities of DivIC<sub>Sa</sub><sup>D92N</sup> and DivIC<sub>Sa</sub><sup>Δ118-130</sup> to *S. aureus* PG with or without WTA (Figure 3.15) were similar to that of wild-type (Figure 3.15). DivIC<sub>Sa</sub><sup>Δ118-130</sup> and DivIC<sub>Sa</sub><sup>D92N</sup> were only observed in the pellet fraction at high PG concentrations without WTA; as the PG concentration decreased, the amount of bound protein decreased, and hence the proteins were found in both the supernatant and pellet fractions (Figure 3.15).

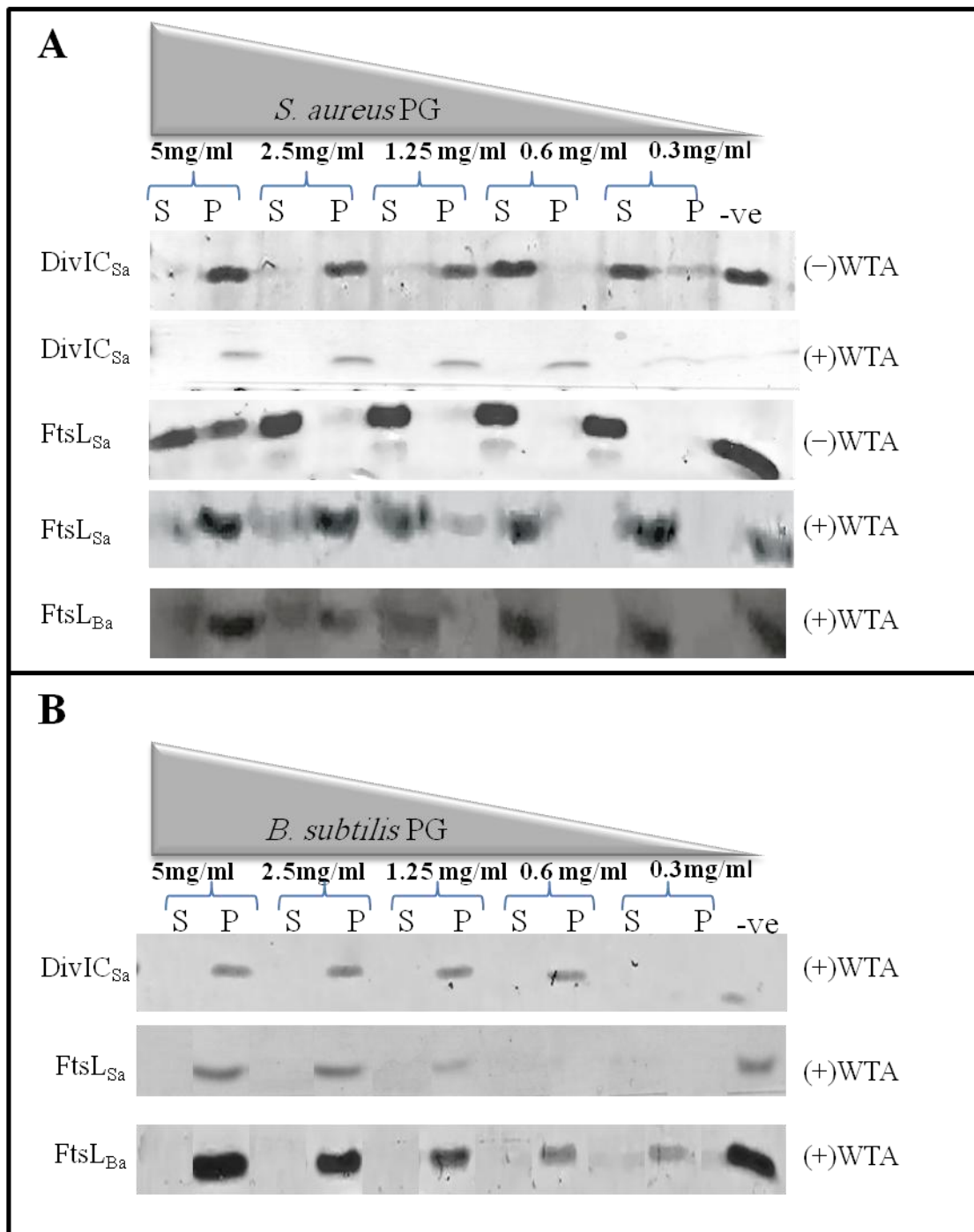


**Figure 3.14 Cell wall affinity binding assay of DivIC<sub>Sa</sub>, FtsL<sub>Sa</sub> and FtsL<sub>Bs</sub>**

The ability of the recombinant proteins to bind to purified *S. aureus* or *B. subtilis* cell walls was examined. The binding buffer consisted of 20 mM sodium citrate at pH 5 and 10 mM MgCl<sub>2</sub>. Several substrate concentrations with and without WTA were incubated with 0.1 mg ml<sup>-1</sup> recombinant protein.

A. *S. aureus* peptidoglycan with and without WTA was incubated with recombinant *S. aureus* DivIC, *S. aureus* FtsL and *B. subtilis* FtsL.

B. *B. subtilis* peptidoglycan with WTA was incubated with recombinant *S. aureus* DivIC, *S. aureus* FtsL and *B. subtilis* FtsL.

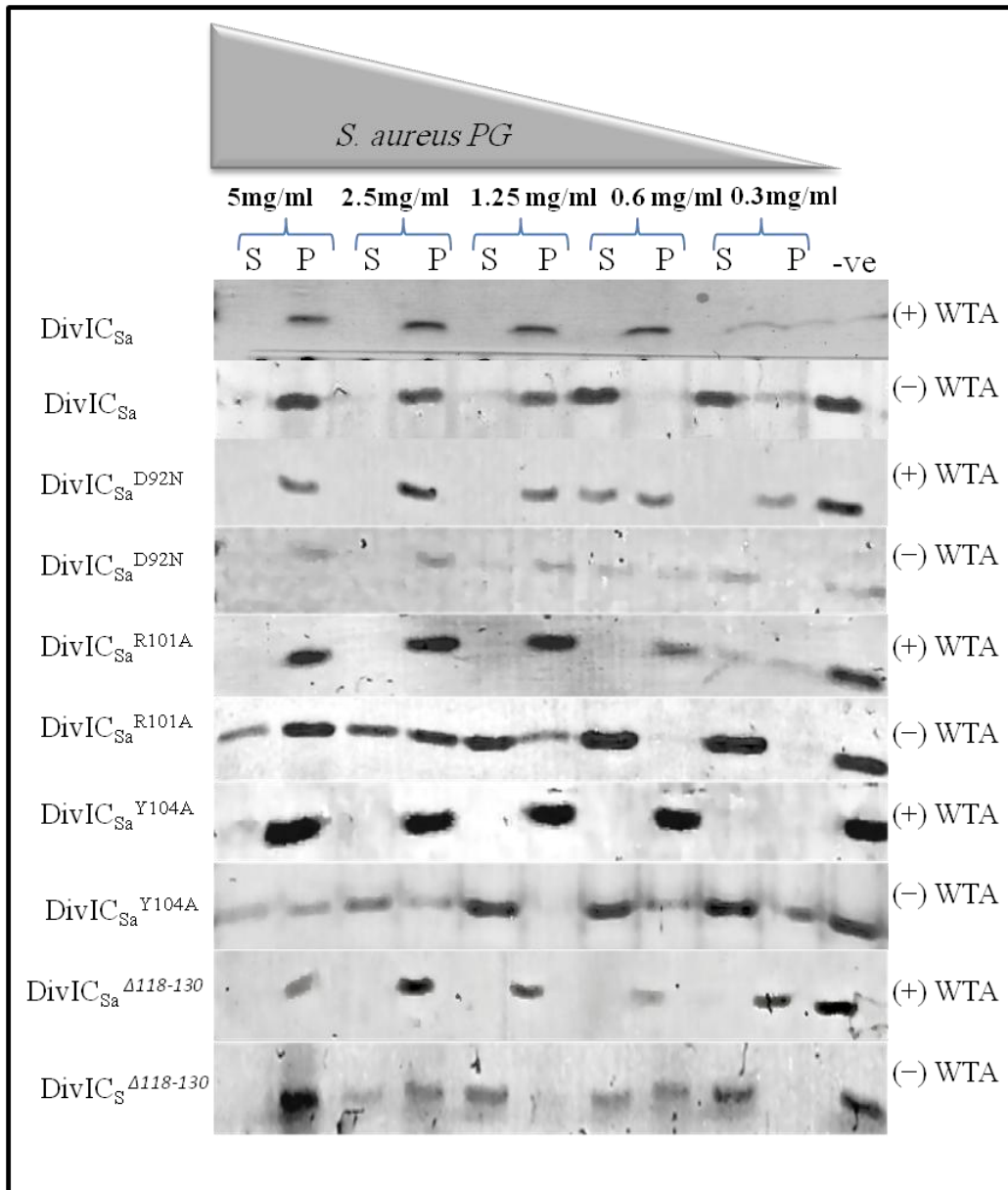


**Figure 3.15 Cell wall affinity binding assays of *S. aureus* DivIC mutants**

The ability of the recombinant proteins to bind to purified *S. aureus* cell walls was examined. The binding buffer consisted of 20 mM sodium citrate at pH 5 and 10 mM MgCl<sub>2</sub>. Several substrate concentrations with and without WTA were incubated with 0.1 mg ml<sup>-1</sup> recombinant protein. *S. aureus* peptidoglycan with and without WTA as incubated with *S. aureus* DivIC, *S. aureus* site-directed mutants and truncated *S. aureus* DivIC.

By contrast, when incubated with *S. aureus* PG plus WTA, the protein was detected in the pellet fraction, similar to wild-type (Figure 3.15). The ability of DivIC<sub>Sa</sub><sup>R101A</sup> and DivIC<sub>Sa</sub><sup>Y104A</sup> to bind to *S. aureus* PG was much lower than that of wild-type (Figure 3.15) as they were detected in the pellet and supernatant fractions at higher PG concentrations. The zymography results (Section 3.2.4.2.3) demonstrated that DivIC<sub>Sa</sub><sup>R101A</sup> and DivIC<sub>Sa</sub><sup>Y104A</sup> did not produce any zone of clearing on the SDS zymogram gel when incubated in pH 5 renaturing buffer without Mg<sup>2+</sup> ions (Figure 3.11B), while activities that were lower than those of wild-type were detected in pH 5 renaturing buffer plus MgCl<sub>2</sub> (Figure 3.11A). These results suggest that point mutations of these residues altered the biochemical activity of the protein. FtsL<sub>Sa</sub> bound *S. aureus* PG only at 5 mg ml<sup>-1</sup> PG (Figure 3.14A), and FtsL<sub>Bs</sub> bound *S. aureus* PG at  $\geq 2.5$  mg ml<sup>-1</sup> PG (Figure 3.14A). FtsL<sub>Sa</sub> bound *S. aureus* PG plus WTA only at  $\geq 1.25$  mg ml<sup>-1</sup> PG (Figure 3.14A), while FtsL<sub>Bs</sub> was detected in the pellet fraction when incubated with *B. subtilis* PG plus WTA (Figure 3.14B).

Interestingly, when FtsL<sub>Sa</sub> was incubated with *B. subtilis* PG plus WTA, the protein was observed in the pellet fraction at all PG concentrations (Figure 3.14B). In contrast, FtsL<sub>Ba</sub> only bound *S. aureus* PG plus WTA at higher concentrations (Figure 3.14A). These results indicate that, FtsL<sub>Sa</sub> binds to the PG-containing WTA of *B. subtilis* with an increased affinity compared to the PG-containing WTA of *S. aureus*. A similar phenomenon was observed for *S. aureus* DivIB, which bound to *B. subtilis* PG plus WTA better than to *S. aureus* PG plus WTA (Bottomley, 2011). In contrast, DivIC<sub>Sa</sub> bound equally well to *S. aureus* and *B. subtilis* PG plus WTA (Figure 3.14A and Figure 3.14B, respectively). The binding affinity of DivIC<sub>Sa</sub> for peptidoglycan was not affected by the difference in the peptidoglycan compositions of *S. aureus* and *B. subtilis*.



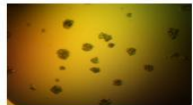
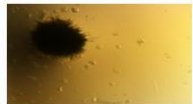


### 3.2.5 Structural analysis

The potential active/binding site of a protein can be mapped by solving the protein's crystal structure. To complement our site-directed mutagenesis data and provide insights into the previous results, we attempted to obtain a crystal structure of DivIC<sub>Sa</sub>. X-ray crystallography is the best established technique for studying the

3D structures of proteins and other biological macromolecules (Smyth and Martin, 2000; Luft *et al.*, 2003). However, it is often challenging to obtain a 3D crystal structure; this process requires the success of a number of steps, including gene cloning, protein overexpression, purification, concentration, quality determination, crystallisation, diffraction and, finally, structure resolution. Crystallisation is usually the main obstacle in this process because well-ordered protein crystals cannot be obtained unless the protein is of sufficiently high quality (Smyth and Martin, 2000; Stevens, 2000; Luft *et al.*, 2003). The protein must also be at high concentration in solution to facilitate its precipitation, and protein crystals form only under certain conditions (Smyth and Martin, 2000). The process of protein crystallisation typically consists of two stages. First, an initial screening of a range of conditions in combination such as buffers, pH, salts and precipitants is performed to identify the optimal conditions for crystal growth. Second, these initial conditions must be optimised for the production of larger crystals for diffraction (Smyth and Martin, 2000; Luft *et al.*, 2003). The overexpression of the recombinant DivIC<sub>Sa</sub> extracellular domain was induced by adding 1 mM IPTG to the culture, followed by incubation for 4 h at 37°C. The protein was first purified by nickel affinity chromatography, and all fractions that gave a positive absorbance and showed the expected size band upon 15% (w/v) SDS-PAGE were pooled (data not shown). The pooled sample was concentrated by centrifugation at 5,300 rpm at 4°C for 10 min in a Vivaspın20 ultrafiltration column (3,000 MWCO PES; Sartorius) that was pre-equilibrated with 50 mM Tris-HCl buffer pH 8. The protein concentration was determined by Bradford assay (Section 2.11.5), and the centrifugation step was repeated until the required protein concentration was reached. The concentrated protein sample was then subjected to gel filtration as a second purification step (Section 2.15). The molecular weight of the protein was determined by comparison with protein standards of known sizes (Gel Filtration Calibration Kit, GE Healthcare). The molecular weight of the protein was then estimated as 19.6 kDa, as described in Section 2.15. The estimated molecular weight of the fraction was larger than the predicted molecular weight of the DivIC<sub>Sa</sub> extracellular domain, 8.9 kDa, consistent with the results obtained in Section 3.2.3. The fractions corresponding to the peak (data not shown) were collected and pooled, and the purity of the sample was analysed by 15% (w/v) SDS-PAGE followed by staining with Coomassie Blue (data not shown).

A purity of at least 90% is desirable because impurities could interfere with crystallisation, for example, by inhibiting the growth of the crystal or producing improper crystals that will not diffract or scatter the X-rays (Benvenuti and Mangani, 2007). A preliminary screening of crystallisation conditions was performed using the sitting-drop vapour diffusion system and a Hydra II automated pipetting robot (Thermo-Scientific). Commercial sparse matrix crystallisation screen plates (Qiagen-Nextal Biotechnology) were used. Each well of the 96-well plate contains a cocktail of different salts, buffers and precipitants at different pH values. Approximately 2 to 4  $\mu\text{g}$  of protein was added to a total of 20  $\mu\text{l}$  of cocktail per plate. The plates were then incubated at 4°C, and the drops were examined under a light microscope for crystal growth after 5 days and approximately once per week thereafter. The results obtained from the initial screening varied; some of the conditions resulted in precipitation, while others did not. Conditions that produced microcrystalline droplets, spherulites, microcrystals, dendritic crystals or tiny crystals were further optimised to obtain larger crystals (Figure 3.16). Drops that resulted in precipitation were checked again after a few weeks for the presence of crystals. Crystals have been reported to grow from precipitates after 1 month (Ng *et al.*, 1996). Furthermore, to optimise the initial conditions and improve the size and shape of the crystals, the successful conditions were reproduced in a 24-well plate.

A number of factors were further optimised, including the buffer pH and the concentrations of protein, salt and precipitant (Smyth and Martin, 2000; Benvenuti and Mangani, 2007). The method of choice for optimisation was hanging-drop vapour diffusion. The crystallisation cocktails were prepared manually based on the initial compositions given by the manufacturer (QIAGEN). The primary factors that were adjusted were the protein concentration, the buffer pH and the concentration of the precipitant. Buffer pH values and precipitant concentrations both below and above those that produced crystals in the initial screening were tested. Different combinations of the mother liquor cocktails, buffer and precipitant were placed in each well. A 40- $\mu\text{l}$  volume of precipitant and 40  $\mu\text{l}$  of buffer were mixed together in water, with a total volume of 400  $\mu\text{l}$  of reservoir buffer per well. A 1- $\mu\text{l}$  aliquot of the protein plus 1  $\mu\text{l}$  of the mother liquor were placed onto pre-siliconised glass coverslips (a hydrophobic surface) and mixed by gentle pipetting.

Morphology	Description	Protein concentration mg ml <sup>-1</sup>	Protein buffer	Crystallisation cocktail
	Dendrite	18	10 mM MES pH6.5	0.2 M Tri-potassium citrate, 20 % (w/v) PEG 3350
	Microcrystalline droplet (Phase separation)	18	10 mM MES pH6.5	0.2 M sodium nitrate, 20 % (w/v) PEG 3350
	Gelatinous precipitate	18	10 mM MES pH6.5	0.1 M MT buffer pH7, 25 % (w/v) PEG 1500
	Spherulites (Sea urchins)	10	10 mM Tris pH7.5	0.1 M MT buffer pH6, 25 % (w/v) PEG 1500
	Microcrystals	10	10 mM Tris pH7.5	0.02 M MgCL <sub>2</sub> , 0.1M HEPES pH7.5, 22 % (w/v) polyacrylic acid 5100, sodium salt
	Microcrystals	10	10 mM Tris pH7.5	0.2 M ammonium acetate, 0.1 M Bis-Tris pH5.5, 25 % (w/v) PEG 3350

**Figure 3.16 Initial crystallisation condition screening results for recombinant *S. aureus* DivIC**

The coverslip was then placed upside-down on top of the well containing the corresponding buffer and sealed. The plate was then incubated at 4°C, and the drops were checked under the microscope for signs of crystallisation after five days and once per week thereafter. Again, the results varied; some conditions yielded precipitation, oils, microcrystals and spherulites (data not shown). Attempts to obtain larger crystals have thus far been unsuccessful due to the complexity of the factors that can affect protein crystallisation. No further structural investigations could be performed due to time limitations.

### **3.3 Discussion**

#### **3.3.1 Oligomeric states of DivIC and FtsL**

Previous work in our laboratory using a bacterial two-hybrid system identified protein-protein interactions between *S. aureus* DivIC and FtsL, including self-interactions and interactions with each other as well as with other cell division proteins (Steele *et al.*, 2011, Figure 1.4A). Gel filtration analysis indicated that the extracellular domains of *S. aureus* DivIC and FtsL likely exist as dimers (Figure 3.5 and Figure 3.6). These analyses of *S. aureus* DivIC and FtsL indicate that self-associations and the interactions between these two proteins are mediated mainly by the extracellular domains of these proteins, which contain coiled coil motifs. The self-association of DivIC and FtsL have been observed in other bacterial species. The periplasmic domains of FtsL and DivIC in *S. pneumoniae* were found to homodimerise when the cytoplasmic and transmembrane domains were replaced by artificial coiled coil motifs (Noirclerc-Savoye *et al.*, 2005). An *E. coli* FtsL homodimer was detected by Western blotting in strains that express only the periplasmic and transmembrane domains, and the introduction of point mutations of two of the leucine residues in the coiled coils region reduces the dimerisation of the protein (Ghigo and Beckwith, 2000). A yeast two-hybrid system revealed that FtsL but not DivIC was self associated (Daniel *et al.*, 2006). Previous work in our lab (Kabli, 2009) demonstrated that there is no direct interaction between the C-terminal domains of DivIC and FtsL under the conditions used in the gel filtration analysis. However, a similar phenomenon was observed for the C-terminal domains of *B. subtilis* FtsL and DivIC, and heterodimerisation of the proteins' extracellular



domains cannot be excluded because these domains contain coiled coil motifs (Robson *et al.*, 2002; Figure 3.1E and Figure 3.2E). *E. coli* two-hybrid and co-immunoprecipitation assays have demonstrated that there is an interaction between full-length FtsL and FtsB, indicating that these proteins exist as a complex *in vivo*, and also demonstrated that this complex interacts with another cell division protein, FtsQ, to form a trimeric FtsL/FtsB/FtsQ complex (DiLallo *et al.*, 2003; Buddelmeijer and Beckwith, 2004). “Swap constructs” were made by swapping similar domains between proteins to characterise the importance of specific domains for interaction and localisation. These experiments confirmed the importance of the periplasmic domain containing the leucine zipper motif and the transmembrane domain of FtsL in the formation of the heterodimer with FtsB (Buddelmeijer and Beckwith, 2004). In *B. subtilis*, an interaction between full-length DivIC and FtsL was observed in a yeast two-hybrid system, and the C-terminal domains of FtsL and DivIC were detected by native SDS-PAGE. Moreover, interactions between DivIB, DivIC and FtsL were also detected using a yeast two-hybrid system (Daniel *et al.*, 2006; Sievers and Errington, 2000b). These results indicate that the oligomeric states of FtsL and DivIC are important for their stability and physiological functions in the organism.

### **3.3.2 DivIC and FtsL peptidoglycan hydrolase activity**

Zymographic analysis of the wild-type and mutant *S. aureus* DivIC (Figure 3.7A and Figure 3.11) revealed that the extracytoplasmic domain has putative peptidoglycan hydrolase activity, in the presence and absence of divalent cations, at acidic pH, the likely pH of the inner wall zone in which this bitopic protein resides. Although the pI of DivIC is greater than 7, it has been suggested that peptidoglycan hydrolases reside in the inner wall zone if their pI is less than 7 and bind to the outer cell wall surface if their pI is greater than 7 (Matias and Beveridge, 2005; Buist *et al.*, 2008). In contrast, the *S. aureus* FtsL extracytoplasmic domain did not exhibit any hydrolase activity as detected by SDS zymogram analysis (Figure 3.7B). Peptidoglycan hydrolases are crucial for cell growth and division. Certain bacteria appear to have numerous hydrolases that exhibit redundant activities (Smith *et al.*, 2000). These hydrolases may have several functions; they participate in daughter cell separation during cell division by cleaving the septum (Heidrich *et al.* 2001; Heidrich *et al.* 2002) and are involved in cell wall turnover, during which

they degrade peptidoglycan to products that can be used by the peptidoglycan biosynthetic enzymes (Vollmer *et al.*, 2008, Biswas *et al.*, 2006; Höltje, 1995; Doyle *et al.*, 1988). The association of hydrolases with septum initiation requires the nicking of the existing cell wall during cell division, followed by the insertion of the new peptidoglycan beneath the existing cell wall (Vollmer *et al.*, 2008). Enzymes that are involved in cell separation have been identified recently in gram-negative bacteria, including endopeptidases that contain the LytM domain and LytC-type amidases such as AmiA, AmiB and AmiC. Mutant cells lacking AmiA, AmiB and AmiC are unable to divide and hence produce long chains of cells (Bernhard and de Boer, 2003; Bernhard and de Boer, 2004; Uehara *et al.*, 2009; Uehara *et al.*, 2010). DipM, another peptidoglycan hydrolase, is essential for the final stage of cell division and has recently been identified in *C. crescentus* (Moll *et al.*, 2010, Goley *et al.* 2010; Poggio *et al.* 2010). The hydrolytic activity of the DipM LytM domain has been demonstrated by zymography assay, although its activity is weak compared to that of the full-length protein (Moll *et al.*, 2010). PBP7 and PBP4 are also peptidoglycan hydrolases that are involved in septum breakage; the lack of these proteins results in a failure of cell division and the production of long chains of non-separated *E. coli* cells (Priyadarshini *et al.*, 2006). EnvC and NlpD are components of the cell division machinery that contain the LytM peptidase domain, which is essential for proper cell separation (Bernhardt and de Boer, 2004; Uehara *et al.*, 2009; Uehara *et al.*, 2010). Although their hydrolytic activities have been detected by zymogram assay (Bernhardt and de Boer, 2004) but not by solution assay, EnvC enhances the activities of AmiA and AmiB, and NlpD enhances the activity of AmiC in solution assays. Several of the residues necessary for catalysis are missing in the LytM domain of EnvC and NlpD (Uehara *et al.*, 2010). Moreover, *B. subtilis* SpoIID, a lytic transglycosylase, produces a zone of clearing on a zymogram gel, indicating hydrolysis; however, it did not exhibit any hydrolase activity in solution-based assays (Morlot *et al.*, 2010). This enzyme cannot hydrolyse glycan strands on its own; it requires another hydrolytic enzyme, SpoIIP, which breaks the cross-links between the cell wall and removes the stem peptides. Thus, the observation of clear zones on the SDS zymogram gels for EnvC, NlpD and SpoIID were most likely due to the binding of the enzyme to the substrate in the gel, resulting in the exclusion of the dye from the area where this enzyme migrates (Morlot *et al.*, 2010; Uehara *et al.*, 2010). A similar phenomenon

might occur for DivIC<sub>Sa</sub>, which also produced an unequivocal zone of clearing by SDS gel zymography assay (Figure 3.7A) but no activity in the RBB release assay (Figure 3.13). A native zymogram assay with pre-stained peptidoglycan was developed to exclude the possibility that false-positive clear zones were obtained in the SDS zymogram gel. However, DivIC<sub>Sa</sub> did not exhibit hydrolytic activity in this assay, while the positive controls displayed an obvious zone of clearing (Figure 3.12). This result does not rule out a hydrolytic function for DivIC<sub>Sa</sub>; this protein might have a function similar to that of EnvC, NlpD or SpoIID (Uehara *et al.*, 2010; Morlot *et al.*, 2010). Therefore, DivIC might work together with another peptidoglycan hydrolase involved in cell division. DivIC<sub>Sa</sub> may also act as a peptidoglycan hydrolase activator during cell division, enhancing or activating peptidoglycan hydrolases, similar to the functions of EnvC and NlpD (Uehara *et al.*, 2010). A temperature-sensitive mutation of DivIC in *B. subtilis* causes septum formation to fail, resulting in a continuation of cell growth without division and eventual cell lysis. The N-terminal and membrane spanning domains of DivIC are crucial for cell division at high temperature, and a small amount of DivIC is required for proper cell division at any temperature (Levin and Losick, 1994; Katis and Wake, 1999). Thus, these previous findings suggest that DivIC is involved in cell division. In contrast, no hydrolytic activity was detected for FtsL using zymography (Figure 3.7B) or solution-based assays (Figure 3.13). However, the *B. subtilis*  $\Delta$ *ftsL* mutant exhibits septation blockage at the early stage of the cell cycle, leading to filamentous growth. Cells lacking FtsL fail to activate sigma factors during sporulation, suggesting the importance of FtsL during sporulation as well as daughter cell separation (Daniel *et al.*, 1998).

### 3.3.3 DivIC and FtsL peptidoglycan binding activity

The unequivocal clear zones observed by zymography for DivIC<sub>Sa</sub> and its mutants but not for FtsL<sub>Sa</sub> or the negative controls suggest that the dye blockage was not random but rather highly specific. Similarly, in the control SDS zymogram gel (Figure 3.7D), DivIB and PBP1 produced obvious zones of clearing, whereas BSA and YdiE did not produce any clear zone. The clear zone could be produced because the strong binding of the enzyme to the cell wall substrate prevented the

dye from access. Similar observations have been made for enzymes such as *E. coli* EnvC and NlpD, *C. crescentus* DipM and *B. subtilis* SpoIID, all of which produce positive results in zymogram gels but not in liquid assays (Uehara *et al.* 2010; Morlot *et al.* 2010; Moll *et al.* 2010). Sedimentation assays have also shown the affinity of DipM and SpoIID for peptidoglycan (Morlot *et al.* 2010; Moll *et al.* 2010). The sedimentation assay in this study showed that FtsL<sub>Sa</sub>, FtsL<sub>Ba</sub>, DivIC<sub>Sa</sub> and DivIC<sub>Sa</sub> site-directed mutants and a truncated DivIC<sub>Sa</sub> fragment (Figure 3.14 and Figure 3.15) bind to peptidoglycan, even though the binding affinity of DivIC<sub>Sa</sub> is higher than that of FtsL<sub>Sa</sub>. This has raised the question of whether DivIC<sub>Sa</sub> and FtsL<sub>Sa</sub> contain peptidoglycan-binding residues in their sequences (Figure 3.1 and Figure 3.2). Many peptidoglycan hydrolases contain domains that bind to peptidoglycan or its associated components and enhance their enzymatic activities. These domains are referred to as cell wall-binding domains (CBDs) (Buist *et al.*, 2008; Moll *et al.*, 2010). FtsN is an essential bitopic cell division protein, and its C-terminal domain contains a CBD (Dai *et al.*, 1996; Wissel and Weiss, 2004; Muller *et al.*, 2007). However, this domain is not required for cell division, even though this binding occurs during division (Ursinus *et al.*, 2004; Moll and Thanbichler, 2009). The presence of the CBDs in some of the cell division proteins is sufficient for binding to the septum to localise these proteins to the septal ring during the cell division process (Arends *et al.*, 2010). Affinity binding assays have shown that the CBDs in *E. coli* and *C. crescentus* FtsN bound to peptidoglycan (Ursinus *et al.*, 2004; Moll and Thanbichler, 2009). In addition, this technique has shown that approximately 80% of recombinant (*E. coli* purified) His-tagged CBDs from DedD, RlpA and DamX, was present in the pellet fraction bound to peptidoglycan (Arends *et al.*, 2010). *A. hydrophila* ExeA contains CBD in its periplasmic region (Li and Howard, 2010). Sedimentation and other assays, including gel filtration, *in vivo* cross-linking and native PAGE, have shown that *A. hydrophila* ExeA interacts with peptidoglycan. Substitution mutations in any of the highly conserved residues in its CBD reduce its binding affinity to peptidoglycan by two-fold *in vitro* (Li and Howard, 2010) and *in vivo* (Howard *et al.*, 2006), indicating the specificity of the binding to the peptidoglycan backbone rather than other associated components and suggesting involvement of these residues in the interaction (Howard *et al.*, 2006; Li and Howard, 2010). To some extent, similar observations were made for the DivIC<sub>Sa</sub> site-directed mutants; DivIC<sub>Sa</sub><sup>R101A</sup> and DivIC<sub>Sa</sub><sup>Y104A</sup> exhibited reduced

binding affinities to peptidoglycan (Figure 3.15) compared with the wild-type DivIC<sub>Sa</sub> (Figure 3.14). This result highlights the importance of these residues. Unfortunately, our attempts to solve the structure of DivIC<sub>Sa</sub> could not be completed due to time limitations, but the determination of this structure would permit a complete analysis of the protein structure. Furthermore, both DivIC<sub>Sa</sub> and FtsL<sub>Sa</sub> bound to *S. aureus* and *B. subtilis* PG with WTA, and these binding events were unaffected by differences in the peptidoglycan composition of *S. aureus* and *B. subtilis*. For instance, the stem peptide in *S. aureus* contains L-lysine, whereas in *B. subtilis*, it contains meso-diaminopimelic acid. The cross-linking of *S. aureus* PG differs from that of *B. subtilis* PG. In *B. subtilis*, the cross-link is formed by the attachment of the D-alanine of one stem peptide to the meso-diaminopimelic acid of another stem peptide, whereas in *S. aureus*, the cross-link is formed via an amino acid bridge that contains five glycine residues. In addition, the degree of stem peptide cross-linking in *S. aureus* is greater than that observed in *B. subtilis*. Approximately 90% of stem peptides are cross-linked in *S. aureus*, whereas approximately 63% are cross-linked in *B. subtilis* (Scheffers and Pinho, 2005). Consequently, FtsL<sub>Sa</sub> and *S. aureus* DivIB might bind more effectively to *B. subtilis* PG compared to *S. aureus* PG, and this might be attributed to the reduced frequency of cross-linked stem peptides in *B. subtilis*, which facilitates the access of the protein to its binding site within the substrate. The ability of DivIC<sub>Sa</sub> to bind to PG in the presence or absence of WTA reveals that this protein may interact with the cell wall directly or via WTA. By contrast, FtsL<sub>Sa</sub> binding to the cell wall is enhanced due to the presence of WTA, suggesting that it has a much lower affinity for PG than DivIC<sub>Sa</sub>. The zymography assays demonstrated that DivIC<sub>Sa</sub> produced an obvious zone of clearing, while FtsL<sub>Sa</sub> did not produce any zone of clearing on a renaturing gel (Figure 3.7), consistent with a stronger cell wall binding affinity for DivIC<sub>Sa</sub> than for FtsL<sub>Sa</sub>.

However, DivIC<sub>Sa</sub> and FtsL<sub>Sa</sub> exhibit reduced binding affinities to *S. aureus* peptidoglycan (i.e., they require increased concentrations to achieve the same level of binding) without WTA, even though the binding affinity of DivIC<sub>Sa</sub> is stronger than that of FtsL<sub>Sa</sub>, indicating that the binding to peptidoglycan is direct, not through indirectly associated components. The environmental pH of the gram-

positive cell wall is likely acidic (Calamita *et al.* 2001). It has been reported that *Lactococcus lactis* AcmD, which contains a CBD, binds to the cell wall at pH 4, which is lower than the pI of the domain (Buist *et al.*, 2008). DivIC<sub>Sa</sub> and FtsL<sub>Sa</sub> were observed to bind to peptidoglycan at pH 5, which is also lower than the pI values of these proteins (Table 3.1), indicating that this binding is mainly due to a non-covalent ionic interaction. The effect of MgCl<sub>2</sub> on binding of the recombinant proteins to peptidoglycan was investigated as this has previously been shown to effect *B. subtilis* CwlA binding to the cell wall (Foster, 1991). Bioinformatic analysis using BLASTp showed that the *S. aureus* DivIC and FtsL amino acid sequences share no similarities with any of the known peptidoglycan hydrolases, peptidoglycan binding domains or proteins containing peptidoglycan binding domains. A similar result was found in our lab for DivIB (Bottomley, 2011). This shows the importance of the C-terminal domains of DivIC and FtsL as a novel peptidoglycan binding motifs.

### 3.4 Future work

This study demonstrates that *S. aureus* DivIC and FtsL represent a new class of peptidoglycan binding protein. Both *S. aureus* DivIC and FtsL and *B. subtilis* FtsL were able to bind to peptidoglycan, suggesting that peptidoglycan binding is conserved in these proteins. Due to time limitations, *B. subtilis* DivIC recombinant protein could not be purified, and its physiological and biochemical function could not be investigated. Nevertheless, it would be interesting to determine whether *B. subtilis* DivIC is able to bind to native and non-native peptidoglycans. *S. aureus* DivIC and FtsL and *B. subtilis* FtsL can all bind to non-native peptidoglycan, indicating that they are likely to bind to conserved peptidoglycan components. The site-directed mutants produced here showed reduced binding affinities to peptidoglycan in sedimentation assays. However, the active site of *S. aureus* DivIC mapped using site-directed mutants could be verified by solving the protein structure. Different techniques could be used to identify what component(s) of the peptidoglycan are recognised by the proteins. Further investigations using surface plasmon resonance (SPR) could determine the affinity of DivIC and FtsL for peptidoglycan substrate using a range of conditions.

## Chapter 4

### Localisation of *S. aureus* DivIC and FtsL

#### 4.1. Introduction

It has been proposed that all the essential cell division proteins localise to form the divisome, responsible for constructing the septum (Ghigo *et al.*, 1999). A number of cell division proteins have been shown to localise at the midpoint of *S. aureus* cells. For example, *S. aureus* FtsZ localisation was demonstrated through immunofluorescence, GFP and cyan fluorescent protein (CFP) fusions, expressed either from ectopic or native chromosomal positions (Liew *et al.*, 2010; Jorge *et al.*, 2011; Veiga *et al.*, 2011). *S. aureus* PBP2 was shown to localise at the septum by immunofluorescence microscopy (Pinho and Errington, 2003), and this localisation was confirmed using the GFP-PBP2 fusion protein (Pinho and Errington, 2005). PBP1 localisation to the septum was also shown by immunofluorescence (Pereira *et al.*, 2007b; Pereira *et al.*, 2009), and EzrA-CFP, EzrA-GFP and EzrA-mCherry were localised to the division septa in *S. aureus* (Pereira *et al.*, 2010; Veiga *et al.*, 2011; Steele *et al.*, 2011).

DivIC/FtsB belongs to the septum formation initiation family of proteins (Pfam 04977) and is essential for cell division in *B. subtilis* and *E. coli*, as the depletion of this protein causes failures in the septum formation at the division site, which produces filamentation and cell lysis (Levin and Losick, 1994; Buddelmeijer *et al.*, 2002). The immunolocalisation of *B. subtilis* DivIC protein showed that DivIC is localised between well-separated nucleoids (Katis *et al.*, 1997). Subcellular localisation analysis has shown that *B. subtilis* DivIC is a membrane-associated protein, and this result was further verified using different approaches, including immunolocalisation and protoplast treatment with proteinase K (Katis *et al.*, 1997). Fluorescence microscopy revealed that the N-terminal GFP fusion to FtsB in *E. coli* is localised to the division site (Buddelmeijer *et al.*, 2002). The localisation of *E. coli* GFP-FtsB was not detected at the septum in *ftsL*<sup>-</sup> and *ftsQ*<sup>-</sup> filament cells; however, the FtsB septal localisation was not affected in *ftsI*<sup>-</sup> and *ftsW*<sup>-</sup> filament cells (Buddelmeijer *et al.*, 2002). The Z-ring formation was not affected by the absence of DivIC in temperature sensitive *divIC* mutants (Daniel *et al.*, 1998; Levin and Losick, 1996). In *B. subtilis* cells, immunofluorescence imaging showed that

the *ftsL* null mutation prevented the localisation of DivIC, DivIB and PBP 2B but did not affect the formation of the FtsZ-ring (Daniel *et al.*, 1998). Western blot analysis revealed that in *B. subtilis ftsL*<sup>-</sup> cells, DivIC quickly disappeared, while DivIB remained in the cells, indicating that DivIC stability is associated with the presence of FtsL in the cells; however, the stability of DivIC is not required for its localisation (Daniel *et al.*, 1998; Katis *et al.*, 2000). The stability dependence on FtsL has been associated with the interaction of these two proteins, as they both contain leucine-zipper motifs that might be required for protein-protein interaction (Daniel *et al.*, 1998; Ghigo and Beckwith, 2000). In *ftsZ*<sup>-</sup> cells, *B. subtilis* DivIC is present in the cell at native amounts; however, this protein does not localise to the site of division, suggesting that the localisation of DivIC to the septum is dependent on FtsZ (Daniel *et al.*, 1998; Katis *et al.*, 2000). The replacement of the cytoplasmic and transmembrane domains of *B. subtilis* DivIC with *E. coli* TolR cytoplasmic and transmembrane domains did not affect the septal localisation of DivIC, albeit the intensity of the localisation was 50% less than the wild-type localisation (Katis and Wake, 1999). In addition, the level and subcellular localisation of *B. subtilis* DivIC in the cell were not affected by the replacement of these domains (Katis and Wake, 1999). Immunofluorescence imaging has shown that *B. subtilis* DivIB requires *B. subtilis* DivIC for its localisation at all temperatures, and this localisation is dependent on the amount of DivIC at the division site (Katis *et al.*, 2000). In contrast, *B. subtilis* DivIC localisation at the septum requires *B. subtilis* DivIB only at high temperature and this localisation is maintained through direct interaction between the two proteins (Katis *et al.*, 2000; Daniel *et al.*, 2006). The *B. subtilis* DivIC abundance in the cell was increased in the absence of *B. subtilis* DivIB, suggesting that DivIB negatively induces the synthesis of DivIC (Katis *et al.*, 2000). In *S. pneumoniae*, immunofluorescence microscopy has shown that DivIC is consistently observed at the cell midpoint, and DivIC remains at the division site during nucleoid segregation and Z-ring formation (Noirclec-Savoie *et al.*, 2005).

FtsL belongs to the cell division family of proteins (Pfam:04999), and this protein is essential in *E. coli* and *B. subtilis* because mutant cells exhibit long-filament phenotypes that lead to cell death (Guzman *et al.*, 1992; Ueki *et al.*, 1992; Daniel *et al.*, 1998). The GFP-FtsL fusion protein localised to the midpoint of *B. subtilis* cells during the early stages of the cell division and remains at the division site during



septum formations; however, FtsL disperses away from the new poles of the daughter cells (Sievers and Errington, 2000b). Deconvolution microscopy showed that *B. subtilis* GFP-FtsL forms ring-like constructs at the division site, analogous to the cytoplasmic Z-ring (Sievers and Errington, 2000b). Immunofluorescence microscopy showed that *B. subtilis* FtsL was co-localised at the division site with FtsZ (Daniel and Errington, 2000). *B. subtilis* FtsL localisation to the division site is dependent on other cell division proteins, such as FtsZ, DivIC, DivIB and PBP 2B (Daniel and Errington, 2000). The localisation of *E. coli* FtsL in wild-type cells using immunofluorescence microscopy revealed that FtsL forms a ring at the division site in 50% of the cells; however, the cross-reactivity of other *E. coli* proteins was observed through Western blot analysis using  $\alpha$ -FtsL antibodies (Ghigo *et al.*, 1999). Furthermore, the functional fusion of GFP to the N-terminal domain of FtsL showed that in 60-75% of cells, FtsL was localised at the mid-point, forming a septal ring that resembles the Z-ring (Ghigo *et al.*, 1999). Nevertheless, 20-40 copies of *E. coli* FtsL protein are present in cells, which is not abundant enough to produce a continuous ring (Ghigo *et al.*, 1999). *gfp-ftsL* was expressed in several *E. coli* Ts mutant strains, including *ftsZ*, *ftsA* and *ftsI*. The localisation of GFP-FtsL at the septum was detected in background of all Ts strains at permissive temperatures, whereas at restrictive temperatures, localisation at the septum was only observed in the *ftsI* Ts background. Accordingly, FtsL septal localisation is dependent on the presence of FtsZ and FtsA but not FtsI; however, the localisation of FtsZ, FtsA and ZipA are not dependent on FtsL (Ghigo *et al.*, 1999). In addition, FtsL localisation in *E. coli* was also dependent on FtsQ, as localisation at the septum was hindered in *ftsQ*<sup>-</sup> cells (Ghigo *et al.*, 1999). GFP-FtsL localisation to the division site was not observed in FtsB-depleted filamentous *E. coli* cells. As previously described, GFP-FtsB was not localised to the septum in FtsL-depleted filamentous *E. coli* cells, suggesting that FtsB and FtsL localisation to the septum occurs in a co-dependent manner (Buddelmeijer *et al.*, 2002). In addition, the localisation of FtsB and FtsL are dependent on the localisation of *E. coli* FtsQ, and these three proteins form a complex in cells and subsequently migrate to the cell mid-point (Buddelmeijer and Beckwith *et al.*, 2004; Buddelmeijer *et al.*, 2002). The transient immunolocalisation of FtsL in *S. pneumoniae* was observed at the division site during Z-ring construction, and it was co-localised with DivIC. However it is present at the cell hemisphere throughout the cell cycle (Noirclerc-Savoie *et al.*,

2005). The localisation dependency of one protein on another and the instability of one protein in the absence of another differs from one organism to another, suggesting that divisome assembly and septation are differentially regulated across the bacteria (Katis *et al.*, 2000).

#### **4.1.1. Aims of this chapter**

- Examine the subcellular localisation of *S. aureus* DivIC
- Examine the subcellular localisation of *S. aureus* FtsL

## **4.2. Results**

### **4.2.1. Generation of anti-DivIC and anti-FtsL antibodies**

Rabbit  $\alpha$ -DivIC and  $\alpha$ -FtsL polyclonal antibodies were raised against purified recombinant DivIC<sub>Sa</sub> and FtsL<sub>Sa</sub> (Section 2.13, Section 3.2.2) at BioServ (University of Sheffield). The recombinant proteins used for immunisation were obtained through the overexpression of His-tag proteins in *E. coli* (Section 3.2.2.3). The overexpressed proteins were then purified using affinity chromatography (Section 3.2.2.4) and dialysis (Section 3.2.2.4).

The reactivity and specificity of  $\alpha$ -DivIC and  $\alpha$ -FtsL antibodies against the recombinant proteins, DivIC<sub>Sa</sub> and FtsL<sub>Sa</sub>, respectively, were investigated. The recombinant proteins DivIC<sub>Sa</sub> and FtsL<sub>Sa</sub> and whole cell lysates of SH1000 *spa::kan* were analysed by Western blotting (Section 2.11.4). The blots were probed with polyclonal  $\alpha$ -DivIC (Figure 4.1A) and  $\alpha$ -FtsL (Figure 4.2A) using a range of serum dilutions from 1:5,000 to 1:50,000. An intense band of reactivity with  $\alpha$ -DivIC antibodies was observed at ~ 14 kDa for recombinant DivIC<sub>Sa</sub>, which is slightly higher than the expected size of 9.68 kDa (Figure 4.1A). A number of bands were observed in the whole cell lysate of SH1000 *spa::kan* using polyclonal  $\alpha$ -DivIC antibodies, however a predominant ~ 15 kDa band, corresponding to the expected size of the native *S. aureus* DivIC, was detected at all the dilutions, suggesting that the polyclonal  $\alpha$ -DivIC reacted with other *S. aureus* proteins (Figure 4.1A).

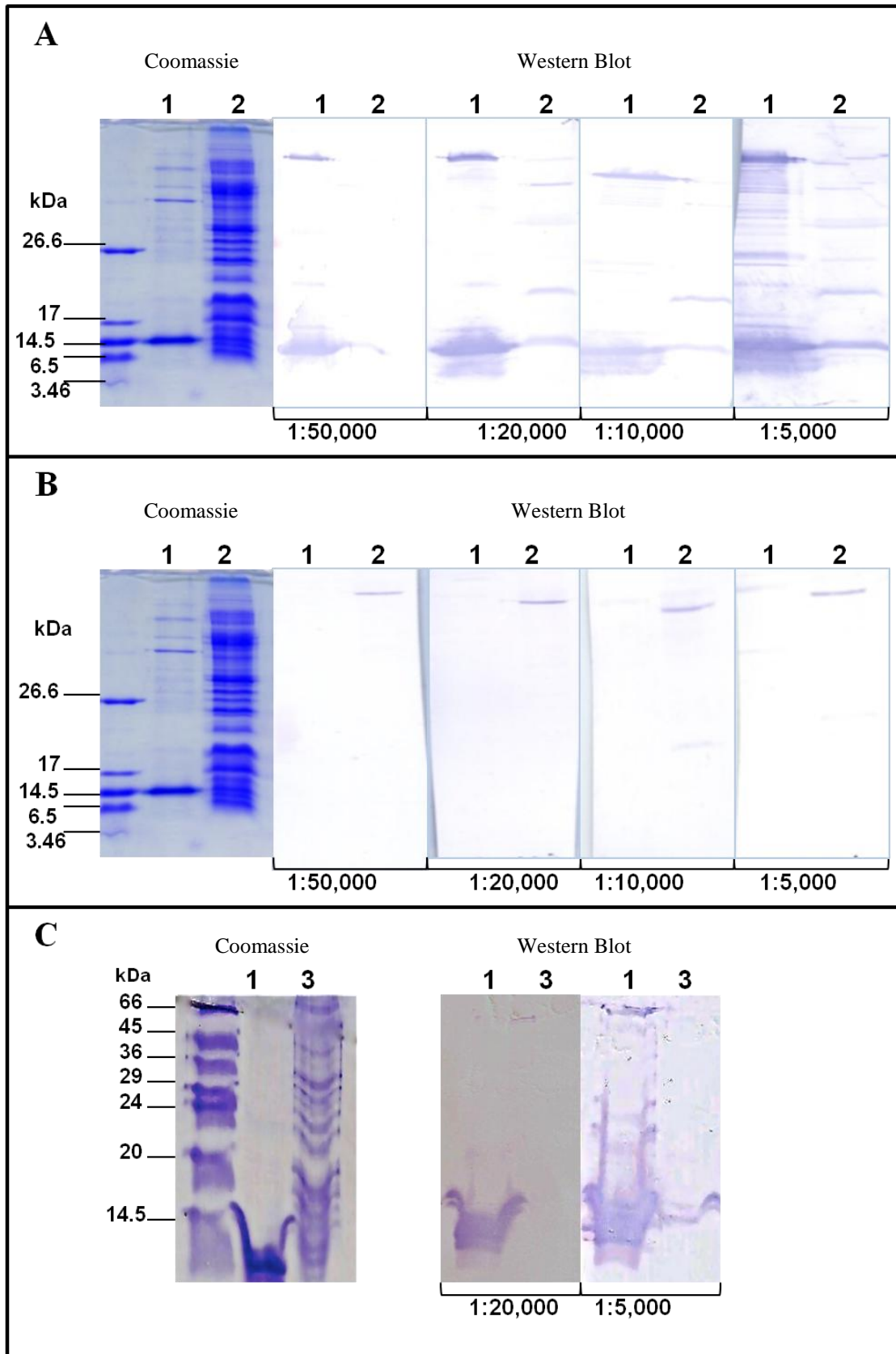


**Figure 4.1 Reactivity of polyclonal  $\alpha$ -DivIC antibodies**

A total of 2  $\mu$ g of recombinant (1) DivIC<sub>Sa</sub> and (2) *S. aureus* SH1000 *spa::kan* or (3) of a membrane fraction of *S. aureus* SH1000 *spa::kan* were analysed 11%

(w/v) SDS-PAGE and Western blotting, which was probed with various antibodies (A-C). The blots were probed with (A) rabbit polyclonal  $\alpha$ -DivIC antibodies at 1:5,000 to 1:50,000, (B) naïve rabbit serum at 1:5,000 to 1:50,000, (C) affinity purified *E. coli* lysate treated  $\alpha$ -DivIC at 1:5,000 and 1:20,000.

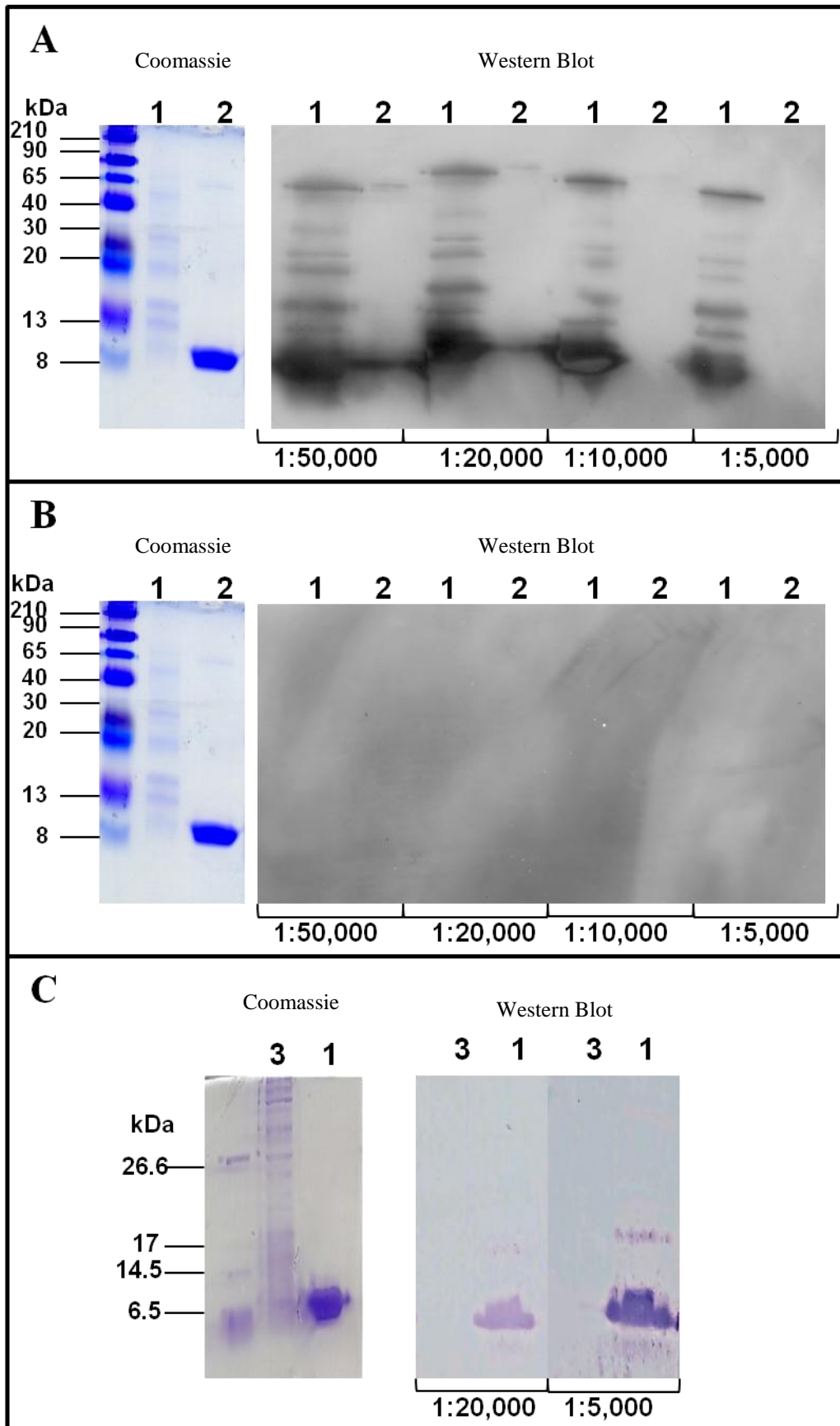


Figure 4.2 Reactivity of polyclonal  $\alpha$ -FtsL antibodies

A total of 2 µg of recombinant (1) FtsL<sub>Sa</sub> and (2) *S. aureus* SH1000 *spa::kan* or (3) of a membrane fraction of *S. aureus* SH1000 *spa::kan* were analysed 11% (w/v) SDS-PAGE and Western blotting, which was probed with various antibodies (A-C). The blots were probed with (A) rabbit polyclonal α-FtsL antibodies at 1:5,000 to 1:50,000, (B) naïve rabbit serum at 1:5,000 to 1:50,000, and (C) affinity purified *E. coli* lysate-treated α-FtsL at 1:5,000 and 1:20,000

A band of reactivity with  $\alpha$ -FtsL antibodies was observed at  $\sim 8$  kDa for recombinant FtsL<sub>Sa</sub>, which is similar to the expected size of 8.45 kDa (Figure 4.2A). A number of bands were observed in the whole cell lysate of SH1000 *spa::kan* using  $\alpha$ -FtsL, however a predominant band of  $\sim 8$  kDa, which is slightly lower than the expected molecular weight of *S. aureus* FtsL, was detected at all the dilutions (Figure 4.2A). Similar blots were also probed with naïve rabbit serum, and no reactive proteins against the recombinant DivIC<sub>Sa</sub> (Figure 4.1B) or FtsL<sub>Sa</sub> (Figure 4.2B) were observed. The reactivity of naïve rabbit serum against *S. aureus* proteins was observed with SH1000 *spa::kan* whole cell lysate (Figure 4.1B), suggesting the cross-reactivity of the serum with *S. aureus* proteins however no bands of reactivity were seen in (Figure 4.2B).

The multiple bands of reactivity, detected on the blots probed with the polyclonal  $\alpha$ -DivIC and  $\alpha$ -FtsL antibodies, could reflect the presence of other antibodies in the serum that react with non-specific proteins, resulting from the contamination of the recombinant protein used for immunisation with other *E. coli* proteins. Accordingly, the polyclonal  $\alpha$ -DivIC and  $\alpha$ -FtsL serums were affinity purified against recombinant DivIC<sub>Sa</sub> and FtsL<sub>Sa</sub>, respectively, at BioServ (University of Sheffield) to reduce cross-reactivity with other *S. aureus* proteins. The affinity-purified antibodies were also treated with *E. coli* lysate for four h at room temperature to remove cross-reactive antibodies (Section 2.13.2.1) after diluting the antibodies in blocking buffer (Section 2.4.8.3) to reduce the unspecific reactivity with other *E. coli* proteins.

The analysis of recombinant DivIC<sub>Sa</sub>, FtsL<sub>Sa</sub> and a membrane fraction of SH1000 *spa::kan* by Western blotting was repeated using affinity-purified and *E. coli* lysate-treated antibodies (Figure 4.1C and Figure 4.2C). A distinctive band of reactivity was observed (the band size was smaller than 14.5 kDa), and no bands of reactivity were observed with the membrane fraction of SH1000 *spa::kan* when the blot was probed with  $\alpha$ -DivIC at 1:20,000 however a band of reactivity was seen at  $\sim 15$  kDa when the blot was probed with  $\alpha$ -DivIC at 1:5,000 (Figure 4.1C). When the membrane fraction of SH1000 *spa::kan* blot was probed with  $\alpha$ -FtsL affinity-purified *E. coli* lysate-treated antibodies, no bands of reactivity were observed;

however, a band was observed for recombinant FtsL<sub>Sa</sub> when probed with  $\alpha$ -FtsL (Figure 4.2C).

#### **4.2.2. Subcellular localisation of DivIC and FtsL**

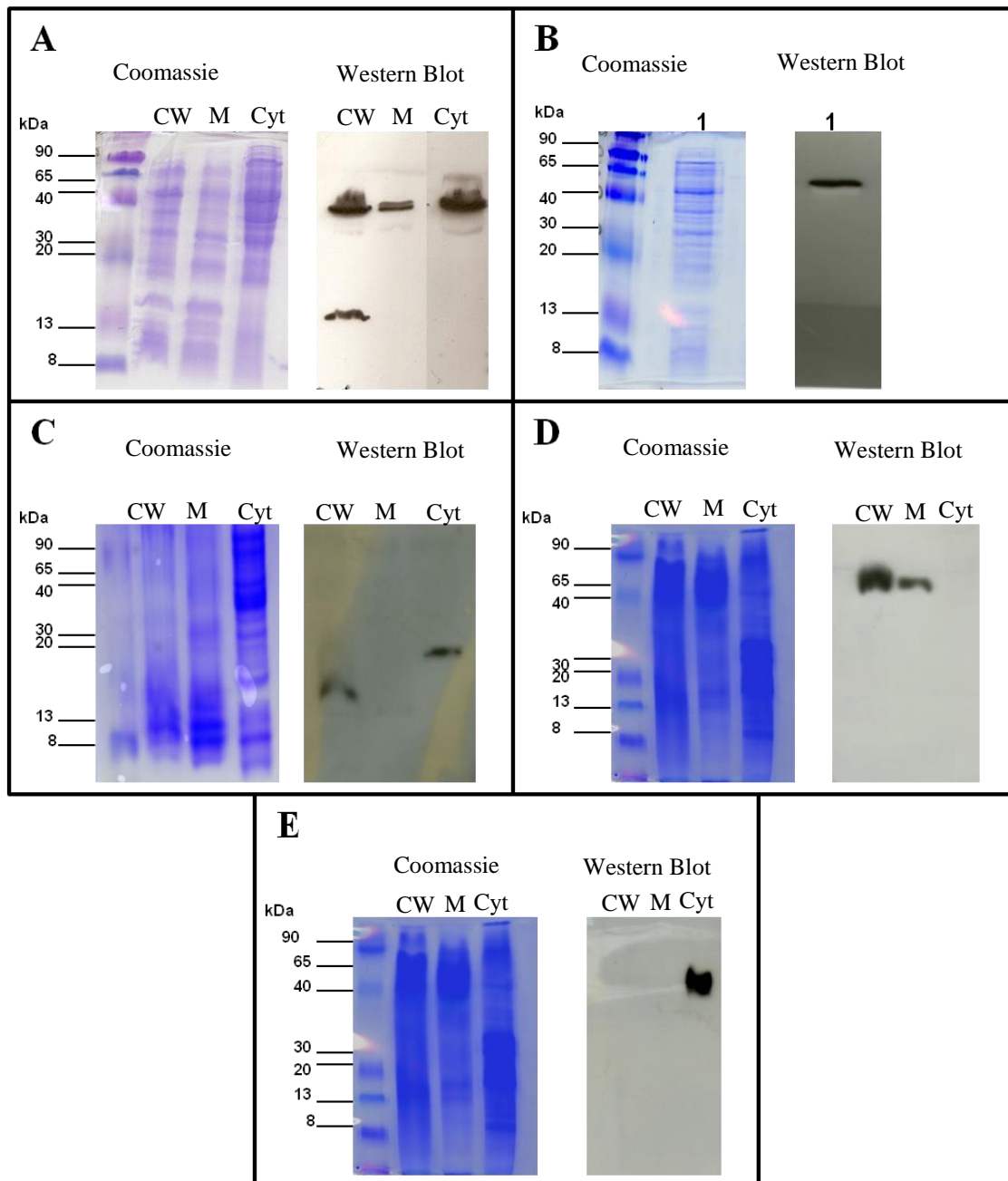
Different techniques were used to determine the subcellular localisation of DivIC and FtsL in *S. aureus*.

##### **4.2.2.1. Western blot analysis of subcellular fractions**

The bioinformatics analysis of DivIC<sub>Sa</sub> (Figure 3.1) showed that this protein contains a putative transmembrane domain at the N-terminus. The *B. subtilis* DivIC protein contains a long stretch of hydrophobic residues, implying its association with the cytoplasmic membrane (Levin and Losick, 1994). In addition, immunoblot analysis of *B. subtilis* DivIC revealed it in the membrane fraction as expected; however, a small amount of the protein was detected in the cell wall and a trace in the cytoplasmic fraction (Katis *et al.*, 1997). Consequently, DivIC<sub>Sa</sub> and FtsL<sub>Sa</sub> localisations were verified through the Western blot analysis of cellular fractions.

Protein A (SpA) was expected to cross-react non-specifically with antibodies, as this protein has a strong binding affinity for the IgG Fc region (Gomez *et al.*, 2006). Thus, cellular fractions of SH1000 *spa::kan* were prepared (Section 2.16), where the *spa* gene was substituted with a kanamycin resistance cassette (Girbe Buist, unpublished). Cell wall (CW), membrane (M) and cytoplasm (CY) fractions were separated by 15% (w/v) SDS-PAGE for Western blotting (Section 2.11.4) and Coomassie staining (Figure 4.3). The blot was probed with affinity-purified *E. coli* lysate-treated rabbit polyclonal  $\alpha$ -DivIC antibodies (Figure 4.3A). A strong band of ~15 kDa was only observed in the cell wall fraction; however, higher bands of ~50 kDa were also observed in all fractions, which is the expected molecular weight of the Sbi protein. The Sbi protein is similar to the SpA in its affinity to the IgG Fc region (Zhang *et al.*, 1998; Gomez *et al.*, 2006; Smith *et al.*, 2011) (Figure 4.3A). Thus, the whole cell lysate of Newman strain, lacking SpA and Sbi proteins was used, and the blot was probed with  $\alpha$ -DivIC.





#### 4.3 Subcellular localisation of DivIC and FtsL in *S. aureus*

A. Cellular fractions of SH1000 *spa::kan*, corresponding to an equal amount of cellular material, were separated by 11% (w/v) SDS-PAGE and subsequently analysed by Western blotting with  $\alpha$ -DivIC at 1:500. CW, cell wall; M, membrane; Cyt, cytoplasm. The sizes of the molecular markers are shown.

B. *S. aureus* Newman *spa- sbi-* whole cell lysate (lane 1) were analysed by 11% (w/v) SDS-PAGE and Western blotting. The blot was probed with affinity purified *E. coli* lysate-treated  $\alpha$ -DivIC at 1:5000.

C, D and E. Cellular fractions of SH1000 *spa::kan*, corresponding to an equal amount of cellular material, were separated by 11% (w/v) SDS-PAGE and subsequently analysed by Western blotting with (C)  $\alpha$ -FtsL at 1:500, (D)  $\alpha$ -glu at 1:500, and (E)  $\alpha$ -FtsZ at 1:500. CW, cell wall; M, membrane; Cyt, cytoplasm. The sizes of the molecular markers are shown.

Similarly, one band of ~ 50 kDa was observed (Figure 4.3B), suggesting that this band did not reflect nonspecific reactivity with the antibodies, but it might be due to the presence of different forms of DivIC<sub>Sa</sub>. This observation was also obtained with *S. aureus* DivIB (Bottomley, 2011) and *S. pneumoniae* DivIB (Noirclerc-Savoie *et al.* 2005) proteins. The slow migration of *S. pneumoniae* DivIB in SDS-PAGE, which exhibited a larger band size than expected, likely reflects the presence of charged and polar residues in the C-terminal and the N-terminal domains (Noirclerc-Savoie *et al.* 2005). Indeed, DivIC<sub>Sa</sub> N-terminal (residues 2-33) and C-terminal (residues 57-130) domains contain polar and charged residues (Figure 3.1), and thus this slow migration of DivIC<sub>Sa</sub> in the SDS-PAGE could also reflect the presence of these residues in the protein. The presence of *S. aureus* DivIC in the cell wall fraction strongly suggests that DivIC is a cell wall-anchored protein, supporting a previous finding that DivIC is a peptidoglycan-binding protein (Section 3.2.4.4). In *B. subtilis*, DivIC is a membrane-associated protein primarily detected in membrane fractions, although a small amount of this protein has been detected in the cell wall and cytoplasmic fractions (Katis *et al.*, 1997). A similar observation was obtained for DivIB, another cell division protein, which has primarily been observed in the membrane fraction, with a small amount detected in the cell wall fraction in *B. subtilis* (Harry and Wake, 1997) and *S. aureus* (Bottomley, 2011).

When the blot was probed with affinity-purified *E. coli* lysate-treated rabbit polyclonal  $\alpha$ -FtsL antibodies, a band of ~ 15 kDa was observed in the cell wall fraction and a high molecular mass band ~ 30 kDa was observed in the cytoplasmic fraction (Figure 4.3C). The subcellular localisation of *B. subtilis* FtsL alkaline phosphatase fusion protein (FtsL-AP) was observed only in the membrane fraction (Guzman, *et al.*, 1992). A similar fractionation study of *B. subtilis* DivIC showed a high molecular mass band in the cytoplasmic fraction (Katis *et al.*, 1997).

A control blot of SH1000 *spa::kan* cellular fractions was probed with different rabbit polyclonal antibodies.  $\alpha$ -Glucosaminidase (glu), a domain that is present in the *S. aureus* Atl protein, was observed in the cell wall and membrane fractions

(Figure 4.3D), whereas  $\alpha$ -FtsZ was only detected in the cytoplasm as expected (Figure 4.3E).

#### **4.2.2.2. Localisation of *S. aureus* GFP-tagged proteins**

The localisation of a specific protein within the cell gives an indication of its role. Localisation can be achieved using GFP fusions as markers demonstrating the localisation of proteins within prokaryotic and eukaryotic cells (Feilmeier *et al.*, 2000; Santini *et al.*, 2001). A study in *E. coli* showed that GFP folds improperly when exported to the extracellular space via the general secretory (Sec) pathway, resulting in a reduction of the level of GFP, and hence the fluorescence signal was not detected (Feilmeier *et al.*, 2000). However, *B. subtilis* LytE-GFP protein was shown to be functional and fluorescent when exported outside the cytoplasm via the Sec pathway, as LytE-GFP complemented the *lytE* null mutation (Carballido-Lopez *et al.*, 2006). In contrast, GFP is properly folded using the twin arginine transport (Tat) pathway when exported outside the cytoplasm (Santini *et al.*, 2001; Thomas *et al.*, 2001). The localisation of *E. coli* AmiA-GFP and AmiC-GFP proteins has been reported using the Tat pathway for exporting the GFP-fused protein to the extracellular space (Bernhardt and de Boer, 2003).

##### **4.2.2.2.1. Localisation of *S. aureus* DivIC-GFP+**

An N-terminal GFP fusion to FtsB in *E. coli* was shown as an obvious line at the cell midpoint indicating localisation to the division site (Buddelmeijer *et al.*, 2002).

To examine the localisation of DivIC in *S. aureus*, Liya Marangattil (University of Sheffield) constructed a C-terminal GFP fusion protein using the pMUTIN-GFP+ vector (Kaltwasser *et al.*, 2002). The ribosome binding site (RBS) and the *S. aureus* *divIC* coding sequence were cloned into the pMUTIN-GFP+ vector to construct an in-frame fusion of *divIC* to *gfp+*. The resulting plasmid, pGL617, was transformed into *S. aureus* RN4420 electrocompetent cells, and the integration of the plasmid into the chromosome occurred via a single crossover event, resulting in a *divIC-gfp+* fusion under the control of the native *divIC* promoter and a native copy of *divIC* under the control of P<sub>Spac</sub> (Figure 4.4).

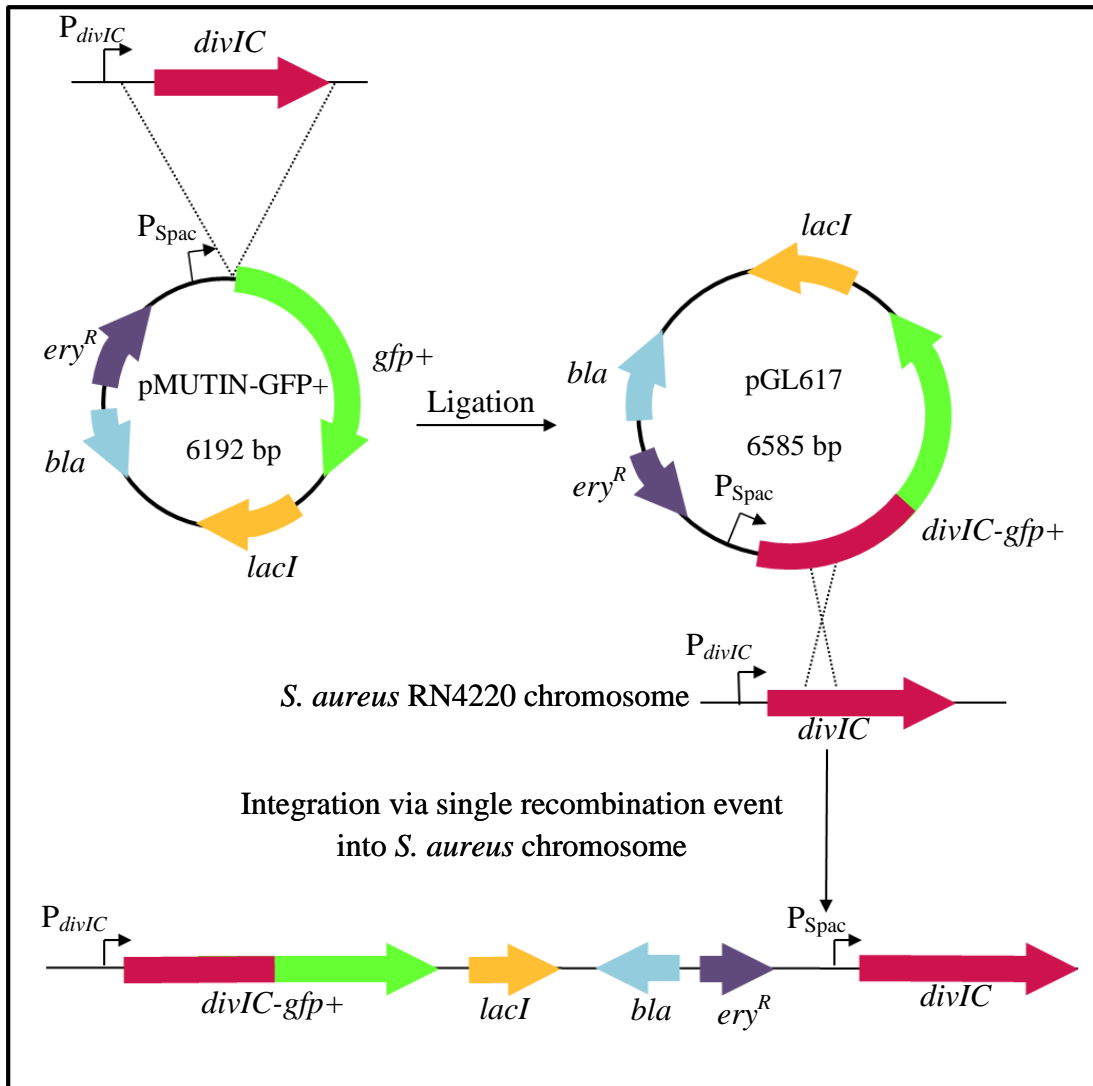


**Figure 4.4 Construction of a *S. aureus* *divIC-gfp+* strain**

Schematic representation of pGL617 construction and the insertion of the plasmid into *S. aureus* RN4220. Liya Marangattil (University of Sheffield) generated this construct.

The plasmid insertion was subsequently transferred into the SH1000 and SH1000 *spa::kan* backgrounds via phage transduction using  $\phi$  11 (Section 2.10.3.4). The resulting strains, AFK1 (SH1000 *divIC-gfp+*) and AFK2 (SH1000 *spa::kan divIC-gfp+*) expressed *S. aureus* DivIC as a C-terminal GFP fusion. *B. subtilis* DivIC C-terminus was shown to be extracellular (Levin and Losick, 1994; Katis *et al.*, 1997). Moreover, prediction indicates that *S. aureus* DivIC has a similar membrane topology to the *B. subtilis* DivIC protein (Figure 3.1).

As previously described, a GFP fusion to a specific protein can cause improper protein folding, incorrect targeting and the loss of protein activity. Consequently, the functionality of the DivIC-GFP+ fusion was assessed before the localisation analysis was performed. The *gfp*-fused gene was under the control of the native promoter (Figure 4.4), and thus when IPTG is not present, the *gfp*-fused gene is the only copy of the gene expressed. Thus, if the native copy of the gene is not expressed, and the GFP fusion protein is not functional, then the cells would likely exhibit a defect in growth. A basal expression level of the native gene from the *spac* promoter ( $P_{Spac}$ ) is likely observed even when the inducer (IPTG) is not present. Thus full repression is achieved through the overexpression of LacI from a multi-copy plasmid. The pMJ8426 plasmid is an *E. coli-S. aureus* shuttle vector carrying the *E. coli lacI* gene under the control of the *Bacillus licheniformis* penicillinase promoter ( $P_{Pcn}$ ), and the LacI protein is constitutively expressed in *S. aureus* (Jana *et al.*, 2000). The pGL485 vector, is a chloramphenicol resistant derivative of pMJ8426 (Cooper *et al.*, 2009) (Figure 4.5), and was introduced into AFK1 (SH1000 *divIC-gfp+*;  $P_{Spac-divIC}$ ) and AFK2 (SH1000 *spa::kan divIC-gfp+*;  $P_{Spac-divIC}$ ) via  $\phi$  11 transduction to create AFK5 (SH1000 *divIC-gfp+* pGL485;  $P_{Spac-divIC}$ ) and AFK6 (SH1000 *spa::kan divIC-gfp+* pGL485;  $P_{Spac-divIC}$ ), respectively. The IPTG dependence of AFK5 (SH1000 *divIC-gfp+* pGL485;  $P_{Spac-divIC}$ ) was tested. AFK5 (SH1000 *divIC-gfp+* pGL485;  $P_{Spac-divIC}$ ) was grown to exponential phase (OD<sub>600</sub> 0.5) in BHI containing 200  $\mu$ M IPTG. The culture was centrifuged to harvest the cells, and the IPTG was removed by washing the cells with fresh BHI. The culture was diluted to  $10^{-6}$  and 50  $\mu$ l was spread onto BHI agar plates in the presence and absence of 1 mM IPTG.

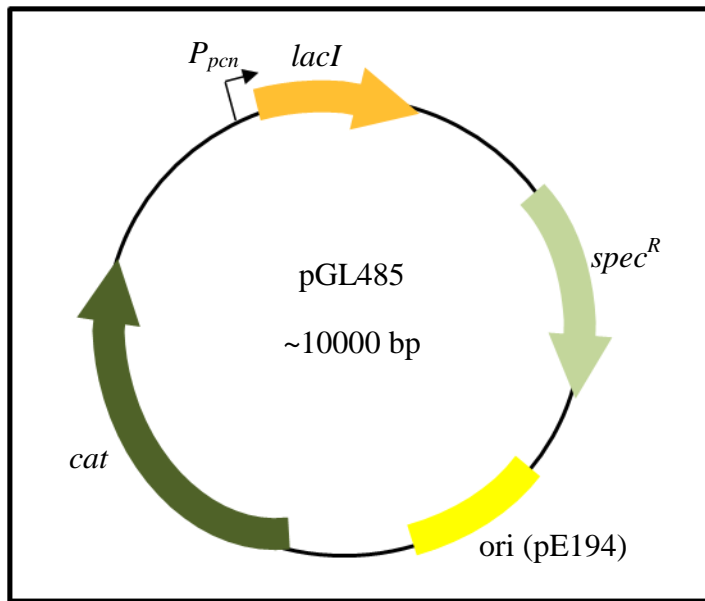


**Figure 4.5 Map of pGL485, the *lacI* expression plasmid**

pGL485 is a chloramphenicol-resistant plasmid and a derivative of pMJ8426, which is an *E. coli-S. aureus* shuttle vector. pGL485 carries the *E. coli lacI* gene under the control of a constitutive *B. licheniformis* penicillinase promoter (P<sub>pen</sub>).

The plates were incubated for 24 h at 37°C. There was no difference in the colony size between colonies grown in 1 mM IPTG and colonies grown without IPTG (Figure 4.6). AFK5 (SH1000 *divIC-gfp+* pGL485; P<sub>Spac</sub>-*divIC*) growth was IPTG-independent, suggesting that the *divIC-gfp+* copy compensates for the lack of the native *divIC* copy and functionally replaced this gene.

The subcellular localisation of *S. aureus* DivIC was visualised using fluorescence microscopy of AFK1 (SH1000 *divIC-gfp+*; P<sub>Spac</sub>-*divIC*), AFK2 (SH1000 *spa::kan divIC-gfp+*; P<sub>Spac</sub>-*divIC*), AFK5 (SH1000 *divIC-gfp+* pGL485; P<sub>Spac</sub>-*divIC*) and AFK6 (SH1000 *spa::kan divIC-gfp+* pGL485; P<sub>Spac</sub>-*divIC*). The cells were grown in BHI at 37°C overnight, re-cultured and incubated at 37°C to exponential phase (OD<sub>600</sub> 0.5). The cells were then centrifuged, resuspended and washed in sdH<sub>2</sub>O prior to staining with either fluorescent vancomycin (Pinho and Errington, 2003) or HADA, a fluorescent hydroxy coumarin derivative of D-alanine (Kuru *et al.*, 2012) that is used to label nascent peptidoglycan. The cells were then washed again in sdH<sub>2</sub>O and subsequently fixed in formaldehyde and glutaraldehyde solution. The samples were examined using deconvolution microscopy. AFK1 (SH1000 *divIC-gfp+*; P<sub>Spac</sub>-*divIC*) showed a surprising localisation pattern (Figure 4.7). DivIC-Gfp<sup>+</sup> was localised away from the division site, appearing mainly as patches around the cell periphery. AFK5 (SH1000 *divIC-gfp+* pGL485; P<sub>Spac</sub>-*divIC*) exhibited slightly different localisation patterns. A summary of the observed localisation patterns of AFK5 (SH1000 *divIC-gfp+* pGL485; P<sub>Spac</sub>-*divIC*) is shown in Figure 4.8 and Figure 4.9: two dots were observed in 21 % of the cells, whereas 32 % one dot existed as central or peripheral. A line was also observed in 6% of the cells, both dots and lines were observed in 17 % of the cells, and 18% of the cells showed multiple dots (three or four dots). The difference in the patterns might reflect specific localisation of DivIC during the cell cycle. Videos showing Z-stack images obtained from these cells are provided in the enclosed CD. The band or the two dot patterns might represent a circumferential DivIC ring at the site of division before the septum has been formed.

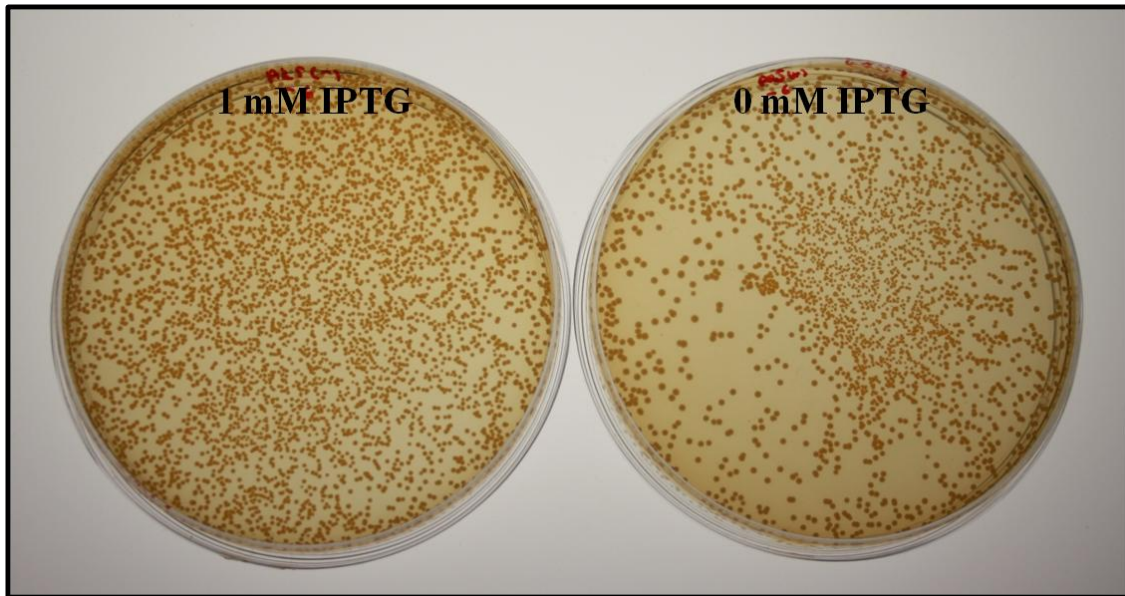


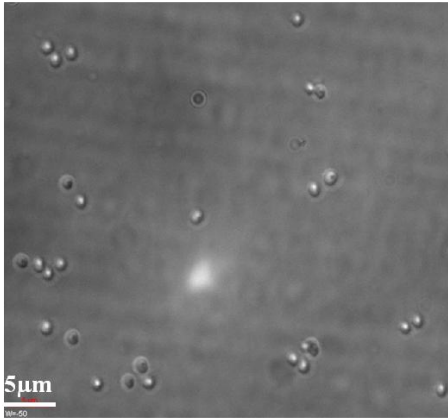
**Figure 4.6 Functionality of the DivIC-GFP+ fusion in *S. aureus***

Growth of AFK5 (*divIC-GFP+*;  $P_{\text{Spac-}divIC}$  pGL485) on BHI agar plates containing  $5 \mu\text{g ml}^{-1}$  erythromycin,  $25 \mu\text{g ml}^{-1}$  lincomycin,  $30 \mu\text{g ml}^{-1}$  chloramphenicol and 0 or 1 mM IPTG.

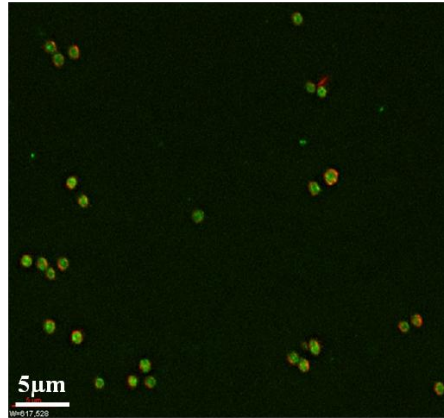


**A.I**

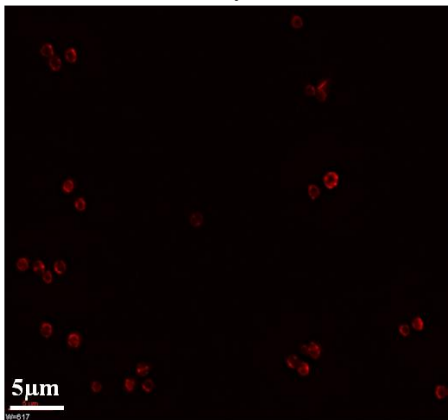
Phase contrast



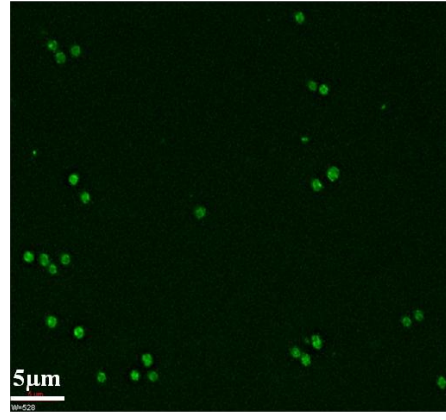
Merge



Vancomycin

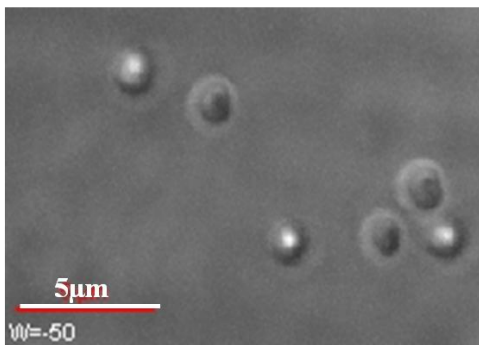


DivIC-GFP+

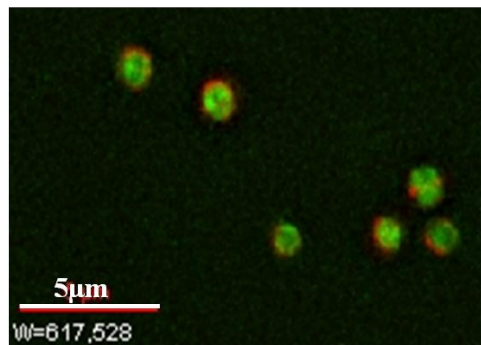


**A.II**

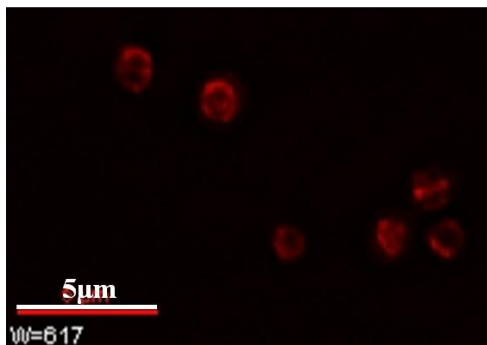
Phase contrast



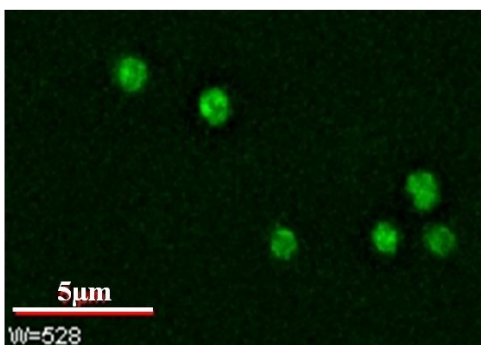
Merge



Vancomycin



DivIC-GFP+



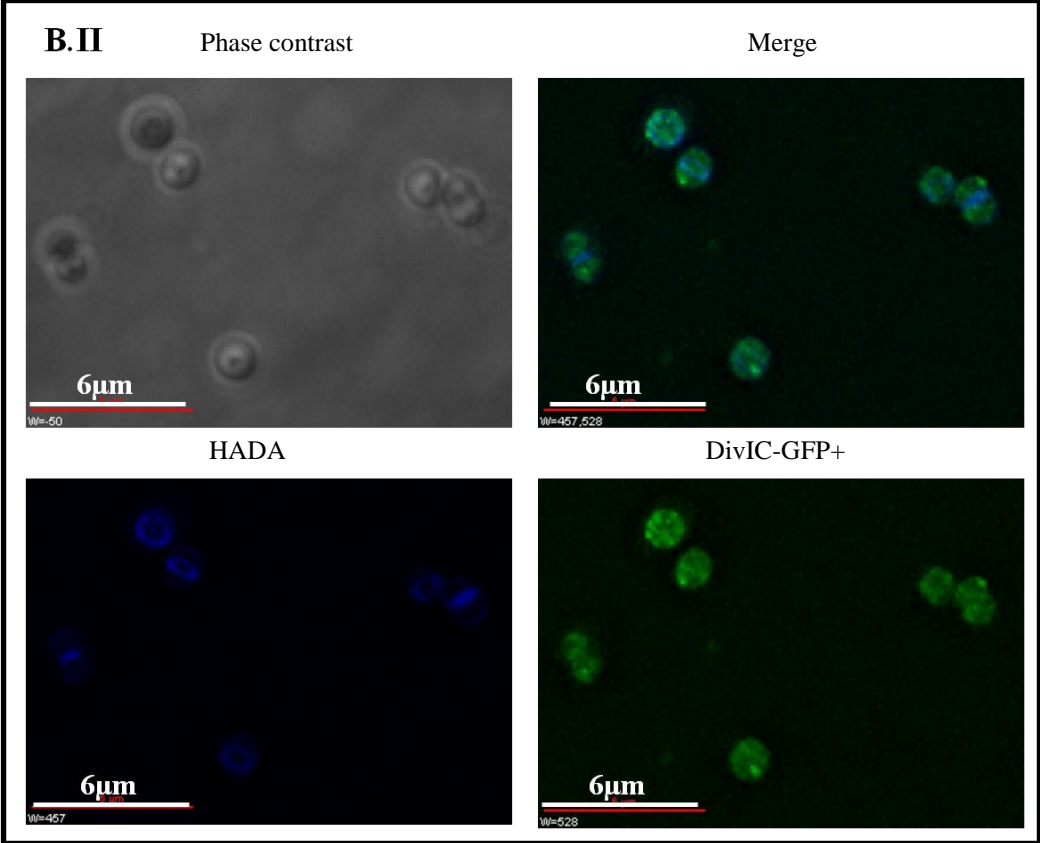
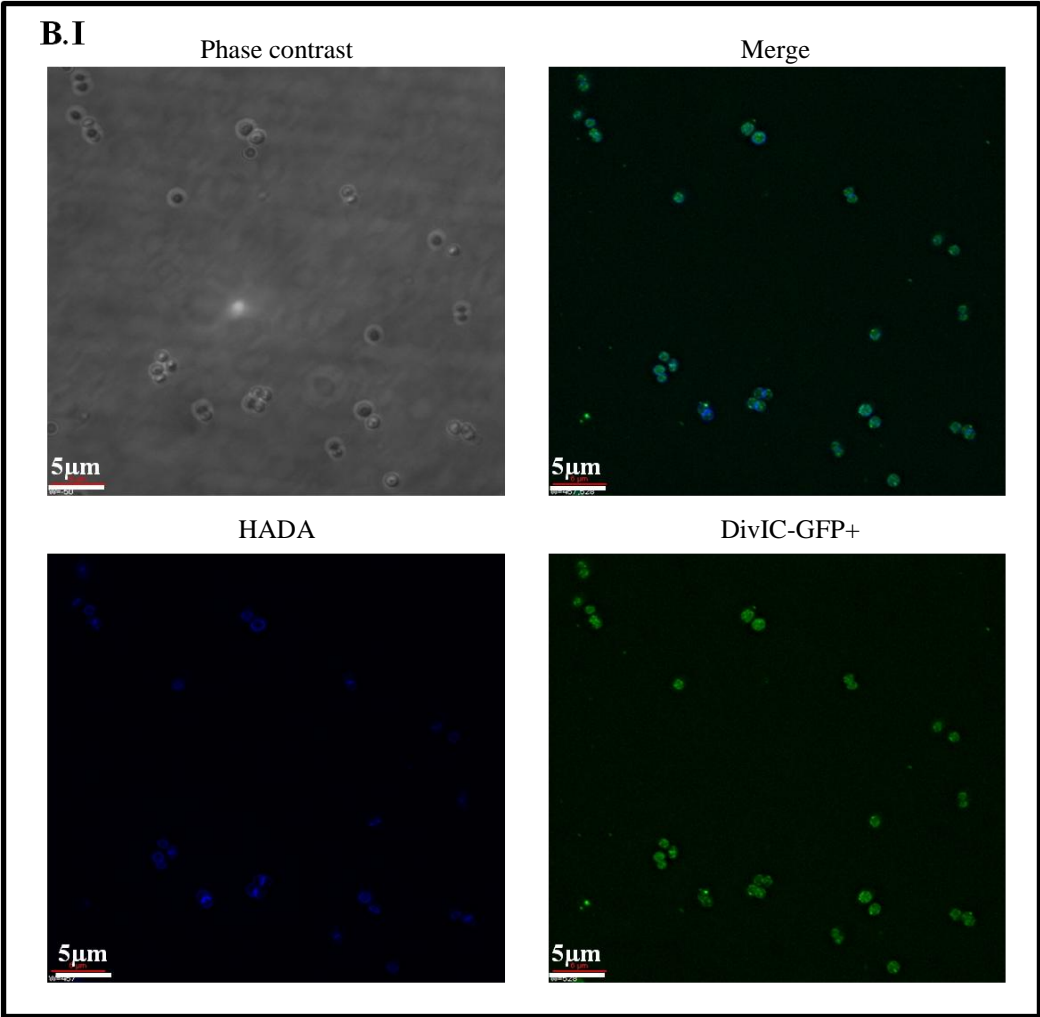


**Figure 4.7 Localisation of DivIC-GFP+ fusion in *S. aureus***

Fluorescence and phase contrast images of AFK1 (*divIC-GFP+*;  $P_{\text{Spac-}divIC}$ ). Peptidoglycan was stained with vancomycin (red; panels A.I and A.II) or HADA (blue; panels B.I and B.II). The DivIC-GFP+ signal is shown in green. Images were acquired using an Olympus IX70 microscope and SoftWoRx 3.5.0 software (Applied Precision). Enlarged images are shown in A.II and B.II. Scale bars are indicated (5 $\mu\text{m}$ ; panels A.I and A.II and B.I; 6  $\mu\text{m}$  panel B.II).

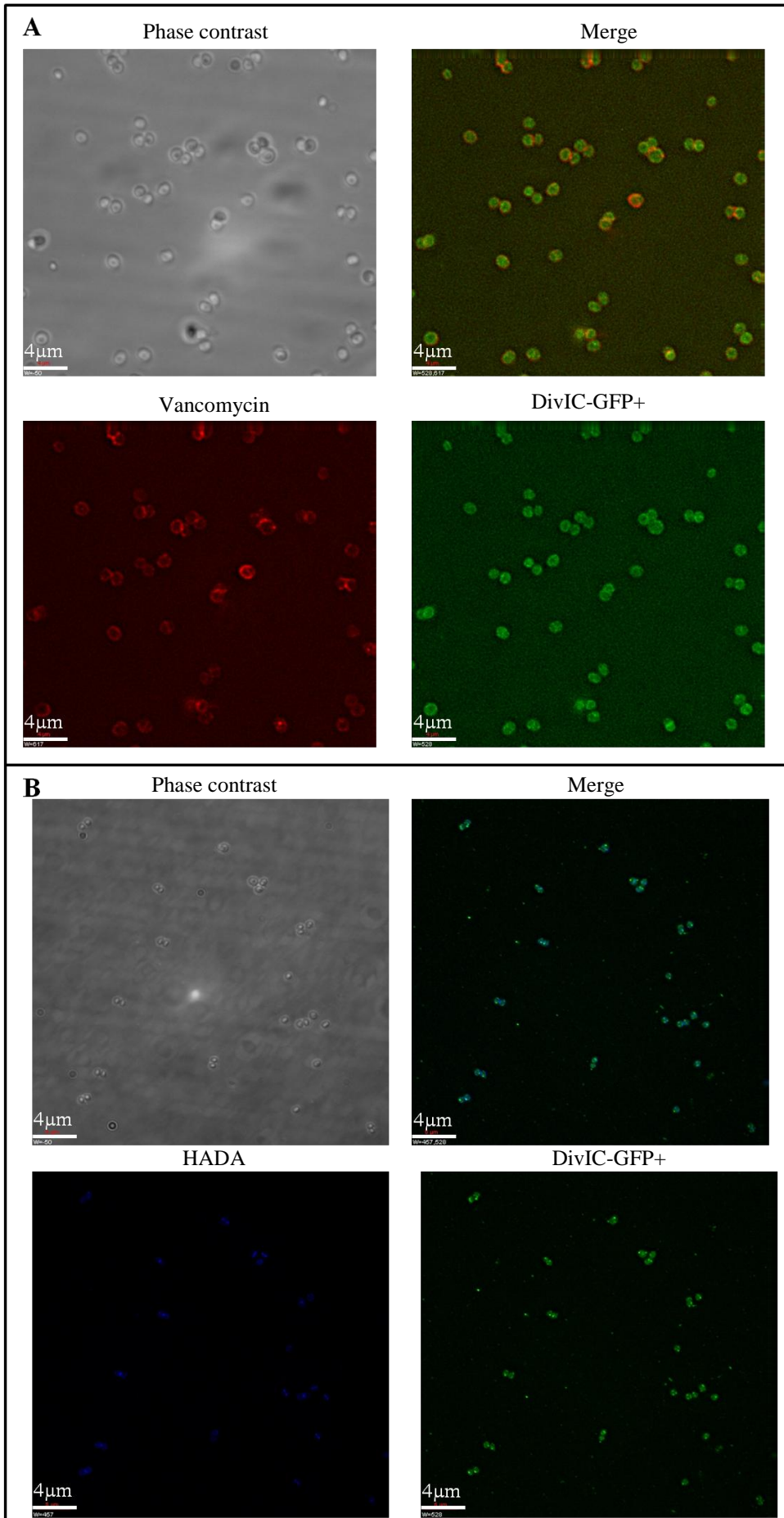


**Figure 4.8 Localisation of DivIC-GFP+ fusion in *S. aureus***

Fluorescence and phase contrast images of AFK5 (*divIC-GFP+*; P<sub>Spac</sub>-*divIC* pGL485). Peptidoglycans were stained with vancomycin (red; panel A) or HADA (blue; panel B). The DivIC-GFP+ signal is shown in green. Images were acquired using an Olympus IX70 microscope and SoftWoRx 3.5.0 software (Applied Precision). Scale bars are indicated.

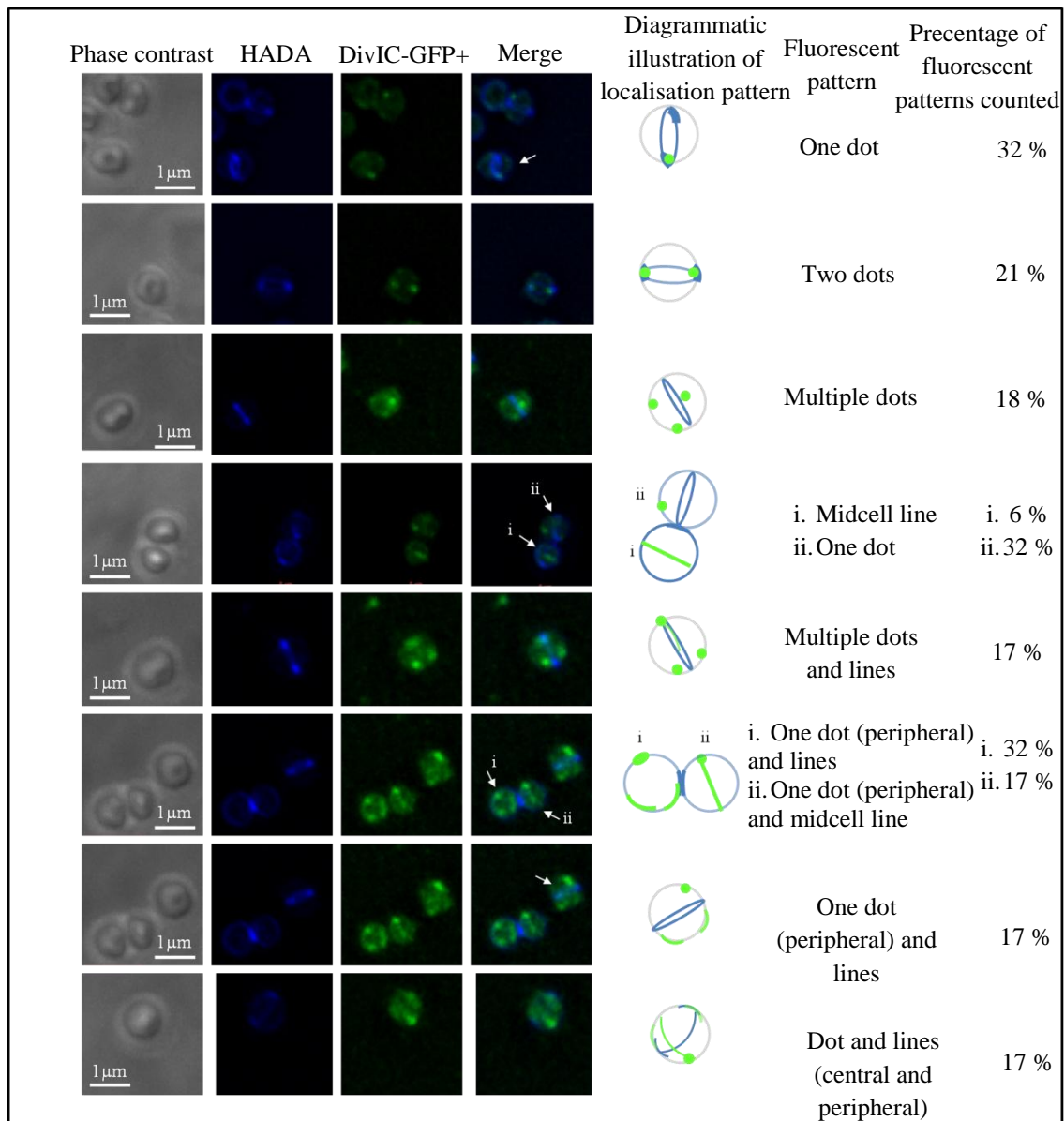


**Figure 4.9 Localisation patterns of DivIC-GFP+ fusion in *S. aureus***

Schematic diagrams of the AFK5 (*divIC-GFP+*;  $P_{\text{Spac}}\text{-divIC}$  pGL485) localisation patterns observed and the percentages counted for each pattern, along with their corresponding representative fluorescent images. Peptidoglycan was stained with HADA (blue). The DivIC-GFP+ signal is shown in green. Images were acquired using an Olympus IX70 microscope and SoftWoRx 3.5.0 software (Applied Precision). Scale bars are indicated.

The localisation of DivIC at the division site might be transient, as the line or the two dots observed were present at the middle of the cell before septum formation, and once septum formation has been initiated, DivIC translocates away from the middle of the cell and appears as patches around the cell wall (Figure 4.7, Figure 4.8 and Figure 4.9). Thus, the formation of a line and two dots at the middle of the cell could indicate a role for DivIC in the early stages of cell division, recruiting other cell division proteins to the division site to form the septum or prevent septum formation from occurring in the wrong place. This finding is interesting because DivIC is a *S. aureus* cell division protein that interacts with the cell division machinery in *S. aureus* (Steele *et al.*, 2011), and DivIC has been localised to the division site in other bacteria, such as *B. subtilis* (Katis *et al.*, 1997), *S. pneumoniae* (Noirclerc-Savoie *et al.*, 2005) and *E. coli* (Buddelmeijer *et al.*, 2002). This result suggests that DivIC might be transiently located at the division site. AFK2 (SH1000 *spa::kan divIC-gfp+*; P<sub>Spac-divIC</sub>) and AFK6 (SH1000 *spa::kan divIC-gfp+* pGL485; P<sub>Spac-divIC</sub>) showed localisation patterns similar to AFK1 (SH1000 *divIC-gfp+*; P<sub>Spac-divIC</sub>) and AFK5 (SH1000 *divIC-gfp+* pGL485; P<sub>Spac-divIC</sub>) (data not shown).

Western blot analysis was performed using whole cell lysates (Section 2.11.7) of SH1000 *spa::kan*, AFK2 (SH1000 *spa::kan divIC-gfp+*; P<sub>Spac-divIC</sub>) and AFK6 (SH1000 *spa::kan divIC-gfp+* pGL485; P<sub>Spac-divIC</sub>) strains grown in BHI media in the presence and absence of IPTG to exponential phase (OD<sub>600</sub> 0.5). A total of 10 µl of a known protein concentration was mixed with 5 µl of SDS loading buffer, boiled for 10 min and centrifuged for 3 min at room temperature at 13,000 rpm. The samples were analysed on 15% (w/v) SDS-PAGE, and the Western blot membranes were probed with affinity-purified α-DivIC and α-Gfp antibodies (Figure 4.10). A band of approximately 15 kDa was detected in the SH1000 *spa::kan* lysate probed with α-DivIC, assumed to be the native DivIC (Figure 4.10A).

In addition, when AFK2 (SH1000 *spa::kan divIC-gfp+*; P<sub>Spac-divIC</sub>) lysate was probed with α-DivIC and α-GFP antibodies, bands of 42 kDa were observed in all samples with and without IPTG (Figure 4.10A), representing the DivIC-GFP+ fusion protein.

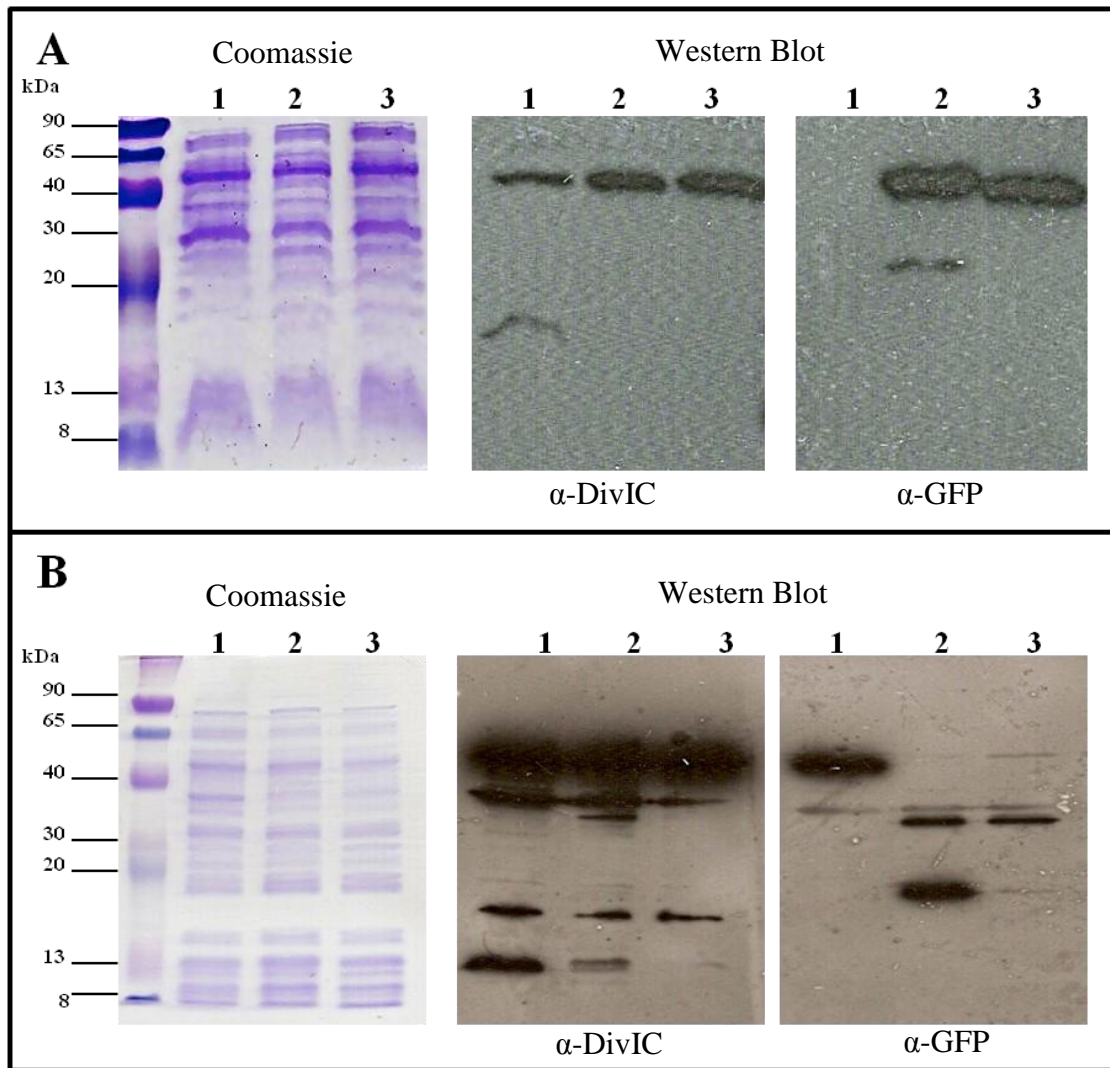


**Figure 4.10 Western blot analysis of a DivIC-GFP+ fusion in *S. aureus***

A. Whole cell lysates of SH1000 *spa::kan* (1) or AFK2 (SH1000 *spa::kan divIC-gfp+*;  $P_{\text{Spac-divIC}}$ ) grown either in the presence of 1 mM IPTG (2) or in the absence of IPTG (3) were separated by 11 % (w/v) SDS-PAGE and then analysed by Western blotting with rabbit polyclonal  $\alpha$ -DivIC at 1:5,000 dilution or with rabbit polyclonal  $\alpha$ -GFP at 1:10,000 dilution. Molecular marker sizes are indicated in kDa.

B. Whole cell lysates of SH1000 *spa::kan* (1) or AFK6 (SH1000 *spa::kan divIC-gfp+* pGL485;  $P_{\text{Spac-divIC}}$ ) grown in the presence of 1 mM IPTG (2) or in the absence of IPTG (3) were separated by 11 % (w/v) SDS-PAGE and then analysed by Western blotting with rabbit polyclonal  $\alpha$ -DivIC at 1:5,000 dilution or with rabbit polyclonal  $\alpha$ -GFP at 1:10,000 dilution. Molecular marker sizes are indicated in kDa.



However, a band of ~ 20 kDa was detected in the AFK2 (SH1000 *spa::kan divIC-gfp+*; P<sub>Spac</sub>-*divIC*) lysate in the presence of IPTG probed with  $\alpha$ -GFP antibodies, likely representing the degradation of the DivIC-GFP+ fusion protein. When AFK6 (SH1000 *spa::kan divIC-gfp+* pGL485; P<sub>Spac</sub>-*divIC*) lysate was probed with  $\alpha$ -DivIC and  $\alpha$ -GFP antibodies, bands of ~ 50 kDa were observed in all the samples probed with  $\alpha$ -DivIC antibodies and only detected in WT and AFK6 plus 1mM IPTG samples probed with  $\alpha$ -GFP antibodies (Figure 4.10B). Other bands of ~ 40 kDa were observed in all the samples probed with  $\alpha$ -DivIC and  $\alpha$ -GFP antibodies (Figure 4.10B). Bands of ~ 33 kDa were observed in AK6 samples induced with IPTG when probed with  $\alpha$ -DivIC antibodies and in AK6 with and without IPTG when probed with  $\alpha$ -GFP antibodies. A band of ~ 20 kDa was only observed in the AFK6 sample induced with IPTG when probed with  $\alpha$ -GFP antibodies. A band of ~ 18 kDa was observed in all the samples probed with  $\alpha$ -DivIC antibodies and a ~ 15 kDa bands was observed in the WT and AFK6 samples induced with IPTG when probed with  $\alpha$ -DivIC antibodies, likely representing the native copy of DivIC (Figure 4.10B).

Additional investigations must be conducted to determine the expression of DivIC-GFP+ in the presence and in the absence of IPTG and to verify that the localisation patterns observed for DivIC-GFP+ were not caused by the degradation of GFP-tagged protein.

#### **4.2.2.2.2. Localisation of *S. aureus* FtsL-GFP**

A functional N-terminal GFP fusion to FtsL was localised to the middle of vegetative *B. subtilis* cells as a ring-like structure and remained at this site throughout division, while in sporulating cells, FtsL was localised at the asymmetric septum (Sievers and Errington, 2000b). N-terminal GFP fusion to *E. coli* FtsL revealed that this protein also forms a ring-like structure at the division septa (Ghigo *et al.*, 1999).

The *gfp-ftsL* fusion gene, under the control of the xylose-inducible promoter (P<sub>xyI</sub>) in *B. subtilis*, was shown to be functional, as it complemented the mutation in *ftsL*<sup>-</sup> cells in the presence of the inducer and the cells divided normally (Sievers and

Errington, 2000b). In *B. subtilis*, the following localisation patterns were observed for GFP-FtsL at the division site: 20% of GFP-FtsL existed as a central dot, 29% of GFP-FtsL was observed as two peripheral dots and 27% of GFP-FtsL was observed as a band across the cell width (Sievers and Errington, 2000b).

To examine the localisation of FtsL in *S. aureus*, a C-terminal GFP fusion protein was constructed (Liya Marangattil; University of Sheffield) using the pMUTIN-GFP+ vector (Kaltwasser *et al.*, 2002). The RBS and *S. aureus ftsL* coding sequence were cloned into the pMUTIN-GFP+ vector to construct an in-frame fusion of *ftsL* to *gfp+*. The resulting plasmid, pGL618, was transformed into *S. aureus* RN4420 electrocompetent cells, and the plasmid was integrated into the chromosome via a single crossover event, resulting in a *ftsL-gfp+* fusion under the control of the native *ftsL* promoter and a native copy of *ftsL* under the control of P<sub>Spac</sub> (Figure 4.11). The plasmid insertion was subsequently transferred into the SH1000 and SH1000 *spa::kan* backgrounds via phage transduction using  $\phi$  11.

The fluorescent signal of FtsL-GFP+ was not intense (data not shown). This observation could potentially reflect either low FtsL-GFP expression, as a higher induction level is likely required to visualise the fluorescent protein was unstable, or the protein was incorrectly folded when exported from the cytoplasm. Due to time limitations, the further investigation of FtsL localisation using the GFP fusion protein was not performed.

### **4.2.3. DivIC and FtsL overexpression in *S. aureus***

#### **4.2.3.1. pLOW system**

pLOW is a low copy number vector that facilitates the overexpression of genes under the control of P<sub>Spac</sub> in *S. aureus* (Liew *et al.*, 2010). pLOW has a multiple cloning site downstream of P<sub>Spac</sub>, which facilitates the insertion of the gene of interest, and the antibiotic markers, *blaM* and *ermC*, for selection in *E. coli* and *S. aureus*, respectively. pLOW also contains the constitutively expressed *lacI* gene under the control of P<sub>Pen</sub>, encoding the Lac repressor protein, which facilitates the regulation of encoded protein production in an IPTG-dependent manner (Liew *et al.*, 2010).

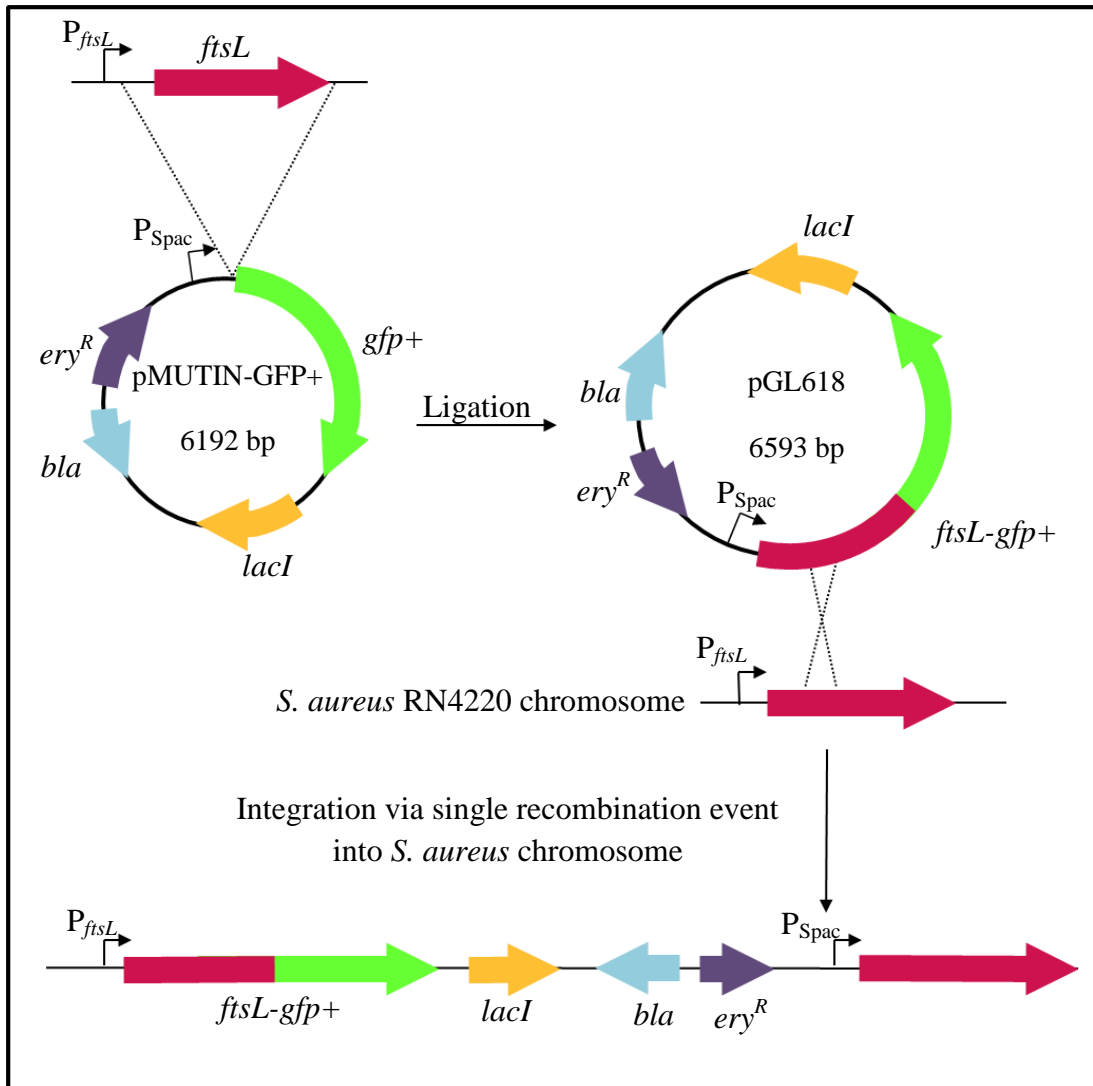


**Figure 4.11 Construction of a *S. aureus* *ftsL-gfp+* strain**

Schematic representation of pGL618 construction and the insertion of the plasmid into *S. aureus* RN4220. Liya Marangattil (University of Sheffield) generated this construct.

pLOW was used to produce the titratable and controllable expression of *S. aureus* genes, such as *ftsZ* and *nusA* (Liew *et al.*, 2010).

#### 4.2.3.2. Construction of overexpression plasmids

The pLOW plasmid was used to examine the effects of *divIC* and *ftsL* overexpression in *S. aureus* cells. The dissociation of the gene from its native promoter while retaining the RBS, which was not encoded within the pLOW vector, was necessary. AK11 and AK13 (Table 2.7) were designed as forward primers to amplify the 5' regions of *divIC* and *ftsL*, respectively.

AK11 was annealed to the region containing the RBS located upstream of *divIC* (Figure 4.12A), while AK13 was annealed within the area encompassing the RBS but overlapping the 3' end of *mraW* (Figure 4.13A). AK12 and AK14 were designed as reverse primers that annealed slightly downstream of *divIC* and *ftsL*, respectively (Figure 4.12A and Figure 4.13A).

The putative RBS and full length *divIC* and *ftsL* genes were amplified from SH1000 genomic DNA using the forward primers AK11 and AK13 and the reverse primers AK12 and AK14 (Table 2.7), and these reactions produced the expected 420 bp *divIC* and 430 bp *ftsL* fragments. The purified products were digested with *Bam*HI and *Eco*RI and ligated into pLOW, previously digested with the same enzymes (Figure 4.12A and Figure 4.13A). The ligation products were transformed into *E. coli* TOP10 electrocompetent cells and selected on LB plates containing ampicillin (100 µg ml<sup>-1</sup>). Positive clones were confirmed through PCR analysis and restriction digests with *Bam*HI and *Eco*RI, and the expected bands were visualised on a 1% (w/v) agarose gel (Figure 4.12B and Figure 4.13B). The positive clones were further verified through DNA sequencing (University of Sheffield). The sequences did not contain any substitutions or mutations.

The resulting plasmids, pAFK4 (pLOW P<sub>Spac</sub>-*divIC*) and pAFK5 (pLOW P<sub>Spac</sub>-*ftsL*), were then transformed into *S. aureus* RN4220 electrocompetent cells. The cells were selected on BHI erythromycin (5 µg ml<sup>-1</sup>) and lincomycin (25 µg ml<sup>-1</sup>) plates.

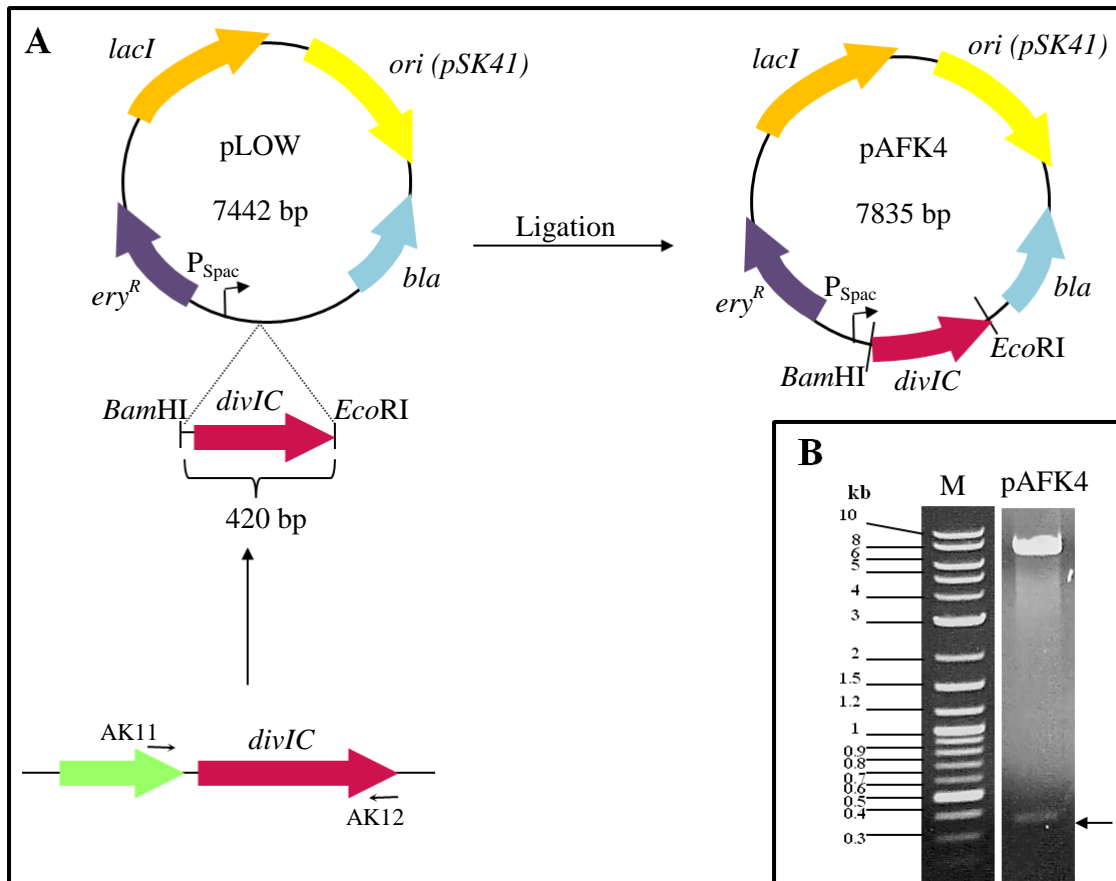


**Figure 4.12 Construction of pAFK4 (pLOW-*S. aureus divIC*) plasmid**

- A. A schematic representation of pAFK4 (pLOW-*S. aureus divIC*) plasmid construction in *E. coli*. The primers and restriction enzymes that were used are indicated (not to scale).
- B. pAFK4 was digested with *Bam*HI and *Eco*RI and subsequently analysed through electrophoresis on a 1% (w/v) TAE agarose gel. A 7,442 bp product, corresponding to the linearised pLOW plasmid, and a 420 bp product, corresponding to the *divIC* insert (indicated by a black arrow) were obtained.

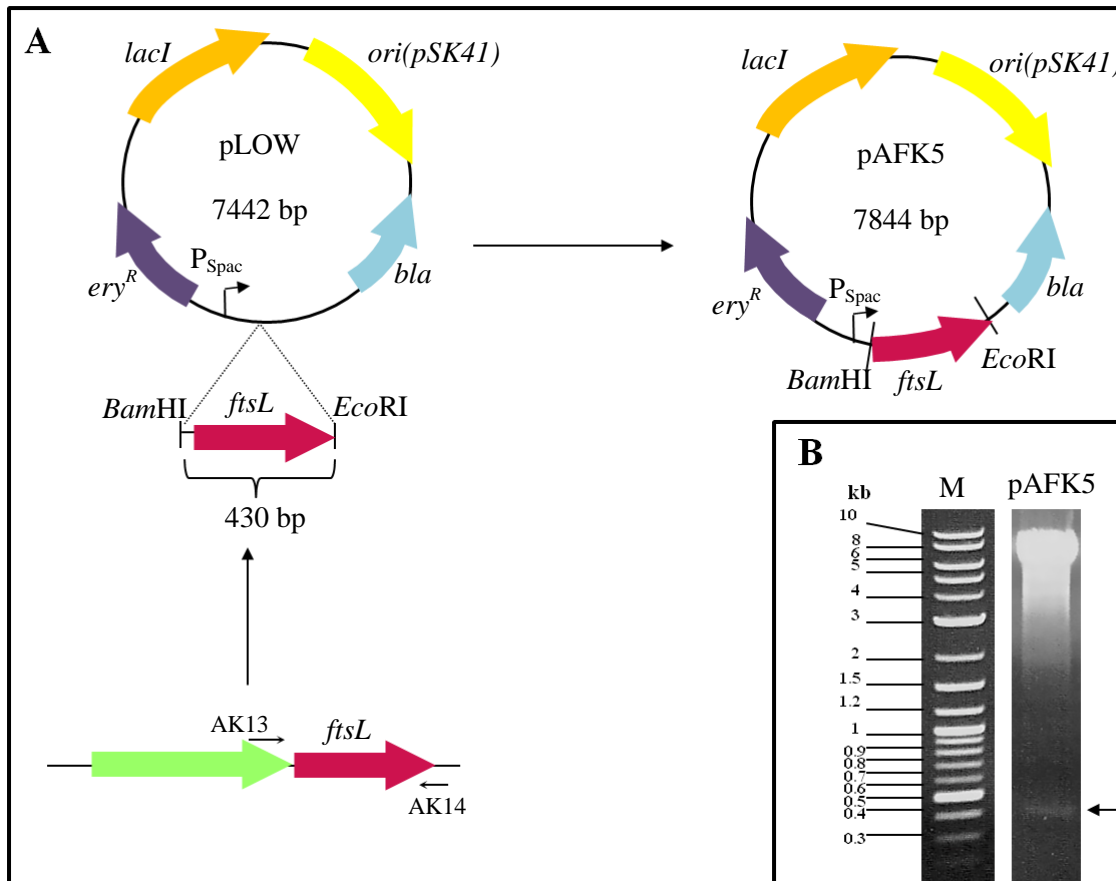


**Figure 4.13 Construction of pAFK5 (pLOW-*S. aureus ftsL*) plasmid**

- A. A schematic representation of pAFK5 (pLOW-*S. aureus ftsL*) plasmid construction in *E. coli*. The primers and restriction enzymes that were used are indicated (not to scale).
- B. pAFK5 was digested with *Bam*HI and *Eco*RI and analysed through electrophoresis on a 1% (w/v) TAE agarose gel. a 7,442 bp product, corresponding to the linearised pLOW plasmid, and a 430 bp product, corresponding to the *ftsL* insert (indicated by a black arrow) were obtained.

The presence of the plasmid was further examined through PCR analysis using primers AK17 and AK18 (Table 2.7) and analysed on a 1% (w/v) agarose gel (data not shown).

Strains AFK9 (RN4200 pAFK4) and AFK10 (RN4220 pAFK5) were lysed with  $\phi$ 11, and plasmids transferred into SH1000 and SH1000 *spa::kan* cells through transduction. The cells in the SH1000 background were selected on BHI erythromycin ( $5 \mu\text{g ml}^{-1}$ ) and lincomycin ( $25 \mu\text{g ml}^{-1}$ ) plates, while the cells in the SH1000 *spa::kan* background were selected on BHI erythromycin ( $5 \mu\text{g ml}^{-1}$ ) and kanamycin ( $50 \mu\text{g ml}^{-1}$ ) plates.

The resulting strains AFK3 (SH1000 pAFK4), AFK4 (SH1000 *spa::kan* pAFK4), AFK11 (SH1000 pAFK5) and AFK12 (SH1000 *spa::kan* pAFK5) were verified for the presence of the plasmids through PCR analysis using primers AK17 and AK18 (Table 2.7) and analysed on a 1% (w/v) agarose gel (data not shown).

#### **4.2.3.3. Induction of protein expression**

To verify the level of DivIC and FtsL expressed from pLOW,  $\alpha$ -DivIC and  $\alpha$ -FtsL antibodies were used for Western blot analysis (Section 2.11.4). SH1000 *spa::kan*, AFK4 (SH1000 *spa::kan* pAFK4) and AFK12 (SH1000 *spa::kan* pAFK5) were grown to exponential phase and whole cell lysates (Section 2.11.7) were analysed through 15% (w/v) SDS-PAGE, transferred to PVDF membranes and subsequently blotted with polyclonal  $\alpha$ -DivIC and  $\alpha$ -FtsL antibodies.

Bands of  $\sim 60$  and  $\sim 40$  kDa were observed in all the samples probed with  $\alpha$ -DivIC antibodies (Figure 4.14A). Faint bands of 15 kDa were detected in all samples, corresponding to the native DivIC (Figure 4.14A). There was hardly any difference between DivIC levels in the presence and the absence of 1 mM IPTG (Figure 4.14A), potentially reflecting the concentration of the repressor, LacI, as too low to effectively suppress  $P_{\text{Spac}}$  (Liew *et al.*, 2010). Two bands lower and higher than 65 kDa were observed in all the samples probed with  $\alpha$ -FtsL antibodies (Figure 4.14B). A faint band of  $\sim 15$  kDa was observed in all samples, likely corresponding to the native FtsL protein (Figure 4.14B).

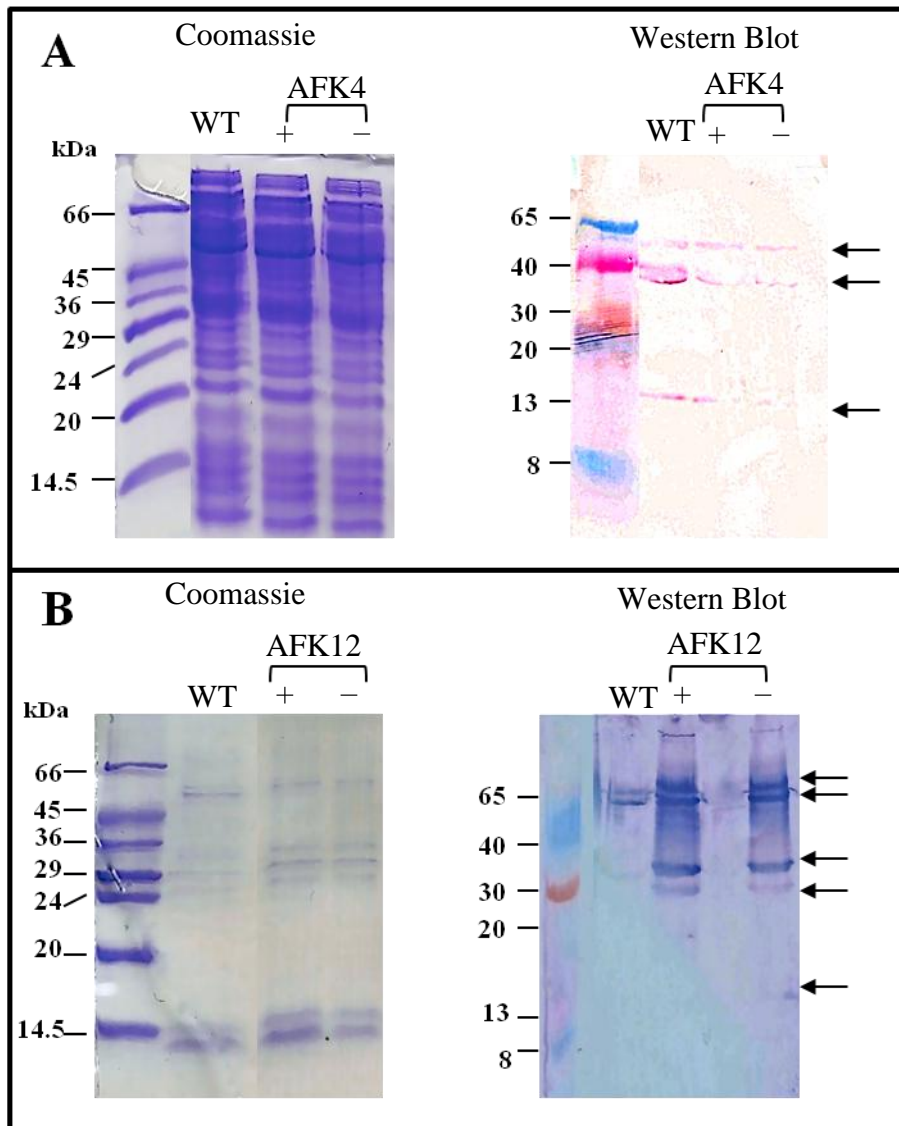


**Figure 4.14 Western blot analysis of AFK4 (SH1000 *spa::kan* pAFK4) and AFK12 (SH1000 *spa::kan* pAFK5)**

A. Whole cell lysates of SH1000 *spa::kan* (WT) and AFK4 (SH1000 *spa::kan* pAFK4) were grown in the presence (+) and absence (-) of 1 mM IPTG and analysed by 15% (w/v) SDS-PAGE. The proteins were transferred to a PVDF membrane and probed with rabbit polyclonal  $\alpha$ -DivIC antibodies at 1:10,000. The expected size of the full length DivIC is 15 kDa.

B. Whole cell lysates of SH1000 *spa::kan* (WT) and AFK12 (SH1000 *spa::kan* pAFK5) were grown in the presence (+) and absence (-) of 1 mM IPTG and analysed by 15% (w/v) SDS-PAGE. The proteins were transferred to a PVDF membrane and probed with rabbit polyclonal  $\alpha$ -FtsL antibodies at 1:10,000. The expected size of the full length FtsL is 15 kDa.



There was no difference between the FtsL levels in the presence and the absence of 1 mM IPTG (Figure 4.14B), potentially reflecting the concentration of the repressor, LacI, as too low to effectively suppress  $P_{\text{Spac}}$  (Liew *et al.*, 2010).

Introducing the multicopy *lacI* plasmid, pGL485, (Figure 4.5) into pLOW generated titratable and IPTG-dependent gene expression from  $P_{\text{Spac}}$  (Liew *et al.*, 2010). Accordingly, to obtain the tight regulation of *divIC* and *ftsL* expression, pGL485 was introduced into AFK4 (SH1000 *spa::kan* pAFK4) and AFK12 (SH1000 *spa::kan* pAFK5). However, due to time limitations this regulation could not be achieved.

#### **4.2.3.4. Phenotypic effect of DivIC and FtsL overexpression in *S. aureus***

To examine the effect of DivIC and FtsL overexpression on *S. aureus* cell morphology, the cells were visualised using optical microscopy. The cell shape and size was examined in the presence and absence of 1 mM IPTG. AFK3 (SH1000 pAFK4) (Figure 4.15A), AFK4 (SH1000 *spa::kan* pAFK4) (data not shown), AFK11 (SH1000 pAFK5) (Figure 4.15B) and AFK12 (SH1000 *spa::kan* pAFK5) (data not shown), were grown overnight in 5 ml of BHI broth containing erythromycin ( $5 \mu\text{g ml}^{-1}$ ) and/or kanamycin ( $50 \mu\text{g ml}^{-1}$ ) and incubated at  $37^\circ\text{C}$  at 250 rpm. The overnight cultures were used to inoculate 5 ml of BHI to an  $\text{OD}_{600}$  of 0.01 in the presence and absence of 1 mM IPTG and incubated at  $37^\circ\text{C}$  to the exponential phase ( $\text{OD}_{600}$  0.5). The cells were centrifuged, resuspended and washed in  $\text{sdH}_2\text{O}$  and subsequently fixed in formaldehyde and glutaraldehyde solution. The samples were examined using deconvolution microscopy. There was no difference in cell size or shape between the samples treated either with or without 1 mM IPTG. Thus, IPTG treatment most likely did not cause many gene expression changes (Figure 4.15). However, as previously mentioned, this effect could reflect the concentration of the repressor, LacI, as too low to effectively suppress  $P_{\text{Spac}}$  and the requirement of the pGL485 plasmid for the tight regulation of gene expression (Liew *et al.*, 2010). Due to time limitations, further investigation could not be achieved.

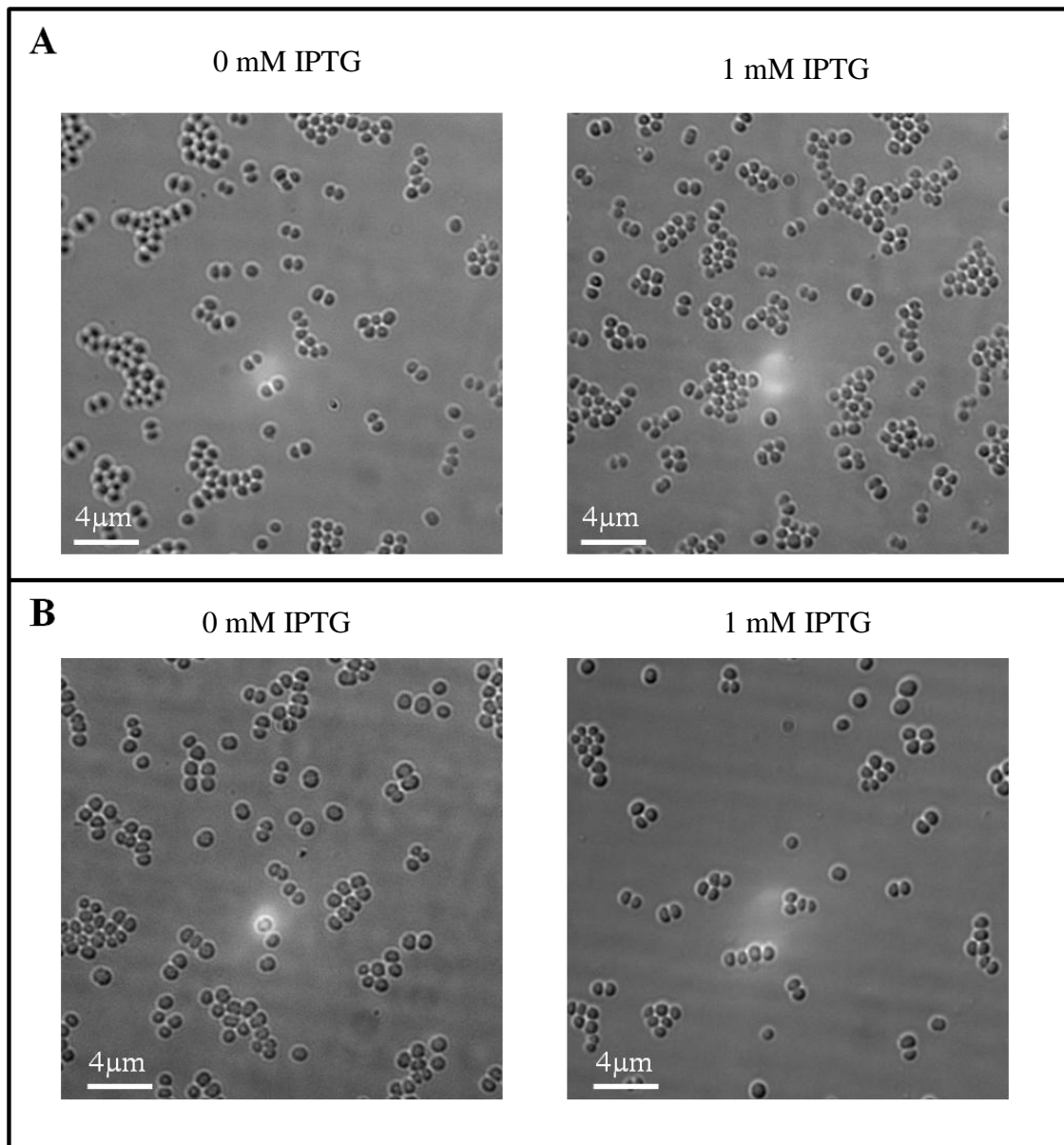


**Figure 4.15 Phenotypic effect of DivIC and FtsL overexpression in *S. aureus***

Phase contrast images of (A) AFK3 (SH1000 pAFK4) and (B) AFK11 (SH1000 pAFK5). Cells were grown in the presence or absence of 1 mM IPTG. Images were acquired using an Olympus IX70 microscope and SoftWoRx 3.5.0 software (Applied Precision). Scale bars are indicated.

#### **4.2.4. Immunolocalisation of *S. aureus* DivIC and FtsL**

##### **4.2.4.1. Immunolocalisation of *S. aureus* DivIC**

In *B. subtilis*, immunofluorescence microscopy showed that 67% of the DivIC protein was localised at the septum between the newly formed daughter cells, while 33% of the protein was localised at the midpoint of non-dividing cells (Katis *et al.*, 1997). The immunolocalisation in *S. pneumoniae* showed that DivIC was consistently localised to the division site during the cell cycle (Noirclerc-Savoie *et al.*, 2005). Therefore, the immunolocalisation of DivIC in *S. aureus* was performed.

Immunolocalisation was performed in accordance with the methods of Pinho and Errington (2003) (Section 2.17.3) in a strain lacking protein A, as this protein was expected to cross-react with the antibodies.

The secondary antibody used was AlexaFluor594-conjugated  $\alpha$ -rabbit IgG (Invitrogen) at a 1:1,000 dilution, to facilitate co-localisation with GFP-tagged proteins when necessary. A range of  $\alpha$ -DivIC antibody concentrations (1:100 to 1:2000) was tested. The cells were incubated with lysostaphin at range of concentrations from 0 to 30 ng ml<sup>-1</sup>. A similar DivIC localisation pattern was observed with immunolocalisation (Figure 4.16) as observed for AFK1 (SH1000 *divIC-gfp*<sup>+</sup>; P<sub>Spac</sub>-*divIC*) (Figure 4.7) and AFK6 (SH1000 *divIC-gfp*<sup>+</sup> pGL485; P<sub>Spac</sub>-*divIC*) (Figure 4.8), confirming the localisation of the DivIC-GFP fusion protein. A negative control without primary antibodies was performed, and no fluorescent cells were detected (data not shown).

##### **4.2.4.2. Immunolocalisation of *S. aureus* FtsL**

Immunofluorescence microscopy showed that *E. coli* FtsL formed a ring-like structure at the division site. The cross-reactivity of the  $\alpha$ -FtsL antibody, observed by Western blotting, did not exclude the fact that the antibodies reacted with other *E. coli* proteins; however, the localisation of FtsL in wild-type cells was demonstrated through the localisation of the GFP-fusion proteins (Ghigo *et al.*, 1999).

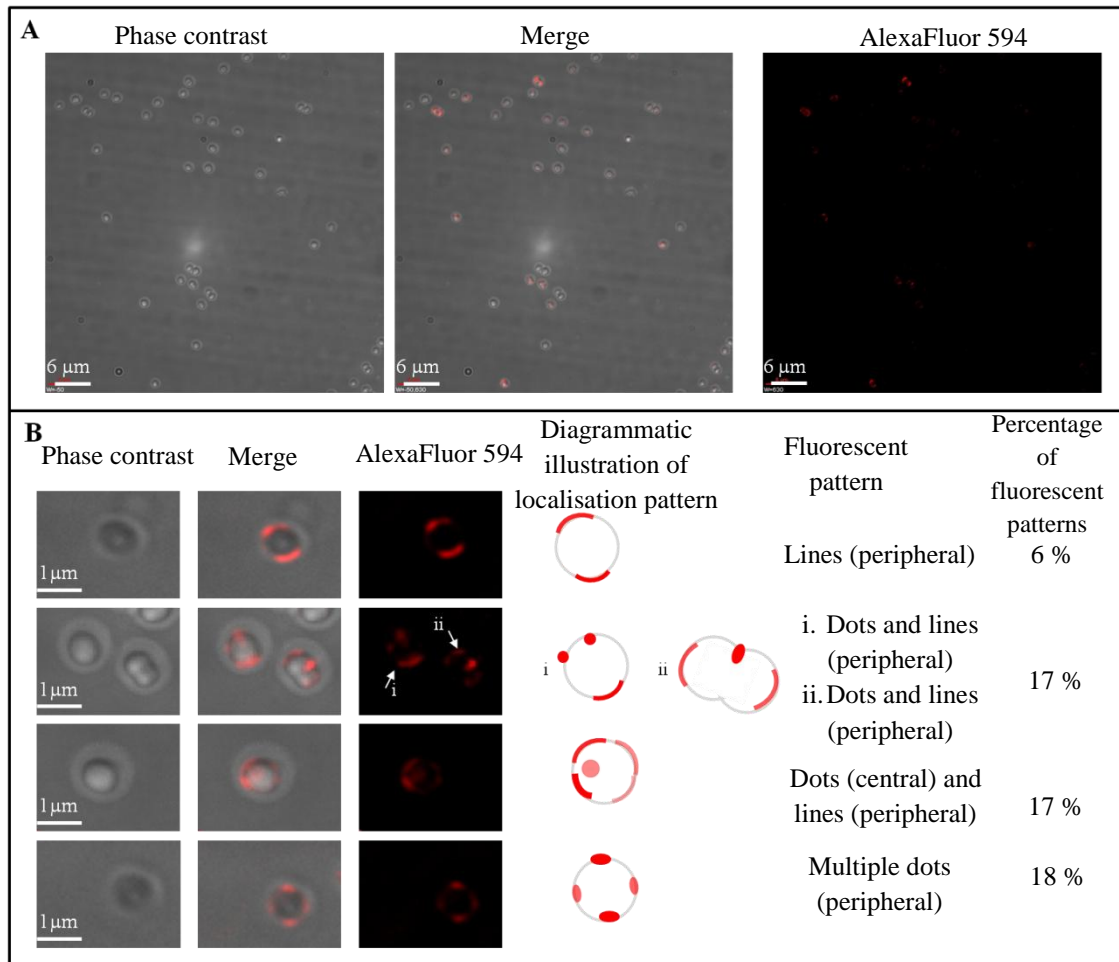


**Figure 4.16 Immunolocalisation of DivIC in *S. aureus***

- A. Fluorescence and phase contrast images of AFK4 (SH1000 *spa::kan* pAFK4) probed with  $\alpha$ - DivIC at 1:400 and detected with the AlexaFluor594-conjugated  $\alpha$ -rabbit IgG (Invitrogen). Images were acquired using Olympus IX70 microscope and SoftWoRx 3.5.0 software (Applied Precision). Scale bars are indicated.
- B. Schematic diagrams of the AFK4 (SH1000 *spa::kan* pAFK4) localisation patterns observed, percentage of patterns counted and their corresponding representative fluorescent images. Images were acquired using an Olympus IX70 microscope and SoftWoRx 3.5.0 software (Applied Precision). Scale bars are indicated.

The HA epitope tag was fused to the C-terminus of *B. subtilis* FtsL, and immunolocalisation was performed using monoclonal anti-HA antibodies. *B. subtilis* FtsL-HA was localised at the division site with FtsZ (Daniel and Errington, 2000). The immunolocalisation of *S. pneumoniae* FtsL showed that FtsL persists at the cell hemisphere; however, this protein migrates to the division site and briefly remains during FtsZ-ring formation, subsequently migrating back to its original location at the cell hemisphere.

The immunolocalisation was performed according to the methods of Pinho and Errington (2003; Section 2.717.3) in a strain lacking protein A, as this protein was expected to cross-react with the antibodies. The secondary antibody was AlexaFluor594-conjugated  $\alpha$ -rabbit IgG (Invitrogen) used at a 1:1,000 dilution, facilitating co-localisation with GFP-tagged proteins when necessary. A range of  $\alpha$ -FtsL antibody concentrations (1:100 to 1:2,000) was tested. The cells were incubated with lysostaphin at a range of concentrations from 0 to 30 ng ml<sup>-1</sup>. The localisation of FtsL (Figure 4.17) was observed as patches around the cell wall; however, only 11% of the FtsL was observed as a band between two dividing cells. A negative control without primary antibodies was performed, and no fluorescent cells were detected (data not shown).

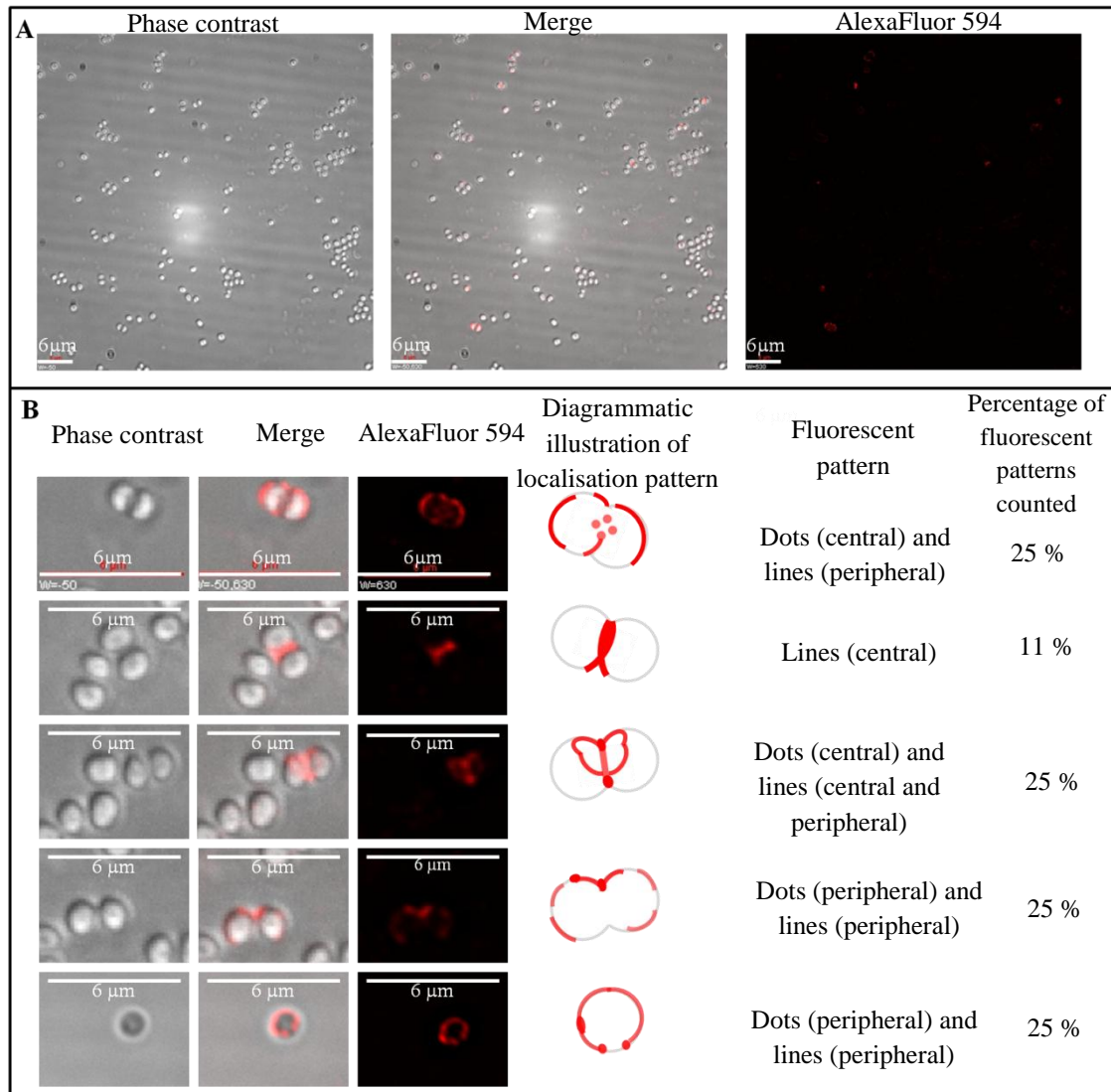


**Figure 4.17 Immunolocalisation of FtsL in *S. aureus***

A. Fluorescence and phase contrast images of AFK12 (SH1000 *spa::kan* pAFK5) probed with  $\alpha$ - FtsL at 1:400 and detected with the AlexaFluor594-conjugated  $\alpha$ -rabbit IgG (Invitrogen). Images were acquired using Olympus IX70 microscope and SoftWoRx 3.5.0 software (Applied Precision). Scale bars are indicated.

B. Schematic diagrams of the AFK12 (SH1000 *spa::kan* pAFK5) localisation patterns that were observed, percentages of patterns counted and their corresponding representative fluorescent images. Images were acquired using an Olympus IX70 microscope and SoftWoRx 3.5.0 software (Applied Precision). Scale bars are indicated.

### 4.3. Discussion

#### 4.3.1. Localisation of DivIC in *S. aureus*

In *B. subtilis*, DivIC was observed as a membrane-associated protein, with lesser amounts in the cell wall and cytoplasm (Katis *et al.*, 1997). The results of the present study showed that *S. aureus* DivIC is associated with the cell wall of *S. aureus* (Figure 4.3). The localisation of the *S. aureus* division protein, DivIC, was unexpected, as most of DivIC was present at the cell periphery, and only 6% of DivIC was localised at the midpoint before the septum is formed, suggesting the presence of DivIC at an early stage of cell division. The localisation of any protein to the division site suggests its involvement in cell division. However, previous studies of localisation in other bacteria have shown that not all cell division proteins are localised at the septum. For example, N-terminal GFP fusion to *E. coli* MinD showed that MinD localises to the cell poles (Raskin and de Boer, 1999a). In *B. subtilis*, Noc-YFP and DivIVA also localise to the cell periphery (Wu *et al.* 2009, Edwards and Errington, 1997). Moreover, immunolocalisation showed that *S. pneumoniae* DivIB and FtsL were localised at the division site only after the Z-ring formation; these protein are otherwise localised at the cell hemisphere throughout the cell cycle (Noirclerc-Savoie *et al.*, 2005). The co-localisation of *S. pneumoniae* DivIB and FtsL with FtsZ and DivIC at the division site was also observed during septation (Noirclerc-Savoie *et al.*, 2005).

It has been reported that DivIC localised to the division sites in *B. subtilis*, *E. coli* and *S. pneumoniae* (Katis *et al.*, 1997; Buddelmeijer *et al.*, 2002; Noirclerc-Savoie *et al.*, 2005). A previous fluorescence microscopy study of *S. aureus*, labelled with fluorescent vancomycin has shown cell wall synthesis exclusively at the cell midpoint (Pinho and Errington, 2003).

In the present study, the co-localisation of DivIC with peptidoglycan synthesis using fluorescent vancomycin and HADA (Figure 4.8 and Figure 4.9) showed that DivIC is present at the midpoint of the cell when no peptidoglycan synthesis was present.

This result suggests two potential mechanisms of DivIC localisation in *S. aureus* cells: DivIC localises to the midpoint of the cell during the early stages of division, indicating where the cell should form the new septum and recruit other cell division proteins to the new division site, followed by migration to the cell periphery once septum formation is initiated. DivIC could also prevent the incorrect placement of the septum or mark previous division sites.

In *S. pneumoniae*, DivIC is consistently localised at the midpoint of the cell, appearing as a distinctive band throughout the cell cycle; however, as soon as FtsZ translocates to the new division site, DivIC appears as a dot in the middle of the cell. Subsequently, DivIC re-joins FtsZ at the new division sites of the daughter cells. The localisation of DivIC in *S. pneumoniae* is similar to the cell division proteins involved in septal peptidoglycan synthesis, such as PBPs and FtsW (Noirclerc-Savoie *et al.*, 2005; Morlot *et al.*, 2004; Morlot *et al.*, 2003).

Immunofluorescence microscopy showed that *B. subtilis* DivIC exists in several localisation patterns. For example, 48% of DivIC existed as two dots in opposition, while 26% were observed as a line across the cell width, 16% appeared as a dot in the centre of the cell and only 8% of DivIC was localised as single dot on the side of the cell (Katis *et al.*, 1997). The existence of DivIC in *B. subtilis* as two dots or a line in dividing cells, suggests early stage localisation during the cell cycle, whereas the centre dot in divided cells represents late stage DivIC localisation during the cell cycle (Katis *et al.*, 1997). The results of previous studies have suggested that the localisation of *B. subtilis* DivIC is associated with a specific stage of cell cycle, such as before, during and after cell division (Katis *et al.*, 1997). *B. subtilis* DivIC localisation is similar to *B. subtilis* DivIB localisation, as both are present at the septum; however, 52% of DivIC existed as two dots at the septum, while only 17% of DivIB existed as two dots at the septum (Katis *et al.*, 1997, Harry and Wake, 1997). The assumption is that *B. subtilis* DivIC migrates to the division site prior to the initiation of division and persists at the division site for longer time periods in dividing cell (Katis *et al.*, 1997). The localisation of DivIC to the division site during early stage cell division reveals the involvement of this protein in distinct processes (Katis *et al.*, 1997).



Previously (Chapter 3; Section 3.2.4.4), DivIC was shown to bind to peptidoglycan, and this protein thus potentially contains a peptidoglycan-binding domain. This domain might bind to new cell wall material or mark previous division planes. This domain might also be involved in recognising a specific peptidoglycan architecture (Turner *et al.*, 2010) and recruiting other cell division proteins through the multiple interactions at the new division site. The involvement of DivIC in setting the division site is discussed later in (Chapter 6).

#### **4.3.2. Localisation of FtsL in *S. aureus***

FtsL is reportedly localised at the midcell throughout the cell cycle in rod-shaped *E. coli* and *B. subtilis* (Sievers and Errington, 2000b; Ghigo *et al.*, 1999). This finding is interesting, as in cocci-shaped *S. pneumoniae* and *S. aureus*, the localisation of FtsL was observed at the cell periphery (Noirclerc-Savoie *et al.* 2005; this study). *S. pneumoniae* FtsL shows a localisation pattern similar to that of DivIB, which is present at the cell hemisphere throughout the cell cycle and only present at the division site when the Z-ring is completely formed and when FtsZ migrates to the equators of daughter cells. Subsequently, both FtsL and DivIB migrate back to the old hemispheres rather than joining FtsZ and DivIC at the future division site (Noirclerc-Savoie *et al.*, 2005). The *B. subtilis* FtsL localisation pattern at the division site was shown either as a band, two dots or single dots. The dots and bands of FtsL present at midcell were also co-localised with FtsZ at the division site (Daniel and Errington, 2000).

#### **4.4. Future work**

Further investigation of the functionality of the DivIC-GFP fusion protein should be performed in a temperature-sensitive mutant of *S. aureus divIC* (Section 5.2.2). Time-lapse microscopy in live cells would be useful technique to investigate the localisation of DivIC during *S. aureus* cell division. As previously described, DivIC binds to peptidoglycan in the presence and absence of WTA, suggesting the involvement of this protein in cell wall recognition or synthesis during division. The identification of the *S. aureus* DivIC binding domain will facilitate the characterisation of the role of this binding in the localisation of DivIC, particularly

when using truncated forms of the protein binding domain to study its effect on protein localisation. In addition, using truncated forms of the DivIC protein in the peptidoglycan-binding domain will provide information concerning the role of DivIC in cell division and recognition of peptidoglycan architecture. The effect of the WTA on DivIC and FtsL localisation should also be investigated, as DivIC and FtsL interact with WTA synthetic machinery (Kent, 2013); hence, DivIC-GFP+ or FtsL-GFP+ should be expressed in a *tagO* *S. aureus* background. Moreover, the effect of DivIC and FtsL localisation when other cell division proteins are depleted should be investigated. Certainly without DivIC and FtsL mutants it is difficult to determine the roles of these proteins in *S. aureus* cell division.

## Chapter 5

### Analysis of the roles of DivIC and FtsL

#### 5.1 Introduction

The bacterial two-hybrid system has revealed multiple interactions between *S. aureus* cell division proteins, including DivIC and FtsL (Figure 1.4A), suggesting that these interactions are involved in stabilising the cell division machinery and the formation of the septum (Steele *et al.*, 2011). Homologues of many cell division proteins have been determined to be crucial for the cell division process in many organisms (Vicente *et al.*, 2006; Zapun *et al.*, 2008).

TMDH has been used to identify a number of *S. aureus* genes that are putatively associated with cell division. This technique identifies transposons within the genome, and genes that lack transposon insertions are then verified by different approaches and confirmed to be essential genes (Chaudhuri *et al.*, 2009). Several newly identified, essential *S. aureus* genes, including *divIC* and *ftsL*, are also essential in *B. subtilis* (Chaudhuri *et al.*, 2009) (Table 1.1); however, the functions of many cell division proteins remain unclear, with the exception of penicillin-binding proteins (Sauvage *et al.*, 2008). In *B. subtilis*, a temperature-sensitive null *divIC* mutant has shown that septum formation in sporulating and vegetative cells is impaired at the non-permissive temperature, and cells exhibit a long filamentous phenotype with no septa. This suggests the necessity of DivIC for cell division and, hence, survival (Levin and Losick, 1994; Mendelson and Cole, 1972). A conditional mutation in *B. subtilis ftsL* has shown that cells were lytic, as the division process ceased at an early stage due to the absence of the septum; therefore, the cells appeared as long filaments. These results indicate the essentiality of *B. subtilis ftsL* for division initiation (Daniel *et al.*, 1998; Daniel *et al.*, 1996; Sievers and Errington, 2000a; Daniel and Errington, 2000). In addition, the lack of *B. subtilis ftsL* and *divIC* hinders the activation of sigma factors that are involved in *B. subtilis* sporulation (Daniel *et al.*, 1998; Levin and Losick, 1994). In *B. subtilis*, mutagenesis of DivIC was performed by replacing the cytoplasmic and membrane-spanning domains of DivIC with TolR, an *E. coli* bitopic transmembrane protein, which demonstrated that the replaced domains are not essential for bacterial cell division, while replacement of the DivIC cytoplasmic

domain with the DivIB cytoplasmic domain resulted in mutant cells that were inefficient at growth at high temperatures (Katis and Wake, 1999). Complementation of an *ftsL* null mutation in *B. subtilis* with heterologous genes from *Bacillus circulans*, *Bacillus badius* and *B. licheniformis* rendered those cells capable of both dividing at high temperatures and sporulating in the absence of native gene expression. However, the *S. aureus* FtsL protein was not complementary in *B. subtilis* (Sievers and Errington, 2000a). Overexpression of *ftsL* in *B. subtilis* restored the cessation of cell growth in *divIB* null mutant cells, which indicated that FtsL can compensate for the loss of DivIB in the cell (Daniel and Errington, 2000). Conditional mutations in *ftsB* (*divIC*) in *E. coli* and *V. cholerae* resulted in a cell division blockage, filamentous growth and lysis of the cells, which suggests the essentiality of these genes in cell division in both organisms (Taschner *et al.*, 1987, Buddelmeijer *et al.*, 2002). An *ftsB* mutant of *E. coli* exhibits an atypical nucleoid segregation structure at non-permissive temperatures, as observed by fluorescence microscopy (Taschner *et al.*, 1987). A temperature-sensitive null mutation in *E. coli ftsL* was considered lethal because it inhibited cell division and led to filamentous growth with no septa and eventually cell death. Complementation of an *ftsL* null mutant restored the wild-type cell phenotype, indicating the essentiality of FtsL in *E. coli* cell division (Guzman *et al.*, 1992; Ueki *et al.*, 1992). In *Streptomyces coelicolor*, marked deletion mutations in *ftsL* and *divIC* have demonstrated that neither gene is essential for bacterial growth or cell viability. However, single and double null mutations in both genes caused division phenotypes that were dependent on the growth medium. Mutant strains that were grown on osmotically enhanced medium exhibited a severe cell division defect (Benett *et al.*, 2007). Additionally, transmission electron microscopy (TEM) has shown that *S. coelicolor divIC* and *ftsL* were required for the effective switch from aerial hyphae to spores (Benett *et al.*, 2007).

### 5.1.1 Aims of this chapter

- To determine the role of *divIC* in *S. aureus*
- To determine the role of *ftsL* in *S. aureus*.

## 5.2 Results

### 5.2.1 Construction of *S. aureus divIC* and *ftsL* conditional lethal mutants

An assumption that *divIC* and *ftsL* were essential genes in *S. aureus* was made because they were essential in other bacteria. In *B. subtilis* and *E. coli* cells, the lack of either *divIC* (*ftsB*) or *ftsL* inhibits bacterial growth that leads to filamentous growth and, ultimately, cell lysis (Sievers and Errington, 2000a, Robichon *et al.*, 2008, Guzman *et al.*, 1992, Buddelmeijer *et al.*, 2002). To determine the essentiality of *divIC* and *ftsL* for *S. aureus* cell growth and to identify their functions in the cell, conditional lethal mutations in both genes were constructed. The essentiality of a gene can be determined in a number of ways, such as by the growth of bacterial cells under certain conditions in which the gene is expressed and growth failure under other sets of conditions in which the gene is not expressed. The gene is placed downstream of a regulatable promoter, which facilitates the construction of a conditional lethal mutant and, hence, verifies whether the gene is essential. This regulated gene expression system should not allow any leakage of gene expression when an inducer is not present; however, in the presence of an inducer, the system should be able to stand excessive gene expression under maximal induction. The P<sub>Spac</sub> is a hybrid between the promoters of the *B. subtilis* SPO1 phage and the *E. coli lac* operator. This promoter controls the expression of downstream genes by IPTG induction and is regulated by the *E. coli lac* repressor (Yansura and Henner, 1984). In *S. aureus*, the P<sub>Spac</sub> system produces titratable and inducible gene expression from a low basal level to a few thousand molecules per cell, which is similar to the physiological levels of many proteins (Zhang *et al.*, 2000). P<sub>Spac</sub> has been used successfully to reveal the essentiality of many *S. aureus* genes, such as *metRS*, *defI* (Zhang *et al.*, 2000), *ftsZ* (Pinho and Errington, 2003), *murE* (Jana *et al.*, 2000) and *pbpI* (Pereira *et al.*, 2007), making the system suitable for constructing conditional *S. aureus divIC* and *ftsL* mutants.

#### 5.2.1.1 Construction of an integrating plasmid containing P<sub>Spac</sub>

pCL84 (Figure 5.1A) is a single-copy integration vector that has a bacteriophage site-specific recombination system, L54a, which integrates into the lipase gene of the host (i.e., *S. aureus*) chromosome through *attP*, which is a viral attachment site,

and *attB*, which is a bacterial attachment site that is proximal to the 3' end of the *S. aureus* lipase structural gene (*geh*). This vector contains antibiotic markers for selection in *E. coli* and *S. aureus* (Lee *et al.*, 1991). The pCL84 vector system is suitable for cloning genes that form lethal overexpression products when they are cloned into multiple-copy vectors (Lee *et al.*, 1991).

The P<sub>Spac</sub> and multiple cloning site (MCS) (488 bp) were PCR-amplified from pAISH1 using primers ALB128 and ALB127 (Table 2.7). The pAISH1 vector (Aish, 2003) is a tetracycline-resistant derivative of pMUTIN4 (Vagner *et al.*, 1998). The purified PCR products were digested with *Bgl*II and *Bam*HI and ligated into pCL84 that had been previously digested with *Bam*HI, and dephosphorylated by alkaline phosphatase to prevent self-ligation of the vector (Figure 5.1A). The ligation mixture was transformed into *E. coli* TOP10 electrocompetent cells, and colonies were selected on LB + spectinomycin (100 mg ml<sup>-1</sup>) plates at 37°C. Positive clones were verified by plasmid extraction, restriction digestion with *Bgl*II and *Bam*HI (Figure 5.1B), PCR using the ALB128 and ALB127 primers and sequencing (Core Genomic Facility, University of Sheffield) (data not shown). The resulting sequences did not contain any substitutions or mutations, and the resulting pAFK7 plasmid was a pCL84 vector containing P<sub>Spac</sub> with downstream MCSs (Figure 5.1).

### 5.2.1.2 Construction of regulatable copies of *divIC* and *ftsL*

Due to the presence of *divIC* and *ftsL* in operons and the potential polarity on downstream genes, the only way to construct conditional lethal mutations is to have a regulatable copy of the gene at the *geh* locus and an in-frame deletion at the native chromosomal locus without affecting the downstream gene expression. Moreover, once integrated in the chromosome, P<sub>Spac</sub> could co-regulate genes downstream of *divIC* and *ftsL* if they were included in operons. Accordingly, *divIC/ftsL* could be misclassified as essential genes if the downstream genes are essential for growth. Analysis of the 105 bp between *divIC* and its downstream gene using the bacterial terminator predictor FindTerm ([www.softberry.com](http://www.softberry.com)) predicted a terminator after the downstream gene.

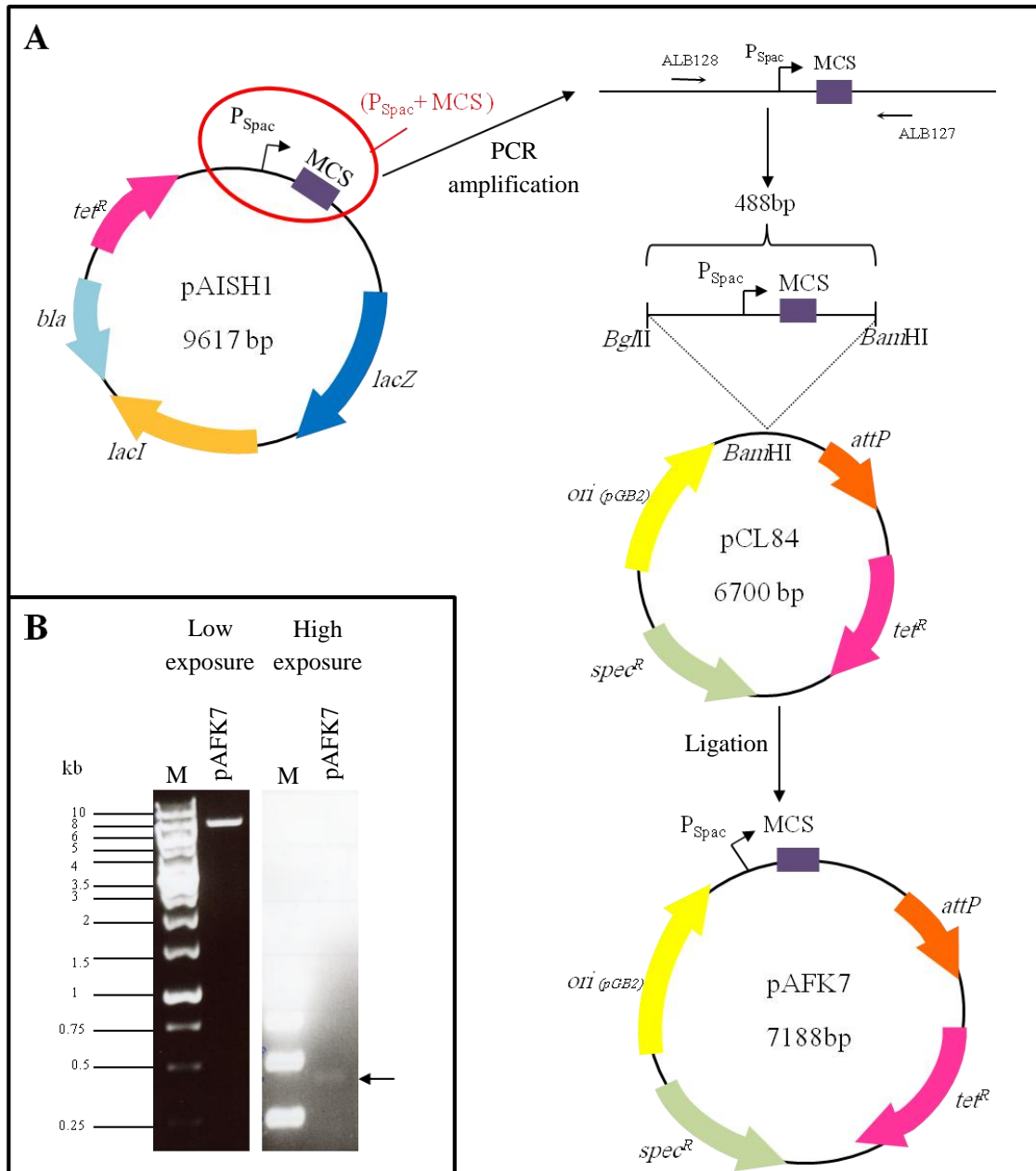


**Figure 5.1 Construction of the  $P_{\text{Spac}}\sim\text{pCL84}$  plasmid (pAFK7)**

A. Diagrammatic representation of the construction of the pAFK7 ( $P_{\text{Spac}}\sim\text{pCL84}$ ) plasmid in *E. coli*. pCL84 was digested with *Bam*HI, treated with alkaline phosphatase, and then ligated with the  $P_{\text{Spac}} + \text{MCS}$  fragment from pAISH1 that was previously digested with *Bgl*II and *Bam*HI. Primers and restriction sites that were used are noted (not to scale).

B. pAFK7 was digested with *Bgl*II and *Bam*HI and then separated by 1% (w/v) TAE-agarose gel electrophoresis. A 6700 bp product that corresponded to linearised pCL84 vector and a 488 bp product that corresponded to  $P_{\text{Spac}} + \text{MCS}$ , indicated by a black arrow, were obtained. A DNA ladder (M) of the sizes shown was used to estimate the fragment size.

Therefore, it is likely that *divIC* is transcribed in an operon with its downstream gene; hence, P<sub>Spac</sub> was placed upstream of the full-length copy of *divIC* at its native locus (Figure 5.2A). In *B. subtilis*, *divIC* is part of an operon that contains the upstream genes *yabP* and *yabQ* and the downstream gene *yabR* (Asai *et al.*, 2001). However, *ftsL* and its downstream gene, *pbp1*, overlap, and using the bacterial terminator predictor, FindTerm, a terminator was predicted to be present after *pbp1* (Figure 5.3A). Therefore, it is likely that *ftsL* is transcribed in an operon with its downstream genes; hence, P<sub>Spac</sub> was placed upstream of the full-length copy of *ftsL* at its native locus. In *E. coli*, *ftsL* is a part of an operon with its downstream gene *ftsI* (Guzman *et al.*, 1992).

Dissociation of the gene from its native promoter while retaining the RBS was necessary to construct a conditional mutation. Promoters were predicted using the bacterial promoter predictor BPROM ([www.softberry.com](http://www.softberry.com)). A putative *divIC* promoter was identified upstream of the hypothetical (*hyp*) gene (Figure 5.2A), and a putative *ftsL* promoter was predicted within *mraW* (Figure 5.3A). The putative RBS of *divIC* was predicted to be located upstream of the *divIC* start codon (Figure 5.2B), while the putative RBS of *ftsL* was predicted to be upstream of the *ftsL* start codon and to overlap with the 3' end of *mraW* (Figure 5.3B). AK29 and AK31 (Table 2.7) were designed as forward primers to amplify the 5' regions of *divIC* and *ftsL*, respectively. AK29 annealed to the region containing the RBS that was located upstream of *divIC* (Figure 5.2B), whilst AK31 annealed within the area encompassing the RBS but overlapping the 3' end of *mraW* (Figure 5.3B). AK30 and AK32 (Table 2.7) were designed as reverse primers that annealed slightly downstream of *divIC* and *ftsL*, respectively (Figure 5.2C and Figure 5.3C).

The putative RBS and full-length *divIC* and *ftsL* were amplified from SH1000 genomic DNA using the forward primers AK29 and AK31 and the reverse primers AK30 and AK32 (Table 2.7), and these reactions produced the expected 420 bp *divIC* and 430 bp *ftsL* fragments. The purified products were digested with *Xma*I and *Sac*II and ligated into pAFK7, which had been digested with the same enzymes (Figure 5.2C and Figure 5.3C). The ligation products were transformed into *E. coli* TOP10 electrocompetent cells and then selected on LB + spectinomycin (100 µg ml<sup>-1</sup>) plates.



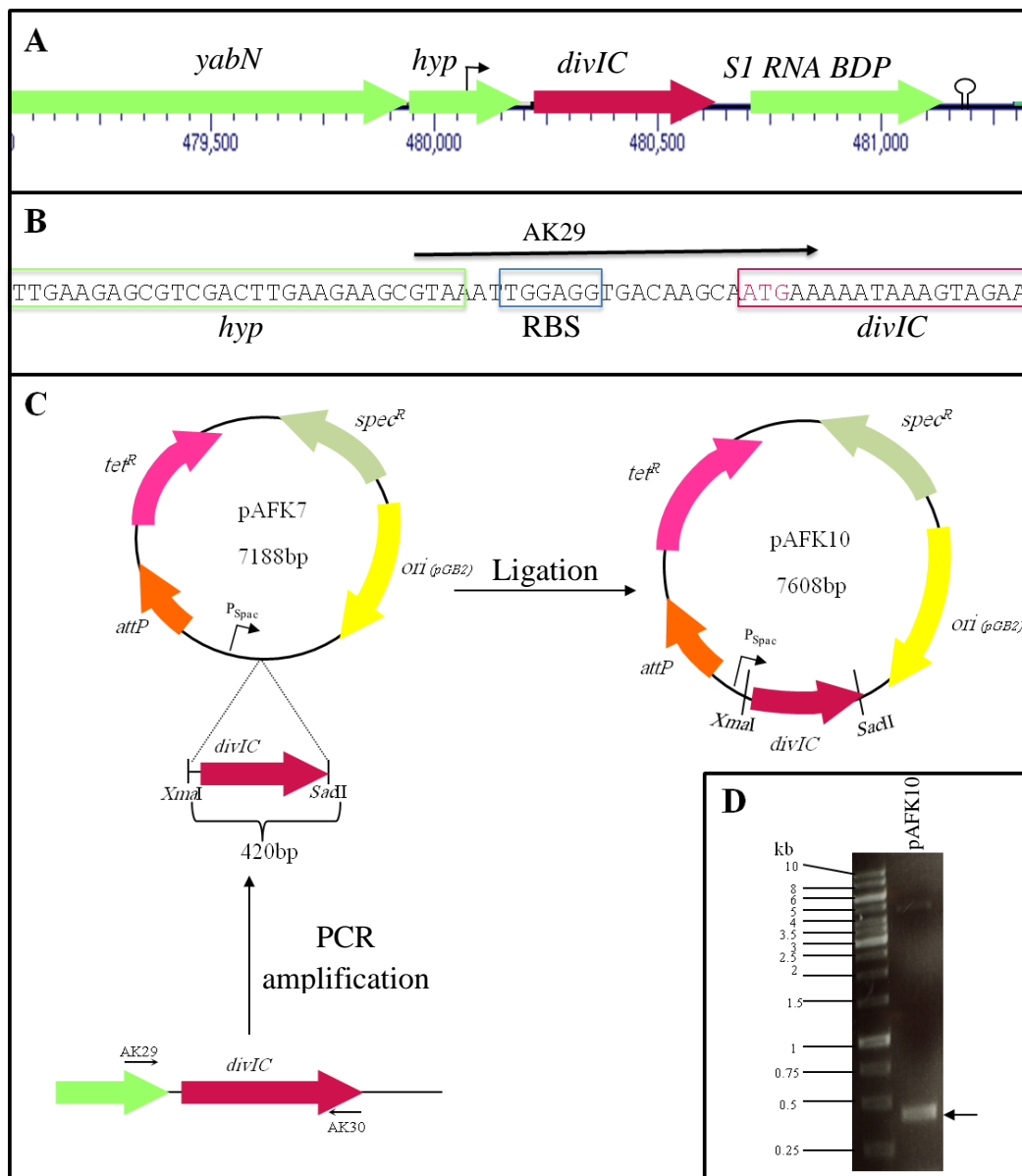


**Figure 5.2 Construction of pAFK10 ( $P_{\text{Spac}}\text{-divIC-pCL84}$ )**

- The chromosomal region of *divIC* in *S. aureus*. The putative terminator is represented as a stem-loop structure, and the putative promoter is shown as an arrow (approximately to scale).
- Site of AK29 annealing to the *S. aureus* chromosome. The RBS is indicated by a blue box; the 3' end of the upstream, hypothetical (*hyp*) gene is indicated by a green box; and *divIC* is indicated by a dark pink box. The *divIC* start codon is highlighted in dark pink.
- Diagrammatic representation of the construction of the pAFK10 (*S. aureus*  $P_{\text{Spac}}\text{-divIC}$ ) plasmid in *E. coli* (not to scale).
- A PCR product of *S. aureus divIC* was amplified from pAFK10 using the AK29 and AK30 primer pairs and then analysed by electrophoresis in a 1% (w/v) TAE agarose gel. A 420 bp product that corresponded to the *divIC* insert was obtained (indicated by a black arrow). DNA standards are of sizes shown in Kb.

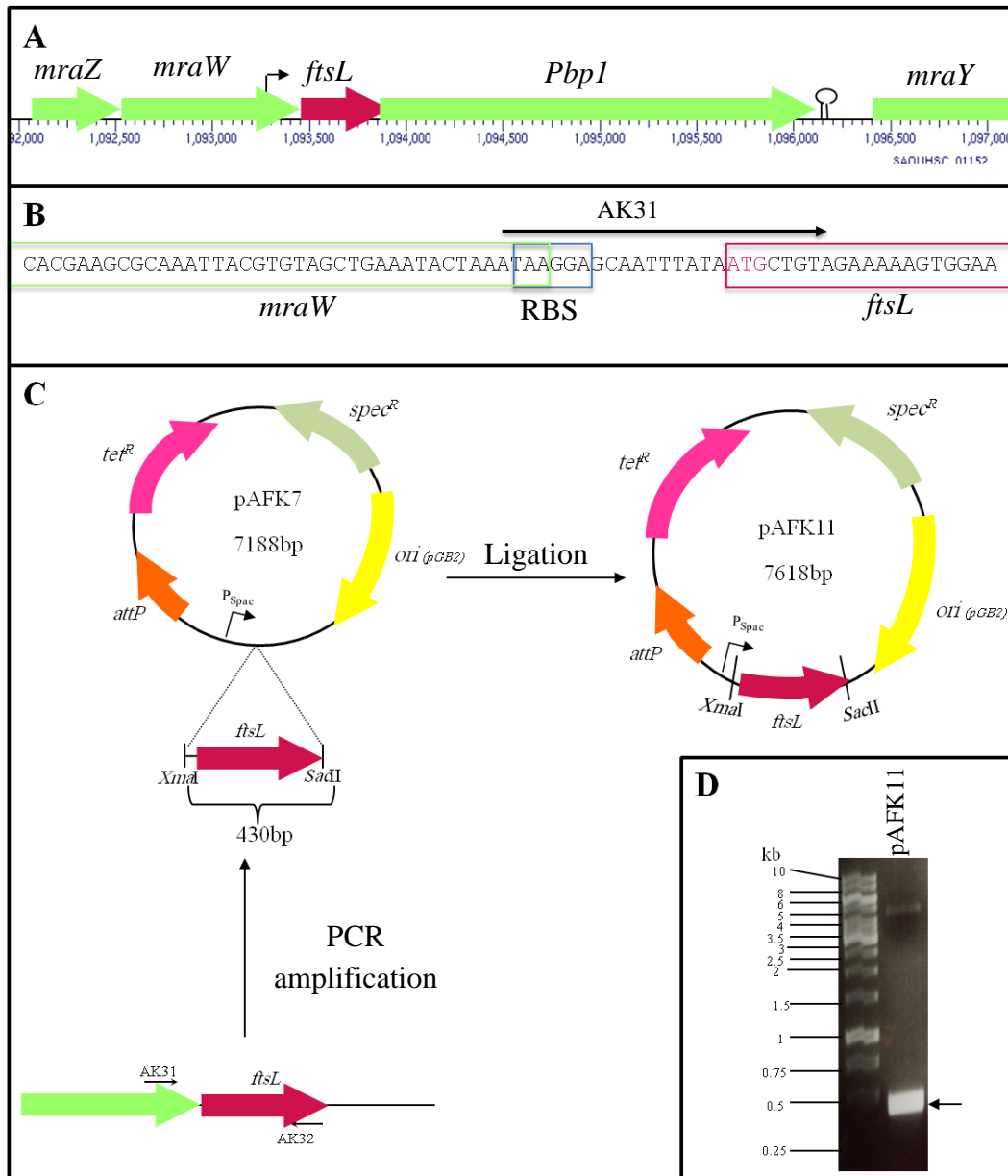


**Figure 5.3 Construction of pAFK11 ( $P_{\text{Spac}}\text{-ftsL}$ -pCL84)**

A. The chromosomal region of *ftsL* in *S. aureus*. The putative terminator is represented as a stem-loop structure, and the putative promoter is shown as an arrow (approximately to scale).

B. The site of AK31 annealing to the *S. aureus* chromosome. The RBS is indicated by a blue box, the 3' end of the *mraW* is indicated by a green box and *ftsL* is represented by a dark pink box. The *ftsL* start codon is highlighted in dark pink.

C. Diagrammatic representation of the construction of the pAFK11 (*S. aureus*  $P_{\text{Spac}}\text{-ftsL}$ ) plasmid in *E. coli* (not to scale).

D. The PCR product of *S. aureus ftsL* was amplified from pAFK11 using the AK31 and AK32 primer pair and then analysed by electrophoresis in a 1% (w/v) TAE agarose gel. A 430 bp product that corresponded to the *ftsL* insert was obtained (indicated by a black arrow). DNA standards are of sizes shown in Kb.

Bacterial growth was evident on the spectinomycin plates, and potential positive clones were verified by PCR analysis using the AK29 and AK30 primer pairs to amplify the *divIC* fragment (Figure 5.2D) and the AK31 and AK32 primer pairs to amplify the *ftsL* fragment (Figure 5.3D). However, verification of the clones by restriction digest or DNA sequencing indicated that the inserts were not present (data not shown); the false-positive PCR products that were observed on the gel could be due to cross-contamination. Therefore, cloning of the *divIC* and *ftsL* fragments into pAFK7 was not successful. After several failed attempts to clone the *divIC* and *ftsL* fragments under the control of P<sub>Spac</sub> in pAFK7, these fragments were cloned into the pAISH1 plasmid (Aish, 2003). The pAISH1 vector (Aish, 2003) encodes antibiotic resistance markers for *E. coli* and *S. aureus*. This plasmid is also non-replicating in *S. aureus* and carries P<sub>Spac</sub> and genes for the *lacI* repressor and *lacZ* reporter to control the inducible gene expression system. The pAISH1 plasmid (Aish, 2003) was chosen as a way to construct regulatable copies of the *divIC* and *ftsL* genes.

The putative RBS and the full-length *divIC* and *ftsL* fragments were amplified using the AK29 and AK30 primer pairs for *divIC* and the AK31 and AK32 primer pairs for *ftsL*. These PCR products were cloned into the MCS after P<sub>Spac</sub> by digesting the purified fragments with *XmaI* and *SacII* and ligating them into pAISH1, which was digested with the same enzymes (Figure 5.4C and Figure 5.5C). The ligation products were transformed into *E. coli* TOP10 electrocompetent cells then selected on LB + ampicillin (100 µg ml<sup>-1</sup>) plates. Positive clones were identified by purifying the plasmid, digesting it with *XmaI* and *SacII* and then confirming the expected bands by separating the reaction in a 1% (w/v) agarose gel (Figure 5.4D and Figure 5.5D). In addition, positive clones were further verified by DNA sequencing (University of Sheffield). The resulting sequences did not contain any substitutions or mutations; therefore, the pAFK12 (TOP10 P<sub>Spac</sub>-*divIC*) and pAFK13 (TOP10 P<sub>Spac</sub>-*ftsL*) plasmids were successfully constructed.

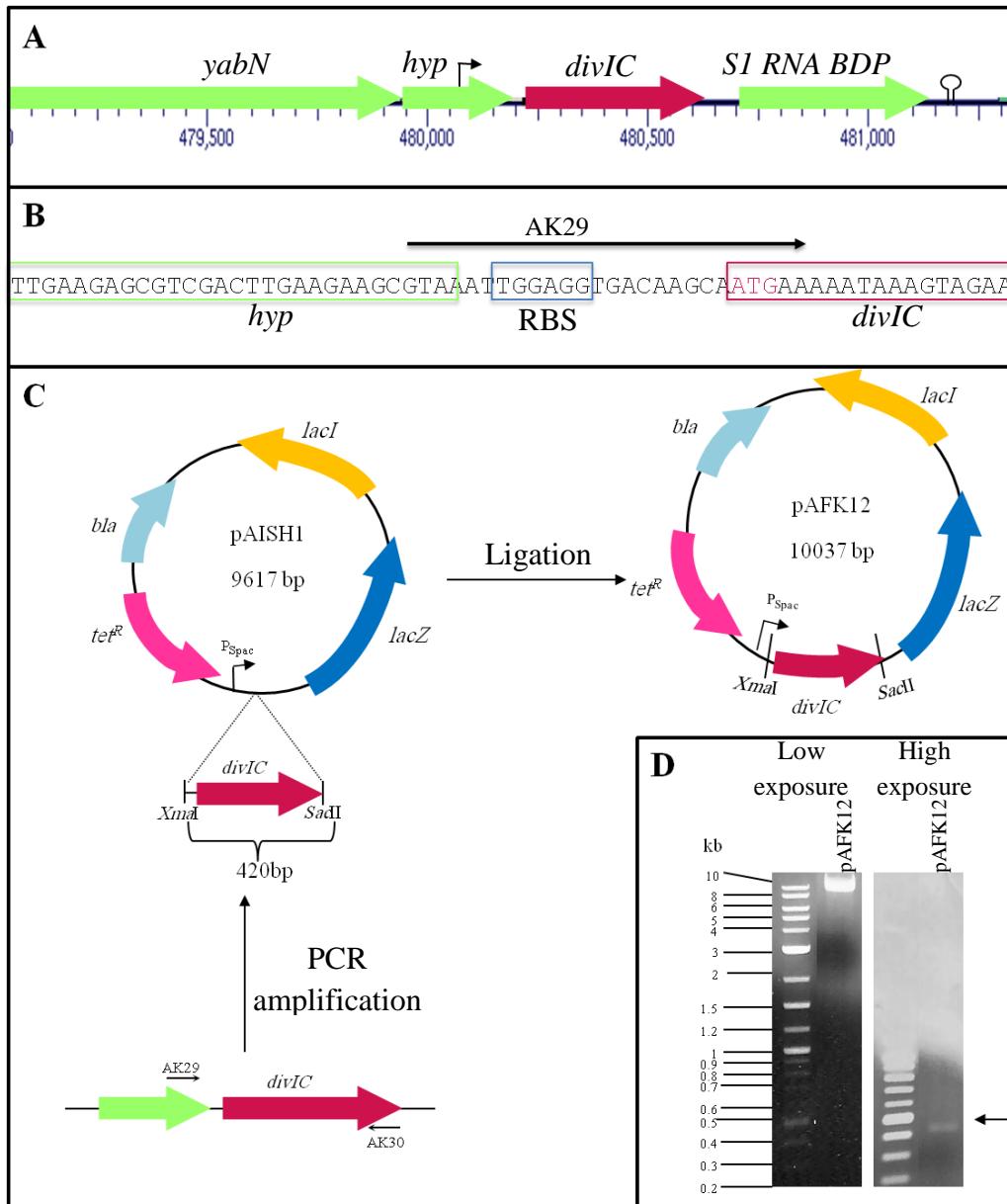


**Figure 5.4 Construction of the  $P_{Spac}$ -*divIC* plasmid pAFK12**

A. The chromosomal region of *divIC* in *S. aureus*. The putative terminator is represented as a stem-loop structure, and the putative promoter is shown as an arrow (approximately to scale).

B. The site of AK29 annealing to the *S. aureus* chromosome. The RBS is indicated by a blue box, the 3' end of the hypothetical (*hyp*) upstream gene is indicated by a green box and *divIC* is indicated by a dark pink box. The *divIC* start codon is highlighted in dark pink.

C. Diagrammatic representation of the construction of the pAFK12 (*S. aureus*  $P_{Spac}$ -*divIC*) plasmid in *E. coli* (not to scale).

D. pAFK12 was digested with *XmaI* and *SacII* and then analysed by electrophoresis in a 1% (w/v) TAE agarose gel. A 9617 bp product that corresponded to the linearised pAISH1 plasmid and a 420 bp product that corresponded to the *divIC* insert (indicated by a black arrow) were obtained. DNA standards are of sizes shown in Kb.

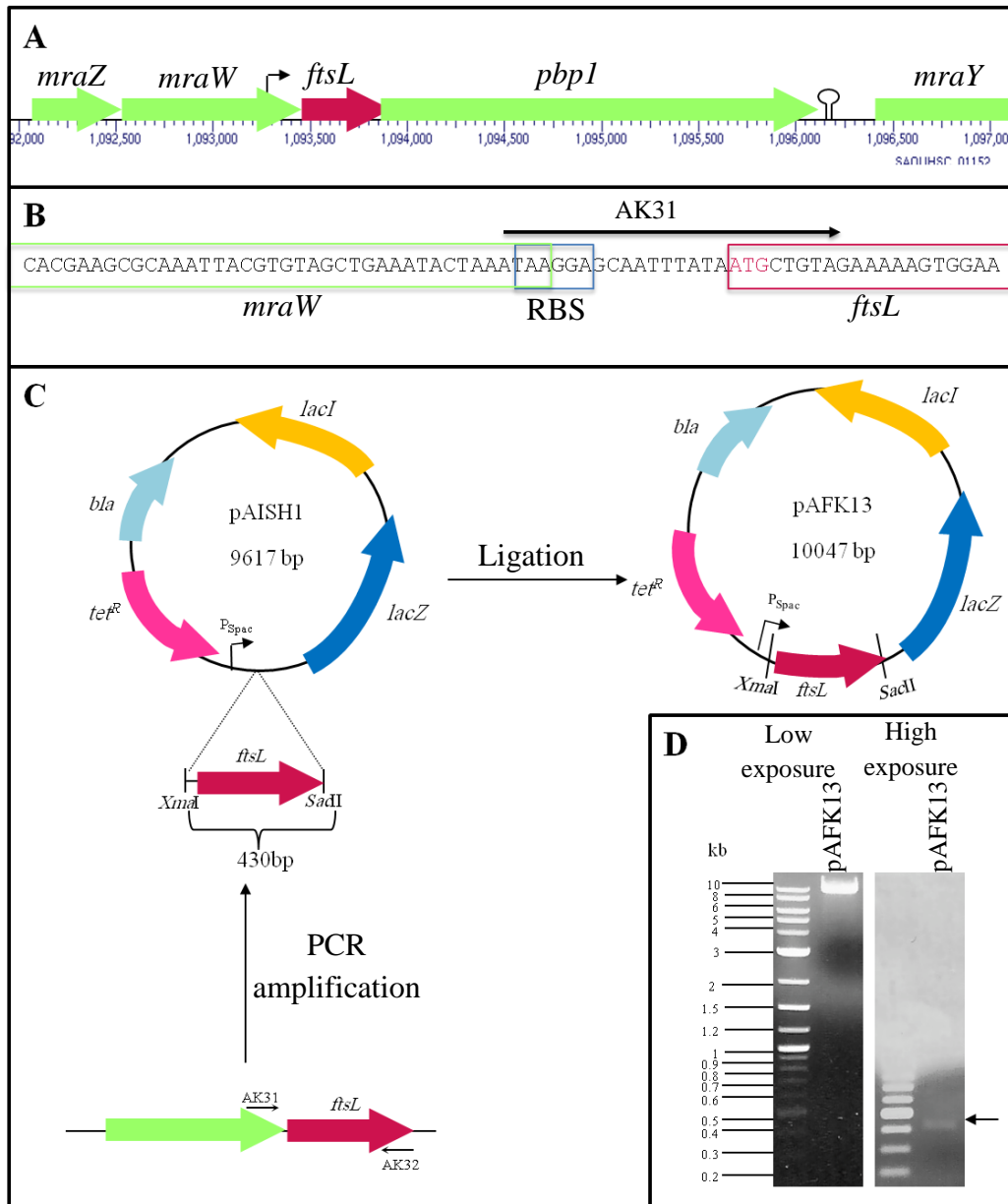


**Figure 5.5 Construction of the  $P_{Spac}$ -*ftsL* plasmid pAFK13**

A. The chromosomal region of *ftsL* in *S. aureus*. The putative terminator is represented as a stem-loop structure, and the putative promoter is shown as an arrow (approximately to scale).

B. The site of AK31 annealing to the *S. aureus* chromosome. The RBS is indicated by a blue box, the 3' end of the *mraW* is indicated by a green box and *ftsL* is indicated by a dark pink box. The *ftsL* start codon is highlighted in dark pink.

C. Diagrammatic representation of the construction of the pAFK11 (*S. aureus*  $P_{Spac}$ -*ftsL*) plasmid in *E. coli* (not to scale).

D. pAFK13 was digested with *XmaI* and *SacII* and then analysed by electrophoresis in a 1% (w/v) TAE agarose gel. A 9617 bp product that corresponded to the linearised pAISH1 plasmid and a 430 bp product that corresponded to the *ftsL* insert (indicated by a black arrow) were obtained. DNA standards are of sizes shown in Kb.

pKASBAR (Figure 5.6) is a hybrid plasmid (K. Wacnik and B. Salamaga, personal communication) that was created by the addition of a DNA fragment of pCL84 (Lee *et al.*, 1991) to the *E. coli* pUC18 (Vieira and Messing, 1982) backbone at the polylinker region, where this fragment bears a gene encoding tetracycline resistance (*tet<sup>R</sup>*), an *attP* site and MCS. pUC18 is a relatively small, high-copy-number plasmid with a versatile MCS that makes it easy to be used as an expression and sequencing vector (Bensasson *et al.*, 2004; Vieira and Messing, 1982).

Plasmid pGM073 (G. McVicker, personal communication, Figure 5.7) is a pKASBAR plasmid derivative with an improved MCS that was designed by Gareth McVicker (University of Sheffield) to make an *ezrA-psmOrange* fusion vector. The *ezrA-psmOrange* fragment encodes the EzrA protein with a C-terminal psmOrange fluorescent protein fusion. The entire fragment was synthesised by the GeneArt® Gene Synthesis service (Life Technologies) and ligated into the *Bam*HI and *Eco*RI sites of pKASBAR (Figure 5.7A). The *ezrA-psmOrange* fragment was then removed by restriction digestion with *Bam*HI and *Eco*RI and separated in a 1% (w/v) agarose gel (Figure 5.7B). The plasmid backbone was extracted from the gel, purified and analysed in a 1% (w/v) agarose gel (Figure 5.7C). This resulting plasmid lacking *ezrA-psmOrange* was termed pAFK22 (Figure 5.7A).

DNA fragments corresponding to the putative RBS and coding regions of *divIC* and *ftsL* were amplified from the pAFK12 (TOP10 P<sub>Spac</sub>-*divIC*) and pAFK13 (TOP10 P<sub>Spac</sub>-*ftsL*) plasmids, respectively, using the AK39 and AK40 primer pairs (Table 2.7). Purified PCR products were digested with *Apa*I and *Asi*SI and ligated into pAFK22, which was digested with the same enzymes (Figure 5.8A and Figure 5.9A). The ligation products were transformed into *E. coli* TOP10 electrocompetent cells and selected for on LB + ampicillin plates (100 µg ml<sup>-1</sup>). Positive clones were verified by plasmid extraction and restriction digestion with *Apa*I and *Asi*SI, and the expected bands were visualised in a 1% (w/v) agarose gel (Figure 5.8B and Figure 5.9B). Positive clones were further confirmed by DNA sequencing (University of Sheffield). The resulting sequences did not contain any substitutions or mutations.

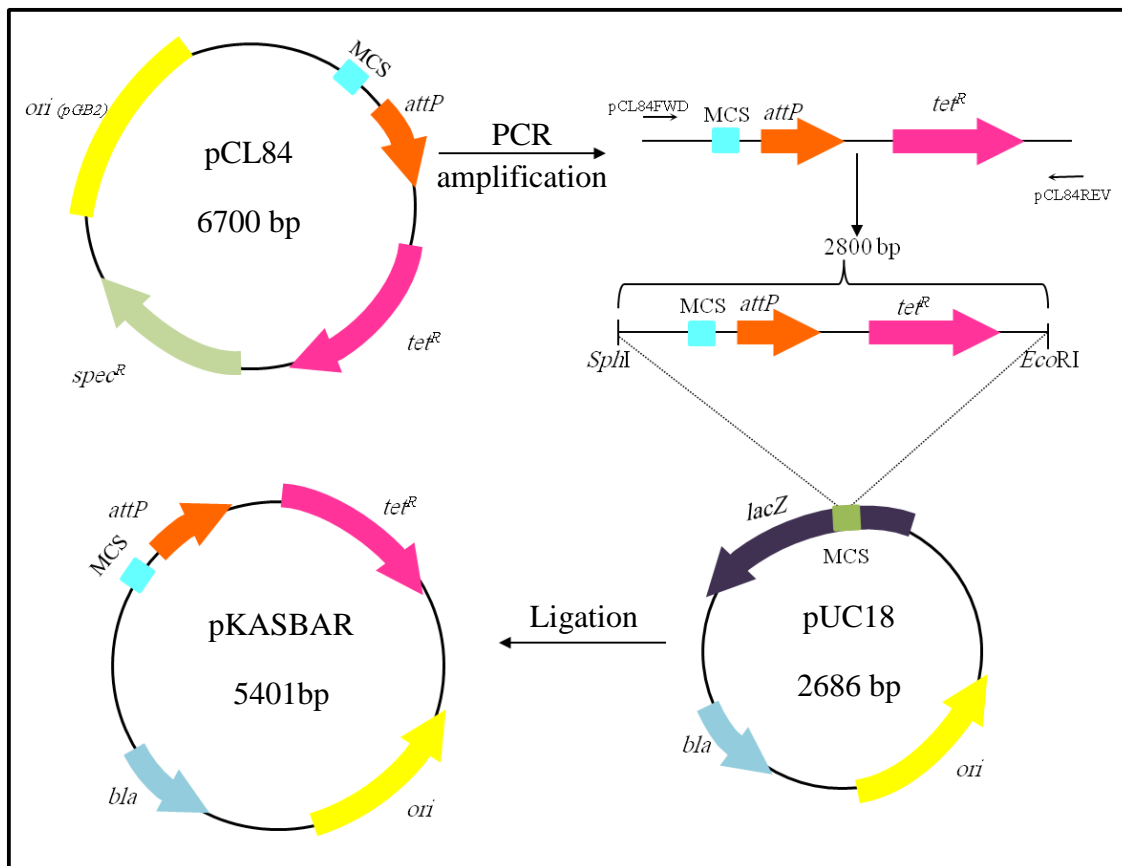


**Figure 5.6 Map of the integrative plasmid, pKASBAR**

pKASBAR is a hybrid plasmid that was created by adding a DNA fragment from pCL84 to the *E. coli* pUC18 backbone at the polylinker region where this fragment bears a *tet<sup>R</sup>* cassette, an *attP* site and MCS. The purified DNA fragment (*tet<sup>R</sup>*+*attP*+ MCS) was digested with *Sph*I and *Eco*RI and ligated into pUC18, which was digested with the same enzymes (map not to scale).

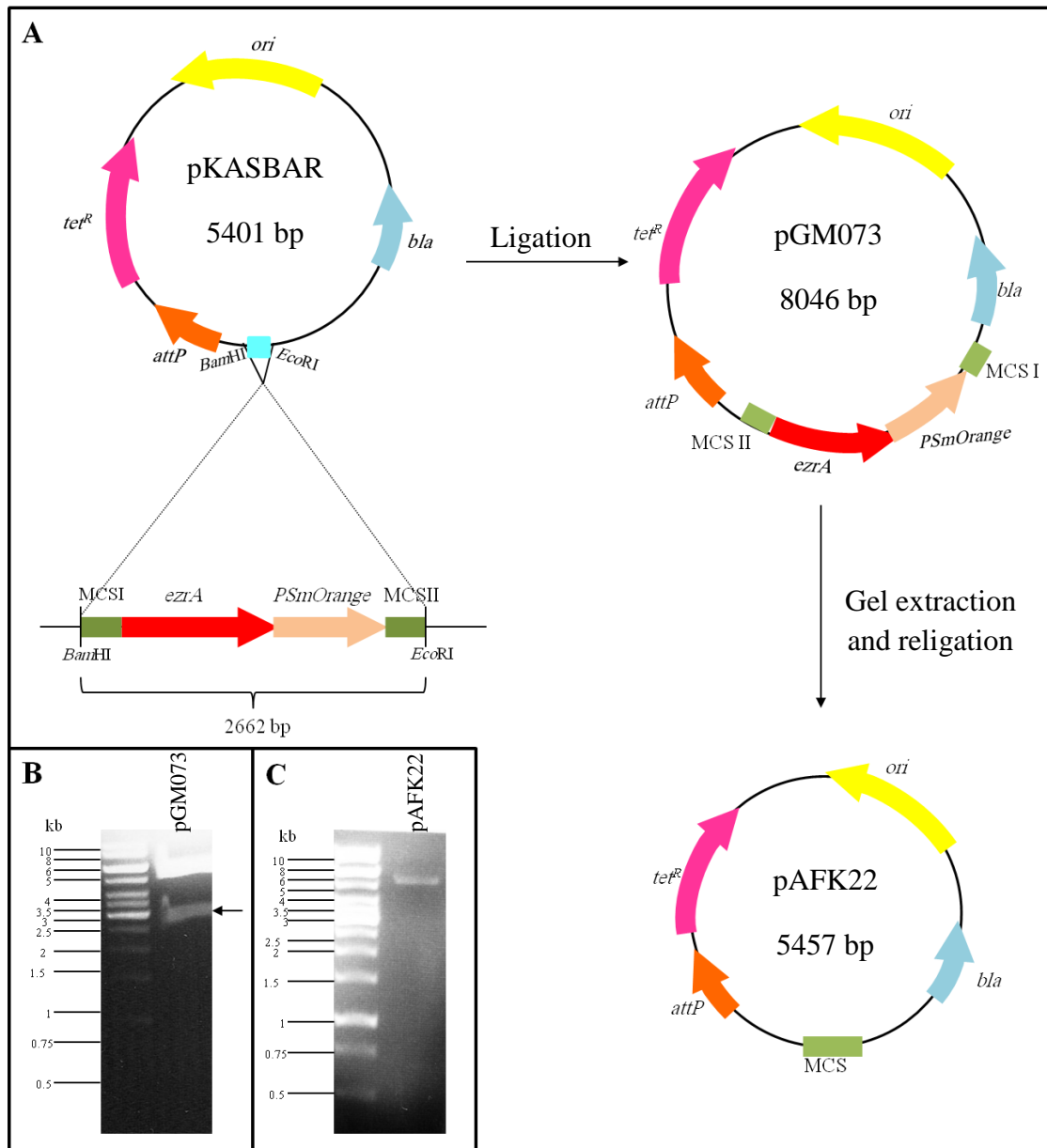


**Figure 5.7 Construction of the integration plasmids pGM073 and pAFK22**

A. Diagrammatic representation of the construction of pGM073 and pAFK22. The *ezra-psmOrange* cassette with the MCS was synthesised by the GeneArt® Gene Synthesis service (Life technologies) and then ligated into the *Bam*HI and *Eco*RI sites of pKASBAR (not to scale).

B. pGM073 was digested with *Bam*HI and *Eco*RI and then analysed by electrophoresis in a 1% (w/v) TAE agarose gel. A 5401 bp product that corresponded to linearised pKASBAR plasmid and a 2662 bp product that corresponded to the *ezra-PSmOrange* insert (indicated by a black arrow) were obtained. DNA standards are of sizes shown in Kb.

C. pAFK22 (pKASBAR including the new MCS) was gel-extracted and then separated by electrophoresis in a 1% (w/v) TAE agarose gel. A 5457 bp product that corresponded to pAFK22 was obtained. DNA standards are of sizes shown in Kb.



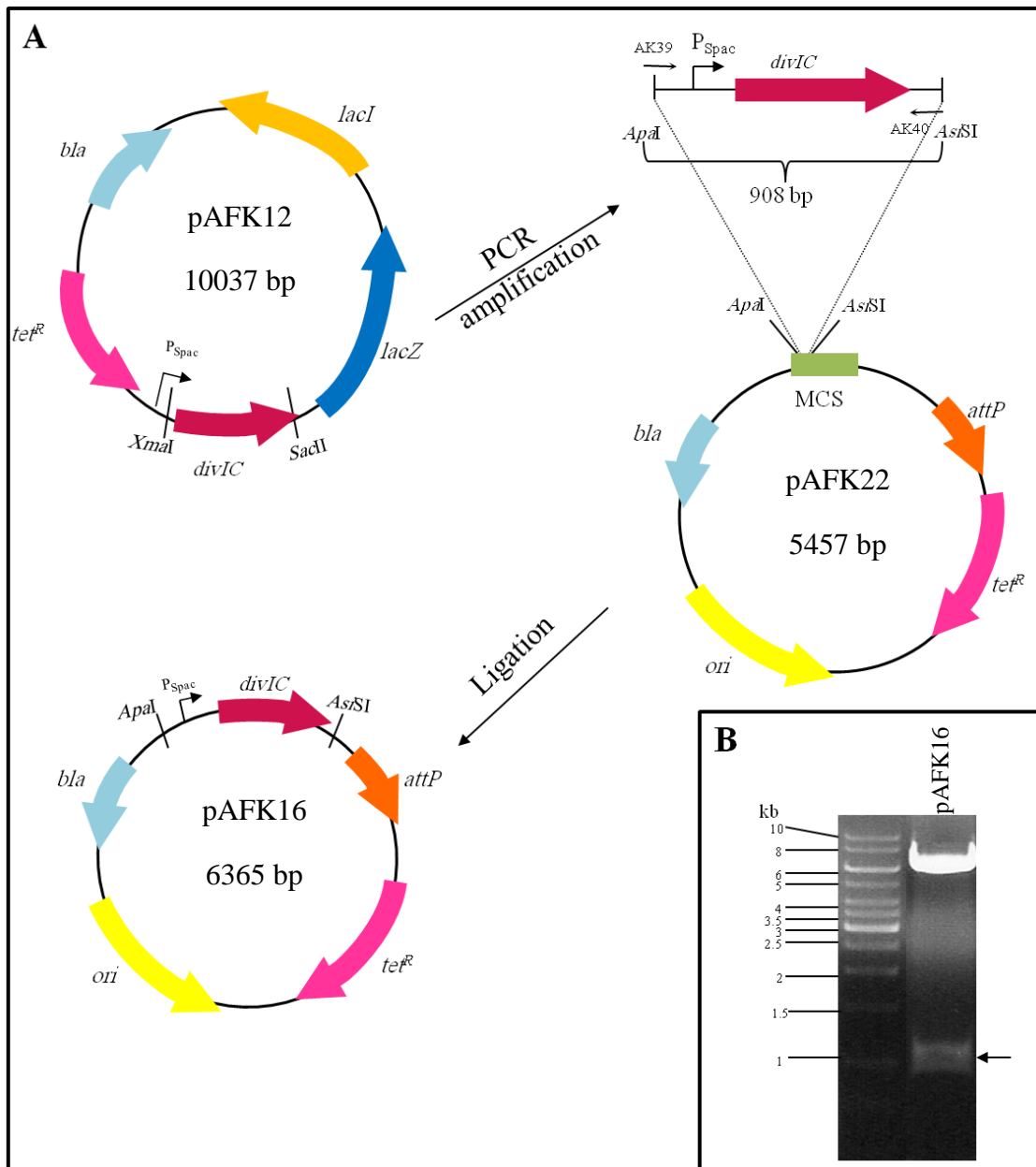


**Figure 5.8 Construction of the pAFK16 ( $P_{\text{Spac}}\text{-divIC}\sim\text{pAFK22}$ ) plasmid**

A. Diagrammatic representation of the construction of the pAFK16 ( $P_{\text{Spac}}\text{-divIC}\sim\text{pAFK22}$ ) plasmid in *E. coli*. Primers and restriction enzymes that were used are indicated (not to scale).

B. pAFK16 was digested with *Apa*I and *Asi*SI and then analysed by electrophoresis in a 1% (w/v) TAE agarose gel. A 5457 bp product that corresponded to linearised pAFK22 plasmid and a 908 bp product that corresponded to the  $P_{\text{Spac}}\text{-divIC}$  insert (indicated by a black arrow) were obtained. DNA standards are of sizes shown in Kb.

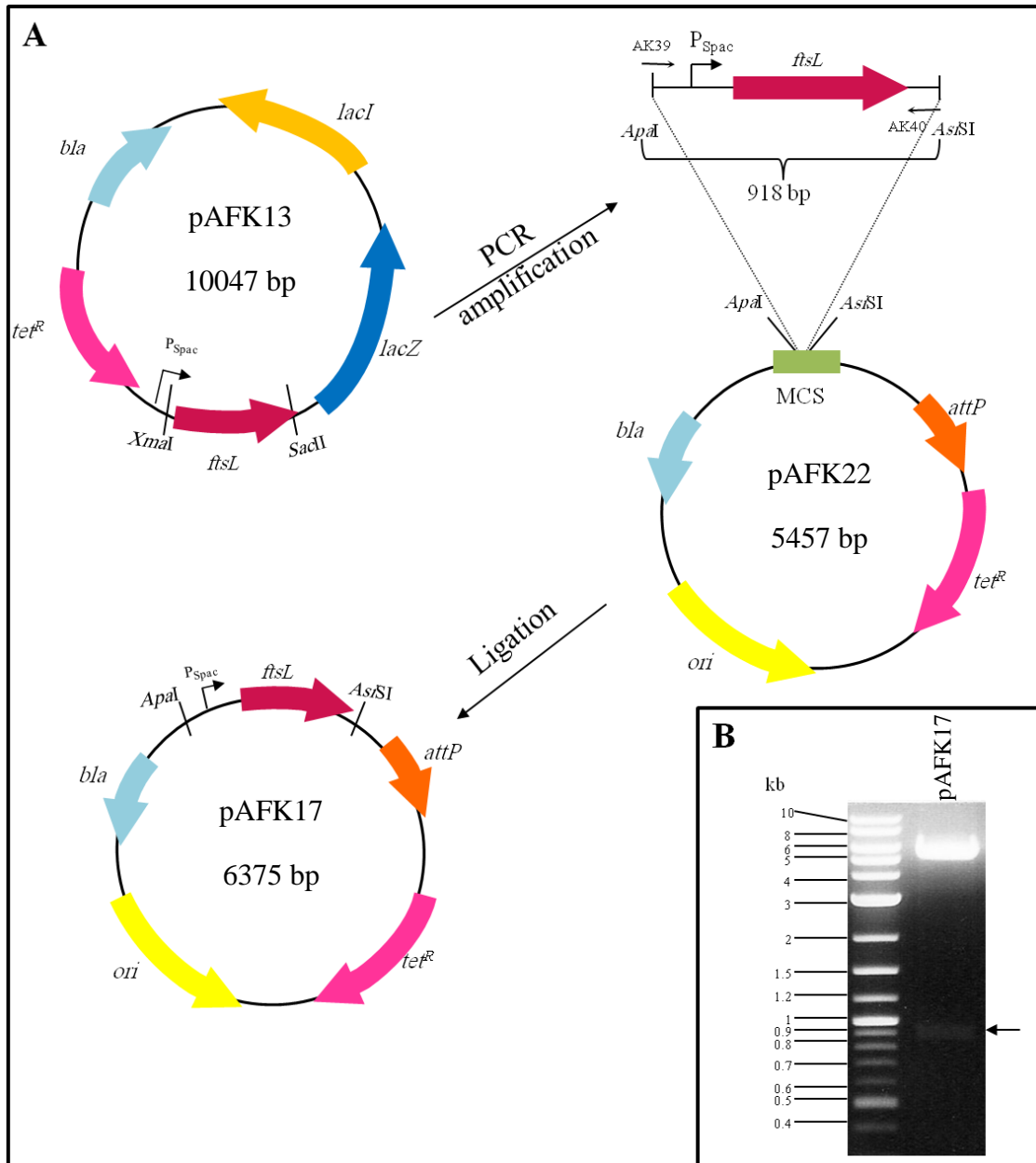


**Figure 5.9 Construction of the pAFK17 ( $P_{Spac}$ -*ftsL*~pAFK22) plasmid**

A. Diagrammatic representation of the construction of the pAFK17 ( $P_{Spac}$ -*ftsL*~pAFK22) plasmid in *E. coli*. Primers and restriction enzymes that were used are indicated (not to scale).

B. pAFK17 was digested with *Apa*I and *Asi*SI and then analysed by electrophoresis in a 1% (w/v) agarose gel. A 5457 bp product that corresponded to the linearised pAFK22 plasmid and a 918 bp product that corresponded to the  $P_{Spac}$ -*ftsL* insert (indicated by a black arrow) were obtained. DNA standards are of sizes shown in Kb.

The resulting plasmids, pAFK16 (pAFK22- P<sub>Spac</sub>-*divIC*) and pAFK17 (pAFK22- P<sub>Spac</sub>-*ftsL*) (Figure 5.10A and Figure 5.11A), were transformed into electrocompetent *S. aureus* RN4220 cells containing pCL112Δ19, which is a multicopy plasmid that carries the L54a integrase gene (*int*) and is expressed constitutively, without an *attP* site (Lee *et al.*, 1991). Selection of the cells took place on BHI + tetracycline (5 μg ml<sup>-1</sup>) plates. Integration of the plasmid into the chromosome was assessed by DNA extraction followed by PCR using the AK39 and AK40 primers (Figure 5.10B and Figure 5.11B). Integration of the plasmid into the chromosome should disrupt lipase production, which was verified by plating the transformants onto Baird-Parker (BPr) medium (Section 2.1.1). *S. aureus* will produce black colonies due to the reduction of the tellurite that is present in the BPr medium, and a zone of precipitation will be produced around the colonies as a result of lipase activity. The transformants showed a loss of lipase activity compared to the positive control (Figure 5.10C and Figure 5.11C), which indicated correct integration of the plasmid into the chromosome at the *geh* gene. Strains AFK17 (RN4220 pCL112Δ19 *geh*::pAFK16) and AFK18 (RN4220 pCL112Δ19 *geh*::pAFK17) were lysed with φ11, and the chromosomal region that contained the plasmid insertion was transferred into SH1000 cells by transduction. The resulting strains AFK19 (SH1000 *geh*::pAFK16) and AFK20 (SH1000 *geh*::pAFK17) were verified both by PCR using the AK39 and AK40 primers and by the loss of lipid hydrolysis on BPr medium (data not shown).

### 5.2.2 Construction of *S. aureus divIC* and *ftsL* deletion mutants

Unmarked, in-frame gene deletions do not impart polar effects on downstream genes. Consequently, constructions of unmarked deletions of *divIC* and *ftsL* were attempted to remove either *divIC* or *ftsL* and prevent any polar effects on their downstream genes encoding the ribosomal-binding (Figure 5.12A) or penicillin-binding proteins (Figure 5.13A), respectively. The deletions were achieved using a two-step approach. Initially, a homologous recombination event occurred between the gene of interest and a homologous DNA sequence on a temperature-sensitive plasmid. After transformation, integration of the plasmid into the chromosome via a single-crossover event occurred by growth at a high, non-permissive temperature whilst maintaining selective pressure.

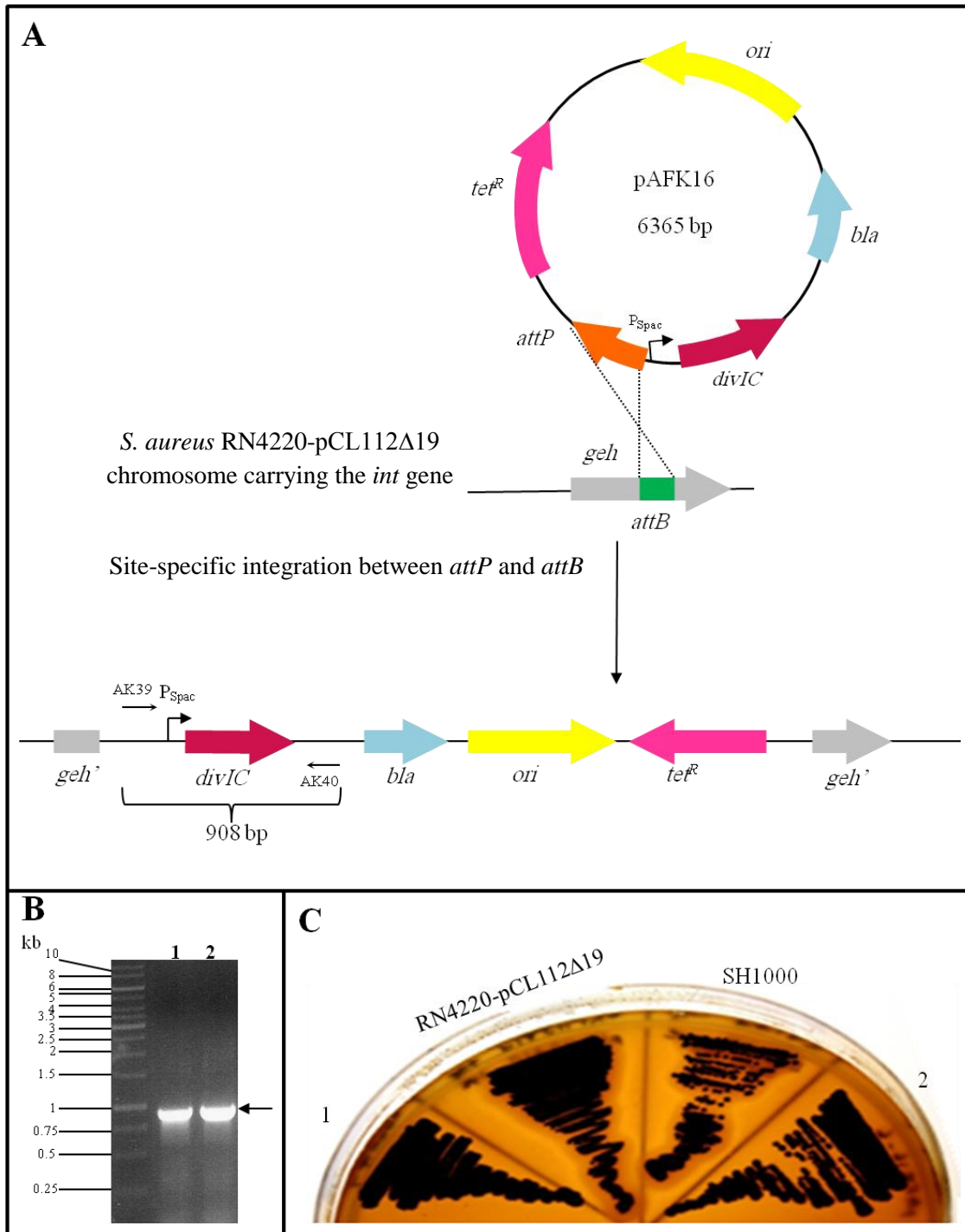


**Figure 5.10 Integration of pAFK16 into the *S. aureus* chromosome**

A. Diagrammatic representation of pAFK16 integration into RN4220-pCL112Δ19, which resulted in strain AFK17. The binding sites for primers AK39 and AK40 are indicated (not to scale).

B. The PCR product of  $P_{Spac}$ -*divIC* was amplified using the AK39 and AK40 primers after genomic DNA extraction and was then analysed by electrophoresis in a 1% TAE (w/v) agarose gel. A 908 bp product that corresponded to the  $P_{Spac}$ -*divIC* insert was obtained (indicated by a black arrow). Lanes 1 and 2 correspond to the clones that were investigated. DNA standards are of sizes shown in Kb.

C. Confirmation of correct pAFK16 integration into the *S. aureus* chromosome by the loss of lipase activity on BPr medium. A precipitation zone, which can be observed around the RN4220pCL112Δ19 and SH1000 colonies, is missing from clones 1 and 2.

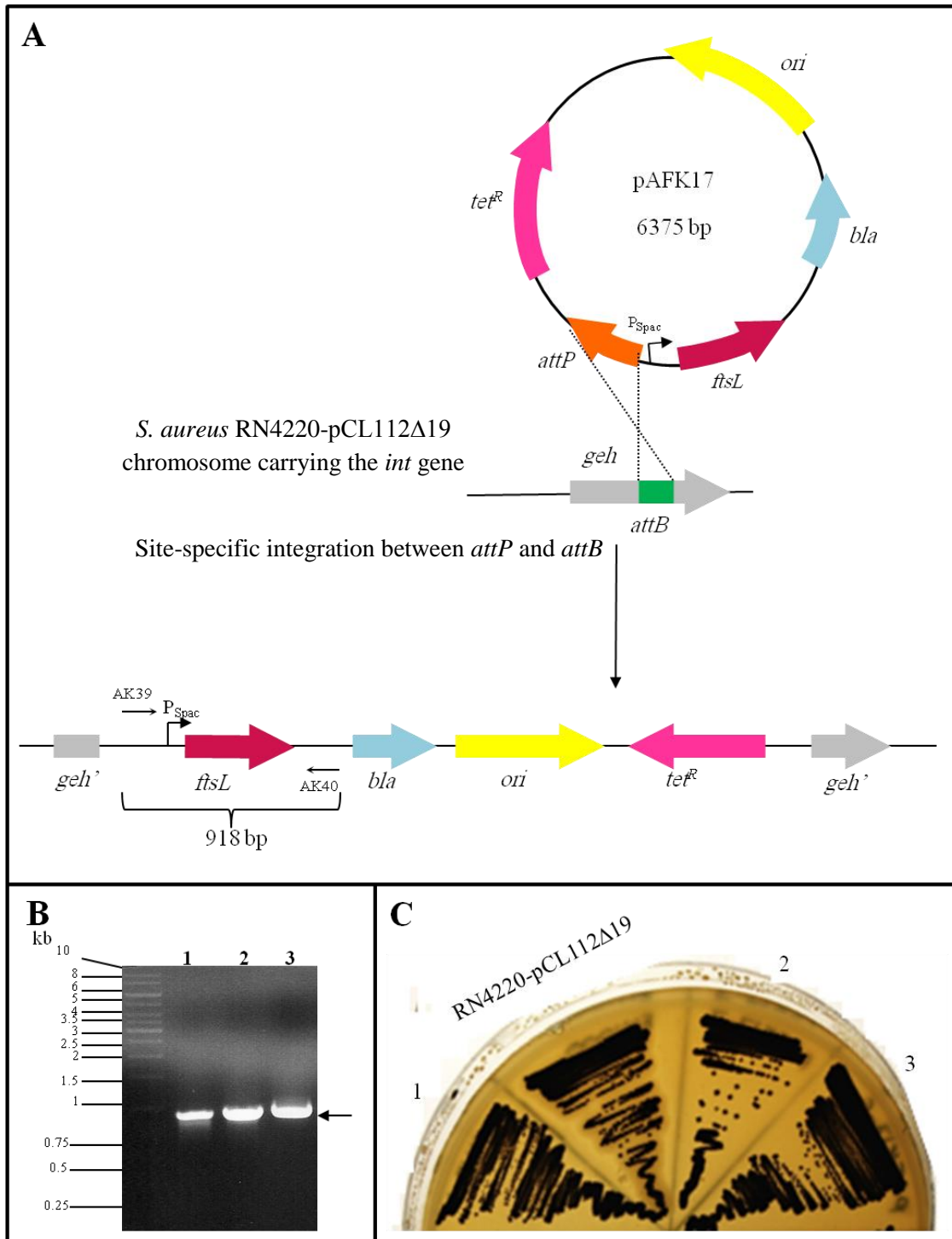


**Figure 5.11 Integration of pAFK17 into the *S. aureus* chromosome**

A. Diagrammatic representation of pAFK17 integration into RN4220-pCL112Δ19, which resulted in strain AFK18. The binding sites for primers AK39 and AK40 are indicated (not to scale).

B. The PCR product of  $P_{Spac}$ -*ftsL* was amplified using the AK39 and AK40 primers after genomic DNA extraction and then analysed by electrophoresis in a 1% TAE (w/v) agarose gel. A 918 bp product that corresponded to the  $P_{Spac}$ -*ftsL* insert was obtained (indicated by a black arrow). Lanes 1 to 3 correspond to the clones that were investigated. DNA standards are of sizes shown in Kb.

C. Confirmation of correct pAFK17 integration into the *S. aureus* chromosome by the loss of lipase activity on BPr medium. A precipitation zone, which can be observed around the RN4220pCL112 $\Delta$ 19 colonies, is missing from clones 1, 2 and 3.

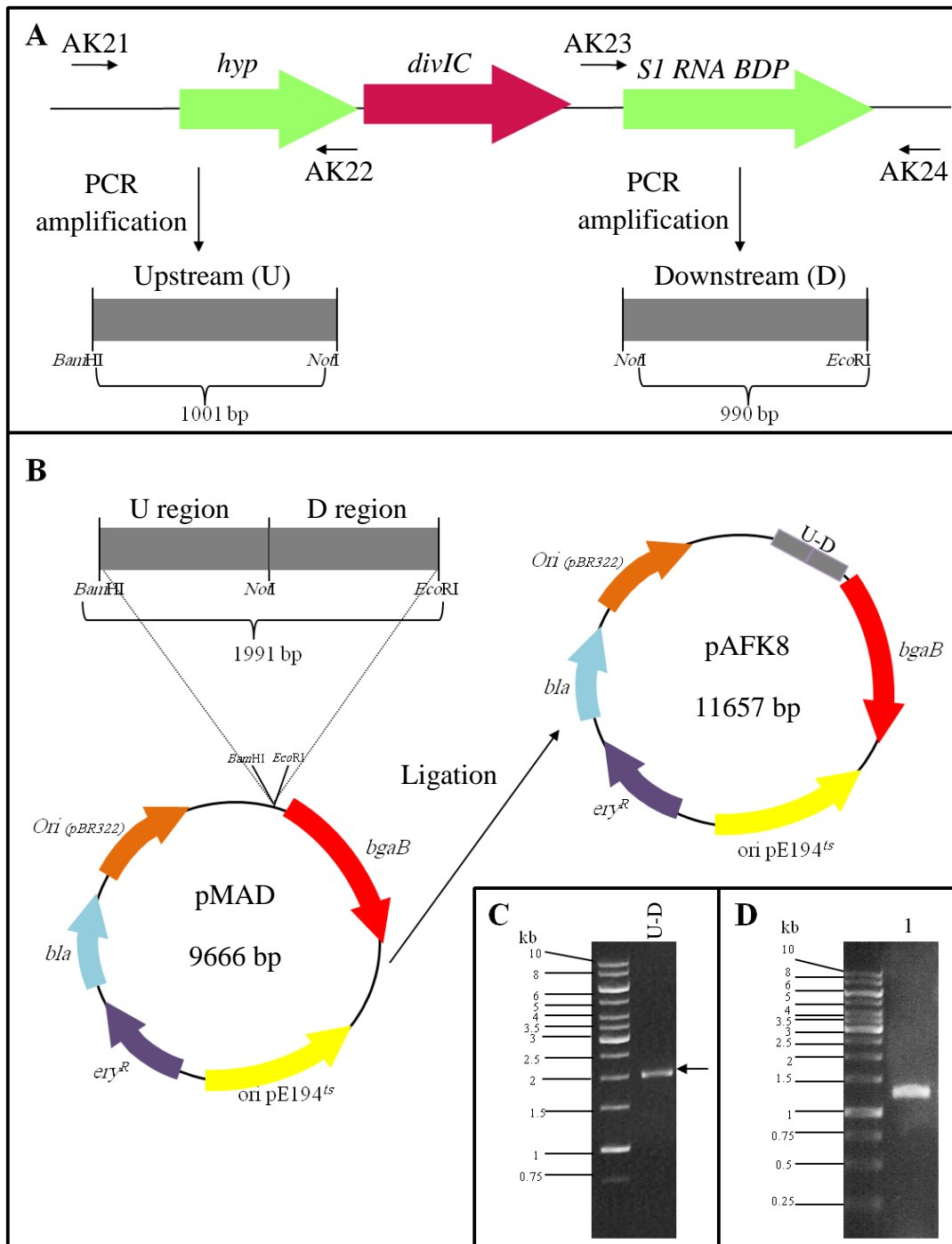


**Figure 5.12 Construction of the *S. aureus divIC* in-frame deletion plasmid, pAFK8**

A. Amplification of the ~1-Kb flanking regions of the *S. aureus divIC* upstream (U) and downstream (D) regions. The locations of the annealing sites of the primers and restriction enzyme sites are indicated.

B. Diagrammatic representation of the construction of pAFK8. The U and D fragments were digested with *NotI* and ligated, and the ligated fragment was amplified to produce a fusion of U and D. The U-D fragment was digested with *BamHI* and *EcoRI* and then inserted into pMAD (not to scale).



C. Following ligation of the U and D fragments, PCR amplification of the ligated fragment was performed, and the fused product was analysed in a 1% (w/v) TAE agarose gel. A 1991 bp product was obtained (indicated by black arrow). DNA standards are of sizes shown in Kb.

D. The PCR product of U-D was PCR-amplified using the AK21 and AK24 primers and then analysed by electrophoresis in a 1% (w/v) TAE agarose gel. Lane 1: A ~1250 bp product of was obtained, which was not the expected size for the U-D fragment. DNA standards are of sizes shown in Kb.

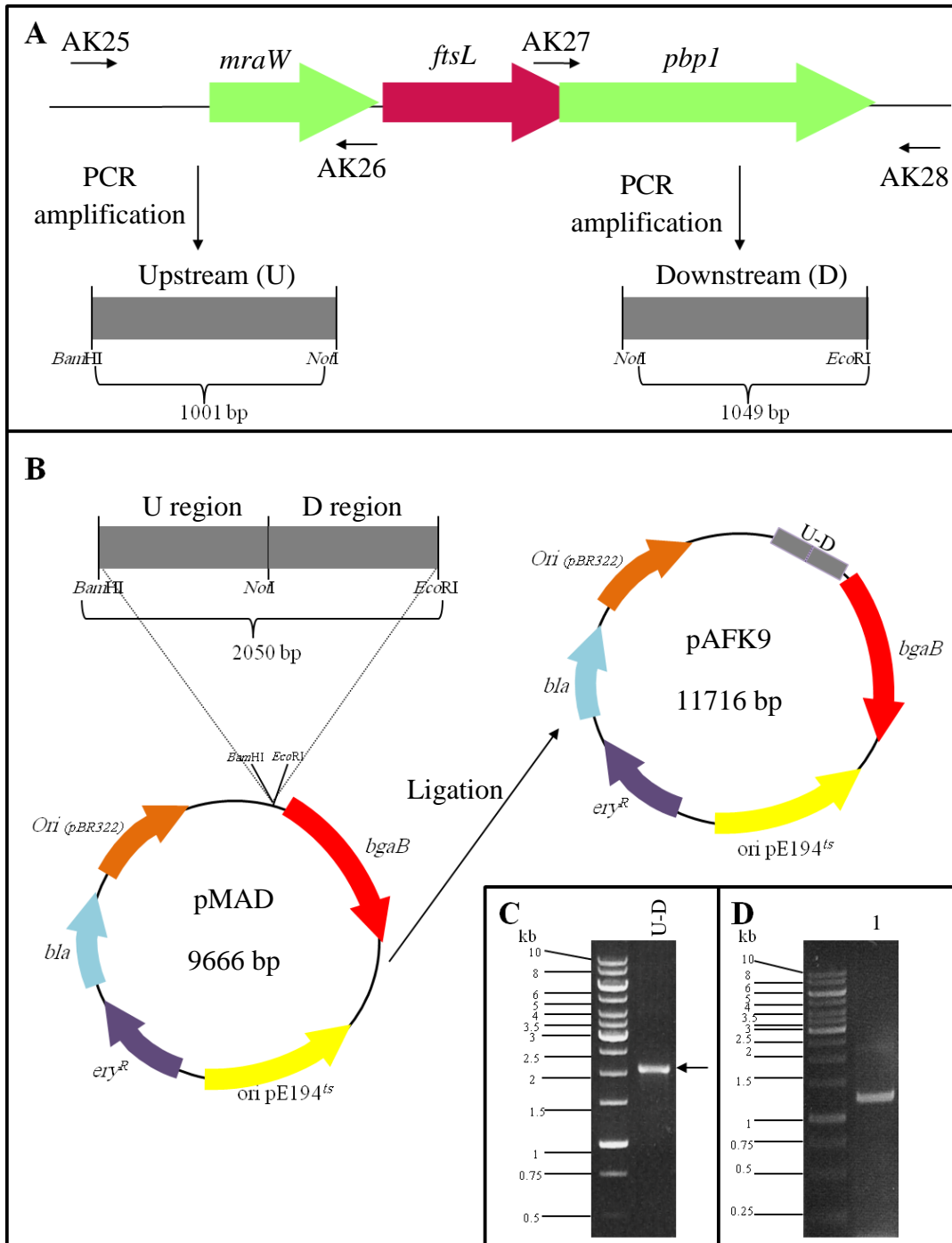


**Figure 5.13 Construction of the *S. aureus ftsL* in-frame deletion plasmid, pAFK9**

A. Amplification of the ~1-Kb flanking regions of the *S. aureus ftsL* upstream (U) and downstream (D) regions. The locations of the primer annealing sites and the restriction enzyme sites are indicated.

B. Diagrammatic representation of the construction of pAFK9. The U and D fragments were digested with *Not*I and ligated, and the ligated fragment was amplified to produce a fusion of U and D. The U-D fragment was digested with *Bam*HI and *Eco*RI and then inserted into pMAD (not to scale).

C. Following the ligation of the U and D fragments, PCR amplification of the ligated fragment was performed, and the fused product was analysed in a 1% (w/v) TAE agarose gel. A 2050 bp product was obtained (indicated by black arrow). DNA standards are of sizes shown in Kb.

D. The PCR product of the U-D fragment was amplified using the AK25 and AK28 primers and then analysed by electrophoresis in a 1% (w/v) agarose gel. Lane 1: A ~1250 bp product was obtained, which was not the expected size for the U-D fragment. DNA standards are of sizes shown in Kb.

Subsequently, growth at a low, permissive temperature could lead to a second recombination event that resulted in the loss of the plasmid from the chromosome. This event could result in either mutant or wild-type alleles being left on the chromosome, whereas the excised plasmid carried the counterpart allele. Clone screening following plasmid resolution was performed using either colorimetric or positive selection (Arnaud *et al.*, 2004; Bae and Schneewind, 2006; Monk *et al.*, 2012; Monk and Foster, 2012). The unmarked in-frame deletion was performed using a vector system termed pMAD (Arnaud *et al.*, 2004). The pMAD vector contains a constitutively expressed *bgaB* transcriptional fusion that encodes  $\beta$ -galactosidase and allows for colorimetric screening of the bacteria on X-Gal (5-bromo-4chloro-3indolyl- $\beta$ -D-galactopyranoside) plates. In addition, the plasmid contains the thermo-sensitive pE194 origin of replication of *S. aureus* and antibiotic resistance markers for selection in *E. coli* and *S. aureus* (Arnaud *et al.*, 2004). Successful replacement of the *S. aureus* vancomycin resistance-associated genes, *vraF* and *vraG*, with a spectinomycin resistance cassette was achieved using pMAD (Arnaud *et al.*, 2004). In addition, pMAD has been used to mutagenise *S. aureus* genes that are involved in biofilm formation (Valle *et al.*, 2003; Toledo-Arana *et al.*, 2005), cell wall biosynthesis (Vergara-Irigaray *et al.*, 2008; Memmi *et al.*, 2008) and antibiotic resistance (Memmi *et al.*, 2008).

A pair of primers was designed to amplify a ~1-Kb region upstream (U) and a 1-Kb region downstream (D) of the gene of interest. These primers were designed to include *Bam*HI and *Eco*RI sites at the 5' and 3' ends of the U and D regions, respectively. *Not*I sites were incorporated at the 3' and 5' ends of the U and D regions, respectively, which allowed for ligation of the U and D regions. The primer pairs AK21/AK22 (U-*divIC*), AK23/AK24 (D-*divIC*), AK25/26 (U-*ftsL*), and AK27/28 (D-*ftsL*) (Table 2.7) were used to amplify the corresponding regions from SH1000 genomic DNA and produced PCR products of 1001 bp and 990 bp for the U and D regions of *divIC* and 1001 bp and 1049 bp for the U and D regions of *ftsL*, respectively (Figure 5.12A and Figure 5.13A). Both U and D PCR products were digested with *Not*I and ligated, and the ligation mixtures were used as PCR templates to amplify the U and D regions of *divIC* and *ftsL* using the respective primer pairs AK21/AK24 and AK25/AK28 to obtain a fused, single 2-Kb fragment (U-D) (Figure 5.12B/C and Figure 5.13B/C). The PCR products were gel extracted

and digested with *Bam*HI and *Eco*RI. The digested fragments were then ligated into pMAD that had been digested with the same enzymes (Figure 5.12B and Figure 5.13B), and the ligation mixtures were then transformed into electrocompetent *E. coli* TOP 10 cells. Positive transformant clones were then selected on LB + ampicillin (100 mg ml<sup>-1</sup>) plates at 30°C. Putative positive clones were identified by PCR analysis with the AK21/24 and AK25/28 primers using the extracted plasmid as template DNA. Although growth was evident on the ampicillin plates, verification of these clones by restriction digestion with *Bam*HI and *Eco*RI or PCR using the AK21/AK24 and AK25/AK28 primer pairs and then separation in a 1 % (w/v) agarose gel revealed bands of unexpected sizes (Figure 5.12D and Figure 5.13D). Cloning the ~2-Kb fragment directly into pMAD was not successful, though, this method was previously reported to be successful in *S. aureus* (Bottomley, 2011; Arnaud *et al.*, 2004; Valle *et al.*, 2003; Toledo-Arana *et al.*, 2005; Vergara-Irigaray *et al.*, 2008; Memmi *et al.*, 2008). The inability to create in-frame mutations in the *divIC* and *ftsL* genes could be due to the toxicity of the fragment in *E. coli*. Other vectors were used to attempt to clone the ~2 Kb fragments into smaller vectors such as pOB or pCR 2.1-TOPO using the TOPO TA cloning kit (Invitrogen), but all of these attempts were also unsuccessful.

pIMAY was constructed to facilitate the manipulation of genetically recalcitrant Gram-positive bacteria. pIMAY is a new, low-copy number, *E. coli*-*S. aureus* shuttle vector that can be used for allelic exchange in *S. aureus* (Monk *et al.*, 2012). pIMAY contains the *p15A* origin, which is a low-copy *E. coli* replication origin, and a highly temperature-sensitive replicon of *S. aureus* (*repA<sup>TS</sup>*) that allows integration of the plasmid into the chromosome at 37°C (Maguin *et al.*, 1992). In addition, pIMAY carries a highly expressed chloramphenicol resistance (*cat<sup>R</sup>*) marker for selection in *E. coli* and *S. aureus* and the tetracycline-inducible, antisense *secY* region (*anti-secY*), which inhibits the growth of any cells that contain the integrated plasmid and, hence, selects cells that do not contain the plasmid (Bae and Schneewind, 2006; Monk *et al.*, 2012). Unmarked deletion mutations in *S. aureus* *hsdR*, which is a type I restriction modification gene, and *sauUSI*, which is a type IV restriction gene, were successfully obtained using the pIMAY vector system (Monk *et al.*, 2012).

U and D regions (~1 Kb each) of *divIC* or *ftsL* were amplified from *S. aureus* SH1000 genomic DNA using the AK35/AK22 (U-*divIC*) and AK37/AK26 (U-*ftsL*) or AK23/AK36 (D-*divIC*) and AK27/AK38 (D-*ftsL*) primer pairs. These primers were designed to include *KpnI* and *SacI* sites at the 5' and 3' ends of the respective U and D regions of *divIC* and *EcoRI* and *AatII* sites at the 5' to 3' ends of the respective U and D regions of *ftsL*. *NotI* sites were incorporated at the 3' and 5' ends of the U and D regions, which allowed for ligation between the U and D regions. The primer pairs AK35/AK22 (U-*divIC*), AK23/AK36 (D-*divIC*), AK37/26 (U-*ftsL*) and AK27/38 (D-*ftsL*) (Table 2.7) were used to amplify their corresponding regions and produced PCR products of 1001 bp (U) and 990 bp (D) of *divIC* and 1001 bp (U) and 1049 bp (D) of *ftsL* (Figure 5.14A and Figure 5.15A). The U and D PCR products were both digested with *NotI* and ligated, and the ligation mixtures were used as PCR templates to amplify the U and D regions of *divIC* and *ftsL* using the respective AK35/AK38 and AK37/AK38 primer pairs to obtain a fused, single ~2-Kb fragment (U-D). The PCR products were gel extracted and digested with *KpnI* and *SacI* or *EcoRI* and *AatII* and were ligated into pIMAY that had been digested with the same enzymes (Figure 5.14B and Figure 5.15B). The ligation mixtures were then transformed into electrocompetent *E. coli* TOP 10 cells and selected on LB + chloramphenicol (15  $\mu\text{g ml}^{-1}$ ) plates at 37°C. Positive clones were identified by DNA sequencing (University of Sheffield), PCR analysis using the extracted plasmid as template DNA and the AK35/36 and AK37/38 primers (data not shown) and restriction digestion with *KpnI* and *SacI* or *EcoRI* and *AatII* then separation in a 1% (w/v) agarose gel (Figure 5.14C and Figure 5.15C).

Ten micrograms of each of the resulting plasmids pAFK14 and pAFK15 was then transformed into *S. aureus* RN4220, and transformants were selected on BHI + chloramphenicol (10  $\mu\text{g ml}^{-1}$ ) plates at 25°C for 48 h. To obtain pure, isolated colonies, 16 colonies were picked and patched onto BHI chloramphenicol (10  $\mu\text{g ml}^{-1}$ ) plates at 25°C, and isolates were verified by plasmid extraction followed by PCR amplification using the MCS FWD and MCS REV primers (Table 2.7) and then analysed by separation in a 1% (w/v) agarose gel (data not shown).

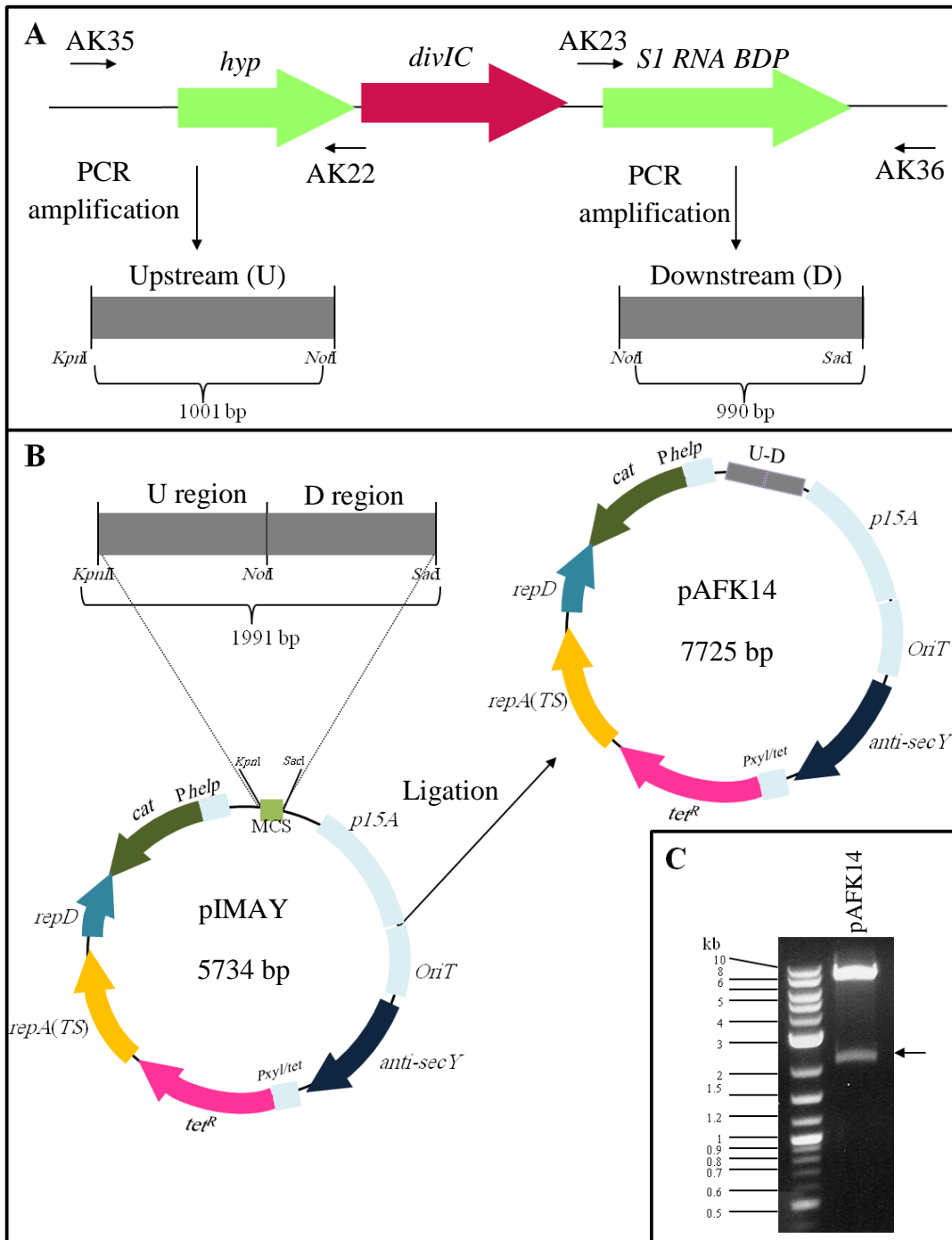


**Figure 5.14 Construction of the *S. aureus* *divIC* in-frame deletion plasmid, pAFK14**

A. Amplification of the ~1-Kb flanking regions of *S. aureus* *divIC* upstream (U) and downstream (D) regions. The locations of the primer annealing sites and restriction enzyme sites are indicated.

B. Diagrammatic representation of the construction of pAFK14. The U and D fragments were digested with *NotI* and ligated, and the ligated fragment was amplified to produce a fusion of U and D. The U-D fragment was digested with *KpnI* and *SacI* and then inserted into pIMAY (not to scale).

C. pAFK14 was digested with *KpnI* and *SacI* and then electrophoresed in a 1% (w/v) TAE agarose gel. A 5734-bp PCR product, which corresponded to the linearised pIMAY vector, and a 1990-bp PCR product, which corresponded to the U-D fragment (indicated by black arrow), were obtained. DNA standards are of sizes shown in kb.



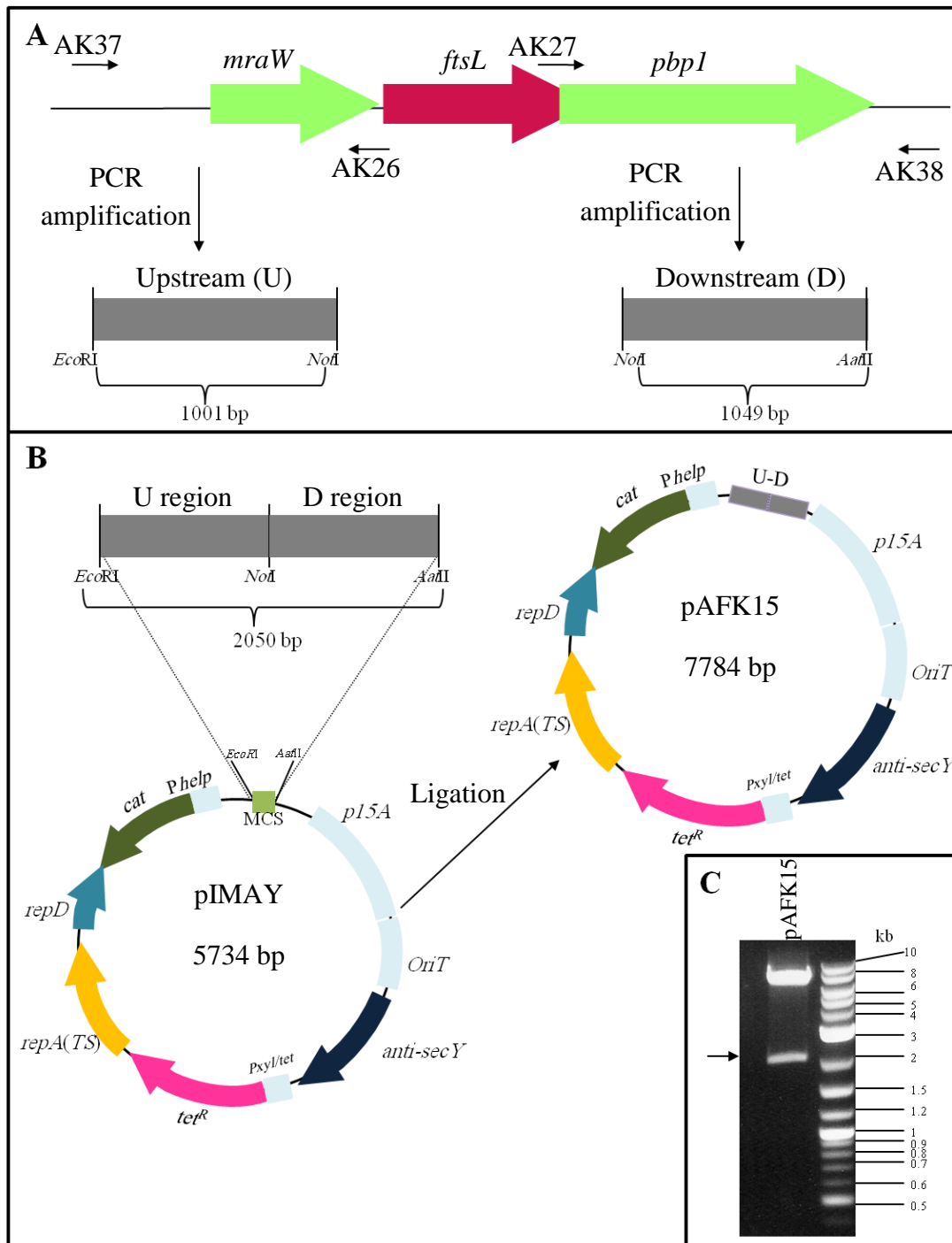


**Figure 5.15 Construction of the *S. aureus ftsL* in-frame deletion plasmid, pAFK15**

A. Amplification of the ~1-Kb flanking regions of *S. aureus ftsL* upstream (U) and downstream (D) regions. The locations of the primer annealing sites and restriction enzyme sites are indicated.

B. Diagrammatic representation of the construction of pAFK15. The U and D fragments were digested with *NotI* and ligated, and the ligated fragment was amplified to produce a fusion of U and D. The U-D fragment was digested with *EcoRI* and *AatII* and then inserted into pIMAY (not to scale).

C. pAFK15 was digested with *EcoRI* and *AatII* and then electrophoresed in a 1 % (w/v) TAE agarose gel. A 5734 bp PCR product, which corresponded to the linearised pIMAY vector, and a 2050 bp PCR product, which corresponded to the U-D fragment (indicated by black arrow), were obtained. DNA standards are of sizes shown in kb.

The strains AFK13 (RN4220 pAK14) and AFK14 (RN4220 pAFK15) were lysed with  $\phi$ 11 (Section 2.10.3.2), and the plasmids were transferred to SH1000 by transduction (Section 2.10.3.4) at 25°C for 48 h (Figure 5.16A and Figure 5.16B). Sixteen transformants were picked and patched onto BHI + chloramphenicol (10  $\mu\text{g ml}^{-1}$ ) plates at 25°C to obtain well-isolated clones. AFK15 (SH1000 pAFK14) and AFK16 (SH1000 pAFK15) were screened for the presence of replicating pAFK14/pAFK15 plasmids by extracting them and then using the plasmid DNAs as templates for PCR amplification with the MCS FWD and MCS REV primers. The expected sizes for the PCR products were observed after separation in 1% (w/v) agarose gels (Figure 5.16C and Figure 5.16D).

Integration of pAFK14/pAFK15 into the *S. aureus* chromosome (Figure 5.17A and Figure 5.18A) was achieved by resuspending single colonies from the pAFK14/pAFK15 25°C plates (AFK15/AFK16) in 200  $\mu\text{l}$  BHI, and the suspensions were diluted  $10^{-1}$ - $10^{-3}$  fold. One hundred microlitres of each diluted suspension was spread onto BHI + chloramphenicol (10  $\mu\text{g ml}^{-1}$ ) plates and incubated at 37°C overnight. Sixteen colonies were picked and subcultured on BHI + chloramphenicol (10  $\mu\text{g ml}^{-1}$ ) plates at 37°C to obtain well-isolated colonies. Putative positive clones were screened for the loss of the replicating plasmid using purified plasmid as a template for PCR analysis and the MCS FWD and MCS REV primer pairs, and the PCR products were separated in a 1% (w/v) agarose gel. No PCR products were observed for the clones, indicating loss of the extrachromosomal plasmid DNA. SH1000 genomic DNA and AFK15/AFK16 genomic DNA controls were included as negative and positive controls and revealed no product (negative control) and the expected product size (positive control) (Figure 5.17B and Figure 5.18B). To determine the sites of plasmid integration, a second PCR was performed for the clones that showed loss of the replicating plasmid. The primer pairs AK43/AK36 or AK35/ AK44 were used to identify the site of pAFK14 integration, and the primer pairs AK45/AK28 or AK37/AK46 were used to identify the site of pAFK15 integration.

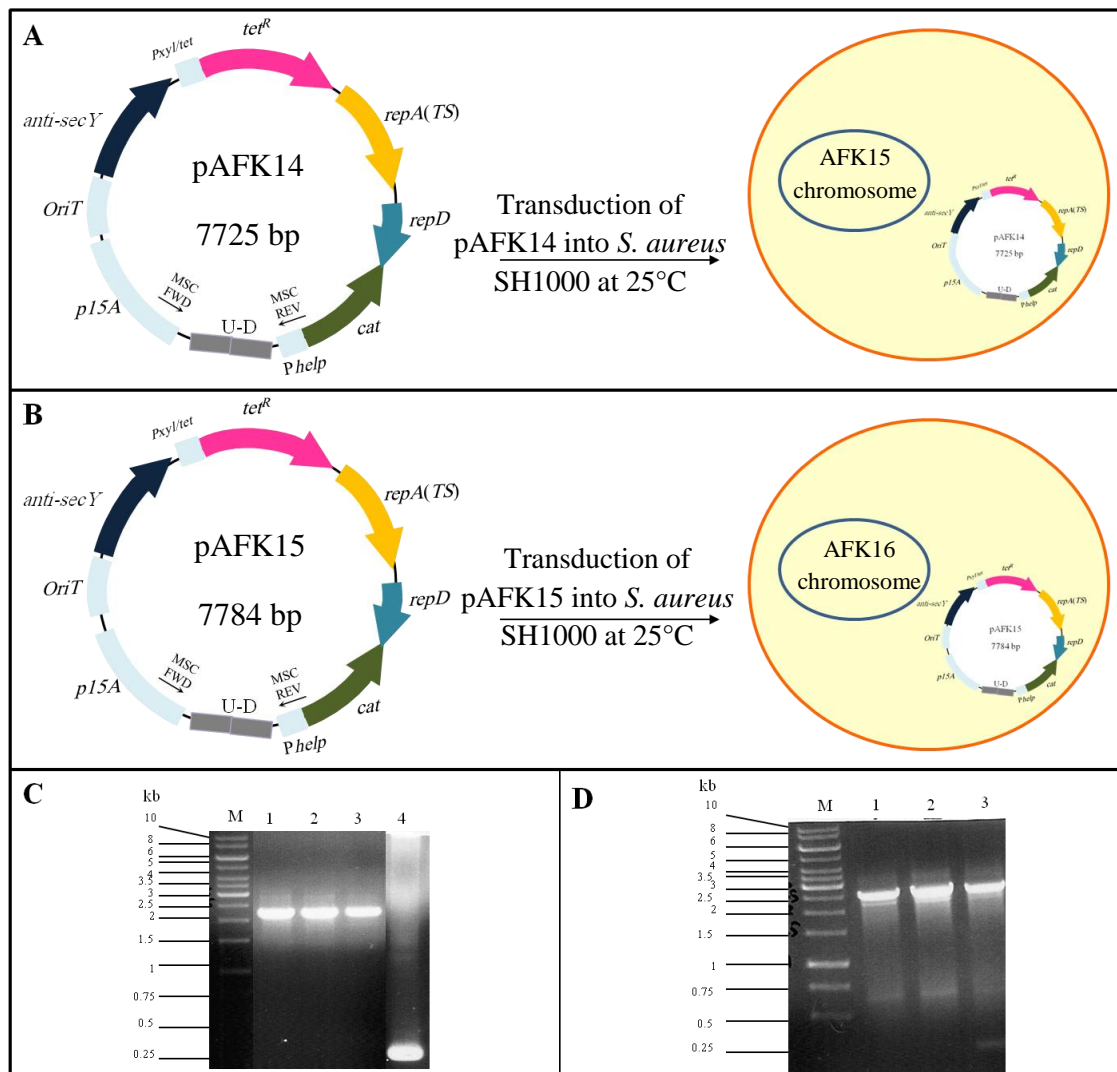


**Figure 5.16 Construction of the pAFK14 and pAFK15 plasmids in *S. aureus***

A. Diagrammatic representation of the construction of pAFK14. pAFK14 was transduced into *S. aureus* SH1000 at 25°C, and the resulting strain was named AFK15 (not to scale).

B. Diagrammatic representation of the construction of pAFK15. pAFK15 was transduced into *S. aureus* SH1000 at 25°C, and the resulting strain was named AFK16 (not to scale).

C. The presence of replicating pAFK14 was confirmed by DNA extraction, and PCR amplification was performed using the MCS FWD and MCS REV primers to produce a 2275-bp fragment (lanes 1 to 3). Lane 4: The MCS was amplified from pIMAY using the MCS FWD and MCS REV primers and produced a 284-bp product. DNA standards are of sizes shown in Kb.

D. The presence of a replicating pAFK15 plasmid was confirmed by DNA extraction, and PCR amplification was performed using the MCS FWD and MCS REV primers to produce a 2334-bp fragment (lanes 1 to 3). DNA standards are of sizes shown in Kb.

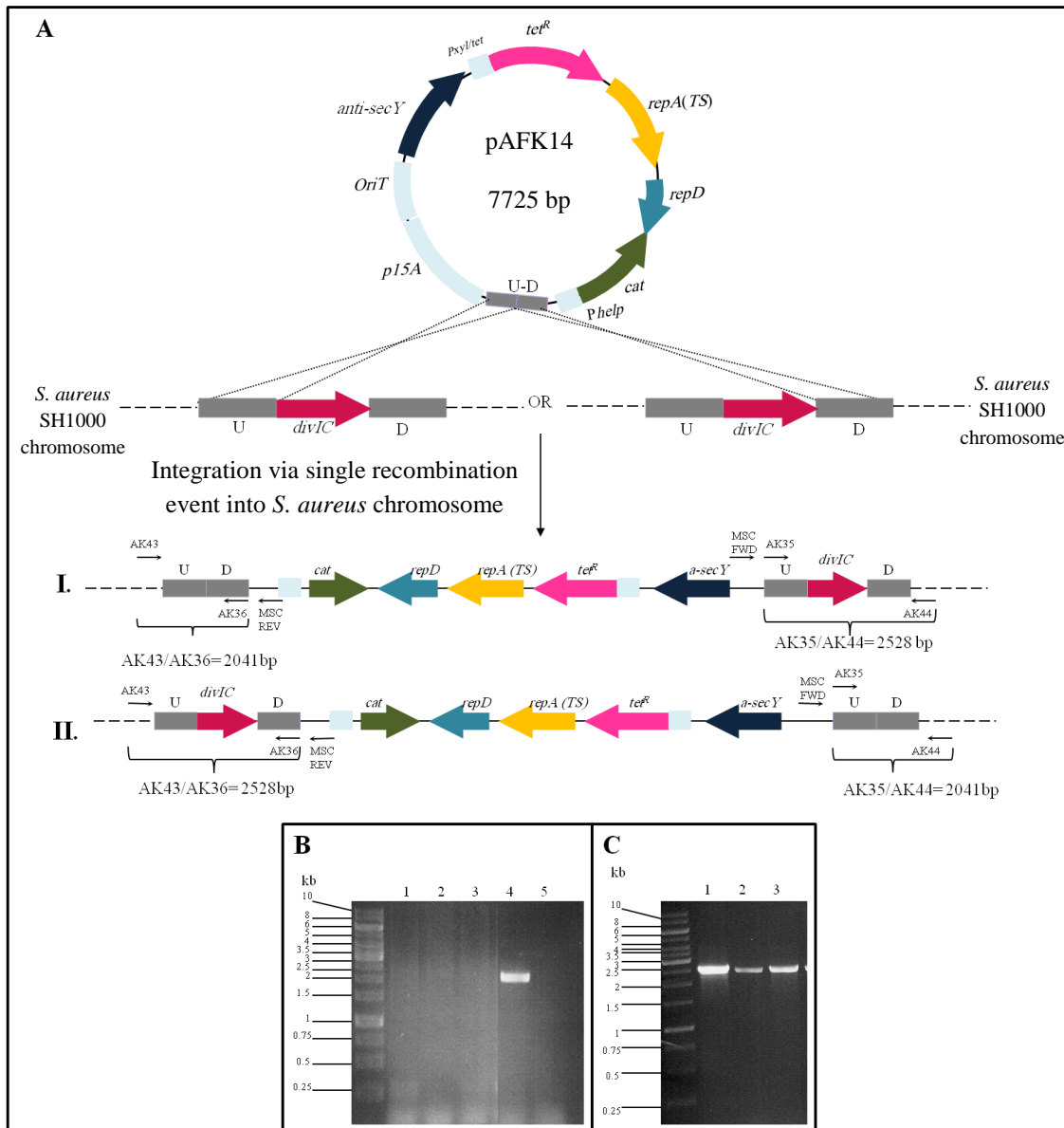


**Figure 5.17 Homologous recombination of pAFK14 into the *S. aureus* SH1000 chromosome**

A. Diagrammatic representation of the likely recombination outcomes of pAFK14 in the *S. aureus* SH1000 chromosome. The primer annealing sites are indicated. A single-crossover event will lead to the following outcomes: I. integration occurs via the upstream region, or II. integration occurs via the downstream region (not to scale).

B. The loss of the replicating pAFK14 plasmid and its integration into the *S. aureus* chromosome was investigated by DNA extraction of randomly selected clones after growth at the non-permissive temperature and subsequent PCR analyses using the MCS FWD and MCS REV primers. The PCR products were electrophoresed in a 1% (w/v) TAE agarose gel. No products should be observed after integration of pAFK14 (Lane 1 to 3). Lane 4: A PCR product from DNA extracted from cells that were grown at 25°C (AFK15) was included as a positive control. A 2275 bp product was obtained. Lane 5: A PCR product from *S. aureus* SH1000 genomic

DNA only. No product was produced due to the absence of the pIMAY vector. DNA standards are of sizes shown in Kb.

C. Clones that lost the replicating plasmid were screened by PCR to determine the site of integration using the AK43 (chromosomal) and AK36 (insert) primers. The PCR products were electrophoresed in a 1% (w/v) TAE agarose gel, and a 2528 bp product was obtained (Lanes 1 to3), which indicates that integration occurred via the downstream region. DNA standards are of sizes shown in Kb.

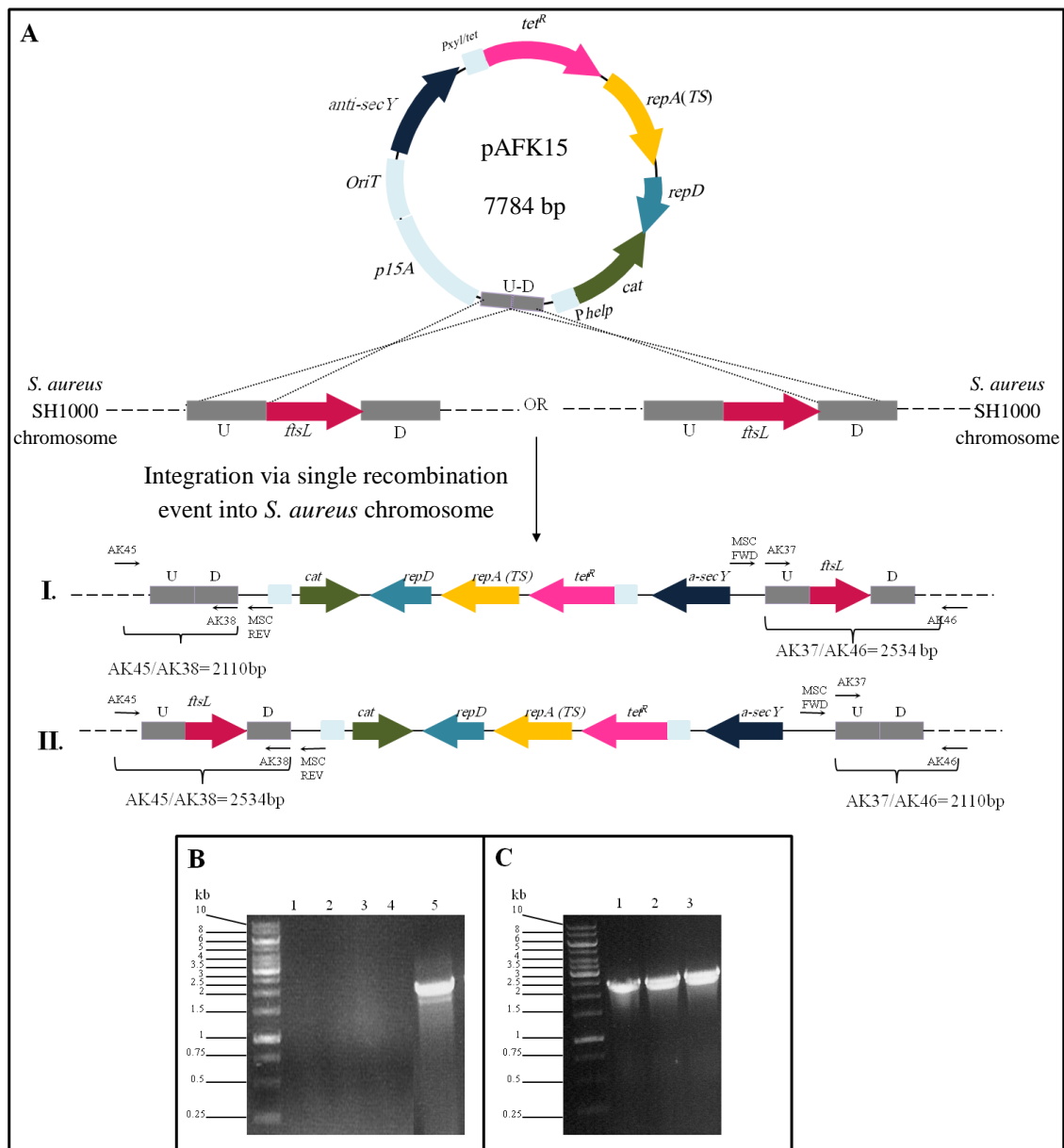


**Figure 5.18 Homologous recombination of pAFK15 into the *S. aureus* SH1000 chromosome**

A. Diagrammatic representation of the likely recombination outcomes of pAFK15 in the *S. aureus* SH1000 chromosome. The primer annealing sites are indicated. A single-crossover event will lead to the following outcomes: I. integration occurs via the upstream region; or II. integration occurs via the downstream region (not to scale).

B. The loss of the replicating pAFK15 plasmid and its integration into the *S. aureus* chromosome was investigated by DNA extraction of randomly selected clones after growth at the non-permissive temperature and subsequent PCR analysis using the MCS FWD and MCS REV primers. The PCR products were separated in a 1% (w/v) TAE agarose gel. No products should be observed after integration of pAFK15 (Lane 1 to 3). Lane 4: A PCR product from DNA extracted from cells that were grown at 25°C (AFK16) was included as a positive control, and a 2334 bp product was obtained. Lane 5: A PCR product using only *S. aureus*

SH1000 genomic DNA. No product was obtained because of the absence of the pIMAY vector. DNA standards are of sizes shown in Kb.

C. Clones that lost the replicating plasmid were screened by PCR to determine the site of integration using the AK45 (chromosomal) and AK38 (insert) primers. The PCR products were analysed in a 1% (w/v) TAE agarose gel, and 2110 bp products were obtained (Lane 1-3), which indicated that integration occurred via the upstream region. DNA standards are of sizes shown in Kb.



The PCR products were analysed in a 1% (w/v) agarose gel, which showed that the integration of pAFK14 occurred via the fragment downstream of *divIC* (Figure 5.17C), while the integration of pAFK15 occurred via the fragment upstream of *ftsL* (Figure 5.18C). A single colony containing either side of the integration and no replicating plasmid was grown without antibiotics overnight at 25°C. The resulting cell culture was then diluted 10-fold to 10<sup>-6</sup> cells, and 50 µl of each of the 10<sup>-4</sup>, 10<sup>-5</sup> and 10<sup>-6</sup> dilutions were plated onto BHI + anhydrotetracycline (1 µg ml<sup>-1</sup>) plates and incubated at 25°C for 48 h. Anhydrotetracycline inhibits the growth of any cells that contain the integrated plasmid (Bae and Schneewind, 2006) and leads to double-crossover events, the resolution of the plasmid and, hence, excision of the targeted gene from the chromosome. During the plasmid excision step, the cells undergo two types of events: a double-crossover event at the upstream region of the target gene or a double-crossover event at the downstream region of the target gene that recreates a wild type or mutated copy of the gene (Figure 5.19A and 5.20A). Potential positive clones were picked and streaked onto BHI + anhydrotetracycline (1 µg ml<sup>-1</sup>) and BHI + chloramphenicol (10 µg ml<sup>-1</sup>) plates and incubated at 37°C overnight. The percentage of colonies that were both chloramphenicol-sensitive and anhydrotetracycline-resistant was low (~ 3%). Genomic DNA was extracted from colonies that grew in the presence of anhydrotetracycline but not in the presence of chloramphenicol and was used as the template for PCR screening using the chromosomal primer pairs AK43/AK44 for screening the  $\Delta divIC$  mutants and AK45/AK46 for screening the  $\Delta ftsL$  mutants. The PCR products were separated in a 1% (w/v) agarose gel, and ~2.5-Kb bands were produced for all of the chloramphenicol-sensitive colonies that were screened for the putative  $\Delta divIC$  and  $\Delta ftsL$  mutants, which corresponds to the expected size of the wild-type chromosomal region (Figure 5.19B and Figure 5.20B). Numerous plasmid excision attempts were performed to isolate a clone that carried the deleted gene, but with no success.

Another attempt was made that included integration of the plasmid and repeating of the plasmid excision steps at 39°C to improve integration; however, all of the clones that were isolated carried the wild-type copy of the gene.

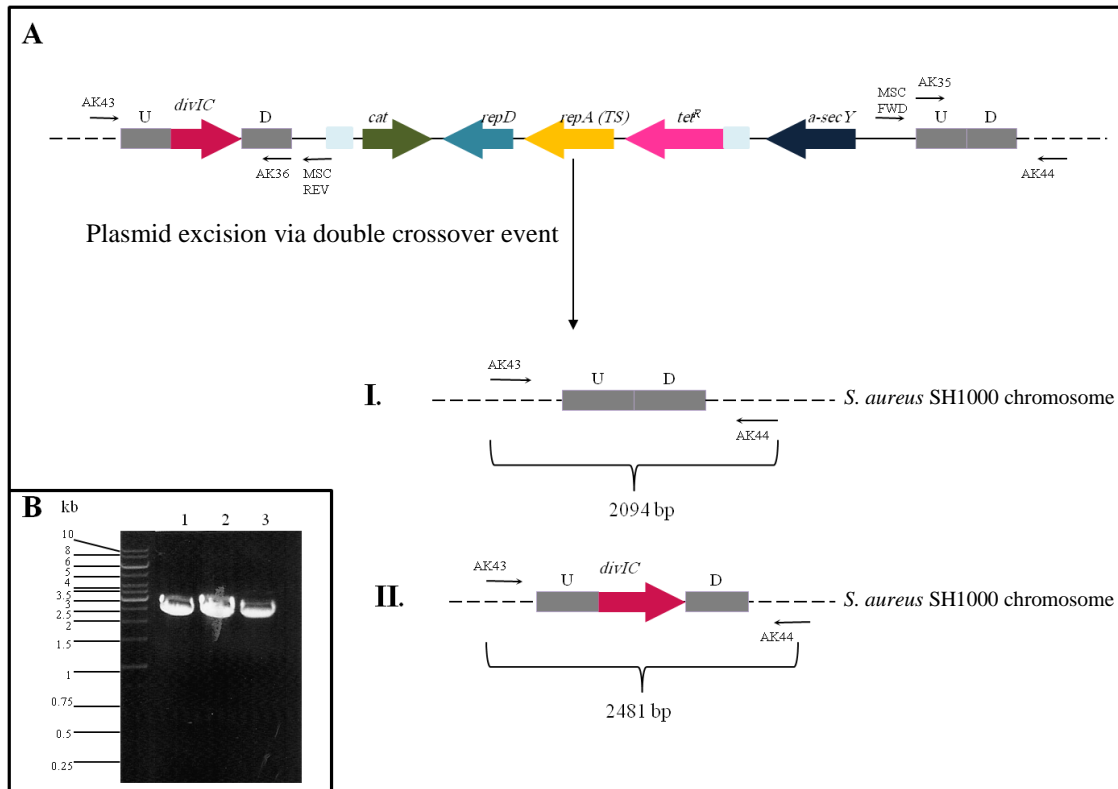


**Figure 5.19** Creation of the *divIC* deletion in *S. aureus* SH1000

A. Diagrammatic representation of the double-crossover outcomes. pAFK14 excision via the upstream side yields a mutant gene (I), while pAFK14 excision via the downstream side produces the wild-type gene (II) (not to scale).

B. Chloramphenicol-sensitive clones were screened by PCR (Lane 1-3) using the AK43 and AK44 chromosomal primer pairs after genomic DNA was extracted from the putative mutants. A 2481 bp product was obtained, which corresponds to the expected size of the wild-type PCR product. DNA standards are of sizes shown in kb.

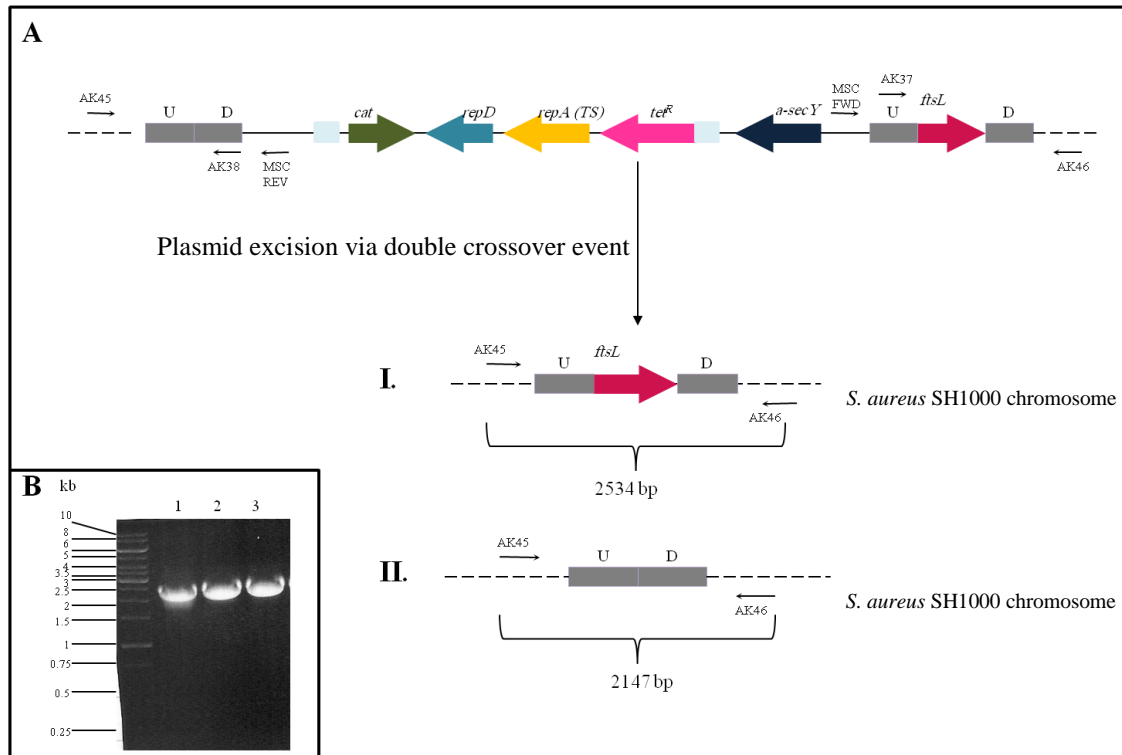


**Figure 5.20** Creation of the *ftsL* deletion in *S. aureus* SH1000

A. Diagrammatic representation of the double-crossover outcomes. pAFK15 excision via the upstream side yields a mutant gene (I), while pAFK15 excision via the downstream side produces the wild-type gene (II) (not to scale).

B. Chloramphenicol-sensitive clones were screened by PCR (Lane 1-3) using the AK45 and AK46 chromosomal primer pairs after genomic DNA was extracted from the putative mutants. Products of 2534 bp were obtained, which corresponded to the wild-type gene. DNA standards are of sizes shown in Kb.

Thousands of potentially positive clones were isolated and screened using chromosomal primers after genomic DNA extraction from the isolates, but none yielded the desired result.

### **5.2.3 Complementation of the *S. aureus divIC* and *ftsL* in-frame deletion mutants**

The resolution of pAFK14 and pAFK15 via homologous recombination and a single-crossover event can lead to gene deletion. If the gene is essential, then the creation of the mutant strain is not possible. Accordingly, deletion of either *S. aureus divIC* or *ftsL* could not be achievable due to the potential essentiality of the genes. To examine the lethality of a target gene deletion, mutation of that gene can be complemented by expression of a functional copy of the gene to maintain cell viability. Therefore, ectopic copies of *divIC* and *ftsL* under the control of P<sub>Spac</sub> were inserted into cells to facilitate gene expression during growth at a permissive temperature in the presence of an inducer (IPTG), thereby permitting the loss of plasmids (pAFK14/pAFK15) from the chromosome.

Strains AFK19 (SH1000 *geh*::pAFK16) and AFK20 (SH1000 *geh*::pAFK17) were lysed with  $\phi$ 11, and the chromosomal regions that included the plasmid insertions were transferred to the SH1000 single-crossover strains AFK21 and AFK22 via transduction at 37°C. The resulting strains, AFK7 and AFK8, included pAFK14/pAFK15 that had been inserted into the chromosome by a single-crossover event and P<sub>Spac</sub>-*divIC* and P<sub>Spac</sub>-*ftsL* that had been ectopically introduced at the gene locus encoding lipase (Figure 5.21A and Figure 5.22A). The insertion of pAFK16/pAFK17 at *geh* was verified for three transductants by the loss of lipid hydrolysis on BPr medium (Figure 5.21B and Figure 5.22B) and by PCR analysis of extracted genomic DNA using the AK39/AK40 primer pairs (Figure 5.21C and Figure 5.22C).

Single colony of AFK7 and AFK8 that did not contain a replicating plasmid were grown without antibiotics overnight at 25°C.

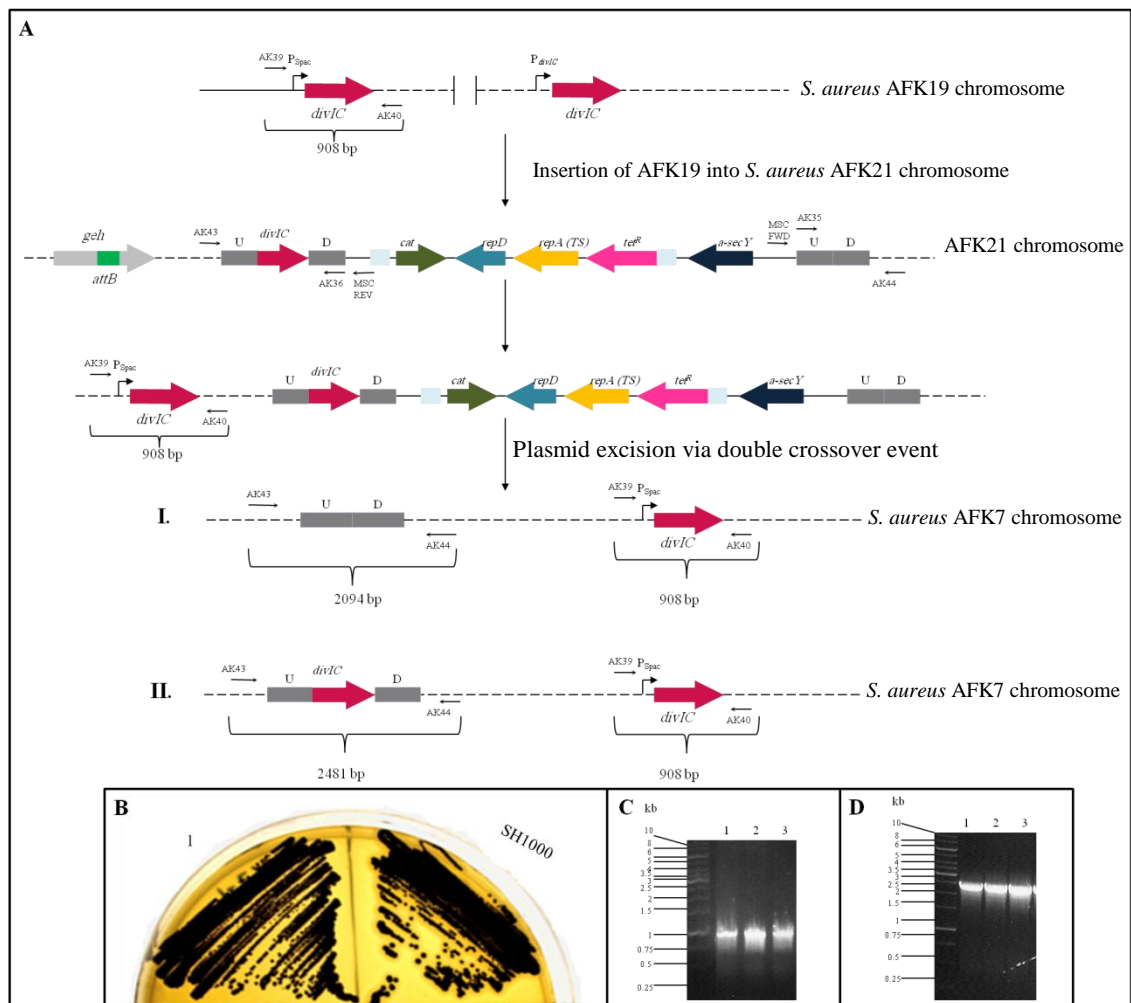


**Figure 5.21 Creation of the conditional *S. aureus divIC* lethal mutant**

A. Diagrammatic representation of insertion of the regulatable copy of *divIC* into AFK21 (pAFK14 single-crossover strain) followed by plasmid excision via a double-crossover event. pAFK14 excision at the upstream side yields a mutant gene (I), while pAFK14 excision via the downstream side produces the wild-type gene (II) (not to scale).

B. Confirmation of correct pAFK16 integration into the *S. aureus* chromosome by the loss of lipase activity on BPr medium. A precipitation zone, which can be observed around the SH1000 colonies, is missing from clone 1.

C. A  $P_{Spac}$ -*divIC* PCR product was amplified using the AK39/AK40 primers after genomic DNA extraction and was then analysed by electrophoresis in a 1% TAE (w/v) agarose gel. A 908 bp product that corresponded to the  $P_{Spac}$ -*divIC* insert was obtained (indicated by a black arrow). Lanes 1 to 3 correspond to the investigated clones. DNA standards are of sizes shown in Kb.

D. Chloramphenicol-sensitive clones were screened by PCR using the chromosomal primer pairs AK43 and AK44 after genomic DNA was extracted from the putative mutants. A 2481 bp product that corresponded to the wild-type gene was obtained. DNA standards are of sizes shown in Kb.

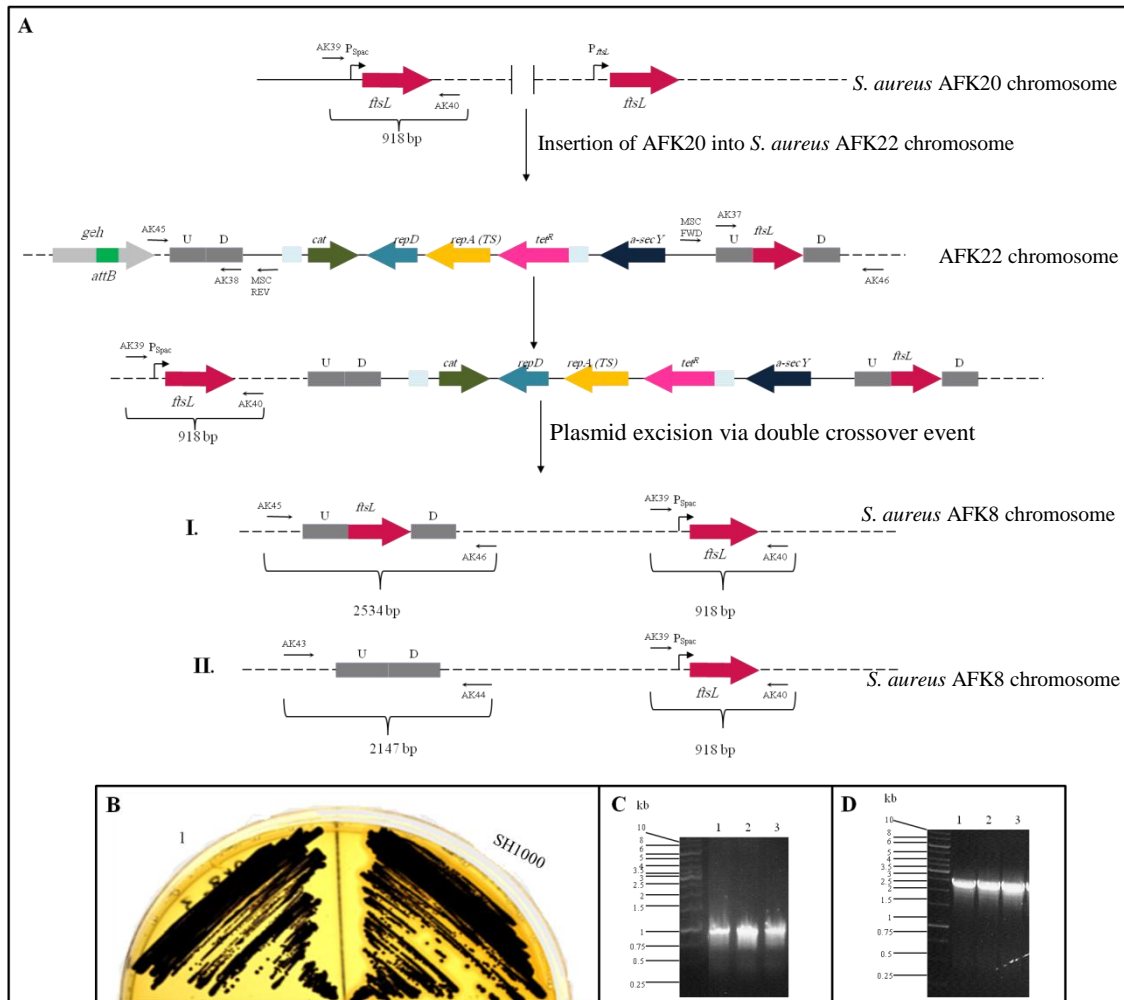


**Figure 5.22 Creation of the conditional *S. aureus ftsL* lethal mutant**

A. Diagrammatic representation of insertion of the regulatable copy of *ftsL* into AFK22 (pAFK15 single-crossover strain) followed by plasmid excision via a double-crossover event. pAFK15 excision at the upstream side yields a mutant gene (I), while pAFK14 excision via the downstream side produces the wild-type gene (II) (not to scale).

B. Confirmation of correct pAFK17 integration into the *S. aureus* chromosome by the loss of lipase activity on BPr medium. A precipitation zone, which can be observed around the SH1000 colonies, is missing from clones 1.

C. A  $P_{\text{Spac}}\text{-}ftsL$  PCR product was amplified using the AK39/AK40 primers after genomic DNA extraction and the products were analysed by electrophoresis in a 1% TAE (w/v) agarose gel. A 918 bp product that corresponded to the  $P_{\text{Spac}}\text{-}ftsL$  insert was obtained (indicated by a black arrow). Lanes 1 to 3 correspond to the investigated clones. DNA standards are of sizes shown in Kb.

D. Chloramphenicol-sensitive clones were screened by PCR using the chromosomal primer pairs AK45/AK46 after genomic DNA was extracted from the putative mutants. A 2534-bp product that corresponded to the wild-type gene was obtained. DNA standards are of sizes shown in Kb.

The cell culture was then diluted  $10^{-1}$ -  $10^{-6}$  fold, and the  $10^{-4}$ ,  $10^{-5}$  and  $10^{-6}$  dilutions (50  $\mu$ l each) were plated on BHI + anhydrotetracycline (1  $\mu$ g ml $^{-1}$ ) + 1 mM IPTG plates and incubated at 25°C for 48 h. Potential positive clones were chosen and streaked onto BHI + anhydrotetracycline (1  $\mu$ g ml $^{-1}$ ) + 1 mM IPTG and BHI + chloramphenicol (10  $\mu$ g ml $^{-1}$ ) + 1 mM IPTG plates and incubated at 37°C overnight. The percentage of colonies that were both chloramphenicol-sensitive and anhydrotetracycline-resistant was  $\sim <3\%$  (79/3,000). Genomic DNA was extracted from colonies that grew in the presence of anhydrotetracycline but not in the presence of chloramphenicol and was used as template for PCR screening. Screening of mutations using the primer pairs AK43/AK44 for the  $\Delta divIC$  mutants and AK45/AK46 for the  $\Delta ftsL$  mutants was performed. The PCR products were then separated in a 1% (w/v) agarose gel, and  $\sim 2.5$ -Kb bands were produced for all of the chloramphenicol-sensitive colonies that were screened, which corresponded to the expected size of the wild-type chromosomal region (Figure 5.21D and Figure 5.22D). Many attempts for plasmid excision were performed to isolate a clone in which the gene had been deleted, but none were successful. Another attempt has been made in which the plasmid excision step was repeated at 39°C to improve integration; however, all of the clones that were isolated encoded a wild-type copy of the gene. Thousands of potential positive clones have been isolated and ( $\sim 120$ ) screened using chromosomal primers after extracting genomic DNA from the isolates, but none have been successful.

### 5.3 Discussion

#### 5.3.1 The essentiality of *divIC* and *ftsL* in *S. aureus*

TMDH was used to analyse the *S. aureus* genome, and 351 putative essential genes for bacterial growth and viability were discovered (Chaudhuri *et al.*, 2009). *S. aureus divIC* and *ftsL* were predicted to be essential due to the absence of the transposons within the genes. PCR footprinting analysis using gene-specific primers and primers based on the transposon sequence were also performed to identify essential genes. Negative PCR products indicated the absence of the transposon; thus, the genes were considered to be essential. However, when PCR products could not be obtained due to gene size (e.g., small genes), a linker PCR was performed to verify several candidate essential genes (Chaudhuri *et al.*, 2009).

However, apparent gene essentiality could be influenced by the experimental conditions used to create the transposon library. For example, *S. aureus* requires prolonged incubation times at 44°C to lose temperature-sensitive replicons; therefore, genes that are needed for survival at higher temperatures are considered to be potentially essential (Chaudhuri *et al.*, 2009).

The functions of DivIC (FtsB) and FtsL have been well studied in rod-shaped organisms such as *B. subtilis* and *E. coli*; however, the exact functions of these proteins in cell division are still unclear. No direct homology between *E. coli* FtsB and *B. subtilis* DivIC has been shown; however, weak homology between *E. coli* FtsB and *B. halodurans* DivIC is evident, and this latter protein is a homologue of *B. subtilis* DivIC (Buddelmeijer *et al.*, 2002). In *S. aureus*, the DivIC protein shares 27% identity with *B. subtilis* DivIC and 14% identity with *E. coli* DivIC. In contrast, *ftsL* in *E. coli* and *B. subtilis* were stated to be analogous based on several factors, among which is the similarity in the chromosomal localisations of the genes in both organisms, that is, *ftsL* lies upstream of the *pbpB/ftsI* gene (Ueki *et al.*, 1992; Guzman *et al.*, 1992; Daniel *et al.*, 1996; Daniel *et al.*, 1998). Additionally, the two upstream genes of the *ftsL* operon, *yllB* and *yllC*, are very similar to the *E. coli* upstream genes of *ftsL* (Daniel *et al.*, 1996). In *S. aureus*, *ftsL* is located upstream of *pbp1* (Figure 5.3A), and the *S. aureus* FtsL protein shares 27% identity with *B. subtilis* FtsL (Figure 5.3B); however, *S. aureus* FtsL shares only very low homology with *E. coli* FtsL (2% identity).

The attempts to make in-frame deletions and thus conditionally lethal mutations of *divIC* and *ftsL* in *S. aureus* (Section 5.2.2 and Section 5.2.3) were unsuccessful. Several reasons might affect the capacity to obtain the desirable mutation. The selection efficiency of the pIMAY plasmid is poor because the percentage of chloramphenicol-sensitive colonies that were also anhydrotetracycline-resistant was low. Additionally, the induction of antisense *secY* gene expression by anhydrotetracycline was likely low; therefore, the counter-selection of pIMAY excision was not efficient because it did not suppress the growth of cells that contained the pIMAY plasmid DNA. Recently, a new cloning technique termed



sequence- and ligation-independent cloning (Li and Elledge, 2007; Monk and Foster, 2012) was applied to a new derivative of pIMAY and resulted in pIMAY-Z, which contains the *lacZ* gene for further colorimetric selection. This new method has improved cloning efficiency because >90% of the screened clones contain inserts; therefore, it decreases the cost and time of laborious mutant screening and deletion construction (Monk and Foster, 2012). Due to time limits, further screening and investigation of the mutants had to be halted.

#### **5.4 Future work**

Creation of *S. aureus* mutants lacking either *divIC* or *ftsL* will help to determine the role of these proteins in the *S. aureus* cell division process; therefore, these proteins can be considered potential targets for inhibitor development. Consequently, pIMAY-Z will be the vector of choice for future attempts at constructing unmarked, in-frame deletions of *S. aureus divIC* and *ftsL*.

## Chapter 6

### General Discussion

#### 6.1 Conservation of the bacterial divisome

An analysis of division and morphogenesis in diverse organisms is helpful for characterising the origin of the division pathway and understanding how mechanisms differ to accommodate changes in cell shape. The cell division apparatus in Eubacteria is assembled via the construction of a macromolecular complex commonly consisting of at least twelve proteins (Nikolaichik and Donachie, 2000; Margolin, 2000; Pinho *et al.*, 2013). A comparison of the genomic sequences of Eubacteria has revealed some differences in the genetic organisation of the gene clusters encoding cell division proteins; however, most of the cell division proteins are highly conserved (Nikolaichik and Donachie, 2000). Ten cell division proteins that are present in nearly all cell wall-containing Eubacteria have been investigated: FtsZ, FtsA, FtsE, FtsX, FtsK, FtsL, FtsB, FtsQ, FtsW and FtsI. However, other proteins may be present (Table 6.1) (Margolin, 2000; Nikolaichik and Donachie, 2000; Gamba *et al.*, 2009; Pinho *et al.*, 2013).

Although bacteria have a range of different shapes, the conservation of many cell division components suggests a degree of similarity in the recruitment and assemblage of the division apparatus at mid-cell. Indeed, the interactions between cell division proteins are conserved in a range of organisms, and these proteins have been found to interact with either one partner or several partners, implying that the division apparatus is stabilised by these interactions (Wang *et al.* 1997; Ma *et al.* 1997; Gaikwad *et al.* 2000; Momynaliev *et al.* 2002; Weiss, 2004; Karimova *et al.*, 2005; Osawa and Erickson 2006; Daniel *et al.*, 2006; D'Ulisse *et al.* 2007; Maggi *et al.* 2008). Recently, the division complex in *S. aureus* was mapped by bacterial two-hybrid analysis. These experiments showed that nearly all the proteins that have been investigated interact with many partners, suggesting a multicomponent division complex (Steele *et al.*, 2011) (Figure 1.4A and Figure 6.1).

Species	Family	FtsZ	FtsA	ZipA	ZapA	EzrA	SepF	FtsW	FtsI	FtsK	FtsL	FtsB	FtsQ	FtsN	FtsEX	GpsB
Eco	$\gamma$ -Proteobacteria	+	+	+	+	-	-	+	+	+	+	+	+	+	+	-
Hin	$\gamma$ -Proteobacteria	+	+	+	+	-	-	+	+	+	+	+	+	+	+	-
Nme	$\beta$ -Proteobacteria	+	+	-	+	-	-	+	+	+	+	+	+	+	+	-
Ccr	$\alpha$ -Proteobacteria	+	+	-	+	-	-	+	+	+	+	+	+	+	+	-
Hpy	$\epsilon$ -Proteobacteria	+	+	-	+	-	-	+	+	+	-	+	-	-	+	-
Ctr	Chlamydiae	-	-	-	-	-	-	+	+	+	+	-	-	-	-	-
Tpa	Spirochaetes	+	+	-	+	-	-	+	+	+	+	-	+	+	+	-
Mtu	+high GC	+	-	-	-	-	+	+	+	+	-	-	+	-	+	-
Mlu	+highGC	+	-	-	-	-	+	+	+	+	-	-	+	-	+	-
Bsu	+low GC	+	+	-	+	+	+	+	+	+	+	+	+	-	+	+
Efa	+lowGC	+	+	-	+	+	+	+	+	+	+	-	+	-	+	+
Sau	+low GC	+	+	-	+	+	+	+	+	+	+	+	+	-	+	+
Spn	+low GC	+	+	-	+	+	+	+	+	+	+	+	+	-	+	+
Ssp	Cyano/chlor	+	+	-	+	+	+	+	+	+	-	-	+	-	+	-
Mja	Euryarchaeota	+	-	-	-	-	+	-	-	-	-	-	-	-	+	+

**Table 6.1 Conservation of divisome components across species**

Eco, *E. coli*; Hin, *H. influenzae*; Nme, *N. meningitidis*; Ccr, *C. crescentus*; Hpy, *Helicobacter pylori*; Ctr, *Chlamydia trachomatis*; Tpa, *Treponema pallidum*; Mtu, *M. tuberculosis*; Mlu, *Micrococcus luteus*; Bsu, *B. subtilis*; Efu, *E. faecalis*; Sau, *S. aureus*; Spn, *S. pneumoniae*; Ssp, *Synechocystis* sp.; Mja, *M. jannaschii*.

Adapted from (Margolin, 2000; Nikolaichik and Donachie, 2000; Pinho *et al.*, 2013). The Protein Knowledgebase (UniprotKB), (<http://www.uniprot.org/>) was used to identify the presence (+) or absence (-) of protein homologues in the above-mentioned species.

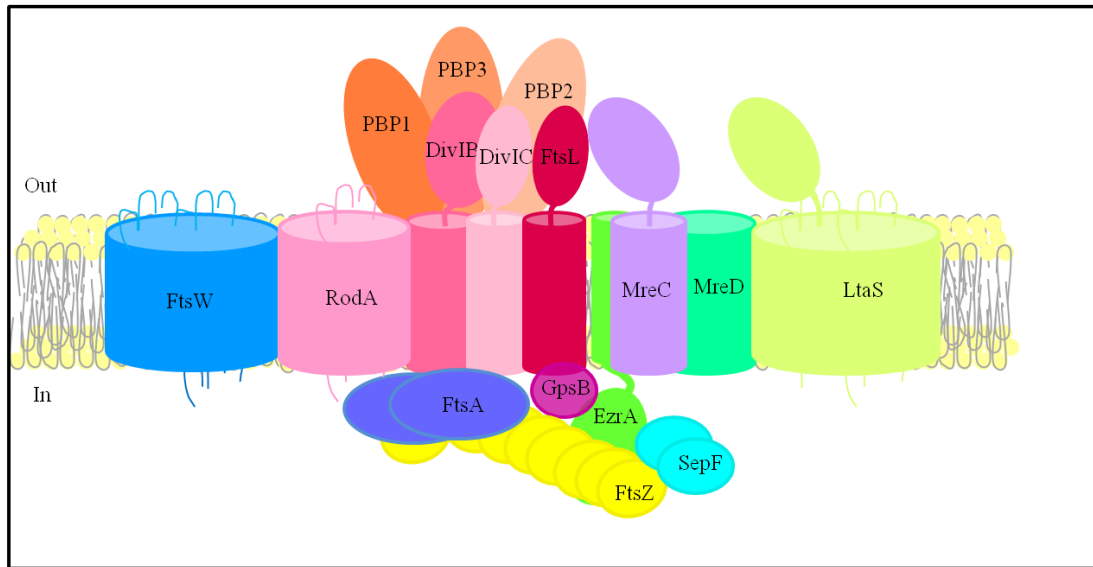


**Figure 6.1 Cell division machinery of *S. aureus***

Schematic representations of the cell division machinery in *S. aureus*. The components were determined based on protein-protein interactions using bacterial two-hybrid assays. Not all known interactions between the division components are shown here. Adapted from (Bottomley, 2011).

Orthologues of the bitopic membrane proteins FtsL, DivIC/FtsB and DivIB/FtsQ were not found in bacteria lacking cell walls (Margolin, 2000). The *ftsL*, *divIC* and *divIB* genes are often located in an operon that is involved in the synthesis of peptidoglycan precursors (Zapun *et al.*, 2008). This finding suggests that these proteins might be involved in the synthesis and/or remodelling of the cell wall. The three proteins form a trimeric complex that is conserved in all the organisms in which division protein interactions have been studied, indicating the functional significance of this complex (Steele *et al.*, 2011; Daniel *et al.*, 2006; Noirclerc-Savoie *et al.*, 2005; Buddelmeijer and Beckwith, 2004). FtsL, DivIC and DivIB are mutually dependent on each other for their stabilisation and localisation to the division site (Daniel *et al.*, 1998; Ghigo *et al.*, 1999; Daniel and Errington, 2000; Buddelmeijer *et al.*, 2002; Daniel *et al.*, 2006). Furthermore, localisation of the FtsL-DivIC-DivIB complex to the mid-cell is dependent on the peptidoglycan biosynthesis machinery (Weiss *et al.*, 1999; Daniel *et al.*, 2000; Rowland *et al.*, 2010; Noirclerc-Savoie *et al.*, 2013).

## **6.2 *S. aureus*, a model of cell division**

The simple cell cycle and morphology of *S. aureus* makes it a potential model in which to study cell division. This bacterium does not undergo cylindrical elongation of the cell wall (Turner *et al.*, 2010); hence, the roles of the cell wall machinery components do not overlap. The synthesis of peptidoglycan only occurs at midcell in an FtsZ-dependent manner (Pinho and Errington, 2003), and the septum becomes the nascent hemispherical poles of the resulting daughter cells after the separation of the parent cell (Figure 6.2). The Min system and nucleoid occlusions select the division site in rod-shaped bacteria by preventing the formation of the FtsZ-ring at the cell poles and above the chromosome, respectively (Errington *et al.*, 2003). No Min homologues have been identified in *S. aureus*; however, DivIVA is present in *S. aureus* but is not essential for division (Pinho and Errington, 2004). Noc was shown to be important for the correct placement of the FtsZ-ring, suggesting that Noc has a role in placing the septum in the correct plane (Veiga *et al.*, 2011). However, nucleoid occlusion alone cannot provide sufficient information to initiate division in the next orthogonal plane.

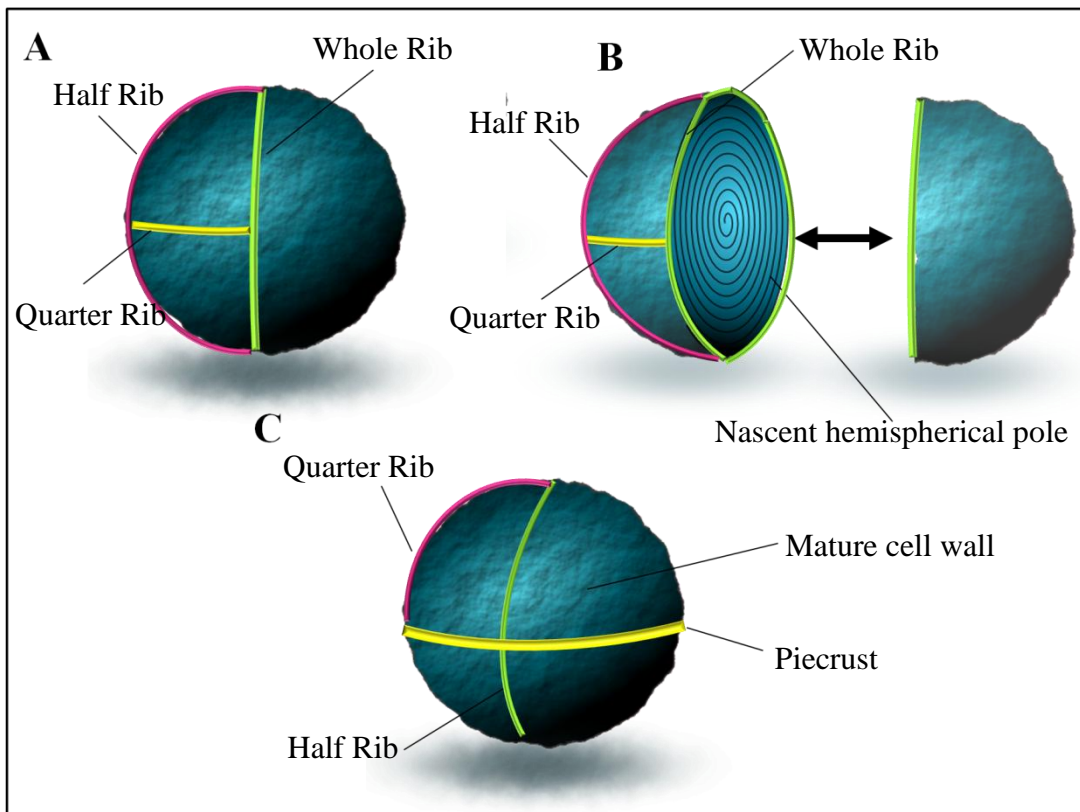


**Figure 6.2 *S. aureus* cell wall architecture and maturation**

A. Mature parent *S. aureus* cells illustrating the planes of division. The whole rib represents the most recent division plane, the half rib represents the second most recent division plane and the quarter rib represents the third most recent and future division planes.

B. After the separation of the daughter cells, the septum forms the nascent hemispherical poles, and each daughter cell will inherit half of the rib.

C. As the cell matures, the peptidoglycan structure undergoes remodelling to allow expansion of the cell. A new piecrust is formed along the plane of the quarter rib, maintaining the characteristics of the three-plane sequence.

Adapted from (Turner *et al.*, 2010; Wheeler, 2012).

Thus, the components of the cell division machinery may recognise certain physical markers within the cell that guide the division machinery to the presumptive division plane. A recent study of *S. aureus* peptidoglycan using AFM has identified important architectural features that reveal potential clues about *S. aureus* cell division (Turner *et al.*, 2010). A thick ring of peptidoglycan was observed and termed “piecrust” because it exhibited a piecrust texture at the presumptive site of septum formation. This piecrust was retained as an orthogonal “rib” after the completion of septum formation. When the cell divides in the next plane, division occurs across the previous septum, resulting in the sectoring of the cell wall material, whereby each sector is delineated by old piecrust materials, the ribs. These ribs contain enough information to mark the previous plane and hence determine the location of the future plane, maintaining the characteristic three-plane sequence (Figure 6.2) (Turner *et al.*, 2010). Thus, the dissimilarities in peptidoglycan structure throughout the cell cycle maybe recognised by different components of the cell division machinery to form the septum. Indeed, the peptidoglycan architectural features of *S. aureus* (piecrust, septal plate and ribs) suggest that the cell division process is not a linear process and not all of the division components interact at the same time, which indicates that the division process occurs in more than one stage (Turner *et al.*, 2010). The synthesis of the septal cell wall in *S. aureus* has been shown to be disorganised in the absence of cell division components such as FtsZ (Pinho and Errington, 2003) and EzrA (Steele *et al.*, 2011). Recent work in our lab has shown that DivIB depletion led to the formation of enlarged “hamburger” cells with multiple or aberrant rings when newly synthesised peptidoglycan was labelled with fluorescent vancomycin (Bottomley *et al.*, unpublished), suggesting the initiation of two septation sites or premature splitting of septa to form daughter cells. Thus, DivIB is not involved in the initiation of septum formation (piecrust) but participates in the progression and completion of septum formation (septal plate). The failure of DivIB-depleted cells to form complete septa was not caused by the delocalisation of peptidoglycan synthetic proteins (PBPs) (Bottomley *et al.*, unpublished), suggesting that DivIB is essential for the progression of cell division at the point of the transition from piecrust formation to septal plate formation.

### 6.3 Cell wall-binding proteins

A number of cell division proteins have been shown to contain a CBD. FtsN is an essential bitopic cell division protein (Dai *et al.*, 1996; Wissel and Weiss, 2004; Muller *et al.*, 2007), and NMR analysis has shown that the C-terminal domain of FtsN shares sequence similarity with the non-catalytic domain of certain peptidoglycan hydrolases, such as the *B. subtilis* amidase CwlC. Two repeat sequences have been identified in the C-terminal domain of CwlC, and these repeats belong to the SPOR family, members of which are found in more than 1500 sporulation- and division-associated proteins, such as FtsN (Yang *et al.*, 2004; Mishima *et al.*, 2005; Arends *et al.*, 2010). The SPOR domains are conserved among various bacterial species and proteobacterial species, such as *C. crescentus*, *Burkholderia thailandensis* and *Myxococcus xanthus* (Moll and Thanbichler, 2009). These tandem repeats play a crucial role in mediating the direct binding of the protein to peptidoglycan (Yang *et al.*, 2004; Mishima *et al.*, 2005; Arends *et al.*, 2010); however, in FtsN, this domain mediates the localisation of the protein to the division site (Ursinus *et al.*, 2004; Moll and Thanbichler, 2009). RlpA, DedD and DamX are *E. coli* proteins that localise to the septum and contain SPOR domains in their C-terminal sequences that mediate this localisation (Gerding *et al.*, 2009; Arends *et al.*, 2010). DedD and DamX are part of the *E. coli* cell division machinery, and the latter was found to interact with other cell division proteins, including FtsQ, using the bacterial two-hybrid method (Gerding *et al.*, 2009; Arends *et al.*, 2010). The presence of SPOR domains in some of the cell division proteins is sufficient for their binding to the septum and for the localisation of these proteins to the septal ring during cell division (Arends *et al.*, 2010). Affinity binding assays have demonstrated that the SPOR domains in *E. coli* and *C. crescentus* FtsN bind to peptidoglycan (Ursinus *et al.*, 2004; Moll and Thanbichler, 2009). In addition, this technique has shown that approximately 80% of recombinant (purified from *E. coli*) His-tagged SPOR domains from DedD, RlpA and DamX, as well as the SPOR domains from *Vibrio parahaemolyticus*, *Cytophaga hutchinsonii* and *Aquifex aeolicus*, were present in the pellet fraction bound to peptidoglycan (Arends *et al.*, 2010). CwlC from *B. subtilis* was shown to bind peptidoglycan via NMR (Mishima *et al.*, 2005). The localisation of the SPOR domain in *E. coli* FtsN is dependent on FtsI and certain amidases, including AmiC, AmiB and AmiA; it has also been suggested that this domain is recruited to septal



peptidoglycan and is transiently present at constriction sites (Gerding *et al.*, 2009). The PASTA domain is a newly identified peptidoglycan-binding domain that consists of four tandem repeats and has been found in *S. coelicolor* and in the C-terminal region of *M. tuberculosis* pKnB. The PASTA domain is also present in the C-termini of other proteins, such as HMW PBPs and eukaryotic-like serine/threonine kinases, which is where the name PASTA originated (Yeats *et al.*, 2002). This domain interacts with the stem peptides of unlinked peptidoglycans and the  $\beta$ -lactam antibiotics that resemble these structures (Yeats *et al.*, 2002; Jones and Dyson, 2006). The lysin motif, or the LysM domain, binds to GlcNAc in a non-covalent manner and is conserved among many cell wall hydrolases (Buist *et al.*, 2008; Moll *et al.*, 2010). The first LysM domain was found in the C-terminal region of the *Bacillus* phage  $\phi$ 29 and consists of 44 amino acid residues (Garvey *et al.*, 1986). DipM and NlpD contain LysM domains that range from 44 to 65 residues in length (Buist *et al.*, 2008). The glycine-tryptophan (GW) domain is another CBD that attaches non-covalently to lipoteichoic acid (LTA) in the cell wall (Scott and Barnett, 2006), as is the CHAP (cysteine, histidine-dependent amidohydrolase/peptidase) domain, which is part of the activity domain of many enzymes (Bateman and Raw, 2003). Numerous peptidoglycan hydrolases contain a choline-binding domain that attaches the enzyme to phosphocholine in the cell wall-associated components WTA and LTA (Vollmer *et al.*, 2008; Mellroth *et al.*, 2012). LytA is an autolysin in *S. pneumoniae* that hydrolyses the lactyl-amide bond connecting the glycan strands and the stem peptide (Mellroth *et al.*, 2012). LytA has a choline-binding domain in its C-terminus that is crucial for its function because the presence of a high concentration of choline in the cell wall inhibits the hydrolytic activity of the enzyme (Giudicelli and Tomasz, 1984). *A. hydrophila* ExeA contains a peptidoglycan-binding domain (Pfam 01471) in its periplasmic region (Li and Howard, 2010). This domain has been found in many cell wall hydrolases, such as *B. subtilis* autolysins, *B. cereus* SleB and a peptidase in *Streptomyces albus*, in which the peptidoglycan binding domain is located in the N-terminal region and a catalytic domain is present in the C-terminal region (Foster, 1991; Charlier *et al.*, 1984; Moriyama *et al.*, 1996; Li and Howard, 2010). Sedimentation assays and other assays, including gel filtration, *in vivo* cross-linking and native PAGE, have shown that *A. hydrophila* ExeA interacts with peptidoglycan. Substitution mutations in any of the highly conserved residues in

this domain reduce the binding affinity of ExeA for peptidoglycan by two-fold *in vitro* (Li and Howard, 2010) and *in vivo* (Howard *et al.*, 2006), which indicates specific binding to the peptidoglycan backbone rather than the other associated components and the involvement of these residues in the interaction (Howard *et al.*, 2006; Li and Howard, 2010).

*S. aureus* DivIC, FtsL (Chapter 3) and DivIB (Bottomley, 2011) bind to peptidoglycan through their C-terminal regions; however, these regions do not have any homology with the previously mentioned CBD, suggesting that DivIC, FtsL and DivIB represent a new class of CBD. *B. subtilis* FtsL (Chapter 3) and *B. subtilis* DivIB (Bottomley, 2011) have been shown to bind peptidoglycan, implying that this binding may be conserved among closely related species. It would be useful to know whether *B. subtilis* DivIC has a binding affinity for the cell wall similar to *S. aureus* DivIC. The binding affinity of DivIC, FtsL (Chapter 3) and DivIB (Bottomley, 2011) for the cell wall is enhanced by the presence of WTA, and a bacterial two-hybrid analysis in *S. aureus* has revealed that DivIC, FtsL and DivIB interact with components of the WTA synthetic machinery, such as TarO (TagO), which is the first enzyme in WTA biosynthesis, as well as SA2103 and SA1195, which are the hypothetical WTA ligases (Kent, 2013). Furthermore, it has been shown that WTA is less abundant at the septum but gradually increases with the distance from the septum (Schlag *et al.*, 2010; Atilano *et al.*, 2010). However, the interaction of the cell division machinery with the WTA biosynthetic machinery (Kent, 2013) and the blockage of WTA biosynthesis cause defects in cell division and separation (Campbell *et al.*, 2011), and the complete absence of WTA from the septum cannot be ruled out.

The localisation patterns of the DivIC, FtsL and DivIB proteins (Chapter 4; Bottomley, 2011) have shown that these proteins are only present transiently at the division site, which is consistent with the accumulation of DivIC, FtsL and DivIB in areas away from the septum where WTA is more abundant. The localisation patterns of DivIC, FtsL and DivIB suggest that they bind to a specific peptidoglycan architecture (piecrust; thick yellow band in Figure 6.2C or ribs;

green, pink and yellow in Figure 6.2A-C). The ribs are then retained as half or quarter ribs in the subsequent divisions, as each daughter cell inherits an old cell pole (Turner *et al.*, 2010). DivIC, FtsL and DivIB might bind to these features (shown as green, pink and yellow bands in Figure 6.2) to either indicate the location of the new division plane or to mark the previous division planes; this can be observed as line patterns or distinct foci depending on the direction of the planes sectoring the cell (Chapter 4, Bottomley *et al.*, unpublished). It has been postulated that the gaps within the WTA layer are due to the ribs and piecrust intersecting the areas where WTA binds; however, the piecrust feature could have less WTA than the ribs (Kent, 2013), which could be due to WTA that was not fully polymerised at the initiation of septum formation (Schlag *et al.*, 2010). Thus, DivIC and FtsL may have roles in either the initial interaction at the beginning of cell division by recognising the existing peptidoglycan template or in directing the cell division machinery to synthesise a particular peptidoglycan architecture.

Katis *et al.*, (1997) suggested two models of DivIC localisation within the *B. subtilis* cell cycle. First, DivIC forms a ring at the septum site before and throughout septation, and once the septum is completely formed, DivIC persists between the newly unseparated daughter cells until cell division is complete. Second, DivIC also exists as a ring at the septum site; however, DivIC is incorporated over the invaginating septum and forms a disc, which degrades once septation is complete, yet a small amount of DivIC remains at the poles of the daughter cells.

#### **6.4 Cell division as an antibacterial target**

The essentiality of the cell division process in nearly all bacteria, particularly those that are pathogenic, makes it an attractive target for antibiotics as disruption of division will cause a loss in cell viability. In addition, the conservation of cell division proteins in a wide range of bacterial species also makes it an ideal target for the development of new therapeutic agents (McDevitt *et al.*, 2002). An optimal target for the development of antimicrobial agents should be conserved, essential and, most important, have no significant homology to mammalian cell division

proteins. Many compounds have been shown (Chapter 1;Section 1.8) to inhibit cell division, and these are under investigation as potential antimicrobial agents (McDevitt *et al.*, 2002; Beuria *et al.*, 2009; Schaffner-Barbero *et al.*, 2011). Some inhibitors have been shown to have anti-tuberculosis (Kumar *et al.*, 2010) and anti-staphylococcal (Haydon *et al.*, 2008) activities. The structural homology of FtsZ and FtsA to eukaryotic tubulin and actin, respectively, could lead to host cell toxicity. Thus, cell division proteins with unknown functions could serve as potential antimicrobial targets when no resistance has been described. DivIC/FtsB and FtsL could serve as putative targets because no homology to eukaryotic proteins has been identified, and they are conserved in bacteria with cell walls. DivIC/FtsB and FtsL were shown to be essential in *B. subtilis* and *E. coli* (Guzman *et al.*, 1992; Levin and Losick, 1994; Daniel *et al.*, 1998; Buddelmeijer *et al.*, 2002) and potentially essential in *S. aureus* (Chaudhuri *et al.*, 2009). Indeed, confirming that these proteins are essential in *S. aureus* will allow them to be considered as potential targets for anti-staphylococcal inhibitors.

Immunological therapies, such as vaccination and therapeutic antibodies, can be used as alternatives to antibiotics. Current and previous active and passive immunisation approaches for the development of *S. aureus* vaccines have targeted several antigens (Otto, 2010; Garcia-Lara and Foster, 2009). These antigens include the following: cell wall targets, including IsdB (V710, Merck), LTA (Pagimaximab, Biosynexus), clumping factor A (Veronate® and Aurexis®, Inhibitex), multi-component surface proteins, such as SdrE, IsdA, SdrD and IsdB (Stranger-Jones *et al.*, 2006), anchorless cell wall proteins, such as enolase, oxoacyl reductase, putative esterase (Glowalla *et al.*, 2009) and protein A (Elusys Therapeutics, Pfizer (ETI211)); capsular targets, including capsular polysaccharide type 5 and type 8 (StaphVAX™, Nabi); membrane targets, such as the ABC transporter GrfA (Aurograb®, Neutec Pharma); extracellular molecules, including  $\alpha$ -toxin, H35L (Bubeck Wardenburg and Schneewind, 2008), Panton-Valentine leukocidin (Brown *et al.*, 2008; Bubeck Wardenburg *et al.*, 2008), enterotoxins and TSST (Hu *et al.*, 2003; Nilsson *et al.* 1999); and surface-associated targets, such as poly-N-acetylglucosamine (Maira-Litran *et al.*, 2005).

Due to the complexity of *S. aureus* pathogenicity and infections, targeting the components mentioned above is often ineffective. Therefore, the search for new targets, such as cell division proteins, is crucial. The ability to utilise membrane proteins as immunological targets for vaccine development suggests that DivIC and FtsL might be useful in this category. Antibodies could inhibit the binding of these proteins to the cell wall and block their functions and hence affect cell division.

## 6.5 Future work

This study has demonstrated that DivIC and FtsL bind peptidoglycan, suggesting that these proteins function in cell wall recognition or synthesis during cell division in *S. aureus*. Localisation studies indicate that DivIC and perhaps FtsL could function as markers of potential division planes or previous division planes, ensuring the assembly of the divisome in the correct plane. Super high-resolution microscopy and AFM will aid in localising DivIC and FtsL to particular *S. aureus* peptidoglycan structures (e.g., piecrust, ribs). In addition, because the binding of DivIC and FtsL to the cell wall was enhanced by the presence of WTA, understanding the role of WTA in mediating the localisation of DivIC and FtsL could clarify the role of WTA in planar division. Further studies using SPR will help to identify the particular component of peptidoglycan that is recognised by these proteins. In addition, the kinetics of binding can be determined by labelling the recombinant proteins with fluorescent dye and subsequently investigating the binding to peptidoglycan at different pHs in the presence or absence of the divalent cations. Although DivIC and FtsL are not highly conserved across bacterial species, it would be useful to investigate the conservation of their function in cell division, especially if the function of these proteins is species-specific. The construction of *divIC* and *ftsL* mutants of *S. aureus* is crucial for verifying the role of DivIC and FtsL in *S. aureus* cell division. Such mutants can be constructed by mutating the chromosome via allelic exchange using Ts plasmids. The mutation can then be complemented by several approaches, such as integration vectors, shuttle plasmids or the induction of gene expression (Monk and Foster, 2012). The depletion of DivIC and FtsL could affect the morphology of the cell and cause a phenotypic change similar to what was observed with the rod-shaped organisms *E. coli* and *B. subtilis*. The present work draws attention to the need to study cell division in

model organisms other than those that are rod-shaped, particularly in those that have different modes of growth. Indeed, studying cell division in clinically relevant pathogens will aid in the identification of putative antibacterial targets and hence further the development of anti-staphylococcal inhibitors.

## References

- Adams, D. W. & Errington, J. (2009)** Bacterial cell division: assembly, maintenance and disassembly of the Z ring. *Nat Rev Microbiol*, 7, 642-53.
- Adams, D. W., Wu, L. J., Czaplowski, L. G. & Errington, J. (2011)** Multiple effects of benzamide antibiotics on FtsZ function. *Mol Microbiol*, 80, 68-84.
- Addinall, S. G., Cao, C. & Lutkenhaus, J. (1997)** FtsN, a late recruit to the septum in *Escherichia coli*. *Mol Microbiol*, 25, 303-9.
- Addinall, S. G. & Lutkenhaus, J. (1996)** FtsA is localized to the septum in an FtsZ-dependent manner. *J Bacteriol*, 178, 7167-72.
- Aish, J. (2003)** Environmental regulation of virulence determinant in *Staphylococcus aureus*, PhD Thesis. University of Sheffield.
- Alber, T. (1992)** Structure of the leucine zipper. *Curr Opin Genet Dev*, 2, 205-10.
- Alyahya, S. A., Alexander, R., Costa, T., Henriques, A. O., Emonet, T. & Jacobs-Wagner, C. (2009)** RodZ, a component of the bacterial core morphogenic apparatus. *Proc Natl Acad Sci U S A*, 106, 1239-44.
- Anderson, D. E., Gueiros-Filho, F. J. & Erickson, H. P. (2004)** Assembly dynamics of FtsZ rings in *Bacillus subtilis* and *Escherichia coli* and effects of FtsZ-regulating proteins. *J Bacteriol*, 186, 5775-81.
- Andreu, J. M., Schaffner-Barbero, C., Huecas, S., Alonso, D., Lopez-Rodriguez, M. L., Ruiz-Avila, L. B., Nunez-Ramirez, R., Llorca, O. & Martin-Galiano, A. J. (2010)** The antibacterial cell division inhibitor PC190723 is an FtsZ polymer-stabilizing agent that induces filament assembly and condensation. *J Biol Chem*, 285, 14239-46.
- Angert, E. R. (2005)** Alternatives to binary fission in bacteria. *Nat Rev Microbiol*, 3, 214-24.
- Angert, E. R. & Losick, R. M. (1998)** Propagation by sporulation in the guinea pig symbiont *Metabacterium polyspora*. *Proc Natl Acad Sci U S A*, 95, 10218-23.
- Archer, G. L. (1998)** *Staphylococcus aureus*: a well-armed pathogen. *Clin Infect Dis*, 26, 1179-81.
- Arends, S. J., Kustus, R. J. & Weiss, D. S. (2009)** ATP-binding site lesions in FtsE impair cell division. *J Bacteriol*, 191, 3772-84.
- Arends, S. J., Williams, K., Scott, R. J., Rolong, S., Popham, D. L. & Weiss, D. S. (2010)** Discovery and characterization of three new *Escherichia coli* septal ring proteins that contain a SPOR domain: DamX, DedD, and RlpA. *J Bacteriol*, 192, 242-55.
- Arnaud, M., Chastanet, A. & Debarbouille, M. (2004)** New vector for efficient allelic replacement in naturally nontransformable, low-GC-content, gram-positive bacteria. *Appl Environ Microbiol*, 70, 6887-91.
- Asai, K., Takamatsu, H., Iwano, M., Kodama, T., Watabe, K. & Ogasawara, N. (2001)** The *Bacillus subtilis* *yabQ* gene is essential for formation of the spore cortex. *Microbiology*, 147, 919-27.
- Atilano, M. L., Pereira, P. M., Yates, J., Reed, P., Veiga, H., Pinho, M. G. & Filipe, S. R. (2010a)** Teichoic acids are temporal and spatial regulators of peptidoglycan cross-linking in *Staphylococcus aureus*. *Proc Natl Acad Sci U S A*, 107, 18991-6.
- Atilano, M. L., Yates, J., Glittenberg, M., Filipe, S. R. & Ligoxygakis, P. (2010b)** Wall teichoic acids of *Staphylococcus aureus* limit recognition by the drosophila peptidoglycan recognition protein-SA to promote pathogenicity. *PLoS Pathog*, 7, e1002421.
- Atrih, A., Bacher, G., Allmaier, G., Williamson, M. P. & Foster, S. J. (1999)** Analysis of peptidoglycan structure from vegetative cells of *Bacillus subtilis* 168 and role of PBP 5 in peptidoglycan maturation. *J Bacteriol*, 181, 3956-66.
- Aussel, L., Barre, F. X., Aroyo, M., Stasiak, A., Stasiak, A. Z. & Sherratt, D. (2002)** FtsK is a DNA motor protein that activates chromosome dimer resolution by switching the catalytic state of the XerC and XerD recombinases. *Cell*, 108, 195-205.
- Bae, T. & Schneewind, O. (2006)** Allelic replacement in *Staphylococcus aureus* with inducible counter-selection. *Plasmid*, 55, 58-63.
- Barber, M. & Rozwadowska-Dowzenko, M. (1948)** Infection by penicillin-resistant *staphylococci*. *Lancet*, 2, 641-4.
- Barbour, A. G. (1981)** Properties of penicillin-binding proteins in *Neisseria gonorrhoeae*. *Antimicrob Agents Chemother*, 19, 316-22.
- Bateman, A. & Rawlings, N. D. (2003)** The CHAP domain: a large family of amidases including GSP amidase and peptidoglycan hydrolases. *Trends Biochem Sci*, 28, 234-7.
- Bayer, A. S., Schneider, T. & Sahl, H. G. (2013)** Mechanisms of daptomycin resistance in *Staphylococcus aureus*: role of the cell membrane and cell wall. *Ann N Y Acad Sci*, 1277, 139-58.
- Beall, B. & Lutkenhaus, J. (1989)** Nucleotide sequence and insertional inactivation of a *Bacillus subtilis* gene that affects cell division, sporulation, and temperature sensitivity. *J Bacteriol*, 171, 6821-34.
- Beall, B. & Lutkenhaus, J. (1991)** FtsZ in *Bacillus subtilis* is required for vegetative septation and for asymmetric septation during sporulation. *Genes Dev*, 5, 447-55.

- Beall, B. & Lutkenhaus, J. (1992)** Impaired cell division and sporulation of a *Bacillus subtilis* strain with the *ftsA* gene deleted. *J Bacteriol*, 174, 2398-403.
- Beech, P. L., Nheu, T., Schultz, T., Herbert, S., Lithgow, T., Gilson, P. R. & Mcfadden, G. I. (2000)** Mitochondrial FtsZ in a chromophyte alga. *Science*, 287, 1276-9.
- Begg, K. J. & Donachie, W. D. (1998)** Division planes alternate in spherical cells of *Escherichia coli*. *J Bacteriol*, 180, 2564-7.
- Ben-Yehuda, S. & Losick, R. (2002)** Asymmetric cell division in *B. subtilis* involves a spiral-like intermediate of the cytokinetic protein FtsZ. *Cell*, 109, 257-66.
- Bendezu, F. O., Hale, C. A., Bernhardt, T. G. & De Boer, P. A. (2009)** RodZ (YfgA) is required for proper assembly of the MreB actin cytoskeleton and cell shape in *E. coli*. *EMBO J*, 28, 193-204.
- Bennett, J. A., Aimino, R. M. & McCormick, J. R. (2007)** *Streptomyces coelicolor* genes *ftsL* and *divIC* play a role in cell division but are dispensable for colony formation. *J Bacteriol*, 189, 8982-92.
- Bensasson, D., Boore, J. L. & Nielsen, K. M. (2004)** Genes without frontiers? *Heredity (Edinb)*, 92, 483-9.
- Benvenuti, M. & Mangani, S. (2007)** Crystallization of soluble proteins in vapor diffusion for x-ray crystallography. *Nat Protoc*, 2, 1633-51.
- Bera, A., Herbert, S., Jakob, A., Vollmer, W. & Gotz, F. (2005)** Why are pathogenic *staphylococci* so lysozyme resistant? The peptidoglycan O-acetyltransferase OatA is the major determinant for lysozyme resistance of *Staphylococcus aureus*. *Mol Microbiol*, 55, 778-87.
- Bernard, C. S., Sadasivam, M., Shiomi, D. & Margolin, W. (2007)** An altered FtsA can compensate for the loss of essential cell division protein FtsN in *Escherichia coli*. *Mol Microbiol*, 64, 1289-305.
- Bernatchez, S., Francis, F. M., Salimnia, H., Beveridge, T. J., Li, H. & Dillon, J. A. (2000)** Genomic, transcriptional and phenotypic analysis of *ftsE* and *ftsX* of *Neisseria gonorrhoeae*. *DNA Res*, 7, 75-81.
- Bernhardt, T. G. & De Boer, P. A. (2003)** The *Escherichia coli* amidase AmiC is a periplasmic septal ring component exported via the twin-arginine transport pathway. *Mol Microbiol*, 48, 1171-82.
- Bernhardt, T. G. & De Boer, P. A. (2004)** Screening for synthetic lethal mutants in *Escherichia coli* and identification of EnvC (YibP) as a periplasmic septal ring factor with murein hydrolase activity. *Mol Microbiol*, 52, 1255-69.
- Bernhardt, T. G. & De Boer, P. A. (2005)** SlmA, a nucleoid-associated, FtsZ binding protein required for blocking septal ring assembly over Chromosomes in *E. coli*. *Mol Cell*, 18, 555-64.
- Beuria, T. K., Santra, M. K. & Panda, D. (2005)** Sanguinarine blocks cytokinesis in bacteria by inhibiting FtsZ assembly and bundling. *Biochemistry*, 44, 16584-93.
- Beuria, T. K., Singh, P., Surolia, A. & Panda, D. (2009)** Promoting assembly and bundling of FtsZ as a strategy to inhibit bacterial cell division: a new approach for developing novel antibacterial drugs. *Biochem J*, 423, 61-9.
- Bi, E. F. & Lutkenhaus, J. (1991)** FtsZ ring structure associated with division in *Escherichia coli*. *Nature*, 354, 161-4.
- Bigot, S., Sivanathan, V., Possoz, C., Barre, F. X. & Cornet, F. (2007)** FtsK, a literate chromosome segregation machine. *Mol Microbiol*, 64, 1434-41.
- Biswas, R., Voggu, L., Simon, U. K., Hentschel, P., Thumm, G. & Gotz, F. (2006)** Activity of the major staphylococcal autolysin Atl. *FEMS Microbiol Lett*, 259, 260-8.
- Blumberg, P. M. & Strominger, J. L. (1974)** Interaction of penicillin with the bacterial cell: penicillin-binding proteins and penicillin-sensitive enzymes. *Bacteriol Rev*, 38, 291-335.
- Bork, P., Sander, C. & Valencia, A. (1992)** An ATPase domain common to prokaryotic cell cycle proteins, sugar kinases, actin, and hsp70 heat shock proteins. *Proc Natl Acad Sci U S A*, 89, 7290-4.
- Bose, K. & Clark, A. C. (2005)** pH effects on the stability and dimerization of procaspase-3. *Protein Sci*, 14, 24-36.
- Bottomley, A. L. (2011)** Identification and characterisation of the cell division machinery in *Staphylococcus aureus*, PhD Thesis. University of Sheffield.
- Boyle, D. S., Khattar, M. M., Addinall, S. G., Lutkenhaus, J. & Donachie, W. D. (1997)** *ftsW* is an essential cell-division gene in *Escherichia coli*. *Mol Microbiol*, 24, 1263-73.
- Bramhill, D. (1997)** Bacterial cell division. *Annu Rev Cell Dev Biol*, 13, 395-424.
- Bramkamp, M., Emmins, R., Weston, L., Donovan, C., Daniel, R. A. & Errington, J. (2008)** A novel component of the division-site selection system of *Bacillus subtilis* and a new mode of action for the division inhibitor MinCD. *Mol Microbiol*, 70, 1556-69.
- Bramkamp, M., Weston, L., Daniel, R. A. & Errington, J. (2006)** Regulated intramembrane proteolysis of FtsL protein and the control of cell division in *Bacillus subtilis*. *Mol Microbiol*, 62, 580-91.
- Brown, E. L., Dumitrescu, O., Thomas, D., Badiou, C., Koers, E. M., Choudhury, P., Vazquez, V., Etienne, J., Lina, G., Vandenesch, F. & Bowden, M. G. (2009)** The Panton-Valentine leukocidin vaccine protects mice against lung and skin infections caused by *Staphylococcus aureus* USA300. *Clin Microbiol Infect*, 15, 156-64.
- Bubeck Wardenburg, J. & Schneewind, O. (2008)** Vaccine protection against *Staphylococcus aureus* pneumonia. *J Exp Med*, 205, 287-94.



**Buddelmeijer, N., Aarsman, M. E., Kolk, A. H., Vicente, M. & Nanninga, N. (1998)** Localization of cell division protein FtsQ by immunofluorescence microscopy in dividing and nondividing cells of *Escherichia coli*. *J Bacteriol*, 180, 6107-16.

**Buddelmeijer, N. & Beckwith, J. (2002)** Assembly of cell division proteins at the *E. coli* cell center. *Curr Opin Microbiol*, 5, 553-7.

**Buddelmeijer, N. & Beckwith, J. (2004)** A complex of the *Escherichia coli* cell division proteins FtsL, FtsB and FtsQ forms independently of its localization to the septal region. *Mol Microbiol*, 52, 1315-27.

**Buddelmeijer, N., Judson, N., Boyd, D., Mekalanos, J. J. & Beckwith, J. (2002)** YgbQ, a cell division protein in *Escherichia coli* and *Vibrio cholerae*, localizes in codependent fashion with FtsL to the division site. *Proc Natl Acad Sci U S A*, 99, 6316-21.

**Bugg, T. D., Dutka-Malen, S., Arthur, M., Courvalin, P. & Walsh, C. T. (1991)** Identification of vancomycin resistance protein VanA as a D-alanine:D-alanine ligase of altered substrate specificity. *Biochemistry*, 30, 2017-21.

**Buist, G., Steen, A., Kok, J. & Kuipers, O. P. (2008)** LysM, a widely distributed protein motif for binding to (peptido)glycans. *Mol Microbiol*, 68, 838-47.

**Cadioux, N. & Kadner, R. J. (1999)** Site-directed disulfide bonding reveals an interaction site between energy-coupling protein TonB and BtuB, the outer membrane cobalamin transporter. *Proc Natl Acad Sci U S A*, 96, 10673-8.

**Cafferkey, M. T., Hone, R. & Keane, C. T. (1982)** Severe staphylococcal infections treated with vancomycin. *J Antimicrob Chemother*, 9, 69-74.

**Calamita, H. G., Ehringer, W. D., Koch, A. L. & Doyle, R. J. (2001)** Evidence that the cell wall of *Bacillus subtilis* is protonated during respiration. *Proc Natl Acad Sci U S A*, 98, 15260-3.

**Campbell, J., Singh, A. K., Santa Maria, J. P., Jr., Kim, Y., Brown, S., Swoboda, J. G., Mylonakis, E., Wilkinson, B. J. & Walker, S. (2011)** Synthetic lethal compound combinations reveal a fundamental connection between wall teichoic acid and peptidoglycan biosyntheses in *Staphylococcus aureus*. *ACS Chem Biol*, 6, 106-16.

**Carballido-Lopez, R. & Formstone, A. (2007)** Shape determination in *Bacillus subtilis*. *Curr Opin Microbiol*, 10, 611-6.

**Carballido-Lopez, R., Formstone, A., Li, Y., Ehrlich, S. D., Noirot, P. & Errington, J. (2006)** Actin homolog MreBH governs cell morphogenesis by localization of the cell wall hydrolase LytE. *Dev Cell*, 11, 399-409.

**Carson, M. J., Barondess, J. & Beckwith, J. (1991)** The FtsQ protein of *Escherichia coli*: membrane topology, abundance, and cell division phenotypes due to overproduction and insertion mutations. *J Bacteriol*, 173, 2187-95.

**Cha, J. H. & Stewart, G. C. (1997)** The *divIVA* minicell locus of *Bacillus subtilis*. *J Bacteriol*, 179, 1671-83.

**Charbonneau, P., Parienti, J. J., Thibon, P., Ramakers, M., Daubin, C., Du Cheyron, D., Lebouvier, G., Le Coutour, X. & Leclercq, R. (2006)** Fluoroquinolone use and methicillin-resistant *Staphylococcus aureus* isolation rates in hospitalized patients: a quasi experimental study. *Clin Infect Dis*, 42, 778-84.

**Charlier, P., Dideberg, O., Jamouille, J. C., Frere, J. M., Ghuysen, J. M., Dive, G. & Lamotte-Brasseur, J. (1984)** Active-site-directed inactivators of the Zn<sup>2+</sup>-containing D-alanyl-D-alanine-cleaving carboxypeptidase of *Streptomyces albus* G. *Biochem J*, 219, 763-72.

**Chastanet, A. & Carballido-Lopez, R. (2012)** The actin-like MreB proteins in *Bacillus subtilis*: a new turn. *Front Biosci (Schol Ed)*, 4, 1582-606.

**Chater, K. F. (1993)** Genetics of differentiation in *Streptomyces*. *Annu Rev Microbiol*, 47, 685-713.

**Chaudhuri, R. R., Allen, A. G., Owen, P. J., Shalom, G., Stone, K., Harrison, M., Burgis, T. A., Lockyer, M., Garcia-Lara, J., Foster, S. J., Pleasance, S. J., Peters, S. E., Maskell, D. J. & Charles, I. G. (2009)** Comprehensive identification of essential *Staphylococcus aureus* genes using Transposon-Mediated Differential Hybridisation (TMDH). *BMC Genomics*, 10, 291.

**Chen, J. C. & Beckwith, J. (2001)** FtsQ, FtsL and FtsI require FtsK, but not FtsN, for co-localization with FtsZ during *Escherichia coli* cell division. *Mol Microbiol*, 42, 395-413.

**Chen, J. C., Minev, M. & Beckwith, J. (2002)** Analysis of ftsQ mutant alleles in *Escherichia coli*: complementation, septal localization, and recruitment of downstream cell division proteins. *J Bacteriol*, 184, 695-705.

**Cho, H. & Bernhardt, T. G. (2013)** Identification of the SlmA active site responsible for blocking bacterial cytokinetic ring assembly over the chromosome. *PLoS Genet*, 9, e1003304.

**Cho, H., Mcmanus, H. R., Dove, S. L. & Bernhardt, T. G. (2011)** Nucleoid occlusion factor SlmA is a DNA-activated FtsZ polymerization antagonist. *Proc Natl Acad Sci U S A*, 108, 3773-8.

**Chung, C. C., Cheng, I. F., Yang, W. H. & Chang, H. C. (2011)** Antibiotic susceptibility test based on the dielectrophoretic behavior of elongated *Escherichia coli* with cephalixin treatment. *Biomicrofluidics*, 5, 21102.

- Chung, H. S., Yao, Z., Goehring, N. W., Kishony, R., Beckwith, J. & Kahne, D. (2009)** Rapid beta-lactam-induced lysis requires successful assembly of the cell division machinery. *Proc Natl Acad Sci U S A*, 106, 21872-7.
- Chung, K. M., Hsu, H. H., Govindan, S. & Chang, B. Y. (2004)** Transcription regulation of *ezrA* and its effect on cell division of *Bacillus subtilis*. *J Bacteriol*, 186, 5926-32.
- Claessen, D., Emmins, R., Hamoen, L. W., Daniel, R. A., Errington, J. & Edwards, D. H. (2008)** Control of the cell elongation-division cycle by shuttling of PBP1 protein in *Bacillus subtilis*. *Mol Microbiol*, 68, 1029-46.
- Cooper, E. L., Garcia-Lara, J. & Foster, S. J. (2009)** YsxC, an essential protein in *Staphylococcus aureus* crucial for ribosome assembly/stability. *BMC Microbiol*, 9, 266.
- Corbin, B. D., Wang, Y., Beuria, T. K. & Margolin, W. (2007)** Interaction between cell division proteins FtsE and FtsZ. *J Bacteriol*, 189, 3026-35.
- Costa, C. S. & Anton, D. N. (1999)** Conditional lethality of cell shape mutations of *Salmonella typhimurium*: *rodA* and *mre* mutants are lethal on solid but not in liquid medium. *Curr Microbiol*, 38, 137-42.
- Costa, T., Priyadarshini, R. & Jacobs-Wagner, C. (2008)** Localization of PBP3 in *Caulobacter crescentus* is highly dynamic and largely relies on its functional transpeptidase domain. *Mol Microbiol*, 70, 634-51.
- Courvalin, P. (2006)** Vancomycin resistance in gram-positive cocci. *Clin Infect Dis*, 42 Suppl 1, S25-34.
- Cui, L., Iwamoto, A., Lian, J. Q., Neoh, H. M., Maruyama, T., Horikawa, Y. & Hiramatsu, K. (2006)** Novel mechanism of antibiotic resistance originating in vancomycin-intermediate *Staphylococcus aureus*. *Antimicrob Agents Chemother*, 50, 428-38.
- Cui, L., Murakami, H., Kuwahara-Arai, K., Hanaki, H. & Hiramatsu, K. (2000)** Contribution of a thickened cell wall and its glutamine nonamidated component to the vancomycin resistance expressed by *Staphylococcus aureus* Mu50. *Antimicrob Agents Chemother*, 44, 2276-85.
- D'ulisse, V., Fagioli, M., Ghelardini, P. & Paolozzi, L. (2007)** Three functional subdomains of the *Escherichia coli* FtsQ protein are involved in its interaction with the other division proteins. *Microbiology*, 153, 124-38.
- Dai, K. & Lutkenhaus, J. (1991)** *ftsZ* is an essential cell division gene in *Escherichia coli*. *J Bacteriol*, 173, 3500-6.
- Dai, K. & Lutkenhaus, J. (1992)** The proper ratio of FtsZ to FtsA is required for cell division to occur in *Escherichia coli*. *J Bacteriol*, 174, 6145-51.
- Dai, K., Xu, Y. & Lutkenhaus, J. (1993)** Cloning and characterization of *ftsN*, an essential cell division gene in *Escherichia coli* isolated as a multicopy suppressor of *ftsA12(Ts)*. *J Bacteriol*, 175, 3790-7.
- Dai, K., Xu, Y. & Lutkenhaus, J. (1996)** Topological characterization of the essential *Escherichia coli* cell division protein FtsN. *J Bacteriol*, 178, 1328-34.
- Dajkovic, A., Pichoff, S., Lutkenhaus, J. & Wirtz, D. (2010)** Cross-linking FtsZ polymers into coherent Z rings. *Mol Microbiol*, 78, 651-68.
- Dancer, S. J. (2008)** The effect of antibiotics on methicillin-resistant *Staphylococcus aureus*. *J Antimicrob Chemother*, 61, 246-53.
- Daniel, R. A. & Errington, J. (2000)** Intrinsic instability of the essential cell division protein FtsL of *Bacillus subtilis* and a role for DivIB protein in FtsL turnover. *Mol Microbiol*, 36, 278-89.
- Daniel, R. A. & Errington, J. (2003)** Control of cell morphogenesis in bacteria: two distinct ways to make a rod-shaped cell. *Cell*, 113, 767-76.
- Daniel, R. A., Harry, E. J. & Errington, J. (2000)** Role of penicillin-binding protein PBP 2B in assembly and functioning of the division machinery of *Bacillus subtilis*. *Mol Microbiol*, 35, 299-311.
- Daniel, R. A., Harry, E. J., Katis, V. L., Wake, R. G. & Errington, J. (1998)** Characterization of the essential cell division gene *ftsL(yIID)* of *Bacillus subtilis* and its role in the assembly of the division apparatus. *Mol Microbiol*, 29, 593-604.
- Daniel, R. A., Noirot-Gros, M. F., Noirot, P. & Errington, J. (2006)** Multiple interactions between the transmembrane division proteins of *Bacillus subtilis* and the role of FtsL instability in divisome assembly. *J Bacteriol*, 188, 7396-404.
- Daniel, R. A., Williams, A. M. & Errington, J. (1996)** A complex four-gene operon containing essential cell division gene *pbpB* in *Bacillus subtilis*. *J Bacteriol*, 178, 2343-50.
- Datta, P., Dasgupta, A., Singh, A. K., Mukherjee, P., Kundu, M. & Basu, J. (2006)** Interaction between FtsW and penicillin-binding protein 3 (PBP3) directs PBP3 to mid-cell, controls cell septation and mediates the formation of a trimeric complex involving FtsZ, FtsW and PBP3 in mycobacteria. *Mol Microbiol*, 62, 1655-73.
- De Boer, P., Crossley, R. & Rothfield, L. (1992a)** The essential bacterial cell-division protein FtsZ is a GTPase. *Nature*, 359, 254-6.
- De Boer, P. A., Crossley, R. E., Hand, A. R. & Rothfield, L. I. (1991)** The MinD protein is a membrane ATPase required for the correct placement of the *Escherichia coli* division site. *EMBO J*, 10, 4371-80.

- De Boer, P. A., Crossley, R. E. & Rothfield, L. I. (1989)** A division inhibitor and a topological specificity factor coded for by the minicell locus determine proper placement of the division septum in *E. coli*. *Cell*, 56, 641-9.
- De Boer, P. A., Crossley, R. E. & Rothfield, L. I. (1992b)** Roles of MinC and MinD in the site-specific septation block mediated by the MinCDE system of *Escherichia coli*. *J Bacteriol*, 174, 63-70.
- De Leeuw, E., Graham, B., Phillips, G. J., Ten Hagen-Jongman, C. M., Oudega, B. & Luirink, J. (1999)** Molecular characterization of *Escherichia coli* FtsE and FtsX. *Mol Microbiol*, 31, 983-93.
- Defeu Soufo, H. J. & Graumann, P. L. (2004)** Dynamic movement of actin-like proteins within bacterial cells. *EMBO Rep*, 5, 789-94.
- Deleo, F. R., Diep, B. A. & Otto, M. (2009)** Host defense and pathogenesis in *Staphylococcus aureus* infections. *Infect Dis Clin North Am*, 23, 17-34.
- Dempwolff, F., Reimold, C., Reth, M. & Graumann, P. L. (2011)** *Bacillus subtilis* MreB orthologs self-organize into filamentous structures underneath the cell membrane in a heterologous cell system. *PLoS One*, 6, e27035.
- Den Blaauwen, T., Buddelmeijer, N., Aarsman, M. E., Hameete, C. M. & Nanninga, N. (1999)** Timing of FtsZ assembly in *Escherichia coli*. *J Bacteriol*, 181, 5167-75.
- Den Blaauwen, T., De Pedro, M. A., Nguyen-Disteche, M. & Ayala, J. A. (2008)** Morphogenesis of rod-shaped sacculi. *FEMS Microbiol Rev*, 32, 321-44.
- Derouaux, A., Wolf, B., Fraipont, C., Breukink, E., Nguyen-Disteche, M. & Terrak, M. (2008)** The monofunctional glycosyltransferase of *Escherichia coli* localizes to the cell division site and interacts with penicillin-binding protein 3, FtsW, and FtsN. *J Bacteriol*, 190, 1831-4.
- Di Lallo, G., Fagioli, M., Barionovi, D., Ghelardini, P. & Paolozzi, L. (2003)** Use of a two-hybrid assay to study the assembly of a complex multicomponent protein machinery: bacterial septosome differentiation. *Microbiology*, 149, 3353-9.
- Din, N., Quardokus, E. M., Sackett, M. J. & Brun, Y. V. (1998)** Dominant C-terminal deletions of FtsZ that affect its ability to localize in *Caulobacter* and its interaction with FtsA. *Mol Microbiol*, 27, 1051-63.
- Divakaruni, A. V., Baida, C., White, C. L. & Gober, J. W. (2007)** The cell shape proteins MreB and MreC control cell morphogenesis by positioning cell wall synthetic complexes. *Mol Microbiol*, 66, 174-88.
- Divakaruni, A. V., Loo, R. R., Xie, Y., Loo, J. A. & Gober, J. W. (2005)** The cell-shape protein MreC interacts with extracytoplasmic proteins including cell wall assembly complexes in *Caulobacter crescentus*. *Proc Natl Acad Sci U S A*, 102, 18602-7.
- Dodson, G. & Wlodawer, A. (1998)** Catalytic triads and their relatives. *Trends Biochem Sci*, 23, 347-52.
- Domadia, P., Swarup, S., Bhunia, A., Sivaraman, J. & Dasgupta, D. (2007)** Inhibition of bacterial cell division protein FtsZ by cinnamaldehyde. *Biochem Pharmacol*, 74, 831-40.
- Dominguez-Escobar, J., Chastanet, A., Crevenna, A. H., Fromion, V., Wedlich-Soldner, R. & Carballido-Lopez, R. (2011)** Processive movement of MreB-associated cell wall biosynthetic complexes in bacteria. *Science*, 333, 225-8.
- Donachie, W. D. & Begg, K. J. (1989)** Cell length, nucleoid separation, and cell division of rod-shaped and spherical cells of *Escherichia coli*. *J Bacteriol*, 171, 4633-9.
- Dowding, J. E. (1977)** Mechanisms of gentamicin resistance in *Staphylococcus aureus*. *Antimicrob Agents Chemother*, 11, 47-50.
- Doyle, R. J., Chaloupka, J. & Vinter, V. (1988)** Turnover of cell walls in microorganisms. *Microbiol Rev*, 52, 554-67.
- Draper, G. C., McLennan, N., Begg, K., Masters, M. & Donachie, W. D. (1998)** Only the N-terminal domain of FtsK functions in cell division. *J Bacteriol*, 180, 4621-7.
- Drew, R. H., Perfect, J. R., Srinath, L., Kurkimilis, E., Dowzicky, M. & Talbot, G. H. (2000)** Treatment of methicillin-resistant *staphylococcus aureus* infections with quinupristin-dalfopristin in patients intolerant of or failing prior therapy. For the Synercid Emergency-Use Study Group. *J Antimicrob Chemother*, 46, 775-84.
- Durand-Heredia, J. M., Yu, H. H., De Carlo, S., Lesser, C. F. & Janakiraman, A. (2011)** Identification and characterization of ZapC, a stabilizer of the FtsZ ring in *Escherichia coli*. *J Bacteriol*, 193, 1405-13.
- Dye, N. A., Pincus, Z., Theriot, J. A., Shapiro, L. & Gitai, Z. (2005)** Two independent spiral structures control cell shape in *Caulobacter*. *Proc Natl Acad Sci U S A*, 102, 18608-13.
- Ebersbach, G., Galli, E., Moller-Jensen, J., Lowe, J. & Gerdes, K. (2008)** Novel coiled-coil cell division factor ZapB stimulates Z ring assembly and cell division. *Mol Microbiol*, 68, 720-35.
- Edwards, D. H. & Errington, J. (1997)** The *Bacillus subtilis* DivIVA protein targets to the division septum and controls the site specificity of cell division. *Mol Microbiol*, 24, 905-15.
- Ehler, K. & Holtje, J. V. (1996)** Role of precursor translocation in coordination of murein and phospholipid synthesis in *Escherichia coli*. *J Bacteriol*, 178, 6766-71.

**Ekici, O. D., Paetzel, M. & Dalbey, R. E. (2008)** Unconventional serine proteases: variations on the catalytic Ser/His/Asp triad configuration. *Protein Sci*, 17, 2023-37.

**Entenza, J. M., Caldelari, I., Glauser, M. P. & Moreillon, P. (1999)** Efficacy of levofloxacin in the treatment of experimental endocarditis caused by viridans group streptococci. *J Antimicrob Chemother*, 44, 775-86.

**Erickson, H. P. (1997)** FtsZ, a tubulin homologue in prokaryote cell division. *Trends Cell Biol*, 7, 362-7.

**Erickson, H. P. (2001)** The FtsZ protofilament and attachment of ZipA--structural constraints on the FtsZ power stroke. *Curr Opin Cell Biol*, 13, 55-60.

**Erickson, H. P., Anderson, D. E. & Osawa, M. (2010)** FtsZ in bacterial cytokinesis: cytoskeleton and force generator all in one. *Microbiol Mol Biol Rev*, 74, 504-28.

**Erickson, H. P., Taylor, D. W., Taylor, K. A. & Bramhill, D. (1996)** Bacterial cell division protein FtsZ assembles into protofilament sheets and minirings, structural homologs of tubulin polymers. *Proc Natl Acad Sci U S A*, 93, 519-23.

**Errington, J., Daniel, R. A. & Scheffers, D. J. (2003)** Cytokinesis in bacteria. *Microbiol Mol Biol Rev*, 67, 52-65. table of contents.

**Fadda, D., Pischedda, C., Caldara, F., Whalen, M. B., Anderluzzi, D., Domenici, E. & Massidda, O. (2003)** Characterization of *divIVA* and other genes located in the chromosomal region downstream of the *dcw* cluster in *Streptococcus pneumoniae*. *J Bacteriol*, 185, 6209-14.

**Fawcett, P., Eichenberger, P., Losick, R. & Youngman, P. (2000)** The transcriptional profile of early to middle sporulation in *Bacillus subtilis*. *Proc Natl Acad Sci U S A*, 97, 8063-8.

**Feilmeier, B. J., Iseminger, G., Schroeder, D., Webber, H. & Phillips, G. J. (2000)** Green fluorescent protein functions as a reporter for protein localization in *Escherichia coli*. *J Bacteriol*, 182, 4068-76.

**Ferrero, L., Cameron, B. & Crouzet, J. (1995)** Analysis of *gyrA* and *glaA* mutations in stepwise-selected ciprofloxacin-resistant mutants of *Staphylococcus aureus*. *Antimicrob Agents Chemother*, 39, 1554-8.

**Feucht, A., Lucet, I., Yudkin, M. D. & Errington, J. (2001)** Cytological and biochemical characterization of the FtsA cell division protein of *Bacillus subtilis*. *Mol Microbiol*, 40, 115-25.

**Feucht, A., Magnin, T., Yudkin, M. D. & Errington, J. (1996)** Bifunctional protein required for asymmetric cell division and cell-specific transcription in *Bacillus subtilis*. *Genes Dev*, 10, 794-803.

**Figge, R. M., Divakaruni, A. V. & Gober, J. W. (2004)** MreB, the cell shape-determining bacterial actin homologue, co-ordinates cell wall morphogenesis in *Caulobacter crescentus*. *Mol Microbiol*, 51, 1321-32.

**Fisher, A. M. (1946)** A study on the mechanism of action of penicillin as shown by its effect on bacterial morphology. *J Bacteriol*, 52, 539-554.

**Fletcher, H., Hickey, I. & Winter, P. (2007)** *Genetics*, New York, Taylor & Francis Group.

**Formstone, A., Carballido-Lopez, R., Noirot, P., Errington, J. & Scheffers, D. J. (2008)** Localization and interactions of teichoic acid synthetic enzymes in *Bacillus subtilis*. *J Bacteriol*, 190, 1812-21.

**Formstone, A. & Errington, J. (2005)** A magnesium-dependent *mreB* null mutant: implications for the role of *mreB* in *Bacillus subtilis*. *Mol Microbiol*, 55, 1646-57.

**Forrest, T. M., Wilson, G. E., Pan, Y. & Schaefer, J. (1991)** Characterization of cross-linking of cell walls of *Bacillus subtilis* by a combination of magic-angle spinning NMR and gas chromatography-mass spectrometry of both intact and hydrolyzed <sup>13</sup>C- and <sup>15</sup>N-labeled cell-wall peptidoglycan. *J Biol Chem*, 266, 24485-91.

**Foster, S. J. (1991)** Cloning, expression, sequence analysis and biochemical characterization of an autolytic amidase of *Bacillus subtilis* 168 trpC2. *J Gen Microbiol*, 137, 1987-98.

**Foster, S. J. (1992)** Analysis of the autolysins of *Bacillus subtilis* 168 during vegetative growth and differentiation by using renaturing polyacrylamide gel electrophoresis. *J Bacteriol*, 174, 464-70.

**Foster, S. J. & Popham, D. L. (2001)** Structure and synthesis of cell wall, spore cortex, teichoic acids, S-layers, and capsules. In Sonenshein, A. L., Hoch, J. A. & Losick, R. (Eds.) *Bacillus subtilis* and Its Close Relative: from genes to cells. Washington, D.C., American Society for Microbiology.

**Foster, T. J. (2005)** Immune evasion by staphylococci. *Nat Rev Microbiol*, 3, 948-58.

**Foster, T. J. & Hook, M. (1998)** Surface protein adhesins of *Staphylococcus aureus*. *Trends Microbiol*, 6, 484-8.

**Fraipont, C., Alexeeva, S., Wolf, B., Van Der Ploeg, R., Schloesser, M., Den Blaauwen, T. & Nguyen-Disteche, M. (2011)** The integral membrane FtsW protein and peptidoglycan synthase PBP3 form a subcomplex in *Escherichia coli*. *Microbiology*, 157, 251-9.

**Frandsen, N., Barak, I., Karmazyn-Campelli, C. & Stragier, P. (1999)** Transient gene asymmetry during sporulation and establishment of cell specificity in *Bacillus subtilis*. *Genes Dev*, 13, 394-9.

**Fu, G., Huang, T., Buss, J., Coltharp, C., Hensel, Z. & Xiao, J. (2010)** *In vivo* structure of the *E. coli* FtsZ-ring revealed by photoactivated localization microscopy (PALM). *PLoS One*, 5, e12682.

**Fu, X., Shih, Y. L., Zhang, Y. & Rothfield, L. I. (2001)** The MinE ring required for proper placement of the division site is a mobile structure that changes its cellular location during the *Escherichia coli* division cycle. *Proc Natl Acad Sci U S A*, 98, 980-5.

- Fuda, C., Suvorov, M., Vakulenko, S. B. & Mobashery, S. (2004)** The basis for resistance to beta-lactam antibiotics by penicillin-binding protein 2a of methicillin-resistant *Staphylococcus aureus*. *J Biol Chem*, 279, 40802-6.
- Fukushima, T., Afkham, A., Kurosawa, S., Tanabe, T., Yamamoto, H. & Sekiguchi, J. (2006)** A new D,L-endopeptidase gene product, YojL (renamed CwlS), plays a role in cell separation with LytE and LytF in *Bacillus subtilis*. *J Bacteriol*, 188, 5541-50.
- Gaikwad, A., Babbarwal, V., Pant, V. & Mukherjee, S. K. (2000)** Pea chloroplast FtsZ can form multimers and correct the thermosensitive defect of an *Escherichia coli* ftsZ mutant. *Mol Gen Genet*, 263, 213-21.
- Galli, E. & Gerdes, K. (2010)** Spatial resolution of two bacterial cell division proteins: ZapA recruits ZapB to the inner face of the Z-ring. *Mol Microbiol*, 76, 1514-26.
- Galli, E. & Gerdes, K. (2012)** FtsZ-ZapA-ZapB interactome of *Escherichia coli*. *J Bacteriol*, 194, 292-302.
- Gamba, P., Veening, J. W., Saunders, N. J., Hamoen, L. W. & Daniel, R. A. (2009)** Two-step assembly dynamics of the *Bacillus subtilis* divisome. *J Bacteriol*, 191, 4186-94.
- Garcia-Lara, J. & Foster, S. J. (2009)** Anti-*Staphylococcus aureus* immunotherapy: current status and prospects. *Curr Opin Pharmacol*, 9, 552-7.
- Garcia-Lara, J., Masalha, M. & Foster, S. J. (2005)** *Staphylococcus aureus*: the search for novel targets. *Drug Discov Today*, 10, 643-51.
- Gardner, A. D. (1940)** Morphological effects of penicillin on bacteria. *Nature*, 146, 837-838.
- Garner, E. C., Bernard, R., Wang, W., Zhuang, X., Rudner, D. Z. & Mitchison, T. (2011)** Coupled, circumferential motions of the cell wall synthesis machinery and MreB filaments in *B. subtilis*. *Science*, 333, 222-5.
- Garti-Levi, S., Hazan, R., Kain, J., Fujita, M. & Ben-Yehuda, S. (2008)** The FtsEX ABC transporter directs cellular differentiation in *Bacillus subtilis*. *Mol Microbiol*, 69, 1018-28.
- Garvey, K. J., Saedi, M. S. & Ito, J. (1986)** Nucleotide sequence of *Bacillus* phage phi 29 genes 14 and 15: homology of gene 15 with other phage lysozymes. *Nucleic Acids Res*, 14, 10001-8.
- Gerard, P., Vernet, T. & Zapun, A. (2002)** Membrane topology of the *Streptococcus pneumoniae* FtsW division protein. *J Bacteriol*, 184, 1925-31.
- Gerding, M. A., Liu, B., Bendezu, F. O., Hale, C. A., Bernhardt, T. G. & De Boer, P. A. (2009)** Self-enhanced accumulation of FtsN at Division Sites and Roles for Other Proteins with a SPOR domain (DamX, DedD, and RlpA) in *Escherichia coli* cell constriction. *J Bacteriol*, 191, 7383-401.
- Ghigo, J. M. & Beckwith, J. (2000)** Cell division in *Escherichia coli*: role of FtsL domains in septal localization, function, and oligomerization. *J Bacteriol*, 182, 116-29.
- Ghigo, J. M., Weiss, D. S., Chen, J. C., Yarrow, J. C. & Beckwith, J. (1999)** Localization of FtsL to the *Escherichia coli* septal ring. *Mol Microbiol*, 31, 725-37.
- Gibson, C. W., Daneo-Moore, L. & Higgins, M. L. (1983)** Cell wall assembly during inhibition of DNA synthesis in *Streptococcus faecium*. *J Bacteriol*, 155, 351-6.
- Giesbrecht, P., Kersten, T., Maidhof, H. & Wecke, J. (1998)** Staphylococcal cell wall: morphogenesis and fatal variations in the presence of penicillin. *Microbiol Mol Biol Rev*, 62, 1371-414.
- Giudicelli, S. & Tomasz, A. (1984)** Attachment of pneumococcal autolysin to wall teichoic acids, an essential step in enzymatic wall degradation. *J Bacteriol*, 158, 1188-90.
- Glowalla, E., Tosetti, B., Kronke, M. & Krut, O. (2009)** Proteomics-based identification of anchorless cell wall proteins as vaccine candidates against *Staphylococcus aureus*. *Infect Immun*, 77, 2719-29.
- Goehring, N. W. & Beckwith, J. (2005)** Diverse paths to midcell: assembly of the bacterial cell division machinery. *Curr Biol*, 15, R514-26.
- Goehring, N. W., Gonzalez, M. D. & Beckwith, J. (2006)** Premature targeting of cell division proteins to midcell reveals hierarchies of protein interactions involved in divisome assembly. *Mol Microbiol*, 61, 33-45.
- Goehring, N. W., Robichon, C. & Beckwith, J. (2007)** Role for the nonessential N terminus of FtsN in divisome assembly. *J Bacteriol*, 189, 646-9.
- Goffin, C., Fraipont, C., Ayala, J., Terrak, M., Nguyen-Disteche, M. & Ghuysen, J. M. (1996)** The non-penicillin-binding module of the tripartite penicillin-binding protein 3 of *Escherichia coli* is required for folding and/or stability of the penicillin-binding module and the membrane-anchoring module confers cell septation activity on the folded structure. *J Bacteriol*, 178, 5402-9.
- Goffin, C. & Ghuysen, J. M. (1998)** Multimodular penicillin-binding proteins: an enigmatic family of orthologs and paralogs. *Microbiol Mol Biol Rev*, 62, 1079-93.
- Goley, E. D., Comolli, L. R., Fero, K. E., Downing, K. H. & Shapiro, L. (2010)** DipM links peptidoglycan remodelling to outer membrane organization in *Caulobacter*. *Mol Microbiol*, 77, 56-73.
- Goley, E. D., Yeh, Y. C., Hong, S. H., Fero, M. J., Abeliuk, E., Mcadams, H. H. & Shapiro, L. (2011)** Assembly of the *Caulobacter* cell division machine. *Mol Microbiol*, 80, 1680-98.

**Gomez, M. I., O'seaghda, M., Magargee, M., Foster, T. J. & Prince, A. S. (2006)** *Staphylococcus aureus* protein A activates TNFR1 signaling through conserved IgG binding domains. *J Biol Chem*, 281, 20190-6.

**Gonzalez, M. D., Akbay, E. A., Boyd, D. & Beckwith, J. (2010)** Multiple interaction domains in FtsL, a protein component of the widely conserved bacterial FtsLBQ cell division complex. *J Bacteriol*, 192, 2757-68.

**Gonzalez, M. D. & Beckwith, J. (2009)** Divisome under construction: distinct domains of the small membrane protein FtsB are necessary for interaction with multiple cell division proteins. *J Bacteriol*, 191, 2815-25.

**Gootz, T. D., Sanders, C. C. & Sanders, W. E., Jr. (1979)** In vitro activity of furazlocillin (Bay k 4999) compared with those of mezlocillin, piperacillin, and standard beta-lactam antibiotics. *Antimicrob Agents Chemother*, 15, 783-91.

**Goranov, A. I., Katz, L., Breier, A. M., Burge, C. B. & Grossman, A. D. (2005)** A transcriptional response to replication status mediated by the conserved bacterial replication protein DnaA. *Proc Natl Acad Sci U S A*, 102, 12932-7.

**Goshima, G. & Kimura, A. (2010)** New look inside the spindle: microtubule-dependent microtubule generation within the spindle. *Curr Opin Cell Biol*, 22, 44-9.

**Graumann, P. L. (2004)** Cytoskeletal elements in bacteria. *Curr Opin Microbiol*, 7, 565-71.

**Greenberg, D. P., Ward, J. I. & Bayer, A. S. (1987)** Influence of *Staphylococcus aureus* antibody on experimental endocarditis in rabbits. *Infect Immun*, 55, 3030-4.

**Grenga, L., Luzi, G., Paolozzi, L. & Ghelardini, P. (2008)** The *Escherichia coli* FtsK functional domains involved in its interaction with its divisome protein partners. *FEMS Microbiol Lett*, 287, 163-7.

**Grover, N. B., Woldringh, C. L., Zaritsky, A. & Rosenberger, R. F. (1977)** Elongation of rod-shaped bacteria. *J Theor Biol*, 67, 181-93.

**Grundling, A. and Schneewind, O. (2007)**. Synthesis of glycerol phosphate lipoteichoic acid in *Staphylococcus aureus*, *Proc Natl Acad Sci U S A*, 104, 8478-83.

**Gueiros-Filho, F. J. & Losick, R. (2002)** A widely conserved bacterial cell division protein that promotes assembly of the tubulin-like protein FtsZ. *Genes Dev*, 16, 2544-56.

**Gundogdu, M. E., Kawai, Y., Pavlendova, N., Ogasawara, N., Errington, J., Scheffers, D. J. & Hamoen, L. W. (2011)** Large ring polymers align FtsZ polymers for normal septum formation. *EMBO J*, 30, 617-26.

**Gutierrez, J., Smith, R. & Pogliano, K. (2010)** SpoIID-mediated peptidoglycan degradation is required throughout engulfment during *Bacillus subtilis* sporulation. *J Bacteriol*, 192, 3174-86.

**Guzman, L. M., Barondess, J. J. & Beckwith, J. (1992)** FtsL, an essential cytoplasmic membrane protein involved in cell division in *Escherichia coli*. *J Bacteriol*, 174, 7716-28.

**Guzman, L. M., Weiss, D. S. & Beckwith, J. (1997)** Domain-swapping analysis of FtsI, FtsL, and FtsQ, bitopic membrane proteins essential for cell division in *Escherichia coli*. *J Bacteriol*, 179, 5094-103.

**Haeusser, D. P., Garza, A. C., Buscher, A. Z. & Levin, P. A. (2007)** The division inhibitor EzrA contains a seven-residue patch required for maintaining the dynamic nature of the medial FtsZ ring. *J Bacteriol*, 189, 9001-10.

**Haeusser, D. P., Schwartz, R. L., Smith, A. M., Oates, M. E. & Levin, P. A. (2004)** EzrA prevents aberrant cell division by modulating assembly of the cytoskeletal protein FtsZ. *Mol Microbiol*, 52, 801-14.

**Hageman, J. C., Pegues, D. A., Jepson, C., Bell, R. L., Guinan, M., Ward, K. W., Cohen, M. D., Hindler, J. A., Tenover, F. C., Mcallister, S. K., Kellum, M. E. & Fridkin, S. K. (2001)** Vancomycin-intermediate *Staphylococcus aureus* in a home health-care patient. *Emerg Infect Dis*, 7, 1023-5.

**Hale, C. A. & De Boer, P. A. (1997)** Direct binding of FtsZ to ZipA, an essential component of the septal ring structure that mediates cell division in *E. coli*. *Cell*, 88, 175-85.

**Hale, C. A. & De Boer, P. A. (1999)** Recruitment of ZipA to the septal ring of *Escherichia coli* is dependent on FtsZ and independent of FtsA. *J Bacteriol*, 181, 167-76.

**Hale, C. A. & De Boer, P. A. (2002)** ZipA is required for recruitment of FtsK, FtsQ, FtsL, and FtsN to the septal ring in *Escherichia coli*. *J Bacteriol*, 184, 2552-6.

**Hale, C. A., Meinhardt, H. & De Boer, P. A. (2001)** Dynamic localization cycle of the cell division regulator MinE in *Escherichia coli*. *EMBO J*, 20, 1563-72.

**Hale, C. A., Rhee, A. C. & De Boer, P. A. (2000)** ZipA-induced bundling of FtsZ polymers mediated by an interaction between C-terminal domains. *J Bacteriol*, 182, 5153-66.

**Hale, C. A., Shiomi, D., Liu, B., Bernhardt, T. G., Margolin, W., Niki, H. & De Boer, P. A. (2011)** Identification of *Escherichia coli* ZapC (YcbW) as a component of the division apparatus that binds and bundles FtsZ polymers. *J Bacteriol*, 193, 1393-404.

**Hamoen, L. W., Meile, J. C., De Jong, W., Noirot, P. & Errington, J. (2006)** SepF, a novel FtsZ-interacting protein required for a late step in cell division. *Mol Microbiol*, 59, 989-99.

- Harris, L. G., Foster, S. J. & Richards, R. G. (2002)** An introduction to *Staphylococcus aureus*, and techniques for identifying and quantifying *S. aureus* adhesins in relation to adhesion to biomaterials: review. *Eur Cell Mater*, 4, 39-60.
- Harry, E. J., Partridge, S. R., Weiss, A. S. & Wake, R. G. (1994)** Conservation of the 168 *divIB* gene in *Bacillus subtilis* W23 and *B. licheniformis*, and evidence for homology to *ftsQ* of *Escherichia coli*. *Gene*, 147, 85-9.
- Harry, E. J., Stewart, B. J. & Wake, R. G. (1993)** Characterization of mutations in *divIB* of *Bacillus subtilis* and cellular localization of the DivIB protein. *Mol Microbiol*, 7, 611-21.
- Harry, E. J. & Wake, R. G. (1989)** Cloning and expression of a *Bacillus subtilis* division initiation gene for which a homolog has not been identified in another organism. *J Bacteriol*, 171, 6835-9.
- Harry, E. J. & Wake, R. G. (1997)** The membrane-bound cell division protein DivIB is localized to the division site in *Bacillus subtilis*. *Mol Microbiol*, 25, 275-83.
- Hayden, M. K., Rezaei, K., Hayes, R. A., Lolans, K., Quinn, J. P. & Weinstein, R. A. (2005)** Development of Daptomycin resistance *in vivo* in methicillin-resistant *Staphylococcus aureus*. *J Clin Microbiol*, 43, 5285-7.
- Haydon, D. J., Stokes, N. R., Ure, R., Galbraith, G., Bennett, J. M., Brown, D. R., Baker, P. J., Barynin, V. V., Rice, D. W., Sedelnikova, S. E., Heal, J. R., Sheridan, J. M., Aiwale, S. T., Chauhan, P. K., Srivastava, A., Taneja, A., Collins, I., Errington, J. & Czaplewski, L. G. (2008)** An inhibitor of FtsZ with potent and selective anti-staphylococcal activity. *Science*, 321, 1673-5.
- Hedge, P. J. & Spratt, B. G. (1985)** Amino acid substitutions that reduce the affinity of penicillin-binding protein 3 of *Escherichia coli* for cephalaxin. *Eur J Biochem*, 151, 111-21.
- Heidrich, C., Templin, M. F., Ursinus, A., Merdanovic, M., Berger, J., Schwarz, H., De Pedro, M. A. & Holtje, J. V. (2001)** Involvement of N-acetylmuramyl-L-alanine amidases in cell separation and antibiotic-induced autolysis of *Escherichia coli*. *Mol Microbiol*, 41, 167-78.
- Heidrich, C., Ursinus, A., Berger, J., Schwarz, H. & Holtje, J. V. (2002)** Effects of multiple deletions of murein hydrolases on viability, septum cleavage, and sensitivity to large toxic molecules in *Escherichia coli*. *J Bacteriol*, 184, 6093-9.
- Hemaiswarya, S., Soudaminikkutty, R., Narasumani, M. L. & Doble, M. (2011)** Phenylpropanoids inhibit protofilament formation of *Escherichia coli* cell division protein FtsZ. *J Med Microbiol*, 60, 1317-25.
- Hennekinne, J. A., De Buyser, M. L. & Dragacci, S. (2012)** *Staphylococcus aureus* and its food poisoning toxins: characterization and outbreak investigation. *FEMS Microbiol Rev*, 36, 815-36.
- Henriques, A. O., Glaser, P., Piggot, P. J. & Moran, C. P., Jr. (1998)** Control of cell shape and elongation by the *rodA* gene in *Bacillus subtilis*. *Mol Microbiol*, 28, 235-47.
- Herbert, S., Bera, A., Nerz, C., Kraus, D., Peschel, A., Goerke, C., Meehl, M., Cheung, A. & Gotz, F. (2007)** Molecular basis of resistance to muramidase and cationic antimicrobial peptide activity of lysozyme in *staphylococci*. *PLoS Pathog*, 3, e102.
- Hett, E. C., Chao, M. C., Deng, L. L. & Rubin, E. J. (2008)** A mycobacterial enzyme essential for cell division synergizes with resuscitation-promoting factor. *PLoS Pathog*, 4, e1000001.
- Hett, E. C., Chao, M. C., Steyn, A. J., Fortune, S. M., Deng, L. L. & Rubin, E. J. (2007)** A partner for the resuscitation-promoting factors of Mycobacterium tuberculosis. *Mol Microbiol*, 66, 658-68.
- Higgins, M. L., Daneo-Moore, L., Boothby, D. & Shockman, G. D. (1974)** Effect of inhibition of deoxyribonucleic acid and protein synthesis on the direction of cell wall growth in *Streptococcus faecalis*. *J Bacteriol*, 118, 681-92.
- Higgins, M. L. & Shockman, G. D. (1970)** Model for cell wall growth of *Streptococcus faecalis*. *J Bacteriol*, 101, 643-8.
- Hilbert, D. W. & Piggot, P. J. (2004)** Compartmentalization of gene expression during *Bacillus subtilis* spore formation. *Microbiol Mol Biol Rev*, 68, 234-62.
- Hill, N. S., Buske, P. J., Shi, Y. & Levin, P. A. (2013)** A moonlighting enzyme links *Escherichia coli* cell size with central metabolism. *PLoS Genet*, 9, e1003663.
- Hiramatsu, K., Aritaka, N., Hanaki, H., Kawasaki, S., Hosoda, Y., Hori, S., Fukuchi, Y. & Kobayashi, I. (1997)** Dissemination in Japanese hospitals of strains of *Staphylococcus aureus* heterogeneously resistant to vancomycin. *Lancet*, 350, 1670-3.
- Hirokawa, T., Boon-Chieng, S. & Mitaku, S. (1998)** SOSUI: classification and secondary structure prediction system for membrane proteins. *Bioinformatics*, 14, 378-9.
- Holtje, J. V. (1995)** From growth to autolysis: the murein hydrolases in *Escherichia coli*. *Arch Microbiol*, 164, 243-54.
- Holtje, J. V. (1998)** Growth of the stress-bearing and shape-maintaining murein sacculus of *Escherichia coli*. *Microbiol Mol Biol Rev*, 62, 181-203.
- Hope, R., Mushtaq, S., James, D., Pillana, T., Warner, M. & Livermore, D. M. (2010)** Tigecycline activity: low resistance rates but problematic disc breakpoints revealed by a multicentre sentinel survey in the UK. *J Antimicrob Chemother*, 65, 2602-9.

- Horsburgh, M. J., Aish, J. L., White, I. J., Shaw, L., Lithgow, J. K., and Foster, S. J. (2002).  $\sigma^B$  modulates virulence determinant expression and stress resistance: characterization of a functional *rsbU* strain derived from *Staphylococcus aureus* 8325-4. *J Bacteriol*, 184, 5457-67.
- Horsburgh, G. J., Atrih, A., Williamson, M. P. & Foster, S. J. (2003) LytG of *Bacillus subtilis* is a novel peptidoglycan hydrolase: the major active glucosaminidase. *Biochemistry*, 42, 257-64.
- Howard, S. P., Gebhart, C., Langen, G. R., Li, G. & Strozen, T. G. (2006) Interactions between peptidoglycan and the ExeAB complex during assembly of the type II secretin of *Aeromonas hydrophila*. *Mol Microbiol*, 59, 1062-72.
- Howell, E. R. & Phillips, C. M. (2007) Cutaneous manifestations of *Staphylococcus aureus* disease. *Skinmed*, 6, 274-9.
- Hsieh, C. W., Lin, T. Y., Lai, H. M., Lin, C. C., Hsieh, T. S. & Shih, Y. L. (2010) Direct MinE-membrane interaction contributes to the proper localization of MinDE in *E. coli*. *Mol Microbiol*, 75, 499-512.
- Hu, D. L., Omoe, K., Shimoda, Y., Nakane, A. & Shinagawa, K. (2003) Induction of emetic response to staphylococcal enterotoxins in the house musk shrew (*Suncus murinus*). *Infect Immun*, 71, 567-70.
- Hu, Z., Gogol, E. P. & Lutkenhaus, J. (2002) Dynamic assembly of MinD on phospholipid vesicles regulated by ATP and MinE. *Proc Natl Acad Sci U S A*, 99, 6761-6.
- Hu, Z. & Lutkenhaus, J. (1999) Topological regulation of cell division in *Escherichia coli* involves rapid pole to pole oscillation of the division inhibitor MinC under the control of MinD and MinE. *Mol Microbiol*, 34, 82-90.
- Hu, Z. & Lutkenhaus, J. (2000) Analysis of MinC reveals two independent domains involved in interaction with MinD and FtsZ. *J Bacteriol*, 182, 3965-71.
- Hu, Z., Mukherjee, A., Pichoff, S. & Lutkenhaus, J. (1999) The MinC component of the division site selection system in *Escherichia coli* interacts with FtsZ to prevent polymerization. *Proc Natl Acad Sci U S A*, 96, 14819-24.
- Huang, W. M., Libbey, J. L., van der hoeven, P., Yu, S. X. (1998). Bipolar localization of *Bacillus subtilis* topoisomerase IV, an enzyme required for chromosome segregation. *Proc Natl Acad Sci U S A*, 95, 4652-57.
- Huard, C., Miranda, G., Redko, Y., Wessner, F., Foster, S. J. & Chapot-Chartier, M. P. (2004) Analysis of the peptidoglycan hydrolase complement of *Lactococcus lactis*: identification of a third N-acetylglucosaminidase, AcmC. *Appl Environ Microbiol*, 70, 3493-9.
- Hunt, A., Rawlins, J. P., Thomaidis, H. B., and Errington, J. (2006). Functional analysis of 11 putative essential genes in *Bacillus subtilis*. *Microbiology*, 152, 2895-907.
- Ikeda, M., Sato, T., Wachi, M., Jung, H. K., Ishino, F., Kobayashi, Y. & Matsushashi, M. (1989) Structural similarity among *Escherichia coli* FtsW and RodA proteins and *Bacillus subtilis* SpoVE protein, which function in cell division, cell elongation, and spore formation, respectively. *J Bacteriol*, 171, 6375-8.
- Inoue, A., Murata, Y., Takahashi, H., Tsuji, N., Fujisaki, S. & Kato, J. (2008) Involvement of an essential gene, *mviN*, in murein synthesis in *Escherichia coli*. *J Bacteriol*, 190, 7298-301.
- Ishikawa, S., Kawai, Y., Hiramatsu, K., Kuwano, M. & Ogasawara, N. (2006) A new FtsZ-interacting protein, YlmF, complements the activity of FtsA during progression of cell division in *Bacillus subtilis*. *Mol Microbiol*, 60, 1364-80.
- Ishino, F., Jung, H. K., Ikeda, M., Doi, M., Wachi, M. & Matsushashi, M. (1989) New mutations *fts-36*, *fts-33*, and *ftsW* clustered in the *mra* region of the *Escherichia coli* chromosome induce thermosensitive cell growth and division. *J Bacteriol*, 171, 5523-30.
- Ishino, F., Park, W., Tomioka, S., Tamaki, S., Takase, I., Kunugita, K., Matsuzawa, H., Asoh, S., Ohta, T., Spratt, B. G. & Et Al. (1986) Peptidoglycan synthetic activities in membranes of *Escherichia coli* caused by overproduction of penicillin-binding protein 2 and rodA protein. *J Biol Chem*, 261, 7024-31.
- Ito, H., Ura, A., Oyamada, Y., Tanitame, A., Yoshida, H., Yamada, S., Wachi, M. & Yamagishi, J. (2006) A 4-aminofurazan derivative-A189-inhibits assembly of bacterial cell division protein FtsZ *in vitro* and *in vivo*. *Microbiol Immunol*, 50, 759-64.
- Jacoby, G. A. (2005) Mechanisms of resistance to quinolones. *Clin Infect Dis*, 41 Suppl 2, S120-6.
- Jaiswal, R., Beuria, T. K., Mohan, R., Mahajan, S. K. & Panda, D. (2007) Totarol inhibits bacterial cytokinesis by perturbing the assembly dynamics of FtsZ. *Biochemistry*, 46, 4211-20.
- Jana, M., Luong, T. T., Komatsuzawa, H., Shigeta, M. & Lee, C. Y. (2000) A method for demonstrating gene essentiality in *Staphylococcus aureus*. *Plasmid*, 44, 100-4.
- Jennings, L. D., Foreman, K. W., Rush, T. S., 3rd, Tsao, D. H., Mosyak, L., Kincaid, S. L., Sukhdeo, M. N., Sutherland, A. G., Ding, W., Kenny, C. H., Sabus, C. L., Liu, H., Dushin, E. G., Moghazeh, S. L., Labthavikul, P., Petersen, P. J., Tuckman, M., Haney, S. A. & Ruzin, A. V. (2004a) Combinatorial synthesis of substituted 3-(2-indolyl)piperidines and 2-phenyl indoles as inhibitors of ZipA-FtsZ interaction. *Bioorg Med Chem*, 12, 5115-31.



Jennings, L. D., Foreman, K. W., Rush, T. S., 3rd, Tsao, D. H., Mosyak, L., Li, Y., Sukhdeo, M. N., Ding, W., Dushin, E. G., Kenny, C. H., Moghazeh, S. L., Petersen, P. J., Ruzin, A. V., Tuckman, M. & Sutherland, A. G. (2004b) Design and synthesis of indolo[2,3-a]quinolizin-7-one inhibitors of the ZipA-FtsZ interaction. *Bioorg Med Chem Lett*, 14, 1427-31.

Jevons, M. P. (1961) "Celbemom"-resistant staphylococci. *Br Med J*, 1, 113-4.

Jevons, M. P., Coe, A. W. & Parker, M. T. (1963) Methicillin resistance in *staphylococci*. *Lancet*, 1, 904-7.

Jones, G. & Dyson, P. (2006) Evolution of transmembrane protein kinases implicated in coordinating remodeling of gram-positive peptidoglycan: inside versus outside. *J Bacteriol*, 188, 7470-6.

Jones, L. J., Carballido-Lopez, R. & Errington, J. (2001) Control of cell shape in bacteria: helical, actin-like filaments in *Bacillus subtilis*. *Cell*, 104, 913-22.

Jorge, A. M., Hoicyk, E., Gomes, J. P. & Pinho, M. G. (2011) EzrA contributes to the regulation of cell size in *Staphylococcus aureus*. *PLoS One*, 6, e27542.

Kaatz, G. W. & Seo, S. M. (1997) Mechanisms of fluoroquinolone resistance in genetically related strains of *Staphylococcus aureus*. *Antimicrob Agents Chemother*, 41, 2733-7.

Kabli, A. F. (2009) *Staphylococcus aureus* cell division-Drugs for bugs, MSc Thesis. University of Sheffield.

Kaltwasser, M., Wiegert, T. & Schumann, W. (2002) Construction and application of epitope- and green fluorescent protein-tagging integration vectors for *Bacillus subtilis*. *Appl Environ Microbiol*, 68, 2624-8.

Kamasaki, T., Osumi, M. & Mabuchi, I. (2007) Three-dimensional arrangement of F-actin in the contractile ring of fission yeast. *J Cell Biol*, 178, 765-71.

Karimova, G., Dautin, N. & Ladant, D. (2005) Interaction network among *Escherichia coli* membrane proteins involved in cell division as revealed by bacterial two-hybrid analysis. *J Bacteriol*, 187, 2233-43.

Katis, V. L., Harry, E. J. & Wake, R. G. (1997) The *Bacillus subtilis* division protein DivIC is a highly abundant membrane-bound protein that localizes to the division site. *Mol Microbiol*, 26, 1047-55.

Katis, V. L. & Wake, R. G. (1999) Membrane-bound division proteins DivIB and DivIC of *Bacillus subtilis* function solely through their external domains in both vegetative and sporulation division. *J Bacteriol*, 181, 2710-8.

Katis, V. L., Wake, R. G. & Harry, E. J. (2000) Septal localization of the membrane-bound division proteins of *Bacillus subtilis* DivIB and DivIC is codependent only at high temperatures and requires FtsZ. *J Bacteriol*, 182, 3607-11.

Kawai, Y., Daniel, R. A. & Errington, J. (2009) Regulation of cell wall morphogenesis in *Bacillus subtilis* by recruitment of PBP1 to the MreB helix. *Mol Microbiol*, 71, 1131-44.

Kawai, Y. & Ogasawara, N. (2006) *Bacillus subtilis* EzrA and FtsL synergistically regulate FtsZ ring dynamics during cell division. *Microbiology*, 152, 1129-41.

Kempf, M. J. & McBride, M. J. (2000) Transposon insertions in the *Flavobacterium johnsoniae* *ftsX* gene disrupt gliding motility and cell division. *J Bacteriol*, 182, 1671-9.

Kent, V. L. (2013) Cell wall architecture and the role of wall teichoic acid in *Staphylococcus aureus*, PhD Thesis. University of Sheffield.

Kern, T., Hediger, S., Muller, P., Giustini, C., Joris, B., Bougault, C., Vollmer, W. & Simorre, J. P. (2008) Toward the characterization of peptidoglycan structure and protein-peptidoglycan interactions by solid-state NMR spectroscopy. *J Am Chem Soc*, 130, 5618-9.

Khaliq, Y. & Zhanel, G. G. (2003) Fluoroquinolone-associated tendinopathy: a critical review of the literature. *Clin Infect Dis*, 36, 1404-10.

Khattar, M. M., Addinall, S. G., Stedul, K. H., Boyle, D. S., Lutkenhaus, J. & Donachie, W. D. (1997) Two polypeptide products of the *Escherichia coli* cell division gene *ftsW* and a possible role for FtsW in FtsZ function. *J Bacteriol*, 179, 784-93.

Kishii, K., Chiba, N., Morozumi, M., Hamano-Hasegawa, K., Kurokawa, I., Masaki, J. & Ubukata, K. (2010) Diverse mutations in the *ftsI* gene in ampicillin-resistant *Haemophilus influenzae* isolates from pediatric patients with acute otitis media. *J Infect Chemother*, 16, 87-93.

Kitano, K. & Tomasz, A. (1979) Triggering of autolytic cell wall degradation in *Escherichia coli* by beta-lactam antibiotics. *Antimicrob Agents Chemother*, 16, 838-48.

Kleiner, D. E. & Stetler-Stevenson, W. G. (1994) Quantitative zymography: detection of picogram quantities of gelatinases. *Anal Biochem*, 218, 325-9.

Kobayashi, K., Ehrlich, S. D., Albertini, A., Amati, G., Andersen, K. K., Arnaud, M., Asai, K., Ashikaga, S., Aymerich, S., Bessieres, P., Boland, F., Brignell, S. C., Bron, S., Bunai, K., Chapuis, J., Christiansen, L. C., Danchin, A., Debarbouille, M., Dervyn, E., Deuerling, E., Devine, K., Devine, S. K., Dreesen, O., Errington, J., Fillinger, S., Foster, S. J., Fujita, Y., Galizzi, A., Gardan, R., Eschevins, C., Fukushima, T., Haga, K., Harwood, C. R., Hecker, M., Hosoya, D., Hullo, M. F., Kakeshita, H., Karamata, D., Kasahara, Y., Kawamura, F., Koga, K., Koski, P., Kuwana, R., Imamura, D., Ishimaru, M., Ishikawa, S., Ishio, I., Le Coq, D., Masson, A., Mael, C., Meima, R., Mellado, R. P., Moir, A., Moriya, S., Nagakawa, E., Nanamiya, H., Nakai, S., Nygaard, P., Ogura,

- M., Ohanan, T., O'reilly, M., O'rourke, M., Pragai, Z., Pooley, H. M., Rapoport, G., Rawlins, J. P., Rivas, L. A., Rivolta, C., Sadaie, A., Sadaie, Y., Sarvas, M., Sato, T., Saxild, H. H., Scanlan, E., Schumann, W., Seegers, J. F., Sekiguchi, J., Sekowska, A., Seror, S. J., Simon, M., Stragier, P., Studer, R., Takamatsu, H., Tanaka, T., Takeuchi, M., Thomaides, H. B., Vagner, V., Van Dijl, J. M., Watabe, K., Wipat, A., Yamamoto, H., Yamamoto, M., Yamamoto, Y., Yamane, K., Yata, K., Yoshida, K., Yoshikawa, H., Zuber, U. & Ogasawara, N. (2003) Essential *Bacillus subtilis* genes. *Proc Natl Acad Sci U S A*, 100, 4678-83.
- Koksharova, O. A. & Wolk, C. P. (2002) A novel gene that bears a DnaJ motif influences cyanobacterial cell division. *J Bacteriol*, 184, 5524-8.
- Kosoy, M., Morway, C., Sheff, K. W., Bai, Y., Colborn, J., Chalcraft, L., Dowell, S. F., Peruski, L. F., Maloney, S. A., Baggett, H., Sutthirattana, S., Sidhirat, A., Maruyama, S., Kabeya, H., Chomel, B. B., Kasten, R., Popov, V., Robinson, J., Kruglov, A. & Petersen, L. R. (2008) *Bartonella tamiae* sp. nov., a newly recognized pathogen isolated from three human patients from Thailand. *J Clin Microbiol*, 46, 772-5.
- Kreis, C. A., Raschke, M. J., Rosslenbroich, S. B., Tholema-Hans, N., Löffler, B. & Fuchs, T. (2013) Therapy of intracellular *Staphylococcus aureus* by tigecyclin. *BMC Infect Dis*, 13, 267.
- Kruse, T., Bork-Jensen, J. & Gerdes, K. (2005) The morphogenetic MreBCD proteins of *Escherichia coli* form an essential membrane-bound complex. *Mol Microbiol*, 55, 78-89.
- Kumar, J. K. (2008) Lysostaphin: an antistaphylococcal agent. *Appl Microbiol Biotechnol*, 80, 555-61.
- Kumar, K., Awasthi, D., Berger, W. T., Tonge, P. J., Slayden, R. A. & Ojima, I. (2010) Discovery of anti-TB agents that target the cell-division protein FtsZ. *Future Med Chem*, 2, 1305-23.
- Kuru, E., Hughes, H. V., Brown, P. J., Hall, E., Tekkam, S., Cava, F., De Pedro, M. A., Brun, Y. V. & Vannieuwenhze, M. S. (2012) In Situ probing of newly synthesized peptidoglycan in live bacteria with fluorescent D-amino acids. *Angew Chem Int Ed Engl*, 51, 12519-23.
- Lacey, R. W. (1975) Antibiotic resistance plasmids of *Staphylococcus aureus* and their clinical importance. *Bacteriol Rev*, 39, 1-32.
- Lackner, L. L., Raskin, D. M. & De Boer, P. A. (2003) ATP-dependent interactions between *Escherichia coli* Min proteins and the phospholipid membrane in vitro. *J Bacteriol*, 185, 735-49.
- Lan, G., Daniels, B. R., Dobrowsky, T. M., Wirtz, D. & Sun, S. X. (2009) Condensation of FtsZ filaments can drive bacterial cell division. *Proc Natl Acad Sci U S A*, 106, 121-6.
- Lappchen, T., Hartog, A. F., Pinas, V. A., Koomen, G. J. & Den Blaauwen, T. (2005) GTP analogue inhibits polymerization and GTPase activity of the bacterial protein FtsZ without affecting its eukaryotic homologue tubulin. *Biochemistry*, 44, 7879-84.
- Lara, B. & Ayala, J. A. (2002) Topological characterization of the essential *Escherichia coli* cell division protein FtsW. *FEMS Microbiol Lett*, 216, 23-32.
- Lara, B., Rico, A. I., Petruzzelli, S., Santona, A., Dumas, J., Biton, J., Vicente, M., Mingorance, J. & Massidda, O. (2005) Cell division in cocci: localization and properties of the *Streptococcus pneumoniae* FtsA protein. *Mol Microbiol*, 55, 699-711.
- Layec, S., Gerard, J., Legue, V., Chapot-Chartier, M. P., Courtin, P., Borges, F., Decaris, B. & Leblond-Bourget, N. (2009) The CHAP domain of Cse functions as an endopeptidase that acts at mature septa to promote *Streptococcus thermophilus* cell separation. *Mol Microbiol*, 71, 1205-17.
- Lazarevic, V. & Karamata, D. (1995) The *tagGH* operon of *Bacillus subtilis* 168 encodes a two-component ABC transporter involved in the metabolism of two wall teichoic acids. *Mol Microbiol*, 16, 345-55.
- Le Gouellec, A., Roux, L., Fadda, D., Massidda, O., Vernet, T. & Zapun, A. (2008) Roles of pneumococcal DivIB in cell division. *J Bacteriol*, 190, 4501-11.
- Le Marechal, C., Jardin, J., Jan, G., Even, S., Pulido, C., Guibert, J. M., Hernandez, D., Francois, P., Schrenzel, J., Demon, D., Meyer, E., Berkova, N., Thiery, R., Vautor, E. & Le Loir, Y. (2011) *Staphylococcus aureus* seroproteomes discriminate ruminant isolates causing mild or severe mastitis. *Vet Res*, 42, 35.
- Leaver, M., Dominguez-Cuevas, P., Coxhead, J. M., Daniel, R. A. & Errington, J. (2009) Life without a wall or division machine in *Bacillus subtilis*. *Nature*, 457, 849-53.
- Leaver, M. & Errington, J. (2005) Roles for MreC and MreD proteins in helical growth of the cylindrical cell wall in *Bacillus subtilis*. *Mol Microbiol*, 57, 1196-209.
- Leclercq, R., Derlot, E., Duval, J. & Courvalin, P. (1988) Plasmid-mediated resistance to vancomycin and teicoplanin in *Enterococcus faecium*. *N Engl J Med*, 319, 157-61.
- Lee, C. Y., Buranen, S. L. & Ye, Z. H. (1991) Construction of single-copy integration vectors for *Staphylococcus aureus*. *Gene*, 103, 101-5.
- Lee, J. C. & Stewart, G. C. (2003) Essential nature of the *mreC* determinant of *Bacillus subtilis*. *J Bacteriol*, 185, 4490-8.
- Lenarcic, R., Halbedel, S., Visser, L., Shaw, M., Wu, L. J., Errington, J., Marenduzzo, D. & Hamoen, L. W. (2009) Localisation of DivIVA by targeting to negatively curved membranes. *EMBO J*, 28, 2272-82.

- Levin, P. A., Kurtser, I. G. & Grossman, A. D. (1999)** Identification and characterization of a negative regulator of FtsZ ring formation in *Bacillus subtilis*. *Proc Natl Acad Sci U S A*, 96, 9642-7.
- Levin, P. A. & Losick, R. (1994)** Characterization of a cell division gene from *Bacillus subtilis* that is required for vegetative and sporulation septum formation. *J Bacteriol*, 176, 1451-9.
- Levin, P. A. & Losick, R. (1996)** Transcription factor Spo0A switches the localization of the cell division protein FtsZ from a medial to a bipolar pattern in *Bacillus subtilis*. *Genes Dev*, 10, 478-88.
- Levin, P. A., Margolis, P. S., Setlow, P., Losick, R. & Sun, D. (1992)** Identification of *Bacillus subtilis* genes for septum placement and shape determination. *J Bacteriol*, 174, 6717-28.
- Li, G. & Howard, S. P. (2010)** ExeA binds to peptidoglycan and forms a multimer for assembly of the type II secretion apparatus in *Aeromonas hydrophila*. *Mol Microbiol*, 76, 772-81.
- Li, M. Z. & Elledge, S. J. (2007)** Harnessing homologous recombination in vitro to generate recombinant DNA via SLIC. *Nat Methods*, 4, 251-6.
- Li, Z., Trimble, M. J., Brun, Y. V. & Jensen, G. J. (2007)** The structure of FtsZ filaments *in vivo* suggests a force-generating role in cell division. *EMBO J*, 26, 4694-708.
- Liew, A. T., Theis, T., Jensen, S. O., Garcia-Lara, J., Foster, S. J., Firth, N., Lewis, P. J. & Harry, E. J. (2010)** A simple plasmid-based system that allows rapid generation of tightly controlled gene expression in *Staphylococcus aureus*. *Microbiology*, 157, 666-76.
- Lim, D. & Strynadka, N. C. (2002)** Structural basis for the beta lactam resistance of PBP2a from methicillin-resistant *Staphylococcus aureus*. *Nat Struct Biol*, 9, 870-6.
- Lleo, M. M., Canepari, P. & Satta, G. (1990)** Bacterial cell shape regulation: testing of additional predictions unique to the two-competing-sites model for peptidoglycan assembly and isolation of conditional rod-shaped mutants from some wild-type cocci. *J Bacteriol*, 172, 3758-71.
- Low, H. H., Moncrieffe, M. C. & Lowe, J. (2004)** The crystal structure of ZapA and its modulation of FtsZ polymerisation. *J Mol Biol*, 341, 839-52.
- Lowe, J. (1998)** Crystal structure determination of FtsZ from *Methanococcus jannaschii*. *J Struct Biol*, 124, 235-43.
- Lowe, J. & Amos, L. A. (1998)** Crystal structure of the bacterial cell-division protein FtsZ. *Nature*, 391, 203-6.
- Lowy, F. D. (1998)** *Staphylococcus aureus* infections. *N Engl J Med*, 339, 520-32.
- Lu, M. & Kleckner, N. (1994)** Molecular cloning and characterization of the *pgm* gene encoding phosphoglucomutase of *Escherichia coli*. *J Bacteriol*, 176, 5847-51.
- Lucet, I., Feucht, A., Yudkin, M. D. & Errington, J. (2000)** Direct interaction between the cell division protein FtsZ and the cell differentiation protein SpoIIIE. *EMBO J*, 19, 1467-75.
- Ludwig, W., Schleifer, K. H. & Whitman, W. B. (2009)** Revised road map to phylum firmicutes. In De Vos, G., Garrity, G., Jones, D., Krieg, N. R., Ludwig, W., Rainey, F. A., Schleifer, K. H. & Whitman, W. B. (Eds.) *Bergey's manual of systematic bacteriology*. 2nd ed. New York, Springer-Verlag.
- Luft, J. R., Collins, R. J., Fehrman, N. A., Lauricella, A. M., Veatch, C. K. & Defitta, G. T. (2003)** A deliberate approach to screening for initial crystallization conditions of biological macromolecules. *J Struct Biol*, 142, 170-9.
- Lupas, A. (1997)** Predicting coiled-coil regions in proteins. *Curr Opin Struct Biol*, 7, 388-93.
- Lutkenhaus, J. (1997)** Bacterial cytokinesis: let the light shine in. *Curr Biol*, 7, R573-5.
- Lutkenhaus, J. & Addinall, S. G. (1997)** Bacterial cell division and the Z ring. *Annu Rev Biochem*, 66, 93-116.
- Lutkenhaus, J., Pichoff, S. & Du, S. (2012)** Bacterial cytokinesis: From Z ring to divisome. *Cytoskeleton (Hoboken)*, 69, 778-90.
- Lutkenhaus, J. F., Wolf-Watz, H. & Donachie, W. D. (1980)** Organization of genes in the *ftsA-envA* region of the *Escherichia coli* genetic map and identification of a new *fts* locus (*ftsZ*). *J Bacteriol*, 142, 615-20.
- Ma, L., King, G. F. & Rothfield, L. (2004)** Positioning of the MinE binding site on the MinD surface suggests a plausible mechanism for activation of the *Escherichia coli* MinD ATPase during division site selection. *Mol Microbiol*, 54, 99-108.
- Ma, X., Ehrhardt, D. W. & Margolin, W. (1996)** Colocalization of cell division proteins FtsZ and FtsA to cytoskeletal structures in living *Escherichia coli* cells by using green fluorescent protein. *Proc Natl Acad Sci U S A*, 93, 12998-3003.
- Madigan, M. T. & Martinko, J. M. (2006)** *Brock Biology of Microorganism* United State of America, Pearson Prentice Hall. Pearson Education Inc.
- Maggi, S., Massidda, O., Luzzi, G., Fadda, D., Paolozzi, L. & Ghelardini, P. (2008)** Division protein interaction web: identification of a phylogenetically conserved common interactome between *Streptococcus pneumoniae* and *Escherichia coli*. *Microbiology*, 154, 3042-52.
- Maguin, E., Duwat, P., Hege, T., Ehrlich, D. & Gruss, A. (1992)** New thermosensitive plasmid for gram-positive bacteria. *J Bacteriol*, 174, 5633-8.

- Maira-Litran, T., Kropec, A., Goldmann, D. A. & Pier, G. B. (2005)** Comparative opsonic and protective activities of *Staphylococcus aureus* conjugate vaccines containing native or deacetylated Staphylococcal Poly-N-acetyl-beta-(1-6)-glucosamine. *Infect Immun*, 73, 6752-62.
- Malbrunyn, B., Canu, A., Bozdogan, B., Fantin, B., Zarrouk, V., Dutka-Malen, S., Feger, C. & Leclercq, R. (2002)** Resistance to quinupristin-dalfopristin due to mutation of L22 ribosomal protein in *Staphylococcus aureus*. *Antimicrob Agents Chemother*, 46, 2200-7.
- Mangili, A., Bica, I., Snyderman, D. R. & Hamer, D. H. (2005)** Daptomycin-resistant, methicillin-resistant *Staphylococcus aureus* bacteremia. *Clin Infect Dis*, 40, 1058-60.
- Mani, N., Tobin, P. & Jayaswal, R. K. (1993)** Isolation and characterization of autolysis-defective mutants of *Staphylococcus aureus* created by Tn917-lacZ mutagenesis. *J Bacteriol*, 175, 1493-9.
- Marbouty, M., Mazouni, K., Saguez, C., Cassier-Chauvat, C. & Chauvat, F. (2009)** Characterization of the *Synechocystis* strain PCC 6803 penicillin-binding proteins and cytokinetic proteins FtsQ and FtsW and their network of interactions with ZipN. *J Bacteriol*, 191, 5123-33.
- Margolin, W. (2000)** Themes and variations in prokaryotic cell division. *FEMS Microbiol Rev*, 24, 531-48.
- Margolin, W. (2001)** Spatial regulation of cytokinesis in bacteria. *Curr Opin Microbiol*, 4, 647-52.
- Marrec-Fairley, M., Piette, A., Gallet, X., Brasseur, R., Hara, H., Fraipont, C., Ghuysen, J. M. & Nguyen-Disteche, M. (2000)** Differential functionalities of amphiphilic peptide segments of the cell-separation penicillin-binding protein 3 of *Escherichia coli*. *Mol Microbiol*, 37, 1019-31.
- Marston, A. L., Thomaides, H. B., Edwards, D. H., Sharpe, M. E. & Errington, J. (1998)** Polar localization of the MinD protein of *Bacillus subtilis* and its role in selection of the mid-cell division site. *Genes Dev*, 12, 3419-30.
- Masson, S., Kern, T., Le Gouellec, A., Giustini, C., Simorre, J. P., Callow, P., Vernet, T., Gabel, F. & Zapun, A. (2009)** Central domain of DivIB caps the C-terminal regions of the FtsL/DivIC coiled-coil rod. *J Biol Chem*, 284, 27687-700.
- Matias, V. R. & Beveridge, T. J. (2005)** Cryo-electron microscopy reveals native polymeric cell wall structure in *Bacillus subtilis* 168 and the existence of a periplasmic space. *Mol Microbiol*, 56, 240-51.
- Matsukawa, M., Kunishima, Y., Takahashi, S., Takeyama, K. & Tsukamoto, T. (2001)** *Staphylococcus aureus* bacteriuria and surgical site infections by methicillin-resistant *Staphylococcus aureus*. *Int J Antimicrob Agents*, 17, 327-9, discussion 329-30.
- Matsuzawa, H., Hayakawa, K., Sato, T. & Imahori, K. (1973)** Characterization and genetic analysis of a mutant of *Escherichia coli* K-12 with rounded morphology. *J Bacteriol*, 115, 436-42.
- Mazouni, K., Domain, F., Cassier-Chauvat, C. & Chauvat, F. (2004)** Molecular analysis of the key cytokinetic components of cyanobacteria: FtsZ, ZipN and MinCDE. *Mol Microbiol*, 52, 1145-58.
- Mcdevitt, D., Payne, D. J., Holmes, D. J. & Rosenberg, M. (2002)** Novel targets for the future development of antibacterial agents. *Symp Ser Soc Appl Microbiol*, 28S-34S.
- McLean, C. L. & Ness, M. G. (2008)** Methicillin-resistant *Staphylococcus aureus* in a veterinary orthopaedic referral hospital: staff nasal colonisation and incidence of clinical cases. *J Small Anim Pract*, 49, 170-7.
- Mcpherson, D. C., Driks, A. & Popham, D. L. (2001)** Two class A high-molecular-weight penicillin-binding proteins of *Bacillus subtilis* play redundant roles in sporulation. *J Bacteriol*, 183, 6046-53.
- Meinhardt, H. & De Boer, P. A. (2001)** Pattern formation in *Escherichia coli*: a model for the pole-to-pole oscillations of Min proteins and the localization of the division site. *Proc Natl Acad Sci U S A*, 98, 14202-7.
- Mellroth, P., Daniels, R., Eberhardt, A., Ronnlund, D., Blom, H., Widengren, J., Normark, S. & Henriques-Normark, B. (2012)** LytA, major autolysin of *Streptococcus pneumoniae*, requires access to nascent peptidoglycan. *J Biol Chem*, 287, 11018-29.
- Memmi, G., Filipe, S. R., Pinho, M. G., Fu, Z. & Cheung, A. (2008)** *Staphylococcus aureus* PBP4 is essential for beta-lactam resistance in community-acquired methicillin-resistant strains. *Antimicrob Agents Chemother*, 52, 3955-66.
- Mendelson, N. H. & Cole, R. M. (1972)** Genetic regulation of cell division initiation in *Bacillus subtilis*. *J Bacteriol*, 112, 994-1003.
- Mengin-Lecreulx, D., Van Heijenoort, J. & Park, J. T. (1996)** Identification of the mpl gene encoding UDP-N-acetylmuramate: L-alanyl-gamma-D-glutamyl-meso-diaminopimelate ligase in *Escherichia coli* and its role in recycling of cell wall peptidoglycan. *J Bacteriol*, 178, 5347-52.
- Mercer, K. L. & Weiss, D. S. (2002)** The *Escherichia coli* cell division protein FtsW is required to recruit its cognate transpeptidase, FtsI (PBP3), to the division site. *J Bacteriol*, 184, 904-12.
- Merino, S., Altarriba, M., Gavin, R., Izquierdo, L. & Tomas, J. M. (2001)** The cell division genes (*ftsE* and *X*) of *Aeromonas hydrophila* and their relationship with opsonophagocytosis. *FEMS Microbiol Lett*, 198, 183-8.
- Meroueh, S. O., Minasov, G., Lee, W., Shoichet, B. K. & Mobashery, S. (2003)** Structural aspects for evolution of beta-lactamases from penicillin-binding proteins. *J Am Chem Soc*, 125, 9612-8.

- Migocki, M. D., Freeman, M. K., Wake, R. G. & Harry, E. J. (2002)** The Min system is not required for precise placement of the midcell Z ring in *Bacillus subtilis*. *EMBO Rep*, 3, 1163-7.
- Mingorance, J., Tadros, M., Vicente, M., Gonzalez, J. M., Rivas, G. & Velez, M. (2005)** Visualization of single *Escherichia coli* FtsZ filament dynamics with atomic force microscopy. *J Biol Chem*, 280, 20909-14.
- Mir, M. A., Rajeswari, H. S., Veeraraghavan, U. & Ajitkumar, P. (2006)** Molecular characterisation of ABC transporter type FtsE and FtsX proteins of *Mycobacterium tuberculosis*. *Arch Microbiol*, 185, 147-58.
- Mishima, M., Shida, T., Yabuki, K., Kato, K., Sekiguchi, J. & Kojima, C. (2005)** Solution structure of the peptidoglycan binding domain of *Bacillus subtilis* cell wall lytic enzyme CwIC: characterization of the sporulation-related repeats by NMR. *Biochemistry*, 44, 10153-63.
- Mohammadi, T., Karczmarek, A., Crouvoisier, M., Bouhss, A., Mengin-Lecreux, D. & Den Blaauwen, T. (2007)** The essential peptidoglycan glycosyltransferase MurG forms a complex with proteins involved in lateral envelope growth as well as with proteins involved in cell division in *Escherichia coli*. *Mol Microbiol*, 65, 1106-21.
- Mohammadi, T., Van Dam, V., Sijbrandi, R., Vernet, T., Zapun, A., Bouhss, A., Diepeveen-De Bruin, M., Nguyen-Disteche, M., De Kruijff, B. & Breukink, E. (2011)** Identification of FtsW as a transporter of lipid-linked cell wall precursors across the membrane. *EMBO J*, 30, 1425-32.
- Moll, A., Schlimpert, S., Briegel, A., Jensen, G. J. & Thanbichler, M. (2010)** DipM, a new factor required for peptidoglycan remodelling during cell division in *Caulobacter crescentus*. *Mol Microbiol*, 77, 90-107.
- Moll, A. & Thanbichler, M. (2009)** FtsN-like proteins are conserved components of the cell division machinery in proteobacteria. *Mol Microbiol*, 72, 1037-53.
- Momynaliev, K. T., Smirnova, O. V., Lazyrev, V. N., Akopian, T. A., Chelysheva, V. V., Ayala, J. A., Simankova, A. N., Borchsenius, S. N. & Govorun, V. M. (2002)** Characterization of the *Mycoplasma hominis* *ftsZ* gene and its sequence variability in mycoplasma clinical isolates. *Biochem Biophys Res Commun*, 293, 155-62.
- Monahan, L. G., Robinson, A. & Harry, E. J. (2009)** Lateral FtsZ association and the assembly of the cytokinetic Z ring in bacteria. *Mol Microbiol*, 74, 1004-17.
- Monk, I. R. & Foster, T. J. (2012)** Genetic manipulation of *Staphylococci*-breaking through the barrier. *Front Cell Infect Microbiol*, 2, 49.
- Monk, I. R., Shah, I. M., Xu, M., Tan, M. W. & Foster, T. J. (2012)** Transforming the untransformable: application of direct transformation to manipulate genetically *Staphylococcus aureus* and *Staphylococcus epidermidis*. *MBio*, 3.
- Moriyama, R., Kudoh, S., Miyata, S., Nonobe, S., Hattori, A. & Makino, S. (1996)** A germination-specific spore cortex-lytic enzyme from *Bacillus cereus* spores: cloning and sequencing of the gene and molecular characterization of the enzyme. *J Bacteriol*, 178, 5330-2.
- Morlot, C., Noirclerc-Savoye, M., Zapun, A., Dideberg, O. & Vernet, T. (2004)** The D,D-carboxypeptidase PBP3 organizes the division process of *Streptococcus pneumoniae*. *Mol Microbiol*, 51, 1641-8.
- Morlot, C., Uehara, T., Marquis, K. A., Bernhardt, T. G. & Rudner, D. Z. (2010)** A highly coordinated cell wall degradation machine governs spore morphogenesis in *Bacillus subtilis*. *Genes Dev*, 24, 411-22.
- Morlot, C., Zapun, A., Dideberg, O. & Vernet, T. (2003)** Growth and division of *Streptococcus pneumoniae*: localization of the high molecular weight penicillin-binding proteins during the cell cycle. *Mol Microbiol*, 50, 845-55.
- Mosyak, L., Zhang, Y., Glasfeld, E., Haney, S., Stahl, M., Seehra, J. & Somers, W. S. (2000)** The bacterial cell-division protein ZipA and its interaction with an FtsZ fragment revealed by X-ray crystallography. *EMBO J*, 19, 3179-91.
- Moy, F. J., Glasfeld, E., Mosyak, L. & Powers, R. (2000)** Solution structure of ZipA, a crucial component of *Escherichia coli* cell division. *Biochemistry*, 39, 9146-56.
- Mukherjee, A. & Lutkenhaus, J. (1998)** Dynamic assembly of FtsZ regulated by GTP hydrolysis. *EMBO J*, 17, 462-9.
- Mulder, E. & Woldringh, C. L. (1989)** Actively replicating nucleoids influence positioning of division sites in *Escherichia coli* filaments forming cells lacking DNA. *J Bacteriol*, 171, 4303-14.
- Muller, P., Ewers, C., Bertsche, U., Anstett, M., Kallis, T., Breukink, E., Fraipont, C., Terrak, M., Nguyen-Disteche, M. & Vollmer, W. (2007)** The essential cell division protein FtsN interacts with the murein (peptidoglycan) synthase PBP1B in *Escherichia coli*. *J Biol Chem*, 282, 36394-402.
- Munoz-Bellido, J. L., Alonzo Manzanares, M., Martinez Andres, J. A., Gutierrez Zufiaurre, M. N., Ortiz, G., Segovia Hernandez, M. & Garcia-Rodriguez, J. A. (1999)** Efflux pump-mediated quinolone resistance in *Staphylococcus aureus* strains wild type for *gyrA*, *gyrB*, *glaA*, and *norA*. *Antimicrob Agents Chemother*, 43, 354-6.

- Murray, R. G., Hall, M. & Thompson, B. G. (1983)** Cell division in *Deinococcus radiodurans* and a method for displaying septa. *Can J Microbiol*, 29, 1412-23.
- Murray, T., Popham, D. L., and Setlow, P. (1997)**. Identification and characterization of *pbpA* encoding *Bacillus subtilis* penicillin-binding protein 2A, *J Bacteriol*, 179, 3021-9.
- Murray, T., Popham, D. L., Setlow, P. (1998)** *Bacillus subtilis* cells lacking penicillin-binding protein 1 require increased levels of divalent cations. *J Bacteriol*, 180, 4555-63.
- Nagai, K., Davies, T. A., Jacobs, M. R. & Appelbaum, P. C. (2002)** Effects of amino acid alterations in penicillin-binding proteins (PBPs) 1a, 2b, and 2x on PBP affinities of penicillin, ampicillin, amoxicillin, cefditoren, cefuroxime, cefprozil, and cefaclor in 18 clinical isolates of penicillin-susceptible, -intermediate, and -resistant *pneumococci*. *Antimicrob Agents Chemother*, 46, 1273-80.
- Naidoo, J. & Noble, W. C. (1978)** Transfer of gentamicin resistance between strains of *Staphylococcus aureus* on skin. *J Gen Microbiol*, 107, 391-3.
- Nanninga, N. (1998) Morphogenesis of *Escherichia coli*. *Microbiol Mol Biol Rev*, 62, 110-29.
- Ng, E. Y., Trucksis, M. & Hooper, D. C. (1994)** Quinolone resistance mediated by *norA*: physiologic characterization and relationship to *flqB*, a quinolone resistance locus on the *Staphylococcus aureus* chromosome. *Antimicrob Agents Chemother*, 38, 1345-55.
- Ng, J. D., Lorber, B., Witz, J., Theobald-Dietrich, A., Kern, D. & Giege, R. (1996)** The crystallization of biological macromolecules from precipitates: evidence for Ostwald ripening. *Journal of Crystal Growth*, 168, 50-62.
- Ng, W. L., Kazmierczak, K. M. & Winkler, M. E. (2004)** Defective cell wall synthesis in *Streptococcus pneumoniae* R6 depleted for the essential PcsB putative murein hydrolase or the VicR (YycF) response regulator. *Mol Microbiol*, 53, 1161-75.
- Niba, E. T., Li, G., Aoki, K. & Kitakawa, M. (2010)** Characterization of *rodZ* mutants: RodZ is not absolutely required for the cell shape and motility. *FEMS Microbiol Lett*, 309, 35-42.
- Nikolaichik, Y. A. & Donachie, W. D. (2000)** Conservation of gene order amongst cell wall and cell division genes in Eubacteria, and ribosomal genes in Eubacteria and Eukaryotic organelles. *Genetica*, 108, 1-7.
- Nilsson, I. M., Verdrengh, M., Ulrich, R. G., Bavari, S. & Tarkowski, A. (1999)** Protection against *Staphylococcus aureus* sepsis by vaccination with recombinant staphylococcal enterotoxin A devoid of superantigenicity. *J Infect Dis*, 180, 1370-3.
- Niu, L. & Yu, J. (2008)** Investigating intracellular dynamics of FtsZ cytoskeleton with photoactivation single-molecule tracking. *Biophys J*, 95, 2009-16.
- Nogales, E., Downing, K. H., Amos, L. A. & Lowe, J. (1998)** Tubulin and FtsZ form a distinct family of GTPases. *Nat Struct Biol*, 5, 451-8.
- Noirclerc-Savoie, M., Lantez, V., Signor, L., Philippe, J., Vernet, T. & Zapun, A. (2013)** Reconstitution of membrane protein complexes involved in pneumococcal septal cell wall assembly. *PLoS One*, 8, e75522.
- Noirclerc-Savoie, M., Le Gouellec, A., Morlot, C., Dideberg, O., Vernet, T. & Zapun, A. (2005)** In vitro reconstitution of a trimeric complex of DivIB, DivIC and FtsL, and their transient co-localization at the division site in *Streptococcus pneumoniae*. *Mol Microbiol*, 55, 413-24.
- Nolan, R. D. & Hildebrandt, J. F. (1979)** Comparison of the penicillin-binding proteins of different strains of *Neisseria gonorrhoeae*. *Antimicrob Agents Chemother*, 16, 336-40.
- Normark, S. (1969)** Mutation in *Escherichia coli* K-12 mediating spherelike envelopes and changes tolerance to ultraviolet irradiation and some antibiotics. *J Bacteriol*, 98, 1274-7.
- Novick, R. P. (1991)** Genetic systems in *staphylococci*. *Methods Enzymol*, 204, 587-636.
- Ohashi, Y., Chijiwa, Y., Suzuki, K., Takahashi, K., Nanamiya, H., Sato, T., Hosoya, Y., Ochi, K. & Kawamura, F. (1999)** The lethal effect of a benzamide derivative, 3-methoxybenzamide, can be suppressed by mutations within a cell division gene, *ftsZ*, in *Bacillus subtilis*. *J Bacteriol*, 181, 1348-51.
- Olijhoek, A. J., Klencke, S., Pas, E., Nanninga, N. & Schwarz, U. (1982)** Volume growth, murein synthesis, and murein cross-linkage during the division cycle of *Escherichia coli* PA3092. *J Bacteriol*, 152, 1248-54.
- Osawa, M. & Erickson, H. P. (2006)** FtsZ from divergent foreign bacteria can function for cell division in *Escherichia coli*. *J Bacteriol*, 188, 7132-40.
- Osteryoung, K. W., Stokes, K. D., Rutherford, S. M., Percival, A. L. & Lee, W. Y. (1998)** Chloroplast division in higher plants requires members of two functionally divergent gene families with homology to bacterial *ftsZ*. *Plant Cell*, 10, 1991-2004.
- Otto, M. (2010)** Novel targeted immunotherapy approaches for staphylococcal infection. *Expert Opin Biol Ther*, 10, 1049-59.
- Palomeque-Messia, P., Englebort, S., Leyh-Bouille, M., Nguyen-Disteche, M., Duez, C., Houba, S., Dideberg, O., Van Beeumen, J. & Ghuyssen, J. M. (1991)** Amino acid sequence of the penicillin-binding protein/DD-peptidase of *Streptomyces* K15. Predicted secondary structures of the low Mr penicillin-binding proteins of class A. *Biochem J*, 279 ( Pt 1), 223-30.
- Pankey, G. A. (2005)** Tigecycline. *J Antimicrob Chemother*, 56, 470-80.

**Paradis-Bleau, C., Sanschagrin, F. & Levesque, R. C. (2005)** Peptide inhibitors of the essential cell division protein FtsA. *Protein Eng Des Sel*, 18, 85-91.

**Pares, S., Mouz, N., Petillot, Y., Hakenbeck, R. & Dideberg, O. (1996)** X-ray structure of *Streptococcus pneumoniae* PBP2x, a primary penicillin target enzyme. *Nat Struct Biol*, 3, 284-9.

**Park, Y. S., Grove, C. I., Gonzalez-Lopez, M., Uргаonkar, S., Fettingер, J. C. & Shaw, J. T. (2011)** Synthesis of (-)-viriditoxin: a 6,6'-binaphthopyran-2-one that targets the bacterial cell division protein FtsZ. *Angew Chem Int Ed Engl*, 50, 3730-3.

**Peacock, S. J., De Silva, I. & Lowy, F. D. (2001)** What determines nasal carriage of *Staphylococcus aureus*? *Trends Microbiol*, 9, 605-10.

**Pease, P. J., Levy, O., Cost, G. J., Gore, J., Ptacin, J. L., Sherratt, D., Bustamante, C. & Cozzarelli, N. R. (2005)** Sequence-directed DNA translocation by purified FtsK. *Science*, 307, 586-90.

**Pedersen, L. B., Angert, E. R. & Setlow, P. (1999)** Septal localization of penicillin-binding protein 1 in *Bacillus subtilis*. *J Bacteriol*, 181, 3201-11.

**Pereira, P. M., Filipe, S. R., Tomasz, A. & Pinho, M. G. (2007a)** Fluorescence ratio imaging microscopy shows decreased access of vancomycin to cell wall synthetic sites in vancomycin-resistant *Staphylococcus aureus*. *Antimicrob Agents Chemother*, 51, 3627-33.

**Pereira, P. M., Veiga, H., Jorge, A. M. & Pinho, M. G. (2010)** Fluorescent reporters for studies of cellular localization of proteins in *Staphylococcus aureus*. *Appl Environ Microbiol*, 76, 4346-53.

**Pereira, S. F., Henriques, A. O., Pinho, M. G., De Lencastre, H. & Tomasz, A. (2007b)** Role of PBP1 in cell division of *Staphylococcus aureus*. *J Bacteriol*, 189, 3525-31.

**Pereira, S. F., Henriques, A. O., Pinho, M. G., De Lencastre, H. & Tomasz, A. (2009)** Evidence for a dual role of PBP1 in the cell division and cell separation of *Staphylococcus aureus*. *Mol Microbiol*, 72, 895-904.

**Peters, N. T., Dinh, T. & Bernhardt, T. G. (2011)** A fail-safe mechanism in the septal ring assembly pathway generated by the sequential recruitment of cell separation amidases and their activators. *J Bacteriol*, 193, 4973-83.

**Peters, P. C., Migocki, M. D., Thoni, C. & Harry, E. J. (2007)** A new assembly pathway for the cytokinetic Z ring from a dynamic helical structure in vegetatively growing cells of *Bacillus subtilis*. *Mol Microbiol*, 64, 487-99.

**Petersen, P. J., Jacobus, N. V., Weiss, W. J., Sum, P. E. & Testa, R. T. (1999)** In vitro and in vivo antibacterial activities of a novel glycylicycline, the 9-t-butylglycylamido derivative of minocycline (GAR-936). *Antimicrob Agents Chemother*, 43, 738-44.

**Pfeiffer, C. A., Kirschbaum, A. & Gardner, W. U. (1940)** Relation of Estrogen to Ossification and the Levels of Serum Calcium and Lipoid in the English Sparrow, *Passer Domesticus*. *Yale J Biol Med*, 13, 279-284 2.

**Pichoff, S. & Lutkenhaus, J. (2002)** Unique and overlapping roles for ZipA and FtsA in septal ring assembly in *Escherichia coli*. *EMBO J*, 21, 685-93.

**Pichoff, S. & Lutkenhaus, J. (2005)** Tethering the Z ring to the membrane through a conserved membrane targeting sequence in FtsA. *Mol Microbiol*, 55, 1722-34.

**Pichoff, S. & Lutkenhaus, J. (2007)** Identification of a region of FtsA required for interaction with FtsZ. *Mol Microbiol*, 64, 1129-38.

**Pinho, M. G. & Errington, J. (2003)** Dispersed mode of *Staphylococcus aureus* cell wall synthesis in the absence of the division machinery. *Mol Microbiol*, 50, 871-81.

**Pinho, M. G. & Errington, J. (2004)** A *divIVA* null mutant of *Staphylococcus aureus* undergoes normal cell division. *FEMS Microbiol Lett*, 240, 145-9.

**Pinho, M. G. & Errington, J. (2005)** Recruitment of penicillin-binding protein PBP2 to the division site of *Staphylococcus aureus* is dependent on its transpeptidation substrates. *Mol Microbiol*, 55, 799-807.

**Pinho, M. G., Kjos, M. & Veening, J. W. (2013)** How to get (a)round: mechanisms controlling growth and division of coccoid bacteria. *Nat Rev Microbiol*, 11, 601-14.

**Plaza, A., Keffer, J. L., Bifulco, G., Lloyd, J. R. & Bewley, C. A. (2010)** Chrysosphaentins A-H, antibacterial bisdiarylbutene macrocycles that inhibit the bacterial cell division protein FtsZ. *J Am Chem Soc*, 132, 9069-77.

**Poggio, S., Takacs, C. N., Vollmer, W. & Jacobs-Wagner, C. (2010)** A protein critical for cell constriction in the Gram-negative bacterium *Caulobacter crescentus* localizes at the division site through its peptidoglycan-binding LysM domains. *Mol Microbiol*, 77, 74-89.

**Priyadarshini, R., Popham, D. L. & Young, K. D. (2006)** Daughter cell separation by penicillin-binding proteins and peptidoglycan amidases in *Escherichia coli*. *J Bacteriol*, 188, 5345-55.

**Rai, D., Singh, J. K., Roy, N. & Panda, D. (2008)** Curcumin inhibits FtsZ assembly: an attractive mechanism for its antibacterial activity. *Biochem J*, 410, 147-55.

**Ramirez-Arcos, S., Salimnia, H., Bergevin, I., Paradis, M. & Dillon, J. A. (2001)** Expression of *Neisseria gonorrhoeae* cell division genes *ftsZ*, *ftsE* and *minD* is influenced by environmental conditions. *Res Microbiol*, 152, 781-91.

- Raskin, D. M. & De Boer, P. A. (1999a)** MinDE-dependent pole-to-pole oscillation of division inhibitor MinC in *Escherichia coli*. *J Bacteriol*, 181, 6419-24.
- Raskin, D. M. & De Boer, P. A. (1999b)** Rapid pole-to-pole oscillation of a protein required for directing division to the middle of *Escherichia coli*. *Proc Natl Acad Sci U S A*, 96, 4971-6.
- Raychaudhuri, D. (1999)** ZipA is a MAP-Tau homolog and is essential for structural integrity of the cytokinetic FtsZ ring during bacterial cell division. *EMBO J*, 18, 2372-83.
- Real, G., Fay, A., Eldar, A., Pinto, S. M., Henriques, A. O. & Dworkin, J. (2008)** Determinants for the subcellular localization and function of a nonessential SEDS protein. *J Bacteriol*, 190, 363-76.
- Reddy, M. (2007)** Role of FtsEX in cell division of *Escherichia coli*: viability of *ftsEX* mutants is dependent on functional SufI or high osmotic strength. *J Bacteriol*, 189, 98-108.
- Rice, L. B. (2006)** Antimicrobial resistance in gram-positive bacteria. *Am J Infect Control*, 34, S11-9; discussion S64-73.
- Robichon, C., Karimova, G., Beckwith, J. & Ladant, D. (2011)** Role of leucine zipper motifs in association of the *Escherichia coli* cell division proteins FtsL and FtsB. *J Bacteriol*, 193, 4988-92.
- Robichon, C., King, G. F., Goehring, N. W. & Beckwith, J. (2008)** Artificial septal targeting of *Bacillus subtilis* cell division proteins in *Escherichia coli*: an interspecies approach to the study of protein-protein interactions in multiprotein complexes. *J Bacteriol*, 190, 6048-59.
- Robson, S. A. & King, G. F. (2006)** Domain architecture and structure of the bacterial cell division protein DivIB. *Proc Natl Acad Sci U S A*, 103, 6700-5.
- Robson, S. A., Michie, K. A., Mackay, J. P., Harry, E. & King, G. F. (2002)** The *Bacillus subtilis* cell division proteins FtsL and DivIC are intrinsically unstable and do not interact with one another in the absence of other septosomal components. *Mol Microbiol*, 44, 663-74.
- Rodloff, A. C., Leclercq, R., Debbia, E. A., Canton, R., Oppenheim, B. A. & Dowzicky, M. J. (2008)** Comparative analysis of antimicrobial susceptibility among organisms from France, Germany, Italy, Spain and the UK as part of the tigecycline evaluation and surveillance trial. *Clin Microbiol Infect*, 14, 307-14.
- Roten, C. A., Brandt, C. & Karamata, D. (1991)** Genes involved in meso-diaminopimelate synthesis in *Bacillus subtilis*: identification of the gene encoding aspartokinase I. *J Gen Microbiol*, 137, 951-62.
- Rothfield, L., Justice, S. & Garcia-Lara, J. (1999)** Bacterial cell division. *Annu Rev Genet*, 33, 423-48.
- Rothfield, L., Taghbalout, A. & Shih, Y. L. (2005)** Spatial control of bacterial division-site placement. *Nat Rev Microbiol*, 3, 959-68.
- Rotun, S. S., Mcmath, V., Schoonmaker, D. J., Maupin, P. S., Tenover, F. C., Hill, B. C. & Ackman, D. M. (1999)** *Staphylococcus aureus* with reduced susceptibility to vancomycin isolated from a patient with fatal bacteremia. *Emerg Infect Dis*, 5, 147-9.
- Rouch, D. A., Byrne, M. E., Kong, Y. C. & Skurray, R. A. (1987)** The *aacA-aphD* gentamicin and kanamycin resistance determinant of Tn4001 from *Staphylococcus aureus*: expression and nucleotide sequence analysis. *J Gen Microbiol*, 133, 3039-52.
- Rowland, S. L., Katis, V. L., Partridge, S. R. & Wake, R. G. (1997)** DivIB, FtsZ and cell division in *Bacillus subtilis*. *Mol Microbiol*, 23, 295-302.
- Rowland, S. L., Wadsworth, K. D., Robson, S. A., Robichon, C., Beckwith, J. & King, G. F. (2010)** Evidence from artificial septal targeting and site-directed mutagenesis that residues in the extracytoplasmic beta domain of DivIB mediate its interaction with the divisomal transpeptidase PBP 2B. *J Bacteriol*, 192, 6116-25.
- Ruiz-Avila, L. B., Huecas, S., Artola, M., Vergonos, A., Ramirez-Aportela, E., Cercenado, E., Barasoain, I., Vazquez-Villa, H., Martin-Fontecha, M., Chacon, P., Lopez-Rodriguez, M. L. & Andreu, J. M. (2013)** Synthetic inhibitors of bacterial cell division targeting the GTP-binding site of FtsZ. *ACS Chem Biol*, 8, 2072-83.
- Ruiz, N. (2008)** Bioinformatics identification of MurJ (MviN) as the peptidoglycan lipid II flippase in *Escherichia coli*. *Proc Natl Acad Sci U S A*, 105, 15553-7.
- Saleh, A. Z., Yamanaka, K., Niki, H., Ogura, T., Yamazoe, M. & Hiraga, S. (1996)** Carboxyl terminal region of the MukB protein in *Escherichia coli* is essential for DNA binding activity. *FEMS Microbiol Lett*, 143, 211-6.
- Sambrook, J. & Russell, D. W. (2001)** *Molecular Cloning: A Laboratory Manual*, New York, Cold Spring Harbor Laboratory Press.
- Sanchez, M., Valencia, A., Ferrandiz, M. J., Sander, C. & Vicente, M. (1994)** Correlation between the structure and biochemical activities of FtsA, an essential cell division protein of the actin family. *EMBO J*, 13, 4919-25.
- Santini, C. L., Bernadac, A., Zhang, M., Chanal, A., Ize, B., Blanco, C. & Wu, L. F. (2001)** Translocation of jellyfish green fluorescent protein via the Tat system of *Escherichia coli* and change of its periplasmic localization in response to osmotic up-shock. *J Biol Chem*, 276, 8159-64.
- Sauvage, E., Kerff, F., Terrak, M., Ayala, J. A. & Charlier, P. (2008)** The penicillin-binding proteins: structure and role in peptidoglycan biosynthesis. *FEMS Microbiol Rev*, 32, 234-58.



**Schaffner-Barbero, C., Martin-Fontecha, M., Chacon, P. & Andreu, J. M. (2011)** Targeting the assembly of bacterial cell division protein FtsZ with small molecules. *ACS Chem Biol*, 7, 269-77.

**Scheffers, D. J. (2008)** The effect of MinC on FtsZ polymerization is pH dependent and can be counteracted by ZapA. *FEBS Lett*, 582, 2601-8.

**Scheffers, D. J., De Wit, J. G., Den Blaauwen, T. & Driessen, A. J. (2002)** GTP hydrolysis of cell division protein FtsZ: evidence that the active site is formed by the association of monomers. *Biochemistry*, 41, 521-9.

**Scheffers, D. J. & Errington, J. (2004)** PBP1 is a component of the *Bacillus subtilis* cell division machinery. *J Bacteriol*, 186, 5153-6.

**Scheffers, D. J. & Pinho, M. G. (2005)** Bacterial cell wall synthesis: new insights from localization studies. *Microbiol Mol Biol Rev*, 69, 585-607.

**Scheffers, D. J., Robichon, C., Haan, G. J., Den Blaauwen, T., Koningstein, G., Van Bloois, E., Beckwith, J. & Luirink, J. (2007)** Contribution of the FtsQ transmembrane segment to localization to the cell division site. *J Bacteriol*, 189, 7273-80.

**Schlag, M., Biswas, R., Krismer, B., Kohler, T., Zoll, S., Yu, W., Schwarz, H., Peschel, A. & Gotz, F. (2010)** Role of staphylococcal wall teichoic acid in targeting the major autolysin Atl. *Mol Microbiol*, 75, 864-73.

**Schmidt, K. L., Peterson, N. D., Kustus, R. J., Wissel, M. C., Graham, B., Phillips, G. J. & Weiss, D. S. (2004)** A predicted ABC transporter, FtsEX, is needed for cell division in *Escherichia coli*. *J Bacteriol*, 186, 785-93.

**Schmidt, L. S., Botta, G. & Park, J. T. (1981)** Effects of furazlocillin, a beta-lactam antibiotic which binds selectively to penicillin-binding protein 3, on *Escherichia coli* mutants deficient in other penicillin-binding proteins. *J Bacteriol*, 145, 632-7.

**Schneider, T., Senn, M. M., Berger-Bachi, B., Tossi, A., Sahl, H. G. & Wiedemann, I. (2004)** In vitro assembly of a complete, pentaglycine interpeptide bridge containing cell wall precursor (lipid II-Gly5) of *Staphylococcus aureus*. *Mol Microbiol*, 53, 675-85.

**Scott, J. R. & Barnett, T. C. (2006)** Surface proteins of gram-positive bacteria and how they get there. *Annu Rev Microbiol*, 60, 397-423.

**Sham, L. T., Barendt, S. M., Kopecky, K. E. & Winkler, M. E. (2011)** Essential PcsB putative peptidoglycan hydrolase interacts with the essential FtsXSpn cell division protein in *Streptococcus pneumoniae* D39. *Proc Natl Acad Sci U S A*, 108, E1061-9.

**Sham, L. T., Jensen, K. R., Bruce, K. E. & Winkler, M. E. (2013)** Involvement of FtsE ATPase and FtsX extracellular loops 1 and 2 in FtsEX-PcsB complex function in cell division of *Streptococcus pneumoniae* D39. *MBio*, 4.

**Sharpe, M. E., Hauser, P. M., Sharpe, R. G. & Errington, J. (1998)** *Bacillus subtilis* cell cycle as studied by fluorescence microscopy: constancy of cell length at initiation of DNA replication and evidence for active nucleoid partitioning. *J Bacteriol*, 180, 547-55.

**Shih, Y. L., Le, T. & Rothfield, L. (2003)** Division site selection in *Escherichia coli* involves dynamic redistribution of Min proteins within coiled structures that extend between the two cell poles. *Proc Natl Acad Sci U S A*, 100, 7865-70.

**Shimotohno, K. W., Kawamura, F., Natori, Y., Nanamiya, H., Magae, J., Ogata, H., Endo, T., Suzuki, T. & Yamaki, H. (2010)** Inhibition of septation in *Bacillus subtilis* by a peptide antibiotic, edeine B(1). *Biol Pharm Bull*, 33, 568-71.

**Shiomi, D., Sakai, M. & Niki, H. (2008)** Determination of bacterial rod shape by a novel cytoskeletal membrane protein. *EMBO J*, 27, 3081-91.

**Siddiqui, R. A., Hoischen, C., Holst, O., Heinze, I., Schlott, B., Gumpert, J., Diekmann, S., Grosse, F. & Platzer, M. (2006)** The analysis of cell division and cell wall synthesis genes reveals mutationally inactivated *ftsQ* and *mraY* in a protoplast-type L-form of *Escherichia coli*. *FEMS Microbiol Lett*, 258, 305-11.

**Sievers, J. & Errington, J. (2000a)** Analysis of the essential cell division gene *ftsL* of *Bacillus subtilis* by mutagenesis and heterologous complementation. *J Bacteriol*, 182, 5572-9.

**Sievers, J. & Errington, J. (2000b)** The *Bacillus subtilis* cell division protein FtsL localizes to sites of septation and interacts with DivIC. *Mol Microbiol*, 36, 846-55.

**Sievert, D. M., Rudrik, J. T., Patel, J. B., McDonald, L. C., Wilkins, M. J. & Hageman, J. C. (2008)** Vancomycin-resistant *Staphylococcus aureus* in the United States, 2002-2006. *Clin Infect Dis*, 46, 668-74.

**Silverman, J. A., Perlmutter, N. G. & Shapiro, H. M. (2003)** Correlation of daptomycin bactericidal activity and membrane depolarization in *Staphylococcus aureus*. *Antimicrob Agents Chemother*, 47, 2538-44.

**Singh, J. K., Makde, R. D., Kumar, V. & Panda, D. (2007)** A membrane protein, EzrA, regulates assembly dynamics of FtsZ by interacting with the C-terminal tail of FtsZ. *Biochemistry*, 46, 11013-22.

- Singh, J. K., Makde, R. D., Kumar, V. & Panda, D. (2008)** SepF increases the assembly and bundling of FtsZ polymers and stabilizes FtsZ protofilaments by binding along its length. *J Biol Chem*, 283, 31116-24.
- Skinner, D. & Keefer, C. S. (1941)** Significance of bacteremia caused by *Staphylococcus aureus*. *Arch Intern Med*, 68, 851-75.
- Small, E., Marrington, R., Rodger, A., Scott, D. J., Sloan, K., Roper, D., Dafforn, T. R. & Addinall, S. G. (2007)** FtsZ polymer-bundling by the *Escherichia coli* ZapA orthologue, YgfE, involves a conformational change in bound GTP. *J Mol Biol*, 369, 210-21.
- Smith, E. J., Visai, L., Kerrigan, S. W., Speziale, P. & Foster, T. J. (2011)** The Sbi protein is a multifunctional immune evasion factor of *Staphylococcus aureus*. *Infect Immun*, 79, 3801-9.
- Smith, T. J., Blackman, S. A. & Foster, S. J. (2000)** Autolysins of *Bacillus subtilis*: multiple enzymes with multiple functions. *Microbiology*, 146 ( Pt 2), 249-62.
- Smith, T. L., Pearson, M. L., Wilcox, K. R., Cruz, C., Lancaster, M. V., Robinson-Dunn, B., Tenover, F. C., Zervos, M. J., Band, J. D., White, E. & Jarvis, W. R. (1999)** Emergence of vancomycin resistance in *Staphylococcus aureus*. Glycopeptide-Intermediate *Staphylococcus aureus* Working Group. *N Engl J Med*, 340, 493-501.
- Smyth, M. S. & Martin, J. H. (2000)** x ray crystallography. *Mol Pathol*, 53, 8-14.
- Snowden, M. A. & Perkins, H. R. (1990) Peptidoglycan cross-linking in *Staphylococcus aureus*. An apparent random polymerisation process. *Eur J Biochem*, 191, 373-7.
- Song, J. H., Ko, K. S., Lee, J. Y., Baek, J. Y., Oh, W. S., Yoon, H. S., Jeong, J. Y. & Chun, J. (2005)** Identification of essential genes in *Streptococcus pneumoniae* by allelic replacement mutagenesis. *Mol Cells*, 19, 365-74.
- Spratt, B. G. (1975)** Distinct penicillin binding proteins involved in the division, elongation, and shape of *Escherichia coli* K12. *Proc Natl Acad Sci U S A*, 72, 2999-3003.
- Spratt, B. G. (1977)** Temperature-sensitive cell division mutants of *Escherichia coli* with thermolabile penicillin-binding proteins. *J Bacteriol*, 131, 293-305.
- Steele, V. R., Bottomley, A. L., Garcia-Lara, J., Kasturiarachchi, J. & Foster, S. J. (2011)** Multiple essential roles for EzrA in cell division of *Staphylococcus aureus*. *Mol Microbiol*, 80, 542-55.
- Stefanova, M. E., Tomberg, J., Davies, C., Nicholas, R. A. & Gutheil, W. G. (2004)** Overexpression and enzymatic characterization of *Neisseria gonorrhoeae* penicillin-binding protein 4. *Eur J Biochem*, 271, 23-32.
- Stevens, R. C. (2000)** High-throughput protein crystallization. *Curr Opin Struct Biol*, 10, 558-63.
- Storrs, M. J., Courvalin, P. & Foster, T. J. (1988)** Genetic analysis of gentamicin resistance in methicillin- and gentamicin-resistant strains of *Staphylococcus aureus* isolated in Dublin hospitals. *Antimicrob Agents Chemother*, 32, 1174-81.
- Stranger-Jones, Y. K., Bae, T. & Schneewind, O. (2006)** Vaccine assembly from surface proteins of *Staphylococcus aureus*. *Proc Natl Acad Sci U S A*, 103, 16942-7.
- Strauss, M. P., Liew, A. T., Turnbull, L., Whitchurch, C. B., Monahan, L. G. & Harry, E. J. (2012)** 3D-SIM super resolution microscopy reveals a bead-like arrangement for FtsZ and the division machinery: implications for triggering cytokinesis. *PLoS Biol*, 10, e1001389.
- Stricker, J., Maddox, P., Salmon, E. D. & Erickson, H. P. (2002)** Rapid assembly dynamics of the *Escherichia coli* FtsZ-ring demonstrated by fluorescence recovery after photobleaching. *Proc Natl Acad Sci U S A*, 99, 3171-5.
- Studier, F. W. & Moffatt, B. A. (1986)** Use of bacteriophage T7 RNA polymerase to direct selective high-level expression of cloned genes. *J Mol Biol*, 189, 113-30.
- Suefuji, K., Valluzzi, R. & Raychaudhuri, D. (2002)** Dynamic assembly of MinD into filament bundles modulated by ATP, phospholipids, and MinE. *Proc Natl Acad Sci U S A*, 99, 16776-81.
- Sun, Q. & Margolin, W. (1998)** FtsZ dynamics during the division cycle of live *Escherichia coli* cells. *J Bacteriol*, 180, 2050-6.
- Sutherland, A. G., Alvarez, J., Ding, W., Foreman, K. W., Kenny, C. H., Labthavikul, P., Mosyak, L., Petersen, P. J., Rush, T. S., 3rd, Ruzin, A., Tsao, D. H. & Wheless, K. L. (2003)** Structure-based design of carboxyphenylindole inhibitors of the ZipA-FtsZ interaction. *Org Biomol Chem*, 1, 4138-40.
- Swoboda, J. G., Meredith, T. C., Campbell, J., Brown, S., Suzuki, T., Bollenbach, T., Malhowski, A. J., Kishony, R., Gilmore, M. S. & Walker, S. (2009)** Discovery of small molecule that blocks wall teichoic acid biosynthesis in *staphylococcus aureus*. *ACS Chem Biol*, 4, 875-83.
- Tally, F. P., Zeckel, M., Wasilewski, M. M., Carini, C., Berman, C. L., Drusano, G. L. & Oleson, F. B., Jr. (1999)** Daptomycin: a novel agent for Gram-positive infections. *Expert Opin Investig Drugs*, 8, 1223-38.
- Tamaki, S., Matsuzawa, H. & Matsubashi, M. (1980)** Cluster of mrdA and mrdB genes responsible for the rod shape and mecillinam sensitivity of *Escherichia coli*. *J Bacteriol*, 141, 52-7.
- Tan, X. X., Rose, K., Margolin, W. & Chen, Y. (2004)** DNA enzyme generated by a novel single-stranded DNA expression vector inhibits expression of the essential bacterial cell division gene ftsZ. *Biochemistry*, 43, 1111-7.

- Taschner, P. E., Verest, J. G. & Woldringh, C. L. (1987)** Genetic and morphological characterization of *ftsB* and *nrdB* mutants of *Escherichia coli*. *J Bacteriol*, 169, 19-25.
- Tavares, J. R., De Souza, R. F., Meira, G. L. & Gueiros-Filho, F. J. (2008)** Cytological characterization of YpsB, a novel component of the *Bacillus subtilis* divisome. *J Bacteriol*, 190, 7096-107.
- Thanedar, S. & Margolin, W. (2004)** FtsZ exhibits rapid movement and oscillation waves in helix-like patterns in *Escherichia coli*. *Curr Biol*, 14, 1167-73.
- Thibessard, A., Fernandez, A., Gintz, B., Leblond-Bourget, N. & Decaris, B. (2002)** Effects of *rodA* and *pbp2b* disruption on cell morphology and oxidative stress response of *Streptococcus thermophilus* CNRZ368. *J Bacteriol*, 184, 2821-6.
- Thomas, J. D., Daniel, R. A., Errington, J. & Robinson, C. (2001)** Export of active green fluorescent protein to the periplasm by the twin-arginine translocase (Tat) pathway in *Escherichia coli*. *Mol Microbiol*, 39, 47-53.
- Thompson, L. S., Beech, P. L., Real, G., Henriques, A. O. & Harry, E. J. (2006)** Requirement for the cell division protein DivIB in polar cell division and engulfment during sporulation in *Bacillus subtilis*. *J Bacteriol*, 188, 7677-85.
- Tiyanont, K., Doan, T., Lazarus, M. B., Fang, X., Rudner, D. Z. & Walker, S. (2006)** Imaging peptidoglycan biosynthesis in *Bacillus subtilis* with fluorescent antibiotics. *Proc Natl Acad Sci U S A*, 103, 11033-8.
- Tokunaga, H., Arakawa, T. & Tokunaga, M. (2008)** Engineering of halophilic enzymes: two acidic amino acid residues at the carboxy-terminal region confer halophilic characteristics to *Halomonas* and *Pseudomonas* nucleoside diphosphate kinases. *Protein Sci*, 17, 1603-10.
- Toledo-Arana, A., Merino, N., Vergara-Irigaray, M., Debarbouille, M., Penades, J. R. & Lasa, I. (2005)** *Staphylococcus aureus* develops an alternative, ica-independent biofilm in the absence of the arlRS two-component system. *J Bacteriol*, 187, 5318-29.
- Tomasz, A., Jamieson, J. D. & Ottolenghi, E. (1964)** The Fine Structure of *Diplococcus Pneumoniae*. *J Cell Biol*, 22, 453-67.
- Tonthat, N. K., Arold, S. T., Pickering, B. F., Van Dyke, M. W., Liang, S., Lu, Y., Beuria, T. K., Margolin, W. & Schumacher, M. A. (2011)** Molecular mechanism by which the nucleoid occlusion factor, SlmA, keeps cytokinesis in check. *EMBO J*, 30, 154-64.
- Toro, E. & Shapiro, L. (2010)** Bacterial chromosome organization and segregation. *Cold Spring Harb Perspect Biol*, 2, a000349.
- Tropsha, A., Bowen, J. P., Brown, F. K. & Kizer, J. S. (1991)** Do interhelical side chain-backbone hydrogen bonds participate in formation of leucine zipper coiled coils? *Proc Natl Acad Sci U S A*, 88, 9488-92.
- Tsiodras, S., Gold, H. S., Sakoulas, G., Eliopoulos, G. M., Wennersten, C., Venkataraman, L., Moellering, R. C. & Ferraro, M. J. (2001)** Linezolid resistance in a clinical isolate of *Staphylococcus aureus*. *Lancet*, 358, 207-8.
- Turner, R. D., Hurd, A. F., Cadby, A., Hobbs, J. K. & Foster, S. J. (2013)** Cell wall elongation mode in Gram-negative bacteria is determined by peptidoglycan architecture. *Nat Commun*, 4, 1496.
- Turner, R. D., Ratcliffe, E. C., Wheeler, R., Golestanian, R., Hobbs, J. K. & Foster, S. J. (2010)** Peptidoglycan architecture can specify division planes in *Staphylococcus aureus*. *Nat Commun*, 1, 26.
- Typas, A., Banzhaf, M., Gross, C. A. & Vollmer, W. (2011)** From the regulation of peptidoglycan synthesis to bacterial growth and morphology. *Nat Rev Microbiol*, 10, 123-36.
- Tzagoloff, H. & Novick, R. (1977)** Geometry of cell division in *Staphylococcus aureus*. *J Bacteriol*, 129, 343-50.
- Uehara, T. & Bernhardt, T. G. (2011)** More than just lysins: peptidoglycan hydrolases tailor the cell wall. *Curr Opin Microbiol*, 14, 698-703.
- Uehara, T., Dinh, T. & Bernhardt, T. G. (2009)** LytM-domain factors are required for daughter cell separation and rapid ampicillin-induced lysis in *Escherichia coli*. *J Bacteriol*, 191, 5094-107.
- Uehara, T., Parzych, K. R., Dinh, T. & Bernhardt, T. G. (2010)** Daughter cell separation is controlled by cytokinetic ring-activated cell wall hydrolysis. *EMBO J*, 29, 1412-22.
- Ueki, M., Wachi, M., Jung, H. K., Ishino, F. & Matsuhashi, M. (1992)** *Escherichia coli mraR* gene involved in cell growth and division. *J Bacteriol*, 174, 7841-3.
- Uhlen, M., Guss, B., Nilsson, B., Gotz, F. & Lindberg, M. (1984)** Expression of the gene encoding protein A in *Staphylococcus aureus* and coagulase-negative staphylococci. *J Bacteriol*, 159, 713-9.
- Ursinus, A., Van Den Ent, F., Brechtel, S., De Pedro, M., Holtje, J. V., Lowe, J. & Vollmer, W. (2004)** Murein (peptidoglycan) binding property of the essential cell division protein FtsN from *Escherichia coli*. *J Bacteriol*, 186, 6728-37.
- Uttley, A. H., Collins, C. H., Naidoo, J. & George, R. C. (1988)** Vancomycin-resistant enterococci. *Lancet*, 1, 57-8.
- Vagner, V., Dervyn, E. & Ehrlich, S. D. (1998)** A vector for systematic gene inactivation in *Bacillus subtilis*. *Microbiology*, 144 ( Pt 11), 3097-104.

- Valle, J., Toledo-Arana, A., Berasain, C., Ghigo, J. M., Amorena, B., Penades, J. R. & Lasa, I. (2003) SarA and not sigmaB is essential for biofilm development by *Staphylococcus aureus*. *Mol Microbiol*, 48, 1075-87.
- Van Den Ent, F., Amos, L. A. & Lowe, J. (2001) Prokaryotic origin of the actin cytoskeleton. *Nature*, 413, 39-44.
- Van Den Ent, F., Johnson, C. M., Persons, L., De Boer, P. & Lowe, J. (2010) Bacterial actin MreB assembles in complex with cell shape protein RodZ. *EMBO J*, 29, 1081-90.
- Van Den Ent, F., Leaver, M., Bendezu, F., Errington, J., De Boer, P. & Lowe, J. (2006) Dimeric structure of the cell shape protein MreC and its functional implications. *Mol Microbiol*, 62, 1631-42.
- Van Den Ent, F. & Lowe, J. (2000) Crystal structure of the cell division protein FtsA from *Thermotoga maritima*. *EMBO J*, 19, 5300-7.
- Van Den Ent, F., Vinkenvleugel, T. M., Ind, A., West, P., Veprintsev, D., Nanninga, N., Den Blaauwen, T. & Lowe, J. (2008) Structural and mutational analysis of the cell division protein FtsQ. *Mol Microbiol*, 68, 110-23.
- Van Der Linden, M. P., De Haan, L., Dideberg, O. & Keck, W. (1994) Site-directed mutagenesis of proposed active-site residues of penicillin-binding protein 5 from *Escherichia coli*. *Biochem J*, 303 ( Pt 2), 357-62.
- Varley, A. W. & Stewart, G. C. (1992) The *divIVB* region of the *Bacillus subtilis* chromosome encodes homologs of *Escherichia coli* septum placement (*minCD*) and cell shape (*mreBCD*) determinants. *J Bacteriol*, 174, 6729-42.
- Varma, A., De Pedro, M. A. & Young, K. D. (2007) FtsZ directs a second mode of peptidoglycan synthesis in *Escherichia coli*. *J Bacteriol*, 189, 5692-704.
- Vaughan, S., Wickstead, B., Gull, K. & Addinall, S. G. (2004) Molecular evolution of FtsZ protein sequences encoded within the genomes of archaea, bacteria, and eukaryota. *J Mol Evol*, 58, 19-29.
- Veiga, H., Jorge, A. M. & Pinho, M. G. (2011) Absence of nucleoid occlusion effector Noc impairs formation of orthogonal FtsZ rings during *Staphylococcus aureus* cell division. *Mol Microbiol*, 80, 1366-80.
- Vergara-Irigaray, M., Maira-Litran, T., Merino, N., Pier, G. B., Penades, J. R. & Lasa, I. (2008) Wall teichoic acids are dispensable for anchoring the PNAG exopolysaccharide to the *Staphylococcus aureus* cell surface. *Microbiology*, 154, 865-77.
- Verkade, E. J., Verhulst, C. J., Huijsdens, X. W. & Kluytmans, J. A. (2010) *In vitro* activity of tigecycline against methicillin-resistant *Staphylococcus aureus*, including livestock-associated strains. *Eur J Clin Microbiol Infect Dis*, 29, 503-7.
- Vicente, M. & Rico, A. I. (2006) The order of the ring: assembly of *Escherichia coli* cell division components. *Mol Microbiol*, 61, 5-8.
- Vieira, J. & Messing, J. (1982) The pUC plasmids, an M13mp7-derived system for insertion mutagenesis and sequencing with synthetic universal primers. *Gene*, 19, 259-68.
- Villanelo, F., Ordenes, A., Brunet, J., Lagos, R. & Monasterio, O. (2011) A model for the *Escherichia coli* FtsB/FtsL/FtsQ cell division complex. *BMC Struct Biol*, 11, 28.
- Vincent, T. L., Green, P. J. & Woolfson, D. N. (2013) LOGICOIL--multi-state prediction of coiled-coil oligomeric state. *Bioinformatics*, 29, 69-76.
- Vollmer, W. (2008) Structural variation in the glycan strands of bacterial peptidoglycan. *FEMS Microbiol Rev*, 32, 287-306.
- Von Kockritz-Blickwede, M., Rohde, M., Oehmcke, S., Miller, L. S., Cheung, A. L., Herwald, H., Foster, S. & Medina, E. (2008) Immunological mechanisms underlying the genetic predisposition to severe *Staphylococcus aureus* infection in the mouse model. *Am J Pathol*, 173, 1657-68.
- Wachi, M., Doi, M., Okada, Y. & Matsushashi, M. (1989) New *mre* genes *mreC* and *mreD*, responsible for formation of the rod shape of *Escherichia coli* cells. *J Bacteriol*, 171, 6511-6.
- Wachi, M., Doi, M., Tamaki, S., Park, W., Nakajima-Iijima, S. & Matsushashi, M. (1987) Mutant isolation and molecular cloning of *mre* genes, which determine cell shape, sensitivity to mecillinam, and amount of penicillin-binding proteins in *Escherichia coli*. *J Bacteriol*, 169, 4935-40.
- Wadenpohl, I. & Bramkamp, M. (2010) DivIC stabilizes FtsL against RasP cleavage. *J Bacteriol*, 192, 5260-3.
- Wadsworth, K. D., Rowland, S. L., Harry, E. J. & King, G. F. (2008) The divisomal protein DivIB contains multiple epitopes that mediate its recruitment to incipient division sites. *Mol Microbiol*, 67, 1143-55.
- Wallace, A. C., Laskowski, R. A. & Thornton, J. M. (1996) Derivation of 3D coordinate templates for searching structural databases: application to Ser-His-Asp catalytic triads in the serine proteinases and lipases. *Protein Sci*, 5, 1001-13.
- Wang, J., Galgoci, A., Kodali, S., Herath, K. B., Jayasuriya, H., Dorso, K., Vicente, F., Gonzalez, A., Cully, D., Bramhill, D. & Singh, S. (2003) Discovery of a small molecule that inhibits cell division by blocking FtsZ, a novel therapeutic target of antibiotics. *J Biol Chem*, 278, 44424-8.

- Wang, J. D. & Levin, P. A. (2009)** Metabolism, cell growth and the bacterial cell cycle. *Nat Rev Microbiol*, 7, 822-7.
- Wang, L., Khattar, M. K., Donachie, W. D. & Lutkenhaus, J. (1998)** FtsI and FtsW are localized to the septum in *Escherichia coli*. *J Bacteriol*, 180, 2810-6.
- Wang, X., Huang, J., Mukherjee, A., Cao, C. & Lutkenhaus, J. (1997)** Analysis of the interaction of FtsZ with itself, GTP, and FtsA. *J Bacteriol*, 179, 5551-9.
- Wang, X. & Lutkenhaus, J. (1996)** FtsZ ring: the eubacterial division apparatus conserved in archaeobacteria. *Mol Microbiol*, 21, 313-9.
- Weart, R. B., Lee, A. H., Chien, A. C., Haeusser, D. P., Hill, N. S. & Levin, P. A. (2007)** A metabolic sensor governing cell size in bacteria. *Cell*, 130, 335-47.
- Weart, R. B. & Levin, P. A. (2003)** Growth rate-dependent regulation of medial FtsZ ring formation. *J Bacteriol*, 185, 2826-34.
- Wei, Y., Havasy, T., Mcpherson, D. C. & Popham, D. L. (2003)** Rod shape determination by the *Bacillus subtilis* class B penicillin-binding proteins encoded by *pbpA* and *pbpH*. *J Bacteriol*, 185, 4717-26.
- Weigel, L. M., Clewell, D. B., Gill, S. R., Clark, N. C., McDougal, L. K., Flannagan, S. E., Kolonay, J. F., Shetty, J., Killgore, G. E. & Tenover, F. C. (2003)** Genetic analysis of a high-level vancomycin-resistant isolate of *Staphylococcus aureus*. *Science*, 302, 1569-71.
- Weiss, D. S. (2004)** Bacterial cell division and the septal ring. *Mol Microbiol*, 54, 588-97.
- Weiss, D. S., Chen, J. C., Ghigo, J. M., Boyd, D. & Beckwith, J. (1999)** Localization of FtsI (PBP3) to the septal ring requires its membrane anchor, the Z ring, FtsA, FtsQ, and FtsL. *J Bacteriol*, 181, 508-20.
- Weiss, D. S., Pogliano, K., Carson, M., Guzman, L. M., Fraipont, C., Nguyen-Disteche, M., Losick, R. & Beckwith, J. (1997)** Localization of the *Escherichia coli* cell division protein FtsI (PBP3) to the division site and cell pole. *Mol Microbiol*, 25, 671-81.
- Werner, G., Cuny, C., Schmitz, F. J. & Witte, W. (2001)** Methicillin-resistant, quinupristin-dalfopristin-resistant *Staphylococcus aureus* with reduced sensitivity to glycopeptides. *J Clin Microbiol*, 39, 3586-90.
- Wheeler, R. (2012)** Peptidoglycan architecture and dynamics in Gram-positive bacteria, PhD thesis. University of Sheffield.
- White, C. L., Kitich, A. & Gober, J. W. (2010)** Positioning cell wall synthetic complexes by the bacterial morphogenetic proteins MreB and MreD. *Mol Microbiol*, 76, 616-33.
- Wilke, M. S., Lovering, A. L. & Strynadka, N. C. (2005)** Beta-lactam antibiotic resistance: a current structural perspective. *Curr Opin Microbiol*, 8, 525-33.
- Wissel, M. C. & Weiss, D. S. (2004)** Genetic analysis of the cell division protein FtsI (PBP3): amino acid substitutions that impair septal localization of FtsI and recruitment of FtsN. *J Bacteriol*, 186, 490-502.
- Witte, W., Bräulke, C. & Strommenger, B. (2008)** Community-associated methicillin-resistant *Staphylococcus aureus* ST8 ("USA300") in an HIV-positive patient in Cologne, Germany, February 2008. *Euro Surveill*, 13.
- Woldringh, C. L., Mulder, E., Valkenburg, J. A., Wientjes, F. B., Zaritsky, A. & Nanninga, N. (1990)** Role of the nucleoid in the toporegulation of division. *Res Microbiol*, 141, 39-49.
- Wright, C. L., Byrne, M. E., Firth, N. & Skurray, R. A. (1998)** A retrospective molecular analysis of gentamicin resistance in *Staphylococcus aureus* strains from UK hospitals. *J Med Microbiol*, 47, 173-8.
- Wu, L. J. & Errington, J. (2004)** Coordination of cell division and chromosome segregation by a nucleoid occlusion protein in *Bacillus subtilis*. *Cell*, 117, 915-25.
- Wu, L. J. & Errington, J. (2011)** Nucleoid occlusion and bacterial cell division. *Nat Rev Microbiol*, 10, 8-12.
- Wu, L. J., Ishikawa, S., Kawai, Y., Oshima, T., Ogasawara, N. & Errington, J. (2009)** Noc protein binds to specific DNA sequences to coordinate cell division with chromosome segregation. *EMBO J*, 28, 1940-52.
- Yamada, S., Sugai, M., Komatsuzawa, H., Nakashima, S., Oshida, T., Matsumoto, A. & Suginaka, H. (1996)** An autolysin ring associated with cell separation of *Staphylococcus aureus*. *J Bacteriol*, 178, 1565-71.
- Yang, D. C., Peters, N. T., Parzych, K. R., Uehara, T., Markovski, M. & Bernhardt, T. G. (2011)** An ATP-binding cassette transporter-like complex governs cell-wall hydrolysis at the bacterial cytokinetic ring. *Proc Natl Acad Sci U S A*, 108, E1052-60.
- Yang, D. C., Tan, K., Joachimiak, A. & Bernhardt, T. G. (2012)** A conformational switch controls cell wall-remodelling enzymes required for bacterial cell division. *Mol Microbiol*, 85, 768-81.
- Yang, J. C., Van Den Ent, F., Neuhaus, D., Brevier, J. & Lowe, J. (2004)** Solution structure and domain architecture of the divisome protein FtsN. *Mol Microbiol*, 52, 651-60.
- Yanouri, A., Daniel, R. A., Errington, J. & Buchanan, C. E. (1993)** Cloning and sequencing of the cell division gene *pbpB*, which encodes penicillin-binding protein 2B in *Bacillus subtilis*. *J Bacteriol*, 175, 7604-16.

- Yansura, D. G. & Henner, D. J. (1984)** Use of the *Escherichia coli lac* repressor and operator to control gene expression in *Bacillus subtilis*. *Proc Natl Acad Sci U S A*, 81, 439-43.
- Yeats, C., Finn, R. D. & Bateman, A. (2002)** The PASTA domain: a beta-lactam-binding domain. *Trends Biochem Sci*, 27, 438.
- Yokogawa, K., Kawata, S., Nishimura, S., Ikeda, Y. & Yoshimura, Y. (1974)** Mutanolysin, bacteriolytic agent for cariogenic *Streptococci*: partial purification and properties. *Antimicrob Agents Chemother*, 6, 156-65.
- Yu, X. C. & Margolin, W. (1999)** FtsZ ring clusters in min and partition mutants: role of both the Min system and the nucleoid in regulating FtsZ ring localization. *Mol Microbiol*, 32, 315-26.
- Yu, X. C., Weihe, E. K. & Margolin, W. (1998)** Role of the C terminus of FtsK in *Escherichia coli* chromosome segregation. *J Bacteriol*, 180, 6424-8.
- Zapun, A., Vernet, T. & Pinho, M. G. (2008)** The different shapes of cocci. *FEMS Microbiol Rev*, 32, 345-60.
- Zhang, L., Fan, F., Palmer, L. M., Lonetto, M. A., Petit, C., Voelker, L. L., St John, A., Bankosky, B., Rosenberg, M. & Mcdevitt, D. (2000)** Regulated gene expression in *Staphylococcus aureus* for identifying conditional lethal phenotypes and antibiotic mode of action. *Gene*, 255, 297-305.
- Zhang, L., Jacobsson, K., Vasi, J., Lindberg, M. & Frykberg, L. (1998)** A second IgG-binding protein in *Staphylococcus aureus*. *Microbiology*, 144 ( Pt 4), 985-91.
- Zhou, R., Chen, S. & Recsei, P. (1988)** A dye release assay for determination of lysostaphin activity. *Anal Biochem*, 171, 141-4.